

**The Response of  
Non-Sway Steel Framed Structures  
with Semi-Rigid Connections**

**Volume I**

by

**Sui Ming LAU**



**A thesis submitted in part fulfilment of the requirement  
for the degree of Doctor of Philosophy**

**Department of Civil and Structural Engineering  
University of Sheffield**

**December, 1993**

**The Response of Non-Sway Steel Framed Structures  
with Semi-Rigid Connections**

**Volume I**

This thesis deposited in the University Library has been divided into two volumes due to the restriction of the new procedures for the microfilming of thesis for the British Library. Volume I contains chapters 1 to 7 and Volume II contains chapters 8 to 11. Apologies for any inconveniences caused to the readers arising from this.

**Sui Ming LAU**

**To Vera, with all my love.**

# Abstract

This thesis describes research work undertaken to examine the influence of joint resistance to in-plane moments on the assessment of five full scale two dimensional steel frames. All the available information has been collected into a form which is readily usable by the wider research community. The findings have been used to develop improved semi-rigid design methods.

Details of the experimental results of five frames are discussed and reported. A variety of joint types were tested, each type of joint exhibited some degree of moment and rotational stiffness, leading to frame responses involving significant interaction between beams and columns. This affects both beam and column deflections, the pattern of frame moments, ultimate capacity of members and collapse modes.

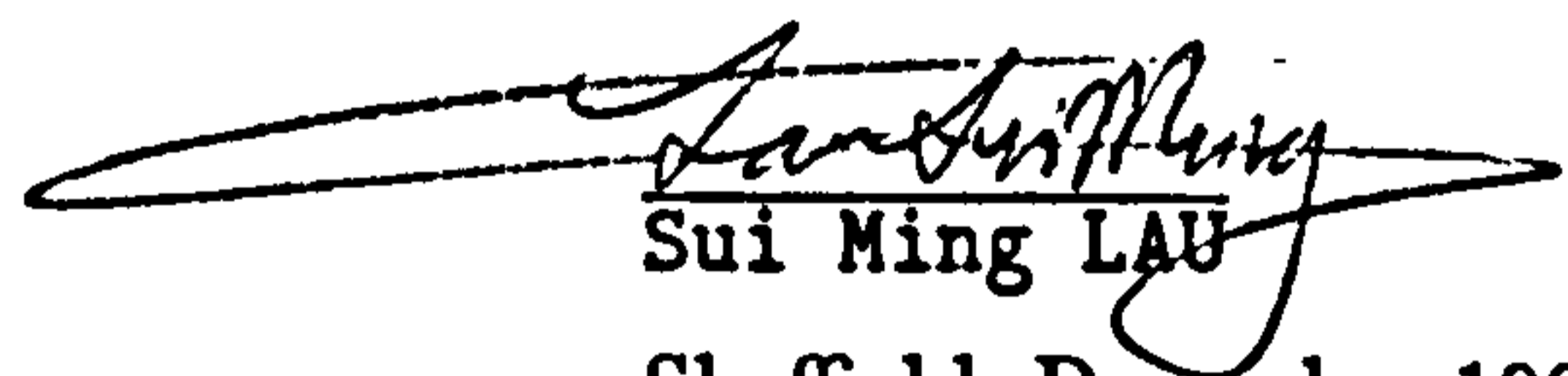
The principal objective of the tests was to provide experimental data against which two in house sophisticated computer analysis programs may be verified. Details of modifications to an existing databank of the moment-rotation test results to provide a more efficient and user friendly tool for research workers are explained.

The main objective of the work described herein was to investigate the influence of semi-rigid connection behaviour on a wide range of subassemblage configurations. A new method for the non-sway column design is developed and validated using the test and analytical results. The new approach is found to be more economical than the existing BS 5950 method but it still essentially conservative. The methods to design the lateral restraint beam including the serviceability and ultimate limit states are also proposed and examined. The most important feature is that the precise form of the  $M-\phi$  responses are not important for the semi-rigid design. Finally, a complete set of design methods is advised to take into account the inherent strength and stiffness of semi-rigid joints.

# Declaration

I hereby declare that the work embodied in this thesis is the result of my own investigations and analysis except where specific reference has been made to the work of others.

No part of this thesis has been submitted to any University or other educational establishment for a Degree, Diploma or other qualification.

  
Sui Ming LAU  
Sheffield, December 1993

# Acknowledgements

I would like to express my enormous appreciation to my supervisor, Dr. P. A. Kirby, for his helpful guidance and encouragement. Thanks are also extended to Dr. J. B. Davison for many helpful discussions particularly on the work of frame tests.

Praise and appreciation is also extended to all the financial supporters. The first research contract is sponsored by European Coal and Steel Community and the British Constructional Steelwork Association on the database during the period from 1-11-90 to 31-3-91. The second contract is sponsored by Building Research Establishment on the assessment of five frames data during the period from 1-4-91 to 31-3-94. I would like to thank the staff at BCSA, notably Mr. P. Allen and Dr. D. Moore in BRE, for their cooperation and technical expertise.

Finally, a special thank you goes to all the librarians of the Applied Science Library, Mrs. Judith Watson for the Faculty Office of Engineering, all Secretaries in the Department specially Mrs. V. Evans and Miss N. Nash whose friendship and support have made my work in University more enjoyable and helpful.

# Contents

Abstract . . . . .	I
Declaration . . . . .	II
Acknowledgements . . . . .	III
Contents . . . . .	IV
Notation . . . . .	XI
List of Tables . . . . .	XIV
List of Figures . . . . .	XIX
<b>1 Introduction</b>	<b>I-1</b>
<b>2 Historical Background</b>	<b>II-1</b>
2.1 Introduction . . . . .	II-1
2.2 Pinned Columns . . . . .	II-1
2.3 End-Restrained Columns . . . . .	II-3
2.4 Frame Tests . . . . .	II-6
<b>3 Databank of Moment-Rotation Test Results</b>	<b>III-1</b>
3.1 Introduction . . . . .	III-1
3.2 Types of Connections . . . . .	III-2
3.3 Structure of Program . . . . .	III-3
3.4 Usage of Database . . . . .	III-3
3.4.1 Scope . . . . .	III-3
3.4.2 Printing the Test Result . . . . .	III-3
3.4.3 Plotting of Moment Rotation Curve . . . . .	III-4
3.4.4 Connection Moment-Rotation Behaviour Modelling . . . . .	III-5
3.4.5 Comparison with Other Tests . . . . .	III-6
3.5 Improvement of Database . . . . .	III-7
3.5.1 General Scope . . . . .	III-7
3.5.2 Greater Efficiency and User Friendliness . . . . .	III-7
3.5.3 Update Test Data . . . . .	III-8

3.5.4	Composite Joint Tests . . . . .	III-8
3.5.5	Program Transfer to Other Centres . . . . .	III-9
3.6	Suggestion for Further Research . . . . .	III-10
<b>4</b>	<b>Tests of Five Full-Scale Steel Frames</b>	<b>IV-1</b>
4.1	Introduction . . . . .	IV-1
4.2	Selection of Frames for Test . . . . .	IV-2
4.3	Fabrication and Material Properties . . . . .	IV-2
4.4	Instrumentation . . . . .	IV-3
4.4.1	Loading and Bracing System . . . . .	IV-3
4.4.2	Strain Measurement . . . . .	IV-4
4.4.3	Rotation Measurement . . . . .	IV-4
4.4.4	Displacement Measurement . . . . .	IV-4
4.4.5	Bolt Force Measurement . . . . .	IV-4
4.5	Data Logging and Storage System . . . . .	IV-5
4.6	Interpretation of the Data . . . . .	IV-6
4.6.1	Analysis of Strains and Determination of Moments . . . . .	IV-6
4.6.2	Beam Moment Calculation . . . . .	IV-7
4.7	A Brief Description of Frame Tests . . . . .	IV-8
<b>5</b>	<b>Behaviour of Two Asymmetrical Frames with End Plate Connection</b>	<b>V-1</b>
5.1	Introduction . . . . .	V-1
5.2	Test Configuration . . . . .	V-1
5.3	Test Set Up and Procedures . . . . .	V-3
5.4	Main Features of Frames 1 and 2 . . . . .	V-4
5.4.1	Test Programme for Frames 1 and 2 . . . . .	V-4
5.4.2	Tightening Procedure in Connections . . . . .	V-5
5.4.3	Observations during Tests . . . . .	V-5
5.5	Behaviour of Frame under Different Load Combinations . . . . .	V-7
5.6	Discussion of Frame Test Results . . . . .	V-9
5.6.1	Parameters and Tests selected for Study . . . . .	V-9
5.6.2	Moment on Beams . . . . .	V-10
5.6.3	Moment Rotation Behaviour of Joints . . . . .	V-11
5.6.4	Beam Deflections . . . . .	V-13
5.6.5	Column Deflection . . . . .	V-14
5.6.6	Sway Displacement . . . . .	V-14
5.6.7	Connection Moment and Bolt Forces . . . . .	V-14



5.7	Tests to Failure in Frame 1 . . . . .	V-15
5.7.1	Test Observations . . . . .	V-15
5.7.2	Bending Moment Distribution around the Frame . . . . .	V-17
5.7.3	Deflected Shape of the Frame . . . . .	V-18
5.7.4	Load vs Moment Relationships in Beams . . . . .	V-19
5.7.5	Load-Deflection Relationships in Beams . . . . .	V-19
5.8	Tests to Failure in Frame 2 . . . . .	V-20
5.8.1	Test Observations . . . . .	V-20
5.8.2	Beam Moment Distribution around the Frame . . . . .	V-21
5.8.3	Deflected Shape of the Frame . . . . .	V-22
5.8.4	Relationship of Load-Moment in Beams . . . . .	V-23
5.8.5	Relationship of Load-Deflection in Beams . . . . .	V-24
5.9	Comparison of Response of Frames 1 and 2 in Tests to Failure . . . . .	V-25
5.10	Concluding Remarks on the Study . . . . .	V-26
<b>6</b>	<b>Behaviour of Two Frames with Flange Cleat Connections</b>	<b>VI-1</b>
6.1	Introduction . . . . .	VI-1
6.2	Test Configuration . . . . .	VI-1
6.3	Test Programme of Frames 3 and 4 . . . . .	VI-3
6.4	Tests to Failure - Frame 3 . . . . .	VI-4
6.4.1	Test Observations . . . . .	VI-4
6.4.2	Problem in the Applied Column Loads . . . . .	VI-4
6.4.3	Bending Moments on Beams . . . . .	VI-7
6.4.4	Relationship of Load-Deflection in Beams . . . . .	VI-7
6.4.5	Bending Moment Distribution around the Frame . . . . .	VI-8
6.4.6	Deflected Shape of the Frame . . . . .	VI-8
6.4.7	Behaviour of Columns as Failure Approached . . . . .	VI-9
6.4.7.1	Failure of Column in Position 2 . . . . .	VI-9
6.4.7.2	Failure of Column in Position 3 . . . . .	VI-10
6.4.8	Tests to Failure of Beams . . . . .	VI-12
6.4.8.1	Accidental Failure of Beam 6 . . . . .	VI-12
6.4.8.2	Failure of Beams 3, 4 and 5 . . . . .	VI-12
6.5	Tests to Failure - Frame 4 . . . . .	VI-13
6.5.1	Test Observations . . . . .	VI-13
6.5.2	Bending Moments on Beams . . . . .	VI-14
6.5.3	Relationship of Load-Deflection in Beams . . . . .	VI-15
6.5.4	Bending Moment Distribution around the Frame . . . . .	VI-15

6.5.5	Deflected Shape of the Frame . . . . .	VI-16
6.5.6	Failure of Column in Position 1 . . . . .	VI-16
6.5.7	Failure of Column in Position 2 . . . . .	VI-17
6.5.8	Test to Failure of the Edge Columns in Position 3 . . . . .	VI-18
6.5.9	Behaviour of Joints in Frame 3 . . . . .	VI-19
6.5.10	Behaviour of Joints in Frame 4 . . . . .	VI-20
6.6	Concluding Remarks on the Study . . . . .	VI-22
<b>7</b>	<b>Behaviour of a Symmetrical Frame with End-Plate Connection</b>	<b>VII-1</b>
7.1	Introduction . . . . .	VII-1
7.2	Test Configuration . . . . .	VII-1
7.3	Tests for Frame 5 . . . . .	VII-2
7.4	Loading Tests . . . . .	VII-3
7.5	Test of Failure . . . . .	VII-4
7.5.1	Test Observations . . . . .	VII-4
7.5.2	Bending Moments on Beams . . . . .	VII-5
7.5.3	Relationship of Load-Deflection in Beams . . . . .	VII-5
7.5.4	Bending Moment Distribution around the Frame . . . . .	VII-6
7.5.5	Deflected Shape of the Frame . . . . .	VII-7
7.5.6	Failure of Column in Position 2 . . . . .	VII-7
7.6	Moment Rotation Behaviour in Joints . . . . .	VII-9
7.6.1	General Behaviour of Connections . . . . .	VII-9
7.6.2	Discussion of Results . . . . .	VII-9
7.6.3	Loading and Unloading Stiffness . . . . .	VII-10
7.6.4	Comparison of the Connection Moment to the Rigid Moment . . . . .	VII-10
7.7	Connection Moment and Bolt Forces . . . . .	VII-11
7.7.1	Objectives . . . . .	VII-11
7.7.2	General Discussions . . . . .	VII-12
7.7.3	General Behaviour of Bolts in Different Connections . . . . .	VII-13
7.8	Concluding Remarks on the Study . . . . .	VII-14
<b>8</b>	<b>Comparisons of Experimental Results with Analytical Predictions</b>	<b>VIII-1</b>
8.1	Declaration . . . . .	VIII-1
8.2	Introduction . . . . .	VIII-1
8.3	Computer Programs Selected for Study . . . . .	VIII-2
8.3.1	SERFA . . . . .	VIII-2
8.3.2	SERVAR . . . . .	VIII-2

8.4	Comparison of Experimental and Predicted Behaviour . . . . .	VIII-2
8.4.1	Frames 1 and 2 . . . . .	VIII-4
8.4.2	Frame 3 . . . . .	VIII-5
8.4.3	Frame 4 . . . . .	VIII-7
8.4.4	Frame 5 . . . . .	VIII-8
8.5	Conclusions and Suggestions for Further Study . . . . .	VIII-10
8.5.1	Conclusions . . . . .	VIII-10
8.5.2	Suggestions for further study . . . . .	VIII-10
<b>9</b>	<b>Parametric Study for Subassemblage Structures</b>	<b>IX-1</b>
9.1	Introduction . . . . .	IX-1
9.2	Development of the Computer Program . . . . .	IX-2
9.3	Validity of the Computer Program . . . . .	IX-3
9.3.1	General . . . . .	IX-3
9.3.2	Comparison with Predicted Results to Actual Test Values for Sub- assemblages . . . . .	IX-3
9.4	Parametric Studies . . . . .	IX-4
9.4.1	General . . . . .	IX-4
9.4.2	Formation of Study . . . . .	IX-5
9.4.3	Subassemblage Configurations . . . . .	IX-5
9.5	First Phase of Study . . . . .	IX-6
9.5.1	Discussion of Result . . . . .	IX-7
9.6	Second Phase of Study . . . . .	IX-9
9.6.1	Discussion of Results . . . . .	IX-13
9.6.2	Conclusions of Second Phase . . . . .	IX-15
9.7	Third Phase of Study . . . . .	IX-15
9.7.1	Using $M-\phi$ Curves from Nominally Connections . . . . .	IX-15
9.7.2	Further Study of Variation of $M-\phi$ Response . . . . .	IX-16
9.7.3	Conclusions of Third Phase . . . . .	IX-17
9.8	Concluding Remarks on the Parametric Study . . . . .	IX-17
<b>10</b>	<b>Development of Semi-Rigid Design Methods</b>	<b>X-1</b>
10.1	Introduction . . . . .	X-1
10.2	Current Design Methods . . . . .	X-1
10.3	$M-\phi$ Characteristics for Beam-to-Column Connections . . . . .	X-2
10.3.1	Current Practice . . . . .	X-3
10.3.2	EC 3 Design Method for End-Plate Connections . . . . .	X-4

10.3.2.1	Design Philosophy . . . . .	X-4
10.3.2.2	Development of the EC 3 Design Method . . . . .	X-5
10.3.2.3	Connection Design Method of EC 3 . . . . .	X-5
10.3.2.4	Comparison the EC 3 predictions to the Experimental Results	X-6
10.3.3	Design Method for Flange Cleat Connections . . . . .	X-10
10.3.4	Joint Classification Systems . . . . .	X-12
10.3.5	General Comments and Conclusions . . . . .	X-15
10.4	The Deformation of Steel Frames under Serviceability Loads . . . . .	X-16
10.4.1	Development of the method to predict the Beam Deformation in Ser- viceability . . . . .	X-16
10.4.1.1	Introduction . . . . .	X-16
10.4.1.2	Development of the Methods . . . . .	X-18
10.4.2	Comparison predicted Beam Deflection at Serviceability to the Ex- perimental Results . . . . .	X-21
10.4.3	General Conclusions . . . . .	X-24
10.5	Ultimate Strength of Laterally Restrained Beams . . . . .	X-24
10.5.1	Introduction . . . . .	X-24
10.5.2	Modified Plastic Hinge Calculation . . . . .	X-25
10.6	Column Design at the Ultimate Limit State . . . . .	X-27
10.6.1	The Current Design Methods . . . . .	X-27
10.6.2	Methods incorporating Semi-Rigid Action . . . . .	X-28
10.6.3	Discussion . . . . .	X-29
10.6.4	Further Validation of the New Approach for the Column Design . .	X-33
10.6.5	Implication for the Design . . . . .	X-39
10.6.6	Recommended Design Procedure . . . . .	X-40
10.6.7	Comments and Conclusions . . . . .	X-41
10.7	Recommendations for a Semi-Rigid Design Method . . . . .	X-42
10.7.1	Procedure for the Design of a Steel Frame using Semi-Rigid Design Methods . . . . .	X-42
10.7.2	Design Methods and Example . . . . .	X-45
10.7.3	Deflection and Capacity Assessment of Frame using Validated Com- puter Program . . . . .	X-52
10.8	Concluding Remarks . . . . .	X-54
<b>11</b>	<b>Conclusions and Recommendations for Further Research</b>	<b>XI-1</b>
11.1	Conclusions . . . . .	XI-2
11.1.1	Connection Behaviour and Frame Response . . . . .	XI-2

11.1.2	Frame Analysis . . . . .	XI-3
11.1.3	Semi-Rigid Frame Design Methods . . . . .	XI-4
11.2	Recommendations for Further Research . . . . .	XI-5
11.2.1	Database . . . . .	XI-5
11.2.2	Frame Tests . . . . .	XI-6
11.2.3	Frame Analysis and Parametric Study . . . . .	XI-6
11.2.4	Frame Design . . . . .	XI-7
	Appendix A Liew and Chen Connection Modelling . . . . .	A-1
	Appendix B Figures . . . . .	B-1

# Notation

In this thesis, the following notation has been used. Notation to the Appendices is described therein.

$A_p$	applied column load
$A_x$	total axial load in column segment
$a_j$	dimensionless exponent
$C'_5, C_5$	secant stiffness of connections at 0.005 rad
$C'_{10}, C_{10}$	secant stiffness of connections at 0.01 rad
$C_c$	secant stiffness defined by Barakat and Chen
$C_i$	initial stiffness of connection
$C_j$	constant parameter
$C_k$	curve-fitting constant
$C_m$	maximum stiffness in the loading stage
$C_t$	loading stiffness
$C_u$	unloading stiffness
$D$	depth of beam
$D_k$	constant parameters for linear fuction
$d_r$	restained displacement
$d_c$	condensed out displacement
$\Delta d^0$	incremental displacement vector
$E$	modulus of elasticity of steel
$ECC$	position of beam end
$F$	force
$F_E$	Euler load (critical load)
$F_c$	condensed applied load
$F_r$	retained applied load
$\Delta F^0$	applied load vector at the proceeding iteration
$H[x]$	Heaviside step function
$I$	second moment of area
$I_b$	second moment of area about the major axis for beam
$I_c$	second moment of area about the relavent axis for column
$I_{cl}$	second moment of area about the relavent axis for lower column
$I_{cu}$	second moment of area about the relavent axis for upper column

$K$	scale factor
$[K^{+1}]$	stiffness matrix
$[K_r], [K_{rc}]$	member stiffness matrices
$[K_c], [K_{cr}]$	member stiffness matrices
$K_b$	beam stiffness
$K_b^1$	modified K factor
$K_c$	column stiffness
$K_i$	non-dimensional factor
$L$	length
$L_b$	length of beam
$L_c$	length of column
$L_{cl}$	length of lower column
$L_{cu}$	length of upper column
$L_o$	original length of column
$L_E$	effective length of column
$LOPD(i)$	applied load positions
$M$	bending moment
$M_1, M_2, M_3, M_4$	moment computer from strain gauges
$M'_1, M'_2, M'_3, M'_4$	calculated moment
$M_{Rd}$	design ultimate moment of beam
$M_E$	end moment for the connection
$M_j$	ultimate capacity of connection
$M_o$	initial moment
$M_p$	fully plastic moment of beam
$M_R$	rigid end connection moment
$M_{SR}$	semi-rigid end connection moment
$M_T$	total number of size parameters
$M_u$	ultimate moment of connection
$M^F$	fixed end moment
$m$	$= \frac{M}{M_u}$
$\bar{m}$	$= \frac{M}{M_p}$
$n$	shape parameter
$P_j$	numerical value of K
$R$	rigidity factor
$R_P$	pinned rotation angle
$R_{SR}$	semi-rigid rotation angle

$SGPO(i)$	stain gauge positions
$S_x$	plastic modulus
$W$	total load on beam
$w$	intensity of uniform distributed beam load
$\alpha$	dimensionless factor = $\frac{M_{SR}}{M_R}$
$\alpha_c$	constant parameter
$\alpha_{pin}$	failure load of a column non-dimensionalised with respect to the failure with pinned end column.
$\alpha_s$	scaling factor
$\beta$	slip factor
$\beta_{10}$	slip factor at 0.01 rad
$\beta_w$	slip factor at working load
$\gamma$	degree of rigidity of connection
$\gamma_{10}$	degree of rigidity of connection at 0.01 rad
$\gamma_w$	degree of rigidity of connection at working load
$\phi$	= $\frac{\phi_j}{\phi_{RP}}$
$\bar{\phi}$	= $\frac{\phi_j}{\phi_P}$
$\phi_b$	rotation of beam
$\phi_{bSR}$	the end rotation for the semi-rigid connection
$\phi_c$	rotation of column
$\phi_j$	rotation of joint
$\phi_P$	= $\frac{M_P}{EI_b}$ or $\frac{M_P}{\frac{5D}{L_b}}$
$\phi'_P$	= reference plastic rotation = $\frac{M_u}{C_i}$
$\phi_s$	calculated end rotation of beam assuming simply support ends
$\delta_P$	mid-span beam deflection for the pinned connected frame
$\delta_R$	mid-span beam deflection for the rigid connected frame
$\delta_{SR}$	mid-span beam deflection for the semi-rigid connected frame
$\theta_K$	startint rotation of linear function
$\lambda$	the ratio of the connection moment to the plastic beam moment



# List of Tables

## Chapter 4

- Table 4.1 Summary of Five Frame Tests  
Table 4.2 Yield Stress measured in Five Frames

## Chapter 5

- Table 5.1 Load Increments up to Design Load in Beams  
Table 5.2 Description of Tests on Frame 1  
Table 5.3 Description of Tests on Frame 2  
Table 5.4 Total Applied Load and Deflection of Beams under Different Load Combinations  
Table 5.5 Beam Moment Distribution in different Tests  
Table 5.6 Tests Selected for Analysis  
Table 5.7 Comparison of Moment in Tests and Rigid Frame Moment  
Table 5.8 Moment Rotation and Stiffness of Joints in Tests 23 and 28 of Frame 1  
Table 5.9 Joint Moment Rotation and Stiffness of Joints in Tests 31 and 40 of Frame 2  
Table 5.10 Comparison Deflection in Tests and Predicted Results  
Table 5.11 Mid-Height Deflection of Columns in Test 28 of Frame 1  
Table 5.12 Sway Displacement between Three Joints in Tests of Frame 2  
Table 5.13 Maximum Loads of Bolts in Two Tests  
Table 5.14 Load History of Frame 1 Test 28  
Table 5.15 Load History of Frame 1 Test 29  
Table 5.16 Load History of Frame 1 Test 30  
Table 5.17 Load History of Frame 2 Test 42  
Table 5.18 Load History of Frame 2 Test 43  
Table 5.19 Comparison of the Results in Test to Failure for Frames 1 and 2  
Table 5.20 Comparison of the Results from Beam 4 in Test to Residual Strength of Frames 1 and 2

## **Chapter 6**

<b>Table 6.1</b>	<b>Load Increments for the Applied Beam Loads in Frames 3 and 4</b>
<b>Table 6.2</b>	<b>Load History of Frame 3 Test 2 (uncorrected)</b>
<b>Table 6.3</b>	<b>Comparison with Different Methods to predict the Applied Column Axial Loads in Test 2</b>
<b>Table 6.4</b>	<b>Comparison of the Total Axial Loads in the Upper Storey with the Results obtained from Methods (1) and (3)</b>
<b>Table 6.5</b>	<b>Axial Load in Columns of Frame 3 Test 2 (Computed from Strain Gauge Readings)</b>
<b>Table 6.6</b>	<b>Comparison of Total Applied Load and Axial Load in Columns above Different Storeys in Test 2 of Frame 3</b>
<b>Table 6.7</b>	<b>Load History of Frame 3 Test 2 (corrected)</b>
<b>Table 6.8</b>	<b>Load History of Frame 3 Test 3</b>
<b>Table 6.9</b>	<b>Load History of Frame 3 Test 4</b>
<b>Table 6.10</b>	<b>Load History of Frame 4 Test 3</b>
<b>Table 6.11</b>	<b>Axial Load of Frame 4 Test 3</b>
<b>Table 6.12</b>	<b>Comparison of Total Applied Load and Axial Load in Columns above Different Storeys in Test 3 of Frame 4</b>
<b>Table 6.13</b>	<b>Load History of Frame 4 Test 4</b>

## **Chapter 7**

<b>Table 7.1</b>	<b>Description of Tests in Frame 5</b>
<b>Table 7.2</b>	<b>Mid-Span Deflection of Beams in Different Tests</b>
<b>Table 7.3</b>	<b>Beam Moment Distribution in Different Tests</b>
<b>Table 7.4</b>	<b>Load History of Frame 5 Test 17</b>
<b>Table 7.5</b>	<b>Axial Load of Frame 5 Test 17</b>
<b>Table 7.6</b>	<b>Comparison of Total Applied Load and Axial Load in Columns above Different Storeys in Test 17 of Frame 5</b>
<b>Table 7.7</b>	<b>End Moments as Percentage of Free Moment at Design Load in Test 17 of Frame 5</b>
<b>Table 7.8</b>	<b>Comparison of the Collapse Load from the Test and BS 5950 for the Central Column</b>
<b>Table 7.9</b>	<b>Comparison of the Stiffness and sustained Moment in Connections in Test 17</b>

- Table 7.10** Comparison of the Rigid connected Frame Moments in Scans 12 and 25 of Test 17
- Table 7.11** Maximum Loads for Bolts in Test 17 (Flush End-Plate)
- Table 7.12** Maximum Loads for Bolts in Test 17 (Extended End-Plate)

## **Chapter 8**

- Table 8.1** Comparison of Experimental and Predicted Results of Ultimate Capacity of Beams using SERFA and SERVAR
- Table 8.2** Comparison of Experimental Results to Predicted Results of Column Failure Loads from SERFA and SERVAR
- Table 8.3** Predicted Results based on Different Factors considered in the Model of SERVAR

## **Chapter 9**

- Table 9.1** Symbols used in the Comparison with Predicted Results to the Subassemblage Test
- Table 9.2** Comparison with the Failure Load predicted by Program
- Table 9.3** Symbols used in the First Phase of Study
- Table 9.4** Predicted Column Failure Load from the First Phase of Study
- Table 9.5** Symbols used in the Second Phase of Study
- Table 9.6** Predicted Column Failure Load with Different Connections for Column Orientation 'B' in the Second Phase of Study
- Table 9.7** Predicted Results from the  $M-\phi$  Curves in Different Tests for Flange Cleats Connections
- Table 9.8** Change of Ultimate Capacity of Columns due to the variation of  $M-\phi$  Response

## **Chapter 10**

- Table 10.1** Current Practice for the Moment Rotation Models
- Table 10.2** Ultimate Capacities predicted by EC 3
- Table 10.3** Moment, Rotation and Stiffness predicted by EC 3 for Frames 1, 2 and 5

Table 10.4	Comparison of EC 3 Predictions to the Frame and Joint Test Results in Frames 1, 2 and 5
Table 10.5	Comparison the predicted Initial Stiffness and Ultimate Moment to the Joint and Frame Test Results used Liew & Chen Models for Frame 3
Table 10.6	Stiffness from the Frame and Joint Tests in Frame 1
Table 10.7	Stiffness from the Frame and Joint Tests in Frame 2
Table 10.8	Stiffness from the Frame and Joint Tests in Frame 3
Table 10.9	Stiffness from the Frame and Joint Tests in Frame 4
Table 10.10	Stiffness from the Frame and Joint Tests in Frame 5
Table 10.11	Dimensionless Factors determined from Five Frame Tests
Table 10.12	Comparison with Mid-Span Deflection to predict Results from different Methods using Frame $M-\phi$ Curves
Table 10.13	Comparison with Mid-Span Deflection to predict Results from different Methods using Joint $M-\phi$ Curves
Table 10.14	Determine the Factor of $\lambda$ from the Tests
Table 10.15	Comparison of the predicted Ultimate Capacity of Beams used the Modified Plastic Hinges Calculation to the Frame Tests
Table 10.16	Slip Factors $\beta$ for the Connections in Frames 3, 4 and 5
Table 10.17	Description of Methods and Cases used in Study
Table 10.18	Comparison with Different Effective Lengths to predict the Failure Load at Columns 4, 5 and 6 in Frame 3
Table 10.19	Comparison with Different Effective Lengths to predict the Failure Load at Columns 7, 8 and 9 in Frame 3
Table 10.20	Comparison with Different Effective Lengths to predict the Failure Load at Columns 1, 2 and 3 in Frame 4
Table 10.21	Comparison with Different Effective Lengths to predict the Failure Load at Columns 4, 5 and 6 in Frame 4
Table 10.22	Comparison with Different Effective Lengths to predict the Failure Load at Columns 4, 5 and 6 in Frame 5
Table 10.23	Comparison of the Ultimate Capacity of Columns for New Design Approach to other Different Methods in Frames 3, 4 and 5
Table 10.24	Comparison of the Ultimate Capacity of Columns for New Design Approach to other Different Methods for 3-D Frames F1 and F2
Table 10.25	Comparison of the Ultimate Capacity of Columns for New Design Approach to other Different Methods for the Parametric Study

Table 10.26	Comparison of the Ultimate Capacity of Columns for New Design Approach to other Different Methods for Trinity Court in Manchester
Table 10.27	Comparison of the Ultimate Capacity of Columns for New Design Approach to other Different Methods for M.R.I. Building in Nottingham
Table 10.28	Comparison of the Ultimate Capacity of Columns used the New Design Approach due to the Variation of the $C_{10}$
Table 10.29	Comparison of the Member Sizes of Frame 5 to the Simple Design Frame and the New Semi-Rigid Design Frame
Table 10.30	Predicted Deflections for New Design Frame used Different Methods
Table 10.31	Comparison of the $\lambda$ value computed from SERFA to the Values used in New Design Frame under Design Load
Table 10.32	Comparison of the Ultimate Capacity of Beams used Different Methods
Table 10.33	Comparison of the Ultimate Capacity of Columns used Different Methods

# List of Figures

## Chapter 2

- Figure 2.1 Variation of Moment Rotation Characteristics for Various of Beam to Column Connections
- Figure 2.2 Influence of Connection Restraint on the Strength of Axially Loaded Columns

## Chapter 3

- Figure 3.1 Single Web Cleat Connection
- Figure 3.2 Double Web Cleats Connection
- Figure 3.3 Single Web Plate Connection
- Figure 3.4 Flange Cleats with Web Cleats Connection
- Figure 3.5 Header Plate Connection
- Figure 3.6 Flush End-Plate Connection
- Figure 3.7 Extended End-Plate Connection
- Figure 3.8 A Example Moment Rotation Curve in Dimensional Form
- Figure 3.9 A Example Moment Rotation Curve in Non-Dimensional Form
- Figure 3.10 Comparison of Test Moment Rotation Curve to Frye-Morris Prediction
- Figure 3.11 Comparison of Test Moment Rotation Curve to B-Spline Curve Fitting
- Figure 3.12 Comparison of Test Moment Rotation Curve to Liu-Chen Fitting
- Figure 3.13 Three Models of Fitting in a Same Plot
- Figure 3.14 Modified Selecting Procedure for Sheffield Database

## Chapter 4

- Figure 4.1 Initial Shape of Frames 3, 4 and 5
- Figure 4.2 Instrumentation of Frames 1 and 2
- Figure 4.3 Hydraulic Beam Loading Arrangement
- Figure 4.4 Column Head Loading Arrangement
- Figure 4.5 Out-of-Plate Action Bracing Locations
- Figure 4.6 Rotation Device
- Figure 4.7 Location of Linear Voltage Displacement Transducers
- Figure 4.8 Strain Gauged Bolt
- Figure 4.9 Strain Gauge Position in Five Frames
- Figure 4.10 Determine of Force Components from measured Strain

- Figure 4.11 Nomenclature of Strain Gauges in the Sections of Beams and Columns  
 Figure 4.12 Notation adopted for Beam Moment Calculation  
 Figure 4.13 Nomenclature of Five Frames

## Chapter 5

- Figure 5.1 Frame 1 views towards the Balcony  
 Figure 5.2 General Arrangement of Frames 1 and 2  
 Figure 5.3 Dimensions of Connections used in Frames 1 and 2  
 Figure 5.4 Stiffeners located in a Column near Connection at Beam Loading Point  
 Figure 5.5 Strain Gauge Positions for Frame 2  
 Figure 5.6 Bolts Tightening Sequence  
 Figure 5.7 Nomenclature and Position of Bolts  
 Figure 5.8 Lack-of-fit Type 1  
 Figure 5.9 Lack-of-fit Type 2  
 Figure 5.10 Lack-of-fit Type 3  
 Figure 5.11 Lack-of-fit Type 4  
 Figure 5.12 Lack-of-fit Type 5  
 Figure 5.13 Lack-of-fit Type 6  
 Figure 5.14 Lack-of-fit Type 7  
 Figure 5.15 Moment Rotation Curve for Test 23 of Frame 1 (Flush End-Plate)  
 Figure 5.16 Moment Rotation Curve for Test 23 of Frame 1 (Extended End-Plate)  
 Figure 5.17 Moment Rotation Curve for Test 28 of Frame 1 (Flush End-Plate)  
 Figure 5.18 Moment Rotation Curve for Test 28 of Frame 1 (Extended End-Plate)  
 Figure 5.19 Moment Rotation Curve for Test 31 of Frame 2 (Flush End-Plate)  
 Figure 5.20 Moment Rotation Curve for Test 31 of Frame 2 (Extended End-Plate)  
 Figure 5.21 Moment Rotation Curve for Test 40 of Frame 2 (Flush End-Plate)  
 Figure 5.22 Moment Rotation Curve for Test 40 of Frame 2 (Extended End-Plate)  
 Figure 5.23 A Typical Moment Rotation Curve  
 Figure 5.24 Moment against Bolt Forces at Joint A for Test 28 of Frame 1  
 Figure 5.25 Moment against Bolt Forces at Joint C for Test 28 of Frame 1  
 Figure 5.26 Moment against Bolt Forces at Joint E for Test 28 of Frame 1  
 Figure 5.27 Moment against Bolt Forces at Joint G for Test 28 of Frame 1  
 Figure 5.28 Moment against Bolt Forces at Joint I for Test 28 of Frame 1  
 Figure 5.29 Moment against Bolt Forces at Joint J for Test 28 of Frame 1  
 Figure 5.30 Moment against Bolt Forces at Joint A for Test 40 of Frame 2

- Figure 5.31 Moment against Bolt Forces at Joint C for Test 40 of Frame 2
- Figure 5.32 Moment against Bolt Forces at Joint E for Test 40 of Frame 2
- Figure 5.33 Moment against Bolt Forces at Joint G for Test 40 of Frame 2
- Figure 5.34 Moment against Bolt Forces at Joint I for Test 40 of Frame 2
- Figure 5.35 Moment against Bolt Forces at Joint J for Test 40 of Frame 2
- Figure 5.36 Frame Moment around the Frame in Test 28 of Frame 1
- Figure 5.37 Frame Moment around the Frame in Test 29 of Frame 1
- Figure 5.38 Frame Moment around the Frame in Test 30 of Frame 1
- Figure 5.39 Change of the Column Head Moment in the Central Column of Test
- Figure 5.40 Frame Deformation around the Frame in Test 28 of Frame 1
- Figure 5.41 Frame Deformation around the Frame in Test 29 of Frame 1
- Figure 5.42 Frame Deformation around the Frame in Test 30 of Frame 1
- Figure 5.43 Total Applied Load vs Bending Moment on Beam 5 in Test 28 of Frame 1
- Figure 5.44 Total Applied Load vs Bending Moment on Beam 6 in Test 28 of Frame 1
- Figure 5.45 Total Applied Load vs Bending Moment on Beam 5 in Test 29 of Frame 1
- Figure 5.46 Total Applied Load vs Bending Moment on Beam 6 in Test 29 of Frame 1
- Figure 5.47 Total Applied Load vs Mid-Span Deflection on Six Beams in Test 28 of Frame 1
- Figure 5.48 Total Applied Load vs Mid-Span Deflection on Six Beams in Test 29 of Frame 1
- Figure 5.49 Total Applied Load vs Mid-Span Deflection on Beams 2, 3 and 4 in Test 28 of Frame 1
- Figure 5.50 Moment against Bolt Forces at Joint I in Test 42 of Frame 2
- Figure 5.51 Frame Moment around the Frame in Test 42 of Frame 2
- Figure 5.52 Frame Moment around the Frame in Test 43 of Frame 2
- Figure 5.53 Frame Deformation around the Frame in Test 42 of Frame 2
- Figure 5.54 Frame Deformation around the Frame in Test 43 of Frame 2
- Figure 5.55 Total Applied Load vs Bending Moment on Beam 5 in Test 42 of Frame 2
- Figure 5.56 Total Applied Load vs Bending Moment on Beam 6 in Test 42 of Frame 2
- Figure 5.57 Total Applied Load vs Bending Moment on Beam 5 in Test 43 of Frame 2
- Figure 5.58 Total Applied Load vs Bending Moment on Beam 6 in Test 43 of Frame 2
- Figure 5.59 Total Applied Load vs Mid-Span Deflection on Six Beams in Test 42 of Frame 2
- Figure 5.60 Total Applied Load vs Mid-Span Deflection on Beams 1 and 4 in Test 42 of Frame 2



## Chapter 6

- Figure 6.1 Frame 3 views towards the Balcony
- Figure 6.2 Frame 4 views towards the Balcony
- Figure 6.3 General Arrangement of Frame 3 (Major Axis Frame)
- Figure 6.4 General Arrangement of Frame 4 (Minor Axis Frame)
- Figure 6.5 Flange Cleat Connection used in Frames 3 and 4
- Figure 6.6 Total Applied Load vs Bending Moment on Beam 2 in Test 3 of Frame 3
- Figure 6.7 Total Applied Load vs Bending Moment on Beam 3 in Test 3 of Frame 3
- Figure 6.8 Total Applied Load vs Bending Moment on Beam 4 in Test 3 of Frame 3
- Figure 6.9 Total Applied Load vs Bending Moment on Beam 5 in Test 3 of Frame 3
- Figure 6.10 Total Applied Load vs Bending Moment on Beam 6 in Test 3 of Frame 3
- Figure 6.11 Bending Moment distribution around Beam 3 in Test 2 of Frame 3 up to End of Beam Load
- Figure 6.12 Total Applied Load vs Mid-Span Deflection on Five Beams in Test 2 of Frame 3
- Figure 6.13 Frame Moment around the Frame in Test 2 of Frame 3 up to End of Beam Load
- Figure 6.14 Frame Moment around the Frame in Test 2 of Frame 3 in Failure of the Central Column in Position 2
- Figure 6.15 Frame Moment around the Frame in Test 2 of Frame 3 in Failure of the Edge Column in Position 3
- Figure 6.16 Moment Equilibrium Check in Frame 3 Test 2
- Figure 6.17 Frame Deformation around the Frame in Test 2 of Frame 3 up to End of the Beam Load
- Figure 6.18 Frame Deformation around the Frame in Test 2 of Frame 3 in Failure of the Central Column in Position 2
- Figure 6.19 Frame Deformation around the Frame in Test 2 of Frame 3 in Failure of the Edge Column in Position 3
- Figure 6.20 Total Axial Load vs the Mid-Height Deflection at Three Lifts of the Central Column (Position 2) in Test 2 of Frame 3
- Figure 6.21 Total Axial Load vs the Column Head Moments at Three Lifts of the Central Column (Position 2) in Test 2 of Frame 3
- Figure 6.22 Total Axial Load vs the Mid-Height Deflection at Three Lifts of the Edge Column (Position 3) in Test 2 of Frame 3

- Figure 6.23** Total Axial Load vs the Column Head Moments at Three Lifts of the Edge Column (Position 3) in Test 2 of Frame 3
- Figure 6.24** Total Applied Load vs Bending Moment on Beam 3 in Test 4 of Frame 3
- Figure 6.25** Total Applied Load vs Bending Moment on Beam 4 in Test 4 of Frame 3
- Figure 6.26** Total Applied Load vs Bending Moment on Beam 5 in Test 4 of Frame 3
- Figure 6.27** Total Applied Load vs Mid-Span Deflection on Beams 3, 4 and 5 in Test 4 of Frame 3
- Figure 6.28** Total Applied Load vs Bending Moment on Beam 1 in Test 3 of Frame 4
- Figure 6.29** Total Applied Load vs Bending Moment on Beam 2 in Test 3 of Frame 4
- Figure 6.30** Total Applied Load vs Bending Moment on Beam 3 in Test 3 of Frame 4
- Figure 6.31** Total Applied Load vs Bending Moment on Beam 4 in Test 3 of Frame 4
- Figure 6.32** Total Applied Load vs Bending Moment on Beam 5 in Test 3 of Frame 4
- Figure 6.33** Total Applied Load vs Bending Moment on Beam 6 in Test 3 of Frame 4
- Figure 6.34** Bending Moment Distribution around Beam 3 in Test 3 of Frame 4 up to End of Beam Load
- Figure 6.35** Total Applied Load vs Mid-Span Deflection on Six Beams in Test 3 of Frame 4
- Figure 6.36** Frame Moment around the Frame in Test 3 of Frame 4 up to End of Beam Load
- Figure 6.37** Frame Moment around the Frame in Test 3 of Frame 4 in Failure of the Edge Column in Position 1
- Figure 6.38** Frame Moment around the Frame in Test 3 of Frame 4 in Failure of the Central Column in Position 2
- Figure 6.39** Moment Equilibrium Check in Frame 4 Test 3
- Figure 6.40** Frame Deformation around the Frame in Test 3 of Frame 4 up to End of the Beam Load
- Figure 6.41** Frame Deformation around the Frame in Test 3 of Frame 4 in Failure of the Edge Column in Position 1
- Figure 6.42** Frame Deformation around the Frame in Test 3 of Frame 4 in Failure of the Central Column in Position 2
- Figure 6.43** Total Axial Load vs the Mid-Height Deflection at Three Lifts of the Edge Column (Position 1) in Test 3 of Frame 4
- Figure 6.44** Total Axial Load vs the Column Head Moments at Three Lifts of the Edge Column (Position 1) in Test 3 of Frame 4
- Figure 6.45** Total Axial Load vs the Mid-Height Deflection at Three Lifts of the Central Column (Position 2) in Test 3 of Frame 4

- Figure 6.46 Total Axial Load vs the Mid-Height Column Moments at Three Lifts of the Central Column (Position 2) in Test 3 of Frame 4
- Figure 6.47 Total Axial Load vs the Mid-Height Deflection at Column 9 of the Edge Column (Position 3) in Test 4 of Frame 4
- Figure 6.48 Moment Rotation Curve for Test 2 of Frame 3 (External Joints C and E)
- Figure 6.49 Moment Rotation Curve for Test 2 of Frame 3 (Internal Joint F)
- Figure 6.50 Moment Rotation Curve for Test 2 of Frame 3 (Internal Joints G, I and K)
- Figure 6.51 Moment Rotation Curve for Test 2 of Frame 3 (External Joints H, J and L)
- Figure 6.52 Moment Rotation Curve for Test 3 of Frame 4 (External Joints A, C and E)
- Figure 6.53 Moment Rotation Curve for Test 3 of Frame 4 (Internal Joints B, D and F)
- Figure 6.54 Moment Rotation Curve for Test 3 of Frame 4 (Internal Joints G, I and K)
- Figure 6.55 Moment Rotation Curve for Test 3 of Frame 4 (External Joints H, J and L)

## Chapter 7

- Figure 7.1 Frame 5 views towards the Balcony
- Figure 7.2 General Arrangement of Frame 5 viewed from the Balcony
- Figure 7.3 Connection Detail in Frame 5
- Figure 7.4 Total Applied Load vs Bending Moment on Beam 1 in Test 17 of Frame 5
- Figure 7.5 Total Applied Load vs Bending Moment on Beam 2 in Test 17 of Frame 5
- Figure 7.6 Total Applied Load vs Bending Moment on Beam 3 in Test 17 of Frame 5
- Figure 7.7 Total Applied Load vs Bending Moment on Beam 4 in Test 17 of Frame 5
- Figure 7.8 Total Applied Load vs Bending Moment on Beam 5 in Test 17 of Frame 5
- Figure 7.9 Total Applied Load vs Bending Moment on Beam 6 in Test 17 of Frame 5
- Figure 7.10 Bending Moment Distribution around Beam 3 in Test 17 of Frame 5 up to End of Beam Load
- Figure 7.11 Total Applied Load vs Mid-Span Deflection on Six Beams in Test 17 of Frame 5
- Figure 7.12 Frame Moment around the Frame in Test 17 of Frame 5 in the End of the Beam Load and Failure of the Central Column
- Figure 7.13 Frame Moment around the Frame in Test 17 of Frame 5 in Failure of the Central Column
- Figure 7.14 Moment Equilibrium Check in Frame 5 Test 17
- Figure 7.15 Frame Deformation around the Frame in Test 17 of Frame 5 in the End of the Beam Load and Failure of the Central Column
- Figure 7.16 Frame Deformation around the Frame in Test 17 of Frame 5 in Failure of the Central Column

- Figure 7.17** Total Axial Load vs the Column Moments at Different Locations at Column 4 in Test 17 of Frame 5
- Figure 7.18** Total Axial Load vs the Column Moments at Different Locations at Column 5 in Test 17 of Frame 5
- Figure 7.19** Total Axial Load vs the Column Moments at Different Locations at Column 6 in Test 17 of Frame 5
- Figure 7.20** Total Axial Load vs the Column Head Moments at Three Lifts of the Central Column (Position 2) in Test 17 of Frame 5
- Figure 7.21** Total Axial Load vs the Column Deflections at Different Locations at Column 6 in Test 17 of Frame 5
- Figure 7.22** Moment Rotation Curve for Test 17 of Frame 5 (External Joints A, C and E)
- Figure 7.23** Moment Rotation Curve for Test 17 of Frame 5 (Internal Joints B, D and F)
- Figure 7.24** Moment Rotation Curve for Test 17 of Frame 5 (Internal Joints G, I and K)
- Figure 7.25** Moment Rotation Curve for Test 17 of Frame 5 (External Joints H and L)
- Figure 7.26** Moment against Bolt Forces at Joint A for Test 17 of Frame 5
- Figure 7.27** Moment against Bolt Forces at Joint C for Test 17 of Frame 5
- Figure 7.28** Moment against Bolt Forces at Joint E for Test 17 of Frame 5
- Figure 7.29** Moment against Bolt Forces at Joint B for Test 17 of Frame 5
- Figure 7.30** Moment against Bolt Forces at Joint D for Test 17 of Frame 5
- Figure 7.31** Moment against Bolt Forces at Joint F for Test 17 of Frame 5
- Figure 7.32** Moment against Bolt Forces at Joint G for Test 17 of Frame 5
- Figure 7.33** Moment against Bolt Forces at Joint I for Test 17 of Frame 5
- Figure 7.34** Moment against Bolt Forces at Joint K for Test 17 of Frame 5
- Figure 7.35** Moment against Bolt Forces at Joint H for Test 17 of Frame 5
- Figure 7.36** Moment against Bolt Forces at Joint J for Test 17 of Frame 5
- Figure 7.37** Moment against Bolt Forces at Joint L for Test 17 of Frame 5

## **Chapter 8**

- Figure 8.1** Model designed for SERFA
- Figure 8.2** Models designed for SERVAV
- Figure 8.3** Linearised Moment Rotation Characteristic used in the Computer Programs
- Figure 8.4** Comparison of Test Moments to Prediction at End of Beam Load Phase in Test 28 of Frame 1 (SERFA)

- Figure 8.5** Comparison of Test Moments to Prediction at Failure of Beams 5 and 6 in Test 42 of Frame 2 (SERFA)
- Figure 8.6** Comparison of Test Moments to Prediction at End of Beam Load Phase in Test 28 of Frame 1 (SERVAR)
- Figure 8.7** Comparison of Test Moments to Prediction at Failure of Beams 5 and 6 in Test 42 of Frame 2 (SERVAR)
- Figure 8.8** Comparison of Predicted and Test Total Applied Load vs the Mid-Span Deflection of Beam 5 in Test 29 of Frame 1
- Figure 8.9** Comparison of Predicted and Test Total Applied Load vs the Mid-Span Deflection of Beam 6 in Test 29 of Frame 1
- Figure 8.10** Comparison of Predicted and Test Total Applied Load vs the Mid-Span Deflection of Beam 5 in Test 42 of Frame 2
- Figure 8.11** Comparison of Predicted and Test Total Applied Load vs the Mid-Span Deflection of Beam 6 in Test 42 of Frame 2
- Figure 8.12** Comparison of Test Moments to Predictions of Frame 3 from SERFA
- Figure 8.13** Comparison of Test Moments to Predictions of Frame 3 from SERVAR
- Figure 8.14** Comparison of Predicted and Test Total Applied Load vs the Mid-Span Deflection of Beam 3 in Test 2 of Frame 3
- Figure 8.15** Comparison of Predicted and Test Axial Load vs the Mid-Height Deflection of Column C4 in Test 2 of Frame 3
- Figure 8.16** Comparison of Predicted and Test Axial Load vs the Mid-Height Deflection of Column C7 in Test 2 of Frame 3
- Figure 8.17** Comparison of Predicted and Test Total Applied Load vs the Mid-Span Deflection of Beam 3 in Test 4 of Frame 3
- Figure 8.18** Comparison of Predicted and Test Total Applied Load vs the Mid-Span Deflection of Beam 4 in Test 4 of Frame 3
- Figure 8.19** Comparison of Predicted and Test Total Applied Load vs the Mid-Span Deflection of Beam 5 in Test 4 of Frame 3
- Figure 8.20** Comparison of Test Moments to Predictions of Frame 4 from SERFA
- Figure 8.21** Comparison of Predicted and Test Axial Load vs the Mid-Height Deflection of Column C1 in Test 3 of Frame 4
- Figure 8.22** Comparison of Predicted and Test Axial Load vs the Mid-Height Deflection of Column C5 in Test 3 of Frame 4
- Figure 8.23** Comparison of Test Moments to Predictions of Frame 5 from SERFA
- Figure 8.24** Comparison of Test Moments to Predictions of Frame 5 from SERVAR

- Figure 8.25** Deformation and Bending Moment Distribution around Frame 5 with Different Predicted and Test Results at Failure of the Central Column
- Figure 8.26** Comparison of Predicted and Test Axial Load vs the Mid-Height Deflection of Column C4 in Test 17 of Frame 5
- Figure 8.27** Pattern of Residual Stress assumed in Column used in the Models of SERFA

## **Chapter 9**

- Figure 9.1** Computer Programs developed in the University of Sheffield
- Figure 9.2** Subassemblage Tests conducted by Gibbons
- Figure 9.3** Comparison of Predicted and Experimental Deflections at the Column Centre of Test S4
- Figure 9.4** Comparison of Predicted and Experimental Moments at the Column Centre of Test S4
- Figure 9.5** The Design Model Arrangement and its Analytical Model
- Figure 9.6** Deflection Mode of Subassemblage in Loading Case (0)
- Figure 9.7** Deflection Mode of Subassemblage in Loading Case (1)
- Figure 9.8** Deflection Mode of Subassemblage in Loading Case (2)
- Figure 9.9** Loading-Unloading Characteristics of Flexible Connections
- Figure 9.10** Moment Rotation Response for Cyclic and Monotonic Loading
- Figure 9.11** Force Distribution and Rotation of Joint for Flexible Connections
- Figure 9.12** Comparison of Moment Rotation Curves of Flush End-Plate Connections (Major axis) from Davison and Celikag
- Figure 9.13** Comparison of Moment Rotation Curves of Flush End-Plate Connections (Minor axis) from Davison and Celikag
- Figure 9.14** Comparison of Moment Rotation Curves of Web and Seat Cleats Connections (Major axis) from Davison and Celikag
- Figure 9.15** Comparison of Moment Rotation Curves of Web and Seat Cleats Connections (Minor axis) from Davison and Celikag
- Figure 9.16** Comparison of Moment Rotation Curves of Double Web Cleats Connections (Major axis) from Davison and Celikag
- Figure 9.17** Comparison of Moment Rotation Curves of Double Web Cleats Connections (Minor axis) from Davison and Celikag
- Figure 9.18** Total Axial Load vs Mid-Height Deflection of Column (Minor Axis) used different Moment Rotation Curves from Davison
- Figure 9.19** Total Axial Load vs Mid-Height Deflection of Column (Minor Axis) used different Moment Rotation Curves from Celikag

- Figure 9.20** Moment Rotation Curves of Flange Cleat Connection (Major Axis ) in different Test Conditions
- Figure 9.21** Moment Rotation Curves of Flange Cleat Connection (Minor Axis ) in different Test Conditions
- Figure 9.22** Total Axial Load vs Mid-Height Deflection of Column used different Moment Rotation Curves (Flange Cleat)
- Figure 9.23** Total Axial Load vs Moment at Column Top used different Moment Rotation Curves (Flange Cleat)
- Figure 9.24** Total Axial Load vs Moment at Column Centre used different Moment Rotation Curves (Flange Cleat)
- Figure 9.25** Variation of the Moment Rotation Responses for Flush End-Plate Connections form Davison and Celikag
- Figure 9.26** Total Axial Load vs Mid-Height Deflection with the Variation of Moment Rotation Curves (Flush End-Plate)
- Figure 9.27** Total Axial Load vs Mid-Height Deflection with the Variation of Moment Rotation Curves (Web and Seat Cleats)
- Figure 9.28** Total Axial Load vs Mid-Height Deflection with the Variation of Moment Rotation Curves (Double Web Cleats)

## **Chapter 10**

- Figure 10.1** Two Approaches for Design of Flush End-Plate Connections
- Figure 10.2**  $M-\phi$  Curves predicted by EC 3 for Frames 1 and 2
- Figure 10.3**  $M-\phi$  Curves predicted by EC 3 for Frame 5
- Figure 10.4** Comparison of EC 3 prediction to Experimental Results (FEP 12mm) of Frame 1
- Figure 10.5** Comparison of EC 3 prediction to Experimental Results (FEP 15mm) of Frame 1
- Figure 10.6** Comparison of EC 3 prediction to Experimental Results (FEP 20mm) of Frame 1
- Figure 10.7** Comparison of EC 3 prediction to Experimental Results (EEP 20mm) of Frame 1
- Figure 10.8** Comparison of EC 3 prediction to Experimental Results (EEP 25mm) of Frame 1
- Figure 10.9** Comparison of EC 3 prediction to Experimental Results (FEP 12mm) of Frame 2

- Figure 10.10 Comparison of EC 3 prediction to Experimental Results (FEP 15mm) of Frame 2
- Figure 10.11 Comparison of EC 3 prediction to Experimental Results (FEP 20mm) of Frame 2
- Figure 10.12 Comparison of EC 3 prediction to Experimental Results (EEP 20mm) of Frame 2
- Figure 10.13 Comparison of EC 3 prediction to Experimental Results (EEP 25mm) of Frame 2
- Figure 10.14 Comparison of EC 3 prediction to Experimental Results (FEP 12mm) of Frame 5
- Figure 10.15 Comparison of EC 3 prediction to Experimental Results (EEP 15mm) of Frame 5
- Figure 10.16 Comparison of prediction from Liew & Chen Model to the Experimental Results (Flange Cleat Connection) of Frame 3
- Figure 10.17 Classification of Connection according to EC 3
- Figure 10.18 Classification of Connection according to Bjorhovde
- Figure 10.19 Classification of Connection in Frame 2 using EC 3
- Figure 10.20 Classification of Connection in Frame 3 using EC 3
- Figure 10.21 Classification of Connection in Frame 4 using EC 3
- Figure 10.22 Classification of Connection in Frame 5 using EC 3
- Figure 10.23 Classification of Connection in Frame 2 using Bjorhovde
- Figure 10.24 Classification of Connection in Frame 3 using Bjorhovde
- Figure 10.25 Classification of Connection in Frame 4 using Bjorhovde
- Figure 10.26 Classification of Connection in Frame 5 using Bjorhovde
- Figure 10.27 Beam-to-Column Sub-frame
- Figure 10.28 Beam Line Method to estimate the Semi-Rigid Moment
- Figure 10.29 Method used for the Secant Stiffness of  $C_i$
- Figure 10.30 Method used for the Secant Stiffness of  $C_{10}$
- Figure 10.31 Method used for the Secant Stiffness of  $C_5$
- Figure 10.32 Method used for the Secant Stiffness of  $C_e$
- Figure 10.33 Behaviour of Beam with Semi-Rigid Connections
- Figure 10.34 The Relationship between the Secant Stiffness of  $C_{10}$  to the Loading  $C_i$  and Unloading  $C_u$  Stiffness of Connections
- Figure 10.35 Development of Semi-Rigid Design Methods
- Figure 10.36 Moment Rotation Curves for Flush End-Plate and Extended End-Plate for Example
- Figure 10.37 Classification of Connections using EC 3 for Example



# Chapter 1

## Introduction

When designing steel frames it is customary to make simplifying assumptions about the behaviour of the beam to column connections and consider them to act either as 'pins' or to achieve full 'rigidity'. In the case of the pin connection, no significant transfer of moment is assumed and the fabrication of such connections is made as simple as possible. For joints assumed to be 'rigid', the connection is considered to have infinite stiffness and transfer the maximum moment possible. The joints need careful detailing, frequently involving the use of stiffeners, with the usual approach being to develop the full moment capacity of the members.

From experimental studies [1.1,1.2] it is evident that most simple beam to column connections are capable of developing some intermediate degree of moment transfer. Such simple connections may therefore be considered as semi-rigid - they possess a rotational stiffness which is intermediate between that of a true pinned connection with zero stiffness and that of a fully fixed connection with infinite stiffness.

The aim of this research project is to understand the influence of semi-rigid joint action on overall frame behaviour by performing both the experimental data assessment from five full scale three storey two bay frame tests and to conduct parametric studies to understand and ultimately quantify, the potential benefits of semi-rigid connection response. One of the objectives is to collate these observations, together with those of other researchers, and to provide further evidence of beam deflections predicted by a convenient and coherent method which is suitable for use in practice. Finally, the aim was to examine the effect of connection stiffness on the load carrying capacity of the steel frame structures.

One objective of the collection of data from the five frame tests is to provide access

to moment-rotation characteristics and corresponding parameters of semi-rigid beam-to-column connections in a convenient computerised form and is the motivation behind the development of a steel beam-to-column connection database at the University of Sheffield. As part of an ECSC contract, work was carried out on the maintenance of the Sheffield database of beam to column joint moment-rotation characteristics. Updated information was entered and a set of computer programs was developed which enable a user to load and unload the test information to and from the Standard Query Language (SQL) system. The database thus can be more easily transferred to other research groups and more readily mounted on a PC. The improvements carried out for this database are presented in chapter 3.

The main objective of this thesis is to discuss and analyse the behaviour of five full scale frame tests and chapters 4 to 7 contain this information. One of the principal objectives of the research project was to use the analysis of the semi-rigid behaviour of frames from the assessment of five full scale test frame data and numerical studies to investigate and where appropriate enhance, existing methods of design. A principal objective of the analytical work for the assessment of the frame test data is to provide results which could be used to investigate the influence of semi-rigid connections on column and frame stability, to examine the existing and new proposed design methods and to verify computer programs capable of incorporating the effects of geometric non-linearity and plasticity.

A direct comparison of the results obtained with the analytical prediction of the existing frame programs [1.3,1.4] is included in chapter 8. After the verification of the subassemblage program [1.5], an investigation of the influence of a wide range parameters on a number of subassemblage models was undertaken as described in chapter 9. Semi-rigid design methods are proposed and the predictions are compared with the test results. This topic is addressed in chapter 10 which presents a brief overview of the current existing design techniques and they appear to achieve a reasonable compromise between accuracy of approach and ease of use. Finally, conclusions are drawn and further studies suggested in chapter 11.

## References

- [1.1] Davison, J. B., 'Strength of Beam-Columns in Flexibly Connected Steel Frames' Ph.D. Thesis, University of Sheffield, June, 1987.
- [1.2] Jones, S. W., Kirby, P. A. and Nethercot, D. A., 'Effect of Semi-Rigid Connections on Steel Column Strength', Journal of Constructional Steel Research, London, England, Vol. 1, No. 1, September, 1980 (pp. 38 -46)
- [1.3] Ahmed, I. 'Semi-Rigid Action of Steel Frames', Ph.D. Thesis, 'Department of Civil and Structural Engineering, University of Sheffield, U.K., September, 1992.
- [1.4] Poggi, C., 'A Finite Element Model for the analysis of Flexibly Connected Plane Steel Frames', International Journal for Numerical Methods in Engineering, Vol. 26, 1988, pp. 2239-2254
- [1.5] Wang, Y. C., 'Ultimate Strength Analysis of Three Dimensional Structures with Flexible Restraints', Ph.D. Thesis, Department of Civil and Structural Engineering, University of Sheffield, U.K., June, 1988

## Chapter 2

# Historical Background

### 2.1 Introduction

This section presents a brief overview of the historical background to the subject and introduces some of the key developments that have played a significant role in advancing the understanding of column and frame behaviour. The present general practice when analysing steel structures is to assume that the connections behave either as perfectly pinned or completely rigid. For the analysis and design of steel framed structures the degree of advantage as a result of the interaction of the beam and column members, due to fixity of the connection, is arguable. The potential for incorporating the benefits of partial fixity of connections in multistorey building frame was identified in the early 1930's, has received attention at various times over the last 50 years and has more recently become more widely appreciated. However, such interaction of components in the frame is not commonly accounted for in steel frame design; simplified, easier to handle solutions being preferred. In this chapter, the history of research on the main area of pin-ended columns, end restrained columns and frame tests is presented.

### 2.2 Pinned Columns

When the flexural buckling of the idealized, pin-ended, uniform column is considered, some assumptions are made as listed.

- The material is linear-elastic.
- The member is initially perfectly straight.
- The applied loading is perfectly axial, i.e. at the centroid of the cross section.

- The member is able to bend only about one principal axis.

Generally, elastic buckling occurs when the average applied compressive stress ( $\sigma_{av} = \frac{F}{A}$ ) in the column load reaches its critical value. However, if the column is slender enough it buckles at a stress below the actual value of the material yield stress. The well known Euler load (critical load) for the pin-ended column is given by

$$F_E = \frac{\pi^2 EI}{L^2} \quad (2.1)$$

where EI is the elastic flexural stiffness and L is the length of the column.

The pin-ended column also represents the classical reference datum on which many experimental appraisals of columns have been based. Early column strength equations were of an empirical nature, based on the results of experimental studies on nominally pinned-ended columns. However, the limitation of such equations was soon realised and an approach with a more theoretical base was sought. It was discovered that, as soon as any axial load is applied to a member having an initial out-of-straightness it sustains a bending moment, which in turn leads to further deformation and a growth in the amplitude of deflection. In practice, both rolled and fabricated sections have residual stress in them due to the heating and cooling processes, that have occurred during forming. It is also noted from the experimental study conducted by Howard that the residual stress reduced the strength of columns with an intermediate slenderness [2.1]. The influence of residual stress on the buckling strength of both rolled members and welded plates was subsequently noted by Salmon and Madsen [2.2,2.3].

Systematic research into the effects of residual stress on column behaviour was initiated in the late 1940's under the guidance of Research Committee A of the Column Research Council (C.R.C.) [2.4,2.5,2.6]. The culmination of these efforts was the publication of Technical Memorandum No.1 which proposed the basic 'C.R.C. Column Strength Curve'. The formula was derived using the concept of an effective tangent modulus to account for residual stress and other material non-linearities, but which ignored the effect of initial deformation. A similar initiative had been taken by the Steel Structures Research Committee with a view to reviewing the contemporary methods of design and applying 'modern' theory to the design of steel structures. The results of this particular Committee's work formed the basis of B.S. 449 [2.7] in 1932.

Further research on the effects of residual stress and initial deformations was brought about by the commercial demand for an ever increasing range of structural section types.

Investigations of column imperfections in the U.S.A. by Bjorhovde and Tall [2.8,2.9] and in Europe by Beer and Shultz [2.10], led to the computation of 112 different strength curves covering a variety of column shapes and material strengths. Comparisons of the appropriate curve with full scale frame test data had shown discrepancies, in terms of strength prediction, of less than 5 %. For the purposes of design, these 112 curves were categorised, primarily depending on the type of section, into a maximum of five distinct design curves. This concept of 'multiple column curves' is much in evidence in a number of current international steelwork design codes [2.11,2.12].

### 2.3 End-Restrained Columns

The Special Committee on Steel Column Research of the American Society of Civil Engineers conducted experimental pin-ended column tests between 1880 and 1925 [2.13]. They noted that the columns had behaved almost as if their remote ends had been fixed. This was attributed to the frictional restraint present in the inadequate spherical supports at the remote ends of the columns. Although unintentional, this experimental error did alert researchers of the time to the beneficial effect of end-restraint.

Design practice has relied upon understanding of the pin-ended column to produce safe column design. In braced structures, with simple connections between beam and column, the column has been assumed to act as a pin-ended column of length equal to the storey height. Column curves relating the slenderness ratio of the column to a safe working stress had then been used to calculate a safe working load. This method has been in general use for many years. However, in many structures 'rigid' connections are used, in some cases to eliminate the need for bracing. Therefore, in order to use a similar design approach, and the same column curves, in situations where the pinned column assumption is not valid, the concept of an 'effective' column length was developed. The real column - restrained by connected members - is replaced by an 'effective' length of pin-ended column, chosen to have the same strength as the real restrained column. The effective length is usually estimated by the designer from considerations of the relative size of members and the type of beam to column connections. This is an obvious limitation of the method, and one which has been recognised for many years. The recent trend towards limit state methods of design has reinforced the need for column design to include the effect of the end restraint from the adjacent structural members which becomes of increased importance as the column approaches failure.

For rigidly connected frames the restraint conditions at the end of the columns are directly related to the stiffness of the interconnecting beams. This led to the derivation of design monographs, also known as alignment charts, which enable the designer to calculate an effective length for a column forming part of a rigidly jointed structure. This method was then adopted in many structural design codes [2.11,2.12].

Research on the end restraint provided by semi-rigid connections commenced seventy-five years ago when Wilson and Moore [2.14] first investigated the flexibility of riveted structural connections. Research workers in Britain, the United States and Canada conducted three separate investigations during 1930s [2.15]. A history of research into the experimental assessment of moment-rotation characteristics of isolated connections is reported in reference [2.16]. Goverdhan [2.17] has collected a large number of test data and provides moment-rotation curves, numeric data and useful information in a single document. Nethercot [2.18] has also summarised the available test data and supplies comprehensive tables containing details of over seven hundred experimental investigations. The Structural Stability Research Council recognised the importance of collecting all the available data on connection tests in order to investigate ways of incorporating their semi-rigid characteristics into design and analysis. They have produced a comprehensive bibliography [2.19], which is also available on computer disk, to enable the reader to identify references on a wide range of tests. Chen and Kishi [2.20] have also produced a comprehensive collection of data on joint tests.

In the early 1960's Galambos [2.21] examined experimentally the behaviour of columns with end moments applied through loading devices and later tested column and beam sub-assemblages with welded joints [2.22]. The purpose of this study was to provide experimental verification of the restrained column theories proposed for use in the plastic design of multi-storey steel frames [2.23]. Cuk et al [2.24] in Australia also conducted a series of nine test on three storey beam columns, subjected to bending moments and axial loads for the same purpose. Experiments on laterally loaded beam-column subassemblages, again with rigid connections between the beam and column, were reported by English and Adams [2.25]. Gent and Milner [2.26] also performed tests on restrained columns with rigid connections. They used machined scale models of column subassemblages tested under biaxial loading conditions to demonstrate the phenomenon of column moment reversal. Here, the beams with initial applied disturbing moments, restrained the rotation at the column ends as failure was induced. The results of the study showed that columns with large initial disturbing moments failed at a higher load than the same column with pinned-end supports. The inference was that the effect of disturbing moments in rigid frames was less than that

implied by the design methods of the time.

Probably the most significant contribution to the experimental evidence of the restraining characteristics of simple connections was provided by Bergquist in 1977 [2.27]. Bergquist tested five subassemblages, each comprising of a column and four beams, connected with web cleats to the column web. The tests, designed to examine the influence of the connections on the column buckling load, have consequently been used by many researchers. However the self contained beam loading arrangement adopted by Bergquist, using tension cables to apply loads to the beams, resulted in an unrealistic load pattern. This deficiency was subsequently addressed by Davison [2.28] who conducted a series of tests on full scale, 2-dimensional, non-sway column subassemblage and frames using a range of connection types and 'realistic' loading arrangements. Even more recently, a comparison study was performed by Gibbons [2.29] on the behaviour on three-dimensional subassemblages incorporating semi-rigid connections.

The principal measure of connection response is the moment-rotation relationship, also known as the  $M-\phi$  curves. Figure 2.1 illustrates the typical range of moment-rotation curves for popular types of connections. It is evident from the curves that the relationship is non-linear, with the tangent to the curve representing the connection stiffness at the loading level. The smallest slope of the web-cleat curve was observed when it was compared to that of the highest stiffness of the extended end-plate. Figure 2.2 (extracted from reference [2.28]) shows the influence of different 'simple' semi-rigid connections on columns of different slendernesses. It is evident from this plot that the most marked increase in strength occurs where the columns have a moderate to high slenderness.

Recently, finite element techniques have been used to predict the behaviour of various type of columns restrained by semi-rigid connections [2.30,2.31,2.32,2.33]. However, due to unreliable results resulting from the complexity of the problem, the moment-rotation relationship for a particular connection are invariably obtained from test data rather than from predictive equations. A finite element computer program was developed by Wang [2.34] and is capable of analysing 3-dimensional column subassemblages with semi-rigid connections. The program successfully predicted the behaviour of rigidly connected, biaxially loaded column subassemblages investigated by Gent and Milner [2.26]. Gibbons [2.29] also used this program to predict the behaviour of 3-dimensional column subassemblages incorporating a range of connection types.



## 2.4 Frame Tests

The earliest frame tests were carried out in the 1920's in the United States. Specifically, measurements were made of the strains in the columns of the Equitable Building, Des Moines, Iowa [2.35], and the American Insurance Union Building, Columbus, Ohio [2.36]. The results of the tests showed observed stresses that were consistently greater than those calculated, the discrepancy being attributed to some error in the theory, although the strain gauge device used, a Berry gauge, appears not to have been particularly accurate and there were problems with temperature corrections which were necessary [2.37].

In Britain, members of the Steel Structures Research Committee were conscious of the fact that the Code of Practice which they had drafted [2.7], did not reflect the true behaviour of real framed structures. Shortly after the draft had been published in 1931, they initiated the investigation of a series of existing 'real' steel structures and purpose made large scale frames. The building of the Geological Museum located in South Kensington London [2.38] was the first to be examined. Measurements of strain were taken on the bare steel frame under load and also for the frame when encased in concrete. The results are presented in reference [2.39]. A number of frames was erected at the Building Research Establishment [2.40,2.41] and comprised a three storey, two bay, one span frame. They incorporated frames with columns bent about both major or minor axes and used a variety of riveted connection details. Although in both cases the connections were considered 'light', both the frames behaved almost as if they were rigidly connected.

The advent of improved strain measurement techniques meant that 'real' steel frames could be appraised during the construction stage with the minimum of disruption. Studies were therefore extended to investigate the Cumberland Hotel at Marble Arch [2.42], Euston Offices [2.43] and a block of London flats [2.44]. Tests were carried out on the bare steel frames under point loads, after the floors had been constructed, after the columns had been encased and finally when the structure was complete. All the structures behaved very nearly as rigidly jointed frames, which highlighted a fundamental problem in the BS 449 design method. It was thus recognised that the analysis and design of steel frame structures should take account of the interaction of the beam and column members due to the fixity of the connections.

In 1964 a Joint Committee of the Institute of Welding and the Institution of Structural Engineers reported a simplified design method for fully rigid multi-storey welded steel frames [2.45]. In order to verify the method, tests were conducted on a full scale, three

storey, two bay, one span rigid frame fabricated from rolled steel sections of Grade 43 steel and located at the Building Research Station. The tests were reported in *The Structural Engineer* [2.46]. A further development of the design method permitted the use of higher grade steels and accordingly a second more extensive test was performed [2.47].

Taylor reports on an experimental study of continuous columns [2.48]. A series of 19 tests on rigidly jointed, 3-dimensional, three storey scale model frames were carried out. The aim of these tests was to verify a simplified collapse criterion for continuous columns.

In the United States a series of four, 2-dimensional, two storey, two bay rigidly connected braced frames was investigated by Yura and Lu [2.49]. The results showed that in each case the failure loads were greater than those predicted from plastic theory with a discrepancy of less than 4 % and demonstrated that plastic methods could be applied to the design of braced multi-storey frames. One of the important findings was that the sequence of plastic hinge formation had little or no effect on the ultimate load. Details of the apparatus used to load the frames can be found in reference [2.50] along with a list of references of rigid steel frame testing conducted in the United States from 1940's to the early 1960's.

Experimental tests on the behaviour of semi-rigid steel frames are much less common. A report of work by Stelmack et al [2.51] was published in 1986. The purpose of the study reported therein was to provide experimental documentation of the validity of analytical methods for predicting the response of flexibly connected steel frames. Ten tests on two frames of two storey, single bay and one storey, two bay were conducted. The frame connections comprised a flange and seat cleat and in each case sway was permitted. The results showed good correlation with the predicted response. However the scope of the work was limited because neither the tests nor the analysis extended beyond the elastic range. Five two dimensional full scale frame tests had been conducted at the Building Research Establishment, Garston, Watford. The tests are the result of a collaborative effort by BRE, Hatfield Polytechnic and the University of Sheffield. The first two frames were designed and tested by Hatfield Polytechnic [2.52], the second pair by the University of Sheffield [2.28] and the fifth frame by BRE [2.53]. An in-depth appraisal of the most significant of the test results from the five frames has been carried out and is reported in this thesis. More recently, two 3-dimensional frames with end-plate connections have been tested by Gibbons [2.29] and some of the results have also been studied by the author [2.54].

## References

- [2.1] Howard, J. E., 'Some Results of the Tests of Steel Columns in Progress at the Watertown Arsenal', Proc. Am. Soc. Test. Mater., Vol. 8,, 1908, pp.336.
- [2.2] Salmon, E. H., 'Columns', Oxford Technical Publishers, London, 1921.
- [2.3] Madsen, I., 'Report of Crane Girder Tests', Iron Steel Engineering, Vol. 18, No. 11, 1941, pp.47.
- [2.4] Osgood, W. R., 'The Effect of Residual Stress on Column Strength', Proc. 1st U.S. Natl. Cong. Appl. Mech., June, 1951, pp.336.
- [2.5] Yang, H., Beedle, L. S. and Johnston, B. G., 'Residual Stress and the Yield Strength of Steel Beams', Weld J., Res. Suppl., Vol. 31, 1952, pp. 224-225.
- [2.6] Beedle, L. S. and Tall, L., 'Basic Column Strength', Journal of Structural Divison, ASCE, Vol. 86, No. ST7, 1960, pp. 139-173.
- [2.7] British Standard BS 449, 'The Use of Structural Steel in Buildings', The British Standards Institution, London, 1932.
- [2.8] Bjorhovde, R., 'Deterministic and Probabilistic Approaches to the Strength of Steel Columns', Ph.D. Thesis, Lehigh University, Fritz Eng. Lab., May, 1972.
- [2.9] Bjorhovde, R. and Tall, L., 'Maximum Column Strength and the Multiple Column Curve Concept,' Rep. No. 337.29, Lehigh University, Fritz Eng. Lab., Bethlehem, Pa., October, 1971.
- [2.10] Beer, H. and Schultz, G., 'Theoretical Basis for the European Column Curves', Constr. Met., No. 3, 1970, pp. 58.
- [2.11] British Standards Institution BS 5950: Part 1: Structural Use of Steelwork in Building. BSI, London, British Standards Institution, 1990.
- [2.12] American Institute of Steel Construction, 'Load and Resistance Factor Design', Manual of Steel Construction, First Edition, 1986.
- [2.13] Progress Report of the Special Committee on Steel Column Research, Trans., ASCE, Vol. 89, 1926, pp. 1526-1536.
- [2.14] Wilson, W. M. and Moore, H. F., 'Tests to Determine the Rigidity of Riveted Joints in Steel Structures', University of Illinois, Engineering Experiment Station, Bulletin No.104, Urbana, USA, 1917.
- [2.15] Nethercot, D. A. and Chen, W. F., 'Effect of Connections on Columns', Journal of Constructional Steel Research, Vol. 10, 1988, pp. 201-239.

- [2.16] Jones, S. W., Kirby, P. A. and Nethercot, D. A., 'The Analysis of Frames with Semi-Rigid Connection - A state of the Art Report', *Journal of Constructional Steel Research*, Vol. 3, No. 2, 1983, pp. 2-13.
- [2.17] Goverdhan, A. V., 'A Collection of Experimental Moment-Rotation Curves and Evaluation of Prediction Equations for Semi-Rigid Connections', Masters Thesis, University of Vanderbilt, Nashville, Tennessee, December, 1983.
- [2.18] Nethercot, D. A., 'Steel Beam to Column Connections - A Review of Test Data and their Applicability to the Evaluation of the Joint Behaviour of the Performance of Steel Frames', CIRIA Project Record, RP 338, 1985.
- [2.19] Structural Stability Research Council, 'Connections Bibliography', Task Group 25, Third Draft, March, 1987.
- [2.20] Kishi, N. and Chen, W. F., 'Data Base of Steel Beam to Column Connections', Vol. I & II, Structural Engineering Report No. CE-STR-86-26, School of Civil Engineering, Purdue University, 1986.
- [2.21] Van, K. R. C. and Galambos, T. V., 'Beam-Column Experiments', *Journal of Structural Division*, ASCE, Vol. 90, April, 1965, pp. 223.
- [2.22] Lay, M. G. and Galambos, T. V., 'The Experimental Behaviour of Restrained Columns', *Welding Research Council, Bulletin No. 110*, November, 1965, pp. 17-38.
- [2.23] Ojalvo, M. and Levi, V., 'Columns in Planar Continuous Structures', *Journal of Structural Division*, ASCE, Vol. 89, ST1, February, 1963.
- [2.24] Cuk, P. E., Roger, D. F. and Trahair, N. S., 'Inelastic Buckling of continuous Steel Beam-Columns', *Journal of Constructional Steel Research*, Vol. 6, No. 1, 1986, pp. 22-50.
- [2.25] English, G. W. and Adams, P. F., 'Experiments on Laterally Loaded Steel Beam-Columns', *Journal of Structural Division*, ASCE, Vol. 99, ST7, July, 1973, pp. 1457-1470.
- [2.26] Gent, A. R. and Milner, H. R., 'The Ultimate Load Capacity of Elastically Restrained H-Columns under Biaxial Bending', *Proceedings of the Institution of Civil Engineers*, No. 41, 1968, pp. 685-704.
- [2.27] Bergquist, D. J., 'Test on Columns Restrained by Beams with Simple Connections', Report No. 1, American Iron and Steel Institute Project No. 189, Department of Civil Engineering, The University of Texas, Austin, Texas, January, 1977.

- [2.28] Davison, J. B., 'Strength of Beam-to-Column in Flexibly Connected Steel Frames', Ph.D. Thesis, University of Sheffield, England, June, 1987.
- [2.29] Gibbons, C., 'The Strength of Biaxially Loaded Beam Columns in Flexibly Connected Steel Frames', Ph.D. Thesis, University of Sheffield, England, December, 1990.
- [2.30] Chen, W. F., 'End Restraint and Column Stability', Journal of Structural Division, ASCE, Vol. 106, No. ST11, November, 1980, pp. 2279-2295.
- [2.31] Jones, S. W., Kirby, P. A. and Nethercot, D. A., 'Effect of Semi-Rigid Connections on Steel Column Strength', Journal of Constructional Steel Research, Vol. 1, No. 1, 1980, pp. 38-46.
- [2.32] Razzaq, Z and Chang, J. G., 'Partially Restrained Imperfect Columns', Additional Papers, Conference on Joints in Structural Steelwork, Teesside, April 1981, Pentech Press Ltd., pp. 6.57-6.80.
- [2.33] Rifai, A. M., 'Behaviour of Columns in Sub-Frames with Semi-Rigid Joints', Ph.D. Thesis, University of Sheffield, England, June, 1990.
- [2.34] Wang, Y. C., 'Ultimate Strength Analysis of Three-Dimensional Column Sub-assemblages with Flexible Connections', Journal of Constructional Steel Research, Vol. 9, No. 4, 1988, pp. 235-264.
- [2.35] Fuller, A. H., 'Measurements of Stresses in Four Steel Columns of the Equitable Building, Des Moines, Iowa', Iowa State College of Agriculture and Mechanic Arts, Engineering experiment Station, Bulletin No. 40, Columbus, 1928.
- [2.36] Morris, C. T., 'Dead Load Stress in the Columns of a Tall Building', Ohio State University, Engineering Experimental Station, Bulletin No. 72, Ames (Iowa), 1924.
- [2.37] Baker, J. F., 'Early Steelwork Research', Journal of Constructional Steel Research, Vol. 1, No. 1, September, 1980, pp. 3-9.
- [2.38] Baker, J. F., 'Examination of Building in Course of Erection', First Report of the Steel Structures Research Committee, H.M.S.O., London, 1931.
- [2.39] Faber, O., 'Report on Observed Stresses in a Steel Frame Structure at the Museum of Practical Geology, South Kensington', Second Report of the Steel Structures Research Committee, H.M.S.O., London, pp. 44-60.
- [2.40] Baker, J. F., 'An Investigation of the Stress Distribution in a Number of Three-Storey Building Frames', Second Report on the Steel Structures Research Committee, H.M.S.O., London, 1934, pp. 241-318.

- [2.41] Lobban, C. H., 'Measurement of Stresses in Experimental Frame', First Report on the Steel Structures Research Committee, H.M.S.O., London, 1931, pp. 191-193.
- [2.42] Baker, J. F., 'An Investigation of the Stress Distribution in the Steel Framework of a Modern Hotel Building', Final Report of the Steel Structures Research Committee, H.M.S.O., London, 1936, pp. 8-139.
- [2.43] Baker, J. F., 'An Investigation of the Stress Distribution in the Steel Framework of a Modern Office Building', Final Report of the Steel Structures Research Committee, H.M.S.O., London, 1936, pp. 140-227.
- [2.44] Baker, J. F., 'An Investigation of the Stress Distribution in the Steel Framework of a Modern Residential Flats Building', Final Report of the Steel Structures Research Committee, H.M.S.O., London, 1936, pp. 228-249.
- [2.45] Joint Committee Report on Fully Rigid, Multi-Storey, welded Steel Frames. The Institution of Structural Engineers, December, 1964.
- [2.46] Wood, R. H., Needham, F. H. and Smith, R. F., 'Tests on a Multi-Storey Rigid Steel Frame', The Structural Engineer, Vol.46, No.4, April, 1968, pp. 107-120.
- [2.47] Smith, R. F. and Roberts, E. H., 'Test of a Full-Scale Rigid-Jointed Multi-storey Frame in High-Yield Steel (BS 4360, grade 50)', B.I.S.R.A. Open Report, Report No. EG/A/17/71.
- [2.48] Taylor, D. A., 'An Experimental Study of continuous Columns', Proceedings of the Institution of Civil Engineers., Vol. 53, 1972, pp. 1-17.
- [2.49] Yura, J. A. and Lu, L. W., 'Ultimate Load Tests on Braced Multi-Storey Frames', Journal of Structural Division, ASCE, Vol. 95, No. ST10, October, 1969.
- [2.50] Yarimci, E., Yura, J. A. and Lu, L. W., 'Techniques for Testing Structures permitted to Sway', Experimental Mechanics, August, 1967, pp. 321-331.
- [2.51] Stelmack, T. W., Marley, M. J. and Gerstle, K. H., 'Analysis and Tests of Flexibly connected Steel Frames', Journal of Structural Engineering, ASCE, Vol. 112, No.7.
- [2.52] Prescott, A. T., 'The Performance of End-Plate Connections in Steel Structures and their Influence on Overall Structural Behaviour', Ph.D. Thesis, Hatfield Polytechnic, July, 1987.
- [2.53] Lennon, T., 'Full-Scale Steel Frame Tests: Load Tests on Frame No.5', Building Research Establishment, Report No. N71/88.
- [2.54] Lau, S. M., 'A Study of Results from a Full Scale Frame Test' MSc(Eng) Dissertation, University of Sheffield, September, 1990.

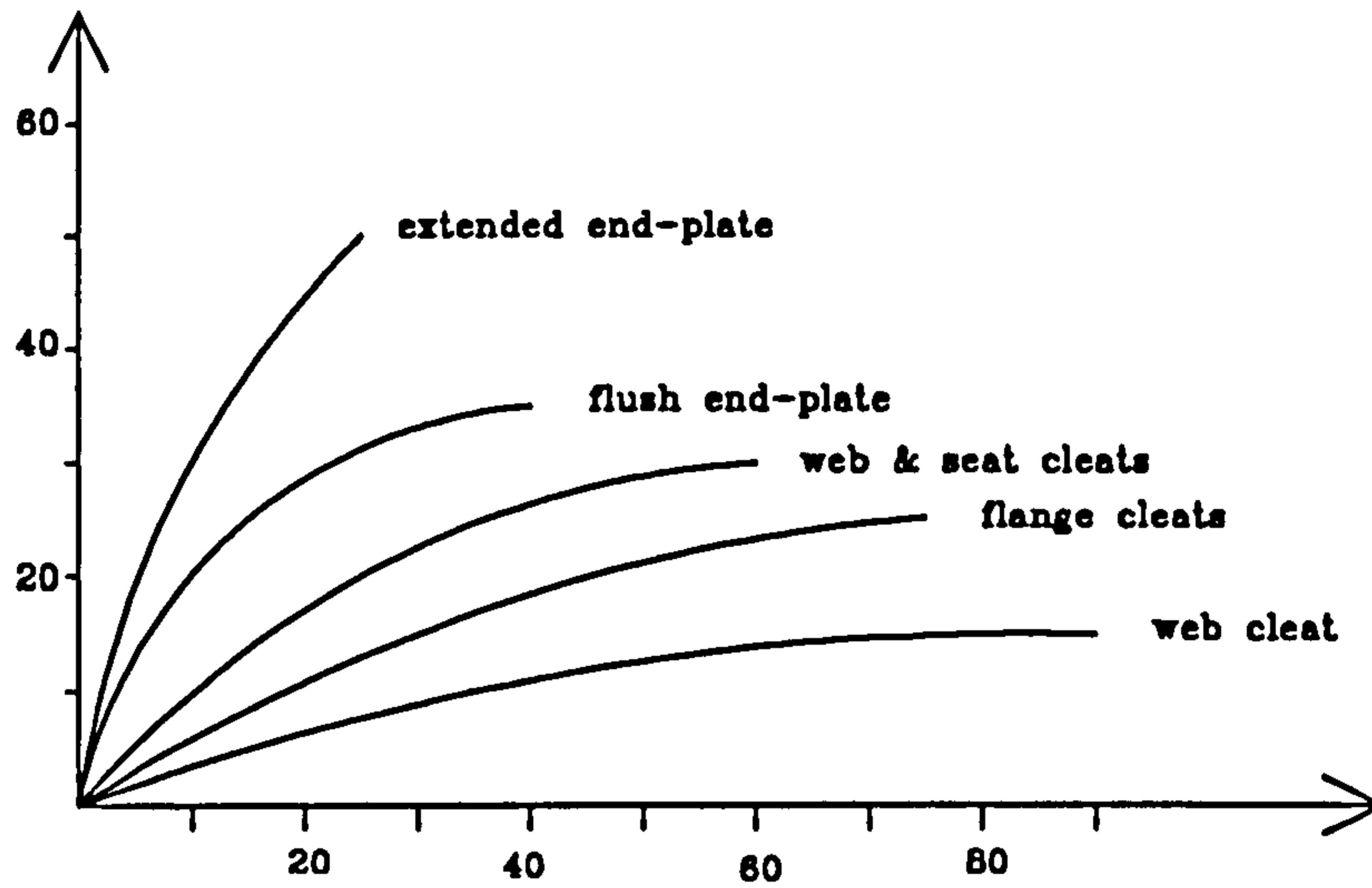


Figure 2.1 : Variation of Moment Rotation Characteristics for Various of Beam to Column Connections

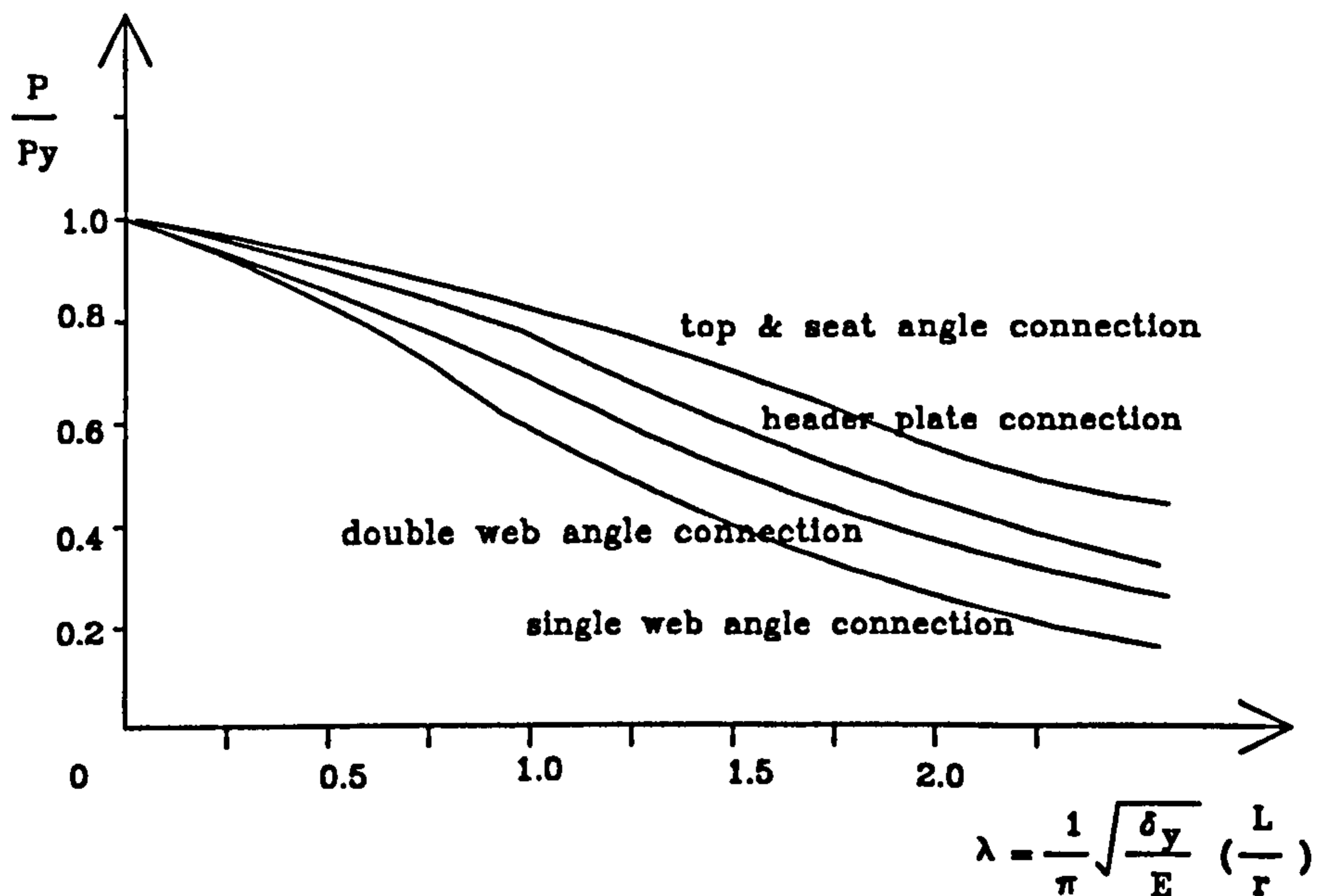


Figure 2.2 : Influence of Connection Restraint on the Strength of Axially Loaded Columns

## **Chapter 3**

# **Databank of Moment-Rotation Test Results**

### **3.1 Introduction**

When designing steel frames it is customary to assume that the beam to column connections perform either as perfect pins or as fully rigid. From experimental studies [3.1] it is evident that most simple beam to column connections are capable of developing some intermediate degree of moment transfer and column restraint. The British design code for structural steelwork [3.2] allows the structure to be designed using one of three methods. The three methods are defined as fully rigid, semi-rigid and simple. When semi-rigid design is used, the connection behaviour must be adequately estimated or predicted.

In the past a large number of connection tests have been performed. Due to the difficulties encountered by designers and researchers in gaining access to test results, the idea of a database was suggested within which test data from the technical literature would be collected. At the University of Sheffield, a system was originally established on an IBM 3083 Mainframe machine by Y. C. Wang.

Three major sources of data were used. The first was that collected by Goverdhan [3.3] which covers tests up to 1983 and which also analyses the effects of various parameters on the connection behaviour. The second is the review of test data compiled by Nethercot [3.4] and the last is the paper database established by Kishi and Chen [3.5] which includes most of the connection tests up to 1985.

The objectives of the data is to provide access to moment-rotation characteristics and



corresponding parameters of semi-rigid beam-to-column connections in a convenient computerised form and is the motivation behind the current steel beam-to-column connection database work at the University of Sheffield.

The database used the technique of the tree selection system to reduce the entries to a brief table. A detailed description of this technique together with the improvement including two options for connection selection procedure will be presented in section 3.5.2. The current data collection includes most of the data published up to the spring of 1991 and facilities were developed to enable new data to be inserted easily. A transfer of this database to other European Community Countries is in hand. To make the program more user friendly, a clearer instruction set has been developed by the Author. Composite structures have become more prevalent in the construction field in all European countries and some joint tests have been performed on connections involving composite action. To increase the versatility of this database, a suggestion in a report format [3.6] has been written by the Author to modify the existing database to incorporate the composite joint test results.

## 3.2 Types of Connections

A survey [3.7] of beam to column connections used throughout the construction industry in the U.K. revealed the seven commonest types of connections currently in use to be;

- Single/Double Web Cleat (Figures 3.1 and 3.2)
- Single Web Plate (Figure 3.3)
- Flange Cleats with/without web cleat (Figure 3.4)
- Header Plate (Figure 3.5)
- Flush End-Plate (Figure 3.6)
- Extended End-Plate (Figure 3.7)

Most of the connection tests reported are for monotonic and cyclic behaviour. Therefore, in the collection of the numerical form of the beam-to-column connection  $M-\phi$  behaviour, only the above seven types of connection under monotonic and cyclic loading are considered.

### **3.3 Structure of Program**

The database is written in Fortran language and at the time of development was implemented on Sheffield University's IBM 3083 mainframe computer. The data is processed using the Standard Query Language (SQL) which had been shown in a study by Necib [3.8] that to be the best to be adopted for this program.

However, the Sheffield IBM main frame computer system was be replaced by a 'SUNC' system in the winter of 1992 and it was impossible to transfer the database to the new system directly due to the lack of the SQL package. A transfer of the database to other centres and transfer to a PC system are considered as described in section 3.5.

Trial use of the program showed that it takes a considerable time to select the required information when using the original detailed selection options set up by Wang. This is inconvenient to users when they need many different sets of data. Thus an alternative way to make the selection procedure more convenient was conceived. The improvement is thus carried out and a description presented in section 3.5; the selecting procedure being reported in section 3.5.2.

### **3.4 Usage of Database**

#### **3.4.1 Scope**

After the required test data has been selected, some of the post-processing features obtainable in the database are:

- Setting and printing the selected test data.
- Plotting the moment rotation curve.
- Connection moment-rotation behaviour modelling.
- Comparison with other moment rotation curves.

#### **3.4.2 Printing the Test Result**

##### **(1) Set and Print the Selected Test Data**

The detail information of the test selected by the user can be printed using an output file named by the user at the beginning of the run. The table lists the major fabrication

details of the connection type. The items from each test registered in the database are listed as:

1. Author, test identification and the date of the test report.
2. Beam and column size and size of beam-to-column components.
3. Material grade or yield stress of these components.
4. Controlling failure mode and test condition.
5. Moment-Rotation data.
6. Reference number and source.

The reference of the source from which the test data was obtained is also printed. Thus the user can check out the required information from this source if necessary. The moment rotation data in different units (kip-in or kN-cm) can also be printed, enabling the user to obtain a hardcopy record of the numerical data. A screen copy is provided for the user to view the test information. The dimensions of the structural members and the plastic moment of the beam are also displayed in the output file.

## **(2) Set and Print Brief Tables**

A general table is prepared for each connection type from which the selection is carried out within the program. The brief table is necessary since the detailed table contains too many variables and the processing of the table is expensive in terms of computer running time and storage. The brief table lists a few important variables chosen as the ones which are found to be most influential and they are varied to distinguish different tests. This type of table can also be viewed on the screen and printed out for reference.

### **3.4.3 Plotting of Moment Rotation Curve**

Moment rotation curves may be plotted either in dimensional or non-dimensional form. For the dimensional form, the moment can be presented in kip-in or kN-cm. For the non-dimensional form, the format of EC 3 Part 1 [3.9] is adopted to classify the connections as rigid, semi-rigid or pinned according to the criteria set out in that document. The connection type, beam size, column size, material grade or yield stress of the connecting components, test author, test identification and the type of framing are displayed with plots in either format. Example plots are shown in Figures 3.8 and 3.9.

### 3.4.4 Connection Moment-Rotation Behaviour Modelling

Currently, three models of fitting the beam-column connection moment-rotation curves are incorporated in the database program. They are:

#### 1. Frye-Morris Polynomial Model

This model [3.10] is in the form of

$$\phi = \sum_{k=1}^n C_k [KM]^k \quad (3.1)$$

where  $C_k$  is a curve-fitting constant,  $K_k$  is a non-dimensional factor depending on the size parameters for the connection type concerned and

$$K = \prod_{j=1}^m P_j^{a_j} \quad (3.2)$$

in which  $P_j$  is the numerical value of  $j$  th size parameter and  $a_j$  a dimensionless exponent indicating the  $j$  th size parameter on the connection moment-rotation behaviour.  $m$  is the total number of size parameters. For each connection test, these curve-fitting coefficients are calculated and recorded in the output file.

#### 2. B-Spline Curve-Fitting

When comparing different curve-fitting techniques, Jones *et al* [3.11] pointed out that the Frye-Morris model could produce negative slopes in some cases, which is unacceptable for the analytical programs. To avoid this negative connection stiffness condition, they proposed the use of a B-Spline model to represent the connection moment-rotation relationship. Using this approach, the rotation is divided into a number of ranges by interior knots prescribed by the user. A cubic spline is then fitted for each range which also ensures the continuity of 1st and 2nd derivatives. This technique is available on the Sheffield main frames through a NAG library routine. A requirement for this method is that the rotation should be in ascending order. The database program also outputs the coefficients of this model. Usually, five interior knots are enough to accurately fit the connection moment-rotation curve. In the program, the rotation values of these interior knots are determined by equally spacing the number of test points to avoid the situation in which no test points (default values) are available between two interior knots.

### 3. Lui-Chen Modified Exponential Equation

Lui-Chen proposed a modified exponential equation, i.e. an exponential equation plus a modifying linear equation, to represent the connection moment-rotation relationship in their study of beam-column connection behaviour. It has the form of:

$$M = M_0 + \sum_{j=1}^m C_j [1 - \exp(\frac{-|\theta_r|}{2j\alpha_c})] + \sum_{k=1}^n D_k (\theta_r - \theta_k) H[\theta_r - \theta_k] \quad (3.3)$$

where  $M_0$  is the initial moment,  $C_j$  and  $\alpha_c$  the constant parameters and the scaling factor for the exponential function,  $D_k$  the constant parameter for linear function,  $\theta_k$  the starting rotations of linear component given by the experimental moment-rotation curve.  $H[x]$  is the Heaviside step function, it is defined as

$$H[x] = 1 \quad \text{for } x \geq 0$$
$$H[x] = 0 \quad \text{for } x < 0$$

It is suggested that  $m$  is taken as 6 and  $n = 3$  for the exponential and linear functions respectively, The starting values are obtained by manual input or dividing the maximum rotation by  $n$ .

These three models may be invoked separately or combined in any order. Figures 3.10, 3.11 and 3.12 show the three individual models and Figure 3.13 shows the three models on the same plot. It is interesting to note that in these figures a large discrepancy of  $M-\phi$  was determined using the Frye-Morris Polynomial Model of fitting. The author has found similar problems when trying to use this curve fitting model. As a result, the Frye-Morris Polynomial Model of fitting is not recommended.

#### 3.4.5 Comparison with Other Tests

Overlaying of moment rotation data for different connections in a plot is frequently required by research workers in order that a comparison can be made of different connection behaviour. This plotting can be done using both formats of moment rotation curves, i.e. using either dimensional or non-dimensional forms. An example is illustrated in Figure 3.13.

## **3.5 Improvement of Database**

### **3.5.1 General Scope**

To increase the usefulness of the Database, some improvements of the existing database have been implemented by the Author. These include:

1. Greater efficiency and user 'friendliness'.
2. Updating of test results.
3. A suggestion for the inclusion of composite joint tests.
4. Transfer of the database to other centres.

### **3.5.2 Greater Efficiency and User Friendliness**

Many users are interested in selecting the test data according to the test author and therefore a new option using the name of the test author has been created. There are now two options for the selection of data by the users. It has been shown that the new option can provide the test data in a quick way with a shorter running time. Thus it provides a more convenient way to access a large set of different types of data.

Instead of using the tree selection system, the technique used in two options of the database is to reduce the entries to a brief table. Once the option and the type of connection of interest has been selected, all of the connection entries in a brief table are shown on screen upon request. This table may then be successively reduced following the technique described in the next section until the number of entries shown on the screen is small enough that the user can specify a connection directly against the reduced brief table.

The reduction procedure starts by giving the user a list of parameters which are the same as the column headings covered in the brief table. Once the user has chosen one parameter, the program will list all of the available values for this parameter stored in the current brief table and the user then makes a selection. The connection test entries associated with the unselected values for this parameter will be deleted from the brief table so that it is reduced. Rather than going through all of the parameters one by one, the user can select the test in any order and may choose a connection test after just a few rounds of reduction, which makes the selection much more efficient.

In some cases, several connection tests with identical connection details may have been performed to investigate the effect of different test conditions, e.g. loading combination,

test arrangement or simply to repeat the test. Only those tests with different conditions are displayed on the screen. Such a group of tests is treated as one entry only in the brief table, but the difference is indicated in the form of test condition once the entry in the brief table is chosen. The reduced brief table is retained and may be used again unless a completely different connection is wanted. Figure 3.14 shows the brief flow-chart of the selection procedure.

Ambiguities in the instructions in the original program caused some difficulties in operation thus a clear and more complete instruction set has been created.

### **3.5.3 Update Test Data**

Updating test data is carried out to collect the additional test data from a literature search. About thirty new test data sets were inserted, making up a total of some 550 sets of data in the database. The collection of new data is a continuous process.

### **3.5.4 Composite Joint Tests**

Although numerous examples of tests conducted on bare steel beam to column connections exist, their applicability is in many cases restricted as nowadays composite structures have become a common feature in typical European buildings. Composite structures, in addition to providing light shallow floors, also assist in the rapid erection of the structure therefore reducing the total construction time.

To increase the usefulness of the Database, the test data for joints with composite members should also be incorporated in order that the additional information is available more readily for researchers. Thus, insertion of test data for joints with composite members is suggested.

Comparing the bare steel members with the composite structural members, the main differences are:-

- Beam - either Steel Beam / Girder or Composite Beam / Composite Girder
- Column - either Steel Column or Reinforced Concrete / Composite Column

(In this context a beam is a rolled section whilst a girder is built up from welded steel plates)

A detailed example of the suggested data input is given in a report [3.6]. The example describes the items of input required for a flange or seat cleat with or without a single or double web cleat connection for a composite steel joint [3.12,3.13,3.14,3.15,3.16]. All other types of connection, e.g. flush end plate, are similar to the original database for the bare steel joint, only the input data for the beam and the column are different. Thus, other types of connection for composite steel joints can be used by incorporating the suggested items for beam and column properties used in this example. The other items can use the original database input for bare steel joints of the same connection type.

Due to the difficulty of describing information in a tabular form, the author strongly recommends the use of drawings to describe the connection, the composite Beam and Column for each individual test inside the database.

Whilst a considerable amount of effort has been employed to produce this proposal it is recognised that it represents a starting point for comments and suggestions for improvements by others. The information has been passed to an EC funded group led by a team at the University of Aachen and suggestions have been incorporated into a set of datasheets being used for input and output of data for a PC mounted version currently under development.

### **3.5.5 Program Transfer to Other Centres**

Clearly the database is a potentially useful source of joint test data. To widen its availability and enable researchers in other countries to use this database, the program is to be transferred to other research centres in the European Coal and Steel Community who funded much of its development.

The database has already been transferred to the University of Liege in Belgium where an operational IBM mainframe machine is still operating. All of the files were loaded in a tape and stored in a file. However, due to the incompatibility of the different main frame systems, this method of transfer of the database proved to be unsuccessful. Thus, another method to solve this problem was devised. A series of Fortran Programs were written in order to directly create the tables in the SQL. The Fortran Program including the program to execute the database and to create the tables in SQL were loaded on a tape which en-



abled the programs to be loaded on the main frame computer in Liege. All tables were then created in SQL/Data system by using the relevant programs.

### **3.6 Suggestion for Further Research**

The modified database was demonstrated at meetings of collaborating partners held in the University of Sheffield in February 1991 and Belgium in May 1991. Further research should be considered in the future to maintain and develop this useful and powerful database.

In the past many tests were reported in insufficient detail and thus not all records are complete. The database contains some data which uses the nominal yield stress of material in joint tests and there may be some difference with the actual yield stress. Also many tests have been conducted in a less than ideal manner and a reappraisal of test data may be required following the suggestions proposed for standardised moment-rotation testing.

Due to the lack of portability of the main frame database, a transfer to a PC based system is also suggested in order that this database can be used more widely. Following the initial suggestion for this, a PC version of the database program for bare steel joint tests is being developed in Aachen, Germany. The basis for the program was demonstrated at a meeting of collaborating partners held in Belgium in May 1991. It was then a very small database which containing only about sixty datasets. Furthermore, it would not be very efficient and convenient to select the data if it contained a large number of datasets. Following an agreement of co-operation, the datasets in the Sheffield database have been transferred and the technique and structure of the Sheffield database has been discussed and made available to the group. A more powerful database in PC version should be available in the near future.

A suggestion to include the composite joint tests in the database is reported and has been examined by the Author. It is recognised that it represents a starting point for comments and suggestions for improvements by others.

## References

- [3.1] Davison, J. B., 'Strength of Beam-Columns in Flexibly Connected Steel Frames' Ph.D. Thesis, University of Sheffield, June, 1987.
- [3.2] BS5950, 'The Structural Use of Structural Steelwork in Buildings', Part 1, London, British Standards, Institution, 1990.
- [3.3] Goverdhan, A. V., 'A Collection of Experimental Moment-Rotation Curves and Evaluation of Prediction Equation for Semi-Rigid Connections', Ph.D. Thesis, University of Illinois, USA, 1984.
- [3.4] Nethercot, D. A., 'Steel Beam to Column Connections - A Review of Test Data and Their Applicability to the Evaluation of the Joint Behaviour of the Performance of Steel Frames', Department of Civil and Structural Engineering, University of Sheffield, U.K., 1985.
- [3.5] Kishi, N. and Chen, W. F., 'Database of Steel Beam-to-column Connections', Structural Engineering Report No. 82-26, School of Civil Engineering, Purdue University, West Lafayette, IN, 1986.
- [3.6] Lau, S. M., 'Database for Semi-Rigid Connection response in Steel Frame with Composite Members', Report, Department of Civil and Structural Engineering, University of Sheffield, U.K.
- [3.7] Research Report - Local Failure in Steelwork Structures, Interim Report, B.R.E. Contract F3/2/256, The Building Research Establishment, Watford, U.K.
- [3.8] Necib, E. P., 'Moment-Rotation Curves for Steel Beam-to-column Connections', M.Phil. Thesis, Department of Civil and Structural Engineering, University of Sheffield, January, 1989.
- [3.9] Draft Euorcode No. 3, 'Design of Steel Structures', Part 1, General Rules and Rules for Buildings, 1985.
- [3.10] Frye, M. J. and Morris, G. A., 'Analysis of Flexibly Connected Steel Frames', Canadian Journal of Civil Engineering, Vol. 2, pp. 280-291, 1975.
- [3.11] Jones, S. W., Kirby, P. A. and Nethercot, D. A., 'Modelling of Semi-Rigid Connection Behaviour and its Influence on Steel Column Behaviour', Joints in Structural Steelwork, ed. by J. H. Howlett, W. M. Jenkins and R. Stainsby, Pentech Press, London, pp. 5.73-5.87
- [3.12] Douglas, J., 'Behaviour of Semi-Rigid Composite Connections', Engineering Journal, American Institute of Steel Construction, Inc., 2nd Quarter, Vol. 24, No. 2, 1987, pp. 53-61.

- [3.13] Wright, H.D. and Francis, R.W., 'Tests on Composite Beams with Low Levels of Shear Connection', *The Structural Engineer*, 7 August, 1990, Vol. 68, No. 15, pp. 293-298.
- [3.14] Davison, J.B. *et. al*, 'Semi-rigid Action of Composite Joints', *The Structural Engineer*, Vol.68, No.24, 18 December, 1990, pp. 489-499.
- [3.15] Tauqir, M. S. *et. al*, 'Beam-Column Moment Connections for Composite Frames Part 1', *Journal of Structural Engineering*, ASCE, Vol. 115, No. 11, November, 1989, pp. 2858-2876.
- [3.16] Gregory, G. D. *et. al*, 'Beam-Column Moment Connections for Composite Frames Part 2', *Journal of Structural Engineering*, American Society of Civil Engineers, Vol. 115, No. 11, November, 1989, pp. 2877-2896.

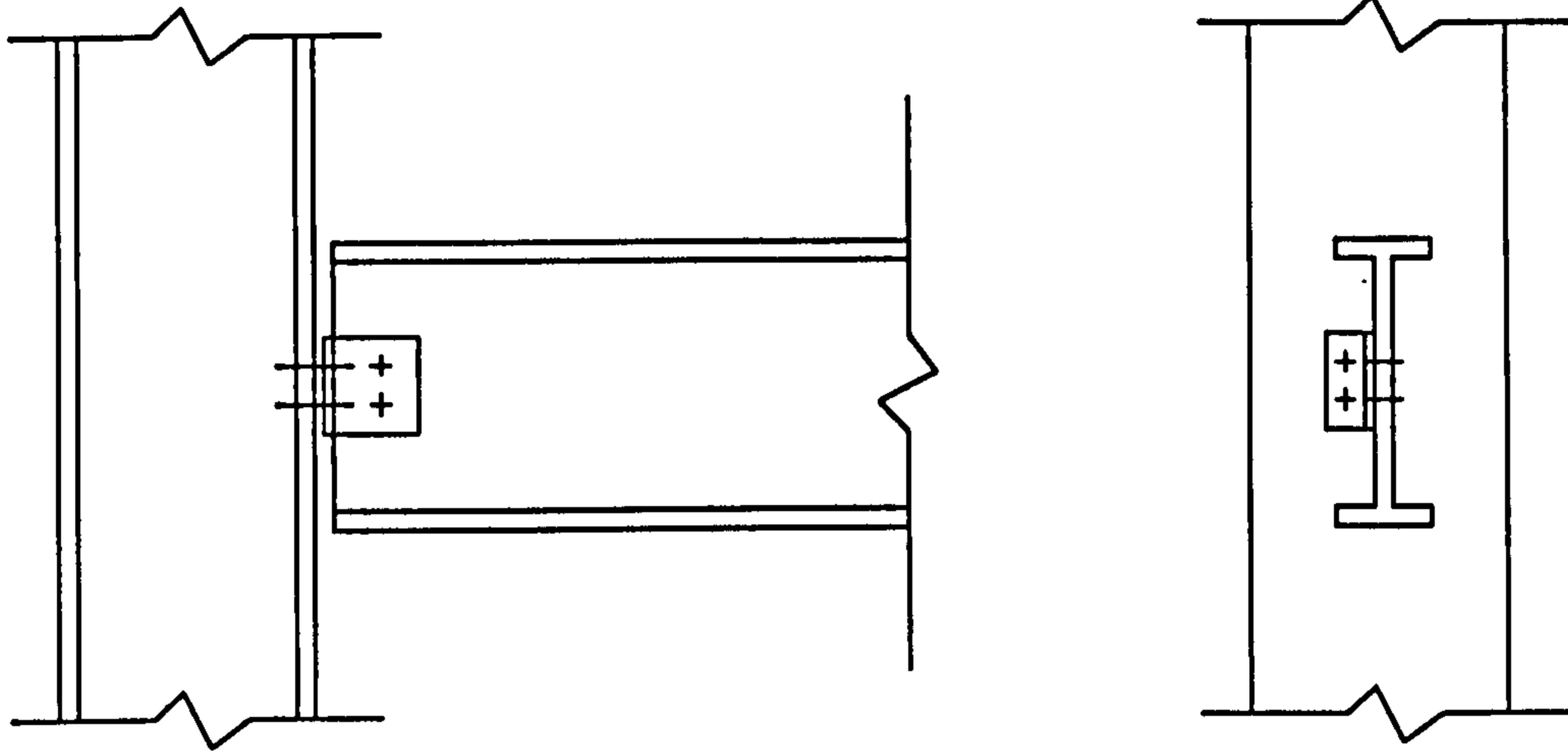


Figure 3.1 : Single Web Cleat Connection

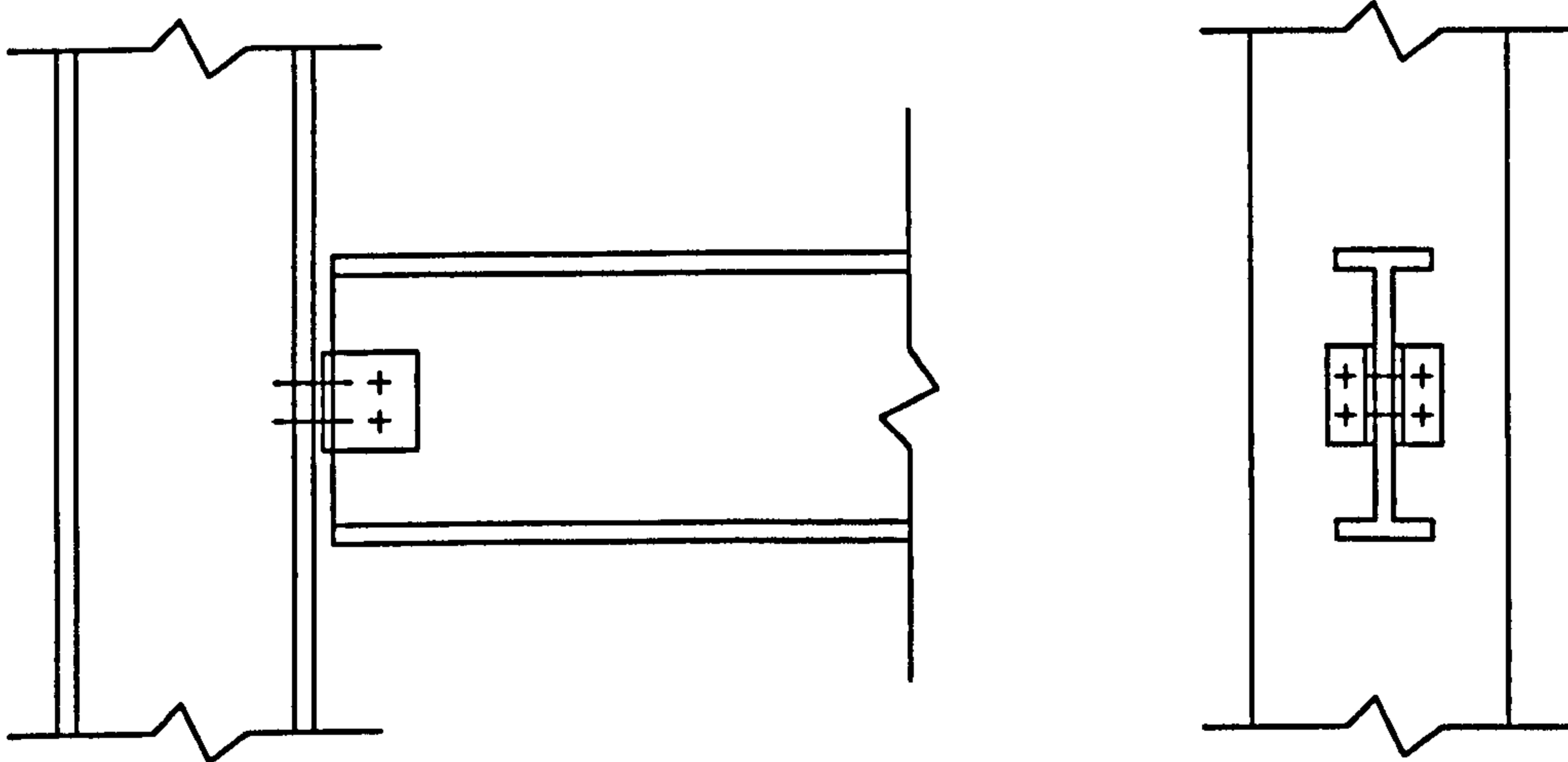


Figure 3.2 : Double Web Cleats Connection

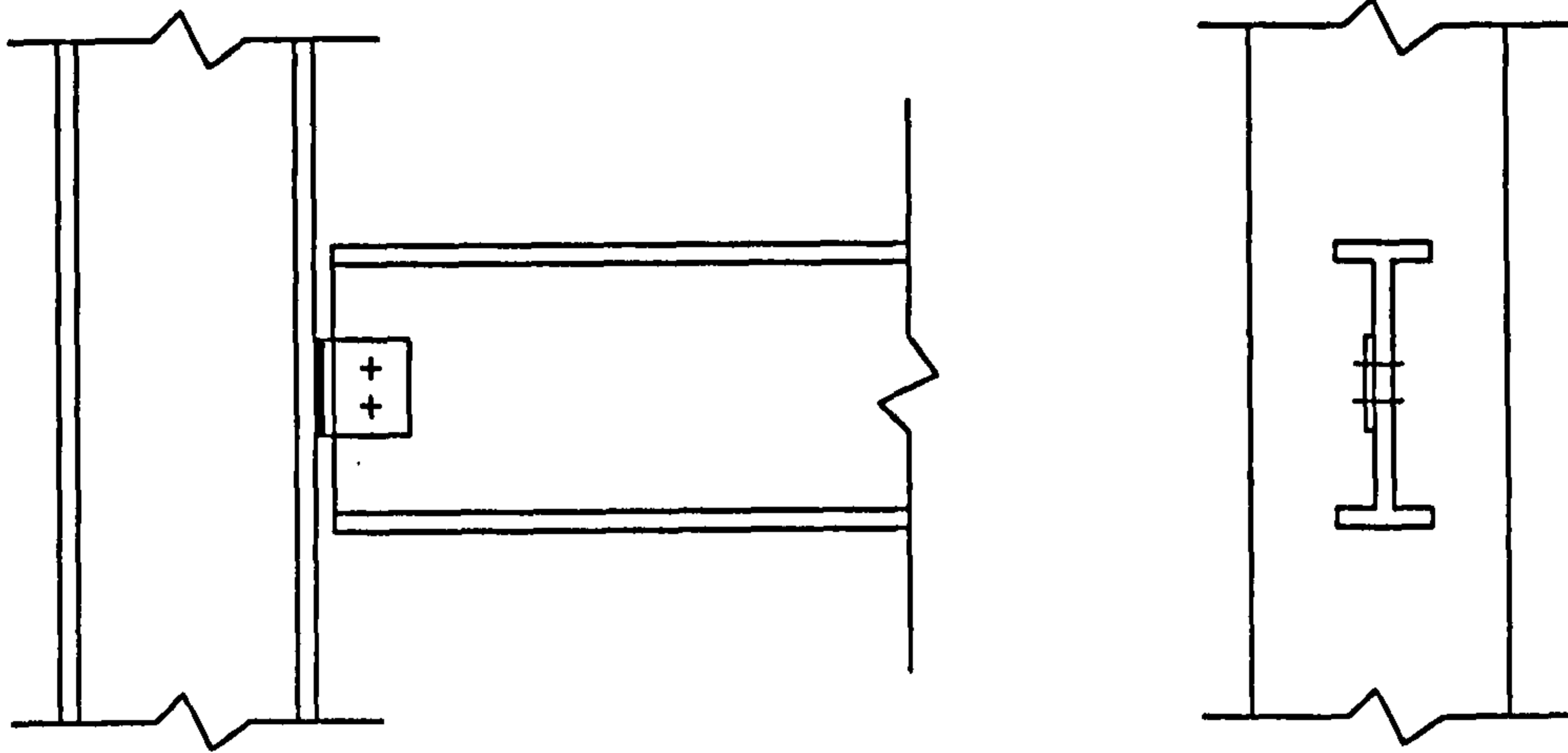


Figure 3.3 : Single Web Plate Connection

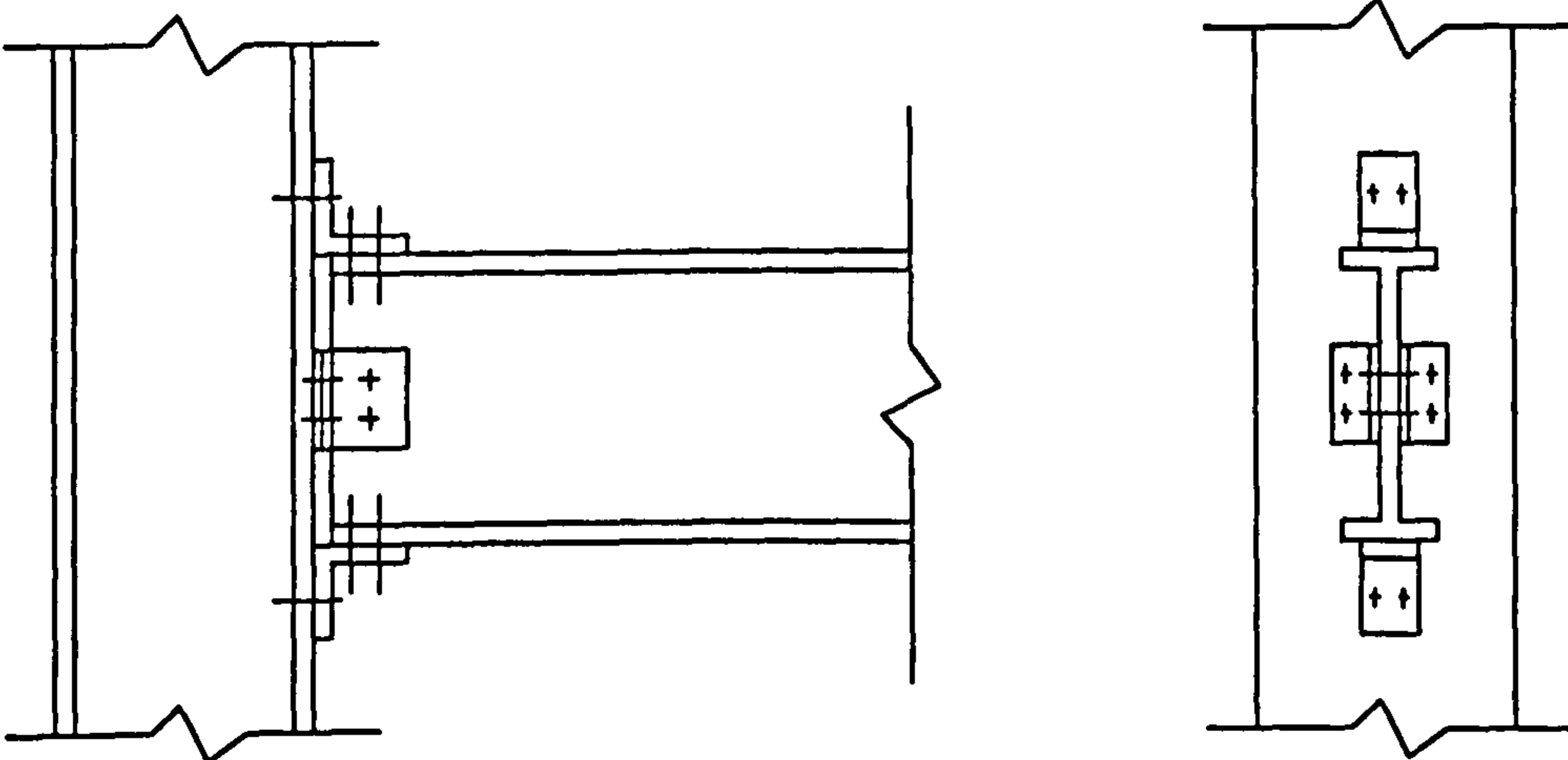


Figure 3.4 : Flange Cleats with Web Cleats Connection

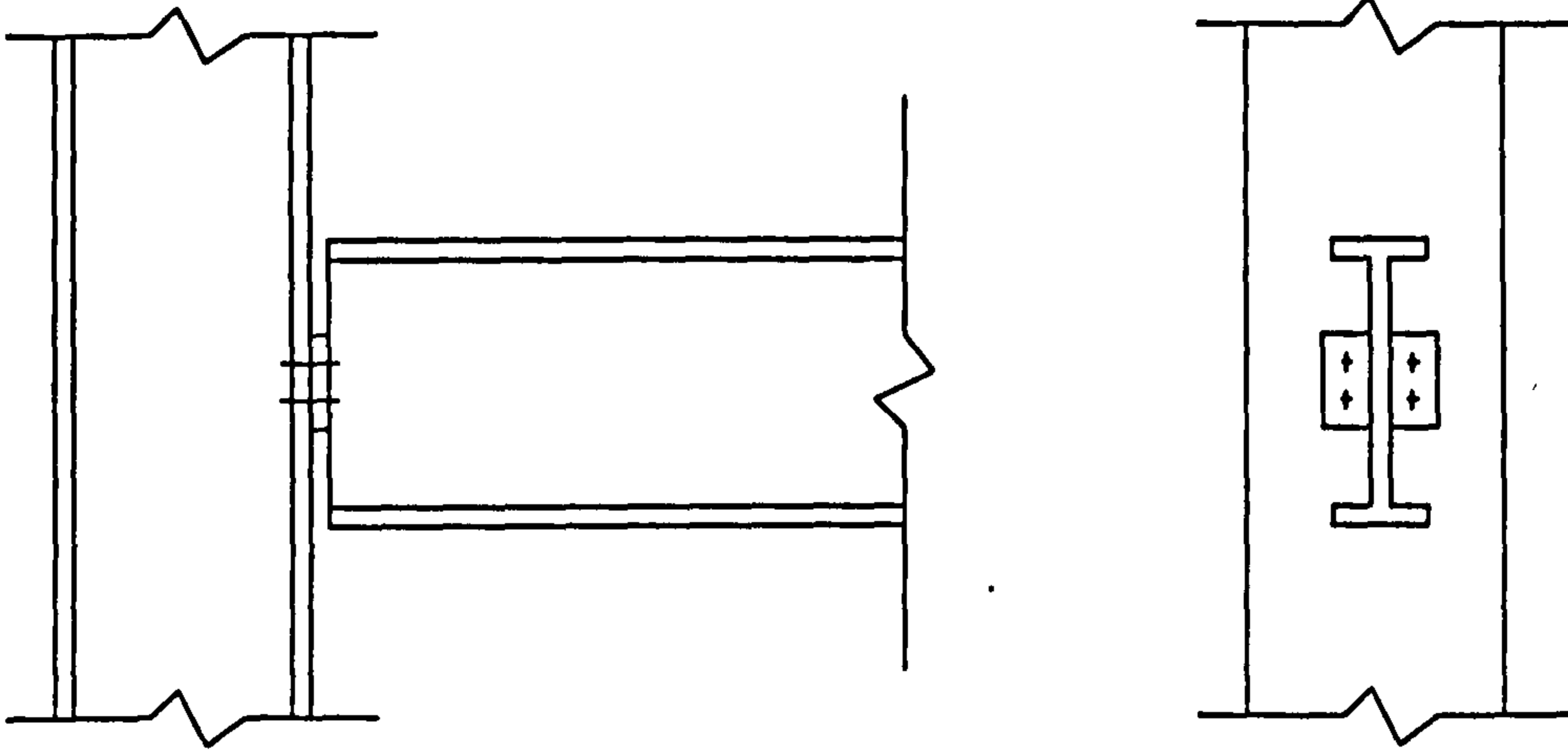


Figure 3.5 : Header Plate Connection

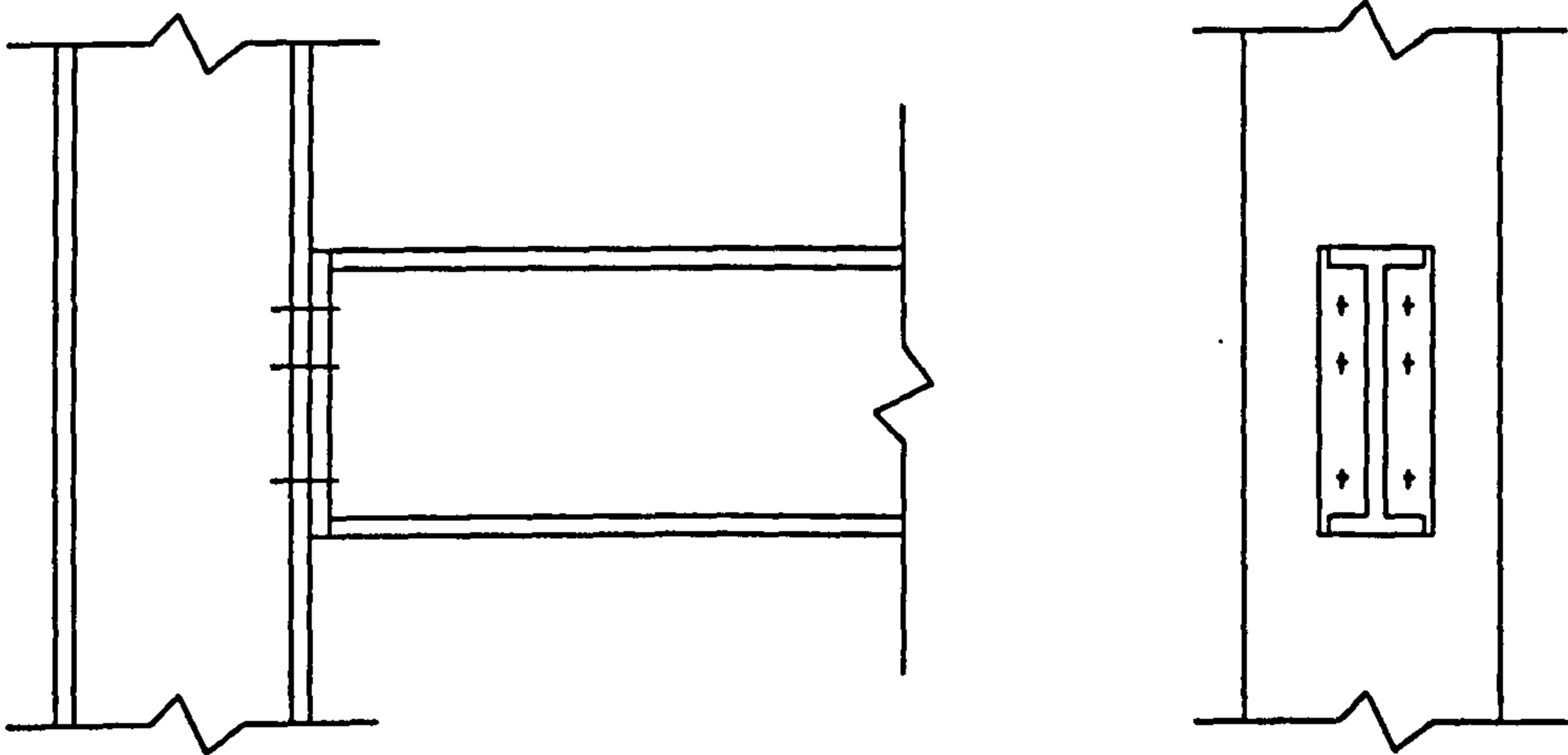


Figure 3.6 : Flush End-Plate Connection

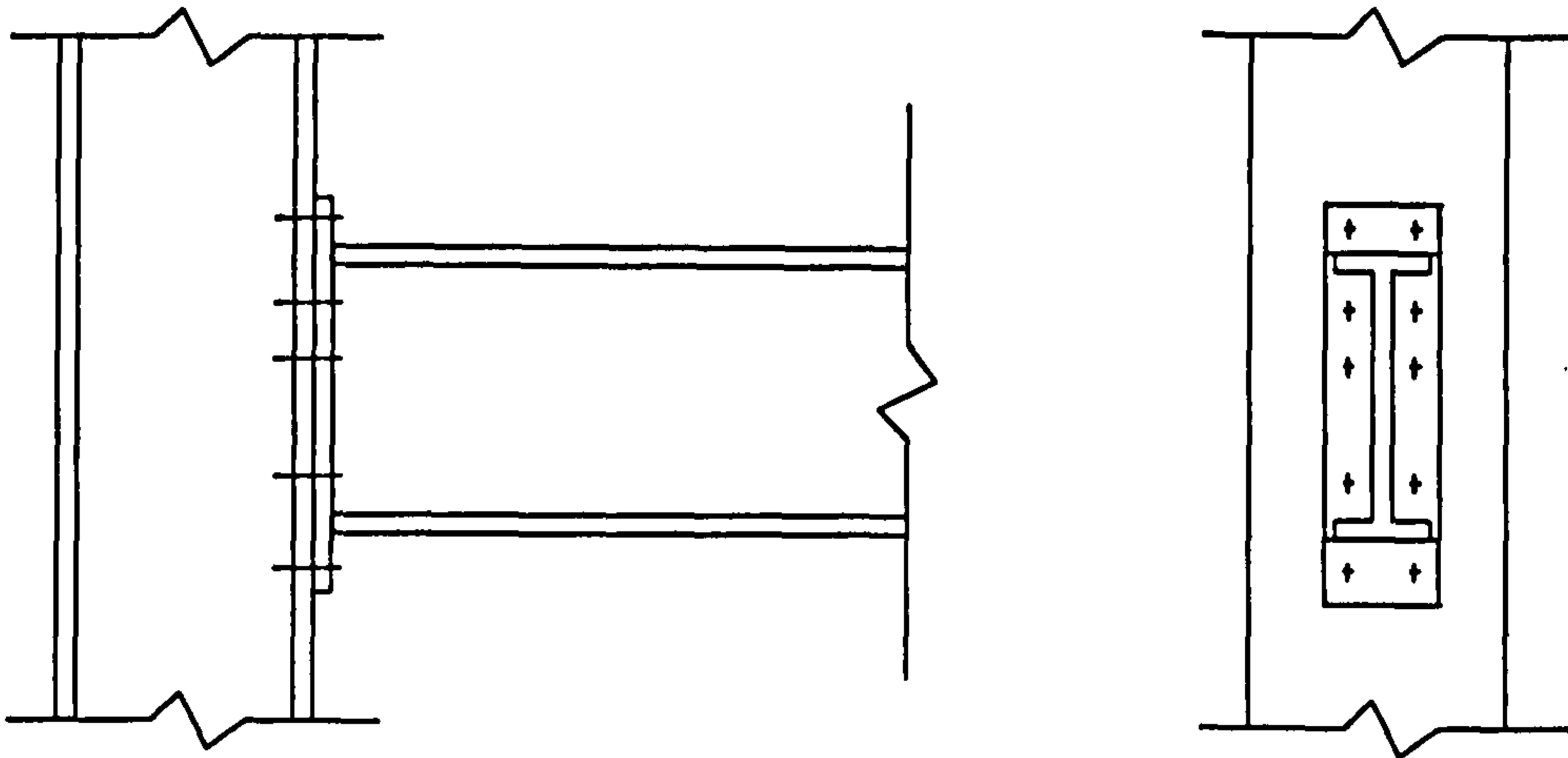


Figure 3.7 : Extended End-Plate Connection

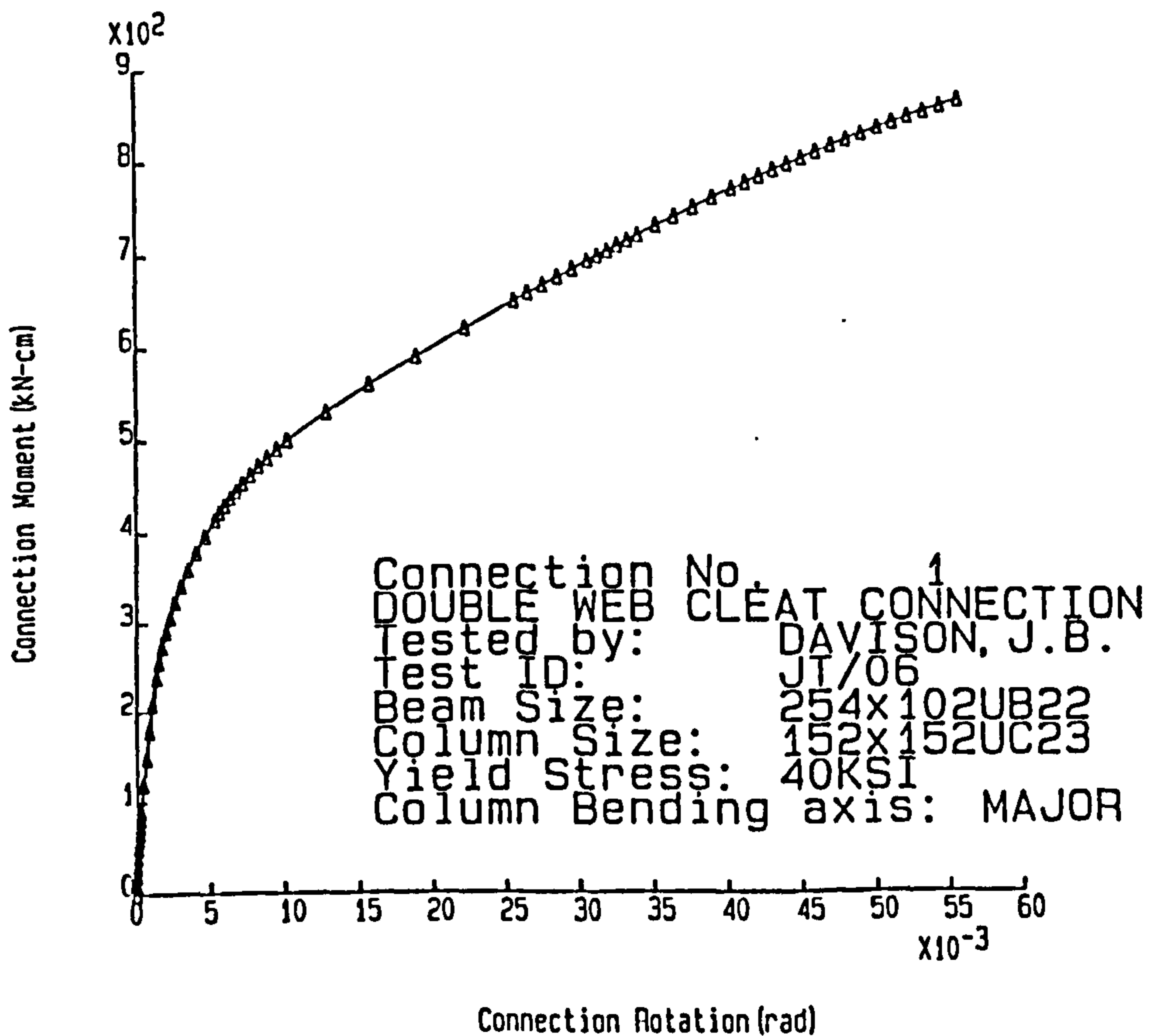


Figure 3.8 : A Example Moment Rotation Curve in Dimensional Form

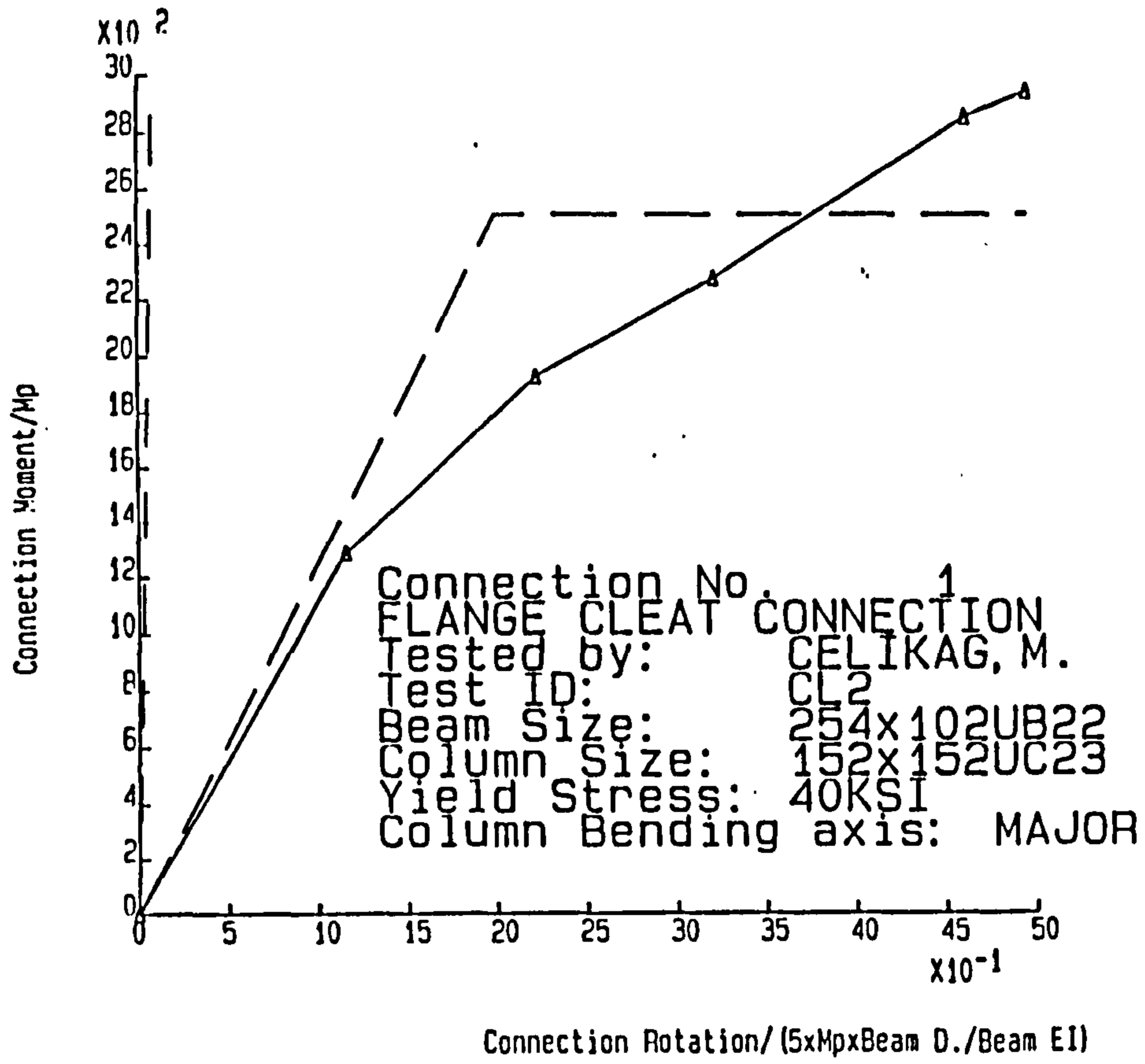


Figure 3.9 : A Example Moment Rotation Curve in Non-Dimensional Form

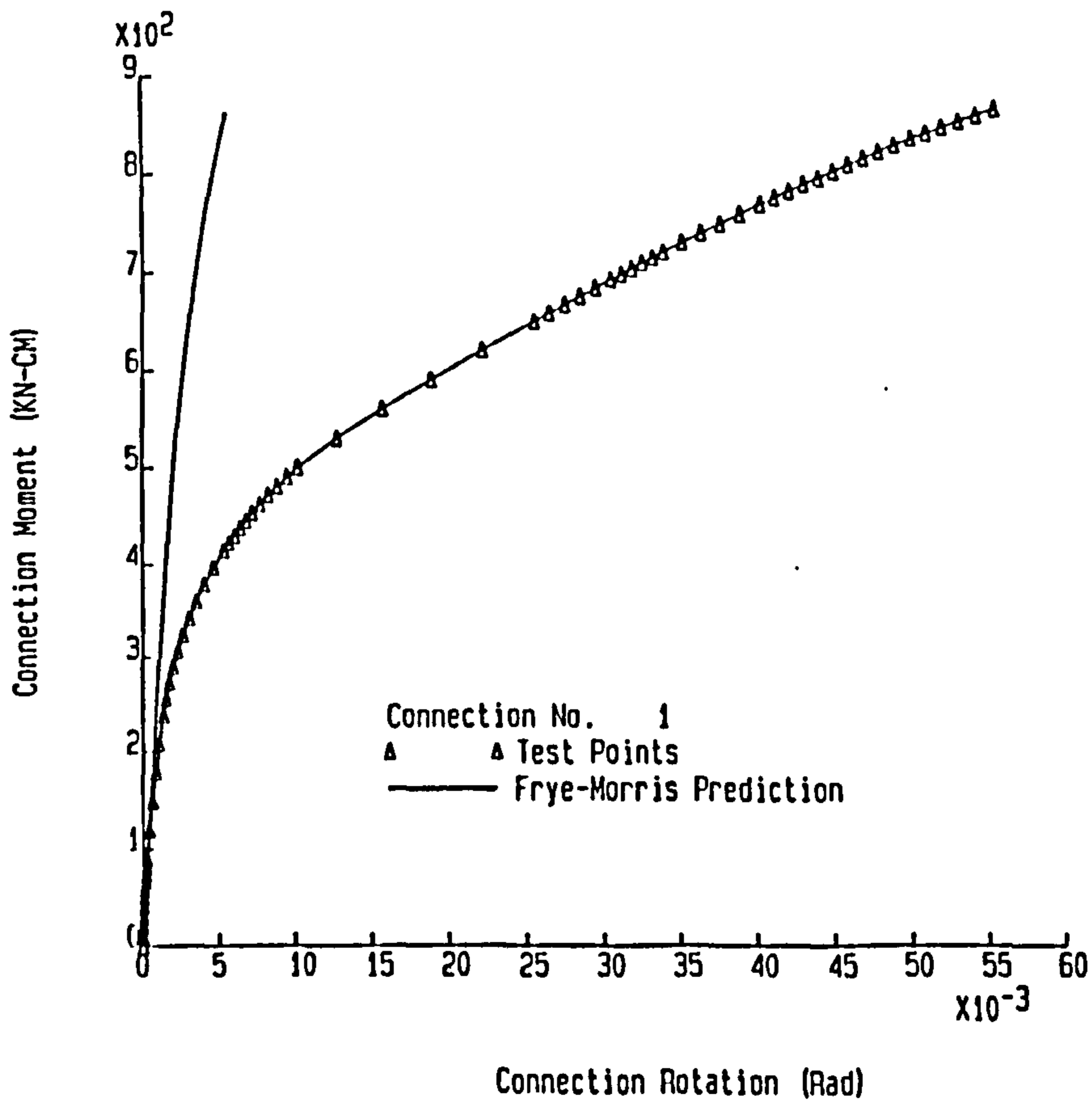


Figure 3.10 : Comparison of Test Moment Rotation Curve to Frye-Morris Prediction



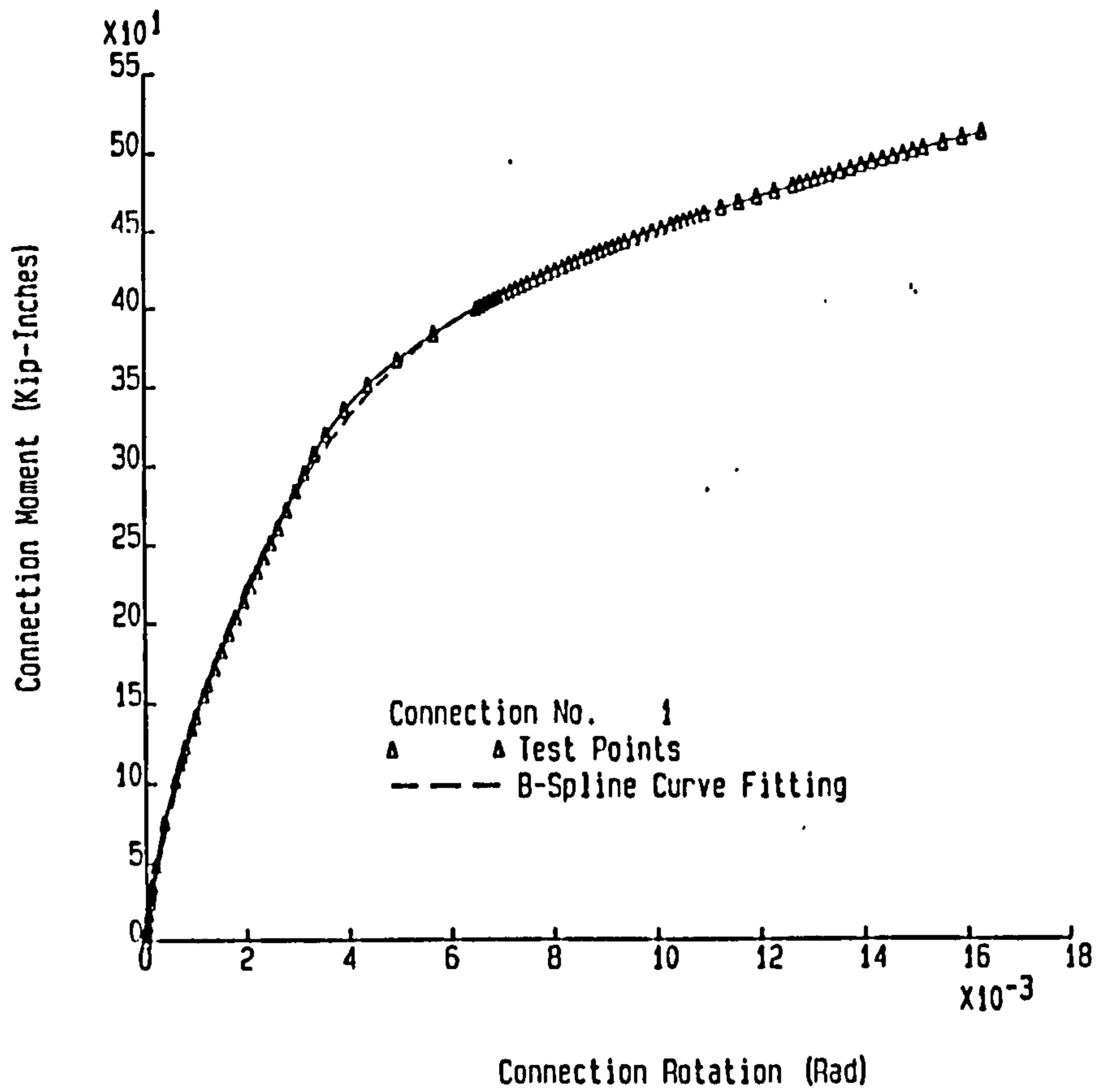


Figure 3.11 : Comparison of Test Moment Rotation Curve to B-Spline Curve Fitting

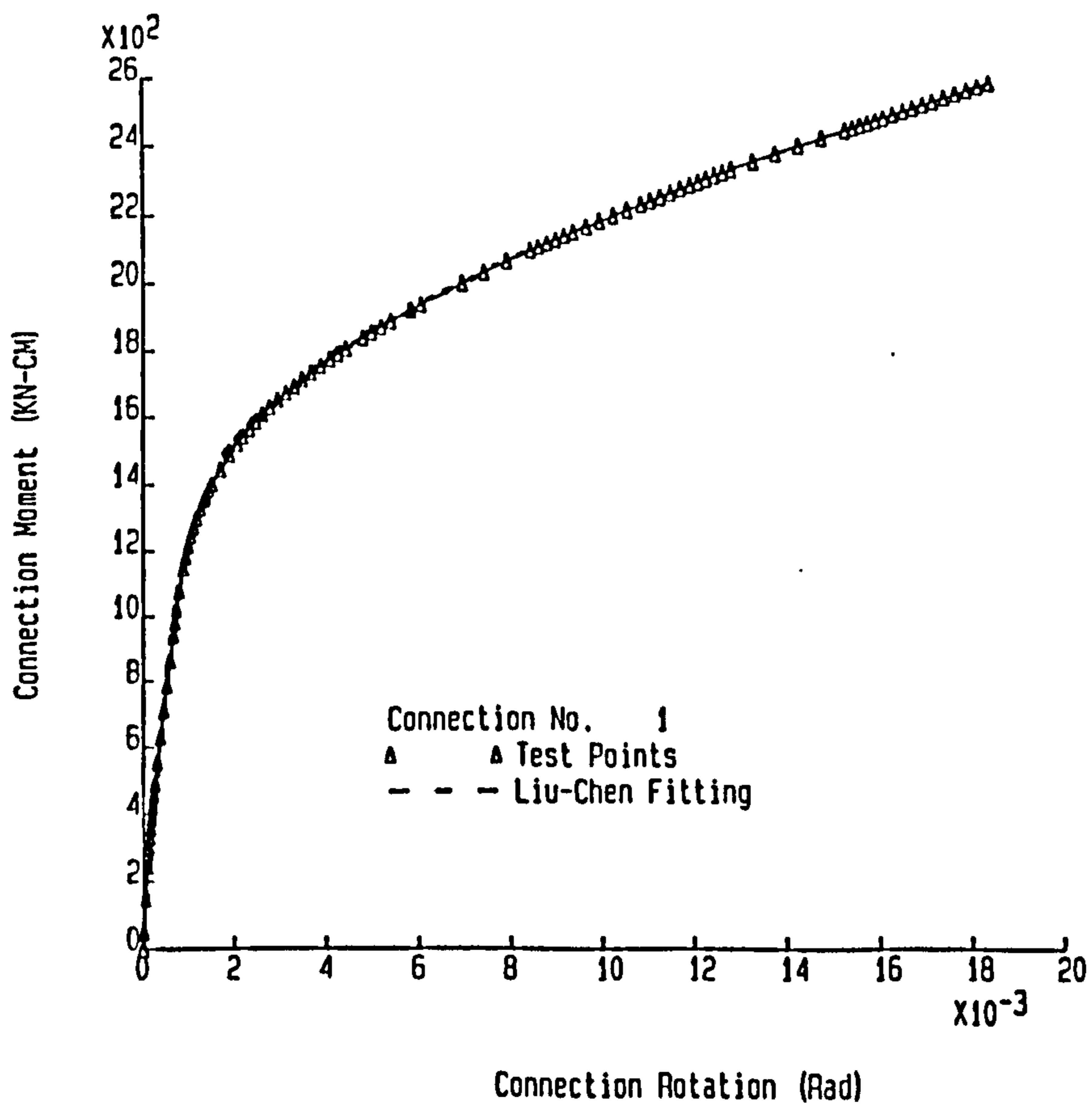


Figure 3.12 : Comparison of Test Moment Rotation Curve to Liu-Chen Fitting

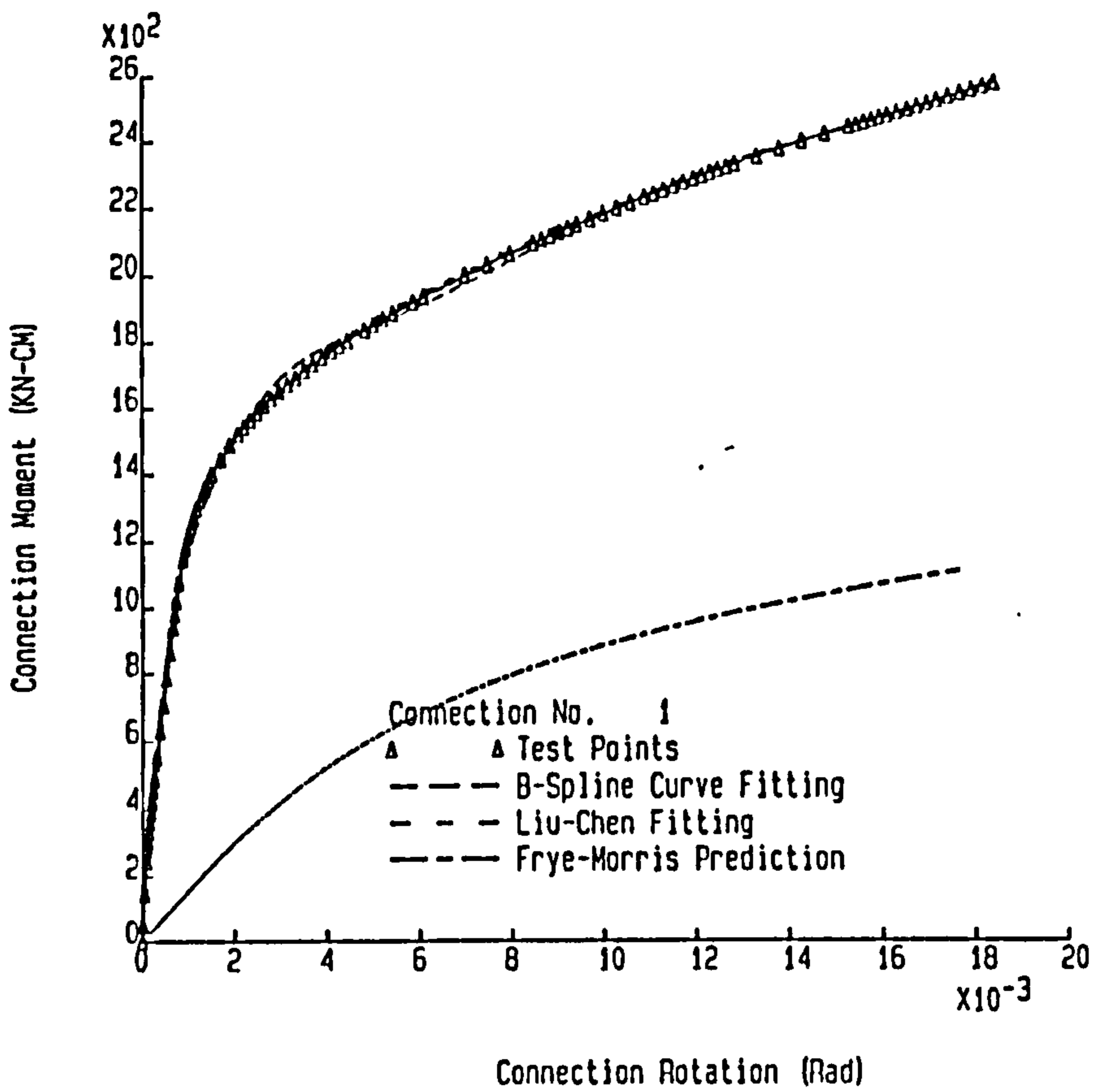


Figure 3.13 : Three Models of Fitting in a Same Plot

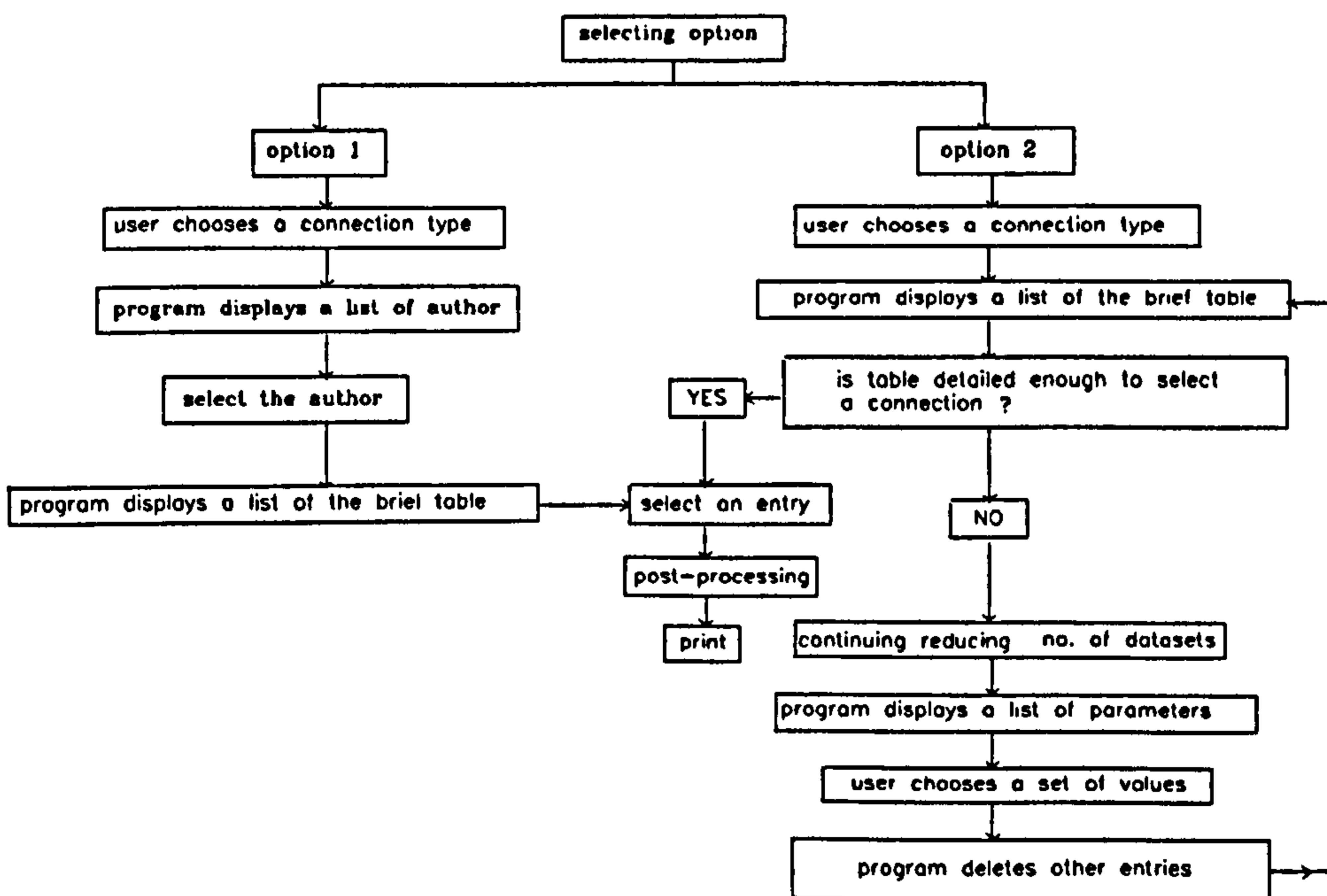


Figure 3.14 : Modified Selecting Procedure for Sheffield Database

## Chapter 4

# Tests of Five Full-Scale Steel Frames

### 4.1 Introduction

Five two dimensional full scale frames have been tested at the Building Research Establishment, Garston, Watford, using a facility developed there. The tests are the result of a collaborative effort by BRE, University of Hertfordshire (formerly, Hatfield Polytechnic) and the University of Sheffield to study the behaviour of frames with semi-rigid bolted connections. The connections varied in stiffness from flange cleats to extended end plates. The first two frames were designed and tested by Hatfield Polytechnic [4.1], the second pair by the University of Sheffield [4.2] and the fifth frame by BRE [4.3]. A large number of tests were carried out for each frame including instrumentation checking tests using different patterns of loading and tests to failure. It was impossible to analyse all of the results, or even most of them, concurrently with the tests due to the limitation of time within the each research project. All data from the five tests were stored at BRE for future study. In 1991, a new research programme suggested by BRE and the University of Sheffield was undertaken in which an in-depth appraisal of the most significant of the test results from the five frames was investigated. The main objective was to study the performance of the connections and their influence on the behaviour of planar frame elements, under practical loading conditions. Comparisons were made with analytical work already carried out with the aim of developing a more realistic design method accounting for connection behaviour.

In this chapter, the rationale behind the selection of the frames is described and then the instrumentation and loading system used for the frame tests are illustrated. Finally, the data logging and storage system and also interpretation methods are explained.

## 4.4 Instrumentation

The main objectives of the instrumentation were to gather sufficient information about the measured applied loads, the distribution of force and moment around the frames, the deflected shape of structure and the  $M-\phi$  relationship of joints to gain an understanding of the behaviour of the different frames. Details of the instrumentation positions for five frames are illustrated in Figure 4.2.

### 4.4.1 Loading and Bracing System

Each beam was loaded individually at its quarter and three-quarter positions using two cables and two hydraulic rams. The steel cables passed through the laboratory floor and were tensioned by two hydraulic rams reacting against the underside of the floor. A pair of hydraulic rams was controlled by a single servo-control valve. The rams were driven at the same hydraulic pressure by splitting the supply into two branches after the oil had left the servo-valve in order to achieve good control. Two load cells possessing similar calibration factors and initial off-set values were used, one for each cable, and were connected together to provide an average feedback signal. Figure 4.3 shows the detail of the hydraulic beam loading arrangement. This chapter presents only a brief summary of this system, a more detailed and technical description is given by Jennings et al [4.4]. A similar loading system was used to apply axial loads to the columns in frames 3, 4 and 5. Two 1000 KN rams were used to load each column. Macalloy bars, instead of steel cables, were used to apply loads to an RHS spreader beam at the column head (Figure 4.4). Control of the system was again achieved by a servo-valve, but the feedback signal was supplied by a displacement transducer arrangement mounted at the head of the column as control by displacement rather than load was considered much safer in the inelastic range near to failure.

All frames were erected adjacent to the laboratory wall so that the balconies could be used to support a bracing system. Nine structural Tee sections were bolted to the balconies and aligned with the bracing positions on each frame. Each frame was restrained by tie-bars attached to one edge column and lying in the plane of the frame for tests in the non-sway condition. They were fitted with threaded ends of different hands so that they could easily be slackened or tightened. Each tie-bar was instrumented so that the distribution and magnitude of the restraining forces could be determined. An additional tie-bar was wired up to act as a temperature compensator. Figure 4.5 shows the bracing system of a test frame.

#### **4.4.2 Strain Measurement**

The distribution of force and moment around the frame was measured using strain gauges located at three sections in each column storey and at four sections along each beam. Four gauges at each section permitted the components of axial strain, bending strains about both major and minor axes, and torsional warping strains to be identified at that section. A linear strain distribution between gauges was assumed. Gauge positions are shown in Figure 4.2.

#### **4.4.3 Rotation Measurement**

Column and beam rotations at connections were measured using pendulum devices similar to ones described by Yarimici [4.5]. Figure 4.6 shows the device in a test frame. Rotation of the beam or column caused the thin metal strip to bend as the weight remained vertical. The relationship between rotation and the resistance of gauges mounted on the strip is linear. A total of 21 of these devices was used for each frame. The device was quite delicate and subject to vibration and therefore an average of fifty readings was taken at a frequency of about twice the natural frequency of the arrangement in order to 'damp' the device. Rotation of the column at the base was measured by an electro level.

#### **4.4.4 Displacement Measurement**

Displacements were measured in both the beams and the columns at the quarter, three-quarter and mid-span positions as shown in Figure 4.7. All of these values were measured relative to points near to the ends of each member. For a non-sway frame test the connection displacements were negligible and so the measurement system was considered to be suitable for the type of test conducted. When the frame is permitted to sway, if axial shortening of the beams is neglected, and the very small vertical displacements ignored, the overall displacement can be deduced knowing the horizontal sway displacement of the outer column and the member displacements relative to their ends. An advantage of the system was that an additional independent instrument supporting frame was not required and left the frame free from visual obstructions.

#### **4.4.5 Bolt Force Measurement**

The bolt forces were measured in frames 1, 2 and 5 in which all 72 bolts, six bolts on each connection, for each frame were monitored, by using precalibrated strain gauged

bolts. A technique similar to that used by previous researchers was employed in these tests [4.6,4.7,4.8,4.9]. The bolts of frame 1 used a single axial strain gauge, bonded in a 2.5 mm diameter by 35 mm deep hole, drilled along the longitudinal axis of the bolt, from the bolt head. These bolts were used in a number of the isolated connection tests. The axial gauge is shown to exhibit a lower reading of bolt force at higher load levels than the surface gauge. This is due to their position on the centre line of the bolt, away from very high bending strains which may be present at the surface. Fracture of all bolts tested to failure occurred in the threaded portion, demonstrating that the presence of the axial gauge did not weaken the bolt in tension.

For frame 2, three strain gauges were individually mounted, longitudinally on the bolt shank at 120° intervals. They were each protected by being positioned in a 0.5 mm milled recess, so that they did not stand proud of the bolt shank. The connection wires from each gauge were passed through a 2 mm diameter hole drilled through the head of the bolt. A 25 mm length of 12 mm diameter stiff plastic tube was threaded into the head of the bolt to a depth of 3 mm. Figure 4.8 shows a bolt.

For frame 5, the method used for frame 2 was adopted with the only difference being that a 3 mm diameter hole was drilled from the centre of bolt head into each gauge recess to avoid interference with the operation of the connection.

The disadvantage of the methods adopted in frames 2 and 5 was the extensive preparation of the bolts needed to fit the three strain gauges. This could be improved used a single axial strain bolt as frame 1.

## 4.5 Data Logging and Storage System

Three Solartron Orion Data Loggers were used to record all the data in the frame tests. Each was connected via an IEEE interface to an LSI 11/73 minicomputer with a 10 mega byte Winchester hard disc and an 8 inch floppy disc drive. This data logging system could log and transfer as many as 1000 channels to hard disk in under 10 seconds, thereby taking a set of readings in a small increment of time which was particularly useful in the elastic plastic range. During this test, around 400 data recording channels were necessary to monitor the frame instrumentation. The first 370 channels, which included the loads, strain gauges and displacement transducers, were recorded first and the rotation gauges were recorded last as they took a greater length of time due to the need to average readings. A pair of

dedicated servo-controlled amplifier units regulated the pressures, and hence load, applied to the individual loading rams and monitored the safety feedback signal. The data logger and the amplifier units were controlled directly from a remote minicomputer. The applied loading scanning of the instrumentation and plotting of the recorded data could be specified by the computer. Information recorded by the data logger was immediately transferred to a hard disk. The mini computer accessed this information and permitted the user to examine the current force and bending moment in any member of the frame or to trace the history of a number of channels through the tests. This facility was extremely useful during the execution of a test particularly near to failure. Detailed information on the data acquisition system and interrogation procedure may be found in Jennings et al [4.4].

At the completion of a test, the information was transferred to an 8 inch floppy disk. For the current study, the data was transferred to a  $5\frac{1}{4}$  inch floppy disk and then sent to the University of Sheffield to be analysed. Here it was transferred onto a Prime main frame computer. A suite of programs, similar to that developed at BRE, was written to interrogate this raw data.

A consistent sign convention has been adopted throughout with the vertical downward movement horizontal movement to the right and clockwise rotations (as defined on Figure 4.2) being taken as positive with the frame view from the adjacent balcony parallel to the frame.

## **4.6 Interpretation of the Data**

### **4.6.1 Analysis of Strains and Determination of Moments**

The distribution of force and moment around the frame was measured using strain gauges located at three sections in each column storey and at four sections along each beam as illustrated in Figure 4.9. Four gauges at each section permitted the components of axial strain, bending strains about major and minor axes and torsional warping strains to be identified at that section. Knowing the total strain at a particular location on the steel section, the individual force components being resisted can be derived. The relationship between the various loading components and the strain is shown in Figure 4.10. Figure 4.11 illustrates the location and the nomenclature of strain gauges in the sections of beam and column.

Assuming a constant gauge factor and a linear relationship between stress and strain until yield, in theory, only four measurements of strain are required to determine the individual load components in the elastic region, one near the edge of each of the flange tips. However, this would be compromised in a local area of high or usual strain distributions. More gauges at each of the relevant sections would overcome this problem as it would effectively provide a degree of redundancy to the monitoring system and hence permit a better interpolation of strain when plastic dislocations occur.

Using this approach, the bending moment at the ends of the members, at the loading points of beams and at the mid-height of columns were calculated. The method used to calculate the beam moment is more fully described next.

#### 4.6.2 Beam Moment Calculation

Moments  $M_1$ ,  $M_2$ ,  $M_3$  and  $M_4$  are computed from strain measurements at strain gauge positions  $SGPO(1)$  to  $SGPO(4)$  indicated on Figure 4.12. The beam moments at each ends ( $M'_1$  and  $M'_4$ ) and the loading points ( $M'_2$  and  $M'_3$ ) are calculated using linear extrapolation. Figure 4.12 shows the moment distribution in a beam and the notation adopted.

To calculate the connection moment, the distance between two gauges points is first calculated by,

$$L_1 = SGPO(2) - SGPO(1) \quad (4.1)$$

The distance between the beam end  $ECC$  and the first gauge point is,

$$D_1 = SGPO(1) - ECC \quad (4.2)$$

The moment at the connection  $M'_1$  is thus obtained as,

$$M'_1 = M_1 + (M_1 - M_2) \frac{1}{L_1} D_1 \quad (4.3)$$

To calculate the moment at the first loading point, the distance between the second gauge point to applied load position  $D_2$  is calculated from,

$$D_2 = LDPO(1) - SGPO(2) \quad (4.4)$$

The moment at the load position  $M'_2$  is obtained as,

$$M'_2 = M_2 + (M_2 - M_1) \frac{1}{L_1} D_2 \quad (4.5)$$



The moments at the second loading point  $M'_3$  and at the connection at the other end of the beam  $M'_4$  are calculated in a corresponding manner.

where  $D_i$  and  $L_i$  are distances along the beam  
LDPO(i) are the applied load positions  
SGPO(i) are the strain gauge positions  
 $M_i$  and  $M'_i$  are the moments at the location points  
 $ECC$  is the position of the beam end

A suite of programs, similar to that developed at BRE written in Fortran language was available to interrogate the raw data on the Prime A computer in University of Sheffield.

## 4.7 A Brief Description of Frame Tests

Frames 1 and 2 were full-scale, two dimensional asymmetric two bay wide by three storey high steel frames with both flush end-plate and extended end-plate connections to the column flange. These two frames were undertaken to examine the influence of the connections on beam response. A detailed analysis will be presented in Chapter 5. For the frames 3, 4 and 5 tests were more concerned with column response. Frames 3 and 4 were full-scale, two dimensional symmetric two bay wide by three storey high steel frames with top and bottom cleat connections. In frame 3 the beams were attached to major axis of the columns and in frame 4 the beams were attached to the column on its minor axis. The results will be discussed in detail in Chapter 6. Finally, frame 5 was a full scale two dimensional symmetric two bay wide by three storey high structure with the connection types used in frames 1 and 2 (no stiffener was adopted). The nomenclature of five frames are shown in Figure 4.13. Details of test results will be the subject in chapter 7.

The provision of all the general information and test results of five frame tests for use by others formed the basis of a paper [4.10].

## References

- [4.1] Prescott, A. T., 'The Performance of End-Plate Connections in Steel Structures and their Influence on Overall Structural Behaviour', Ph.D. Thesis, Hatfield Polytechnic, July, 1987.
- [4.2] Davison, J. B., 'Strength of Beam-Columns in Flexibly Connected Steel Frames' Ph.D. Thesis, University of Sheffield, June, 1987.
- [4.3] Lennon, T., 'Full-Scale Steel Frame Tests: Load Tests on Frame No.5', Building Research Establishment, Report No. N71/88.
- [4.4] Jennings, D. A., Moore, D. B. and Sims, P. A. C., 'Instrumenting and Testing Bolted Steel Frame Structures', Proceedings, Determination of Dangerous Stress Levels and Safe Operation Condition, Edinburgh, August, 1986.
- [4.5] Yarimici, E., Yura, J. A. and Lu, L. W., 'Rotation Gauge for Structural Research', Experimental Mechanics, November, 1968, pp. 525-526.
- [4.6] Nair, R. S., Birkemoe, P.C. and Munse, W. H., 'High Strength Bolts subject to Tension and Prying', Journal of Structural Division, ASCE, Vol. 100, ST2, 1974.
- [4.7] Surtees, J. O. and Mann, A. P., 'End Plate Connections in Plastically Designed Structures', Conference on Joints in Structures, University of Sheffield, U.K., 1970.
- [4.8] Mann, A. P. and Morris, L. J., 'Significance of Lack of Fit-Flush Beam-Column Connections', International Conference on Joints in Structural Steelwork, Teesside Polytechnic, U.K., 1981.
- [4.9] Bahia, C. S., Graham, J. and Martin, L. H., 'Experiments on Rigid Beam to Column Connections subject to Shear and Bending Forces', International Conference on Joints in Structural Steelwork, Teesside Polytechnic, U.K., 1981.
- [4.10] Lau, S. M., Davison, J. B., Kirby, P. A. and Moore, D. B., 'Behaviour of Non-Sway Frames with Semi-Rigid Connections under Beam Load', in press.

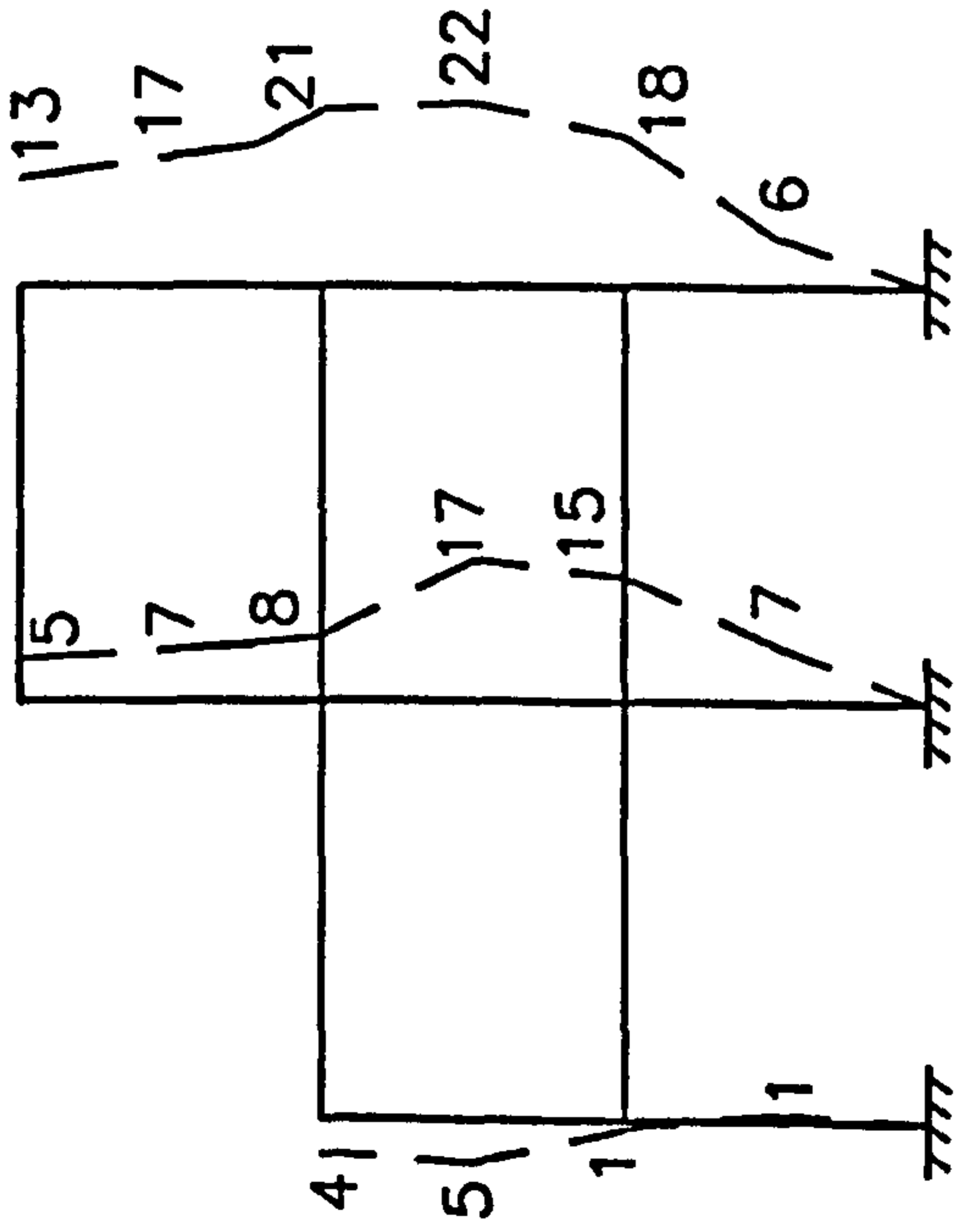
Frame	Axis	Symmetrical (S) / Asymmetrical (As)	Mode	Beam Size	Column Size	Connection Type
1	Major	As	Non-Sway & Sway	254x146UB43	203x203UC71	End-Plate
2	Major	As	Non-Sway & Sway	254x146UB43	203x203UC71	End-Plate
3	Major	S	Non-Sway	254x102UB22	152x152UC23	Flange Cleats
4	Minor	S	Non-Sway	254x102UB22	152x152UC23	Flange Cleats
5	Major	S	Non-Sway	254x146UB37 254x102UB28	152x152UC37	End-Plate

Table 4.1 : Summary of Five Frame Tests

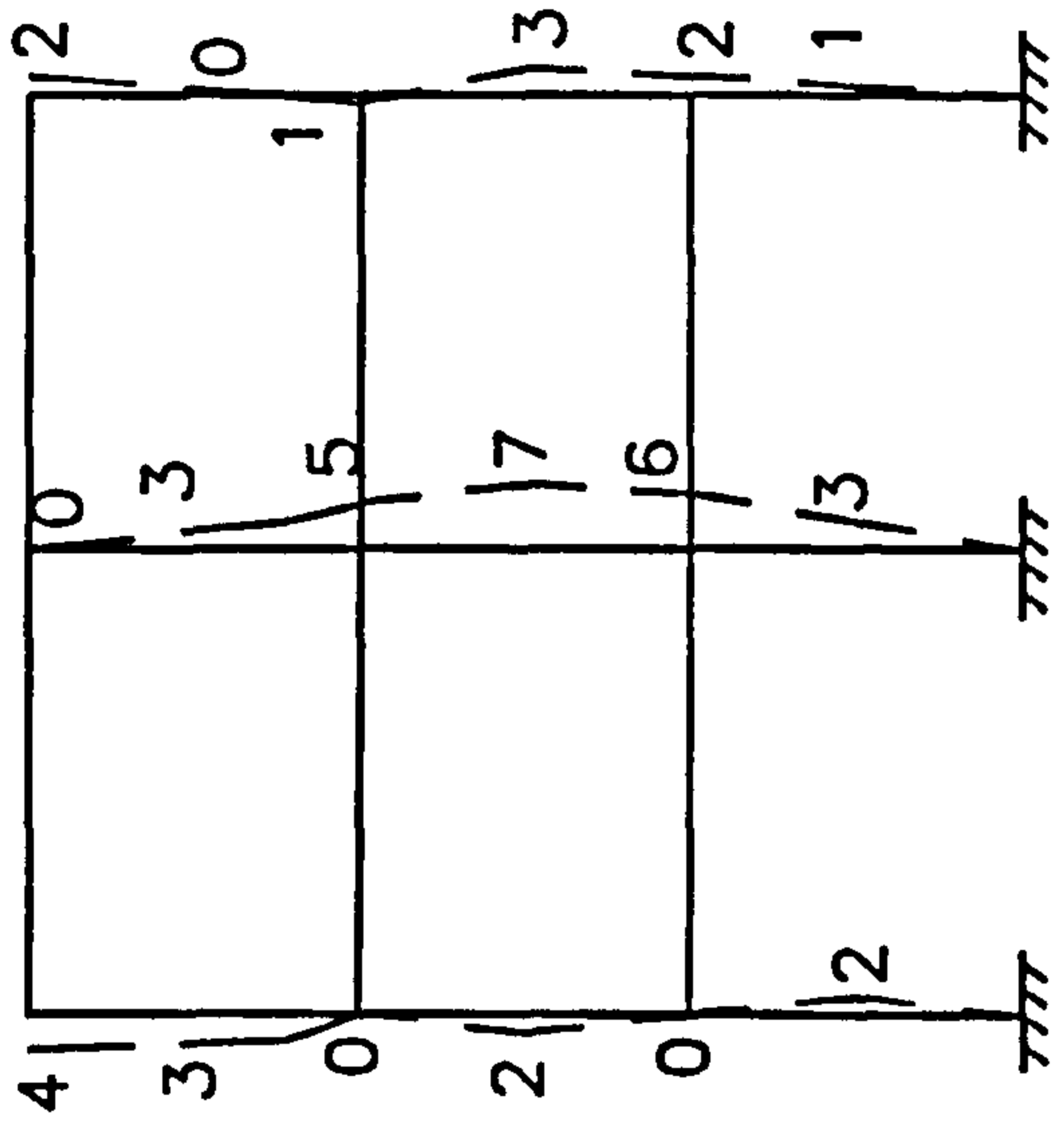
Type	Member	Material Yield Stress ( $N/mm^2$ )				
		Frame No.				
		1	2	3	4	5
Beam	1	323.9	326.0	-	295.4	357.0
	2	316.0	329.0	267.4	300.3	362.3
	3	324.5	324.0	269.3	296.0	354.3
	4	323.9	326.0	271.5	287.5	275.3
	5	316.0	329.0	269.5	286.9	262.9
	6	324.5	324.0	267.2	287.8	270.9
Column	1	274.0	272.4	252.5	298.8	246.0
	2	269.0	269.6	263.3	293.4	269.0
	3	286.0	272.5	262.3	278.1	250.0

Remark : Frame Samples taking from Member Flanges

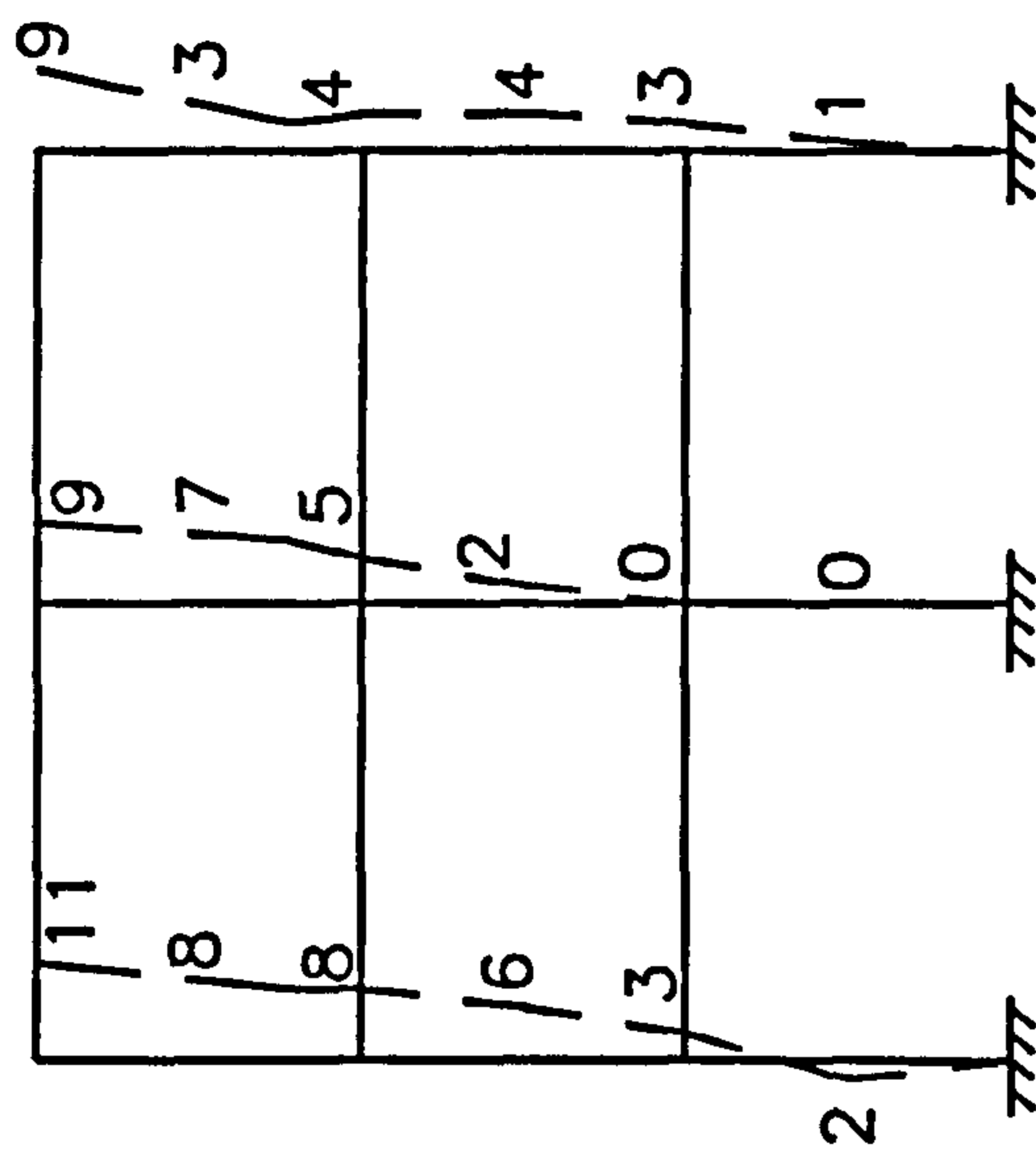
Table 4.2 : Yield Stress measured in Five Frames



Frame 3

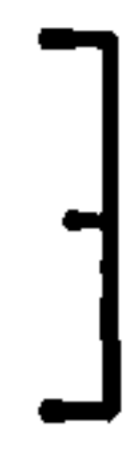


Frame 4



Frame 5

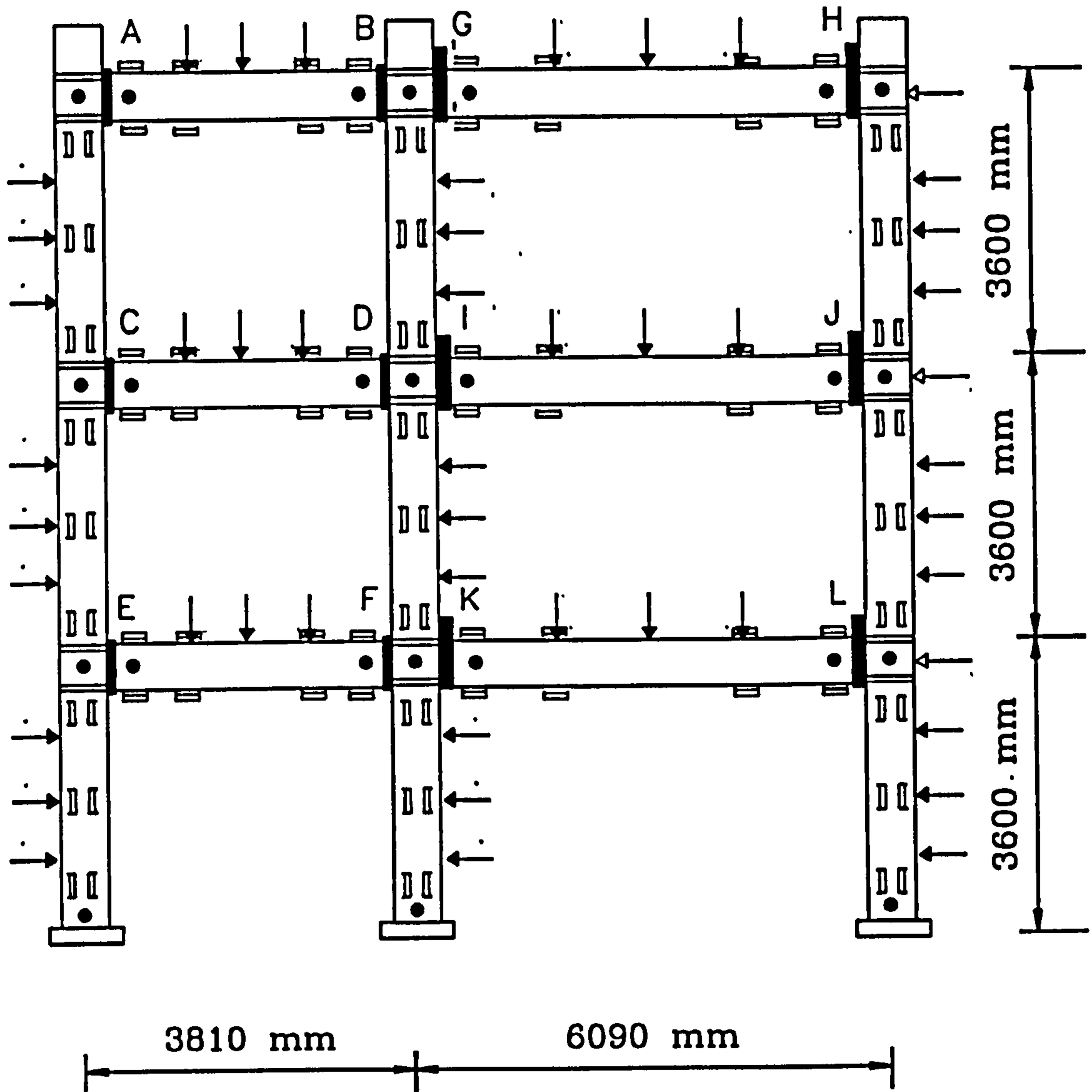
Scale



0 10 20  
in mm

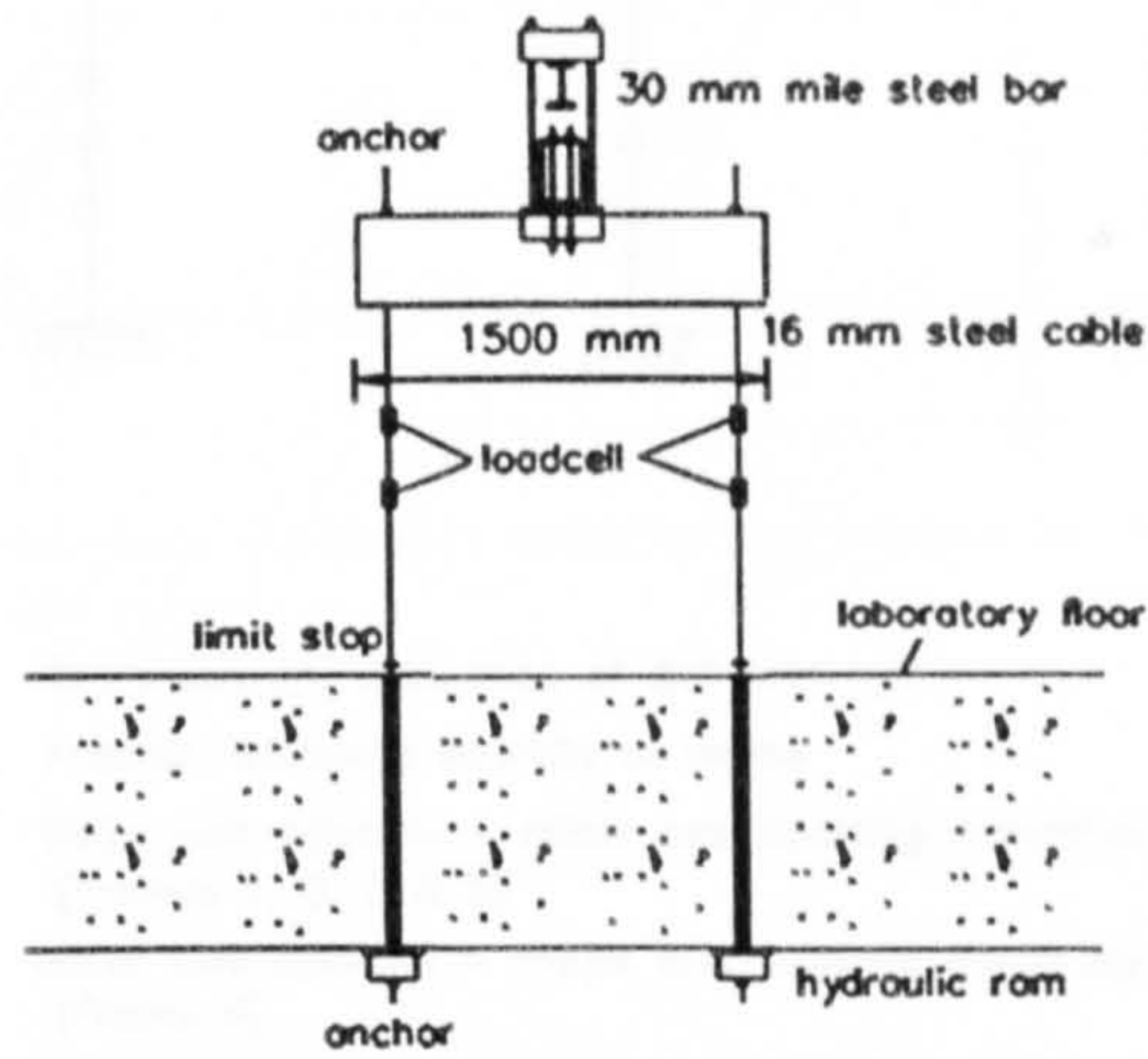
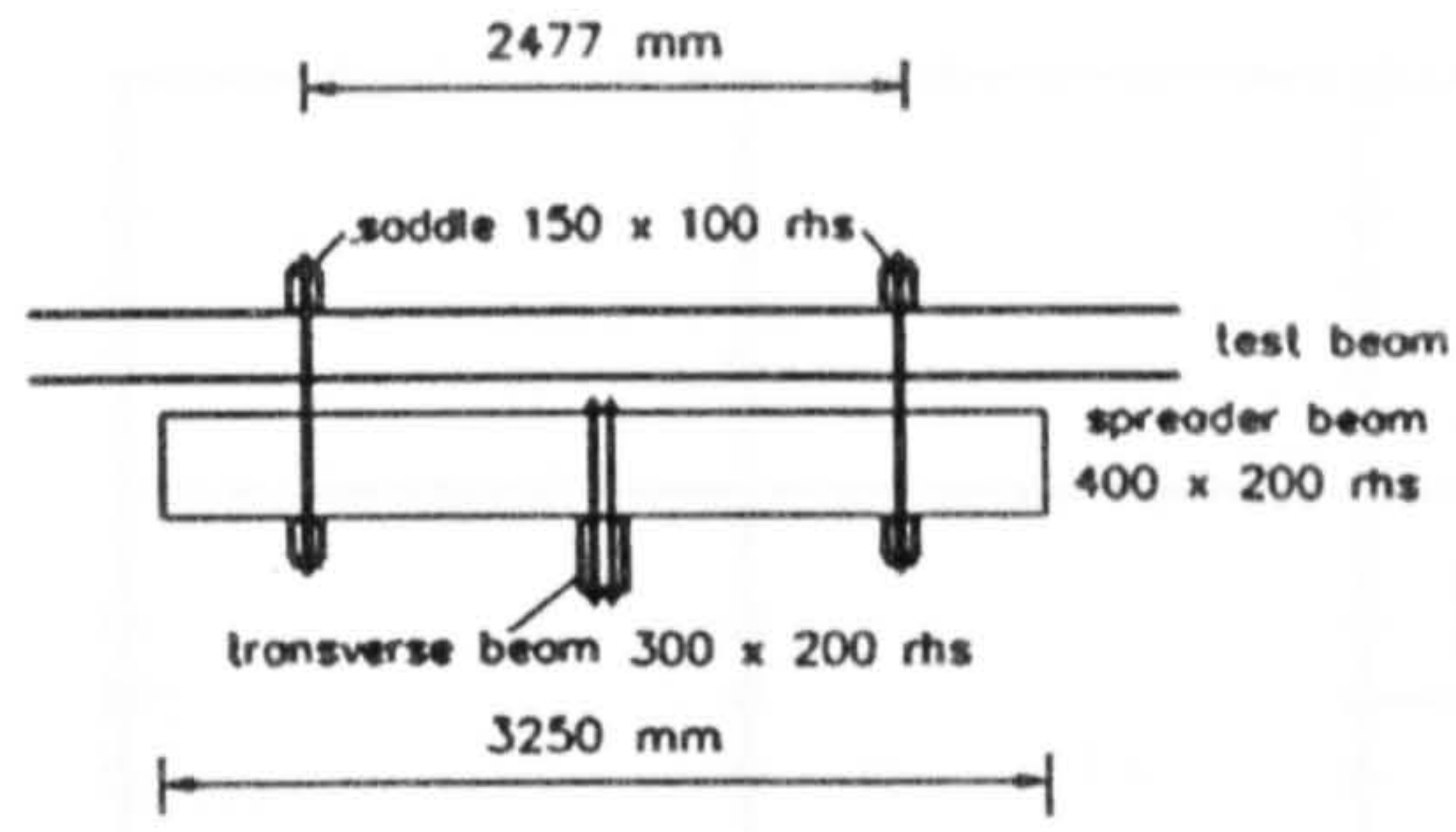
(All Frames viewed from Balcony)

Figure 4.1 : Initial Shape of Frame 3, 4 and 5



- Beam / Column Displacements
- Rotation Devices
- Strain Gauges
- ← Sway Restraint Bars

Figure 4.2 : Instrumentation of Frames 1 and 2



SECTION

Figure 4.3 : Hydraulic Beam Loading Arrangement

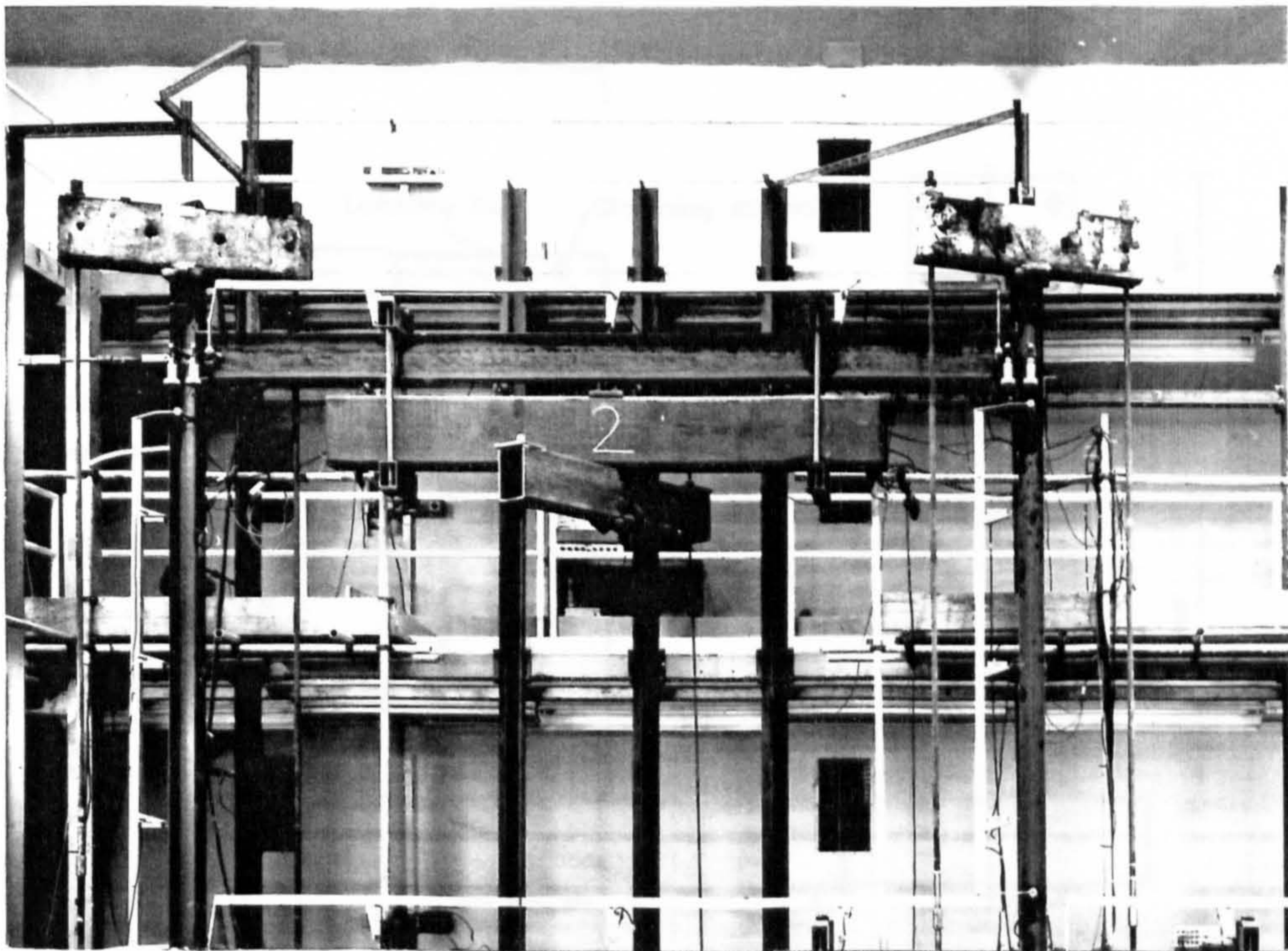
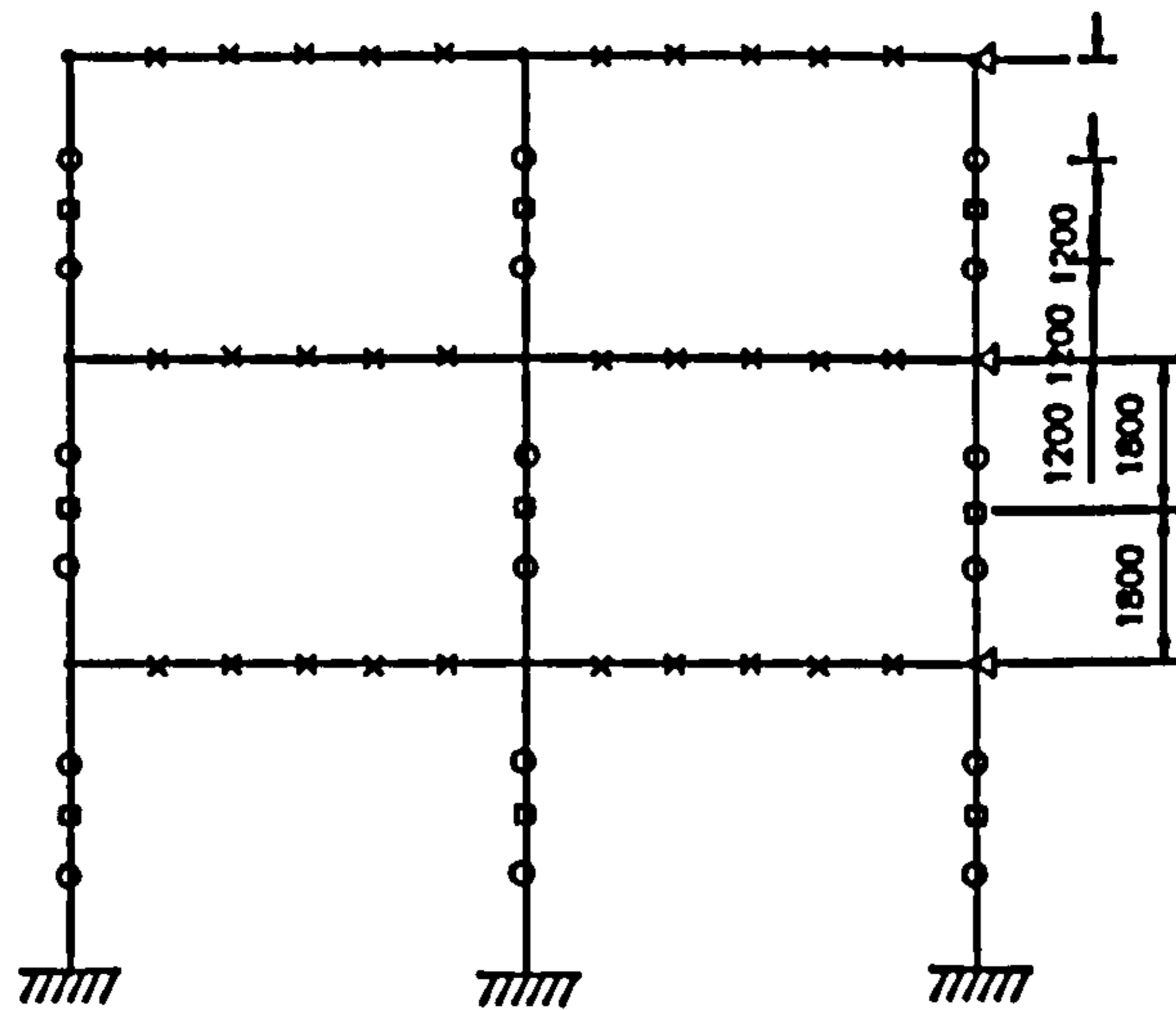


Figure 4.4 : Column Head Loading Arrangement



Beam laterally restrained at 812 mm c/c \*  
 Frames restrained laterally at nodes .  
 Major axis columns - minor axis buckling prevented at O  
 (Frames 1, 2, 3 & 5)  
 Minor axis columns - major axis buckling prevented at □  
 (Frame 4)  
 Sway bracing ←

(view from balcony)

Figure 4.5 : Out-of-Plate Action Bracing Locations

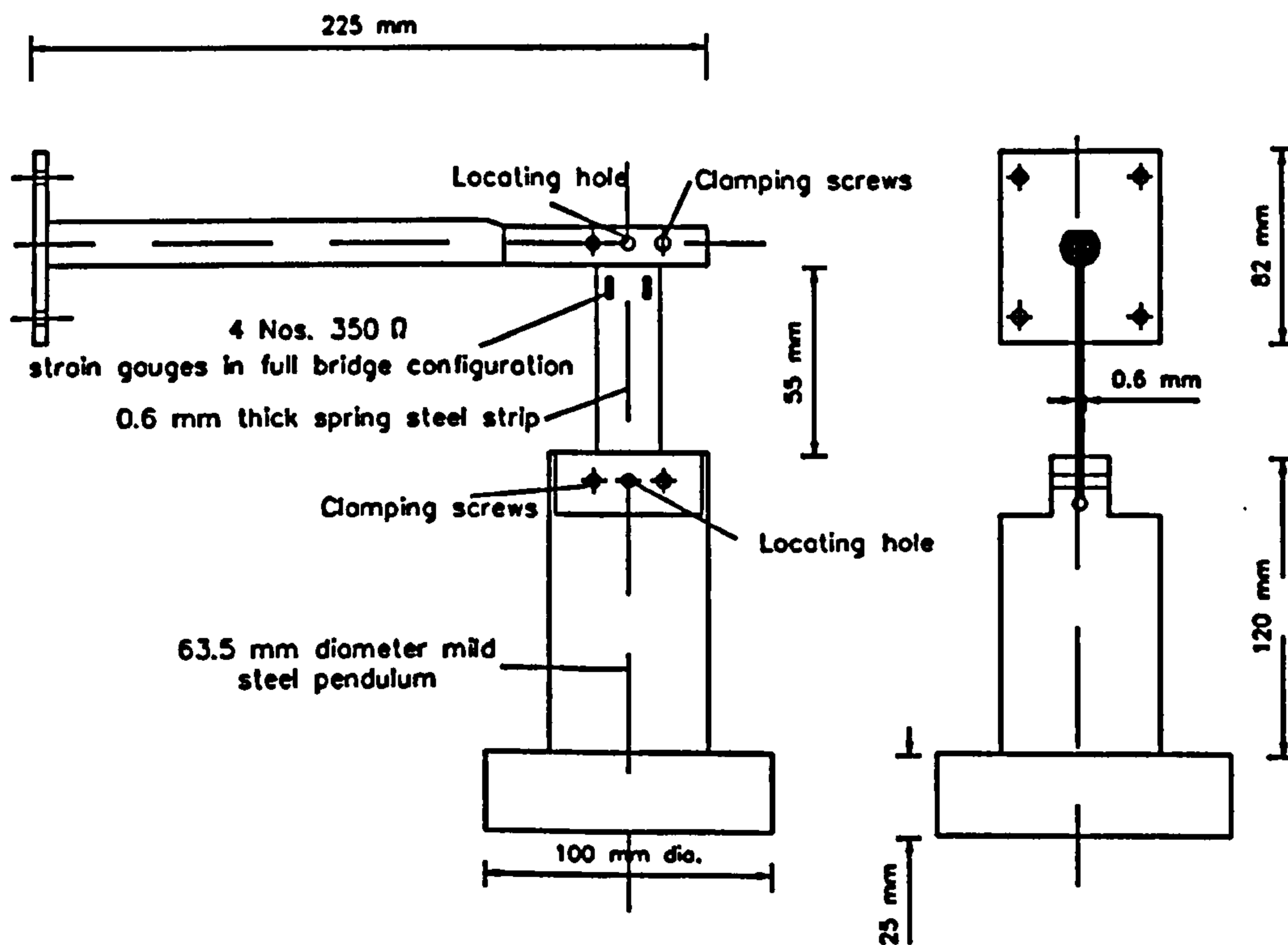


Figure 4.6 : Rotation Device

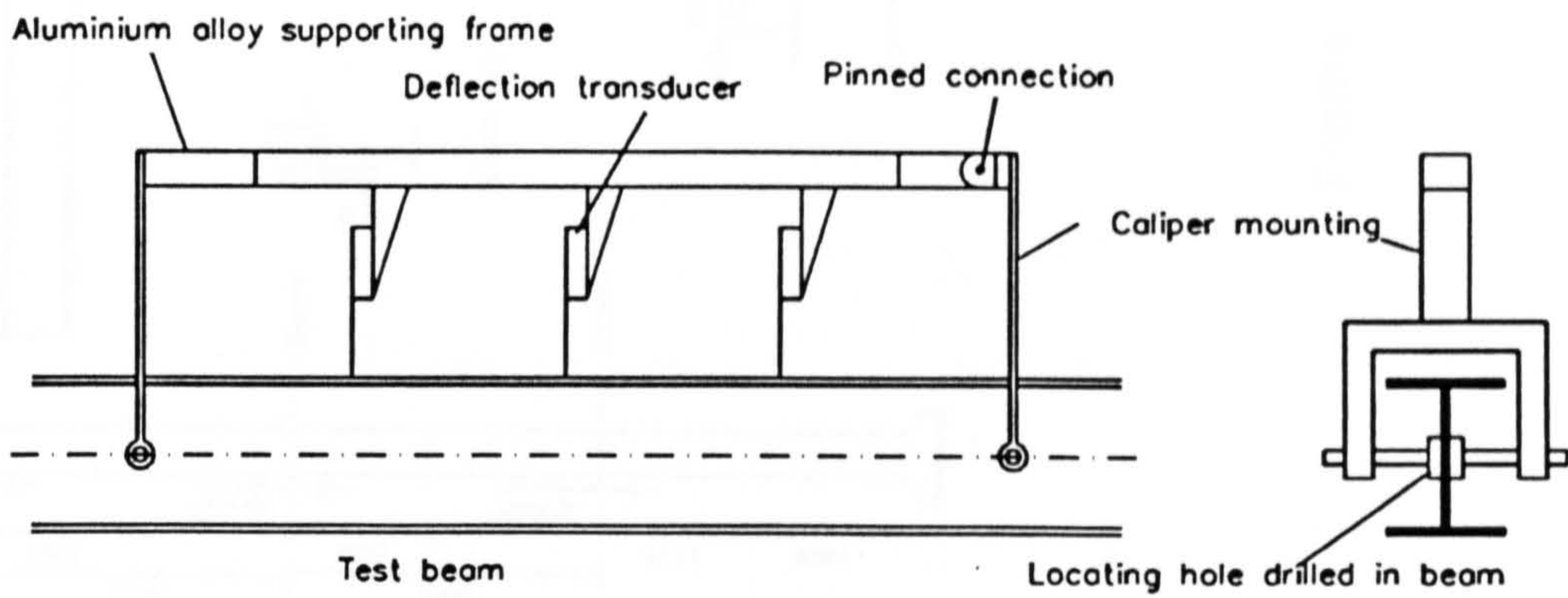


Figure 4.7 : Location of Linear Voltage Displacement Transducers

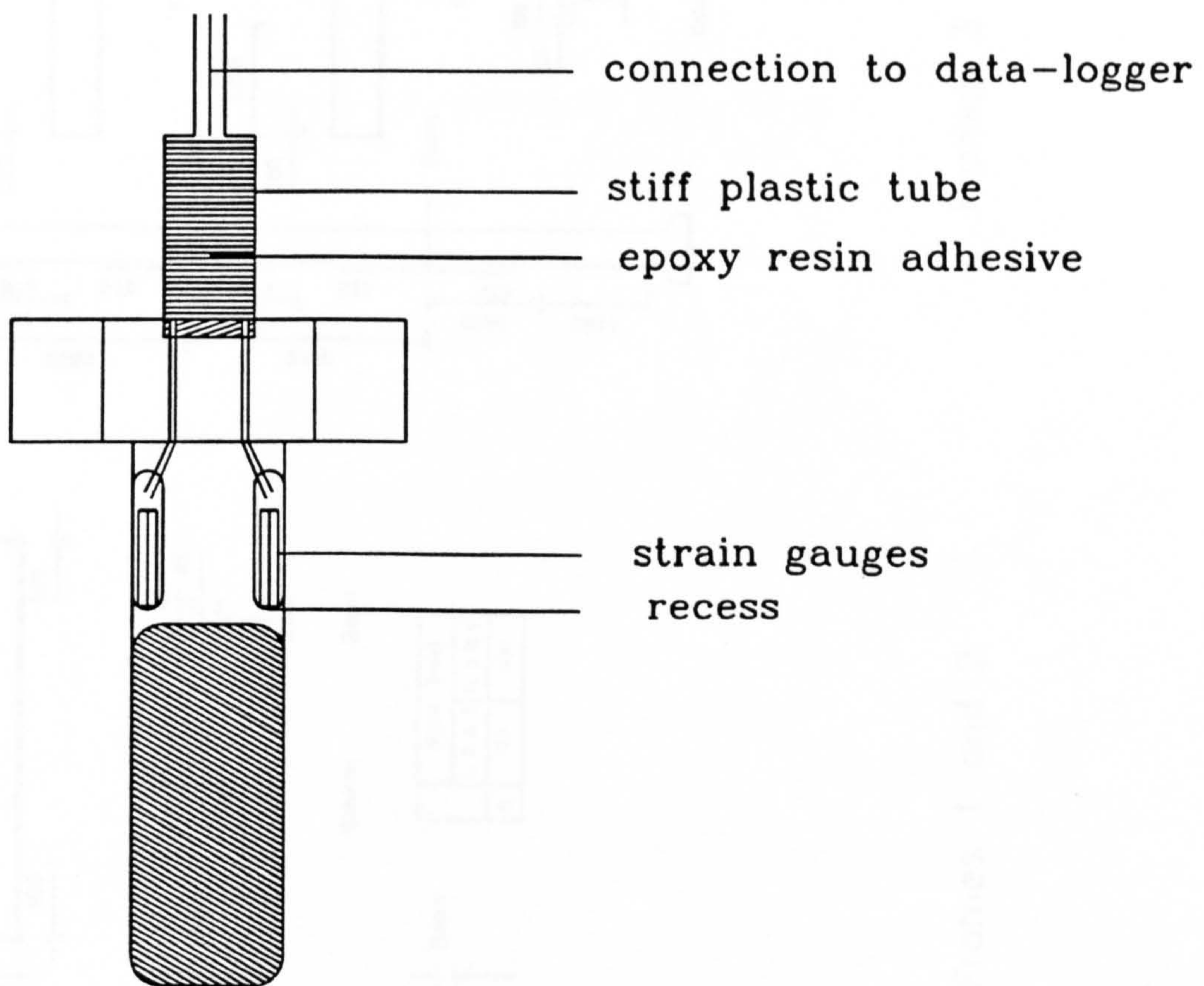
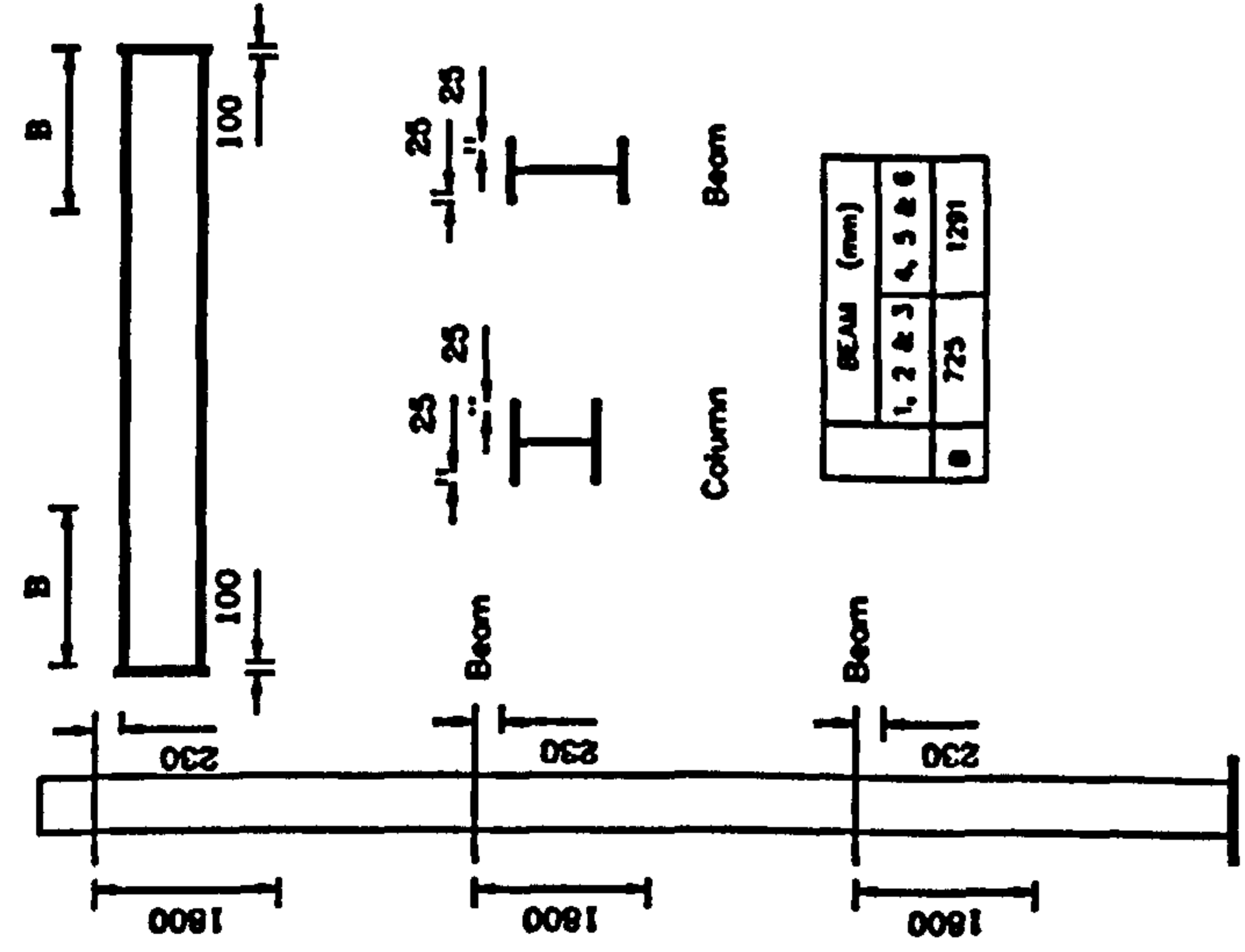
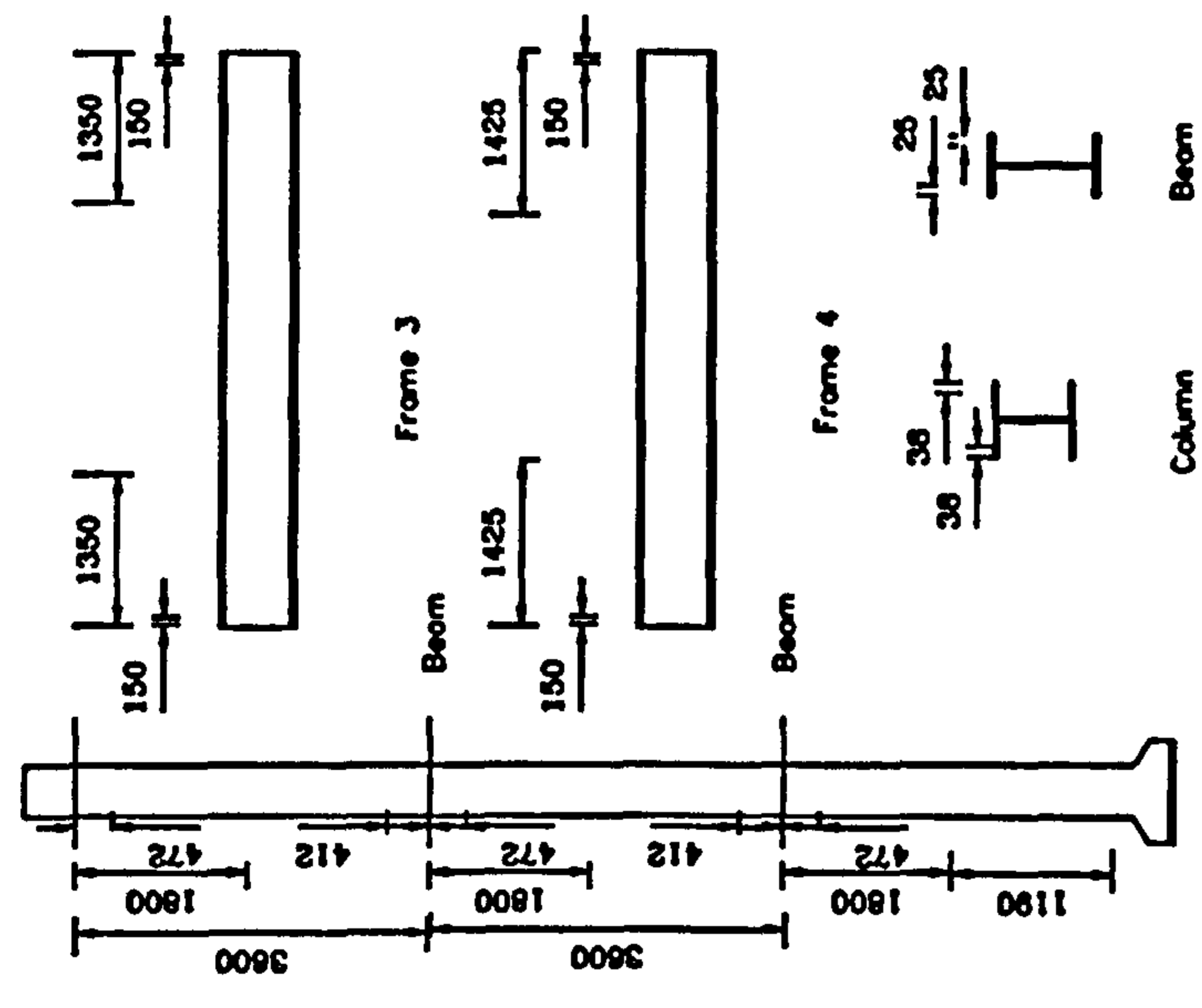


Figure 4.8 : Strain Gauged Bolt

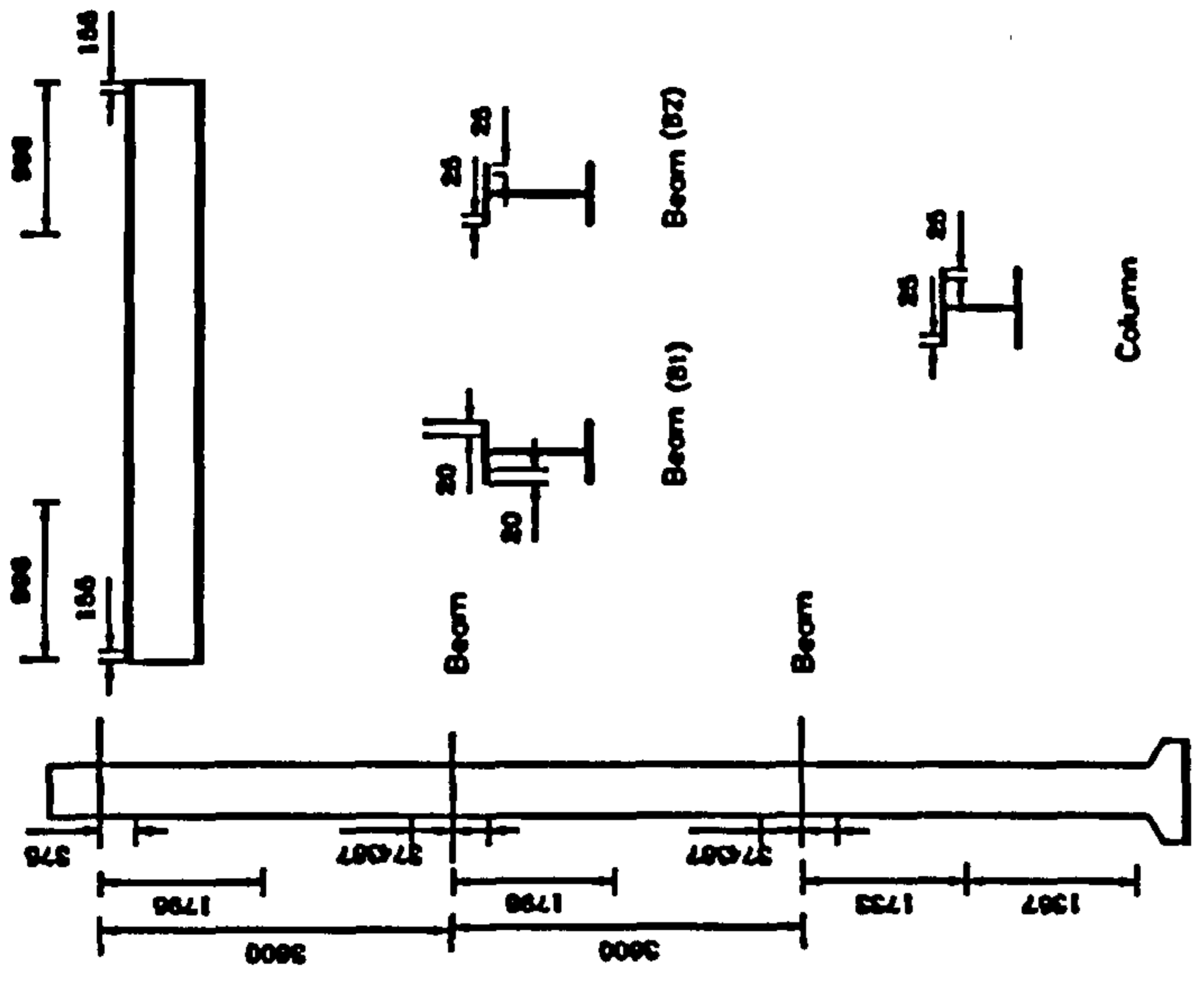




Frames 1 and 2

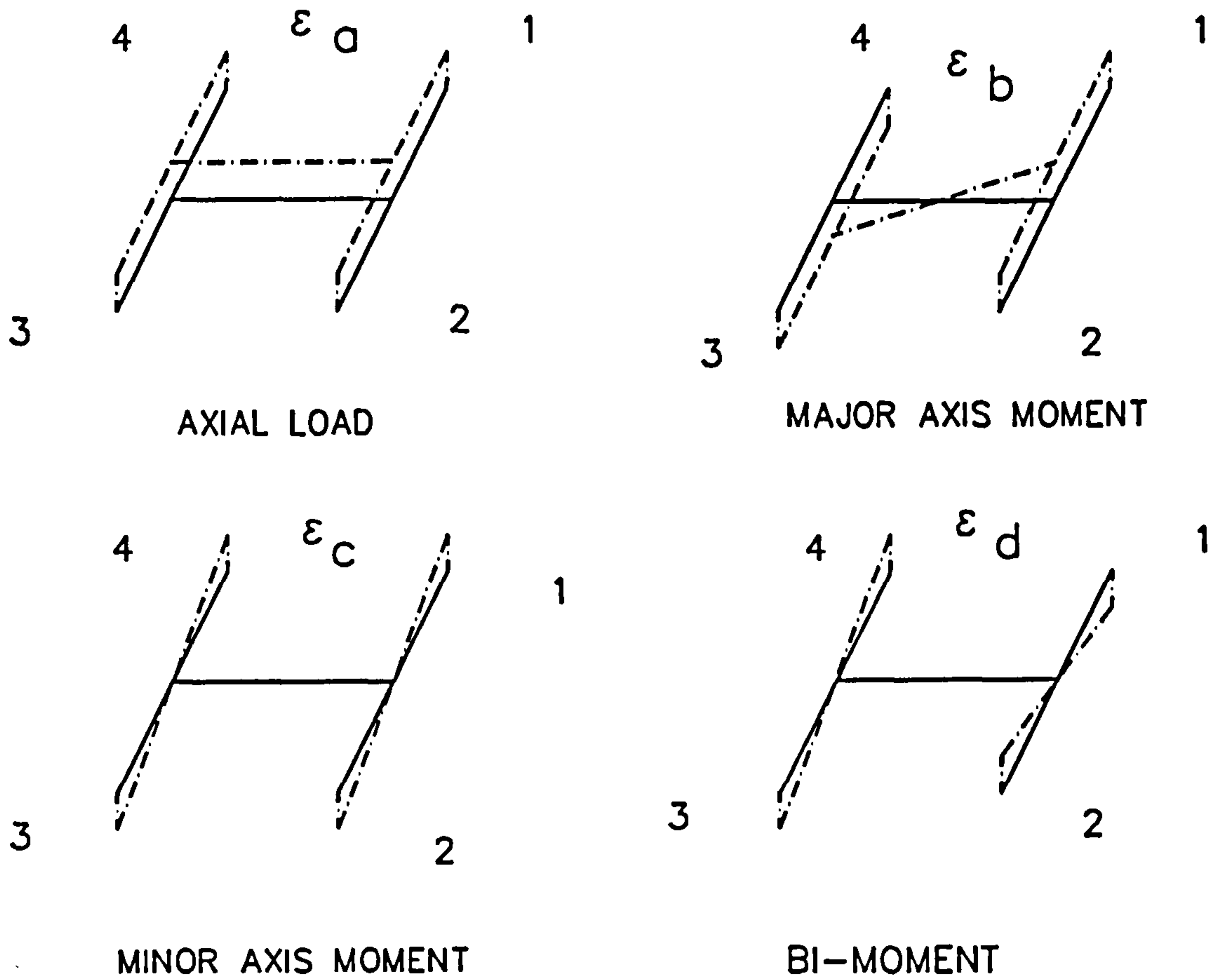


Frames 3 and 4



Frame 5

Figure 4.9 : Strain Gauge Position in Five Frames



STRAIN COMPATIBILITY EQUATIONS :

$$\epsilon_1 = \epsilon_a + \epsilon_b + \epsilon_c - \epsilon_d$$

$$\epsilon_2 = \epsilon_a + \epsilon_b - \epsilon_c + \epsilon_d$$

$$\epsilon_3 = \epsilon_a - \epsilon_b - \epsilon_c - \epsilon_d$$

$$\epsilon_4 = \epsilon_a - \epsilon_b + \epsilon_c + \epsilon_d$$

FORCE EQUATIONS :

$$P = \frac{EA}{4} (\epsilon_1 + \epsilon_2 + \epsilon_3 + \epsilon_4)$$

$$M_x = \frac{EZ_x}{4} (\epsilon_1 + \epsilon_2 - \epsilon_3 - \epsilon_4)$$

$$M_y = \frac{EZ_y}{4} (-\epsilon_1 + \epsilon_2 + \epsilon_3 - \epsilon_4)$$

$$M_w = \frac{EZ_w}{4} (-\epsilon_1 + \epsilon_2 - \epsilon_3 + \epsilon_4)$$

Figure 4.10 : Determine of Force Components from measured Strain

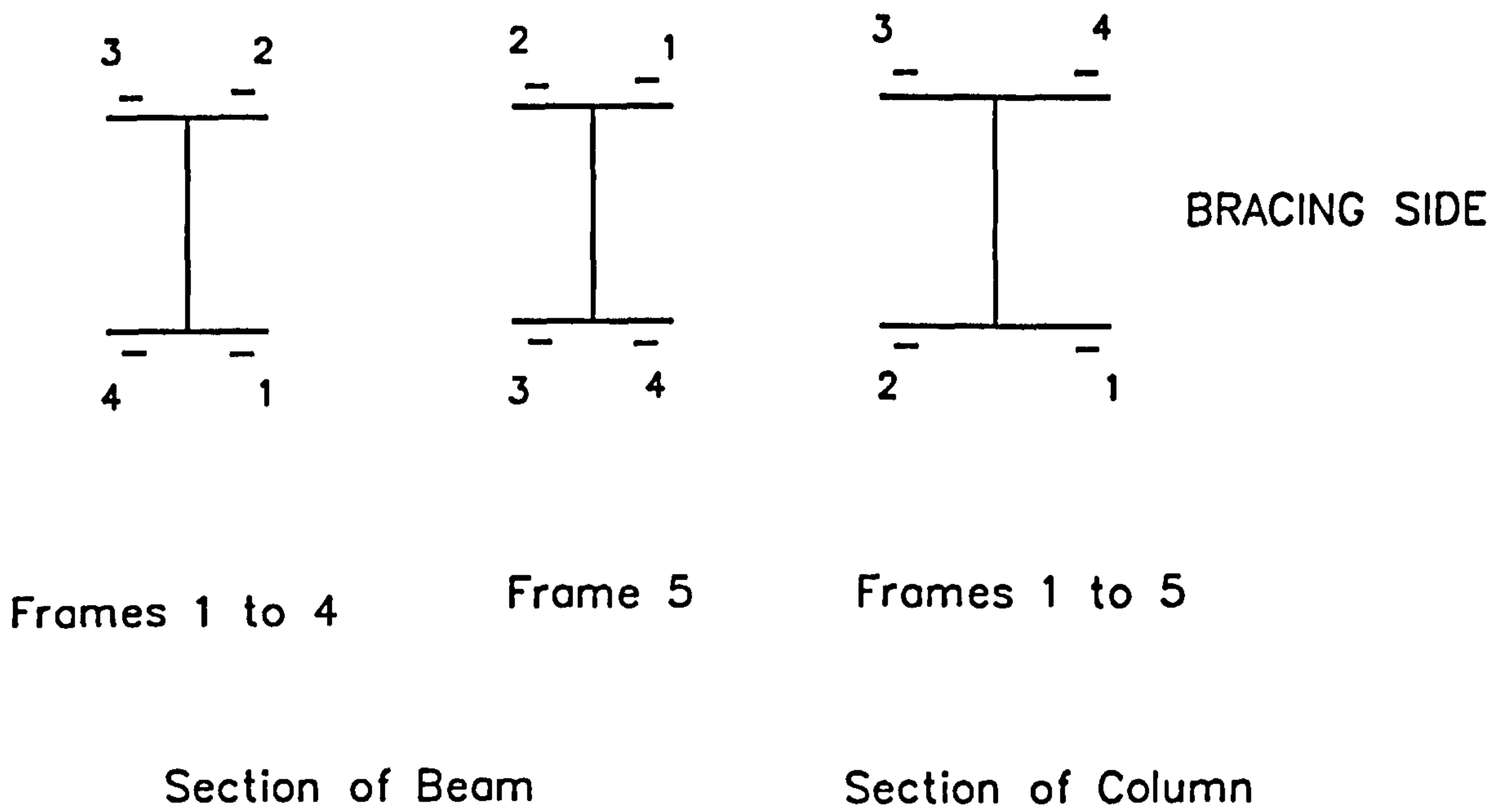


Figure 4.11 : Nomenclature of Strain Gauges in the Sections of Beam and Column

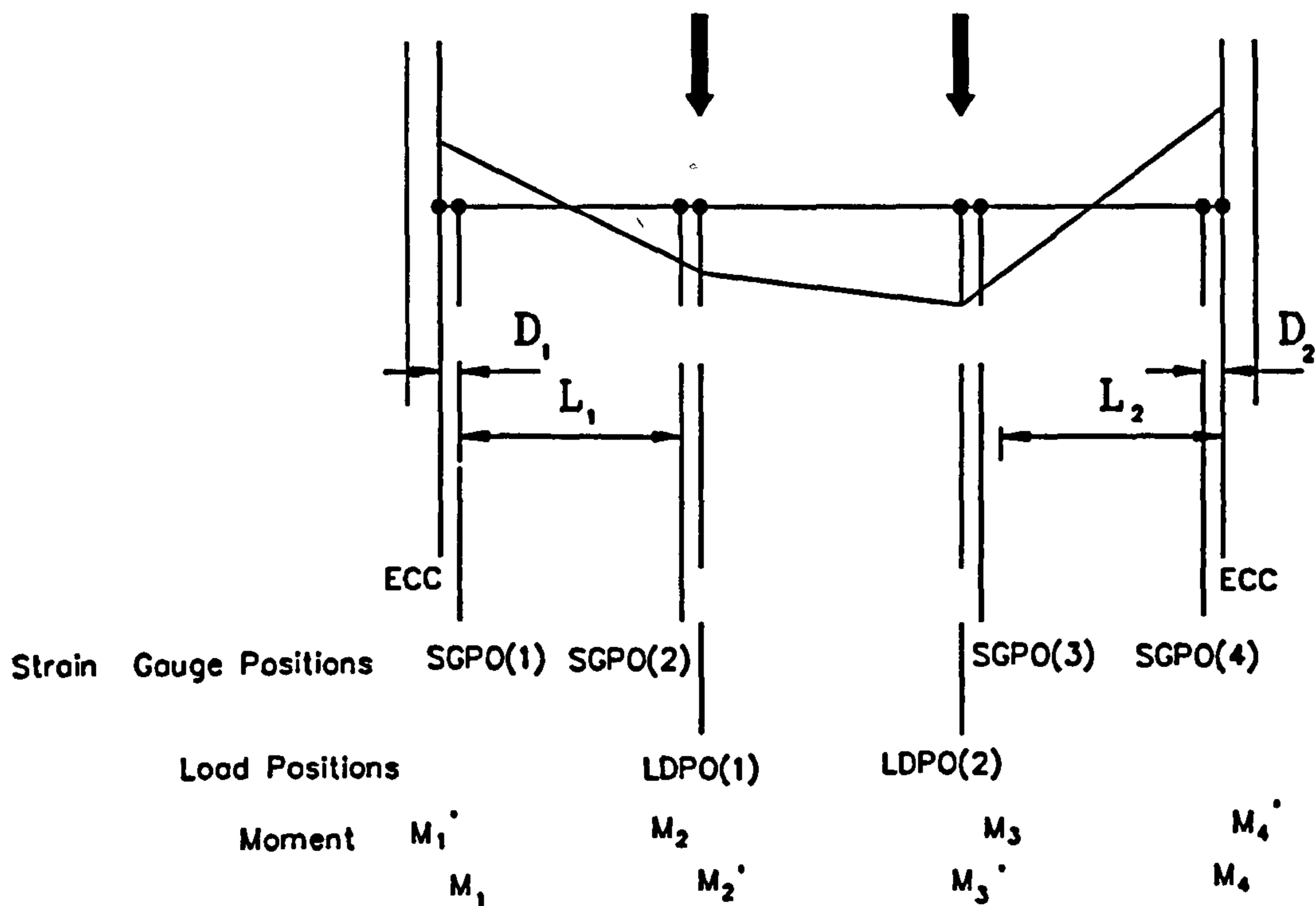
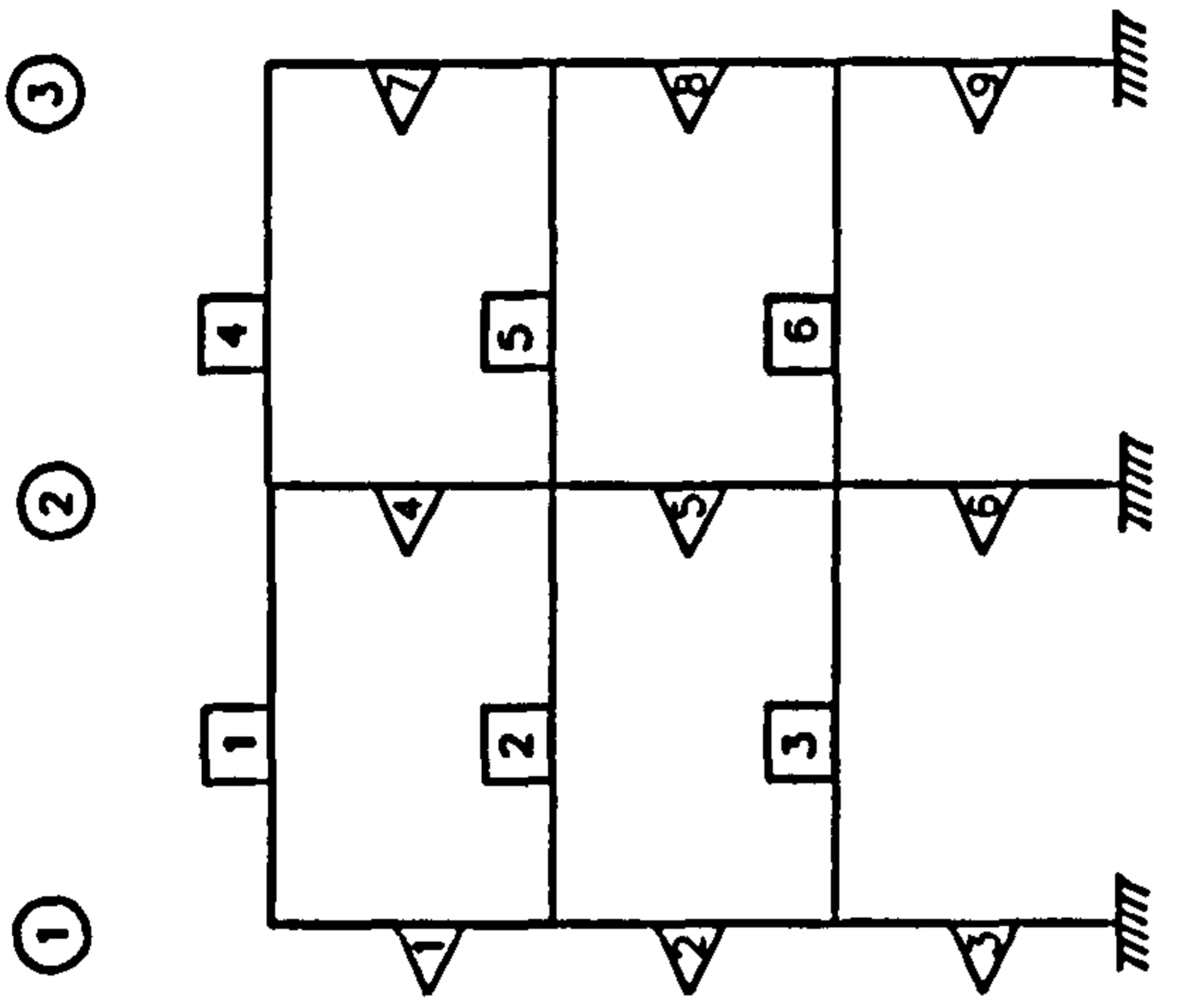
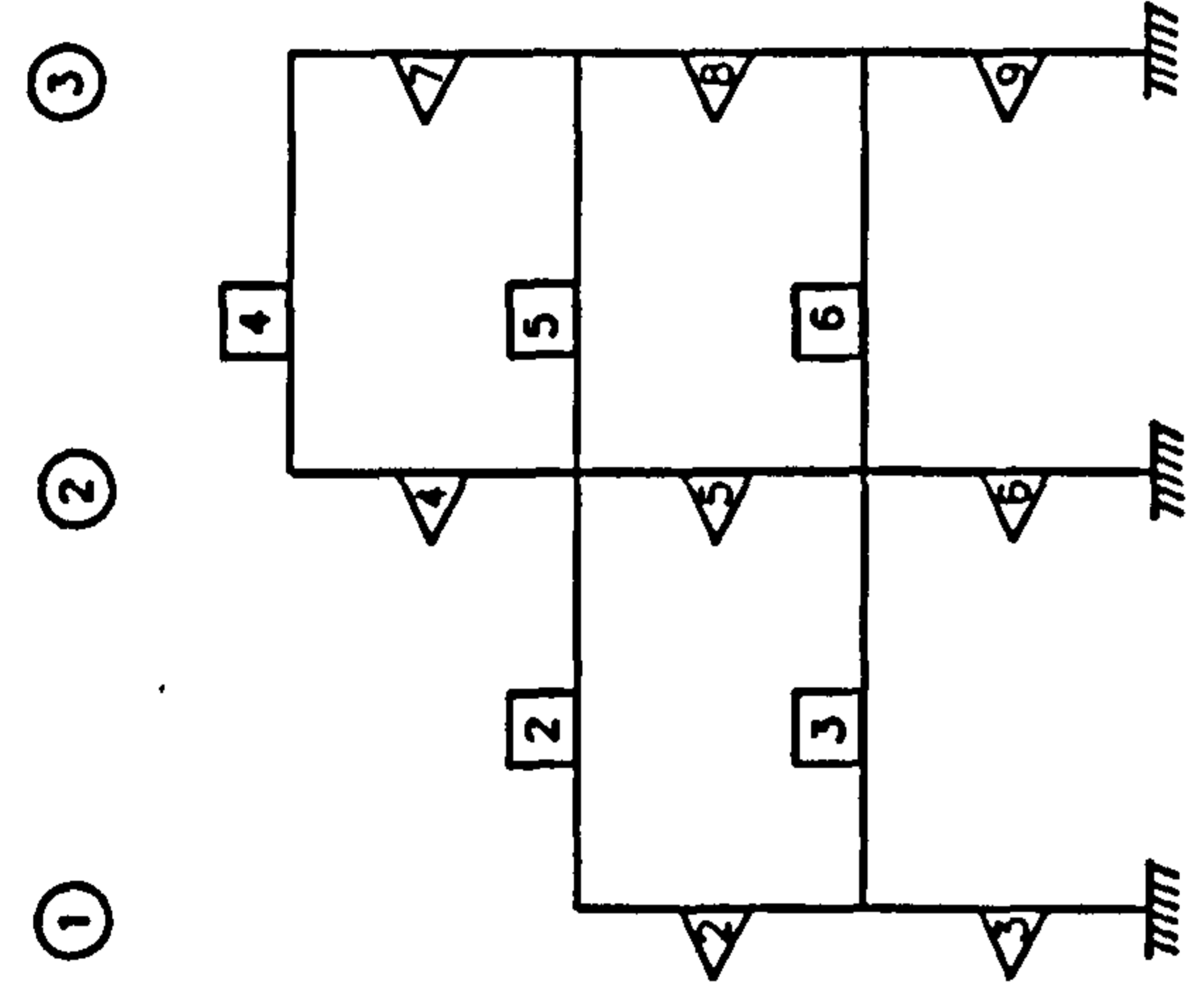


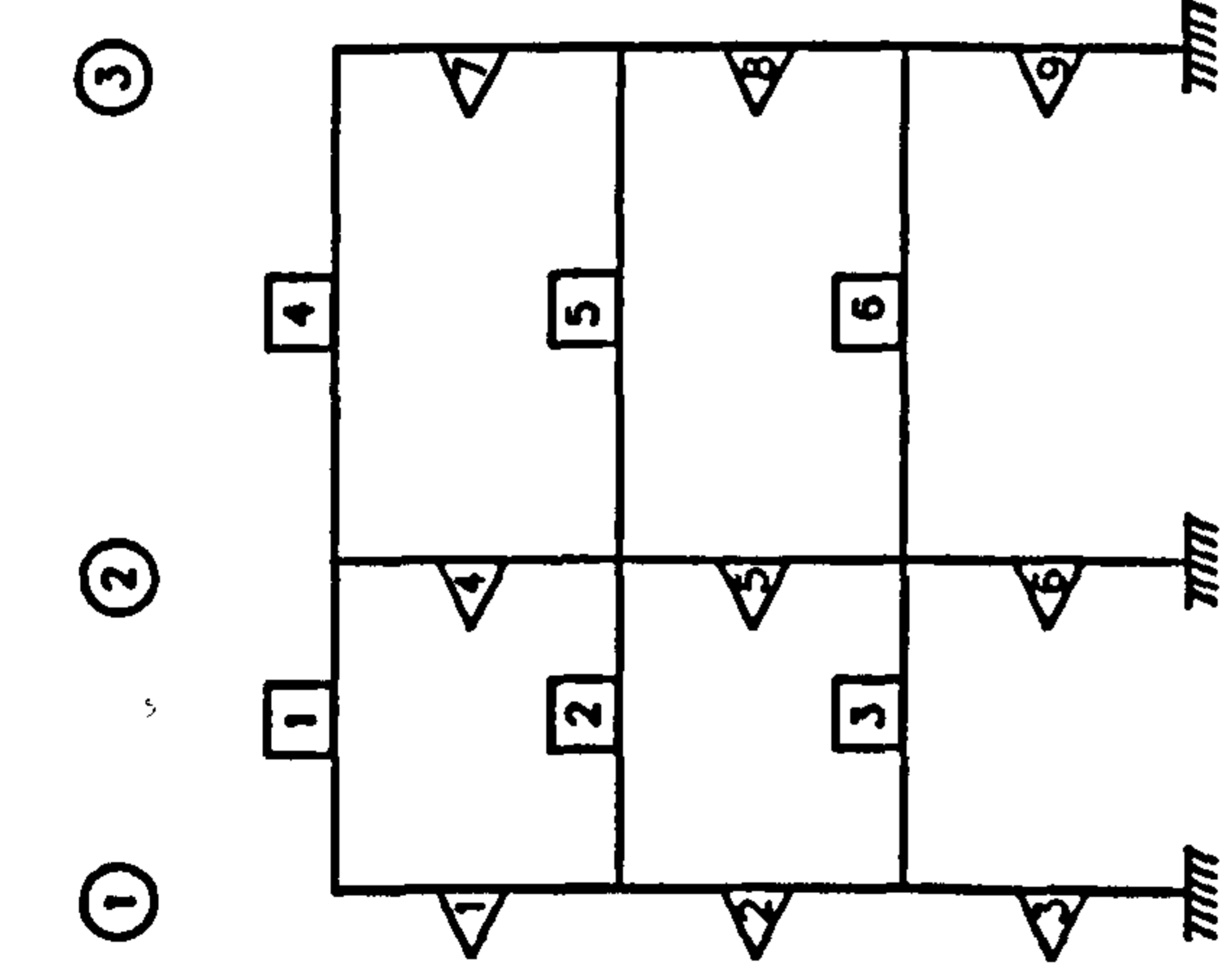
Figure 4.12 : Notation adopted for Beam Moment Calculation



Frames 1 and 2



Frame 3



Frames 4 and 5

- ③ Column Position
- 4 Beam Number
- 1 Column Number

(view from balcony)

Figure 4.13 : Nomenclature of Five Frames

## Chapter 5

# Behaviour of Two Asymmetrical Frames with End Plate Connection

### 5.1 Introduction

This chapter describes the test results from two full scale frames incorporating flush and extended end-plate beam-to-column connections designed and tested by the former Hatfield Polytechnic [5.1]. The first frame was used to investigate the overall behaviour of a structure, in particular the response of stiff connections and the influence of their flexibility on beam behaviour, whilst the second frame was used to make a comparison between two frames and investigate in greater depth any anomalies arising detected in the first frame [5.2,5.3,5.4,5.5]. In this chapter, the behaviour of the frame under different load combinations is discussed. Some relationships such as the moment distribution around the beams, the  $M-\phi$  response of the joints, the deflection of the beams and columns, the load-side-sway displacement between the frame and the relationship of the connection moment and the bolt forces are then selected for study. Finally, the tests to failure are analysed in detail.

### 5.2 Test Configuration

Frames 1 and 2, shown in Figure 5.1, were two storey structures of approximate overall dimension 10 m wide x 11 m high. Figure 5.2 shows the general arrangement of the frame and identifies the joint nomenclature. A suitable storey height for such a building was assessed to be 3.6 m. Unequal beam spans of 4 m and 6 m were selected as these values were

deemed sufficient to produce failure in the beams according to design calculations. Due to the discrete nature of the holding down system and the loading systems in the laboratory these exact span dimensions were not possible and they were thus adjusted to 3.810 m and 6.096 m. The advantage of using beams of two different lengths was the ability to design the beams with different end restraints. Thus the shorter span of beams were designed as flush end-plate connections (joints A to F) whilst the longer span of beams were designed with extended end-plate connections (joints G to L). The dimensions of the connections used are shown in Figure 5.3.

Two frames were constructed using 203 x 203 UC 71 sections for columns and 254 x 146 UB 43 sections for beams. All steel was nominally grade 43A throughout. The end-plates were attached to the ends of the beams with fillet welds - 12 mm in frame 1 and 20 mm in frame 2 - and to the columns with M20 grade 8.8 bolts in 22 mm diameter clearance holes. Different thicknesses of plates were adopted and Figure 5.3 also summaries the plate dimensions. The column base plates were assumed to be pinned in the analysis. This was simulated in the laboratory by using two bolts, positioned on the centre-lines of each column major axis, to hold down the base plate. All beams were framed into the column flanges. All columns were stiffened using conventional horizontal stiffeners positioned directly in line with the connected beam flanges. Stiffeners were used at the loading points in all beams in order to prevent web buckling due to applied loads (Figure 5.4).

Both frames were designed to represent the top three storeys of a much larger multi-storey office block and, as such, the top storey beams were considered to be the roof. The realistic design loads were determined using CP 3 [5.6] as follows, -

- 1. **Dead Load**
  - Floor and roof beams 21.2 kN/m
  - (150 mm slab, 50 mm finishes, ceiling and services)
  
- 2. **Live Load**
  - Floor beams (Offices general use) 10.0 kN/m
  - Roof beams (cleaning, repair and snow) 3.0 kN/m

In practice, the loads would be applied to the beams as uniformly distributed loads (u.d.l.), however in the laboratory it was more practical to use two points loads at the quarter and three-quarter points of the beam in this test. This configuration was chosen, because it represents the free moment diagram for a u.d.l. load in the mid-span of beam i.e.  $M = \frac{WL}{8}$  with reasonable accuracy.

No loads were applied directly to the columns in either frame test. Two frame tests were tested to failure in an in plane non-sway condition. Frame 1 used hand-tightened bolts throughout but, in the second test, both hand-tightened and pre-loaded bolt were adopted using the procedure outlined in the second progress report [5.2]. Two torques were established, 25 kNm for the hand-tightened bolts (frames 1 and 2) and 100 kNm for the pre-loaded bolts (frame 2), in order to compare the overall behaviour of frames under the different bolt forces.

Strain gauges were installed in the same positions on the beams of the two frames. However, different positions were used for the columns in frame 2. Little information on local areas of high or unusual strain distributions around the connections was obtained in the first frame although the overall distribution of the stress resultant was as expected. The strain distributions around the connections on the central column were studied in greater depth for the second frame and enabled a comparison with the first frame to be made. Unfortunately, due to the limitation of the logging system, it was only possible to equip five sections with twelve gauges; above and below joints D / I and F / K on the central column and below joint H. The latter location was specifically chosen because of anomalies arising in the first frame. Column web strains were measured by three 120° rosettes positioned at joint J as described by Prescott [5.1]. Thus column flange bending was studied above and below joints D and J. Gauges were positioned 25 mm from the tips of both sides of the flange, at sections 50 mm above and below the section of twelve gauges. The beam web strains were monitored at two sections in the web at joints D and I. Figure 5.5 illustrates the strain gauge positions for frame 2.

### 5.3 Test Set Up and Procedures

Each beam was loaded at its quarter and three-quarter points using the loading system as described in the first progress report [5.7]. A pattern of beam loads was applied in increments to a pre-determined value or up to failure for each test. Table 5.1 summarises the load levels applied to the beams up to their design values.

The main objective of the frame tests was to gain an understanding of the changing behaviour of the frames under the measured applied loads, the distribution of force and moment around the frames, the deflected shape of the structure and the  $M-\phi$  relationship of joints. Investigations undertaken on the isolated connection tests by Prescott [5.1] suggested that the strain gauges should be positioned about 100 mm away from the edge of the

end-plate in order to avoid measuring very high local stresses due to flange bending. Thus the gauges on the beam were positioned 100 mm away from the edge of the end-plate and the same distance away from the loading position on the side nearest the connection. The gauges at the column ends were also positioned 100 mm away from the top and bottom of the adjacent end-plate. Four gauges were located at each of these sections and positioned on the outer tips of the flange, 25 mm from the end. The strain gauge positions in two frames are illustrated in Figure 4.9. A detailed description is also given in chapter 4.

The rotation transducer readings were initialised to zero by using the data logger's initialisation procedure. The load cell reading was also set to zero by subtracting the initial value registered by the load cell in the Data Logger when the specimen was not loaded. The rotation devices were sensitive to ambient vibration and therefore needed damping to minimise such effects while readings were being taken.

Each beam could be loaded independently to give any desired pattern of beam loads. After specifying the required increments, all beams loads were applied simultaneously. The loads were then checked against measurements from the independent load-cells in each cable. The logger was then scanned to confirm that the loads applied were satisfactory. It was possible to scan one or more of the individual channels. A hard copy of the raw data was then printed out but could only be viewed on the VDU in tabular form due to the format used. The data logging and storage system are described in chapter 4.

## **5.4 Main Features of Frames 1 and 2**

### **5.4.1 Test Programme for Frames 1 and 2**

A total of 30 tests were conducted on frame 1 and 43 on frame 2. Tables 5.2 and 5.3 give a simple description of each individual test. The tests of two frames can be divided into 4 stages.

#### **1. Stage 1 : Preliminary Testing**

Tests in both sway and non-sway modes on frame 1. The different patterns of low loads were applied in order that the instrumentation and equilibrium could be carefully checked.

#### **2. Stage 2 : Working Load Tests**

Tests were conducted with and without sway bracing. Dead load and dead load plus imposed load were applied to the beams in different patterns.



### **3. Stage 3 : Design Load Tests**

Tests in the sway and non-sway modes. Full design load was applied to the beams.

### **4. Stage 4 : Tests to Failure**

Loads were applied to the beams to cause the failure of the frame - all tests conducted in a non-sway mode.

## **5.4.2 Tightening Procedure in Connections**

Ungauged bolts were used when the frame was erected. At each connection two un-gauged bolts were then removed and replaced by strain gauged bolts. This method was used to protect the strain gauged bolts from damage during the erection of frame. This presented an ideal opportunity to investigate how the pre-loading of one bolt affects the pre-load in all other bolts in this frame. The bolt replacement procedure started at the centre column, first floor and proceeded to the two external columns. This procedure was then repeated at the middle and upper levels. At each connection, all bolts were loosely in position and then a standard sequence of bolt tightening was employed. Initially the centre bolt on one side of the web was torqued to the required tension, 25 kNm for hand-tight bolts and 100 kNm for pre-loaded bolts. Then the bolts above and below were tightened to their correct values. Reading of the pre-load in all of the bolts was checked after tightening each bolt. This procedure was repeated until the pre-load was within  $\pm 20\%$  of the required values in these three bolts. An identical procedure was adopted for the bolts on the opposite side. When all of the bolt forces satisfied the requirement, the next connection was tightened. The effect of changing the force in a particular bolt was minimal on other bolts positioned either across the width of the end-plate or in another connection. However, this was not true for those bolts directly above or below the one being tightened. Prescott [5.1] concluded that their preload either decreased or increased significantly dependent upon whether the adjacent bolt was tightened or slackened respectively. Figure 5.6 shows the tightening procedure adopted for each connection.

## **5.4.3 Observations during Tests**

References [5.1,5.8] record that, prior to the tests, some lack-of-fit in connections was observed in a number of joints in different tests although other joints showed good fit up. Generally, lack-of-fits does not appear to cause problems to a building in practice [5.9]. In this section, some type of lack-of-fit in connections are discussed - a detailed record of the

type of lack-of-fit observed in the connections in different tests is presented in a BRE report [5.8] and Prescott's thesis [5.1]. Figure 5.7 illustrates the notations adopted for the bolt position and different bolt rows in both flush end-plate and extended end-plate connections. Based on the reference [5.1], the lack-of-fit in connections were not recorded systematically in Frame 1. In frame 2, seven types of connection lack-of-fit were encountered, these are as follows:-

1. For flush end-plates, a bow was found in the end-plate between the beam tension flange and the middle bolt row. The maximum gap was found at the level of the top row of bolts (Figure 5.8).
2. For extended end-plates, a bow was found between these two rows within the beam depth. The maximum gap was found between these two rows of bolts (Figure 5.9).
3. For flush end-plates, a gap existed at the top of the end-plate extending downwards to the top row of bolts. The maximum gap was found at the top of the flush end-plate (Figure 5.10).
4. A gap existed at the top of the end-plate and extended downward to the middle row of bolt, i.e.  $T_2$  row for the flush end-plate and  $T_1$  row for the extended end-plate. The maximum gap was found at the top of the end-plate (Figure 5.11).
5. A gap existed in the top of the end-plate and extended downward to the bottom of the bolt rows. The maximum gap was found at the top of the end-plate (Figure 5.12).
6. A gap was found from the beam tension flange and extended to the bottom of the end-plate. The maximum gap was found at the bottom of the end-plate (Figure 5.13).
7. A gap was found from the lowest row of bolt and extended to the bottom of the end-plate. The maximum gap was found at the bottom of the end-plate (Figure 5.14).

Although the phenomenon of lack-of-fit in connections has been recorded by others, a general discussion based on reference [5.1] is outlined here. The first and second types of lack-of-fit in connections for typical end-plate distortion were due to welding of the joints. For the isolated tests done conducted by Prescott [5.1], it was found that the bows in the end-plate of the frame tests were relatively common in the majority of connection tests

conducted in isolation. The distortion was found to be larger in the thinner end-plates but required a smaller increase in bolt force to produce a better fit up of the connection. An increase in bolt pre-load eliminated the distortion in all of those connections where it was originally present under the lower tension. Fortunately, these two types of lack-of-fit had no significant effect on the behaviour of the connections.

Lack-of-fit problems type 3, 4 and 5 were due to poor fit up within the frame itself as opposed to local connection deformations. The distortion remained visible in some of the connection tests under medium to high levels of moment and was very dependent on the thickness of the end-plate. The distortion reduced by increasing bolt pre-load. The bolt force increased immediately after the first loading increment was applied, resulting in high bolt force. These differences between the bolt force should be equal to the additional bolt force required to close the gap in the initial lack of fit [5.1].

The last two types of lack-of-fit in connections were less straightforward, affected the overall behaviour of structure and influenced the distribution of moment within the frame. With increasing applied beam load, the gap at the bottom of the end plate closed until eventually the end plate made contact with the column flange. Thus initially the stiffness of the connection was lower than anticipated but this stiffness increased dramatically as the gap was closed and the behaviour of connection reverted back to normal. Detail records and analysis of the lack-of-fit in the connections in different tests was presented and discussed by Prescott [5.1], thus no further analysis was carried out by the author.

## **5.5 Behaviour of Frame under Different Load Combinations**

In the design of a steel frame, the ultimate capacity (axial load and moment) of the members and the deflections at key locations are the principal factors to be considered. Deflections are usually required at serviceability conditions due to unfactored imposed loads and are usually derived from elastic bending theory assuming either pin-ended beams in simple construction or fully rigid connections in continuous constructions. Although some computer programs can accurately predict response with real semi-rigid joints, it is not easy for designers to accept the results without verification.

This section investigated the affect of the frame response due to different load combinations. Two series of tests are included the pre-loaded and hand-tightened bolts in connections. Each series contained two parts, loading of all six beams followed by loading

of each beam individually, to examine the behaviour of the frame under different load combinations. Table 5.4 shows the load and the mid-span deflection of beams under different load combinations in two series of the tests. It is noted that a significant larger mid-span deflection are determined in the tests when load applied separately. This is due to larger restraint provided by the adjacent beam under load in each beam when it was compared with the results under beam loaded separately. Thus smaller mid-span deflections were observed. As a result, it provides an evidence the mid-span beam deflections obtained in the tests under load separately should be considered for the beam deformation check in the serviceability limit state.

It is of interest to compare the mid-span deflection in the tests under beam load individually to the predictions from a simply supported beam to indicated benefits of the semi-rigid design. The predictions of 4.7 mm is obtained for the shorter span beam and 31 mm for the long span beam. The deflections recorded the tests are significantly less than the prediction from a simple supported beam. A minimum reduction of 45 % deflection was determined and thus the economics is still possible using this pattern of load for design.

Table 5.5 shows the moment distribution around the frame under different load combinations in the two series of tests. For the first series of tests, more moment was attracted to the connections, thus reducing the moment at the two loading points on each beam, in test 10 when compared with the connection moment in tests 14 to 19. The same phenomenon was observed in the second series of tests. Due to the larger restraint provided by the adjacent beam in tests 10 and 32, more moment was thus attracted to the beam ends near connections.

At the load level corresponding to the dead load for the beam, the free moment is determined as 38.6 kNm in the shorter beams (beams 1 to 3) and 99 kNm in the longer beams (beams 4 to 6). In the tests, moments were attracted to connections, leading to reduced mid-span moments due to the stiffness of the end-plate. The results from the tests which load applied to each beam individually, shown in Table 5.5 indicate that beam ends with flush end-plate connection reduce by 30 % of free mid-span moment and 34 % for the extended end-plate connected beams.

## **5.6 Discussion of Frame Test Results**

Selected test results will now be discussed in terms of different parameters. Firstly, tests are selected according to the different test conditions (sway or non-sway and hand-tightened or pre-loaded bolts used in connections) and the pattern or level of the applied beam loads. Secondly, one test result is taken as a reference and is discussed and compared with the other selected tests. Finally, the results are compared with the values obtained from analyses using a elastic rigid frame computer program which was developed in the University of Sheffield to determine two extreme cases of joint response, i.e. assuming the connection to be fully rigid or pinned. The results assuming the fully rigid connections are determined from a two dimensional rigid jointed frame but with pinned bases for the lower columns whilst the pinned connection responses are calculated from individual single beams with simply supported end conditions.

### **5.6.1 Parameters and Tests selected for Study**

The moment distribution around the beams is the first characteristic selected for study. Test 3 of frame 2 corresponds to a non-sway frame using hand-tightened bolts in the connections under dead, dead plus imposed and also with additional load on each beams. Test 11 of frame 2 corresponds to a sway frame using hand-tightened bolts in the connections under dead plus imposed loads on each beam: Tests 40 and 41 correspond to a frame with sway and non-sway modes using pre-loaded bolts in the connections under design loads on each beam.

To examine the importance of the actual moment-rotation response of the joints, the results obtained in tests 23 and 28 of frame 1, tests 31 and 40 of frame 2, corresponding to different test conditions, are selected. Thus the moment rotation curves under sway and non-sway conditions using hand-tightened and pre-loaded bolts in connections can be compared to each other. The stiffnesses of the connections at the initial, maximum and unloading stages are determined for each test.

In practice, the deflection of beams is an important factor to be considered by designers and a set of typical beam deflection results are discussed. Four tests, tests 3, 11, 31 and 40 in frame 2, have been chosen for study.

The aim of the tests to failure for this frame was to investigate the behaviour of beams close to the critical load condition. When designing the frame, a heavy column section was thus selected when compared with the size of beam and stiffness of connection used. To

prove this point, test 28 of frame 1 which corresponds to a non-sway frame under very high load (greater than the design load) in each beam, is used to show that the central deflection of each column segment was very much small.

Sway displacements of joints H, J and L (at the upper, middle and lower joints at the edge of column in the longer span side) are also discussed. It is interesting to investigate the effect of pre-loaded and hand tightened bolts adopted in the connections on the side displacement of the frame. Tests 11, 21 and 40 of frame 2 are selected for study.

The distribution of bolt forces in the connections with the change of the connections moment are of interest and the general behaviour of bolt forces in different connections under varying moments are discussed. As different thicknesses of end-plate are used in the two frames, joints A, C, E, G, I and J are thus selected to represent each different thickness of end-plate in test 28 of frame 1 and test 40 of frame 2. Details of the tests selected for study are presented in Table 5.6.

## 5.6.2 Moment on Beams

Table 5.7 presents the end and span moments for the tests and the results from the rigid frame analysis. Larger moments were attracted to the extended end-plate due to the stiffer connection adopted and larger moment levels were associated with longer beams. The internal joints attracted more moment than the external joints due to the internal joint being restrained by the adjacent beams on both sides. As expected, at a given load level, the connection moment from the rigid frame analysis was greater than that in the test due to the semi-rigid nature of the real connections.

In tests 3 and 11 which incorporated hand-tightened bolts in connections with non-sway and sway conditions, it is noted in Table 5.7 that, whilst there is same variation for individual beam on average, there is no significant difference in the beam moments between these two tests. The flush end-plate connections attracted about 64 % rigid moment whilst the extended end-plate connections attracted about 82 % . Comparing the results in tests 40 and 41, it is again found that there is no significant difference for the connection moments existing between the two tests and this confirms that the stiffness of the extended end-plate was larger than the flush end-plate. The extended end-plate connection attracted very high moments. Examining the results show that the internal and external connections attracted moment in a similar ratio to that in the rigid frame. The results also show in Table 5.7

that greater moments were attracted to left hand side joints in test 40 due to sway of the asymmetrical frame.

A comparison of tests 11 and 40, which represent a sway frame with hand-tightened and pre-loaded bolts in the connections, under dead plus imposed loads in each beam is next considered. Results from both tests show that higher moments were sustained near the extended end-plate connections of beams 4, 5 and 6 with a resulting reduction in moment in the span of the beams.

### **5.6.3 Moment Rotation Behaviour of Joints**

The behaviour of a beam-to-column connection is dependent on a number of different parameters including the type of connection, the grade of steel, the size of beam and column and the axis of bending. The behaviour of the connection is best illustrated by the relationship between the moment transmitted by the connection at all levels of load. Two types of connections, flush end-plate and extended end-plate, were used in two frames as follows :-

#### **1. Flush End-Plate Connection**

The flush end-plate used in the short span of beams is currently the most popular type of connection in the U.K., principally because of relatively straightforward fabrication and erection, although convenience in containing the joint within the beam depth is also a factor. This connection is normally used simply as a shear joint and no advantage is normally taken of its inherent stiffness.

#### **2. Extended End-Plate Connection**

The extended end-plate connection with a row of tension bolts outside the beam flange has greater moment capacity than a flush end-plate due to the increased lever arm of the resultant tensile force. Despite the disadvantage of the connection projecting above the top flange of the beam, the extended end-plate is very popular when connections are required to transfer beam moments into columns.

Both flush end-plate and extended end-plate connections have significant stiffness, particularly the latter which has a very high value. Also in this test the strength of the extended end-plate connection exceeds that of the attached beam and thus it may be considered as providing a realistic upper bound of practical connections associated with a semi-rigid design approach.

Figures 5.15 to 5.22 presents the selected moment-rotation curves for tests 23 and 28 of frame 1, tests 31 and 40 of frame 2. The four selected tests are based on different conditions; non-sway and sway with hand-tightened and pre-loaded bolts in the connections. As some instrumentation faults occurred during the test not all parameters have been determined for all joints. A number of key parameters, the maximum moment sustained, the corresponding rotation, initial stiffness ( $C_i$ ), the maximum stiffness in the loading stage ( $C_m$ ) and the unloading stiffness ( $C_u$ ) for each joint are presented in Tables 5.8 and 5.9. Figure 5.23 shows a typical  $M-\phi$  curve response of semi-rigid connection.

Generally, the initial stiffness is often regarded as being the maximum stiffness in the loading stage. Due to the lack of fit observed in some of the joints in the tests, non-linear relationships were observed for some of the joints even in the 'elastic' regions. Thus after an initial stiffness at the commencement of loading, these joints stiffened giving a higher value for ( $C_m$ ). Where pre-loaded bolts were used in the connections, the problem of lack-of-fit in the joints was largely overcome and the maximum stiffness was thus obtained in the initial stage. Frequently, the unloading stiffness is regarded as being similar to the initial stiffness [5.9,5.10,5.11] and here the maximum stiffness is also compared with the unloading stiffness for the particular cases studied. From the results the following observations are made.

First comparing the loading and unloading stiffnesses of the external joint for the flush end-plate connections in tests 23 and 28 of frame 1 (Table 5.8), surprisingly both stiffnesses reduce as the thickness of the plate increases. Conversely, both stiffnesses increases with the increases of the plate thickness in the internal joint for the external end-plate connection. Due to the irregular moment rotation responses obtained for some joints, no comparison can be made for the external joint for the extended plate connections and the internal joint for the flush end-plate connections. The maximum stiffness was found at the some point but not the initial stage of the loading path of the  $M-\phi$  curves in connections (see Figures 5.15 to 5.18).

Turning to compare the loading and unloading stiffnesses of the external joint for the flush end-plate connections in tests 31 and 40 of frame 2 (Table 5.9), their maximum stiffness was presented in the lowest joint E (15 mm thickness of plate). The stiffness of connections were observed significant effect for the thickness of plates. As discussed before, both stiffnesses reduced with increase of the plate thickness in the external joint of the extended end-plate connection. Generally, similar initial stiffness were determined in two tests in non-sway and sway conditions. The maximum stiffness was found in the initial stage of the



$M-\phi$  curves for the pre-loaded bolt adopted in connections. Non-linear curves existed at joint C in both tests, and at joint L in test 40, perhaps due to the lack-of-fit in the connections (Figures 5.19 to 5.22). It is difficult to determine the unloading stiffness in most of the joints due to the variation of the unloading curves. Generally, reduced unloading stiffness was determined for joints when compared with the maximum or initial stiffnesses in the test.

#### 5.6.4 Beam Deflections

Steel frames have usually been designed on the basis that beam-to-column connections are either pinned or rigid. The actual stiffness thought will fall somewhere between these extremes, giving what is generally termed 'semi-rigid' behaviour. Due to the semi-rigid action, the mid-span deflection of beams are always less than the predictions from a simply supported beam. This section highlights the feature from the test results.

Deflections computed using two extreme cases, a rigid frame and a simply supported beam are compared with the test results in Table 5.10 together with the ratio of the test result to the rigid frame deflection and the simply supported deflection to the test value. When the deflection in the tests was compared with the deflection predicted from the rigid frame, the ratios were determined in a range of 1.00 to 1.54 in the short span beams and 1.08 to 1.45 in the long span beams. (The ratio in beam 1 determined lesser than 1 suggest a small degree of experimental error.) Turning to compared the ratio of the predictions from the simply supported beams to the test results, a range of 2.35 to 4.38 for the short span beams and 2.22 to 3.70 for the long span beams were calculated. There was no significant difference of the results between the short and long spans conditions. This results clearly show that the actual deflections, lie between the two extreme cases but are noticeably much closer to the rigid case than the simply supported case.

The effect of sway on beam deflections was studied by comparing tests 31 and 40 (see Table 5.10), it was found no significant different. It is interesting to investigate the effect of beam deflection due to adopt the pre-loaded bolts in connections, tests 11 and 40 were thus selected. When the longer span is considered, an average reduction of 24 % is determined for the top beam (beam 4) and 10 % for the lower storeys (beams 5 and 6). Same phenomenon is observed in the short span beams. Thus it suggests that the preload is more effective at reducing deflections for the thinner, more flexible end-plate connections.

### **5.6.5 Column Deflection**

Table 5.11 shows the maximum deflection at the mid-height of columns in Test 28 of frame 1 which was in a non-sway mode under high beam loads. The deflections can be seen to be very small - all were recorded as below 2.1 mm which is well below the generally accepted initial lack of straightness value of  $L/1000$  which is 3.6 mm. This is not surprising as the columns were intended to provide high restraint to the connections and were not subjected to axial loads and the magnitude of the deflections which occurred indicated that this requirement was attained.

### **5.6.6 Sway Displacement**

To investigate the effect of side displacement of the frame between the cases with hand-tightened and pre-loaded bolts in connections, three tests were selected based on different conditions. Test 11 of frame 2 was the frame tested in sway mode, hand-tightened bolts in connections under their dead plus imposed loads to each beam; test 21 of frame 2 was under the same test conditions with pre-loaded bolts in the connections; Test 40 of frame 2 which corresponds to a sway frame with pre-loaded connection bolts and loaded to its design load. Table 5.12 presents the results. Comparison of tests 11 and 21 shows a larger side displacement was observed in the top storey (joint H) in test 11 due to reduced stiffness provided by the hand-tightened bolts in connections. Larger applied beam loads are required to produce a similar side sway in the top storey for the frame with pre-loaded bolts in the connections as evident by comparison of the results of tests 11 and 40. Thus the pre-loaded bolts used in connections reduced the side displacement in the top storey of the frame.

### **5.6.7 Connection Moment and Bolt Forces**

Figures 5.24 to 5.35 present the resulting moment bolt force plots for each bolt of the connections in test 28 of frame 1 and test 40 of frame 2. All of these forces are zeroed at the start of the tests i.e. any pre-load is discounted. Thus an apparent compression of bolts in these figures could actually be a reduction in pre-load in connections. Joints A, C and E which have three different thicknesses of flush end-plates and Joints G, I and J which use the three different thicknesses of extended end-plates are selected for analysis. Figure 5.7 presents the bolt nomenclature for the connections in the two frames. Table 5.13 gives the maximum recorded bolt forces in the tests.

From Table 5.13, most of the tension force was sustained in the first row  $T_1$ . Very small compression forces were observed in connections A and C in test 28 of frame 1 and connection C of test 40 of frame 2 at the middle and lower rows on the balcony side (Bolt nos. 3 and 5). Most of the bolts are under tension when the maximum moment was applied to the connections. The results show that the upper row of bolts in the flush end-plate sustained most of the tension force, with the middle row sustaining a reduced tension force or even a compression force depending on the location. The lowest row  $T_3$  sustained a lowest tension force or even compression force. In fact, the thickest plates attract more bending in the plate within the depth of beam (see Table 5.13) and the bolts are comparatively stiffer and hence carry higher force. This was again supported by the higher force sustained in the connection C than the connection A in two tests. Comparison with the results for frames 1 and 2, the difference can be explained by the fact that test 40 of frame 2 used the pre-loaded bolts in connections and was tested in sway conditions .

The experimental results of Prescott [5.1] showed that the middle row of the extended end-plate connections was used to sustain most of the tension force under applied beam load. This is evident from the results shown in Table 5.13 in which bolts in row  $T_1$  and  $T_2$  were subjected to the highest tension force.  $T_2$  was observed to be under very similar but slightly less tension than  $T_1$  in connections G and J. As the flush end-plate described in the previous paragraph, the lowest row  $T_3$  was used to sustain any compression force. In connection I, larger tension forces were observed in  $T_2$ . Rows  $T_1$  and  $T_2$  are subjected to a larger bolt force when they were compared with the bolts force in the same rows of connection J. Due to the larger restraining forces provided by the adjacent beam in internal column, the bending of the connection was different. The larger bolt force in the upper row of connection I was thought due to increased bending in the top of the plate. Again, a higher force was sustained in row  $T_1$  of the connection I (25 mm in thickness of plate) than in the connection G (20 mm) due to the higher moment attracted to connection with the thicker plate.

## 5.7 Tests to Failure in Frame 1

### 5.7.1 Test Observations

To analyse the behaviour of the frame up to failure of the beams, three tests were conducted under applied beam load only. After taking the initial readings, loads were applied to all beams in small increments, and a scan was taken after each load step. The loading

histories of these tests are illustrated in Tables 5.14 to 5.16. In test 28, all the beams were loaded up to their design load and additional loads were then applied. At scan 32, the test was terminated although no failure had occurred but the maximum safe working capacity of the loading system was reached. The frame was then unloaded.

As the frame had not been failed in test 28, test 29 was then conducted with the loads moved from the quarter and three-quarter points to the third and two-third points in beams 5 and 6 in order that the failure load could be reduced as the beam loads were applied closer to the mid-span causing a more severe loading arrangement, thus reducing the total failure load of these beams. The change of the loading positions was performed only on the longer span beams. There were lower moment levels associated with the shorter spans with the flush end-plate connections. Therefore failure was attained only in the longer span beams with the extended end-plate connections. At scan 20 and at a recorded beam load of 259 kN, beam 5 failed without warning. The failure was due to weld fracture in the region of connections I and J. Loading of beam 5 was then reduced to a safe limit of about 180 kN (below dead plus imposed loads) and the test was continued with an increase of loads to the other beams. At scan 25 and a recorded beam load of 297 kN, beam 6 failed without warning. A similar failure mode, a weld fracture in the region of connections K and L was observed. The applied load on beam 6 was then reduced to a safe limit of about 170 kN (below dead plus imposed loads) and loading was continued on beams 1, 2, 3 and 4 using the increments shown in Table 5.15. At scan 35, an error was observed in the reading of the load cell on one of the loading cables of beam 1, as it showed a large negative reading. Thus, no further readings of applied load in this beam were obtained. Fortunately, it had no great effect on the usefulness of this test. At scan 38, none of the other beams showed any sign of failure and it was thus decided to terminate the test. All beams were then unloaded.

The unexpected mode of failure was due to the lack of adequate leg length of the weld in connections K and L (12 mm). An increase in the leg length of these welds to 20 mm was then adopted for the next frame in order to investigate the behaviour of beam failure.

The revised residual strength of the frame was determined in test 30. To reduce the applied load required to cause failure from the experience of the previous tests, the loads position were again moved from the quarter and three-quarter points to the third and two-third points in beams of the shorter spans (beams 1 to 3). Beams 1 to 3 were loaded to their design load plus a further seventeen increments beyond this condition. An additional load was then applied to beam 4 in order to induce additional moments into the shorter span's

side connections. An error in the applied beam load on beam 1 was found in test 30 due to a problem with one loading cable. In this test, a large value of recorded applied beam load observed on beam 1 which was due to the effect noted in the previous test. Thus it gave a larger value of reading, approximately 150 kN more than the actual value at the maximum applied load. Fortunately, it did not greatly influence the other results. After an additional load of 66 kN was applied to beam 4 in one increment in scan 29, it was apparent that this frame had a considerable reserve of strength in the short span beams and the failure load was above the capacity of the loading system. The target load of this test was reached and the frame was then unloaded.

### 5.7.2 Bending Moment Distribution around the Frame

To investigate the influence of semi-rigid action of the connections, the distribution of the bending moment around the frame is discussed. Figures 5.36 to 5.38 show the distribution of bending moments in these three tests. In test 28, the moments at four levels of loads are plotted on the same figure in order to compare the distribution of the frame moment under different loading arrangements; scan number 10 which corresponds to dead load, run number 16 which corresponds to dead load plus imposed load, run number 23 which corresponds to design load and run number 32, at which the maximum load was applied as shown in Figure 5.36. The corresponding load levels i.e. dead load, dead plus imposed loads and design load were selected for Test 29 as illustrated in Figure 5.37 with the addition of the runs at the failures of beams 5 and 6 and used to plot the distribution of frame moment diagrams. In test 30, the distributions of frame moments were plotted at runs 28 and 29 which correspond to very high loads applied in beams 1, 2 and 3 and an additional load applied to beam 4 as shown in Figure 5.38.

It is observed in Figure 5.36 that the net moments attracted by the connections were transferred into columns. The apparent out-of-balance at the beam-column intersection is due to the additional moment induced at the column centreline by the eccentricity of the beam end reaction. In Figure 5.37, the same form of moment distribution was observed around the frame up to the failure which occurred in beams 5 and 6 in Test 29. After failure of beam 5, no moment was sustained in Joint J due to the loss of the stiffness of connection after the failure of the weld in the connection. However, some moment was recorded at joint I due to either the restraint of the adjacent beam and column or an incomplete failure of this connection. As a result, more moment was transferred to the mid-span of this beam.

In test 30, the most interesting feature is the effect of moment distribution after additional load was applied to beam 4 (see Figure 5.38). It can be seen that larger moments were attracted to the connections at the ends of the shorter span due to the higher applied beam loads. Due to the beam load being applied at one side of the frame (beams 1, 2 and 3), the disturbing moments  $M_{b1}$ ,  $M_{b2}$  and  $M_{b3}$  which occurred at the internal column of the beam-to-column intersection were of the same sign (anti-clockwise). They were of the opposite sign to the moments in these three columns when compared with the previous tests. In tests 28 and 29, more loads were applied to the longer spans and thus a clockwise disturbing moment occurred in each internal column connection. After additional load was applied to beam 4, a clockwise disturbing moment  $M_{b4}$  occurred at the top of column 4. It has a slight effect on the connection moment in the beam at the other side of the column (Joint B). However, it decreased the moment at the column head. The plot of the major axis moment at the central columns illustrates the phenomenon of the disturbing moment in column 4 after the additional load was applied to beam 4 as presented in Figure 5.39.

### 5.7.3 Deflected Shape of the Frame

Figures 5.40 to 5.42 show the deflected shapes of the frame at various stages during these tests. For each test, the deflections at the various levels of load are plotted on the same diagram corresponding to the loading scans as described in previous section. Thus the changes of frame deflection under the different stages of applied loading can be observed.

In Figure 5.41, the same deflected shape was recorded in test 29 (Figure 5.40) as was found in test 28 up to the failure which occurred in beams 5 and 6. After failure of beam 5, an apparent upwards deflection was recorded in this beam due to an error in the transducer reading. The bending moment distribution around the frame shown in Figure 5.37 provides further evidence of this error since there is no change of sign in the moments at connections I and J after failure occurred in this beam. Comparison with the deflections of the frame in test 28 up to the failure which occurred in beams 5 and 6 shows that larger deflections were recorded in beams 5 and 6 although less load was applied to these two beams due to the loading positions being at the more severe positions (third and two-third points rather than the quarter and three quarter locations). The column rotations at J increased after the failure of beam 5 due to the loss of stiffness of this joint.

In Figure 5.42, significant deflections were recorded in the shorter beams only due to the application of loads to these beams only. Very small deflections were recorded in all

columns and the longer beams (except for scan 29 at which point a single increment of load was applied to beam 4) which caused a further moment (clockwise) to occur in the head of the central column 4. This not only decreased the column head moment but also decreased the central deflection of column 4.

#### 5.7.4 Load vs Moment Relationships in Beams

Figures 5.43 and 5.44 show how the moments in beams 5 and 6 varied with load in test 28. The plots obtained for these two beams at the different locations are essentially linear until the connection moment reached 140 kNm in Joint I and 130 kNm in Joint L (the plastic capacity of beam  $M_p = 143$  kNm was determined by Prescott [5.1]). For Joints I and L, the curve then became non-linear with a smaller increase of moment with the corresponding increment of applied beam loads. Plastic hinges were formed adjacent to joints I, J and K when the maximum applied load was approached.

Figures 5.45 to 5.46 show how the moments in beams 5 and 6 vary with load in test 29. In Figure 5.45, a linear load characteristic was obtained up to the applied load of 230 kN on beam 5. Plastic hinges were then formed at joints I and J. The failure of the joints by welding fracture of the connections without warning caused the sudden reduction of moments at Joints I and J with moment shed to the mid-span. Same phenomenon was observed in beam 6 with plastic hinges formed at joints K and L (Figure 5.46). The failure of joints by welding fracture of the connections without warning caused the sudden reduction of moments at Joints K and L.

#### 5.7.5 Load-Deflection Relationships in Beams

Figure 5.47 shows the load deflection curves for all beams in test 28 in a single plot. Essentially linear load-deflection relationships were obtained for all beams except beams 5 and 6 exhibited some nonlinearity at very high applied loads after 290 kN. The characteristics were then show a loss of stiffness of the beams and indicate that the connections were tending to failure under very high applied beam loads. However, this experiment was not continued to failure but was terminated due to the maximum safe capacity of loading system being reached.

In test 29, the loading positions on beams 5 and 6 were moved from the quarter and three-quarter points to third and two-third points in order to reduce the load to cause

failure. The load deflection relationships of the beams are illustrated in Figures 5.48. Essentially linear load-deflection relationships are obtained initially for all beams before failure occurred in beams 5 and 6 although some indications of non-linearity can be seen just prior to failure. For beam 5, a linear characteristic was observed up to applied load of 240 kN followed by a non-linear curve. At applied load of 259 kN, on this beam, one connection suddenly failed without warning and the effect is evident in this figure. A maximum mid-span deflection of 65 mm was observed in this beam. After applied load of 180 kN (scan 22), an unexpected upwards deflection was recorded in that beam due to an erroneous transducer reading as explained in section 5.7.3. The sign of the connection moments at Joints I and J did not change after failure, thus there was no change in the direction of deflection of this beam. It can be seen that there are sudden increases of deflection in beams 2 and 4 which were due to the effect of the failure of beam 5. After that a linear curve with a larger increasing rate of deflection was observed. Beam 6 also failed without warning at applied load of 297 kN due welding fracture at the connection.

Due to this unexpected failure, a larger weld leg length was specified for all connections designed for the next frame in order that the behaviour of true beam failure could be investigated.

The load-deflection plots for beams 2 to 4 in test 30 are shown in Figure 5.49. The error in the output from the load cell of the loading cable was observed in beam 1 and the result is thus meaningless and will not be discussed. Beam 4 was subjected to a single increment of load about 66 kN between scans 28 and 29 which caused a deflection of about 7 mm. Further increments of load on other beams did not influence the deflection of beam 4.

## **5.8 Tests to Failure in Frame 2**

### **5.8.1 Test Observations**

Test 42 was used to investigate the behaviour of the frame up to failure in the non-sway mode. Due to the experience obtained from the frame 1, the loading positions were again moved from the quarter and three-quarter points to the third and two-third points in order to reduce the beam failure load and enable this frame to attain its full plastic capacity within the limitation of the loading cables. As for frame 1, no load was applied to any column. Thus only beam failure could be studied and a comparison of the results made with these from the first frame. Table 5.17 shows the load history for this test. After



taking the initial readings, loads were applied to all six beams in small increments to their full dead load (scan 10) and additional loads were applied to their dead plus imposed loads (scan 15). All the beams were then subjected to their design load (scan 23). Finally the maximum load was applied to the frame up to the failure of beams 5 and 6 (scan 32). The frame was then unloaded. Plastic hinges were found to have formed at both ends of beams 5 and 6 near joints I, J, K and L. The shedding of moment to the mid-spans of beams 5 and 6 was a result of the plastic hinges near the beam ends. Thus a mechanism may have been developed if further load increments had been applied to these beams with plastic hinges forming in the mid-span region of the beams. However, as the safe capacity of the loading cable had been reached, no further loads were applied to beam and the frame was then unloaded. After the test, the top and middle bolts in the extended end-plate connection at joint I were found to have yielded. Figure 5.50 shows a single plot of the connection moment and the forces in bolts 1 to 4 (top and middle rows). The linear relationships existed up to the connection moment of 140 kNm in joint I. In the non-linear region, a large increase in the bolt force occurs for a small corresponding increase in moment. Failure was attained for these bolts at a maximum sustained moment of 143 kNm. Observations made after the test showed that significant deformation had occurred in the end-plates of joints D and I. Furthermore permanent mid-span deflections for beams 5 and 6 were recorded as 40 and 27 mm respectively after the test. This provides evidence for the failure of beam.

As in the first frame, test 43 was undertaken to examine the residual strength of the already failed frame and attempted to fail beam 4. This test again used the non-sway mode. Detail of the loading history of this test is illustrated in Table 5.18. Beams 1 and 4 were loaded to their dead load (scan 4) and additional loads were applied up to the dead plus imposed values in scan 5 and the frame was loaded to fail beam 4 which occurred at scan 15 due to lateral-torsional buckling. The frame was then unloaded.

### 5.8.2 Beam Moment Distribution around the Frame

Figures 5.51 and 5.52 show the distribution of beam moments around the frame in tests 42 and 43. In test 42, the moments at four levels of load, dead load (D.L.) at scan 10, dead plus imposed loads (D.L. + L.L.) at scan 15, design load (1.4 x D.L. + 1.6 x L.L.) at scan 23 and all six beams subjected to their maximum load (1.4 x D.L. + 2.3 x L.L.) at scan 32, are plotted on the same graph in order to compare the variation of beam moment at different locations and at various levels of loads for the frame test. From Figure 5.51 it can be seen that for the longer beams more moments were attracted to the connections with

the extended end-plates due to the stiffer connections adopted. These moments were then transferred to the columns. A complete picture of the strain distribution at all locations in the columns could not be determined due to the limitation of the logging system as described in section 5.2.

In Figure 5.51, the moments in the connections and at the loading positions can be seen to increase with increasing applied loads for the first three levels of loading plotted. However, from scans 23 to 32, it can be observed that no change of moment occurred at joints I, J, K and L. This was due to the formation of plastic hinges near the connections at these locations at scan 23.

Figure 5.52 shows the bending moment distribution on the beams at scans 4, 5 and 15 in test 43. Loads were applied to beams 1 and 4 in an attempt to fail beam 4. The distributions of beam moment are plotted at scan 4 which corresponds to dead load, scan number 5 which corresponds to dead plus imposed loads and scan number 15, at which beams 1 and 4 were under maximum applied load. In Figure 5.52, the moments at the end of the two beams and the loading points increased with the increasing of the applied load for the first two level of loads. Larger moments were attracted to beam 4 due to the longer span with extended end connections as discussed for test 42. A slightly smaller increase of moment at the mid-span of beam 4 was observed from the scan 5 to 15 due to the reduction of the strength of beam 4 under very high applied beam load.

### 5.8.3 Deflected Shape of the Frame

Figures 5.53 and 5.54 indicate the deflected shapes of frame in tests 42 and 43 with linear interpolation between points of measurement and nodes. The deflection at the four levels of load are plotted in the same figure and correspond to the loading scans described in section 5.8.2.

In Figure 5.53, the mid-span deflections for beams and columns increased approximately proportionally to the increase of the applied load for the first three levels of load. However, larger mid-span deflections of beams 5 and 6 were observed from scans 23 to 32, again due to the formation plastic hinges at the two ends of the beams. The larger increases of the central deflections in columns 5, 6, 8 and 9 were due to the effect of the failure of the connections.

In Figure 5.54, it can be seen that the mid-span deflection of beam 4 increased steadily with the applied load for the first two level of loads, but then increased rapidly from scan 5 to scan 15 due to the failure of this beam in lateral torsional buckling during the last loading increment. Larger corresponding increases of the central deflections in columns 4 and 7 were due to the loss of restraint of the adjacent beam after the failure of beam 4.

#### 5.8.4 Relationship of Load-Moment in Beams

Figures 5.55 and 5.56 show the load moment plots for beams 5 and 6 in test 42. For moderate loads, linear load moment relationships were obtained for all beams at the different locations. However, the relationships ceased to be linear as the formation of the plastic hinges at two ends of the beams near joints I, J, K and L was approached. Subsequently, non-linear curves resulted with larger increases in applied beam loads for the corresponding increment of moment due to the plastic hinges being formed at both ends of the beams near these joints. Corresponding nonlinearities occurred for other locations. The maximum moment sustained at ends K and L of beam 6 was recorded as 143 kNm. This was attained at an applied load of 225 kN for joint K causing a redistribution of bending moment with non-linearities in the relationships for the two loading points on beam 6 - the more pronounced deviation occurring for the left hand load. The non-linearity is barely detectable at the right hand end joint L. It is evident from Figure 5.55 that plastic hinges occurred in beam 5 at the same level of moment - at the right hand end at a load of just over 230 kN and at the left hand end at about 240 kN with consequent non-linearities in the plots for the applied load points. The plastic hinges may have been formed in the spans of these beams if further load increments had been applied. However, as the limiting capacity of the loading cable had been reached, the frame was unloaded.

Figures 5.57 and 5.58 show the corresponding load moment plots for beams 1 and 4 in test 43. A linear relationship was obtained for beam 1 up to the maximum applied load. However, the relationship obtained for beam 4 was essentially linear up to the point at which the moment at joint G reached 143 kNm. After that, a slight reduction of rate of moment increase occurred at the left hand side of the loading point. At the stage of maximum applied beam load, a large reduction of moment occurred at the left hand side and this was due to the failure of beam 4. More moment was shed to the ends of the beam.

### 5.8.5 Relationship of Load-Deflection in Beams

Figure 5.59 shows the load deflection plots for the six beams in test 42. A slightly irregular record of the deflection due to the applied beam loads was obtained in the early scans probably due to the taking up of slack in both specimens and loading devices. All the curves shown then followed a linear route up to high applied loads. Subsequently, the variation to non-linear curves, having larger increments of deflection for corresponding increases of the applied load, reflected a loss of stiffness due to the formation of hinges. This figure shows a linear response up to the maximum applied beam load for beam 1 in which the maximum mid-span deflection was recorded as 1.7 mm. Beams 2 to 4 show linear response up to applied beam loading of 150 kN for beams 2 and 3 and 190 kN for beam 4. The relationships then varied non-linearly showing larger increases in deflection for the corresponding load increments. The maximum mid-span deflections were recorded as 4.2 mm for beam 2, 3.5 mm for beam 3 and 27 mm for beam 4 when under maximum loads. In this figure, the response for beam 5 was linear up to an applied beam load of 250 kN. A non-linear response was obtained after that with the maximum mid-span deflection being recorded as 67 mm. A similar response was obtained for beam 6 and the linear relationship existing up to the record of applied beam load of 220 kN. A non-linear response was then obtained up to the maximum applied load with the mid-span deflection reaching 60 mm. As explained in section 5.8.4, a non-linear curve resulted, with larger increases in applied beam load for the corresponding increment of mid-span deflection in beams 5 and 6 due to the plastic hinges being formed at the ends of the two beams near the connections. The mid-span linear response limit and the maximum deflections were 25 mm to 67 mm for beam 5 respectively and 20 mm to 60 mm for beam 6. There was evidence of large plastic deformations in these two beams at maximum loads which suggested that plastic hinges had formed at the two ends of these beams.

Figure 5.60 shows the load deflection plots for beams 1 and 4 in test 43. This figure shows that for beam 2 the load deflection relationship is essentially linear up to the maximum applied load for which only 2 mm mid-span deflection was recorded. Beam 4 showed a similar response having linear characteristics up to the recorded applied beam load of 220 kN. After that it becomes non-linear due to the plastic hinge formed in the beam end near joint G as explained in section 5.8.4 and showing a large increase in deflection from 27 mm to 57 mm.

## 5.9 Comparison of Response of Frames 1 and 2 in Tests to Failure

Two full-scale frame tests undertaken by Hatfield Polytechnic have been examined by the author in this chapter. Due to the importance of the tests to failure for both frames, a comparison of the actual behaviour of the steel frames is made. In the initial tests to failure, test 29 in frame 1 and test 42 in frame 2, the maximum applied loads, connection moments at the mid-span and two ends and the mid-span deflections in beams 5 and 6 are compared.

In test 29 of frame 1, beams 5 and 6 failed without warning at scans 20 and 26. They failed due to welding fracture in the region of the connections at joints I, J, K and L. For test 42 in frame 2, plastic hinges were formed at the connections of joint I, J, K and L at the two ends of beams 5 and 6. The shedding of moment to the mid-span and the permanent deformation of mid-span for these beams are evident.

For test 30 of frame 1, the residual strength of the failed frame was tested with the maximum load applied to beams 1 to 3. After that beam 4 was subjected to applied load in one increment. Residual strength in the short span beams was observed, but the failure condition was above the capacity of the loading cables. For test 43 of frame 2, only beams 1 and 4 were loaded to try to fail beam 4. At scan 16, beam 4 failed in lateral torsional buckling indicating insufficient out of plane bracing.

Table 5.19 shows the comparison of the moment and deflection at the selected positions in beams 5 and 6 under their dead plus imposed loads and failure. When dead plus imposed loads was applied, the moment sustained was 124 kNm and 120 kNm at joints I and J, 85 kNm at mid-span in test 29 and 120 kNm and 126 kNm at joints I and J, 75 kNm at mid-span in test 42. Although pre-loaded bolts were used in the connections of test 42, there was little difference between the moment distributions in beam 5 for each of the tests. The deflection of beam 5 was recorded as 20 mm in test 29 and 19 mm in test 42. Comparing the results for beam 6 in the two tests, it can be seen that the moment sustained at joints K and L was 116 kNm and 112 kNm, 87 kNm at mid-span in test 29 and 129 kNm and 110 kNm at joints K and L, 75 kNm at mid-span in test 42. The same mid-span deflection of 20 mm was recorded in tests 29 and 42 and showed that there was no significant difference in response between the pre-load bolts or hand-tightened bolts adopted in connections. At the failure load of beams 5 and 6, joints I, J, K and L are all attained their plastic capacity with high moment in the mid-span of beam.

Table 5.20 shows the comparison with the applied beam loads, moments and deflections at the selected positions in beam 4. The maximum value of applied load was 66.1 kN in test 30 and 299.9 kN in test 43. Beams 1 to 4 were loaded in test 30 whilst only beams 1 and 4 were loaded in test 43. The applied load on the shorter span side provided larger restraint to the adjacent side, thus the mid-span deflection in beam 4 was reduced. From Table 5.20, the mid-span deflection was 7 mm in test 30 and 57 mm in test 43. Clearly a comparison of values at these two levels of loading is relatively meaningless and so values corresponding to an applied beam load of 66.1 kN are given in parentheses for test 43 of frame 2. A recorded mid-span deflection in test 43 of 8 mm at the applied beam load of 66.1 kN supports this point. At an applied beam load of 66.1 kN, the moment at joints G and H were recorded as about 30 kNm for both tests. However, the mid-span moment was recorded as 25 kNm in test 30 whilst it was 30 kNm in test 43. A difference moment distribution around beam 4 occurred in the two tests due to the different loading arrangement which renders direct comparison of tests results at comparable load levels questionable.

## 5.10 Concluding Remarks on the Study

Frames 1 and 2 has been analysed and a comparison was made between the behaviour of the two frames. Seven types of the lack-of-fit were observed in connections in the tests. However preloading of the bolts had the effect of making the behaviour repeatable and increasing the bolt force linearly from the start of loading, independent of bolt pre-load.

The load applied to individual beams produced a larger mid-span deflection than when all beams were loaded together. This implied that the results determined from this loading arrangement should be considered for the beam deformation check in the serviceability limit state.

Only the central deflection for each column was observed to be small which was due to the large column section adopted as the test was designed to investigate beam failure. In the unbraced condition, side sway displacement in the top storey of frame was reduced when the connection bolts were pre-loaded.

Although end plates are usually considered to operate in shear only, the flush end-plates are seen to have significant stiffness and moment resistance and, as such, can be classified as semi-rigid. The moments at the beam ends are smaller than those suggested by a rigid

frame analysis and the beam deflections are significantly reduced when compared with the simply supported beam values. However, for the extended end-plate, the end moments are very close to the rigid moments and thus the extended end plate connections used could be regarded as 'rigid' and extended end-plate connection of these proportions are suitable for rigid design.

In frame 1, there was significant non-linearity in some of the  $M-\phi$  curves obtained which in part may be due to some lack of fit occurring in connections. With use of pre-loaded bolts used in connections in part of the tests of frame 2, the maximum stiffness was observed in the initial stage. Thus the deflection of the beams can be reduced by use of pre-loaded bolts in connections at low levels of load. It might be expected that the use of the pre-loaded bolts would lead to a larger connection stiffness which could be expected to attract more moment and also reduce the moment at mid-span, however, there was no significant difference between the moment distribution at comparable higher load levels in beams 5 and 6 found in test 29 of frame 1 (hand tight bolts) and test 42 of frame 2 (pre-loaded bolts).

An unexpected mode of failure the fracture, of welds in two connections occurred in frame 1. The leg length of weld was then increased from 12 mm to 20 mm for the second frame in order to avoid the connection failure. In frame 2, once plastic hinges had formed near the connections at the two ends of a beam, larger deformations occurred in the mid-span of beam for a given increment of load. Very high moment was sustained in the mid-span of beams. It is noted that loading applied to the shorter span beam provided a larger restraint to the adjacent longer span beam thus reducing the mid-span deflection in the longer span.

The result of the frame tests are compared with the prediction of some in house finite element analysis program in chapter 8. New design methods will be developed and checked using all test results, as addressed in chapter 10.

## References

- [5.1] Prescott, A. T., 'The Performance of End-Plate Connections in Steel Structures and their Influence on Overall Structural Behaviour', Ph.D. Thesis, Hatfield Polytechnic, July, 1987.
- [5.2] Lau, S. M., 'Full Scale Frame Tests with Semi-Rigid Connections', Progress Report no.2, Department of Civil and Structural Engineering, University of Sheffield.
- [5.3] Lau, S. M., 'Full Scale Frame Tests with Semi-Rigid Connections', Progress Report no.3, Department of Civil and Structural Engineering, University of Sheffield.
- [5.4] Lau, S. M., 'Full Scale Frame Tests with Semi-Rigid Connections', Progress Report no.4, Department of Civil and Structural Engineering, University of Sheffield.
- [5.5] Lau, S. M., 'Full Scale Frame Tests with Semi-Rigid Connections', Progress Report no.5, Department of Civil and Structural Engineering, University of Sheffield.
- [5.6] CP3, 'Code of Basic Data for the Design of Buildings : Chapter V : Part 1 : Dead and Imposed Loads', British Standards Institution, London, 1986.
- [5.7] Lau, S. M., 'Full Scale Frame Tests with Semi-Rigid Connections', Progress Report no.1, Department of Civil and Structural Engineering, University of Sheffield.
- [5.8] Lennon, T., 'Full-Scale Steel Frame Tests: Tests on Strain Gauged Bolts', Building Research Establishment, Note no. N 3/88, January, 1988.
- [5.9] Davison, J. B., 'Strength of Beam-Columns in Flexibly Connected Steel Frames', Ph.D. Thesis, University of Sheffield, June, 1987.
- [5.10] Gibbons, C., 'The Strength of Biaxially Loaded Beam-Columns in Flexibly Connected Steel Frames', Ph.D. Thesis, University of Sheffield, December, 1990.
- [5.11] Jones, S. W., Kirby, P. A. and Nethercot, D. A., 'Effect of Semi-Rigid Connections on Steel Column Strength', Journal of Constructional Steel Research, London, England, Vol. 1, No. 1, September, 1980 (pp. 38-46).



Total Load per Beam (kN)				Comments
Beam no.				
1	2 and 3	4	5 and 6	
10.1	10.1	16.2	16.2	
20.2	20.2	32.3	32.3	
30.3	30.3	48.5	48.5	
40.4	40.4	64.6	64.6	
50.5	50.5	80.8	80.8	
60.6	60.6	96.9	96.9	
70.7	70.7	113.1	113.1	
80.8	80.8	129.2	129.2	Dead Load
83.7	90.4	133.8	144.5	
86.5	99.9	138.3	159.7	
89.4	109.5	142.9	175.0	
92.2	119.0	147.4	190.2	Dead Load plus Live Load
97.1	125.9	155.3	201.2	
102.0	132.8	163.2	212.3	
106.9	139.7	171.1	223.3	
111.8	146.6	179.0	234.4	
116.7	153.5	186.9	245.4	
121.6	160.0	194.8	256.5	
126.5	167.3	202.7	267.5	
131.4	174.2	210.6	278.0	Design Load

Remark:

$$\text{Dead Load} = 1.0 \text{ D.L.}$$

$$\text{Dead Load plus Live Load} = 1.0 \text{ D.L.} + 1.0 \text{ L.L.}$$

$$\text{Design Load} = 1.4 \text{ D.L.} + 1.6 \text{ L.L.}$$

Table 5.1 : Load Increments up to Design Load in Beams

Test No.	Mode	Load Position	loaded Beam No.	Max. Load
1	Non-sway	1/4 pts.	All	Low
2	Sway	1/4 pts.	3,6	Low
3	Sway	1/4 pts.	All	Low
4	Sway	1/4 pts.	All	D.L.
5	Sway	1/4 pts.	1,4,5	Low
6	Sway	1/4 pts.	1,2,4	Low
7	Sway	1/4 pts.	1,2,4,5	Low
8	Sway	1/4 pts.	1,4,5	Low
9	Sway	1/4 pts.	All	Low
10	Sway	1/4 pts.	All	D.L.
11	Non-sway	1/4 pts.	All	D.L.
12	Non-sway	1/4 pts.	All	D.L.
13	Sway	1/4 pts.	All	D.L.
14	Sway	1/4 pts.	1	D.L.
15	Sway	1/4 pts.	2	D.L.
16	Sway	1/4 pts.	3	D.L.
17	Sway	1/4 pts.	4	D.L.
18	Sway	1/4 pts.	5	D.L.
19	Sway	1/4 pts.	6	D.L.
20	Sway	1/4 pts.	All	D.L.
21	Sway	1/4 pts.	All	D.L.
22	Sway	1/4 pts.	All	D.L. + L.L.
23	Sway	1/4 pts.	All	D.L. + L.L.
24	Non-sway	1/4 pts.	All	D.L.
25	Non-sway	1/4 pts.	All	D.L.
26	Non-sway	1/4 pts.	All	D.L. + L.L.
27	Non-sway	1/4 pts.	All	Design
28	Non-sway	1/4 pts.	All	Failure
29	Non-sway	1/3 pts.	All	Failure
30	Non-sway	1/3 pts.	1,2,3,4	Failure

Table 5.2 : Description of Tests in Frame 1

Test No.	Mode	Load Position	loaded Beam No.	Max. Load	Bolt Force
1	Non-sway	1/4 pts.	All	D.L.	Hand-tightened
2	Non-sway	1/4 pts.	All	D.L.	Hand-tightened
3	Non-sway	1/4 pts.	All	D.L. + L.L.	Hand-tightened
4	Non-sway	1/4 pts.	1	D.L.	Hand-tightened
5	Non-sway	1/4 pts.	2	D.L.	Hand-tightened
6	Non-sway	1/4 pts.	3	D.L.	Hand-tightened
7	Non-sway	1/4 pts.	4	D.L.	Hand-tightened
8	Non-sway	1/4 pts.	5	D.L.	Hand-tightened
9	Non-sway	1/4 pts.	6	D.L.	Hand-tightened
10	Sway	1/4 pts.	All	D.L.	Hand-tightened
11	Sway	1/4 pts.	All	D.L. + L.L.	Hand-tightened
12	Sway	1/4 pts.	4	D.L.	Hand-tightened
13	Sway	1/4 pts.	All	D.L. + L.L.	Hand-tightened
14	Sway	1/4 pts.	1	D.L.	Hand-tightened
15	Sway	1/4 pts.	2	D.L.	Hand-tightened
16	Sway	1/4 pts.	3	D.L.	Hand-tightened
17	Sway	1/4 pts.	4	D.L.	Hand-tightened
18	Sway	1/4 pts.	5	D.L.	Hand-tightened
19	Sway	1/4 pts.	6	D.L.	Hand-tightened
20	Sway	1/4 pts.	All	D.L.	Pre-loaded
21	Sway	1/4 pts.	All	D.L. + L.L.	Pre-loaded
22	Sway	1/4 pts.	All	D.L.	Pre-loaded
23	Sway	1/4 pts.	All	D.L. + L.L.	Pre-loaded
24	Sway	1/4 pts.	1	D.L.	Pre-loaded
25	Sway	1/4 pts.	2	D.L.	Pre-loaded
26	Sway	1/4 pts.	3	D.L.	Pre-loaded
27	Sway	1/4 pts.	4	D.L.	Pre-loaded
28	Sway	1/4 pts.	5	D.L.	Pre-loaded
29	Sway	1/4 pts.	6	D.L.	Pre-loaded
30	Non-sway	1/4 pts.	All	D.L.	Pre-loaded
31	Non-sway	1/4 pts.	All	D.L. + L.L.	Pre-loaded
32	Non-sway	1/4 pts.	All	D.L.	Pre-loaded
33	Non-sway	1/4 pts.	All	D.L. + L.L.	Pre-loaded
34	Non-sway	1/4 pts.	1	D.L.	Pre-loaded
35	Non-sway	1/4 pts.	2	D.L.	Pre-loaded
36	Non-sway	1/4 pts.	3	D.L.	Pre-loaded
37	Non-sway	1/4 pts.	4	D.L.	Pre-loaded
38	Non-sway	1/4 pts.	5	D.L.	Pre-loaded
39	Non-sway	1/4 pts.	6	D.L.	Pre-loaded
40	Sway	1/4 pts.	All	Design	Pre-loaded
41	Non-sway	1/4 pts.	All	Design	Pre-loaded
42	Non-sway	1/3 pts.	All	Failure	Pre-loaded
43	Non-sway	1/3 pts.	1, 4	Failure	Pre-loaded

Table 5.3 : Description of Tests on Frame 2

Series	Test	Mid-Span Deflection of Beam (mm)					
		1	2	3	4	5	6
1	10	2.1	1.9	1.5	14.3	9.7	10.1
	14	2.6	-	-	-	-	-
	15	-	2.4	-	-	-	-
	16	-	-	2.2	-	-	-
	17	-	-	-	13.3	-	-
	18	-	-	-	-	11.3	-
	19	-	-	-	-	-	10.9
2	32	1.3	1.8	1.2	10.9	8.5	9.1
	34	2.3	-	-	-	-	-
	35	-	2.3	-	-	-	-
	36	-	-	1.9	-	-	-
	37	-	-	-	12.2	-	-
	38	-	-	-	-	10.3	-
	39	-	-	-	-	-	9.9

(a) Mid-Span Deflection

Series	Test	Total Applied Load on Beam (kN)					
		1	2	3	4	5	6
1	10	80.7	80.9	80.3	131.2	136.3	130.0
	14	81.0	-	-	-	-	-
	15	-	80.7	-	-	-	-
	16	-	-	80.9	-	-	-
	17	-	-	-	131.0	-	-
	18	-	-	-	-	136.8	-
	19	-	-	-	-	-	130.0
2	32	80.6	80.8	81.6	131.5	135.6	129.6
	34	80.5	-	-	-	-	-
	35	-	80.7	-	-	-	-
	36	-	-	80.8	-	-	-
	37	-	-	-	131.1	-	-
	38	-	-	-	-	136.3	-
	39	-	-	-	-	-	130.1

(b) Total Applied Beam Loads

Table 5.4 : Total Applied Load and Deflection of Beams under Different Load Combinations

Series	Test	Beam	Moment (kNm)			
			Left End	Left Load	Right Load	Right End
1	10	1	-16.24	20.44	19.84	-17.76
		2	-15.82	17.77	18.23	-18.31
		3	-16.06	17.78	10.14	-29.86
		4	-36.14	61.86	53.71	-49.99
		5	-65.29	37.28	39.03	-60.65
		6	-64.74	36.04	43.20	-48.93
	14	1	-10.61	26.92	25.47	-14.00
		2	-10.47	22.98	23.48	-12.56
		3	-15.85	20.40	20.45	-15.57
		4	-48.22	51.23	52.48	-46.26
		5	-57.97	42.70	41.66	-58.35
		6	-61.86	38.69	44.05	-49.04
		2	32	1	-11.63	19.54
2	-10.94			18.95	15.65	-23.07
3	-15.40			16.25	5.74	-36.32
4	-57.99			41.98	45.49	-50.76
5	-60.84			37.88	31.65	-69.37
6	-65.08			27.94	38.36	-54.02
34	1		-11.22	24.73	21.68	-16.20
	2		-9.02	22.33	21.70	-15.21
	3		-18.14	17.38	17.67	-18.85
	4		-51.34	47.49	48.82	-47.93
	5		-57.01	42.28	37.38	-61.71
	6		-63.51	29.58	39.89	-52.41

Table 5.5 : Beam Moment Distribution in Different Tests

Frame	Test	Applied Load (kN)	Mode	Bolt	Analysis
1	23	D.L. + L.L.	Sway	Hand-Tightened	Moment Rotation
1	28	Design	Non-Sway	Hand-Tightened	Column Deflection Moment Bolt Force Moment Rotation
2	3	D.L. + L.L. + Additional	Non-Sway	Hand-Tightened	Beam Moment Beam Deflection
2	11	D.L. + L.L.	Sway	Hand-Tightened	Beam Moment Beam Deflection Sway Displacement
2	21	D.L. + L.L.	Sway	Pre-Loaded	Sway Displacement
2	31	D.L. + L.L.	Non-Sway	Pre-Loaded	Beam Deflection Moment Rotation
2	40	Design Load	Sway	Pre-Loaded	Beam Moment Beam Deflection Moment Rotation Sway Displacement Moment Bolt Force
2	41	Design Load	Non-Sway	Pre-Loaded	Beam Moment

Table 5.6 : Tests Selected for Analysis

Test	Beam	Applied Load	Test Moment (kN)				Rigid Frame Moment (kN)			
			1	2	3	4	1	2	3	4
3 (Non-sway) (Hand-tightened Bolt)	1	94.9	-15.8	25.8	20.2	-26.6	-19.0	17.7	0.5	-53.4
	2	130.1	-18.9	32.5	26.4	-31.8	-35.4	20.4	7.8	-60.6
	3	129.8	-24.7	28.8	19.2	-41.1	29.4	22.9	3.9	-67.4
	4	154.7	-44.9	70.0	60.9	-59.24	-87.3	35.1	44.0	-69.5
	5	217.5	-128.0	68.3	62.9	-98.2	-121.3	46.2	35.1	-44.0
	6	207.7	-93.1	61.2	66.5	-82.2	-118.1	44.5	53.1	-101.0
11 (Sway) (Hand-tightened Bolt)	1	92.3	-18.4	22.8	21.5	-21.5	-22.5	15.0	2.1	-48.5
	2	119.5	-22.4	26.8	25.4	-28.9	-39.1	15.3	10.0	-49.6
	3	120.0	-21.5	27.4	16.4	-41.6	-32.6	18.4	5.9	-57.4
	4	149.9	-45.8	66.4	59.2	-57.0	-87.5	32.8	44.7	-63.6
	5	201.6	-94.5	55.8	57.6	-88.5	-116.3	41.0	32.8	-44.7
	6	192.1	-94.0	53.7	62.6	-73.5	-112.6	39.7	51.2	-89.5
40 (Sway) (Pre-loaded Bolt)	1	92.2	-16.9	20.8	8.8	-37.5	-22.7	15.0	2.5	-49.0
	2	119.5	-22.2	24.7	22.6	-32.4	-39.1	15.3	10.2	-49.4
	3	120.3	-25.1	22.1	7.2	-54.2	-31.8	18.6	4.7	-59.6
	4	150.4	-72.3	44.7	52.9	-55.1	-87.8	32.8	44.8	-63.7
	5	201.7	-96.4	53.5	51.5	-94.1	-116.3	41.0	32.8	-44.8
	6	192.4	-108.0	37.1	58.0	-76.9	-118.2	43.8	51.0	-92.0
41 (Non-sway) (Pre-loaded Bolt)	1	92.7	-14.1	22.8	7.3	-41.6	-18.2	17.3	0.3	-52.2
	2	120.5	-17.9	27.5	21.1	-35.0	-32.7	18.5	7.1	-55.4
	3	119.3	-24.5	23.6	11.6	-47.4	-27.2	21.2	3.6	-62.5
	4	151.1	-69.2	46.0	50.9	-58.6	-84.9	34.0	42.9	-67.1
	5	202.1	-89.9	56.4	49.4	-98.0	-112.3	42.9	34.0	-42.9
	6	192.6	-95.4	41.7	57.4	-79.6	-109.6	41.3	49.3	-93.6

Remark: (1) Left Joint  
(2) Left Loading Point  
(3) Right Loading Point  
(4) Right Joint

(Moments in the applied beam load due to dead and imposed loads)

Table 5.7 : Comparison of Moment in Tests and Rigid Frame Moment

Test	Joint	Type	$t_p$	Moment (kNm)	Rotation (mrad)	Stiffness (kNm/mrad)		
						$C_i$	$C_m$	$C_u$
23	A	F	12	17.06	1.15	22700	28400	12200
	B	F	20	34.13	-	-	-	-
	C	F	20	30.19	8.44	1600	5600	4300
	D	F	20	39.19	3.90	10200	10200	11500
	E	F	15	23.68	2.98	9800	9800	7900
	F	F	20	38.24	6.38	5300	8800	10300
	G	E	20	72.92	4.46	7800	21100	21100
	H	E	20	59.83	-	-	-	-
	I	E	25	142.75	3.55	49500	49500	45300
	J	E	25	111.89	2.11	64300	88900	66300
	K	E	25	116.50	2.31	41800	63600	51600
	L	E	25	102.72	3.68	33900	33900	38700
28	A	F	12	19.06	-	-	-	-
	B	F	20	46.11	3.52	24100	24100	10500
	C	F	20	32.95	4.05	4100	6000	5400
	D	F	20	51.21	17.48	9900	9900	11100
	E	F	15	25.56	2.91	9500	9500	8400
	F	F	20	53.28	8.21	5200	9600	11200
	G	E	20	94.49	5.61	8200	25100	25900
	H	E	20	82.99	-	-	-	-
	I	E	25	168.75	4.58	35300	41700	34300
	J	E	25	164.45	3.71	28900	76500	64200
	K	E	25	159.69	2.85	42600	42600	47200
	L	E	25	125.98	5.04	33000	33000	37900

Remark: Test 23 - Sway, D.L. + L.L.  
Test 28 - Non-Sway, Failure  
F = Flush End-Plate  
E = Extended End-Plate

Table 5.8 : Moment Rotation and Stiffness of Joints in Tests 23 and 28 of Frame 1



Test	Joint	Type	$t_p$	Moment (kNm)	Rotation ( $\times 10^{-3}$ rad)	Stiffness (kNm/mrad)		
						$C_i$	$C_m$	$C_u$
31	A	F	12	13.75	1.15	5000	5000	-
	B	F	20	41.05	-	-	-	-
	C	F	20	18.08	8.44	6700	9200	9000
	D	F	20	32.80	3.90	18700	18700	18700
	E	F	15	24.26	2.98	60000	-	37820
	F	F	20	53.06	6.38	69200	69200	14600
	G	E	20	69.51	4.46	-	-	-
	H	E	20	57.50	-	-	-	80000
	I	E	25	90.77	3.55	28500	30500	33200
	J	E	25	99.35	2.11	64500	64500	56800
	K	E	25	95.96	2.31	66000	66000	61400
	L	E	25	79.11	3.68	30000	30000	28200
40	A	F	12	18.68	5.82	8000	8000	8700
	B	F	20	55.48	0.17	-	-	-
	C	F	20	31.04	3.46	6700	13200	12000
	D	F	20	34.88	4.14	22400	22400	12000
	E	F	15	35.40	8.98	55200	55200	24500
	F	F	20	58.12	4.15	75000	75000	14900
	G	E	20	-	-	-	-	-
	H	E	20	61.34	1.38	-	-	61900
	I	E	25	143.00	0.52	-	-	-
	J	E	25	143.00	4.57	60600	60600	61100
	K	E	25	143.00	4.50	61000	61000	33800
	L	E	25	111.00	5.12	26600	32300	29800

Remark : Test 31 - Non-sway, D.L. + L.L.  
Test 40 - Sway, 1.4 D.L. + 1.6 L.L.  
F = Flush End-Plate  
E = Extended End-Plate

Table 5.9 : Joint Moment Rotation and Stiffness of Joints in Tests 31  
40 of Frame 2

Test	Beam	Applied Load (kN)	Mid-span Deflection (mm)			Ratio	
			Test (1)	Rigid (2)	Pinned (3)	(1)/(2)	(3)/(1)
3 (Non-sway) (Hand-tightened Bolt)	1	94.9	2.3	1.9	5.5	1.20	2.39
	2	130.1	3.1	2.2	7.6	1.41	2.45
	3	129.8	2.6	1.7	7.6	1.54	2.92
	4	154.7	16.6	11.4	36.9	1.45	2.22
	5	217.5	17.1	12.9	51.9	1.33	3.04
	6	207.7	16.8	12.9	49.5	1.30	2.95
11 (Sway) (Hand-tightened Bolt)	1	92.3	2.3	1.8	5.4	1.22	2.35
	2	119.5	2.7	2.0	7.0	1.35	2.59
	3	120.0	2.3	1.6	7.0	1.43	3.04
	4	149.9	16.0	11.3	35.8	1.41	2.24
	5	201.6	14.5	12.0	48.1	1.20	3.31
	6	192.1	14.7	12.0	45.9	1.22	3.12
31 (Non-sway) (Pre-loaded Bolt)	1	92.4	1.6	1.8	5.4	0.88	3.38
	2	119.3	2.6	2.0	7.0	1.30	2.69
	3	120.1	1.7	1.6	7.0	1.06	4.12
	4	150.2	12.1	11.2	35.8	1.08	2.96
	5	201.7	13.0	11.9	48.1	1.09	3.70
	6	192.8	13.3	11.9	45.9	1.12	3.45
40 (Sway) (Pre-loaded Bolt)	1	92.2	1.5	1.8	5.4	0.83	3.60
	2	119.5	2.5	2.0	7.0	1.25	2.80
	3	120.3	1.6	1.6	7.0	1.00	4.38
	4	150.4	12.2	11.3	35.8	1.08	2.93
	5	201.7	13.1	12.0	48.1	1.09	3.67
	6	192.4	13.4	12.0	45.9	1.11	3.43

(Results in the applied beam load of dead plus imposed loads)

Table 5.10 : Comparison Deflection in Tests and Predicted Results

Column	Mid-Height Deflection (mm)
1	0.1
2	0.1
3	0.5
4	0.4
5	0.1
6	2.1
7	0.9
8	0.3
9	1.3

Table 5.11 : Mid-Height Deflection of Columns in Test 28 of Frame 1

Test	Joint	Maximum Sway (mm)	Remarks
11	H	6.60	hand tightened, D.L. + L.L.
	J	0.76	
	L	-0.26	
21	H	5.25	preloaded, D.L. + L.L.
	J	1.40	
	L	0.56	
40	H	6.22	preloaded, 1.4 D.L. + 1.6 L.L.
	J	1.26	
	L	-1.27	

Table 5.12 : Sway Displacement between Three Joints in Tests of Frame 2

Connection	Thickness (mm)	Row	Bolt	Maximum Load (kN)	
				Frame 1 Test 28	Frame 2 Test 40
A  (FEP)	12	1	1	16.6	38.4
		1	2	14.8	33.4
		2	3	-0.7	3.8
		2	4	-1.6	6.3
		3	5	-5.8	8.8
		3	6	2.6	8.0
C  (FEP)	20	1	1	40.0	53.6
		1	2	15.0	39.6
		2	3	-2.0	-0.5
		2	4	-5.4	3.1
		3	5	-8.0	-2.4
		3	6	-17.0	0.1
E  (FEP)	15	1	1	47.5	4.8
		1	2	72.5	8.2
		2	3	14.2	0.9
		2	4	5.3	1.4
		3	5	5.0	0.3
		3	6	4.9	0.3
G  (EEP)	20	1	3	89.0	2.7
		1	4	104.0	18.6
		2	1	70.0	1.5
		2	2	94.0	17.4
		3	5	-16.0	-33.0
		3	6	-9.4	-58.7
I  (EEP)	25	1	3	147.0	154.0
		1	4	139.0	70.5
		2	1	142.0	350.0
		2	2	127.0	209.0
		3	5	1.6	2.7
		3	6	4.1	2.2
J  (EEP)	25	1	3	147.5	35.5
		1	4	139.0	46.0
		2	1	115.0	39.5
		2	2	95.0	45.0
		3	5	-3.0	-2.8
		3	6	-12.7	-21.5

Table 5.13 : Maximum Loads for Bolts in Two Tests

SCAN	APPLIED LOAD (kN)					
	BEAM 1	BEAM 2	BEAM 3	BEAM 4	BEAM 5	BEAM 6
1	0.0	0.0	0.0	0.0	0.0	0.0
2	0.0	0.0	0.0	0.0	0.0	0.0
3	9.8	10.1	9.3	16.2	16.4	16.8
4	19.9	20.3	19.2	32.5	32.7	33.2
5	30.2	30.6	29.4	49.0	49.3	49.8
6	40.4	40.8	39.5	65.5	65.9	66.5
7	50.7	51.2	49.7	80.1	82.4	83.1
8	60.9	61.4	59.7	98.6	99.0	99.7
9	71.3	71.8	70.0	115.1	115.6	116.3
10	81.4	82.0	80.0	131.7	132.4	132.9
11	84.4	91.8	89.7	136.3	148.0	148.6
12	87.3	101.5	99.3	140.7	163.7	164.1
13	90.1	111.2	108.8	145.4	179.4	179.7
14	93.0	120.9	118.3	150.1	194.9	195.4
15	93.0	120.9	118.2	150.1	194.9	195.2
16	98.0	128.1	125.5	158.2	206.4	206.7
17	103.0	135.3	132.5	166.2	217.6	217.9
18	108.0	142.2	139.5	174.2	229.0	229.1
19	113.0	149.2	146.2	182.4	240.4	240.5
20	117.9	156.2	153.3	190.5	251.8	251.8
21	122.9	163.4	160.3	198.4	263.0	263.1
22	127.9	170.3	167.3	206.5	274.4	274.4
23	132.9	177.5	174.2	214.5	285.6	285.6
24	134.0	181.3	178.1	216.4	292.0	291.8
25	135.1	185.3	182.0	218.2	298.3	298.1
26	136.2	189.0	185.7	220.0	304.6	308.0
27	137.4	193.0	189.8	221.0	310.7	314.1
28	137.4	193.0	189.6	221.0	310.7	314.0
29	138.5	196.9	193.5	222.7	317.1	320.3
30	138.5	197.0	193.5	222.8	317.1	320.3
31	139.7	200.7	197.2	224.6	323.4	326.5
32	139.6	200.7	197.2	224.6	323.5	326.7
33	137.3	193.2	189.8	221.1	310.9	313.8
34	135.1	185.5	182.3	218.5	298.4	297.6
35	132.8	177.8	174.8	214.8	285.8	285.1
36	122.9	163.7	160.6	198.9	263.3	262.5
37	113.1	149.5	146.6	182.9	240.6	239.8
38	103.1	135.6	132.8	166.7	217.9	217.1
39	93.2	121.3	118.6	150.7	195.3	194.6
40	87.4	101.9	99.5	141.4	163.9	163.3
41	81.6	82.3	80.2	132.2	132.6	132.1
42	61.0	61.7	59.8	99.1	99.3	99.0
43	40.5	41.1	39.6	65.9	66.0	65.9
44	19.9	20.5	19.3	32.7	32.8	32.8
45	1.0	0.3	1.4	0.0	1.2	0.3

Table 5.14 : Load History of Frame 1 Test 28

SCAN	APPLIED LOAD (kN)					
	BEAM 1	BEAM 2	BEAM 3	BEAM 4	BEAM 5	BEAM 6
1	0.0	0.0	0.0	0.0	0.0	0.0
2	0.0	0.0	0.0	0.0	0.0	0.0
3	10.0	9.5	10.0	16.6	16.8	16.2
4	20.1	19.6	19.8	32.8	33.6	32.4
5	30.4	30.0	29.9	49.4	50.7	49.0
6	40.7	40.2	40.0	65.9	67.8	65.6
7	51.0	50.6	50.1	82.5	85.0	82.2
8	61.1	60.8	60.2	99.1	102.1	98.8
9	71.5	71.2	70.5	115.6	119.0	115.4
10	81.8	81.4	80.6	132.2	136.1	132.0
11	84.7	91.3	90.2	136.8	152.2	147.6
12	87.7	101.0	99.8	141.3	168.2	163.1
13	90.5	110.6	109.3	146.0	184.3	178.6
14	93.4	120.4	118.9	150.8	200.5	194.3
15	98.3	127.6	126.0	158.9	212.3	205.7
16	103.3	134.8	133.1	166.8	223.8	216.8
17	108.3	141.7	140.0	174.9	235.3	228.1
18	113.2	148.7	146.9	183.0	247.0	239.4
19	113.2	148.7	146.8	183.0	247.1	239.0
20	118.1	155.7	153.6	191.1	258.6	250.6
21	123.2	162.9	160.9	198.8	186.4	261.9
22	128.2	169.9	167.7	207.0	179.8	273.2
23	133.3	177.1	174.8	214.9	179.3	284.2
24	134.2	180.8	178.5	216.9	178.9	290.5
25	135.5	184.7	182.5	218.7	178.7	296.8
26	136.5	188.5	185.8	220.5	176.9	182.5
27	142.3	196.9	194.5	230.2	176.4	166.9
28	148.8	205.7	203.0	240.3	176.4	166.6
29	155.0	214.3	211.5	250.6	176.5	166.4
30	168.0	232.1	229.0	271.2	176.4	166.1
31	180.7	249.7	246.3	291.8	176.3	165.8
32	193.3	267.5	263.9	315.9	175.9	165.4
33	96.9	267.7	264.0	315.8	175.5	165.1
34	99.1	267.7	264.0	315.9	175.4	165.0
35	-	267.8	264.0	316.0	175.2	164.9
36	-	267.8	263.9	316.0	175.1	164.8
37	-	267.8	263.9	316.1	175.2	164.8
38	-	267.8	263.8	316.1	175.3	164.8
39	-	232.7	229.5	272.1	174.9	165.0
40	-	197.6	194.9	231.3	174.6	165.2
41	-	185.5	182.8	219.8	174.5	165.3
42	-	177.8	175.1	215.9	174.4	165.3

Table 5.15 : Load History of Frame 1 Test 29

SCAN	APPLIED LOAD (kN)					
	BEAM 1	BEAM 2	BEAM 3	BEAM 4	BEAM 5	BEAM 6
1	0.0	0.0	0.0	0.0	0.0	0.0
2	0.0	0.0	0.0	0.0	0.0	0.0
3	91.6	20.0	20.5	0.3	-0.1	-0.3
4	99.1	40.7	40.7	0.3	-0.1	-0.5
5	86.0	61.3	61.0	0.3	-0.1	-0.6
6	99.5	82.0	81.3	0.4	-0.1	-0.7
7	147.6	101.6	100.5	0.4	-0.1	-0.7
8	216.4	121.0	119.6	0.4	-0.1	-0.7
9	129.8	135.4	133.6	0.4	-0.1	-0.8
10	139.1	149.4	147.5	0.4	-0.1	-0.8
11	258.8	163.5	161.4	0.4	-0.1	-0.8
12	174.8	177.6	175.2	0.4	-0.1	-0.8
13	290.1	185.3	183.0	0.3	-0.1	-0.8
14	209.4	193.3	190.7	0.4	-0.1	-0.8
15	299.0	201.0	198.6	0.4	-0.1	-0.8
16	305.6	209.0	206.2	0.3	-0.1	-0.8
17	289.6	216.6	214.0	0.4	-0.1	-0.8
18	225.8	224.5	221.7	0.4	-0.1	-0.8
19	230.8	232.3	229.2	0.4	-0.1	-0.8
20	205.8	240.1	237.0	0.4	-0.1	-0.8
21	311.7	247.9	244.7	0.4	-0.1	-0.8
22	257.1	255.7	252.3	0.3	0.0	-0.8
23	275.7	263.6	260.2	0.3	-0.1	-0.9
24	304.3	271.3	267.6	0.4	0.0	-0.8
25	218.9	279.3	275.7	0.4	0.0	-0.9
26	305.1	287.0	283.1	0.4	0.0	-0.8
27	270.8	294.9	291.1	0.4	0.0	-0.8
28	353.7	306.3	298.4	0.4	0.0	-0.8
29	241.9	306.4	298.2	66.1	0.0	-1.0
30	186.1	306.4	298.2	1.1	-0.1	-0.6
31	234.4	271.9	268.1	0.9	-0.1	-0.6
32	280.5	240.8	234.5	0.8	-0.1	-0.6
33	216.4	209.6	108.1	0.8	-0.1	-0.6
34	218.7	178.3	175.9	0.8	-0.1	-0.6
35	-22.6	150.2	52.2	0.7	-0.1	-0.5
36	56.5	121.7	-4.5	0.7	-0.1	-0.5
37	102.9	82.7	-107.0	0.9	-0.1	-0.4
38	252.7	41.3	-92.9	0.8	-0.1	-0.2
39	151.9	0.4	1.7	0.8	0.1	0.2

Table 5.16 : Load History of Frame 1 Test 30

SCAN	APPLIED LOAD (kN)						REMARK
	BEAM 1	BEAM 2	BEAM 3	BEAM 4	BEAM 5	BEAM 6	
1	0.0	0.0	0.0	0.0	0.0	0.0	
2	0.0	0.0	0.0	0.0	0.0	0.0	
3	9.6	9.2	9.6	16.1	16.9	12.9	
4	19.6	19.3	19.5	32.4	33.7	29.3	
5	29.9	29.6	29.7	49.0	51.0	46.1	
6	40.0	39.8	39.8	65.5	68.2	62.9	
7	50.2	50.1	50.0	82.1	85.4	79.6	
8	60.3	60.3	60.2	98.7	102.6	96.2	
9	70.5	70.6	70.5	115.3	119.7	112.7	
10	80.6	80.8	80.7	131.8	136.9	129.3	D.L.
11	83.5	90.6	90.4	136.5	153.1	144.9	
12	86.4	100.3	100.1	141.0	169.1	160.3	
13	89.1	109.9	109.6	145.7	185.3	175.9	
14	92.0	119.6	119.1	150.4	201.6	191.5	
15	92.0	119.7	119.1	150.5	201.9	191.4	D.L. + L.L.
16	97.0	126.8	126.2	158.6	213.6	202.9	
17	102.0	134.0	133.4	166.5	225.1	214.0	
18	106.9	140.9	140.4	174.6	236.4	225.3	
19	111.8	148.0	147.4	182.8	248.1	236.6	
20	116.5	155.0	154.4	191.0	259.9	247.9	
21	121.4	162.1	161.5	198.9	271.6	259.2	
22	126.2	169.1	168.5	207.0	283.3	270.5	
23	131.2	176.3	175.6	215.0	294.8	281.7	DESIGN
24	132.3	180.1	179.3	217.1	301.3	287.9	
25	133.4	184.1	183.2	218.8	307.8	294.1	
26	134.5	187.8	186.9	220.7	314.8	300.4	
27	135.4	191.8	190.7	221.6	321.1	306.5	
28	136.6	195.7	194.6	223.5	327.5	316.3	
29	137.7	199.4	198.3	225.2	333.8	322.4	
30	138.9	203.4	202.2	227.0	343.8	328.6	
31	139.8	207.4	206.1	229.0	350.0	334.8	
32	139.8	207.4	206.0	229.0	349.9	334.8	FAILURE
33	135.3	191.9	190.3	221.7	320.2	306.0	
34	130.9	176.6	174.8	215.4	294.3	280.9	
35	111.3	148.5	147.1	183.3	247.5	235.5	
36	91.4	120.4	119.0	151.1	200.7	190.4	
37	79.9	81.6	80.2	132.5	136.0	128.3	
38	39.5	40.6	39.6	66.1	67.6	62.2	
39	0.1	1.4	1.9	4.3	4.8	2.3	

Table 5.17 : Load History of Frame 2 Test 42



SCAN	APPLIED LOAD (kN)						REMARK
	BEAM 1	BEAM 2	BEAM 3	BEAM 4	BEAM 5	BEAM 6	
1	0.0	0.0	0.0	0.0	0.0	0.0	
2	0.0	0.0	0.0	0.0	0.0	0.0	
3	39.8	0.6	0.1	65.4	0.9	-0.4	
4	80.4	0.5	0.1	131.8	1.2	-0.4	D.L.
5	118.8	0.4	0.0	194.5	1.3	-0.6	D.L. + L.L.
6	125.8	0.5	-0.1	205.9	1.2	-0.6	
7	132.8	0.4	-0.2	217.2	1.1	-0.6	
8	139.6	0.4	-0.3	228.6	1.1	-0.6	
9	146.4	0.4	-0.2	240.0	1.1	-0.7	
10	153.1	0.4	-0.3	251.4	1.1	-0.7	
11	160.2	0.4	-0.4	262.8	1.1	-0.8	
12	167.0	0.4	-0.3	274.2	1.1	-0.8	
13	174.0	0.4	-0.3	285.4	1.1	-0.8	
14	180.8	0.5	-0.3	296.9	1.1	-0.8	
15	187.5	0.5	-0.3	299.9	1.0	-0.7	FAILURE
16	145.6	0.9	0.1	240.6	0.6	-0.2	
17	117.7	1.1	0.1	195.5	0.3	0.1	
18	79.4	1.1	0.2	133.2	0.1	0.6	
19	39.3	1.1	0.3	67.4	7.3	1.2	
20	1.6	1.1	0.3	15.1	0.2	0.9	

Table 5.18 : Load History of Frame 2 Test 43

	Beam no.	Loading	Moment (kNm)			Mid-Span Deflection (mm)
			Left End	Mid-Span	Right End	
Frame 1 (Test 29)	5	D.L + L.L.	124	85	120	20
		Failure	143	125	143	28
	6	D.L + L.L.	116	87	112	21
		Failure	143	140	143	38
Frame 2 (Test 42)	5	D.L + L.L.	120	75	126	19
		Failure	143	160	143	67
	6	D.L + L.L.	129	75	110	21
		Failure	143	135	143	60

Table 5.19 : Comparison of the Results in Test to Failure for Frames 1 and 2

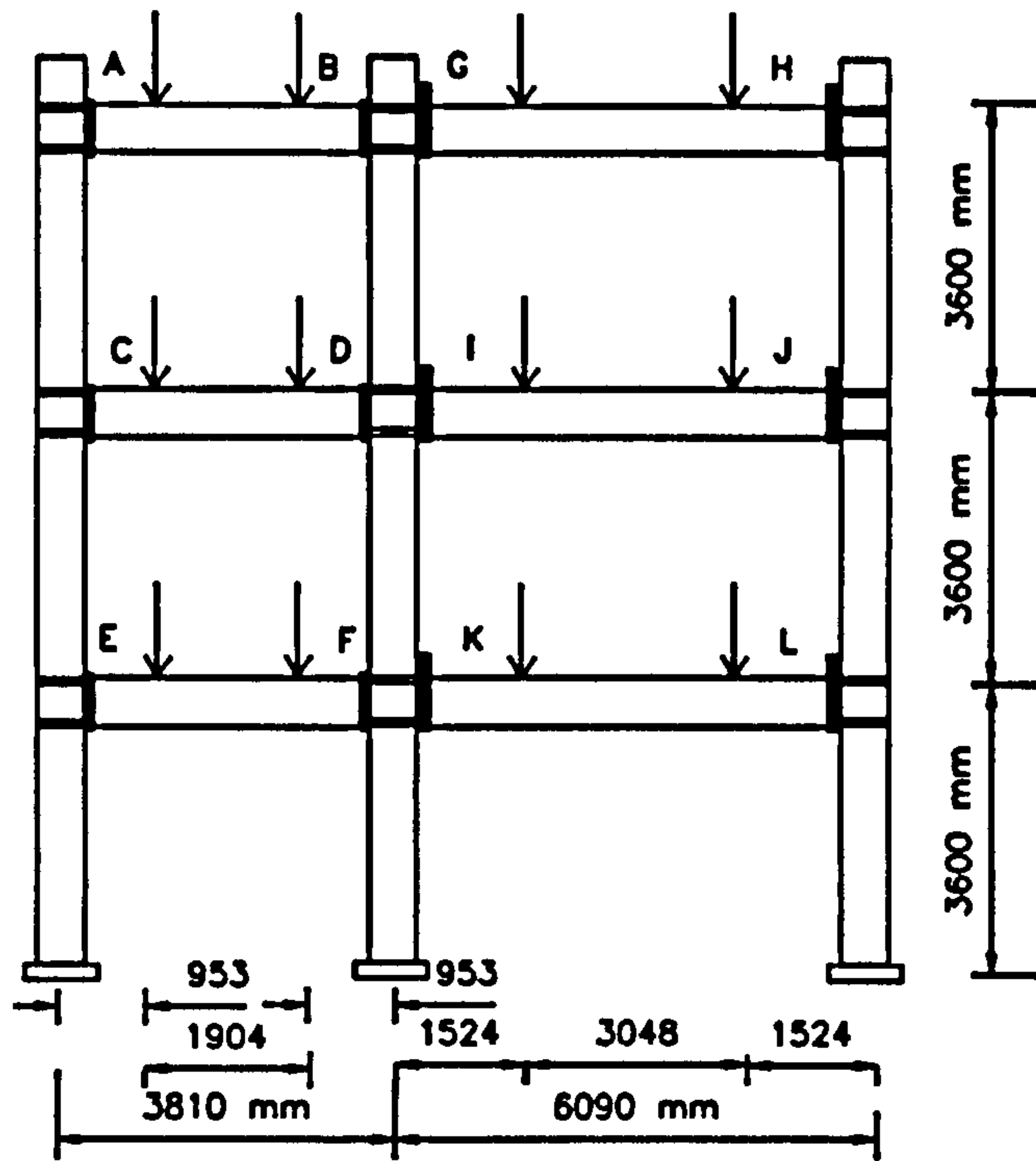
	Moment (kNm)			Mid-Span Deflection (mm)	Applied Beam Load (kN)
	Joint G	Mid-Span	Joint H		
Frame 1 (Test 30)	30	25	28	7	66.1
Frame 2 (Test 43)	143 (36)	125 (30)	143 (30)	57 (8)	229.0 (66.1)

( ) data from the applied beam load of 66.1 kN

Table 5.20 : Comparison of the Results from Beam 4 in Test to Residual Strength of Frames 1 and 2



Figure 5.1 : Frame 1 viewed towards the Balcony



Column 203 x 203 x 71 UC  
 Beam 254 x 146 x 43 UB  
 All Grade 43A Steel

Figure 5.2 : General Arrangement of Frames 1 and 2

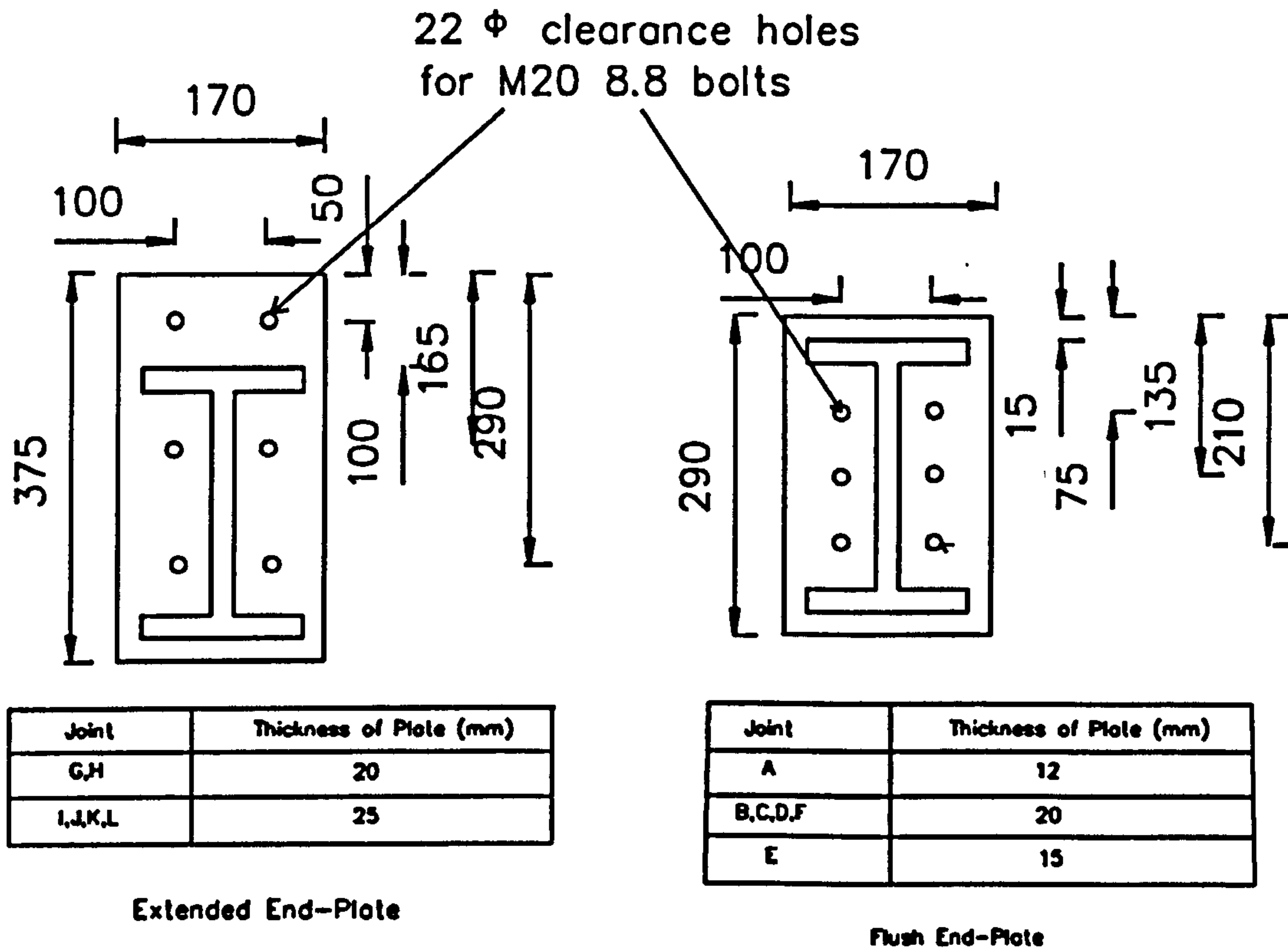


Figure 5.3 : Dimensions of Connections used in Frames 1 and 2

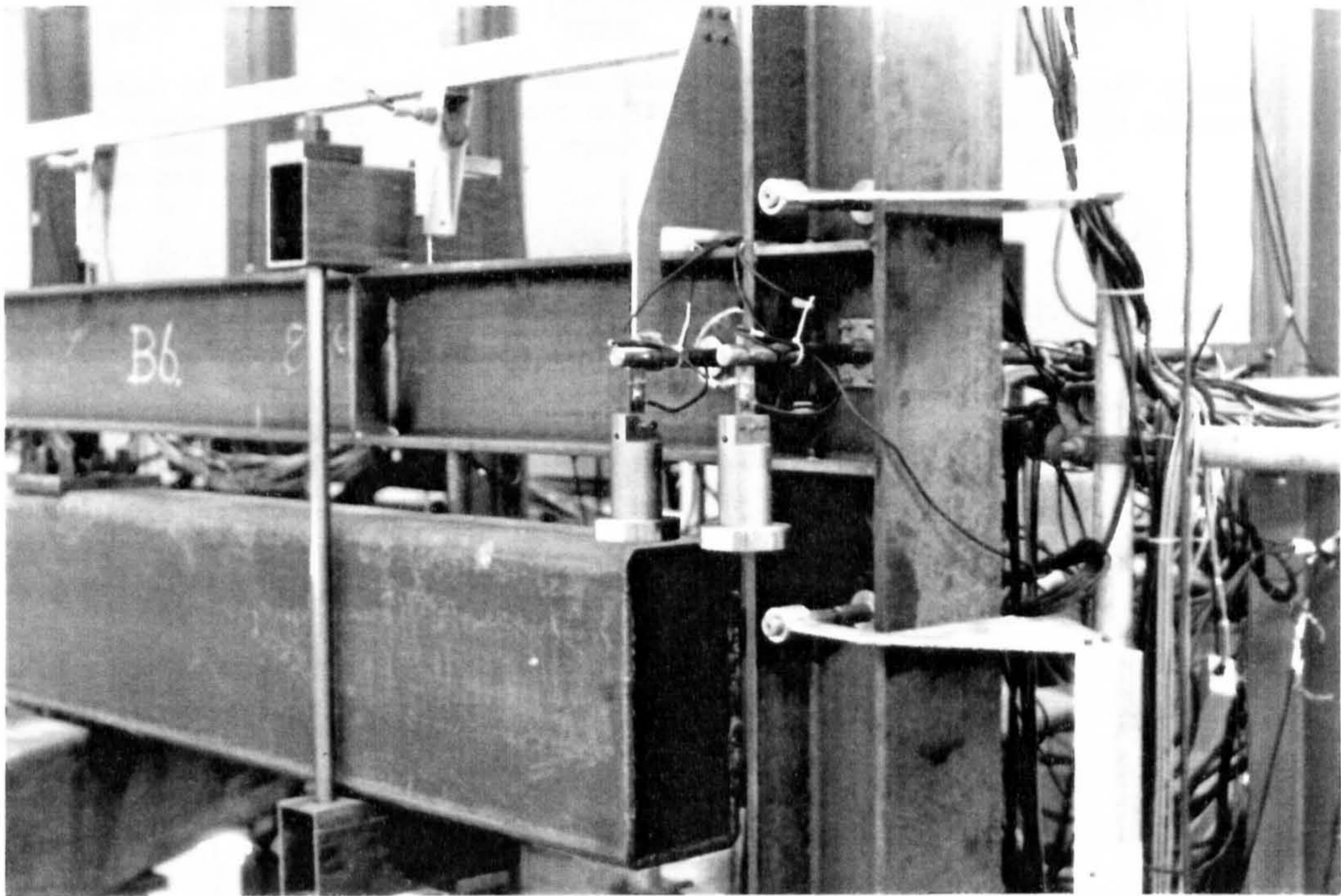
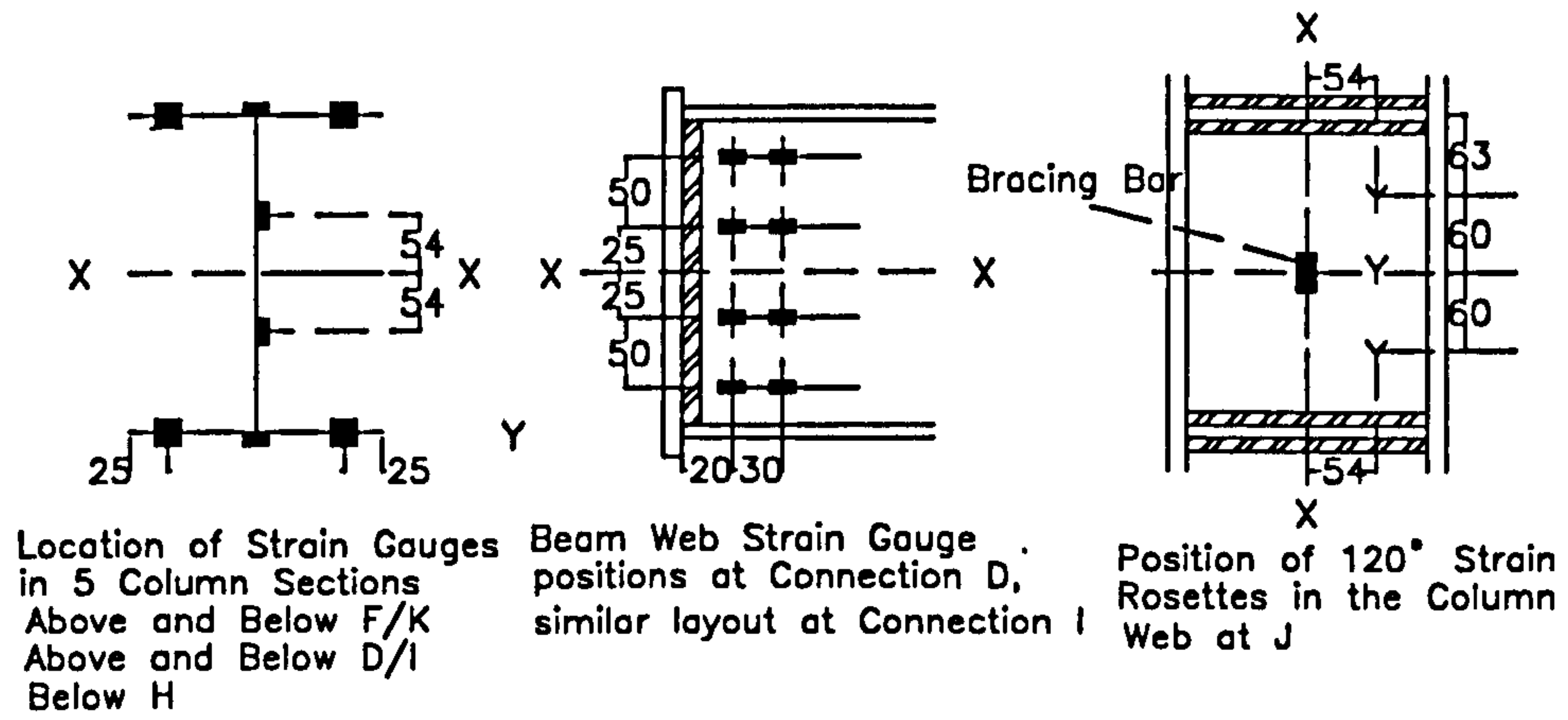


Figure 5.4 : Stiffeners located in a Column near Connection at Beam Loading Point



(All Dimensions in mm)

Figure 5.5 : Stain Gauge Positions for Frame 2

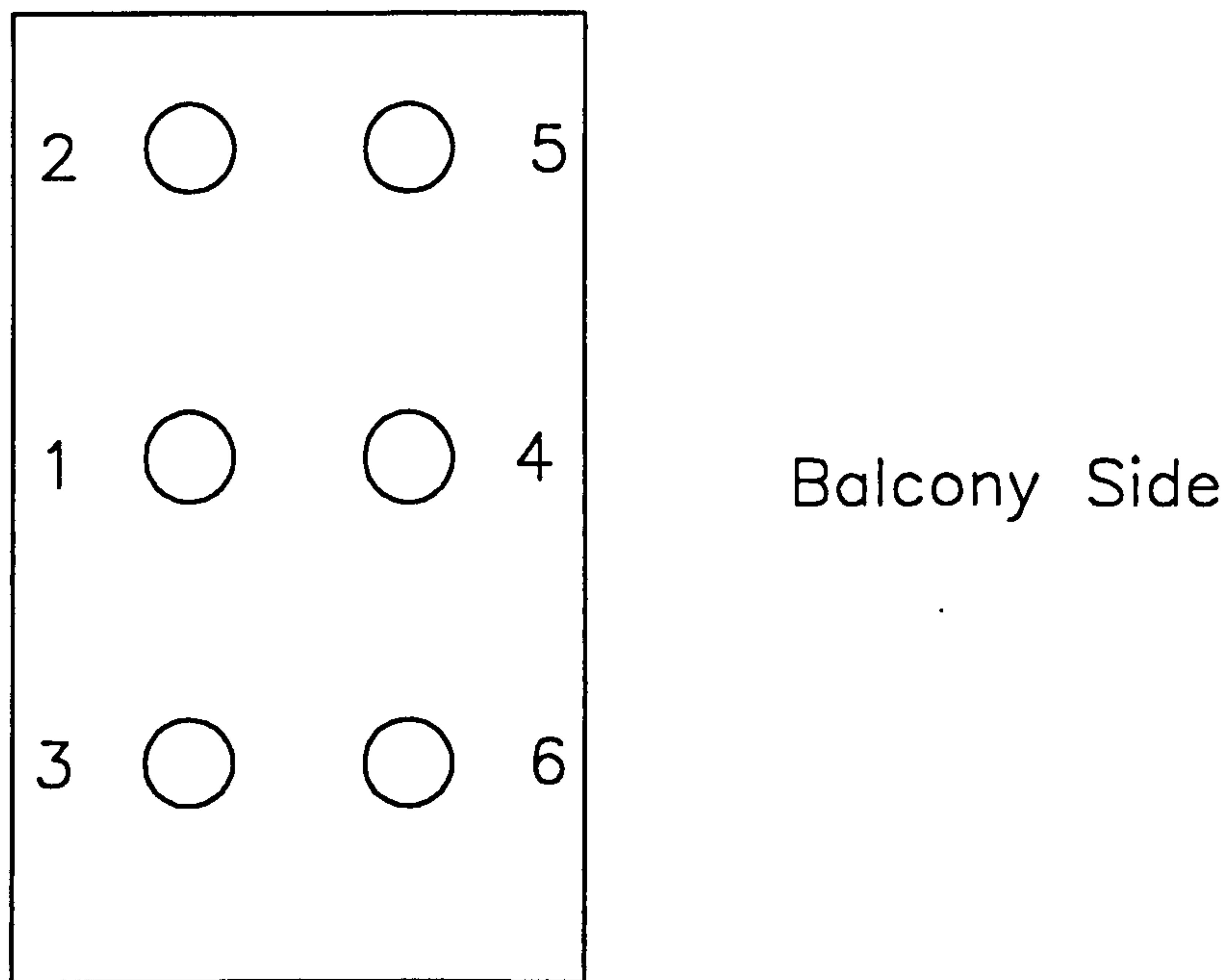
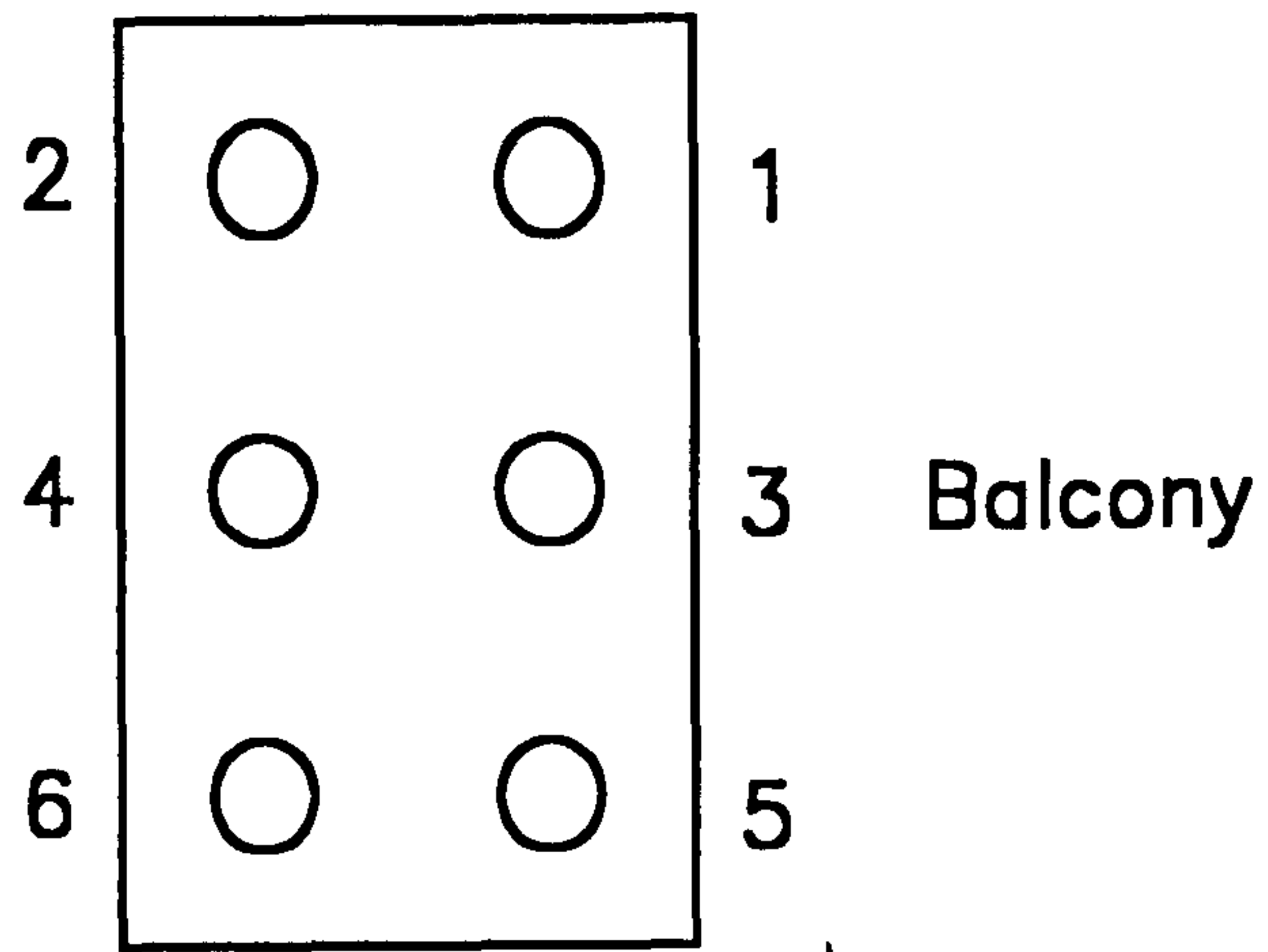
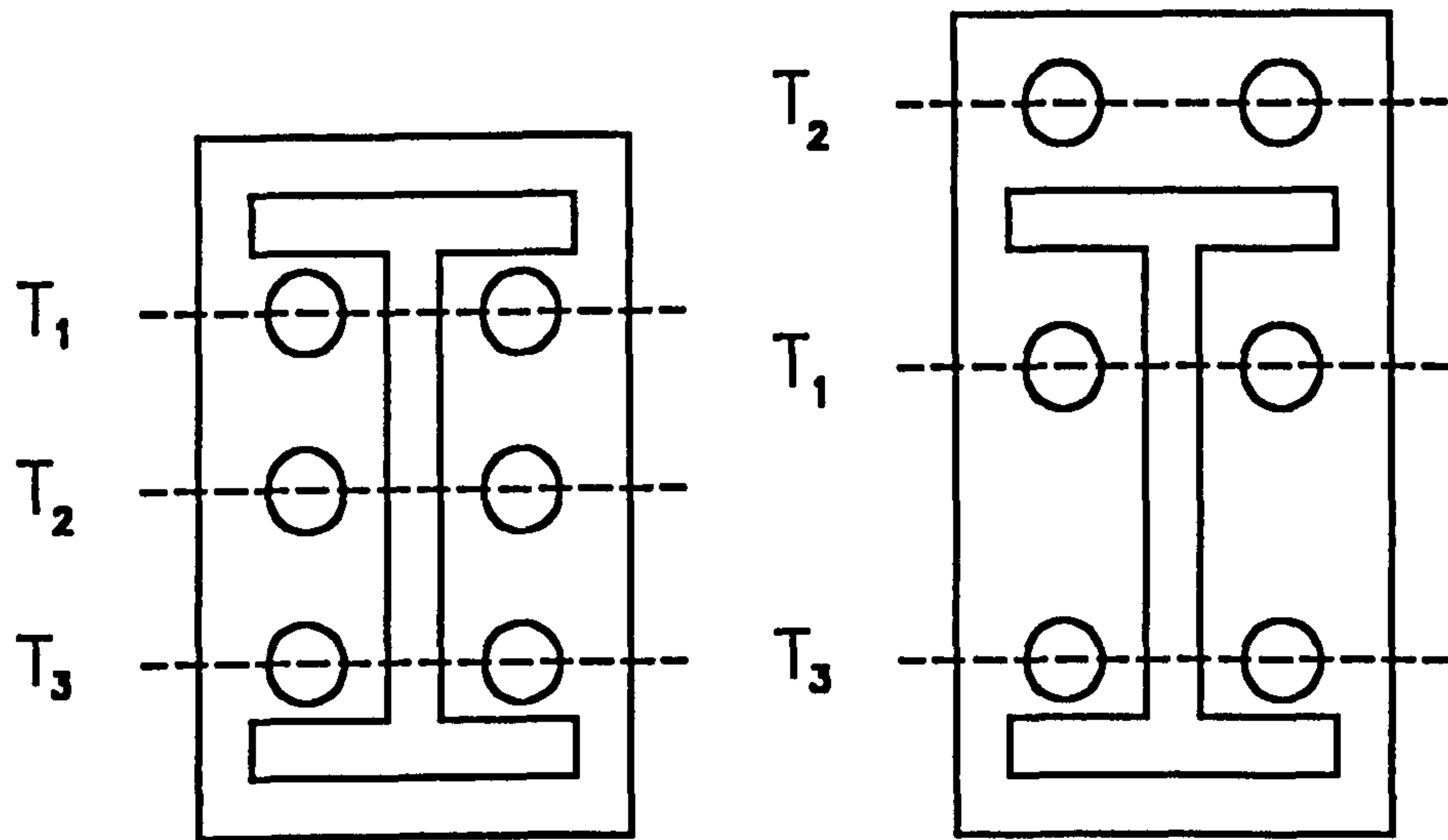


Figure 5.6 : Bolts Tightening Sequence



Nomenclature of Bolts



Position of Bolt Rows

Figure 5.7 : Nomenclature and Position of Bolts

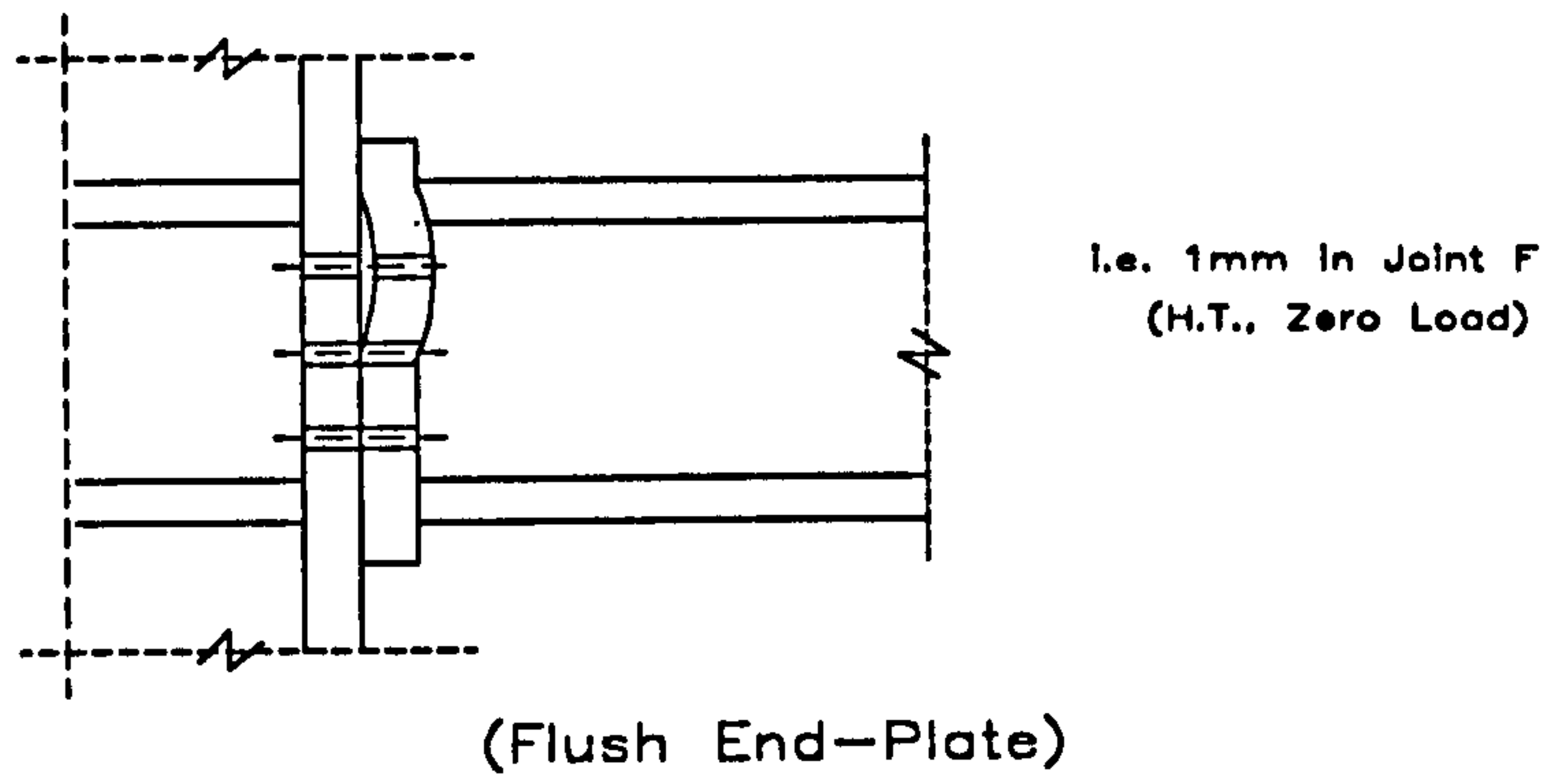


Figure 5.8 : Lack-of-fit Type 1

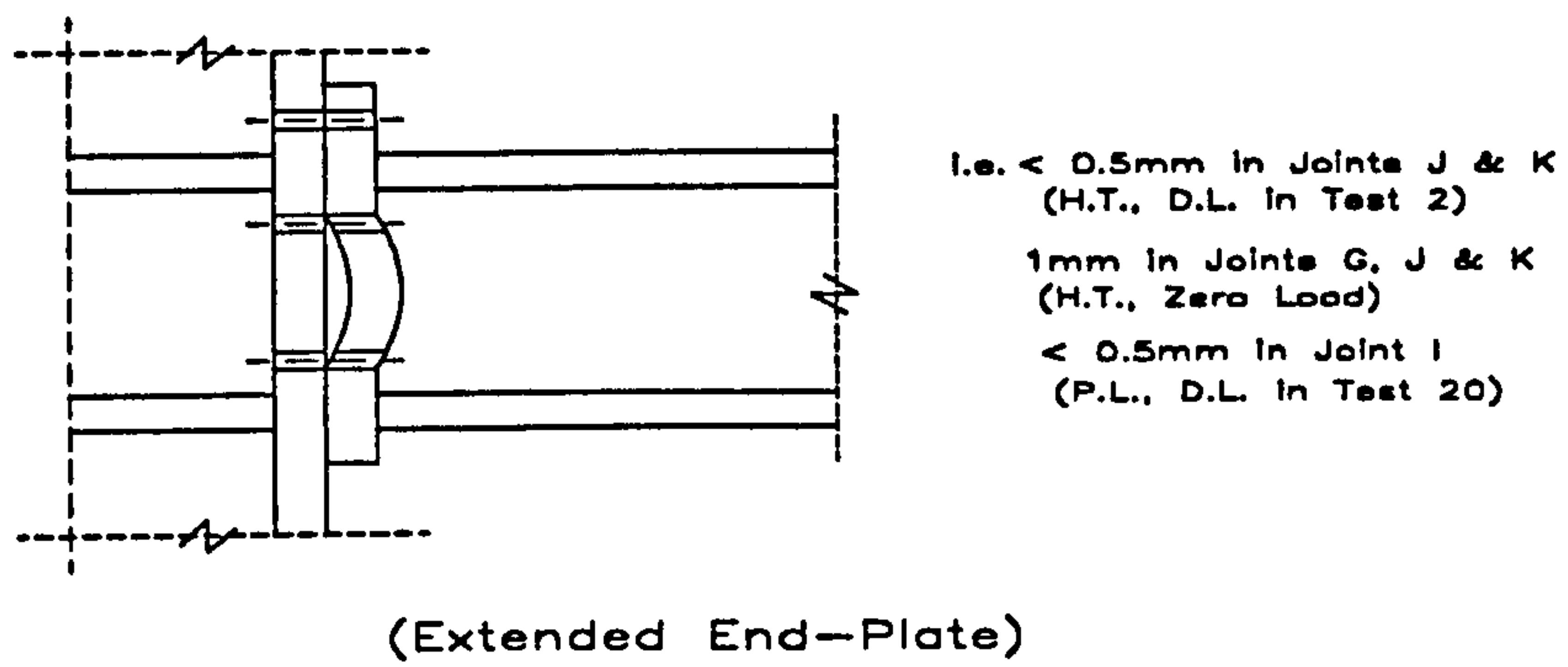


Figure 5.9 : Lack-of-fit Type 2

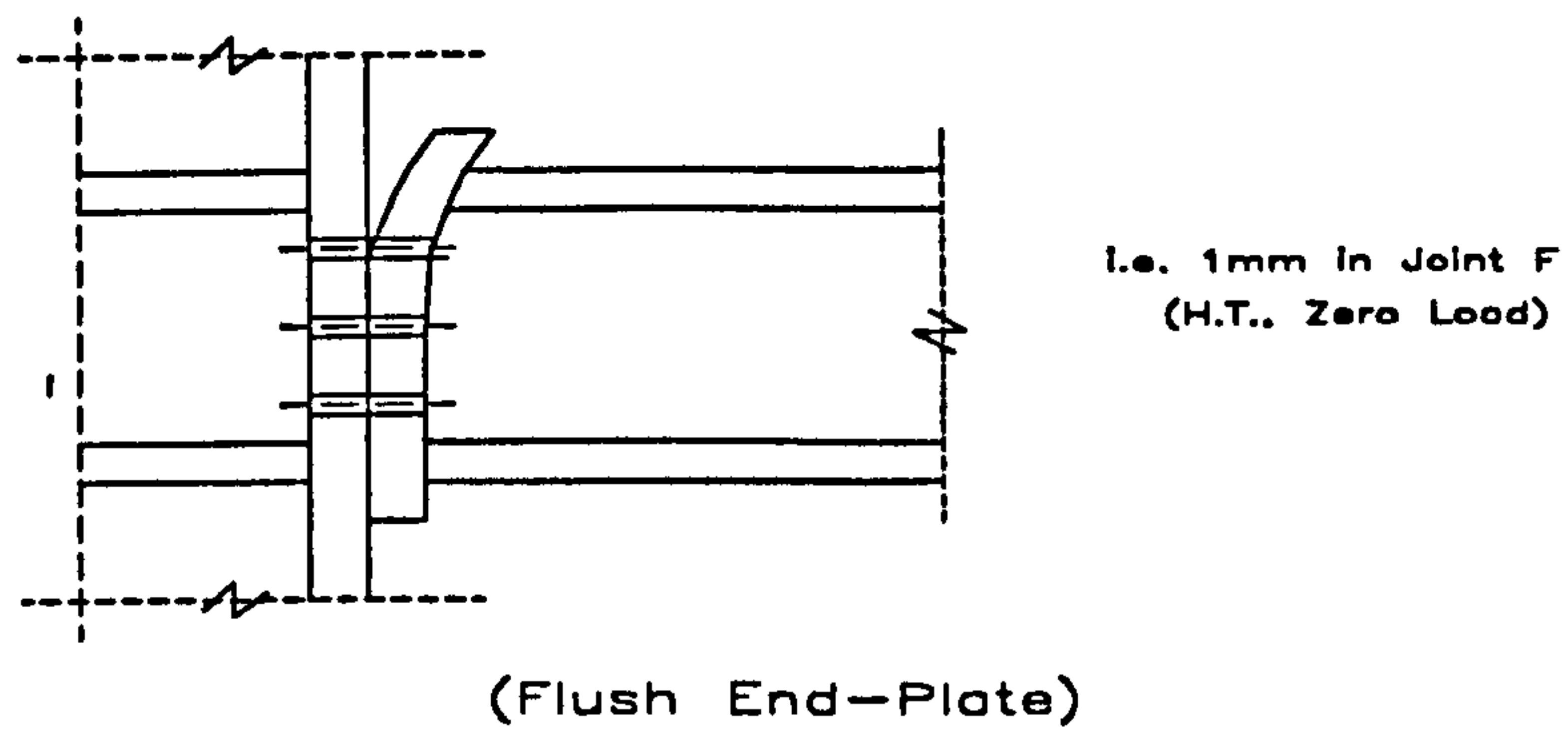


Figure 5.10 : Lack-of-fit Type 3



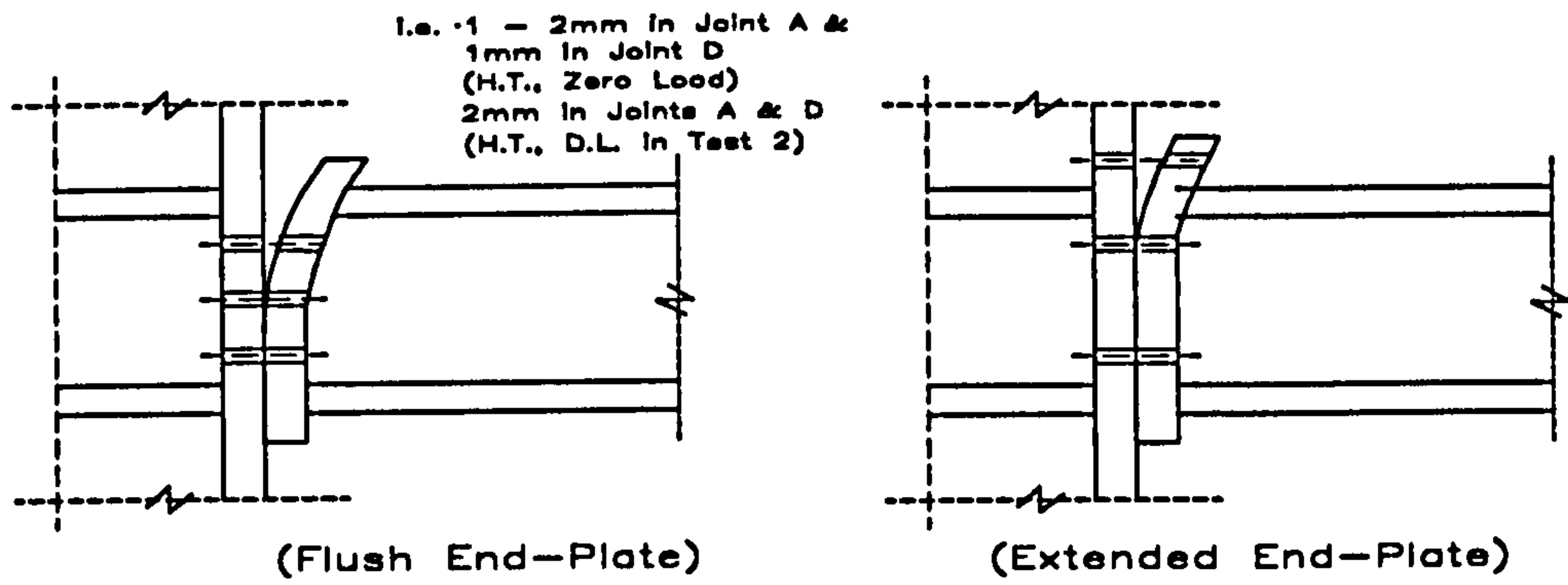


Figure 5.11 : Lack-of-fit Type 4

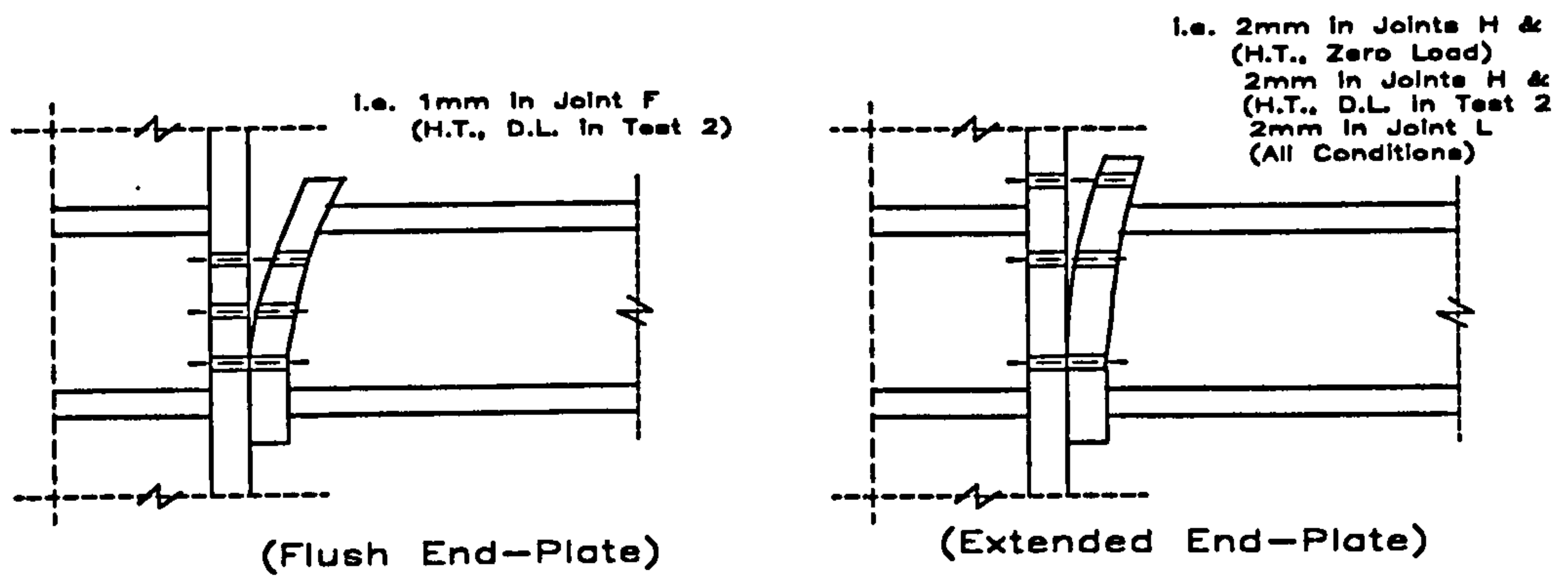


Figure 5.12 : Lack-of-fit Type 5

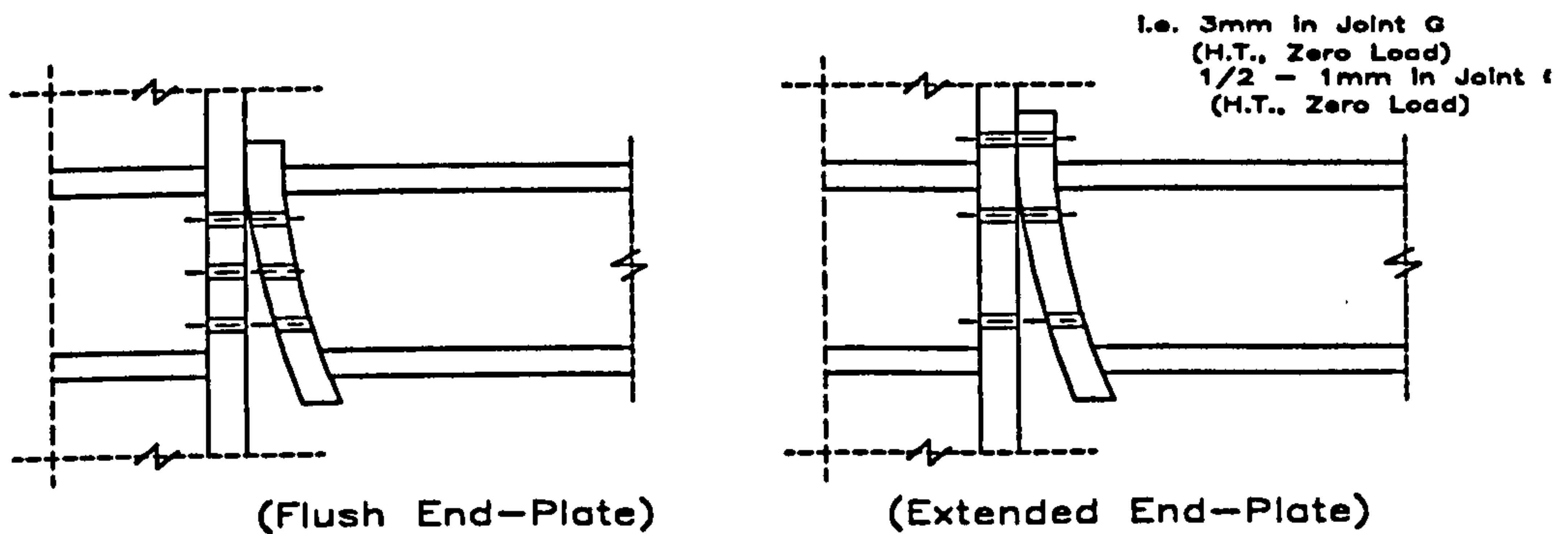


Figure 5.13 : Lack-of-fit Type 6

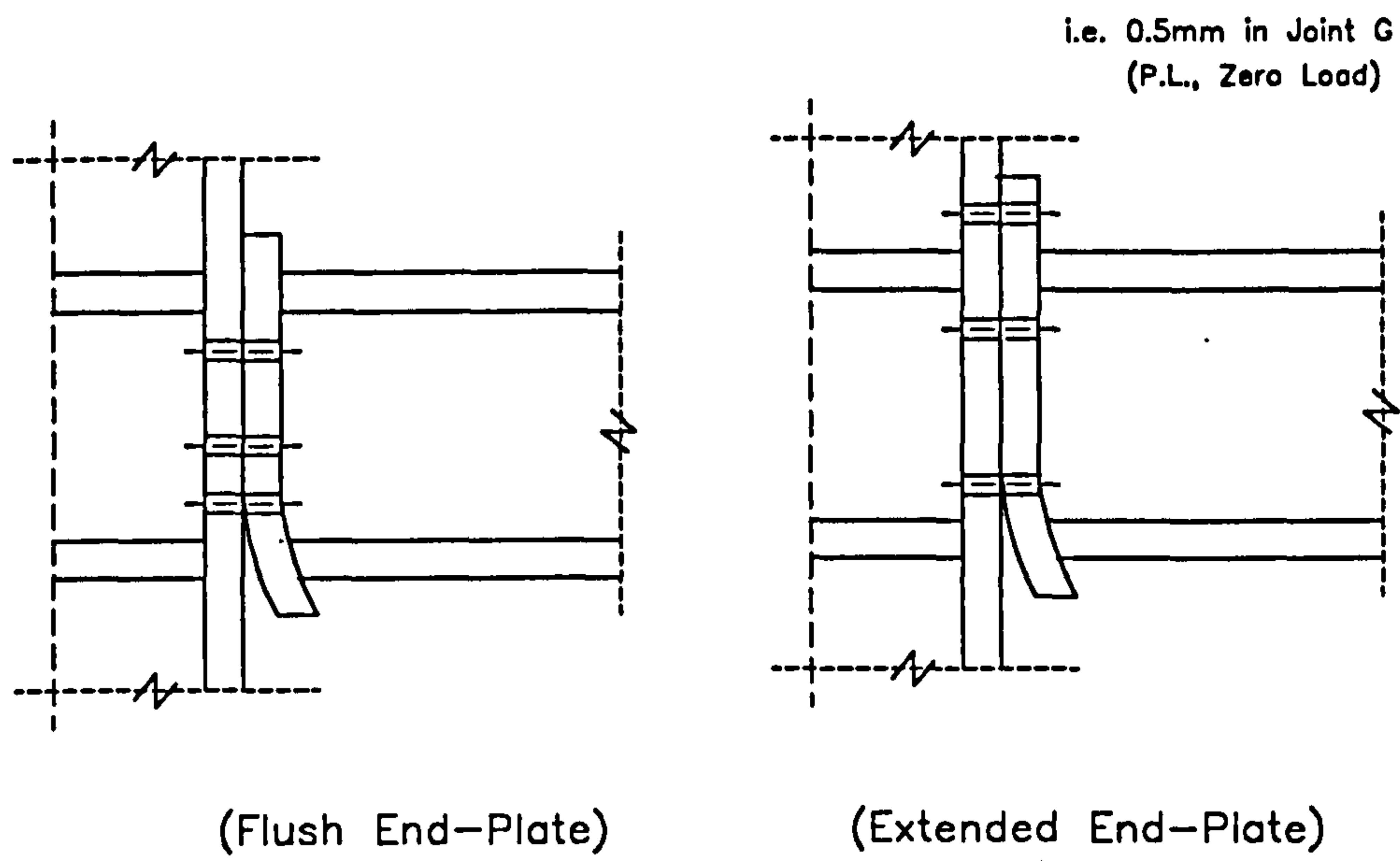


Figure 5.14 : Lack-of-fit Type 7

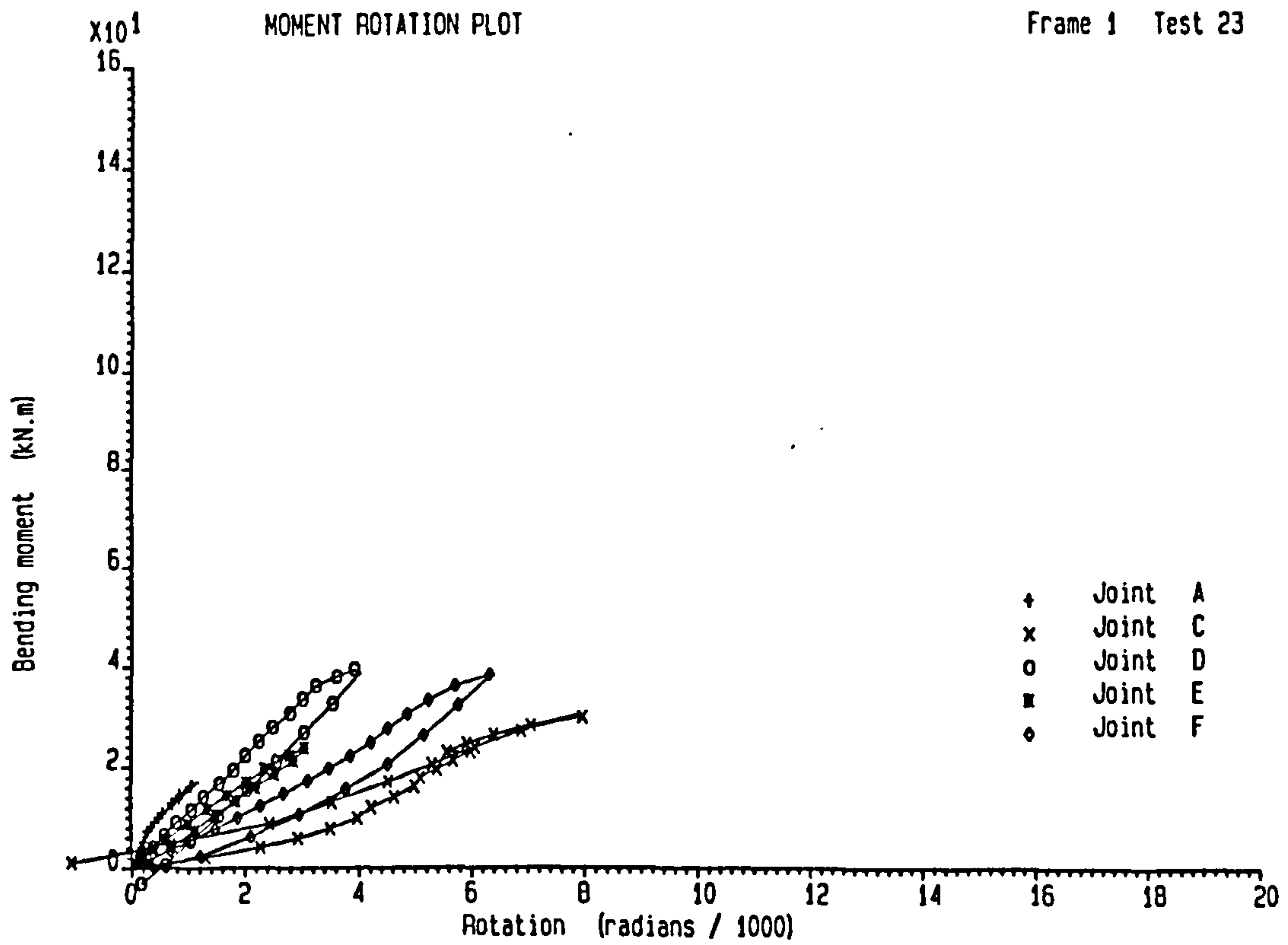


Figure 5.15 : Moment Rotation Curve for Test 23 of Frame 1 (Flush End-Plate)

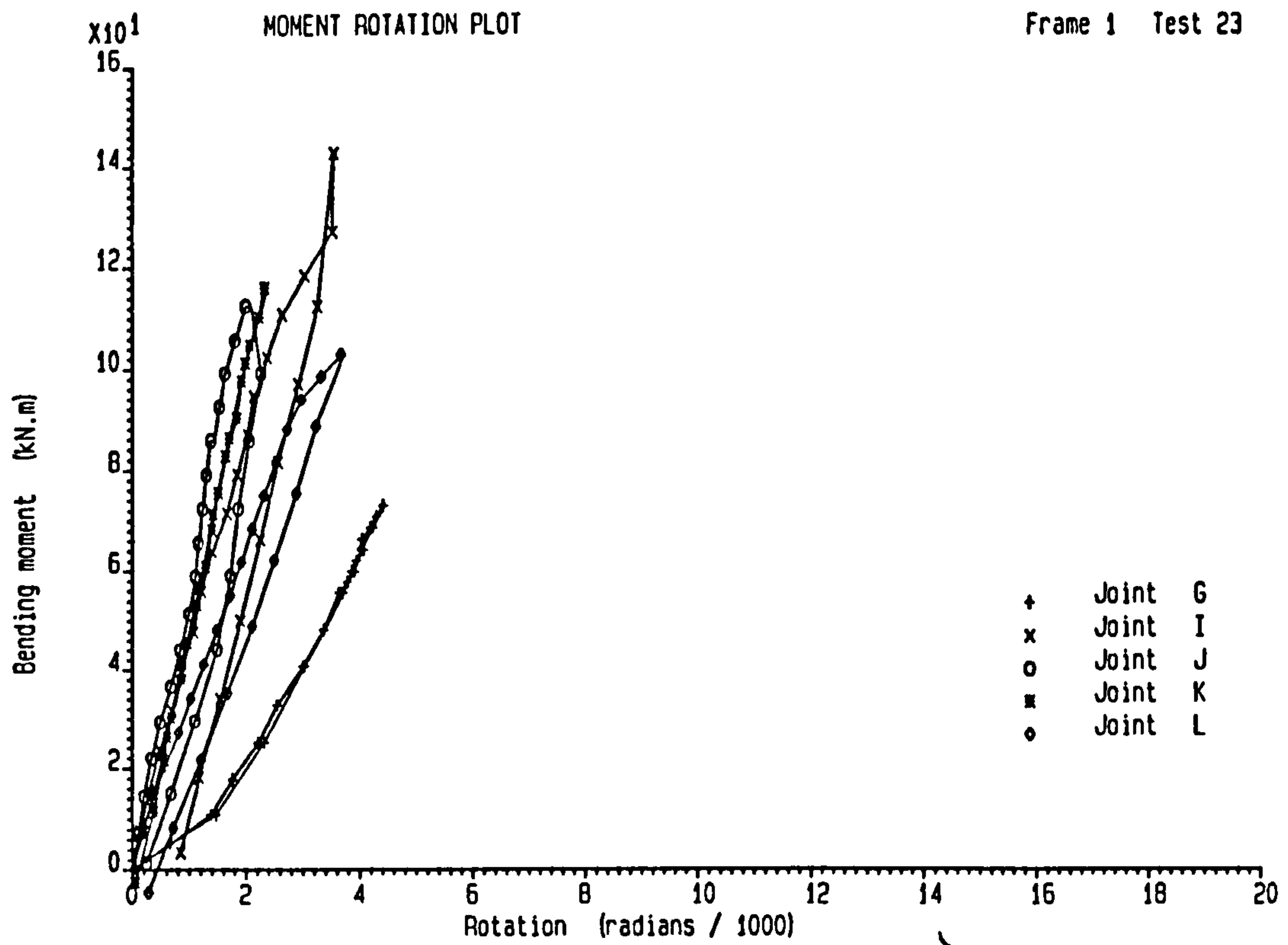


Figure 5.16 : Moment Rotation Curve for Test 23 of Frame 1  
(Extended End-Plate)

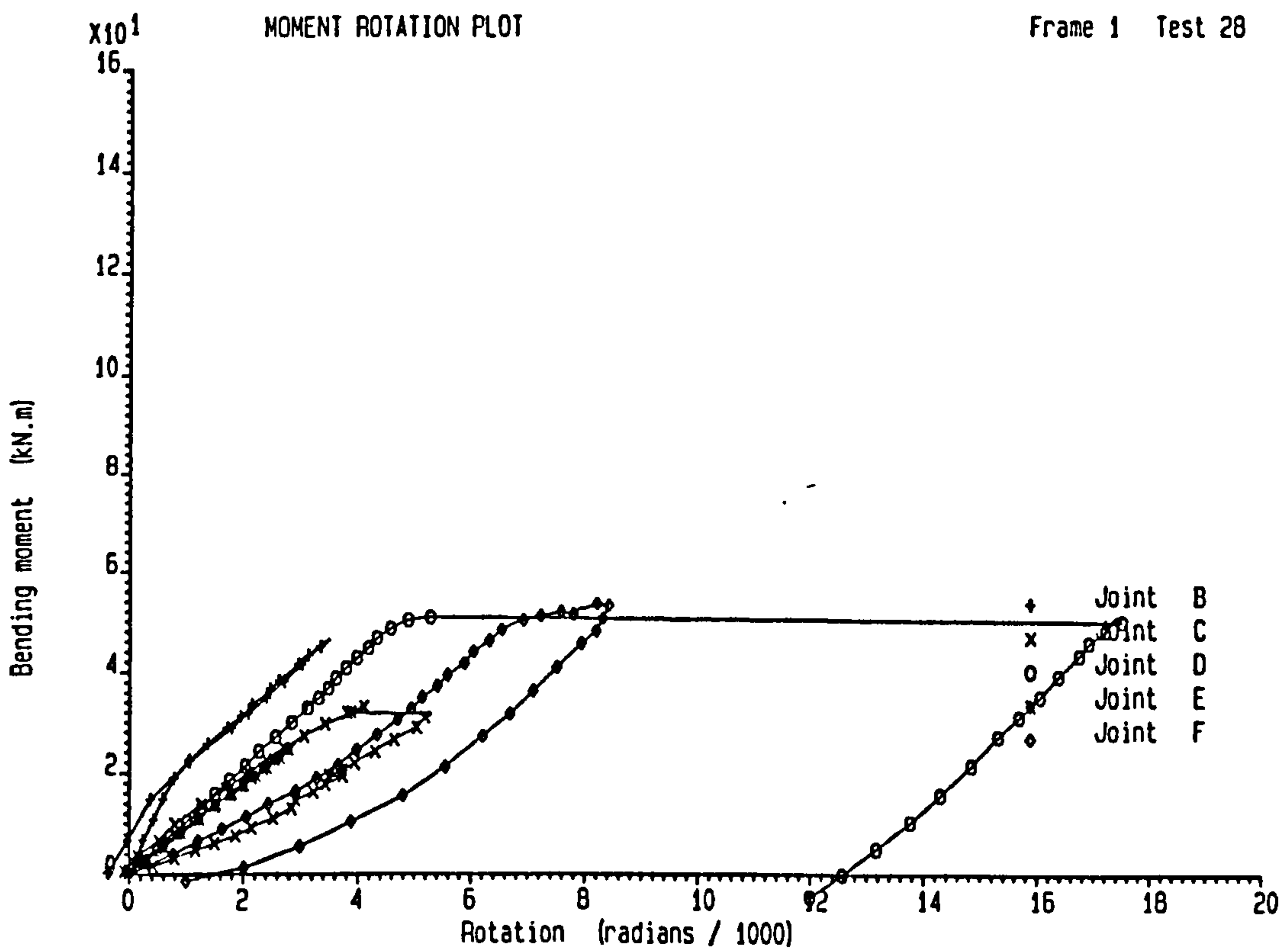


Figure 5.17 : Moment Rotation Curve for Test 28 of Frame 1  
(Flush End-Plate)

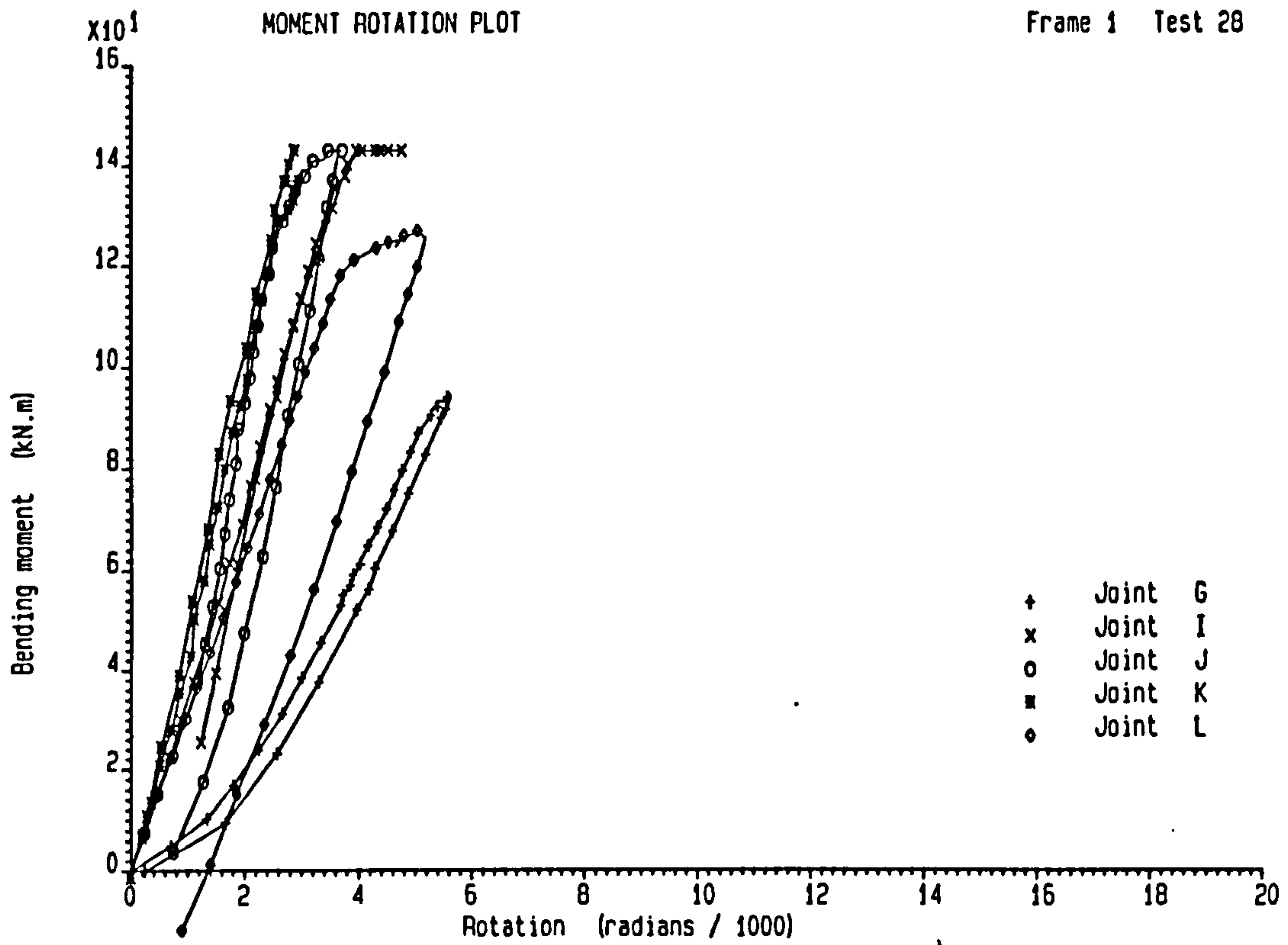


Figure 5.18 : Moment Rotation Curve for Test 28 of Frame 1  
(Extended End-Plate)

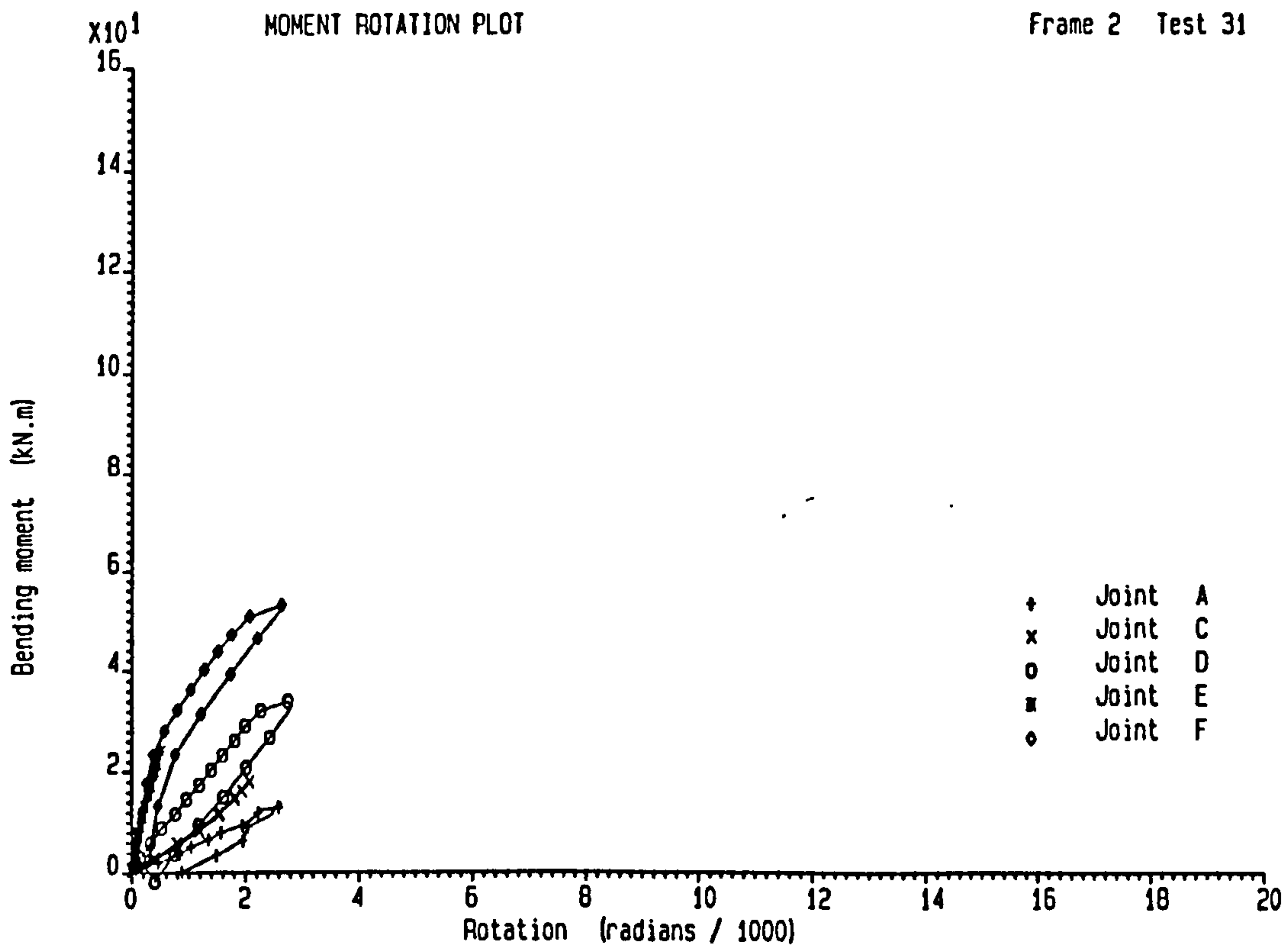


Figure 5.19 : Moment Rotation Curve for Test 31 of Frame 2  
(Flush End-Plate)

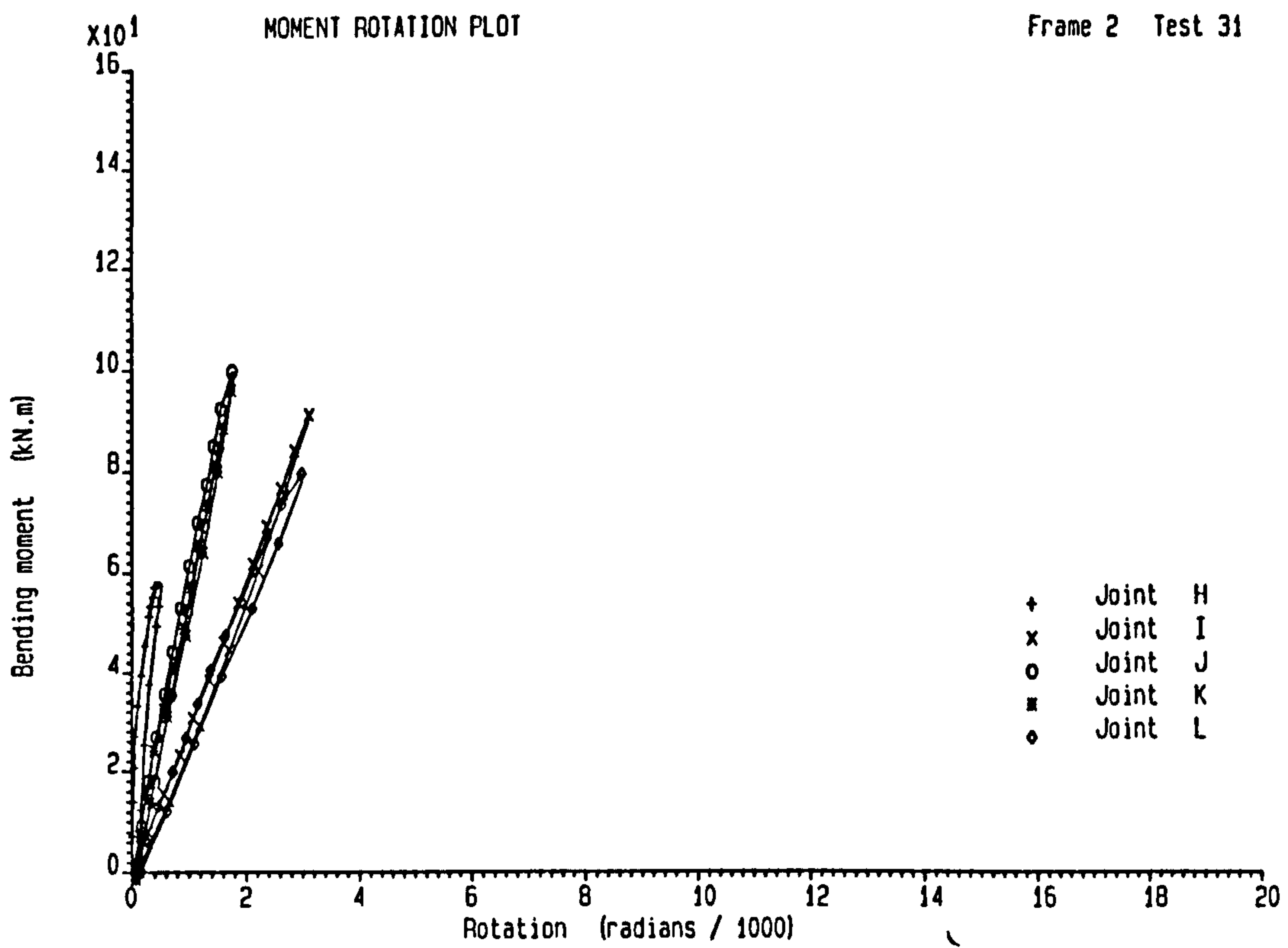


Figure 5.20 : Moment Rotation Curve for Test 31 of Frame 2  
(Extended End-Plate)

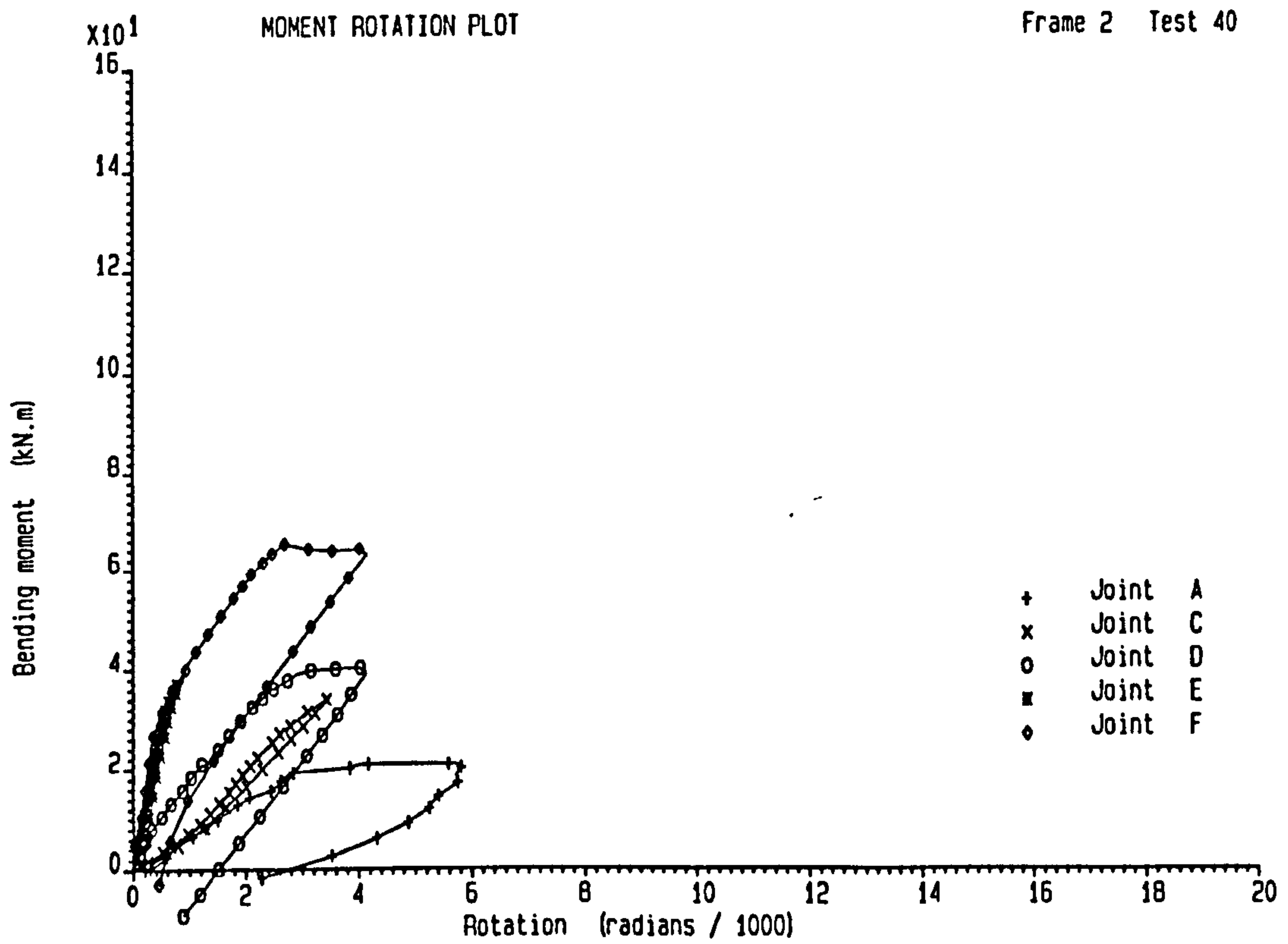


Figure 5.21 : Moment Rotation Curve for Test 40 of Frame 2  
(Flush End-Plate)

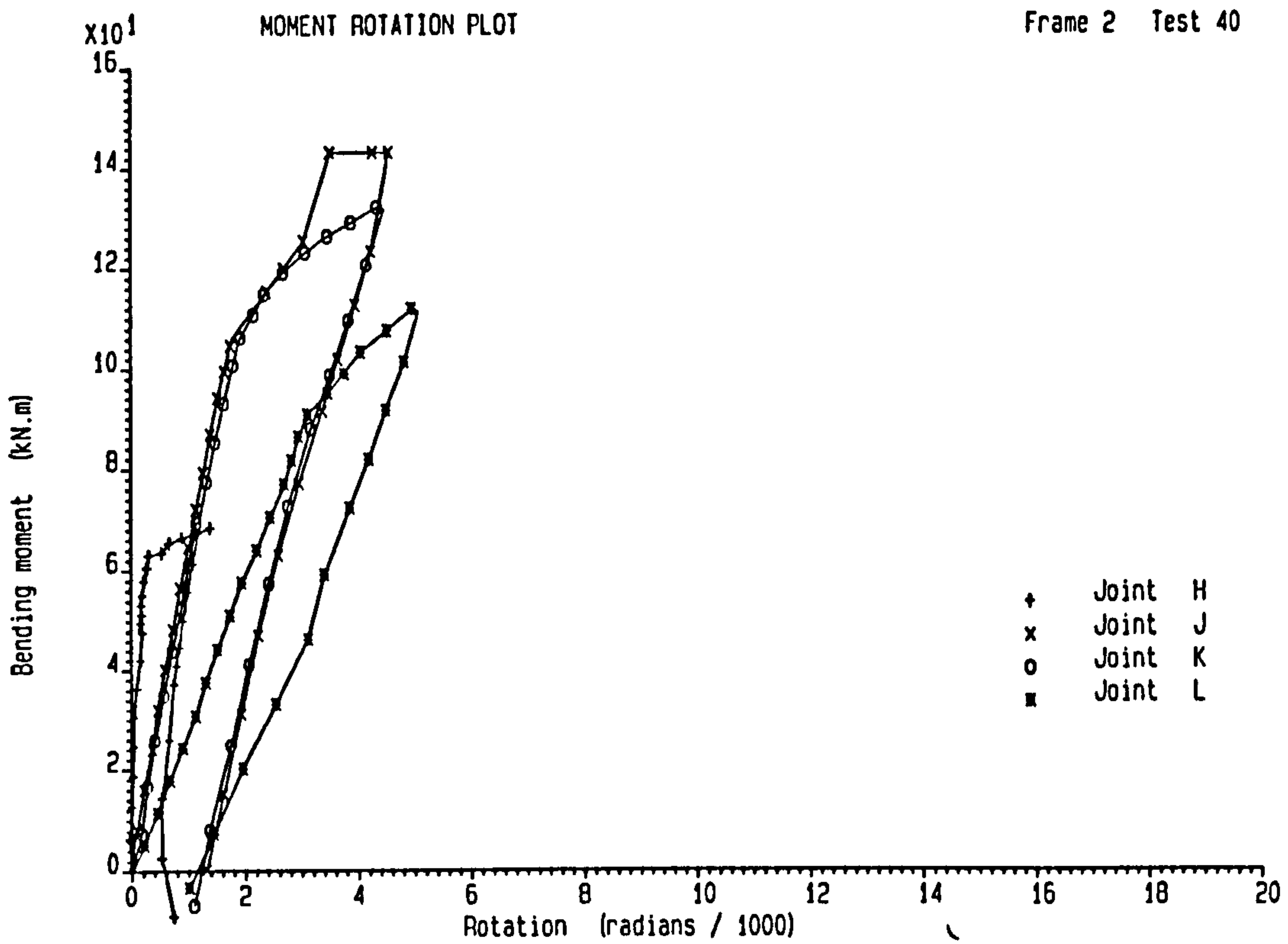
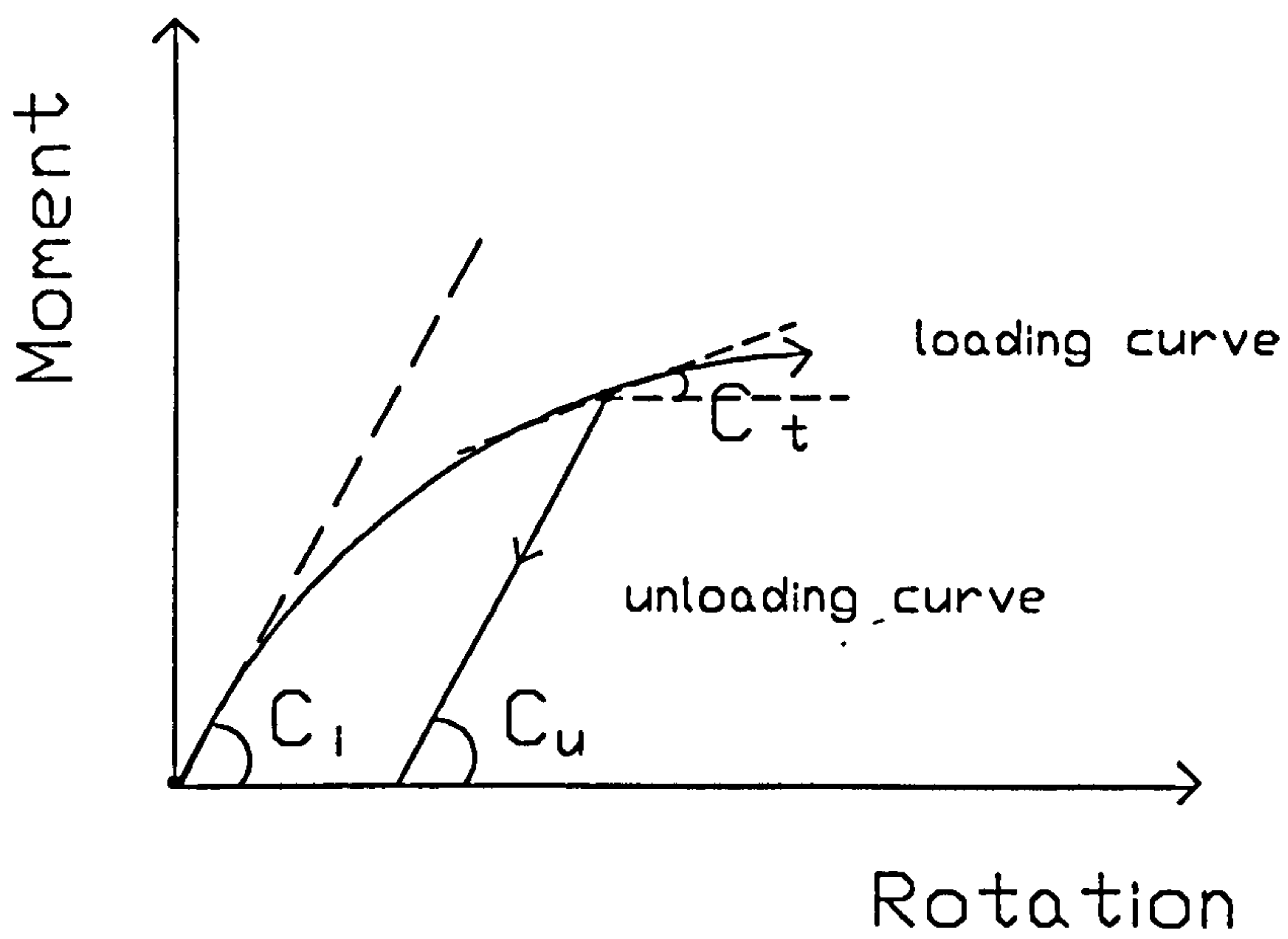


Figure 5.22 : Moment Rotation Curves for Test 40 of Frame 2 (Extended End-Plate)



Where  $C_i = C_u$

Figure 5.23 : A Typical Moment Rotation Curve

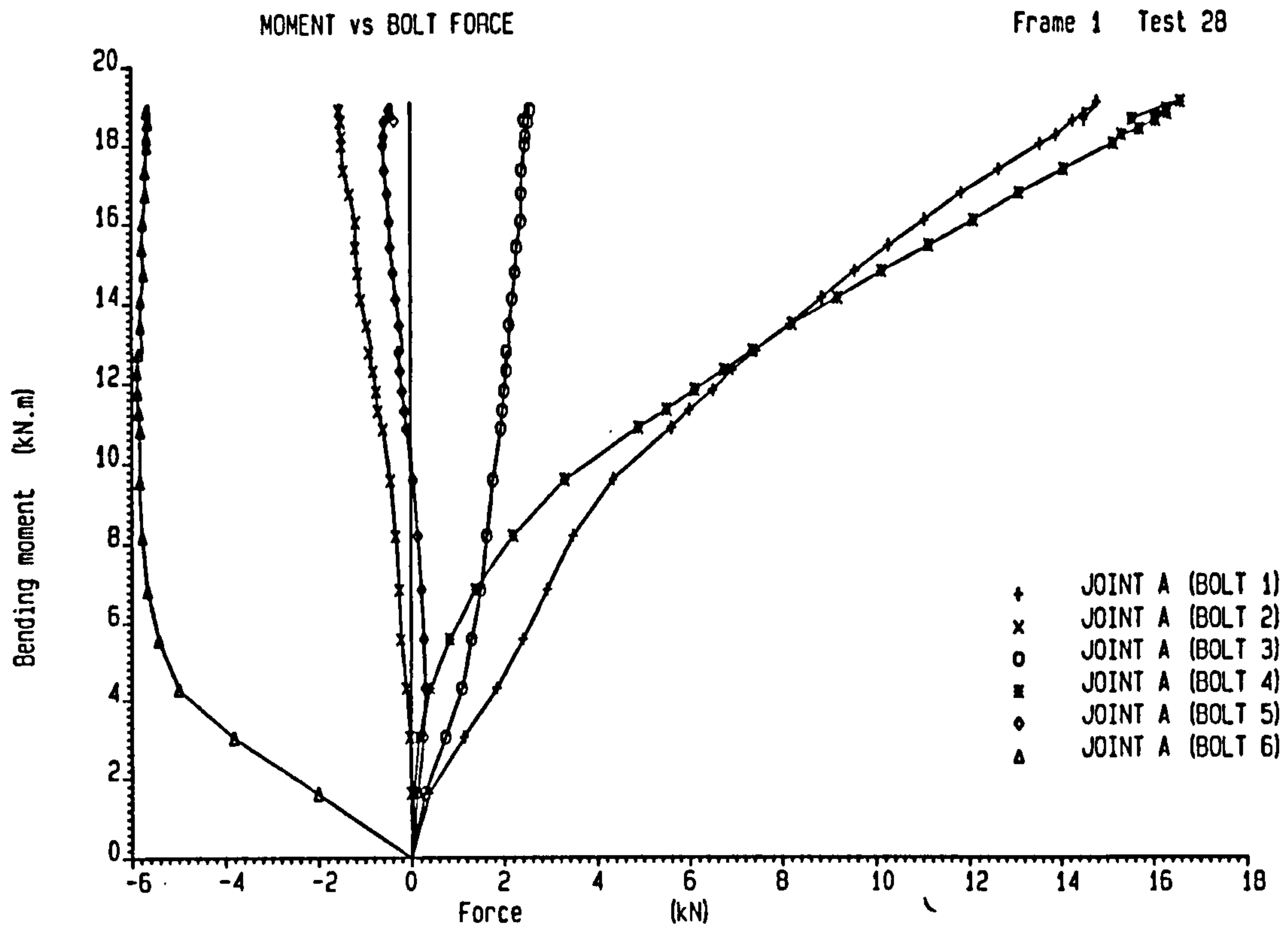


Figure 5.24 : Moment against Bolt Forces at Joint A for Test 28 of Frame 1

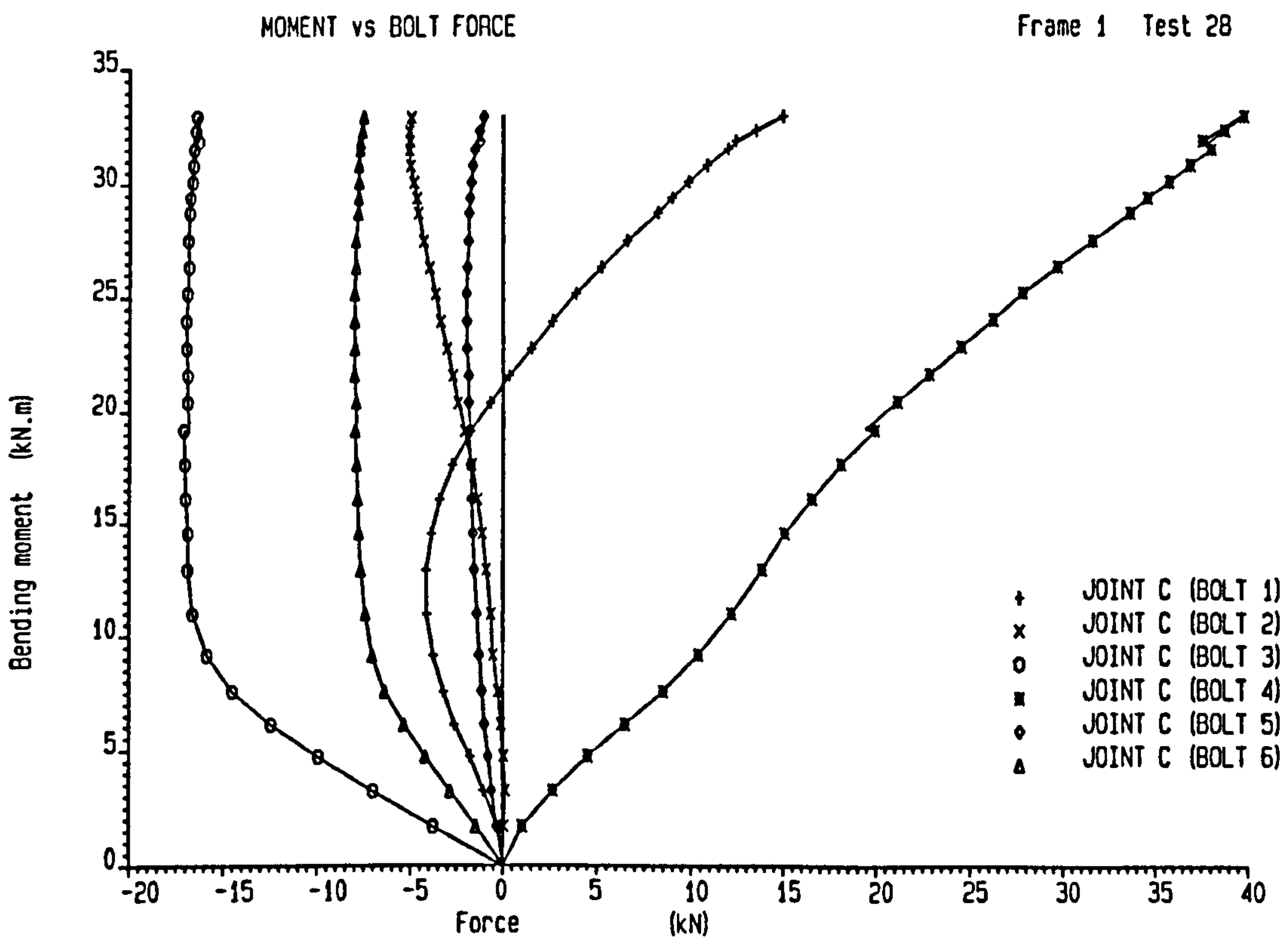


Figure 5.25 : Moment against Bolt Forces at Joint C for Test 28 of Frame 1

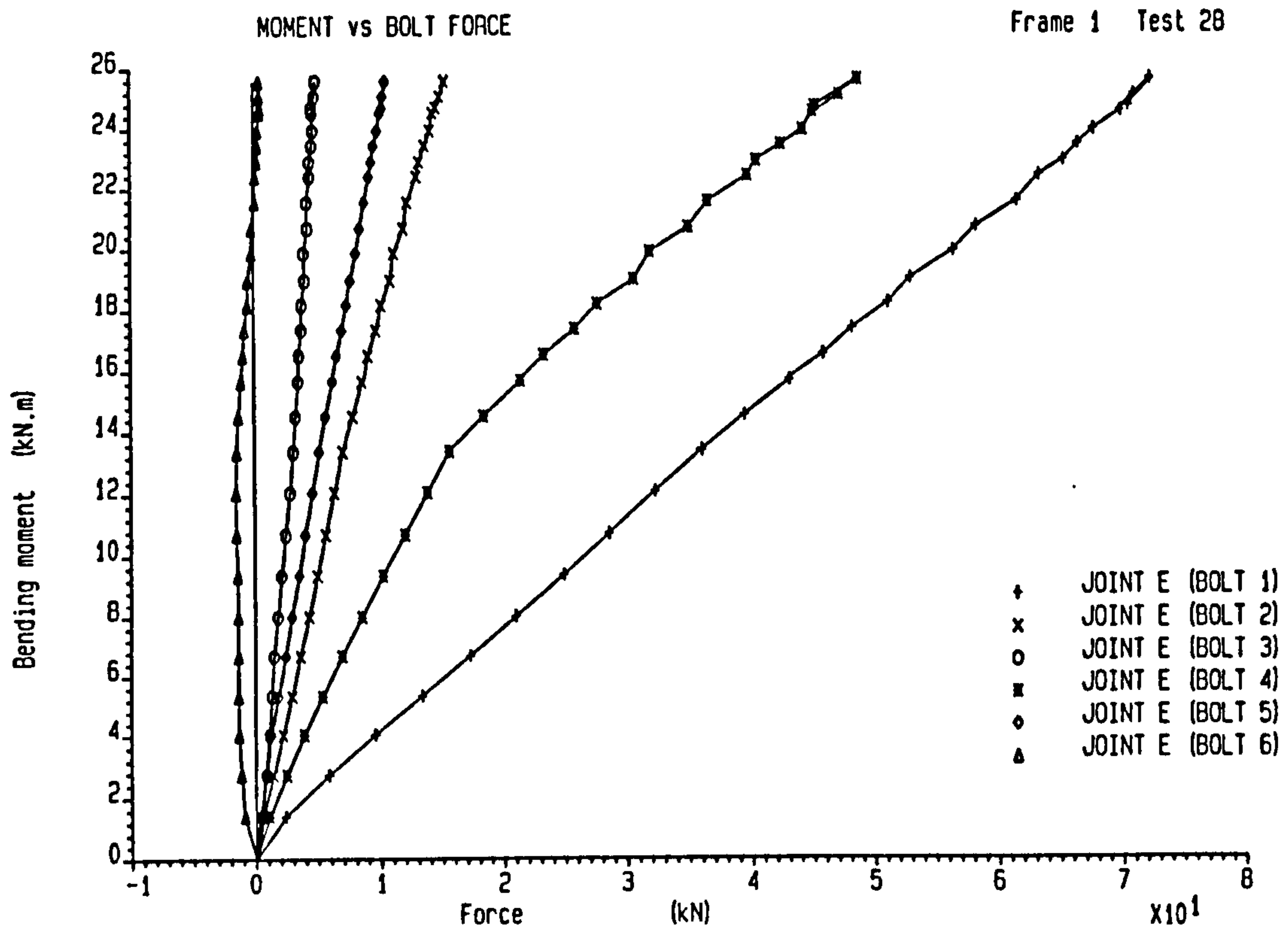


Figure 5.26 : Moment against Bolt Forces at Joint E for Test 28 of Frame 1

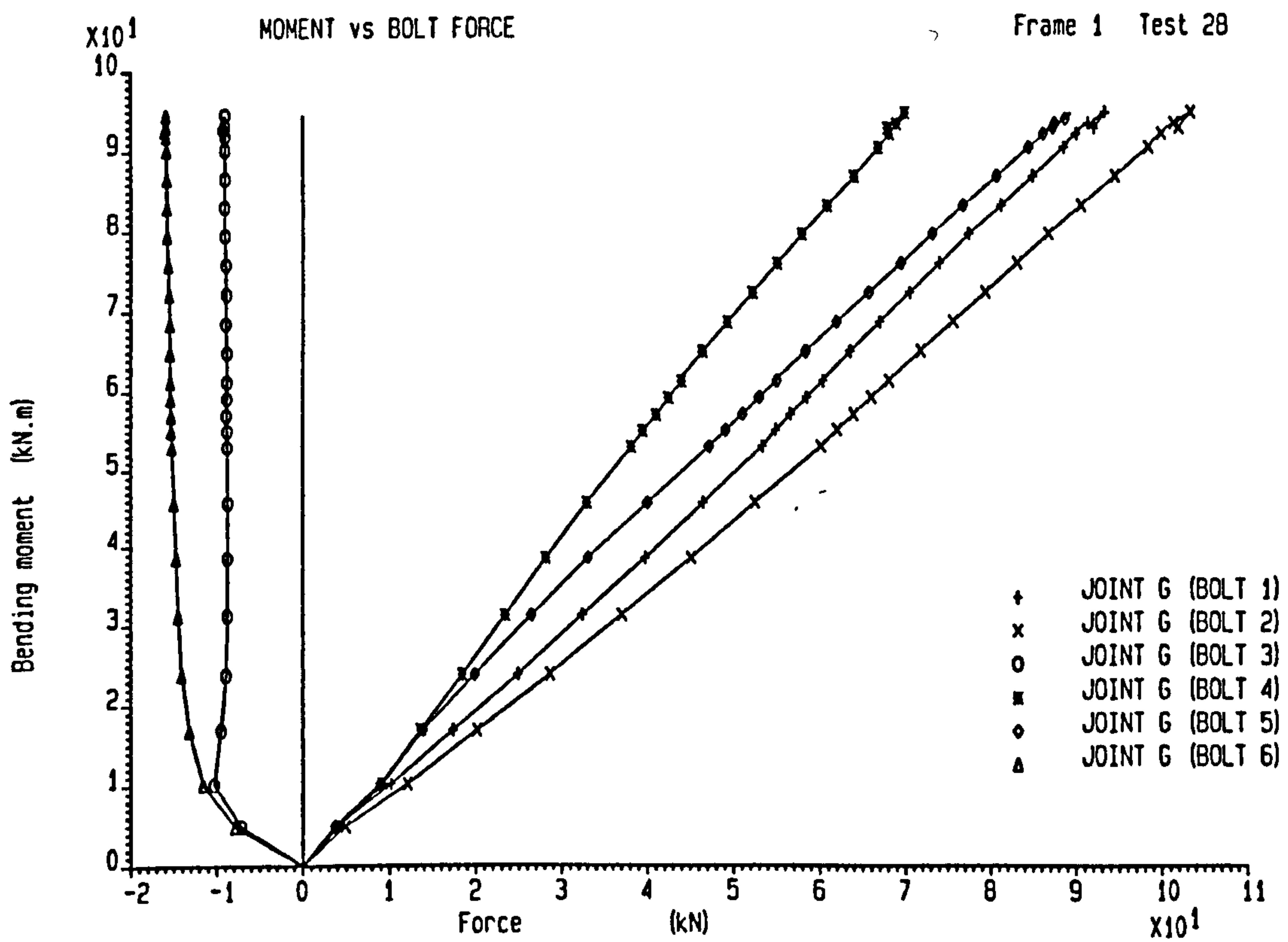


Figure 5.27 : Moment against Bolt Forces at Joint G for Test 28 of Frame 1



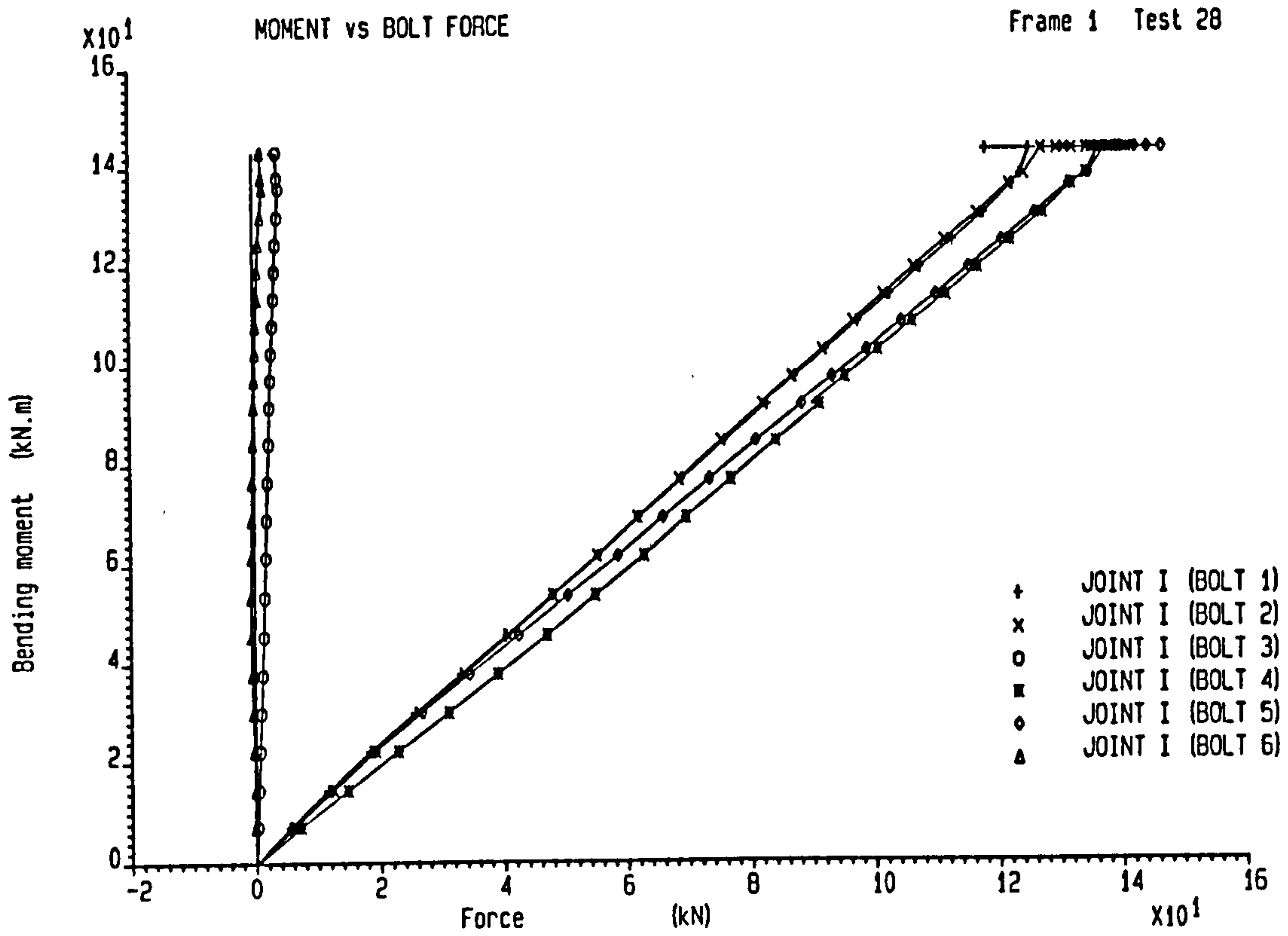


Figure 5.28 : Moment against Bolt Forces at Joint I for Test 28 of Frame 1

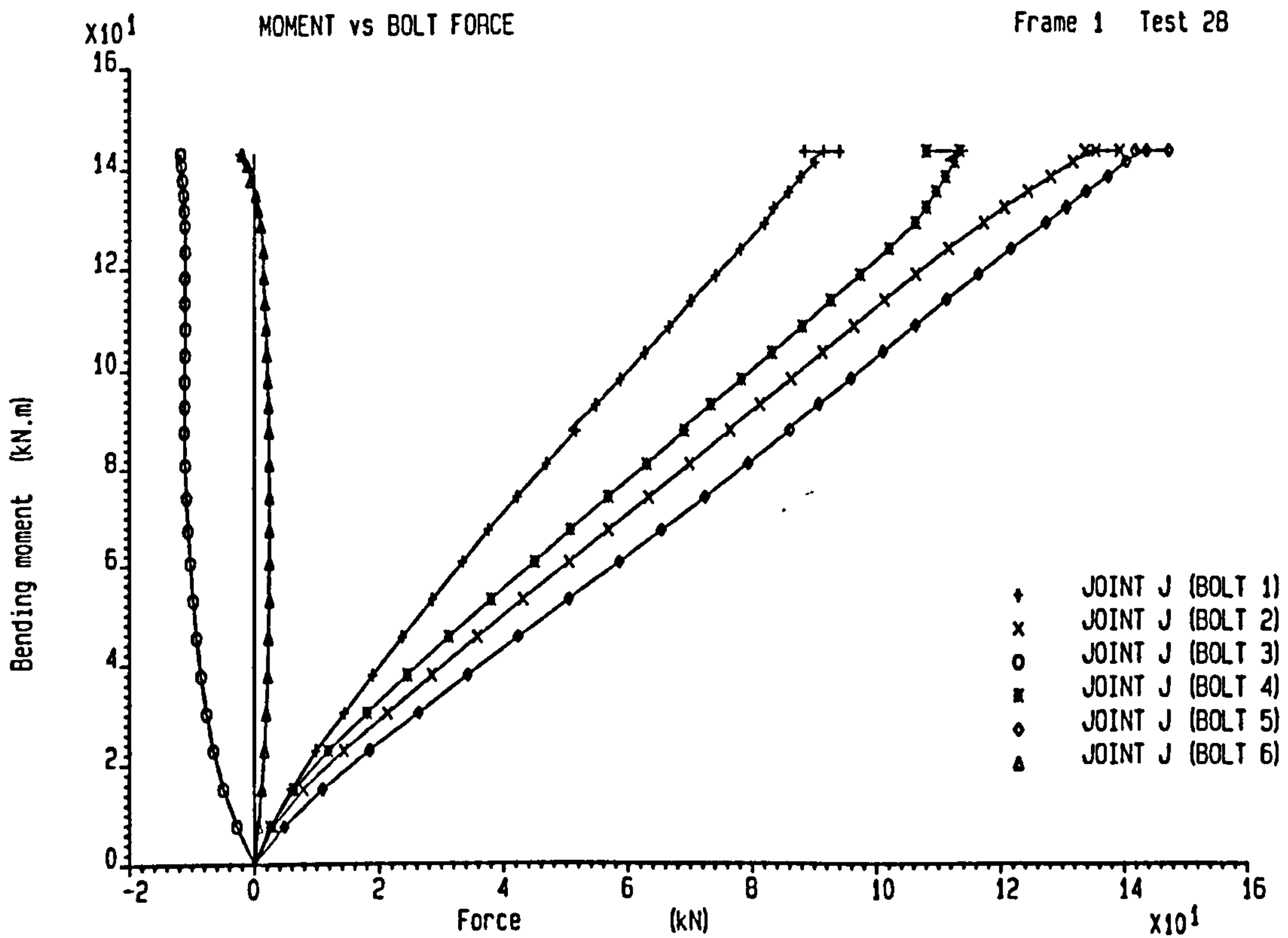


Figure 5.29 : Moment against Bolt Forces at Joint J for Test 28 of Frame 1

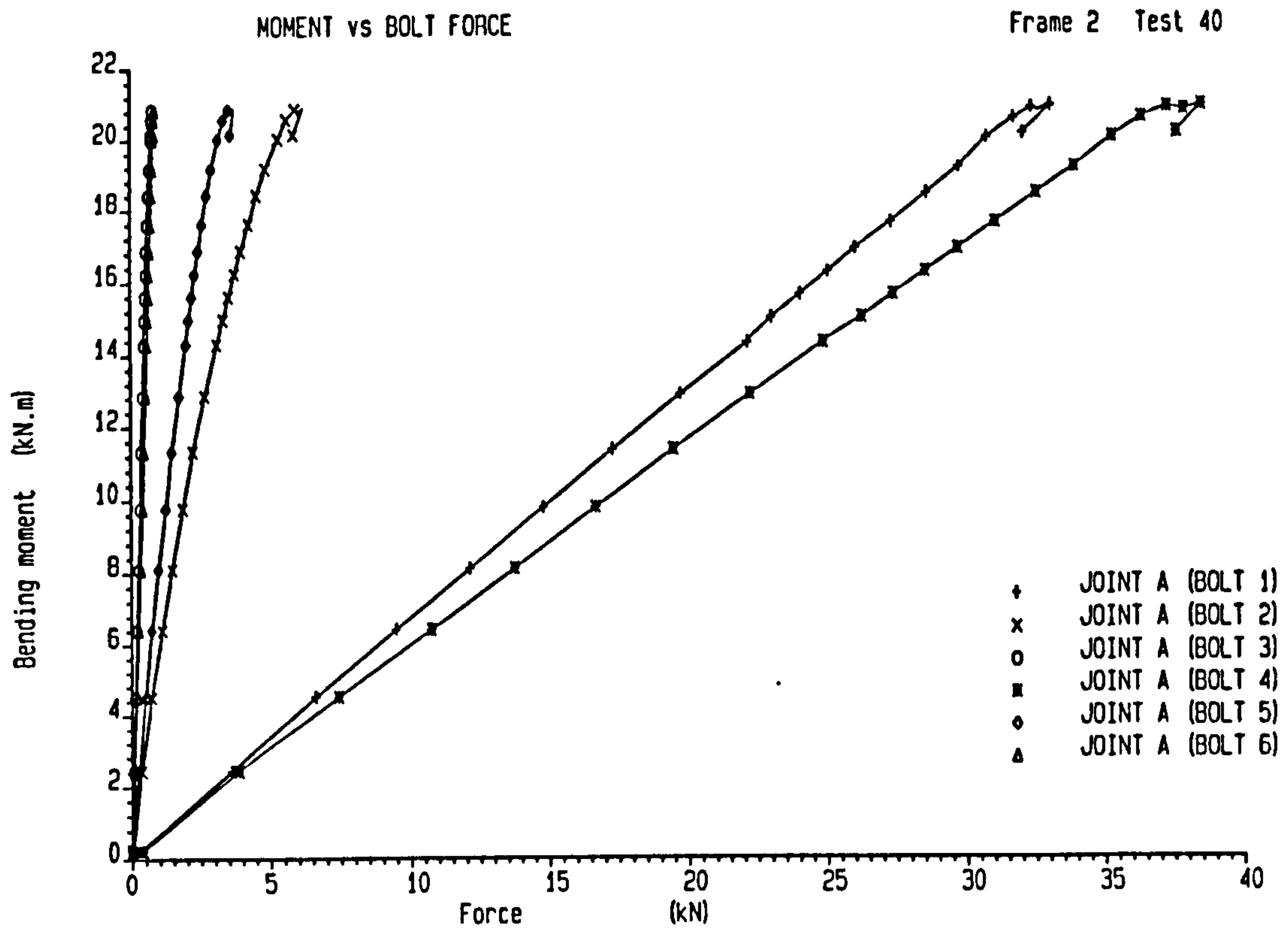


Figure 5.30 : Moment against Bolt Forces at Joint A for Test 40 of Frame 2

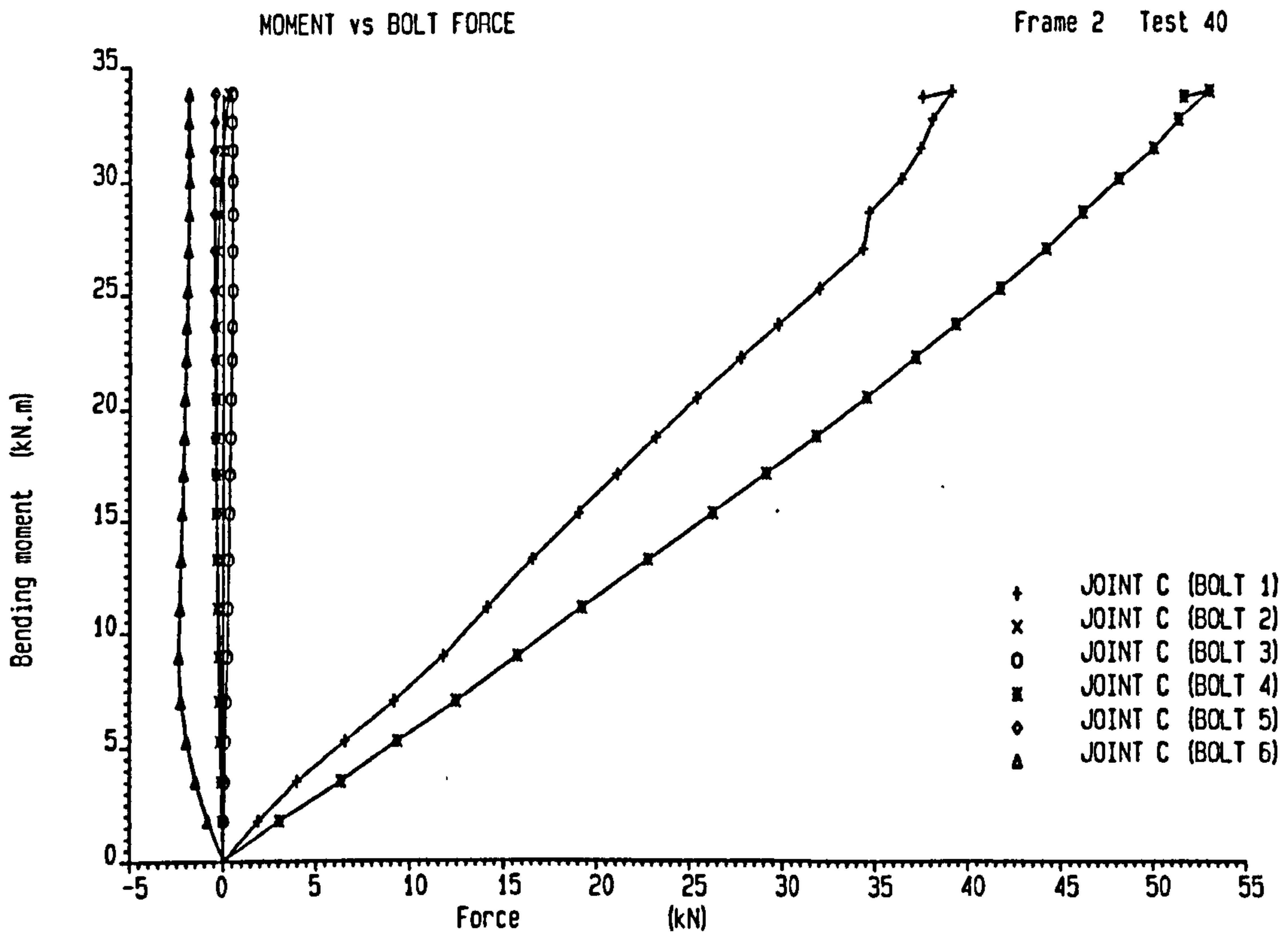


Figure 5.31 : Moment against Bolt Forces at Joint C for Test 40 of Frame 2

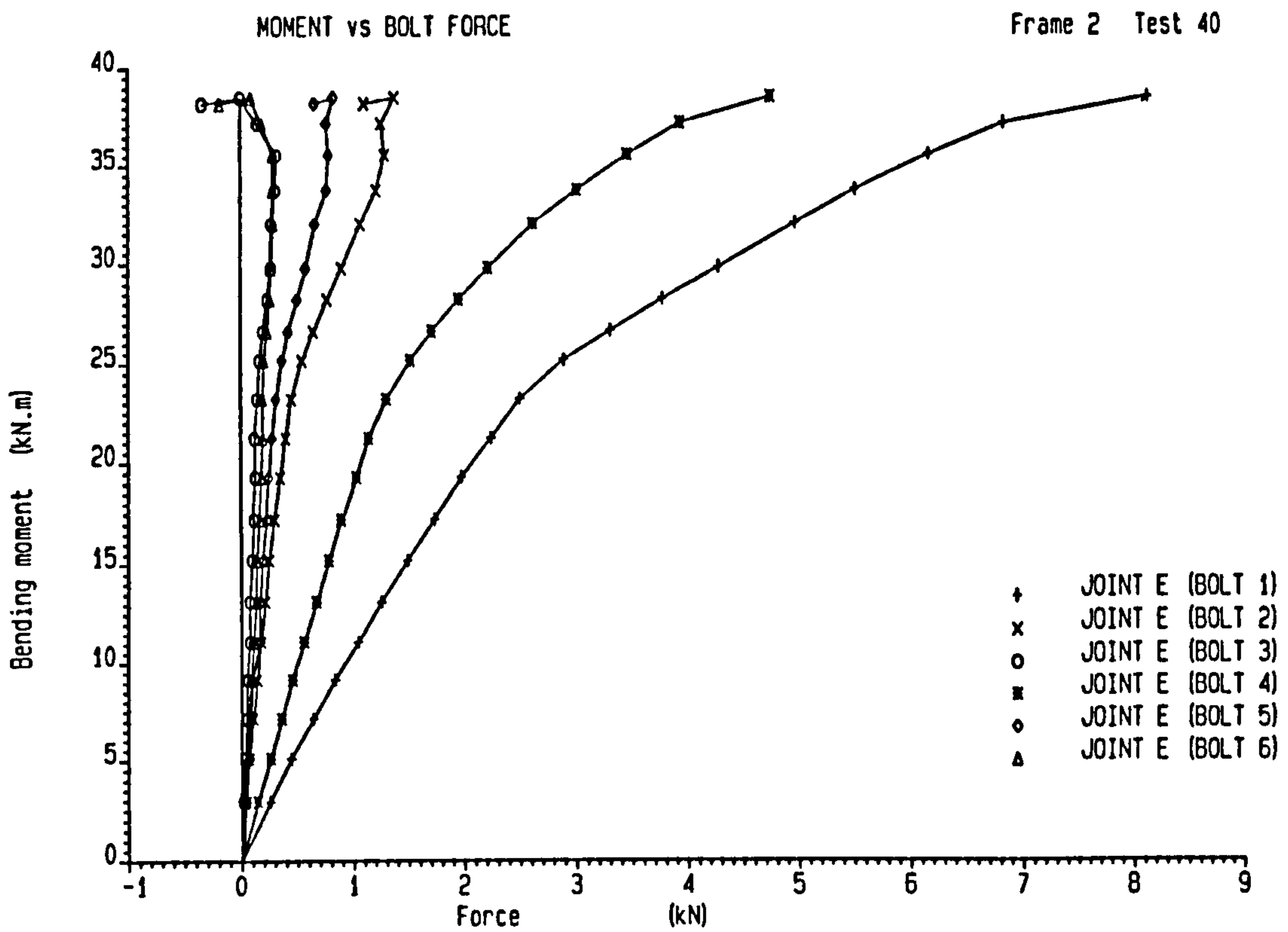


Figure 5.32 : Moment against Bolt Forces at Joint E for Test 40 of Frame 2

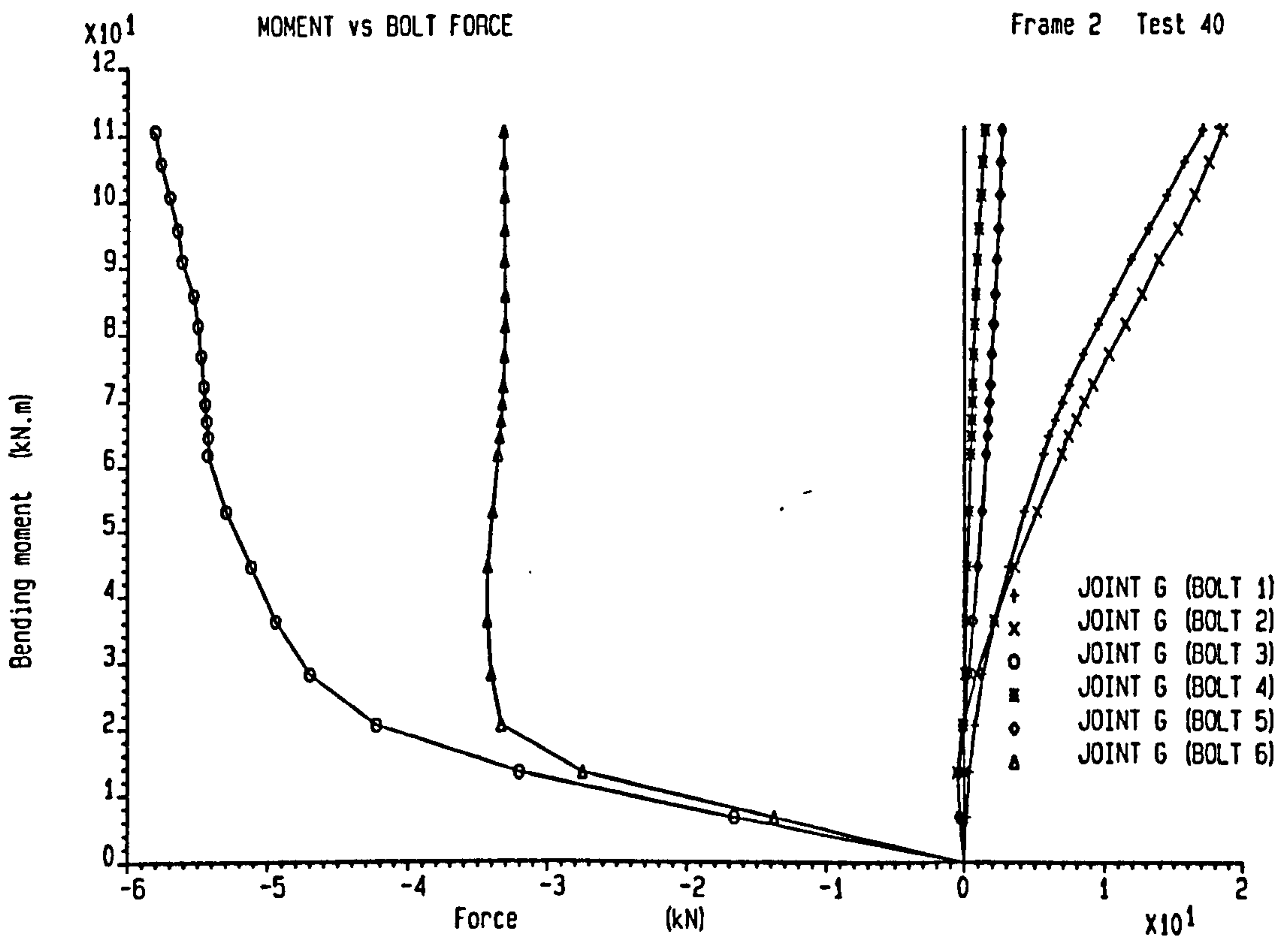


Figure 5.33 : Moment against Bolt Forces at Joint G for Test 40 of Frame 2

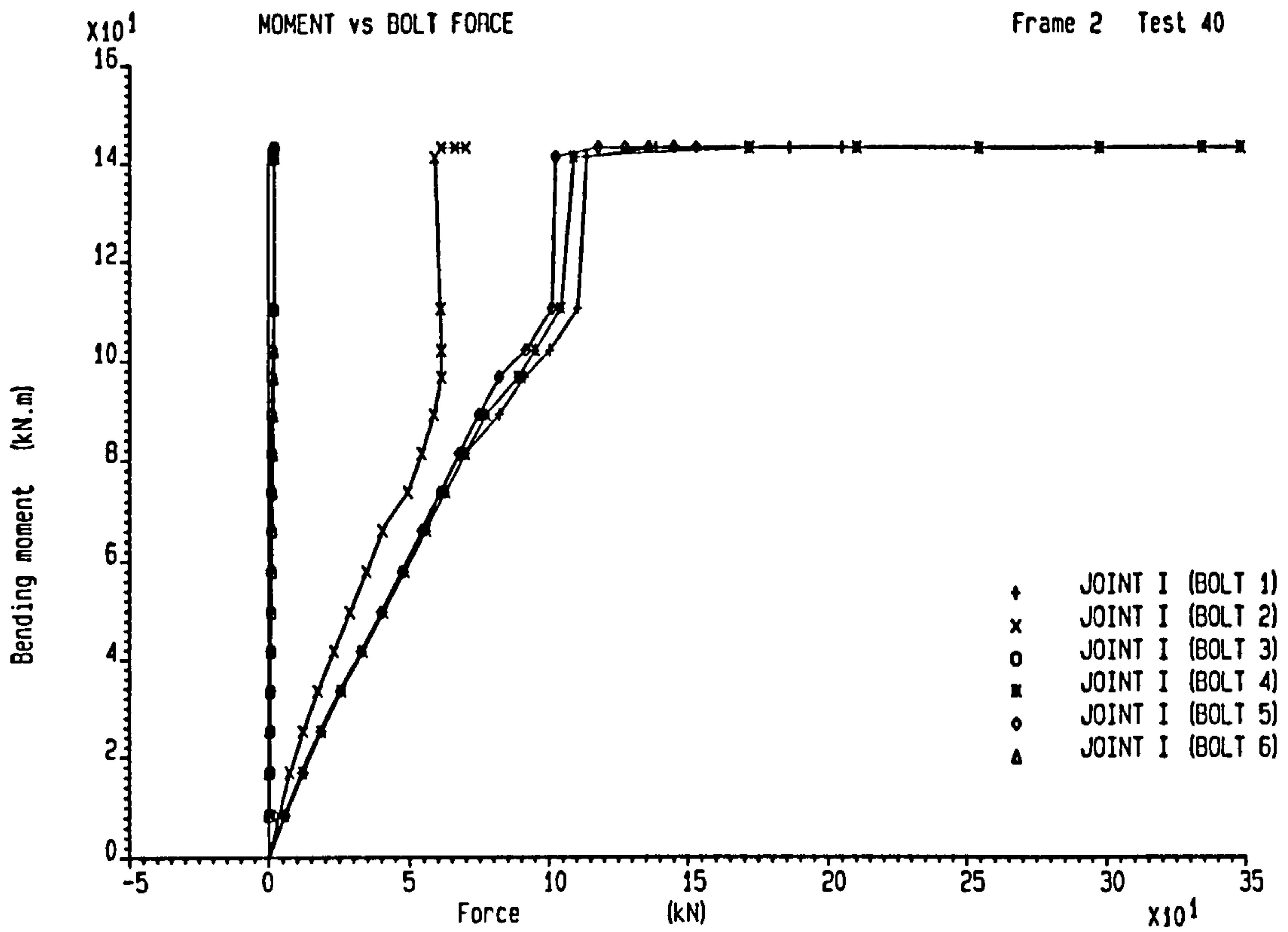


Figure 5.34 : Moment against Bolt Forces at Joint I for Test 40 of Frame 2

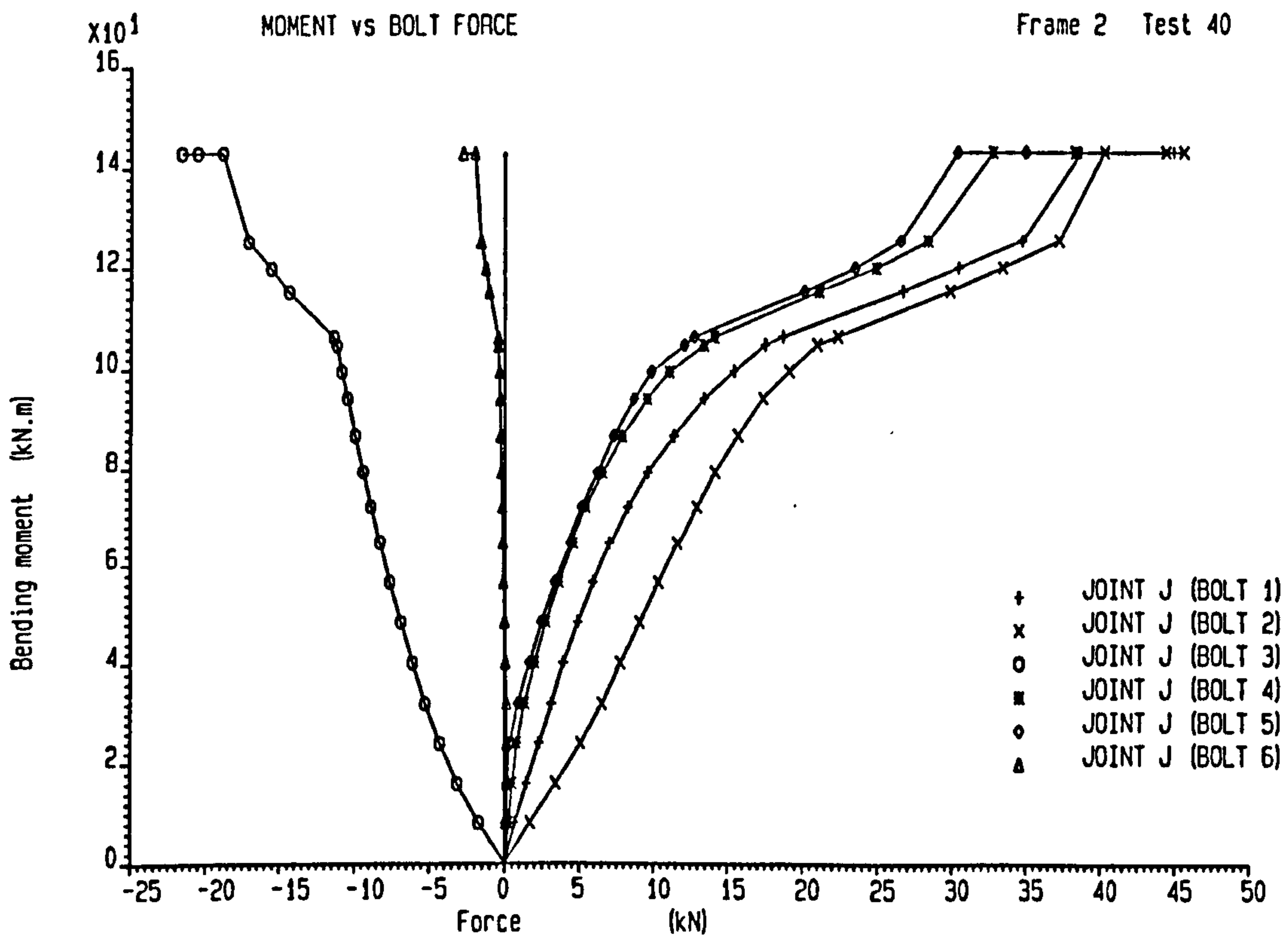


Figure 5.35 : Moment against Bolt Forces at Joint J for Test 40 of Frame 2

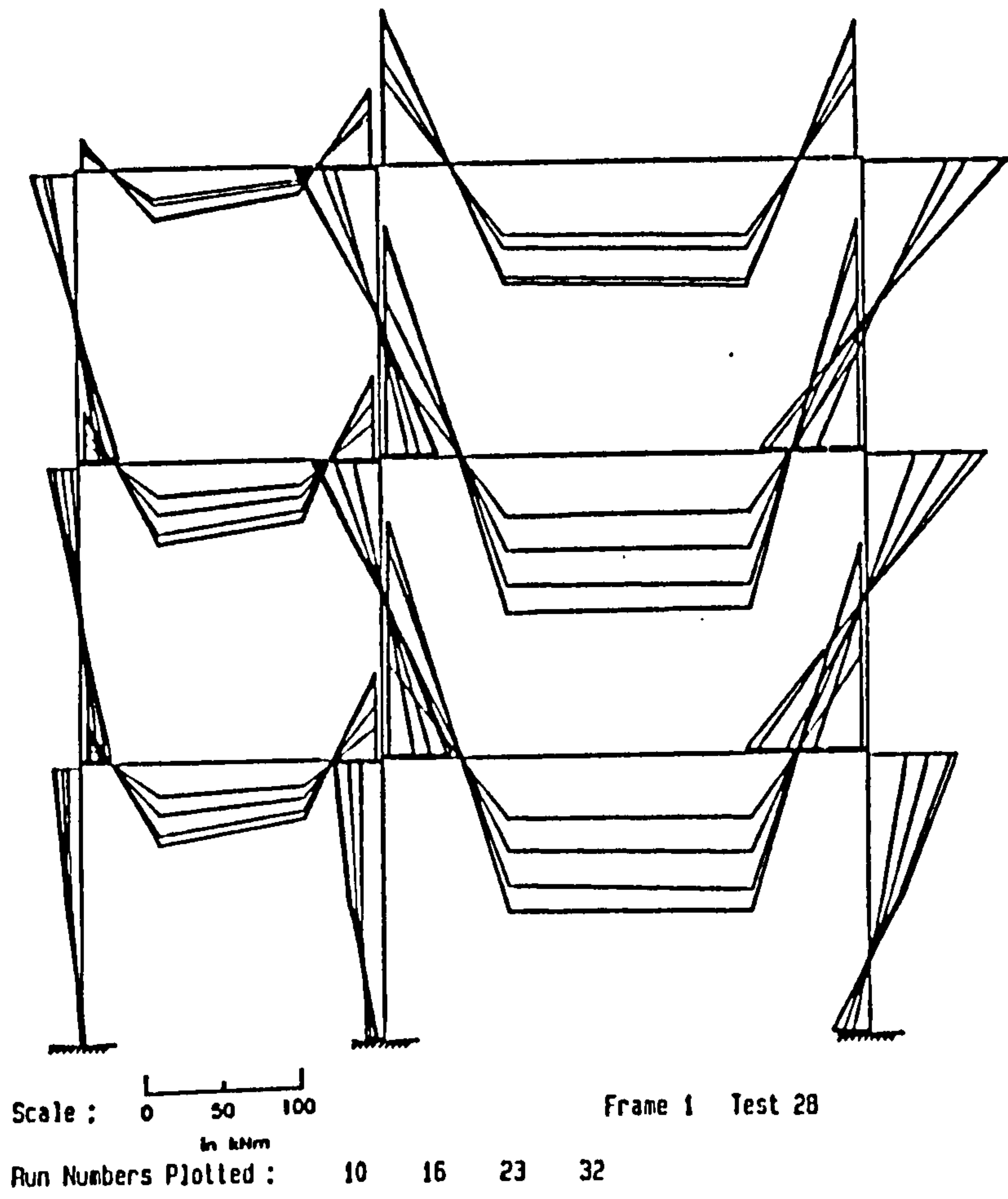


Figure 5.36 : Frame Moment around the Frame in Test 28 of Frame 1

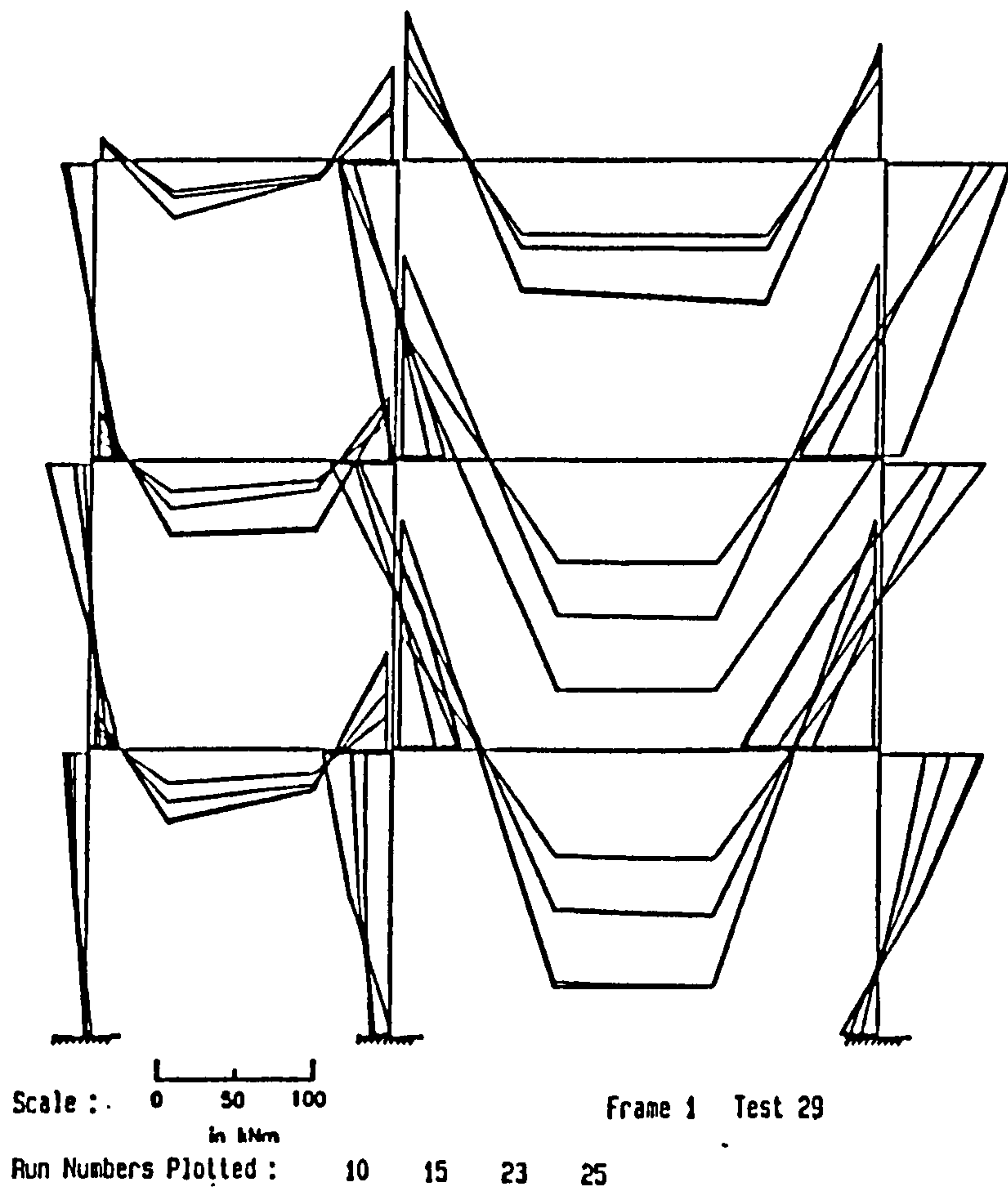
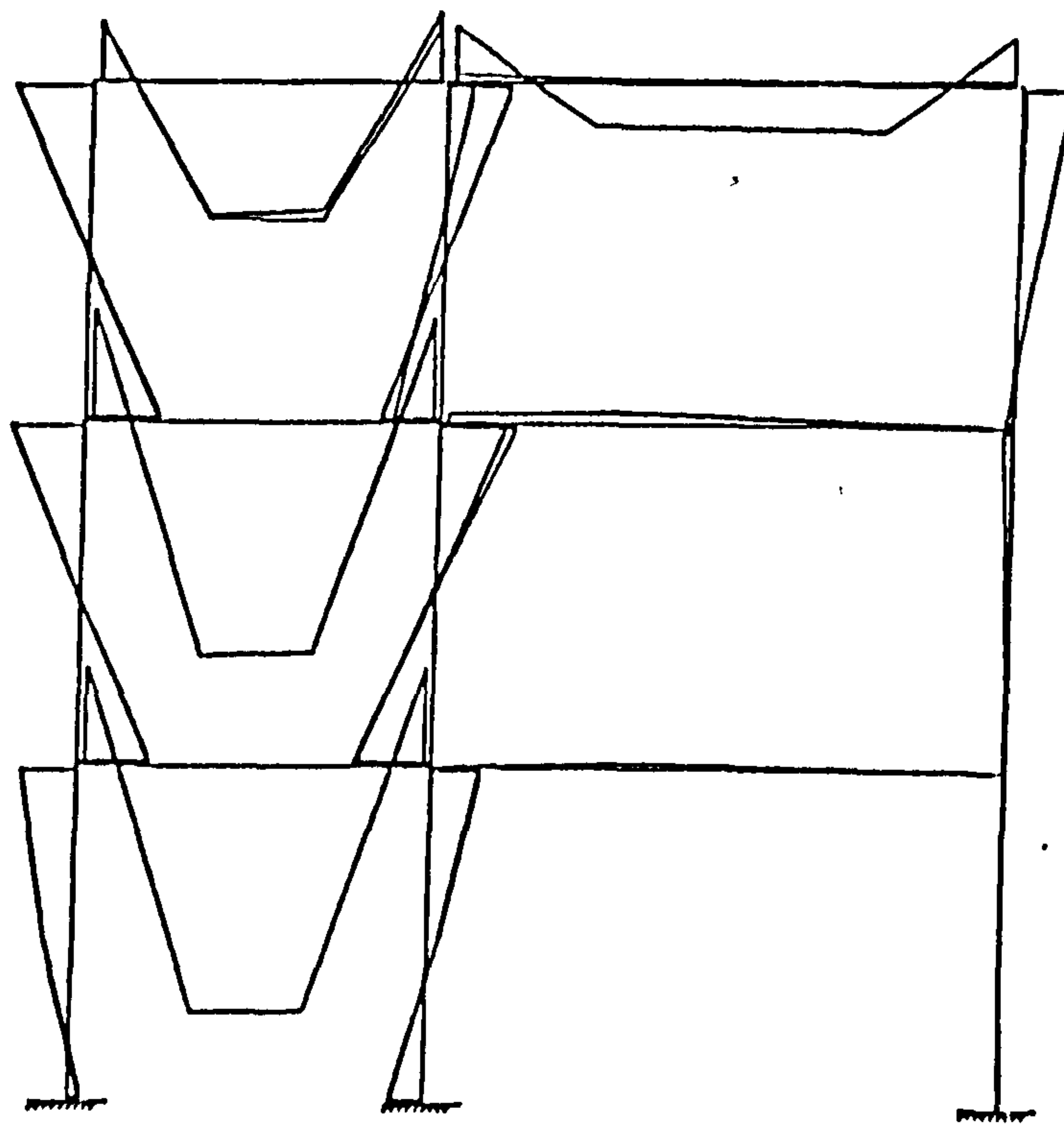
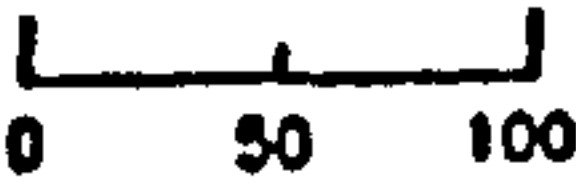


Figure 5.37 : Frame Moment around the Frame in Test 29 of Frame 1

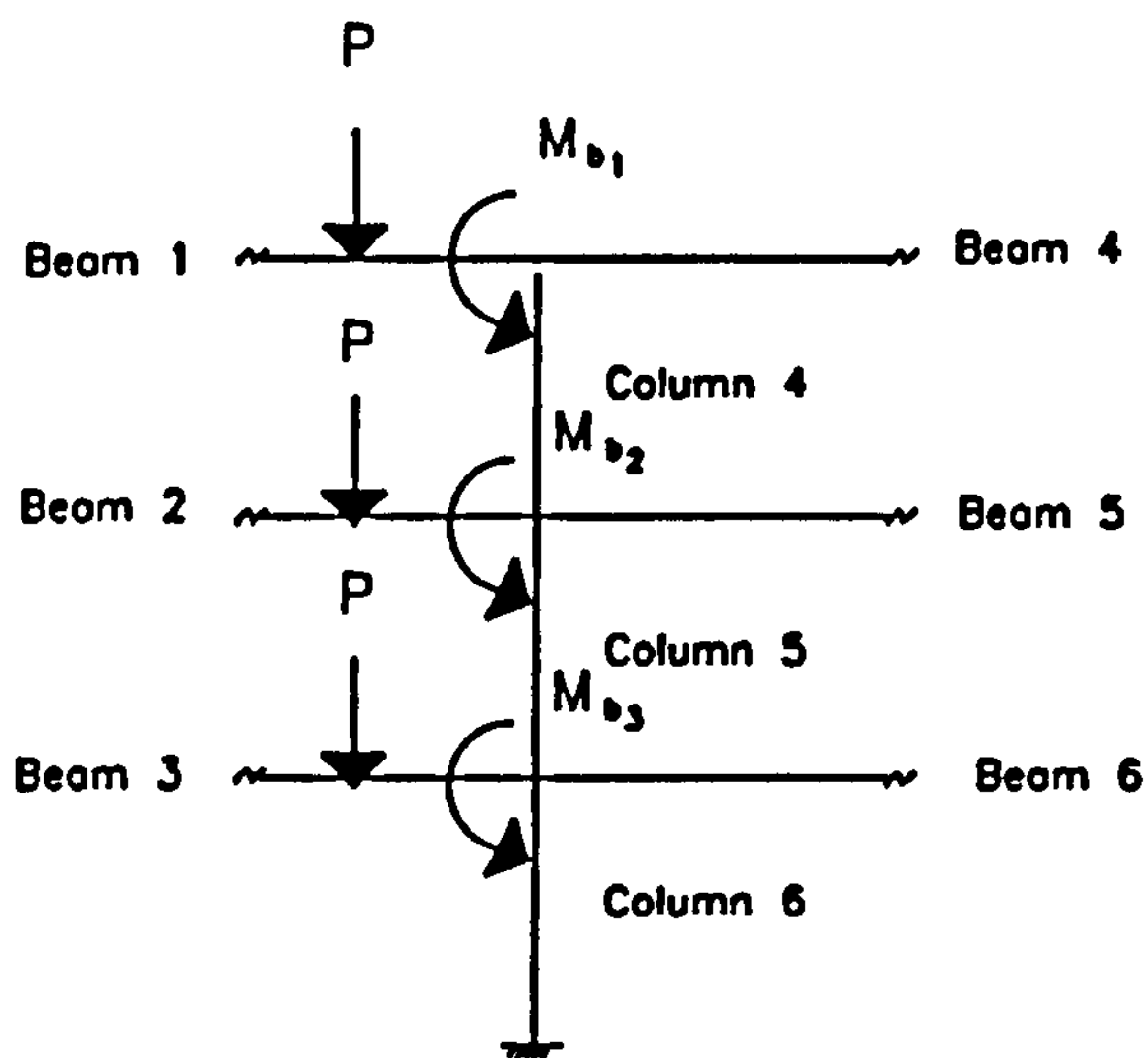


Scale :   
in kNm

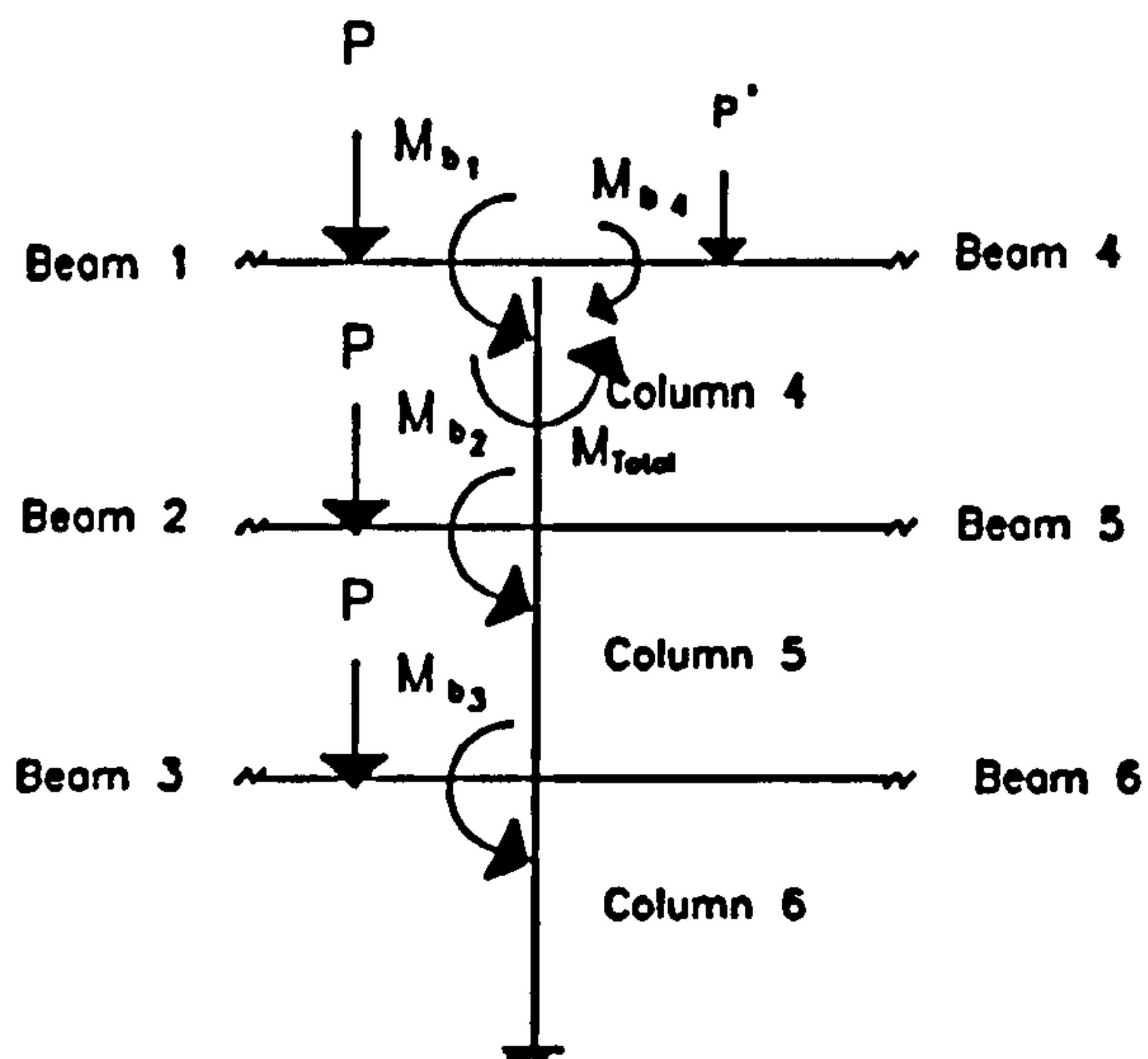
Frame 1 Test 30

Run Numbers Plotted : 28 29

Figure 5.38 : Frame Moment around the Frame in Test 30 of Frame 1

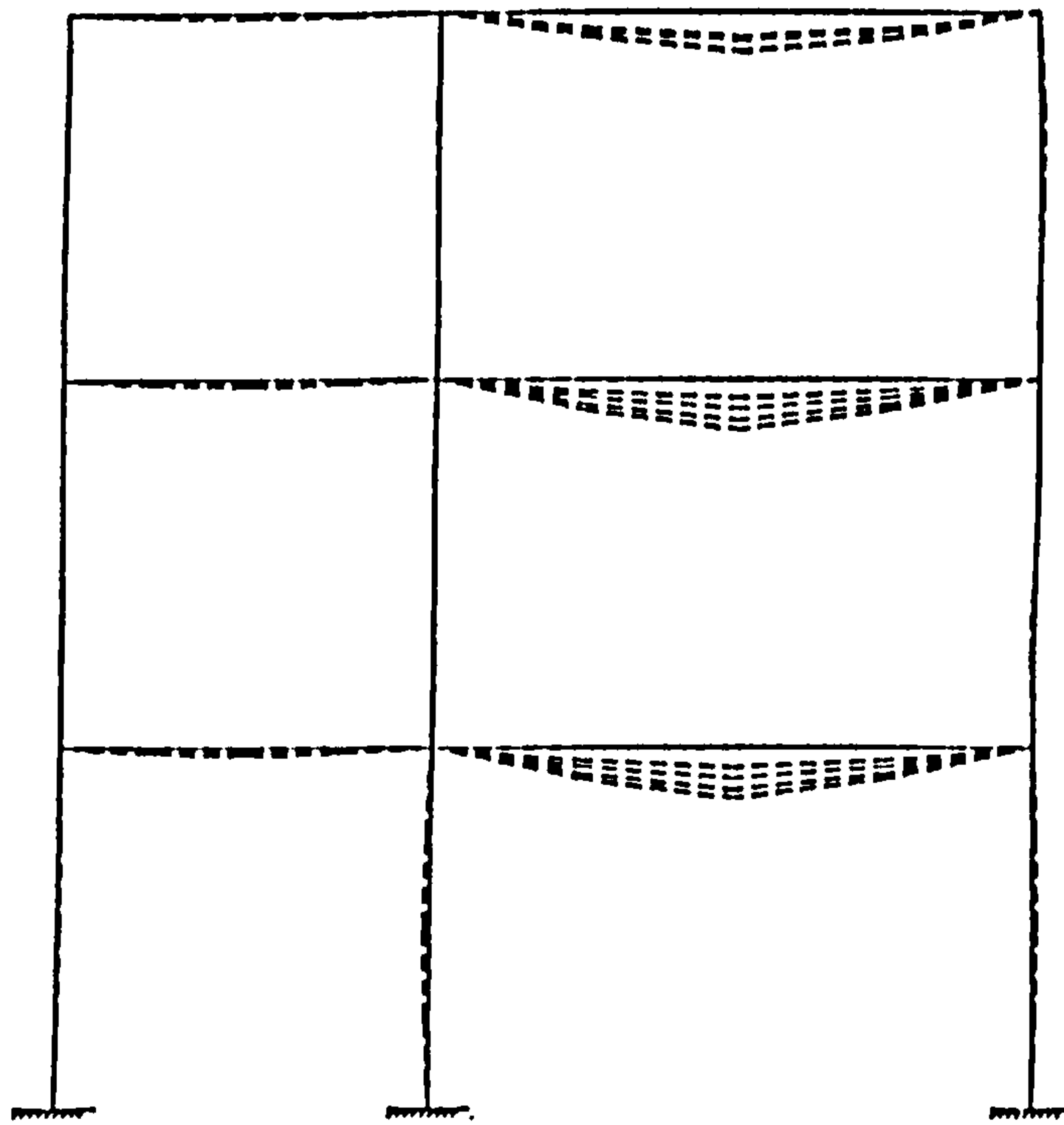


Anti-clockwise Disturbing Moment at the column head was due to the loads applied in shorter span



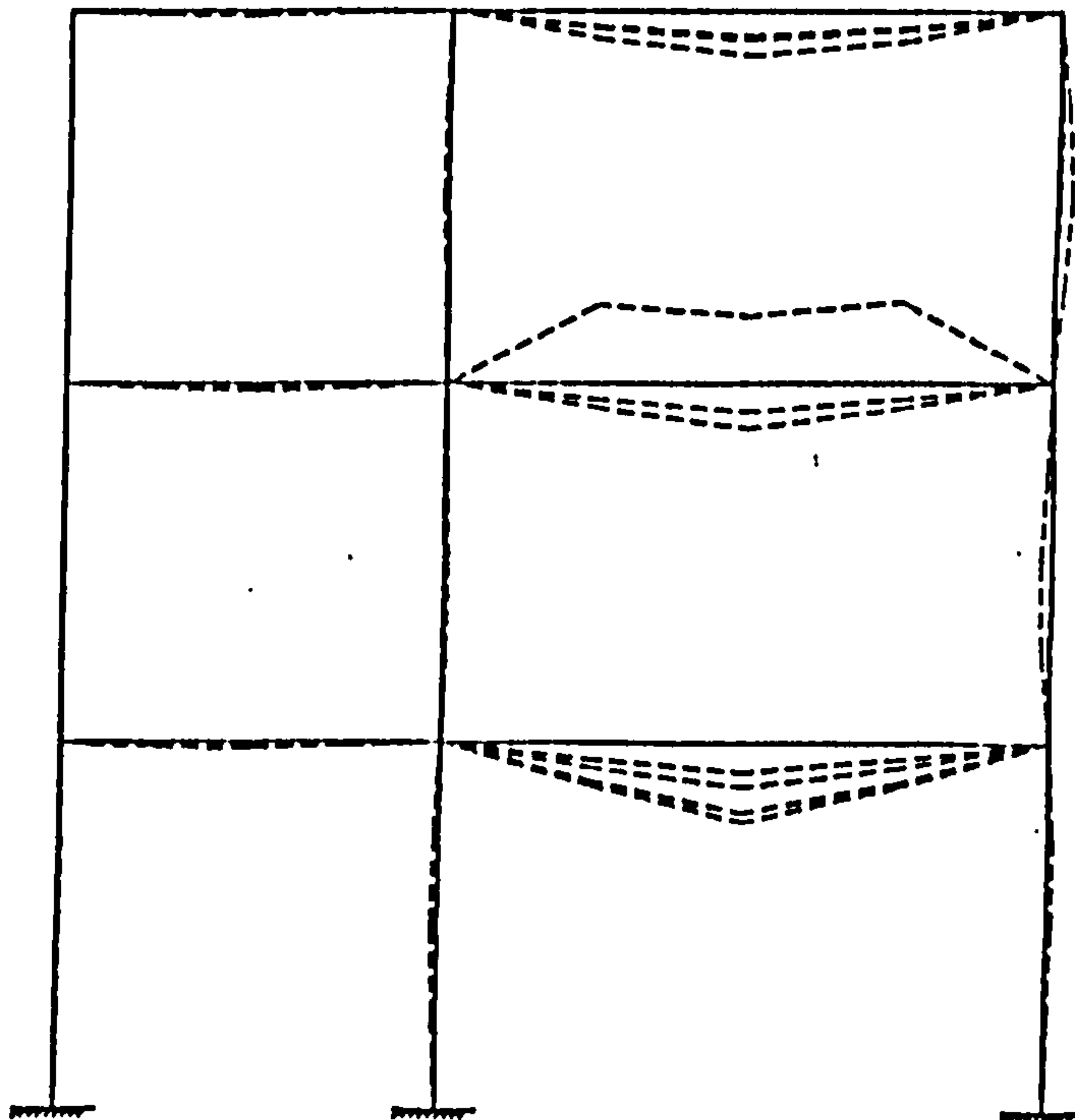
After an additional load applied in Beam 4, a clockwise disturbing moment formed in the end of Beam 4. It decreased the moment in column head ( $M_{Total}$ )

Figure 5.39 : Change of the Column Head Moment in the Central Column of Test



Horizontal deflections 0  $\frac{25}{50}$  in mm  
 Vertical deflections 0  $\frac{50}{100}$  in mm  
 Frame 1 Test 28  
 Run Numbers Plotted : 10 16 23 32

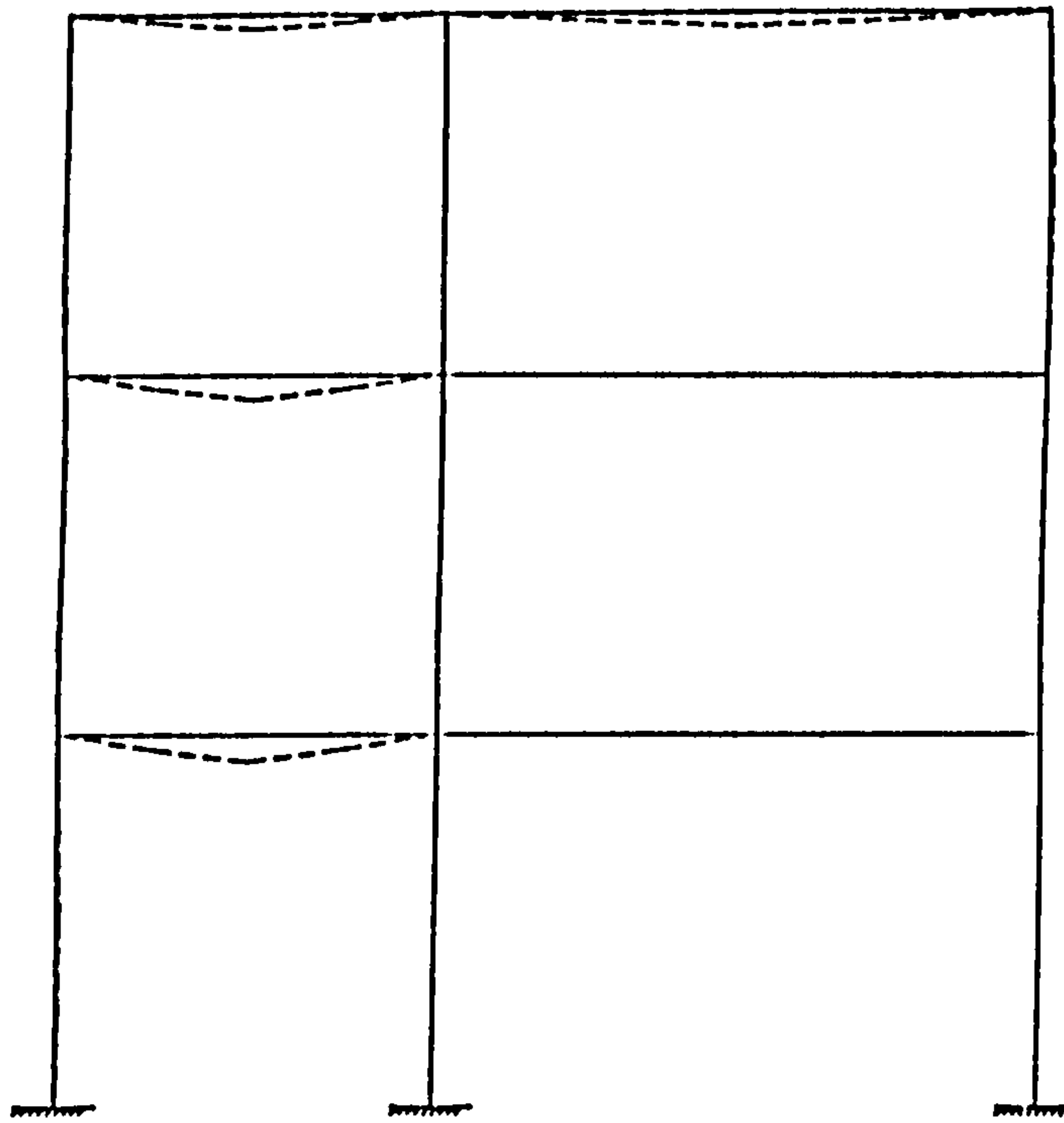
Figure 5.40 : Frame Deformation around the Frame in Test 28 of Frame 1



Horizontal deflections 0  $\frac{25}{50}$  in mm  
 Vertical deflections 0  $\frac{50}{100}$  in mm  
 Frame 1 Test 29  
 Run Numbers Plotted : 10 15 23 25

Figure 5.41 : Frame Deformation around the Frame in Test 29 of Frame 1





Horizontal deflections of 0 25 50  
 Vertical deflections 0 50 100 in mm  
 Run Numbers Plotted : 20 29  
 Frame 1 Test 30

Figure 5.42 : Frame Deformation around the Frame in Test 30 of Frame 1

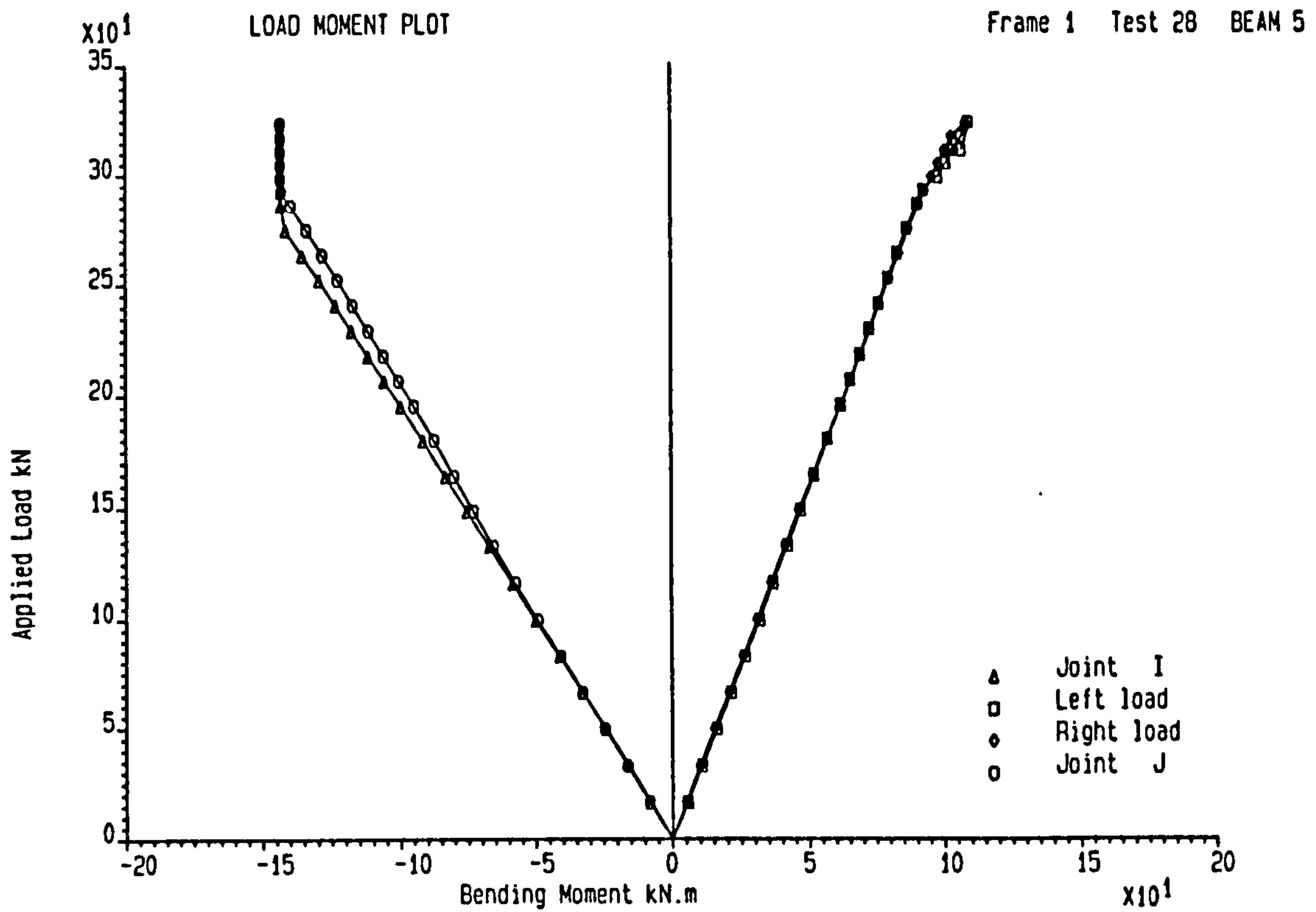


Figure 5.43 : Total Applied Load against Bending Moment on Beam 5  
in Test 28 of Frame 1

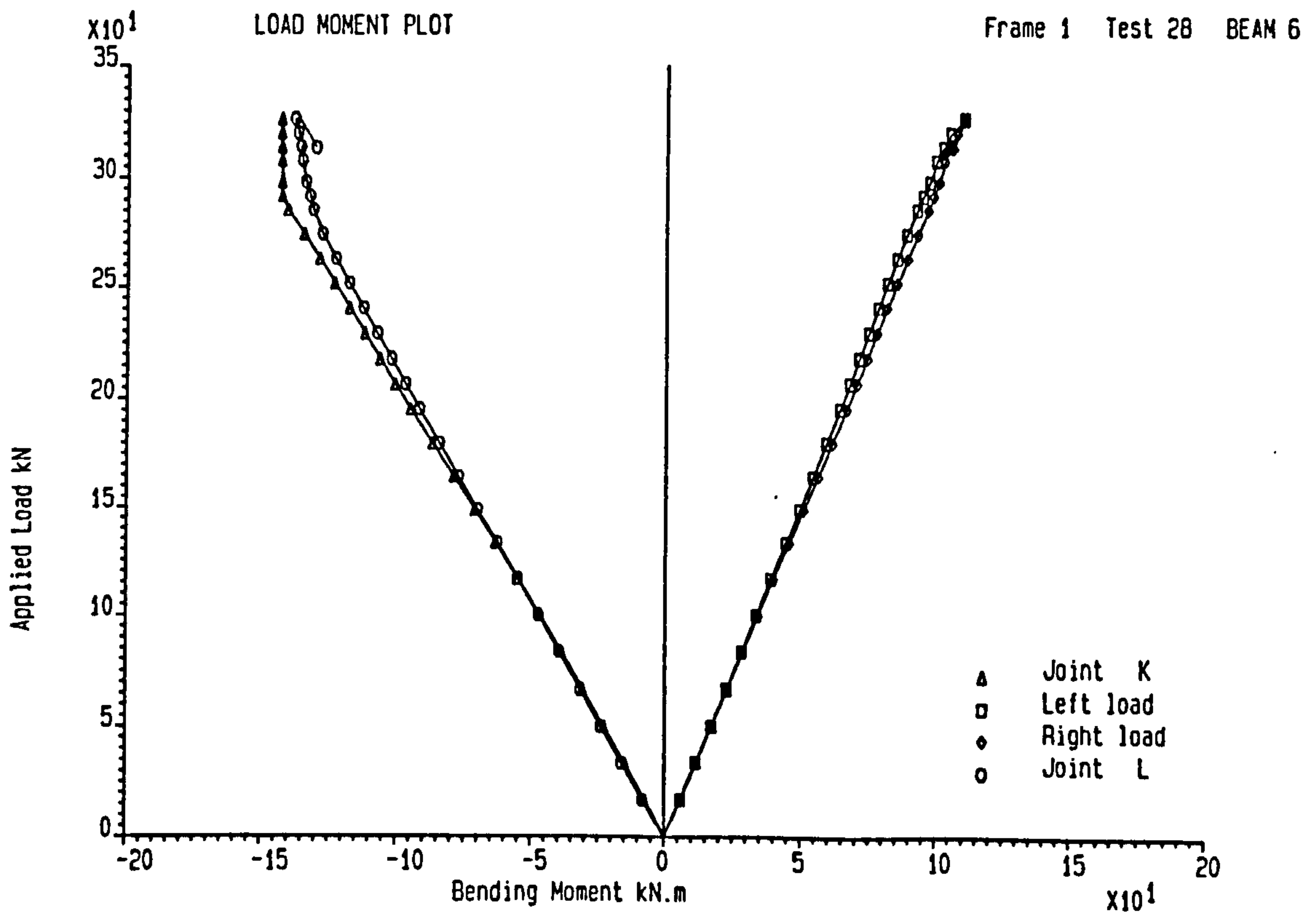


Figure 5.44 : Total Applied Load against Bending Moment on Beam 6  
in Test 28 of Frame 1

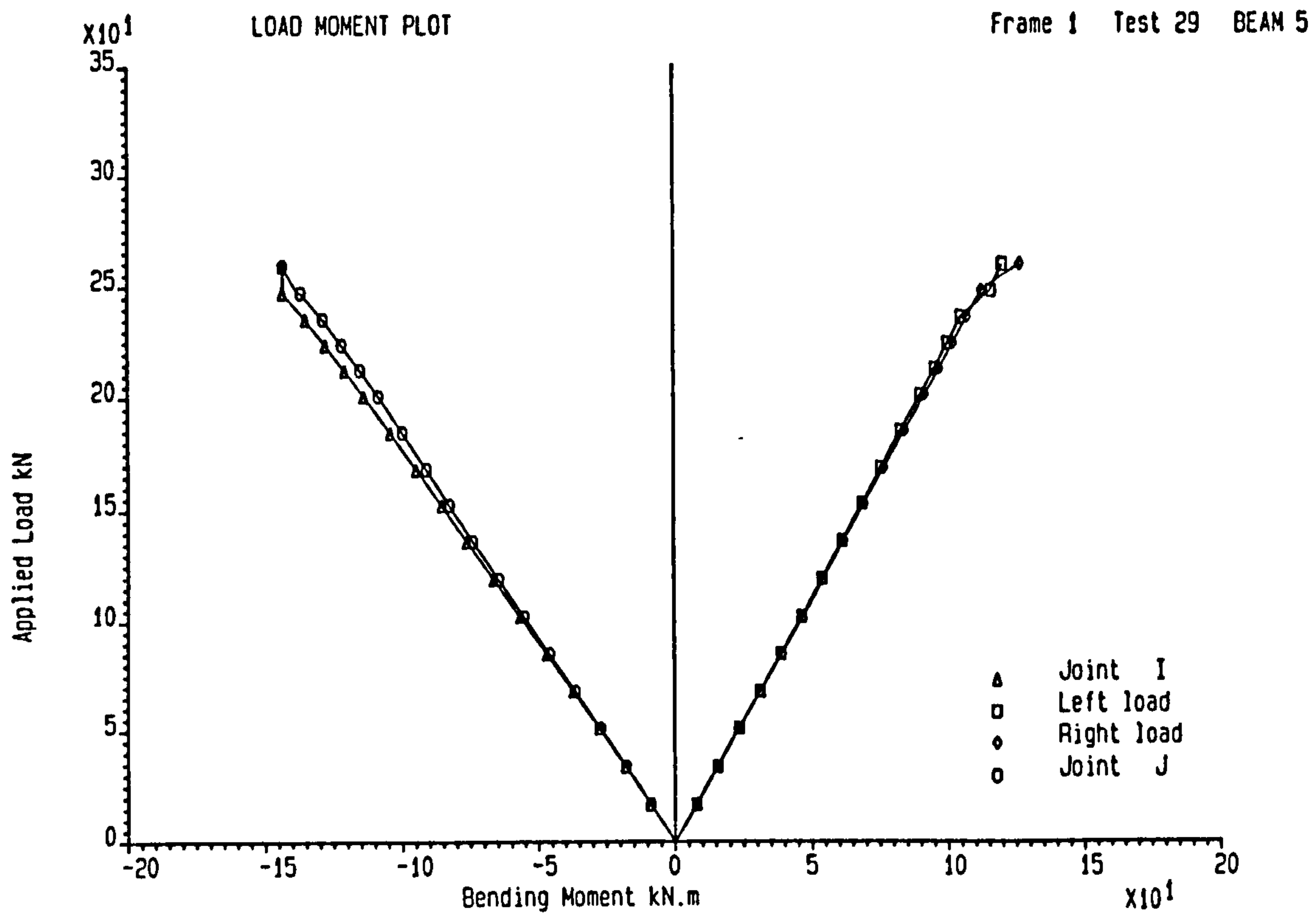


Figure 5.45 : Total Applied Load against Bending Moment on Beam 5  
in Test 29 of Frame 1

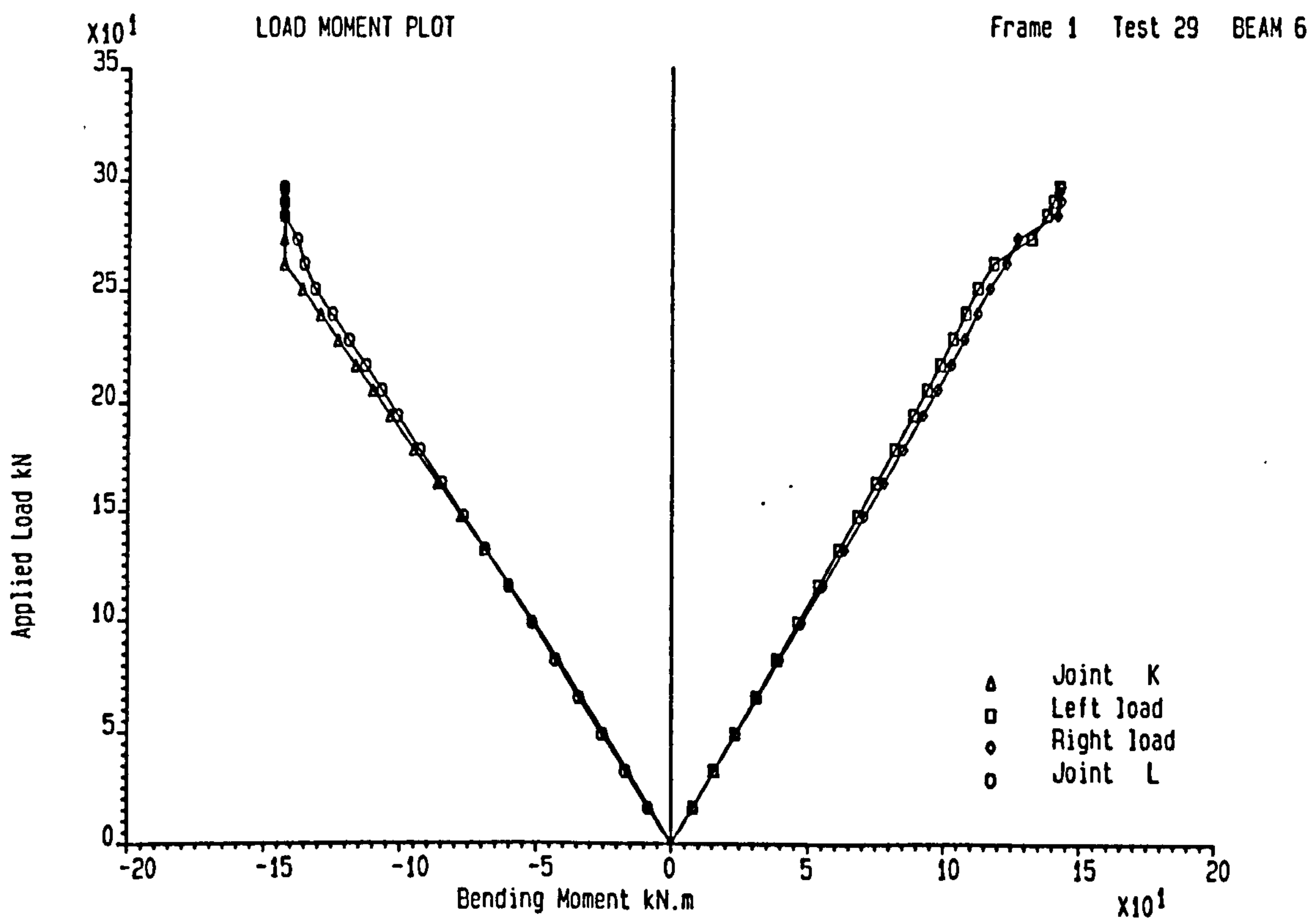


Figure 5.46 : Total Applied Load against Bending Moment on Beam 6  
in Test 29 of Frame 1

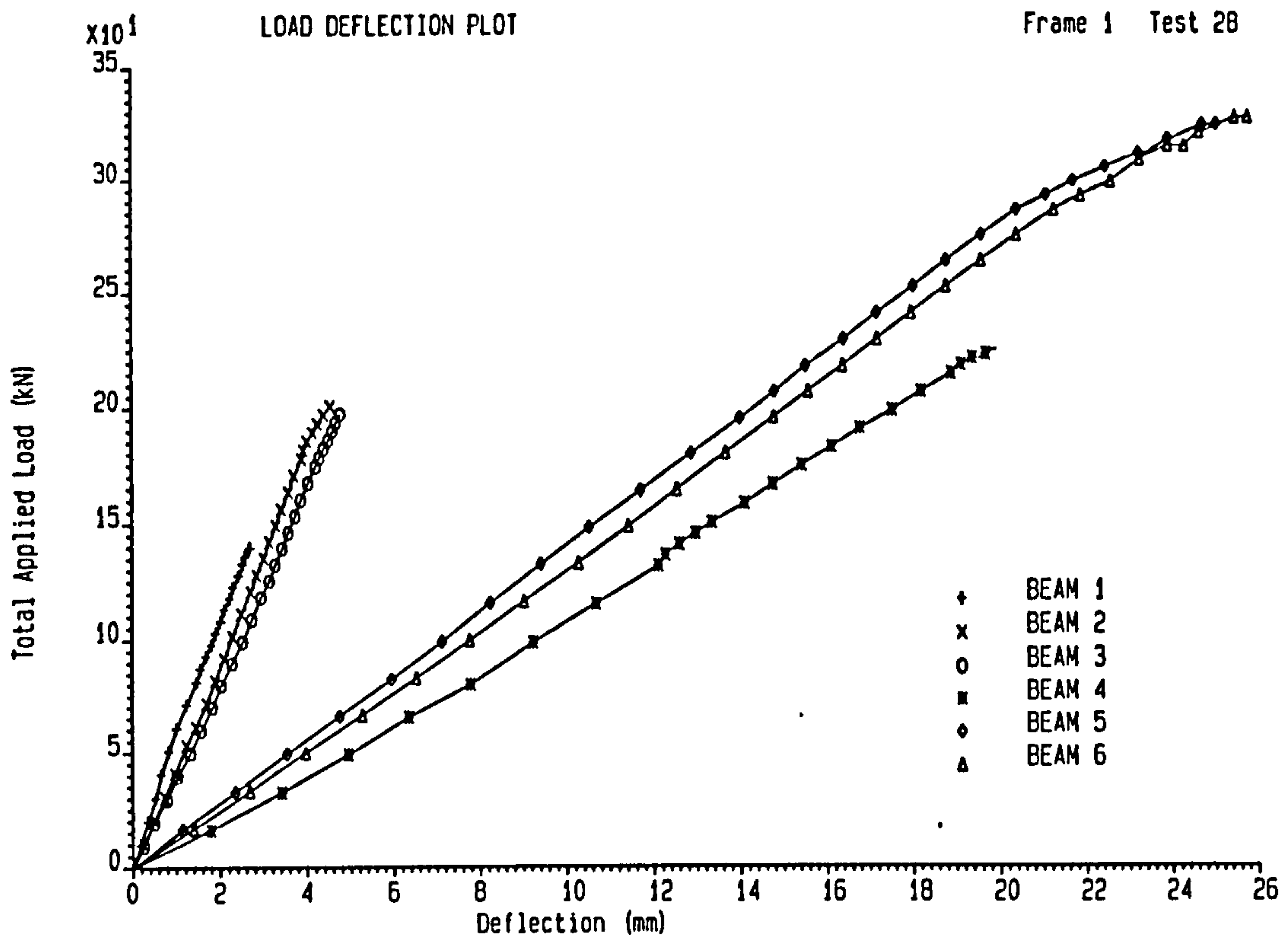


Figure 5.47 : Total Applied Load against Mid-Span Deflection on Six Beams in Test 28 of Frame 1

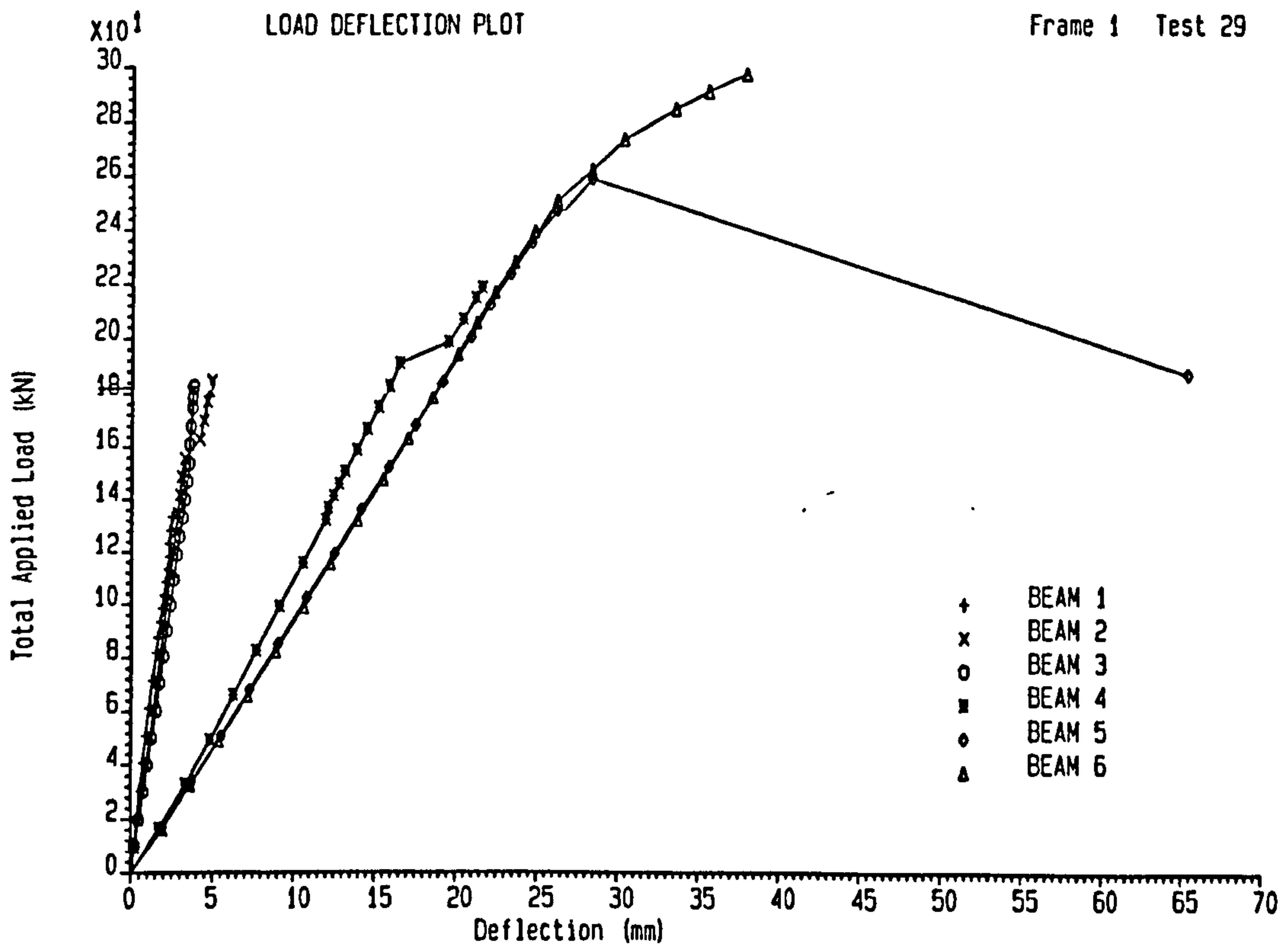


Figure 5.48 : Total Applied Load against Mid-Span Deflection on Six Beams in Test 29 of Frame 1

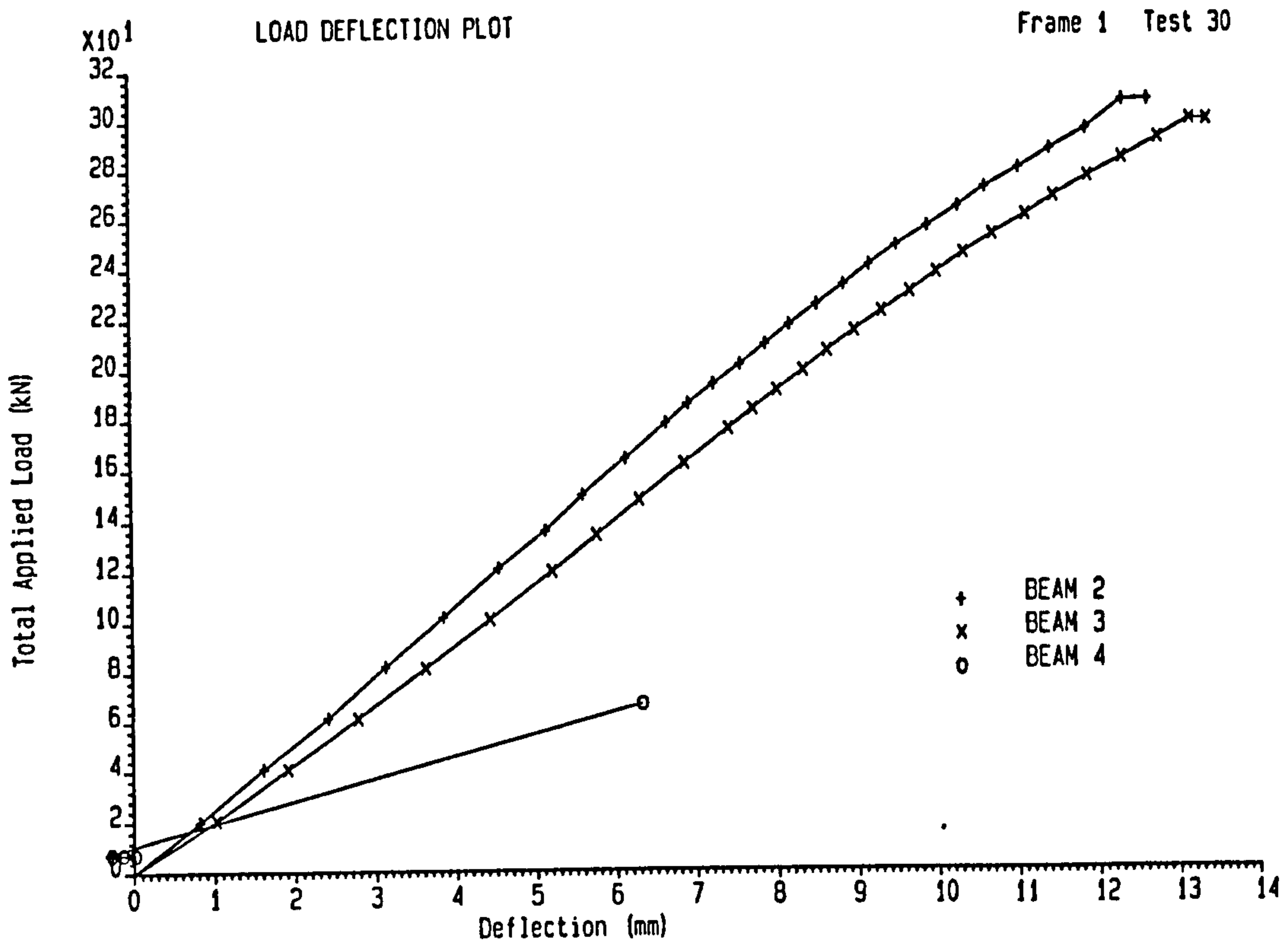


Figure 5.49 : Total Applied Load against Mid-Span Deflection on Beams 2, 3 and 4 in Test 28 of Frame 1

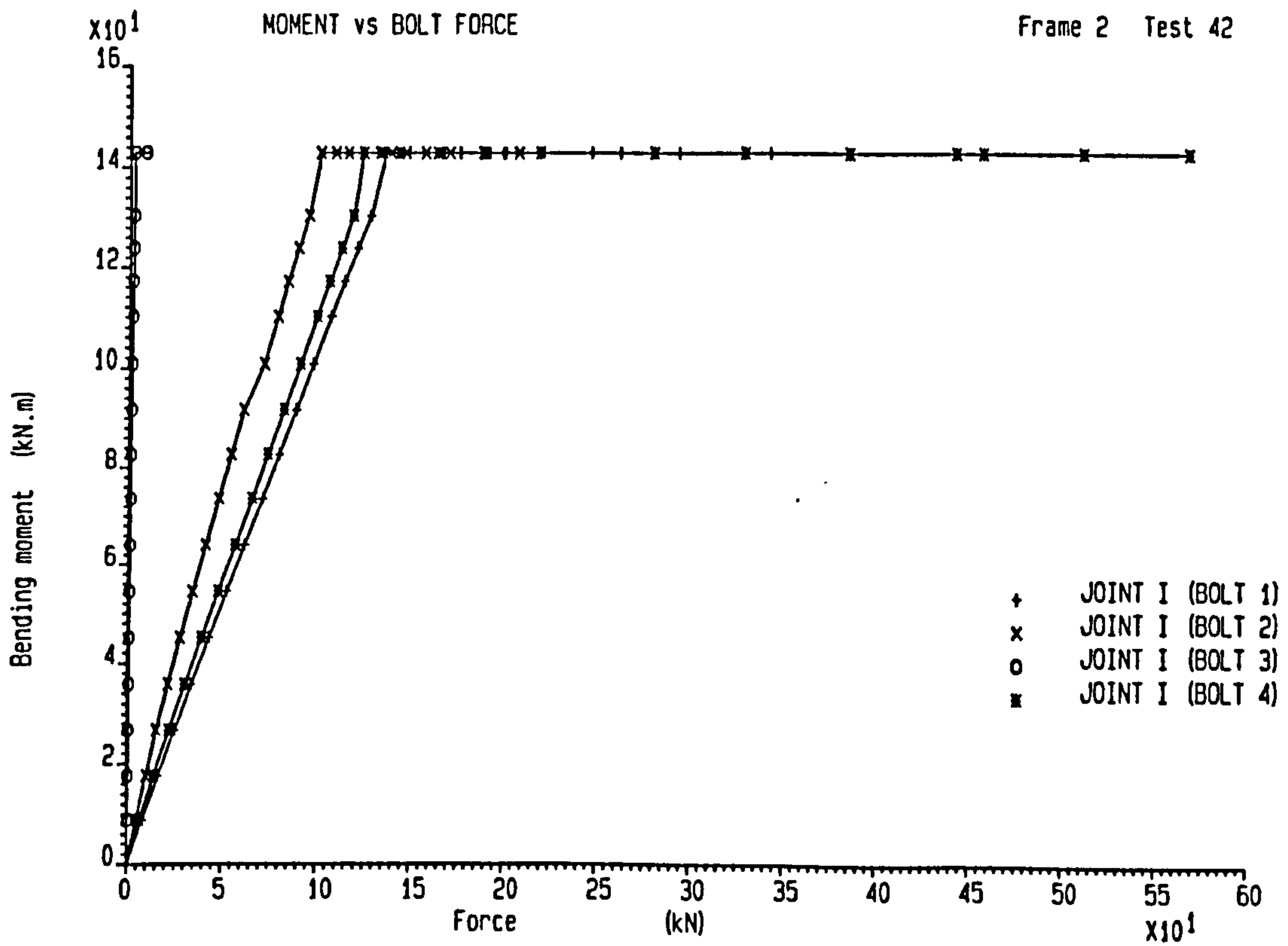


Figure 5.50 : Moment against Bolt Forces at Joint I in Test 42 of Frame 2

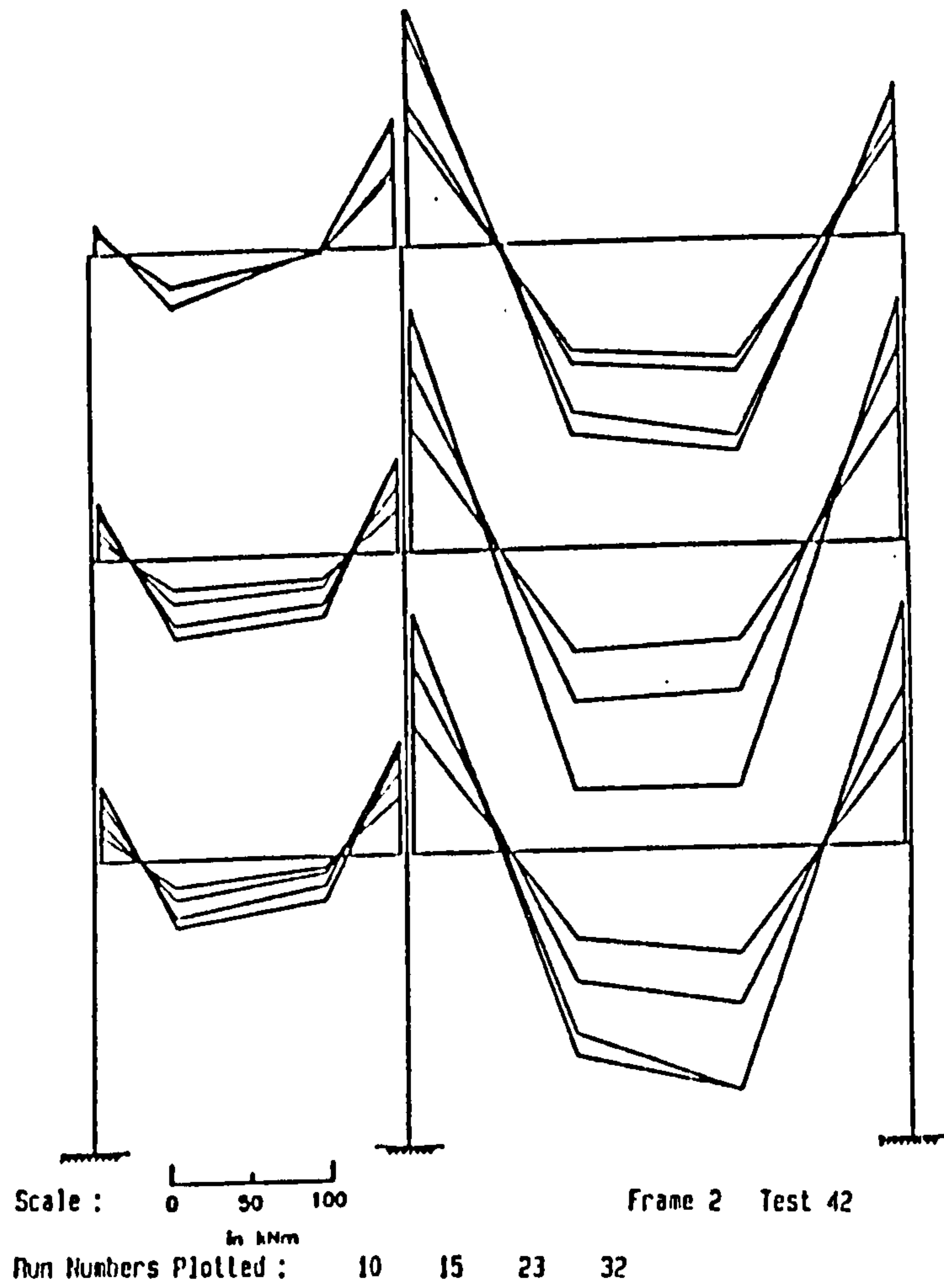


Figure 5.51 : Frame Moment around the Frame in Test 42 of Frame 2

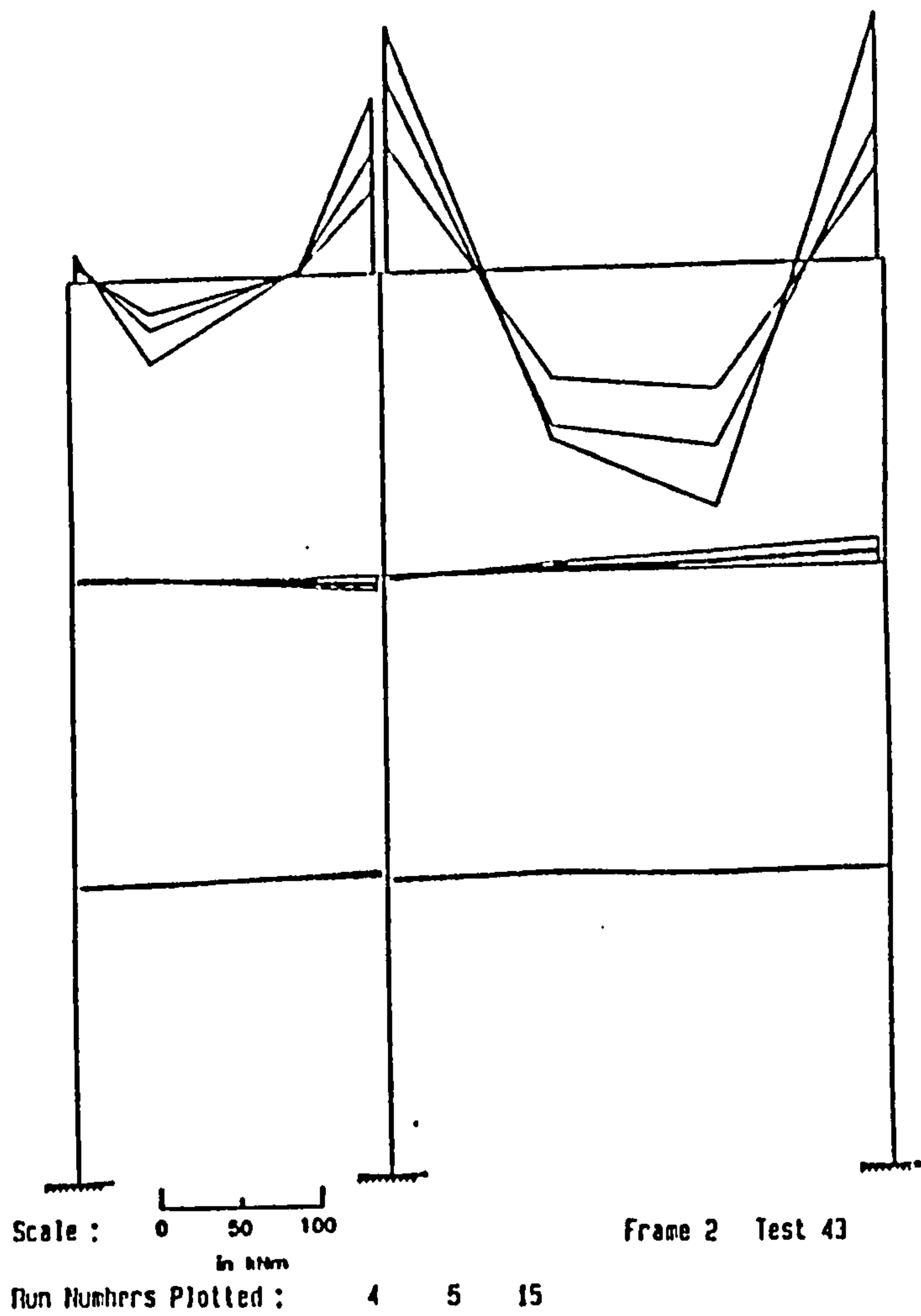
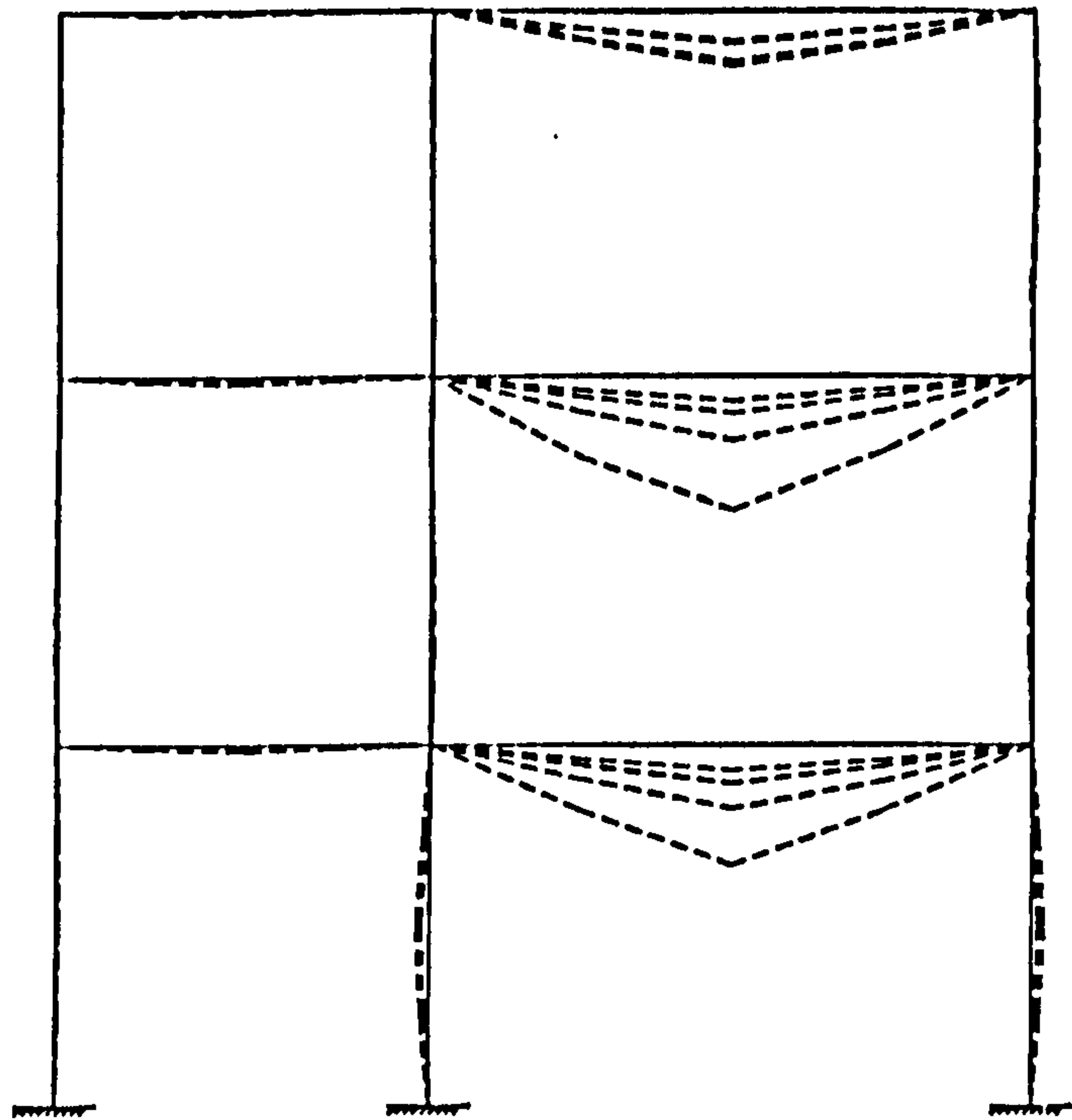
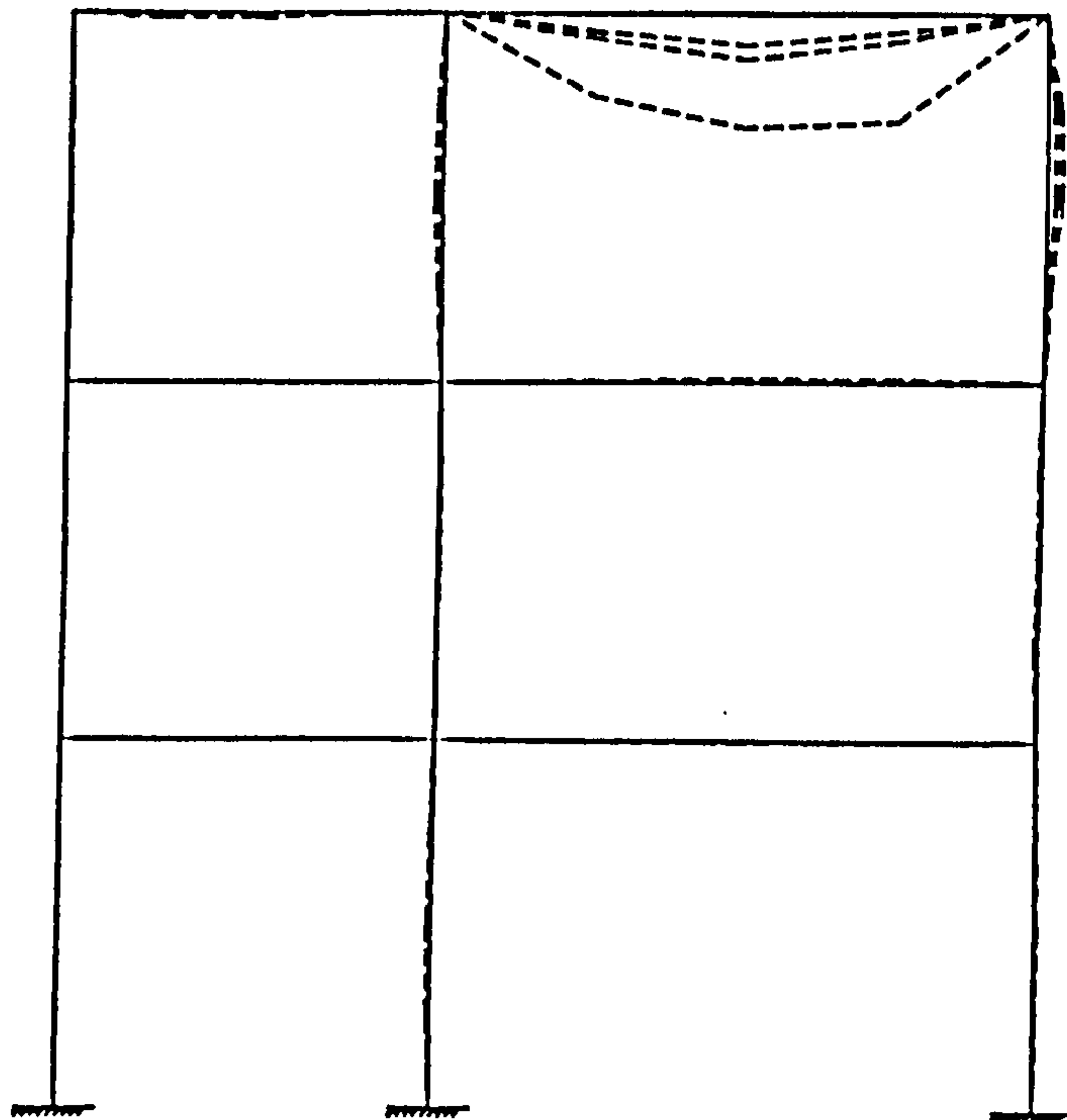


Figure 5.52 : Frame Moment around the Frame in Test 43 of Frame 2



Horizontal deflections 0 | 25 | 50 in mm  
 Vertical deflections 0 | 50 | 100 in mm  
 Frame 2 Test 42  
 Run Numbers Plotted : 10 15 23 32

Figure 5.53 : Frame Deformation around the Frame in Test 42 of Frame 2



Horizontal deflections 0 | 25 | 50 in mm  
 Vertical deflections 0 | 50 | 100 in mm  
 Frame 2 Test 43  
 Run Numbers Plotted : 4 5 15

Figure 5.54 : Frame Deformation around the Frame in Test 43 of Frame 2

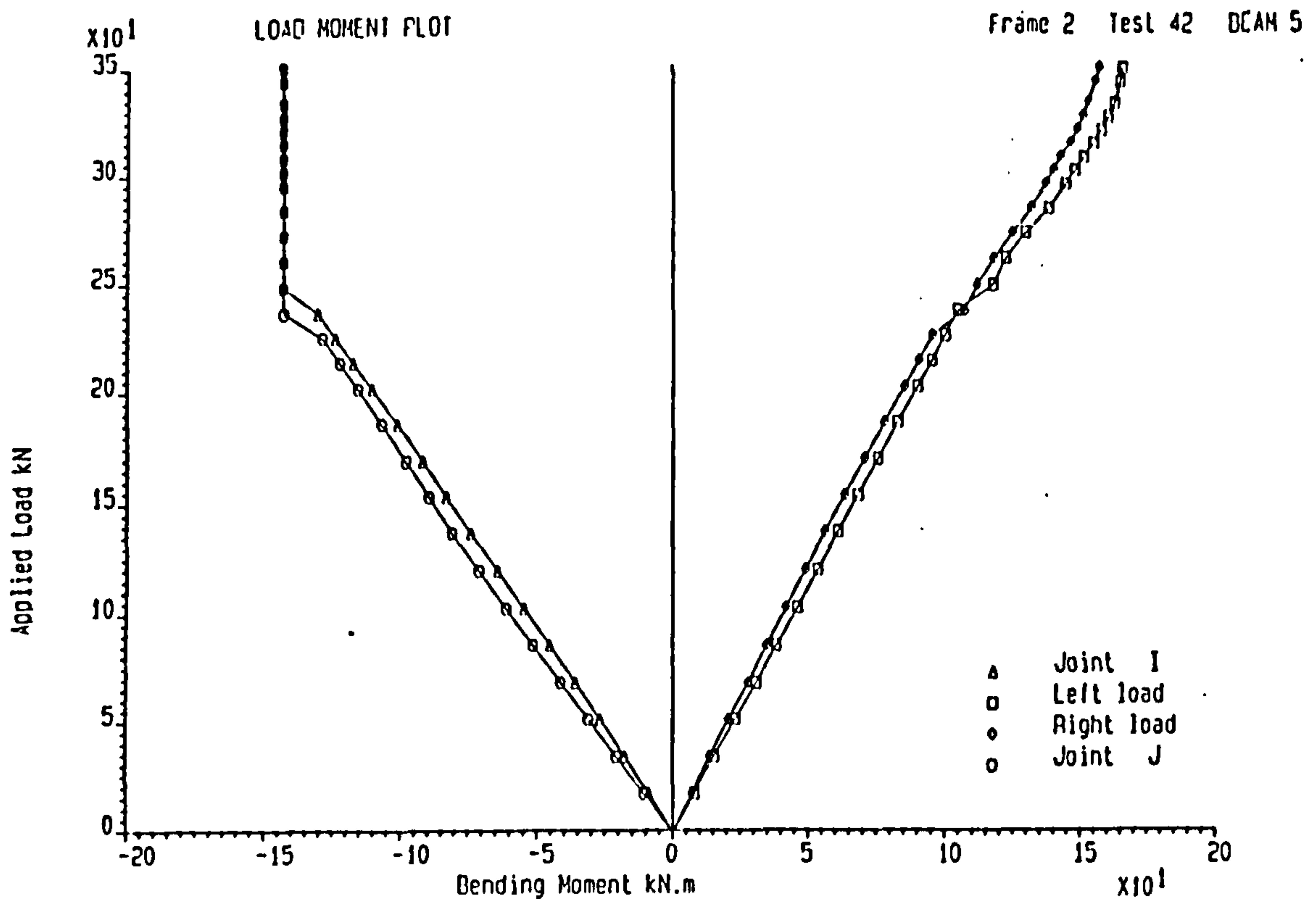


Figure 5.55 : Total Applied Load against Bending Moment on Beam 5  
in Test 42 of Frame 2

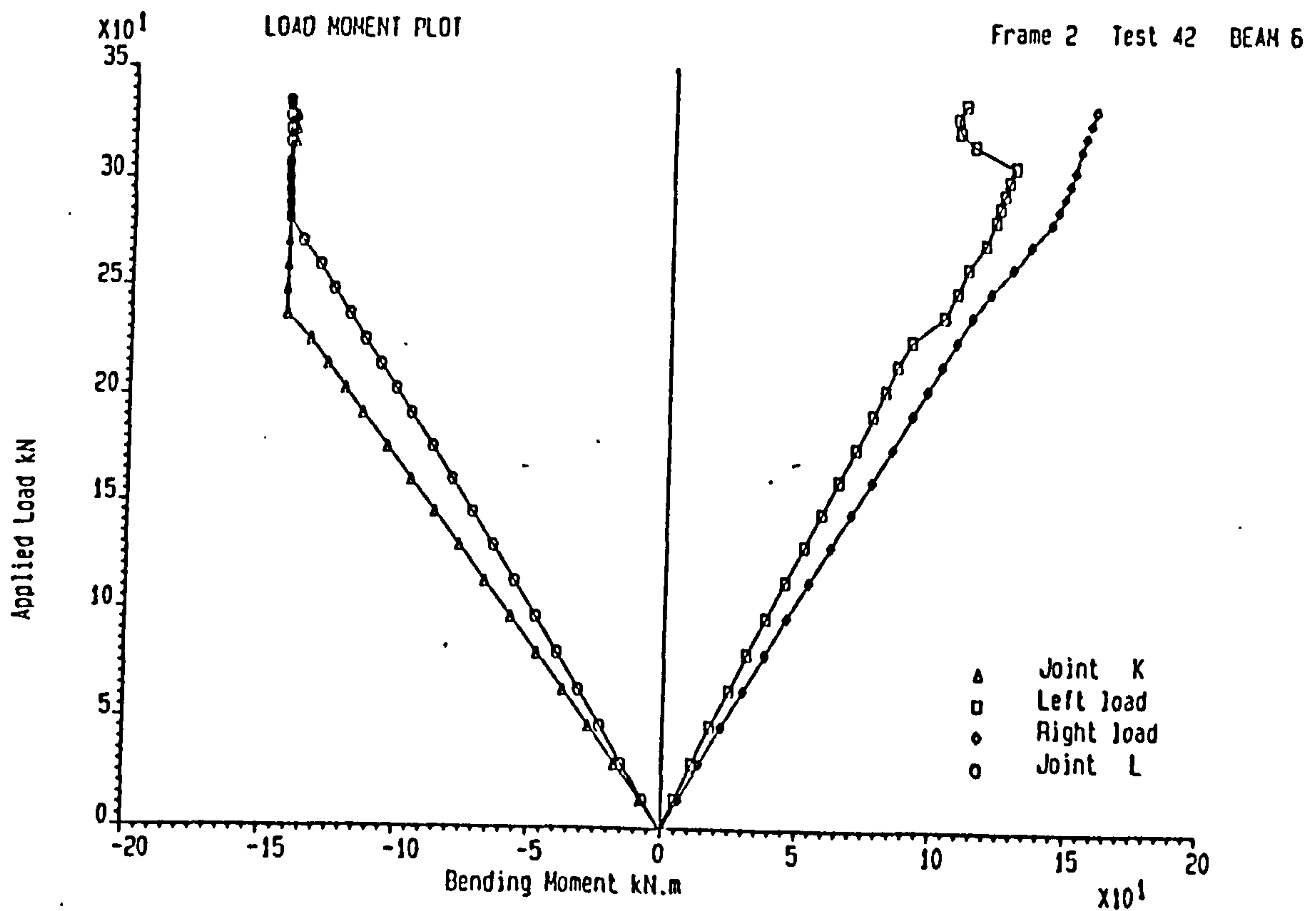


Figure 5.56 : Total Applied Load against Bending Moment on Beam 6  
in Test 42 of Frame 2



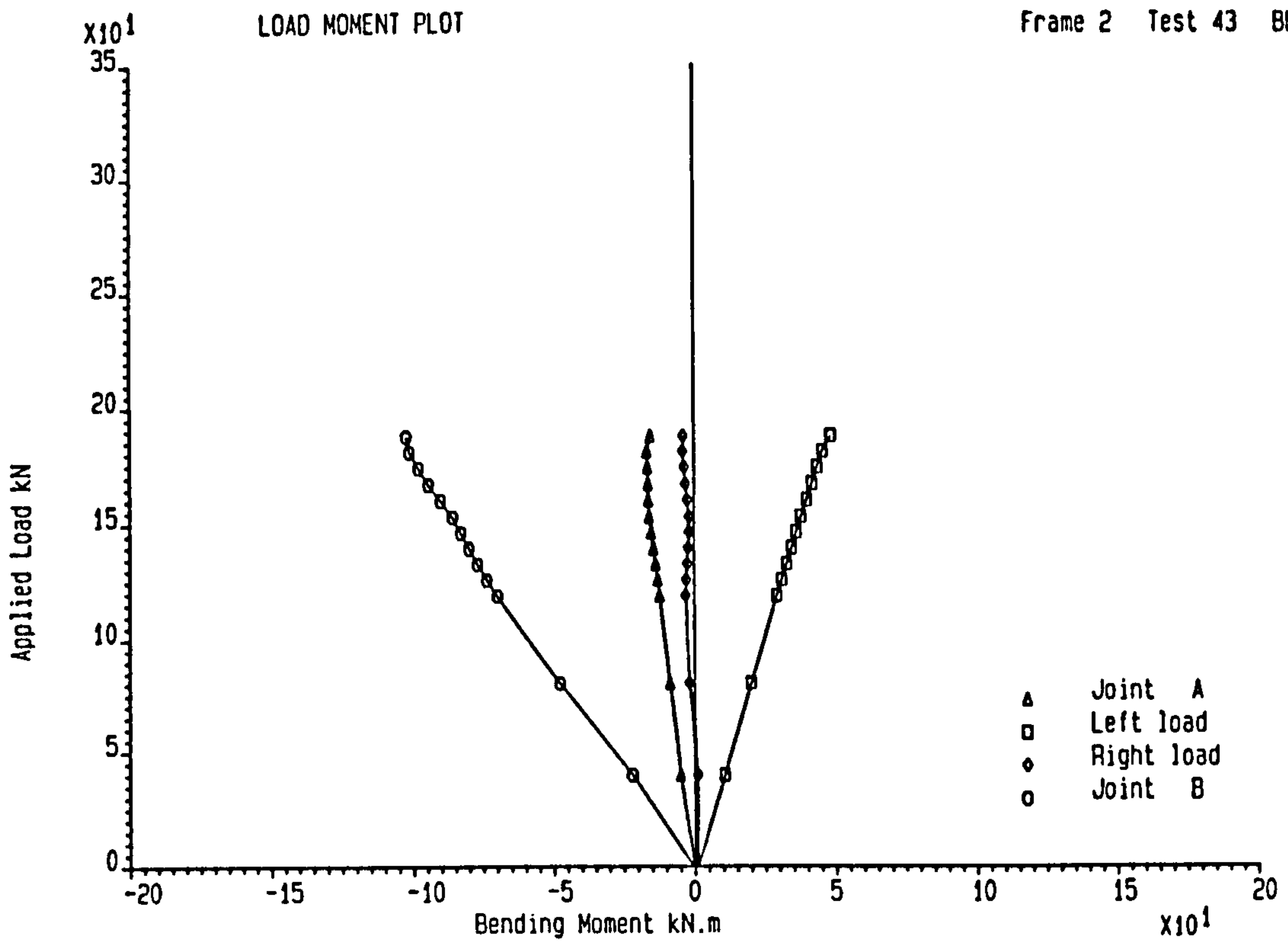


Figure 5.57 : Total Applied Load against Bending Moment on Beam 5  
in Test 43 of Frame 2

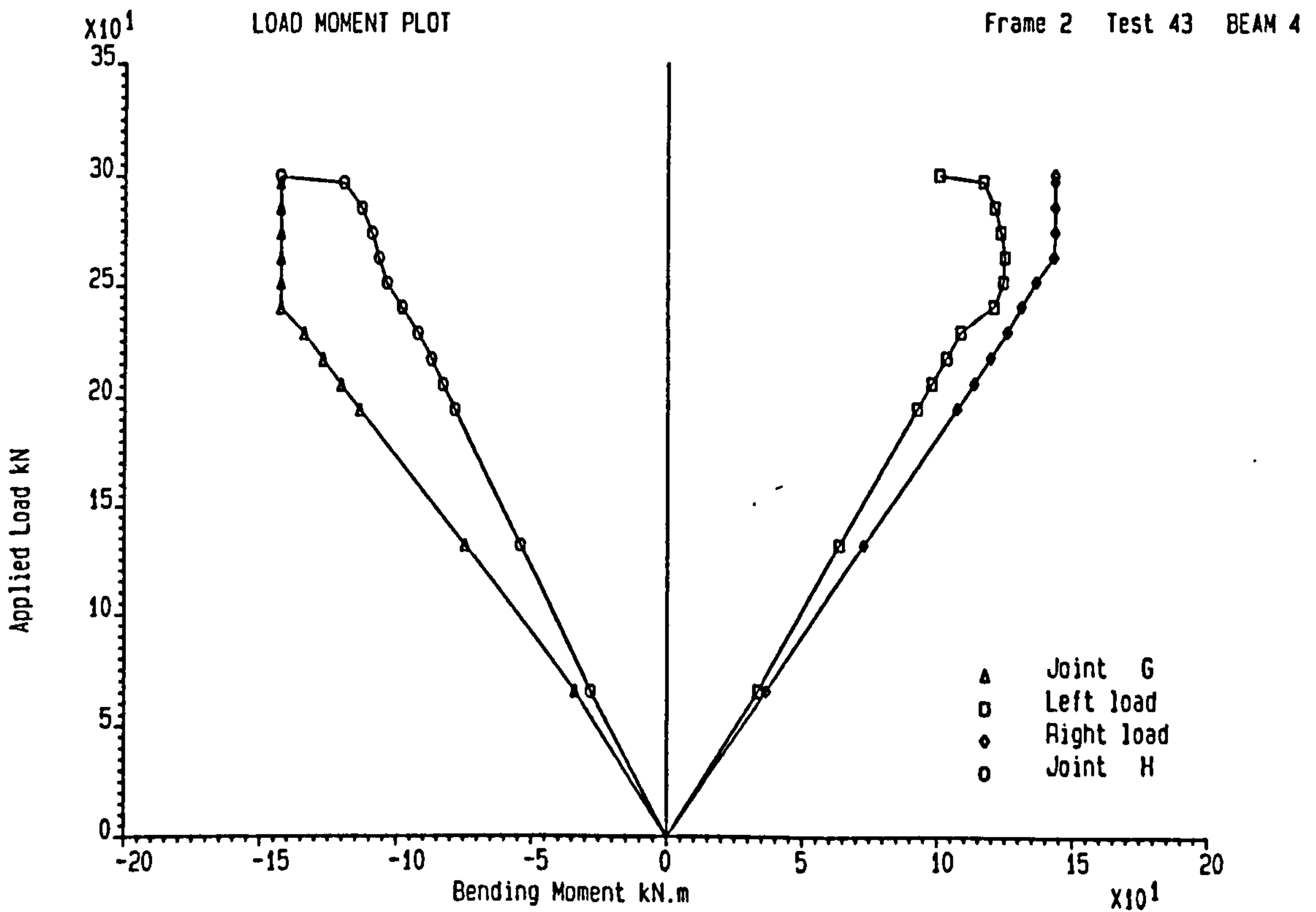


Figure 5.58 : Total Applied Load against Bending Moment on Beam 6  
in Test 43 of Frame 2

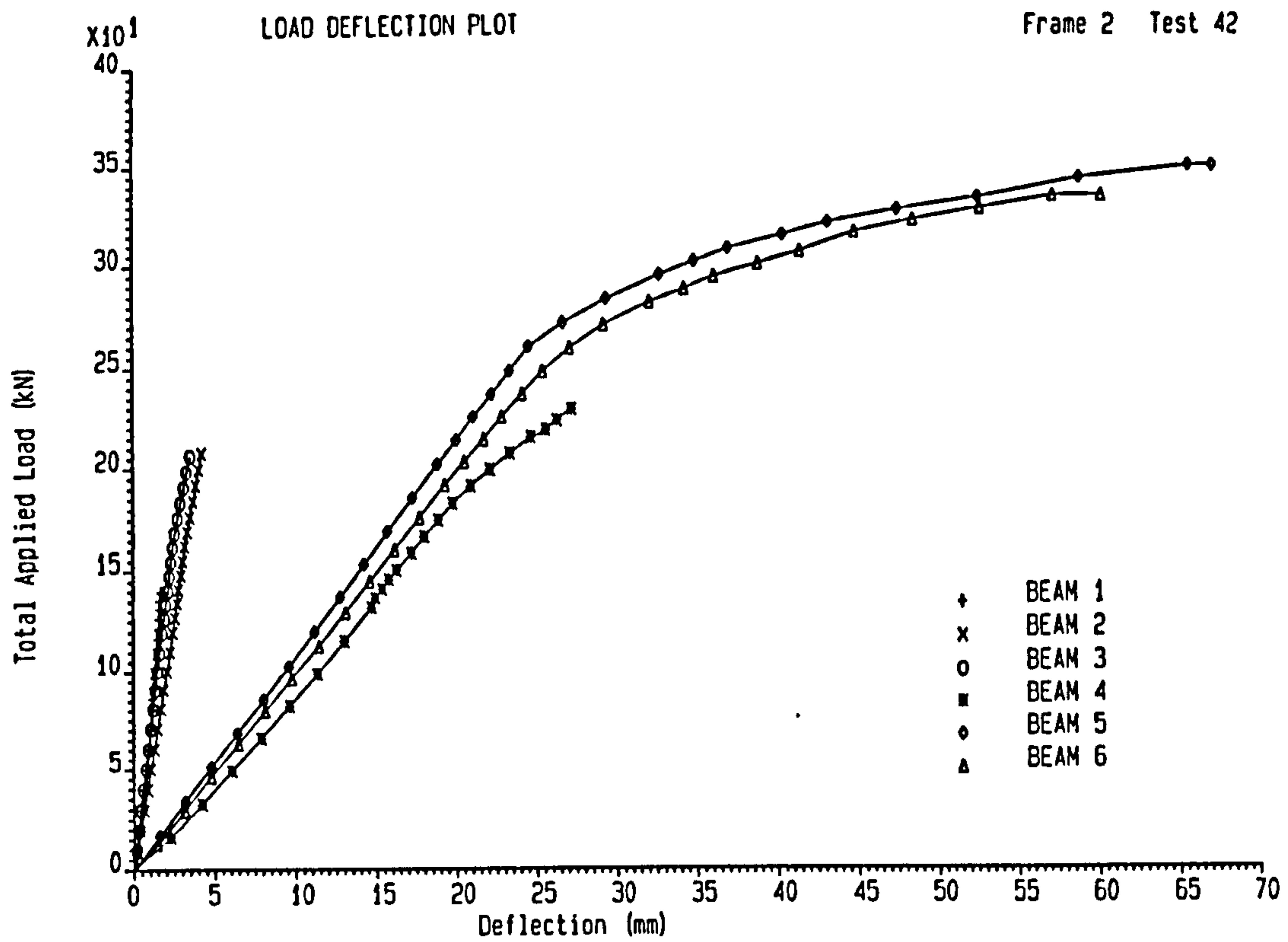


Figure 5.59 : Total Applied Load against Mid-Span Deflection on Six Beams  
in Test 42 of Frame 2

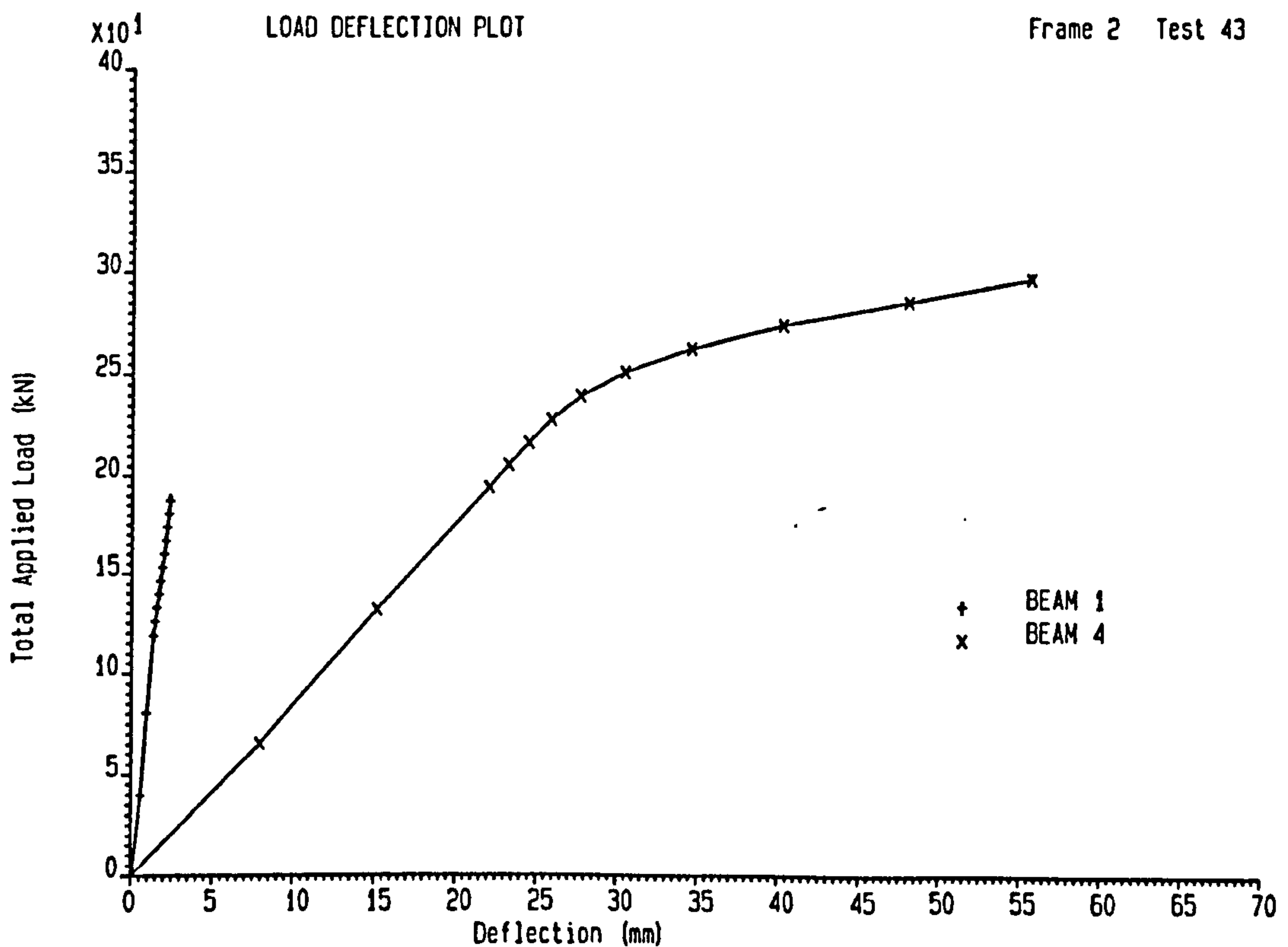


Figure 5.60 : Total Applied Load against Mid-Span Deflection on Beams 1  
and 4 in Test 43 of Frame 2

## Chapter 6

# Behaviour of Two Frames with Flange Cleat Connections

### 6.1 Introduction

This chapter investigates the behaviour of two full scale frames, designed by the University of Sheffield and tested at the Building Research Establishment in 1986. Both frames incorporated flange cleat connections between the beams and columns, connections which lie towards the centre of the semi-rigid stiffness spectrum. The objective of the two frame tests was to investigate the overall behaviour of structures, concentrating specifically on the capacity of the columns under non-sway conditions and comparing the response of columns buckling about their major and minor axes [6.1]. In this chapter, the frame is introduced briefly and then the specimens and test set up are described. The tests to failure are analysed in detail and the moment rotation characteristics of the joints are discussed.

### 6.2 Test Configuration

The Sheffield frames, shown in Figures 6.1 and 6.2, were three storey structures of approximate overall dimension 10 m wide x 11 m high which represents the maximum frame size which could be tested conveniently in the laboratory at BRE. Figures 6.3 and 6.4 show the general arrangement of the two frames when viewed from the balcony whilst the preceding photographs view towards the balcony. A suitable storey height for this frame was assessed to be 3.6 m, a figure selected as being representative of current building practice. Two equal bay widths were adopted with beam spans of 5 m and the beams were designed to frame into the column flanges in frame 3 and column webs in frame 4. Thus a comparison

of the behaviour was obtained for different column orientations.

Both frames were constructed using 152 x 152 UC 23 sections for the columns and 254 x 102 UB 22 sections for the beams. All steel was nominally grade 43A throughout. As the principal aim of the work was to examine the effect of the inherent, but usually neglected, stiffness of 'simple' connections the flange cleat type of connection was selected as being in the centre of the semi-rigid stiffness spectrum. At the time, seat and top cleats was, according to a survey [6.1,6.2], quite widely used in steel frame construction, often because of the usefulness of the seat cleat and the inherent tolerance on dimensional accuracy during erection. Figure 6.5 illustrates the flange cleat adopted in the connection of this frame. At the present time, header plates and tab plates have overtaken it in popularity.

All bolts were M16 grade 4.6 and were symmetrically tightened from 80 N.m to 160 N.m in 40 N.m increments. The method of assembly, though different from that in practice, should not significantly affect the resulting moment rotation curves because the bottom cleat was fixed tightly to the beam flange before bolting the cleat to the column, thus ensuring good contact between the cleat and the beam flange. All the columns had a 'fixed' base detail with heavy base plates bolted to the laboratory floor through the existing grid of holes spaced at 381 mm centres.

The two Sheffield frames had no stiffeners in the column, unlike the two Hatfield frames which had stiffened column joints using conventional horizontal stiffeners positioned directly in line with the connected beam flanges (see Figure 5.4). The two Sheffield frames were tested in-plane and in a non-sway condition. Bracing was used to prevent both out-of-plane buckling of members and lateral displacement of the frame. The nodes of the right-hand column were braced to the adjacent balcony (see Figure 4.5). As for the two Hatfield frames, stiffeners were used at the loading points in all beams (see Figure 5.4) in order to prevent web buckling due to the applied loads.

Both Sheffield frames were designed to BS 5950 Part 1 : 1985 [6.3] and BS 449 Part 2 : 1969 [6.4]. The calculations were used to determine an appropriate level of beam loading, to ensure that the selected beam section would sustain this load neglecting joint stiffness and to estimate the 'design' capacity of the columns. Two points loads were applied at the quarter and three-quarter points of the beam in these tests as previously explained in section 5.2 for the Hatfield frames.

Each beam was loaded at its quarter and three-quarter points using a loading system

similar to that described in chapter 4. Two important effects of connection behaviour on columns are moment transfer and end-restraint. Both of these effects have been studied by Nethercot [6.5], who concluded that different forms of column behaviour could be attained by changing the sequence of loading. Two loading cases investigated were axial column load only and beam load applied first, followed by axial load to failure. His study showed that when the beams are loaded first these loads induce end-rotations, which takes up much of the initial stiff portion of the connection  $M-\phi$  curves with the result that the effects of a change in connection type are more pronounced. For this reason, the beam load was applied whilst load was applied in increments to a pre-determined value after which column loads were applied to failure using displacement to control the hydraulic system. A detailed description of the loading arrangement in the frame tests is given in chapter 4. Table 6.1 summarises the load levels applied to the beams up to their design loads. The data logging and storage system is explained in chapter 4. A detailed description of the instrumentation is recorded in the reference [6.6].

### **6.3 Test Programme of Frames 3 and 4**

The tests can be divided into 3 stages; preliminary tests, tests to failure and calibration tests. In this chapter, only the tests to failure of frames 3 and 4 are discussed and a detailed checking of the preliminary tests and calibration tests was reported in progress report nos 6 and 7 [6.7,6.8].

During a preliminary test in frame 3, an accidental failure of the upper storey of the left hand edge column (viewed from balcony) occurred due to an inadvertent overload. The failed part of the column and the beam connected to it were removed. Fortunately, it was found that [6.9] the failure had not affected the frame other than the two members removed.

## **6.4 Tests to Failure - Frame 3**

### **6.4.1 Test Observations**

Test 2 was used to investigate the behaviour of the frame up to the failure of both full height columns in the non-sway mode under a combination of beam and column loads. Two

scans of readings were taken at zero load (one with the hydraulic pump off and one with the pump on) and at a beam loading of 60 kN on beams 2, 3, 4 and 6. All five beams were then loaded to their full dead load in small increments. Beams 2, 3, 4 and 6 were then loaded to their full design load with the load on beam 5 remaining at its dead load value. Table 6.2 summarises the load levels applied to the beams at each scan. After the applied beam load phase, all of the connections around the frame were inspected for signs of distress. During the beam loading phase, a few audible slips were observed in the connections, but none were dramatic or unduly affected the frame. Additional loads were then added to the columns at heads of positions 2 and 3. Displacement rather than load was employed to control the hydraulic system used to apply the axial deformation to the column. This gave greater control in the region of failure and, consequently, enhanced safety. Two full height columns were loaded to about 250 kN in five increments. The column in position 2 was then loaded up to failure. Further load increments were required to fail the edge column primarily because a lower load was transferred into the edge column from the adjacent beams than was applied to the central column. After failure of the columns in positions 2 and 3, the axial loads applied to the columns were released and all the beam loads were then reduced to about 53 kN before all loading was removed from the frame. An examination of the strain gauges indicated failure by instability in the upper storey of the central column and lowest storey of the edge column.

#### **6.4.2 Problem in the Applied Column Loads**

After the test, a problem associated with the computed column axial loads was discovered since both sets of load cells implied higher applied axial loads in two columns than the axial loads obtained from the strain gauges. A discrepancy up to 7 % of the column load was observed.

From a BRE report [6.10], the calibration figures were amended to take account of the difference in voltage used in the calibration and frame test i.e. 6v was used in the calibration test and 10v in the frame test - so the calibration factor used in the frame test should be divided by 1.67. When the uncorrected calibration factor was adopted, the computed column loads were larger than those which actually occurred in reality. The incorrect applied column loads were recorded in the data logger. Table 6.2 presents the uncorrected applied column loads obtained in test 2.

To overcome this problem, three methods are considered by the author. The first

method is to use a simple correction factor as mentioned above which is the ratio of the calibration factor in each loading cable between the true value and the uncorrected value used in the test. Thus, the correction factor changes the recorded value of the applied column load to the corrected value. The second method uses the axial load in the upper storey of columns, predicted by the strain gauges, to determine the applied column loads. Finally, method three uses a computer program to convert the recorded column axial load from the data file back to a voltage which is then used to predict the corrected column loads which gives slightly different values due to the non-linearity in the calibration curve. The corrected data is then saved in a new data file. Details of these three methods and the results obtained (shown in Table 6.3) are discussed as follows:-

1. Method 1 :

This method is based on using a corrected factor for each column to determine the actual applied column axial load. The graph from the BRE report [6.10] represents the actual calibration factor for each loading cable from the BRE report which is compared with the calibration factor adopted during the test [6.11]. A ratio is then determined to represent the correction factor for the column load. Each uncorrected load times the correction factor then gives the actual applied axial load. This method was used by Davison for the analysis of both Sheffield Frames [6.1].

2. Method 2 :

This method uses the axial load in each column determined from the strain gauges. The total axial load in columns of each storey should of course be equal to the total applied beam and column loads. The total axial load for both of the upper storey column was used to determine to the total applied load. The actual applied column load was obtained by subtracting the axial load obtained from the scan at the end of the beam load phase from the value at each scan. For example, the applied load at column in position 2 at scan 16 can be determined as the axial load in column 4 at scan 16 minus the axial load in column 4 at scan 14.

3. Method 3 :

This method is thought to most accurately predict the applied column axial loads. A computer program was written to take the logged column load from the uncorrected data file and convert the readings back to a voltage. The voltages are then used as the independent variable in a polynomial expression for the

load. The polynomial is based on the calibration data obtained from the latest BRE report [6.10].

From Table 6.3, it can be observed that the three methods predict similar results for the column in position 2. In scan 19 (where the same total load was applied to both columns), methods 1 and 3 predict a similar result for the applied column load in position 2 and also predict a similar result for the applied column load in position 3. As failure was approached for the column in position 2 (scan 24), the three methods predict a similar failure load. However, only methods 1 and 3 predict a similar failure load of 620 kN as failure was approached in the column in position 3 (scan 38) whilst method 2 predicts a load of 673.2 kN.

Table 6.4 shows a comparison between the axial load determined by the strain gauges in the upper storey with the result obtained from methods 1 and 3. A large discrepancy of results obtained was found. The axial loads predicted by the strain gauge are higher than those from the load cells, which suggested that the value of  $E$  measured in the stub column test ( $E = 222 \text{ kN/mm}^2$ ) may be rather high. Furthermore, the large discrepancy may be also due to the combined effect of unreliable nature of results obtained from the strain gauges after material yield. The axial load in each column lift during the test and determined by the strain gauges is presented in Table 6.5. A comparison of the total applied beam and columns loads in each storey using results from method 3 and the axial load computer from strain gauge readings in the columns at this level are shown in Table 6.6. Examination of the results show differences of up to about 10 % in the various storeys up to the end of beam load phase. However, an even larger discrepancy up to 15 % was observed in high applied column load due to the problems of the unreliable nature of results obtained from the strain gauges after material yield as described above. A more detailed discussion of this problem together with a method to improve the results is presented in section 6.4.7.2. In conclusion, it is noted that methods 1 and 3 yield similar results for the applied column loads for test 2 whilst different axial loads are determined from the strain gauges measurements in this study. Method 3 is thought to most correctly interpret the applied axial load due to the technique adopted and will be used for further analysis. Finally, the corrected load history using results from method three is shown in Table 6.7.

### 6.4.3 Bending Moments on Beams

Figures 6.6 to 6.10 show the load moment plots for beams 2 to 6 in Test 2. Each figure shows the change of moment at the four strain gauged sections, two near the connections



and two near the loading points, along each beam as load was applied to the frame. The value of load plotted on the vertical axis is the sum of both loads on the beam as measured by the load cells in the loading rods. The connections at the two ends of each beam attracted moment due to the stiffness of joints, leading to a decrease in the moment at two loading points below the free bending moment.

For moderate loads, non-linear curves were obtained for all five beams at the beam ends and near the connections and consequently the load moment relationships were non-linear. Figure 6.11 shows the distribution of moment in beam 3 as the applied beam load increased. This figure displays the bending moment distribution for scans 4, 6, 8, 10, 12 and 14 which cover the beam loading phase. At the load level corresponding to the design load for beam, the connections sustained a moment of approximately 20 % of the free bending moment in the mid-span of the beam.

After the axial column load was applied (Figures 6.6 to 6.10), an increase of the moment in two loading points for each beam was observed with no increase in applied beam load. Thus, the failure of the column required either further rotation or relaxation of the connection moment with a consequent shift of moment to the mid-span of beam.

#### 6.4.4 Relationship of Load-Deflection in Beams

Figure 6.12 shows the load deflection curves in a single plot for all five beams in Test 2. All curves shown follow a non-linear route up to the end of the beam loading phase. After that, an increase in the mid-span deflection for each beam was observed with no further increase of the applied beam load. As explained in section 6.4.3, the failure of the columns required either further rotation of the connection or a relaxation of end moment which caused an increase of the mid-span deflection of the beam. Deflections of 23 to 25 mm were observed in beams 2, 3, 4 and 6 when they were under their design load before the application of any applied column load. Comparison with the mid-span deflection from a simply supported beam showed a typical deflection value of 33 mm. Thus the result of this frame test showed a reduction of over 24 % the mid-span deflection of the beams due to the restraint provided by the semi-rigid joints.

#### 6.4.5 Bending Moment Distribution around the Frame

Figures 6.13 to 6.15 show the distribution of bending moment around the frame. In Figure 6.13, the moments at three levels of load are plotted on the same graph in order to compare the variation of frame moment at different locations and at various levels of loads. Scan number 7, which corresponds to the dead load (D.L.), scan number 11, which corresponds to the dead plus imposed loads (D.L. + L.L.), and scan number 14 which corresponds to the design load (1.4 D.L. + 1.6 L.L.) are used. In Figure 6.16, the moments in each beam and column are shown. The apparent out-of-balance at the beam-column intersection is due to the additional moment induced at the column centreline by the eccentricity of the beam end reaction. Figures 6.14 and 6.15 show the frame moment at the level of load corresponding to the failure of columns in positions 2 (scan 24) and 3 (scan 38) respectively. Very high moment was observed in the top of the central column in the upper storey (Figure 6.14) and the top of the edge column in the lowest storey (Figure 6.15). The two failure modes are discussed in section 6.4.7.

#### 6.4.6 Deflected Shape of the Frame

Deflections were recorded at the mid-span, quarter and three-quarter points of the beams and the mid-heights of the columns. Figures 6.17 to 6.19 show the deflections of the frame at different load levels. In Figure 6.17, the deflections during the beam loading phase are plotted in the same figure; the load levels corresponding to the scans are as described in Figure 6.13 and section 6.4.5. The mid-span deflections for the beams and the columns all increased approximately proportionately to the applied load. In Figure 6.18, the mid-span deflection at three levels of load are plotted on the same graph in which scan 14 represents the end of the beam load phase, scan 19 represents the condition at which the loading applied to the two columns was at its maximum equal value and scan 24 represents the load at failure for the column in position 2. In Figure 6.19, the mid-span deflection at three levels of load are plotted on the same graph in which scan 14 and scan 19 are as described above and scan 38 represents the load at failure of column in position 3. These two figures illustrate the change of deflection from the end of beam load phase up to the failure of the columns. There was a modest change in the mid-height deflection from the end of beam load phase to the end of the equal loading applied to the two columns. However, substantially larger mid-height deflections were observed between the last two levels of loads as failure was approached for each of the two columns.

## 6.4.7 Behaviour of Columns as Failure Approached

### 6.4.7.1 Failure of Column in Position 2

Figure 6.20 shows the total load against the mid-height deflection for the three lifts in column position 2. After the load was applied to the head of the central column, it is evident that there is a lesser change in the mid-height deflection of columns 4 and 5. The marked change of slope in the load-deflection behaviour at the end of the beam load phase and the commencement of axial load applied to the column head can be observed for both upper column lengths. As column 4 sustained a larger moment from the single beam connected at its head, as shown in Figures 6.13 and 6.14, it underwent the largest mid-height deflection of about 6 mm. The smallest mid-height deflection of about 3 mm was observed in column 5 due to the reduced moments introduced at the first and second floor levels. In Figure 6.20, very little mid-height deflection was observed in column 6 (1.5 mm) during the beam load phase. This was due to the balanced beam loads introduced at the first floor level and, to a lesser extent due to the stiffness of the column base. When axial load was applied at the column head in position 2, the mid-height deflection of column 6 increased steadily throughout the beam and column loading phase as throughout, it mainly experienced additional axial loading due to the balance natured of the beam loading. Failure occurred when the central column was unable to sustain a steady axial column load. As the failure was approached, the recorded applied column load was 464 kN and the strain gauged cross sections gave the total axial load in columns 4, 5 and 6 as 542 kN, 644 kN and 789 kN respectively. These values correspond to 523 kN, 609 kN and 727 kN as computed from 464 kN plus half of the loads applied to each connecting beam above the section.

Figure 6.21 shows the axial load against the bending moment at the tops of columns 4, 5 and 6. No loss of stiffness was observed in any of the three columns during the beam load phase. When load was applied to the top of the central column, column 4 exhibited a loss of stiffness until failure was produced in that column segment. However, for columns 5 and 6 no significant change of the column head moment was seen. Thus failure was reached in column 4 resulting from the loss of stiffness due to the application of the highest out of balance beam moment being transferred to the column head due to the rotation of the column head during the beam load phase. This phenomenon was due to the discontinuity of the beam on the adjacent side and exacerbated because no column extended above that level to share the high applied moment as shown in Figure 6.14. Thus the failure was initiated in that column section due to the arrangement of the test frame. However, such a failure would be less likely in a real structure. Although edge columns always exists, for such high axial loading to be introduced, the column would need to be extended above that

floor level and thus the applied moment would be shared between two column ends. The test condition therefore represents an extreme adverse condition.

#### **6.4.7.2 Failure of Column in Position 3**

Figure 6.22 shows the total load against the mid-height deflection of columns 7, 8 and 9 in position 3. The large mid-height deflection observed in column 7 was due to the large moment transmitted to the edge column between the second to third floor levels. Inspection of the plot reveals that the major part of the deflection occurred during the beam load phase. When the load was applied equally to both columns, the mid-height deflection reduced slightly and then kept at essentially the same value. After that additional column load was applied continuously to the top of the column in position 2 with a same applied load holding at the top of the column in position 3, an increase of deflection was observed. Having failed the internal column, extra load was then applied to the edge column in position 3. A non-linear curve with an increasing deflection was observed for equal increments of applied axial load. Finally, a maximum value of mid-height deflection of 3.5 mm was determined as failure was approached for that column.

In column 8, the deflections were very small and showed some scatter initially, followed by the same value at different levels of load. A similar form of behaviour was obtained for column 9. However the principal feature is that the deflections were very small (less than 0.1 mm).

Figure 6.23 shows axial load against bending moment at the top of column lift nos 7, 8 and 9 which make up the column in position 3. Constant stiffness was observed for all three columns up to the maximum dead load applied to each beam. After that, a reversal of moment occurred in column 8 as the load in beam 5 was kept constant whilst the loads applied to beams 4 and 6 were increased. Columns 7 and 9 showed no change of stiffness during the beam load phase. When the column load was applied to the top of the edge column, column 9 exhibited a loss of stiffness until failure was produced in that column segment. However, for column 7 there was no significant change of the column head moment while a reversal of the head moment was produced in column 8 during the application of the column head load. Thus it may be argued that failure was reached in column 9 which resulted from the continual loss of stiffness due to the increasing moment formed at the column head.

As failure was approached in the edge column, the record of applied column load was 620 kN and the total axial load in each of the column lifts 7, 8 and 9 was determined as 732

kN, 782 kN and 891 kN respectively. These values correspond to 679 kN, 706 kN and 766 kN as computed from the 620 kN head load plus half of the loads applied to each connecting beam above the section.

A close inspection of the strain gauge readings after the test suggests that the failure occurred in the column in the ground to the first floor level at the total axial load of 891 kN. A large discrepancy was found when it was compared with the failure load obtained from the load cell. As discussed in section 6.4.2, the axial loads predicted by the strain gauges are higher than those from the load cells, which suggested that the value of E measured in the stub column test may be rather high. The reliability of the strain gauge readings after plasticity may be an additional reason causing an over-prediction of the failure load. The readings from strain gauges in yield zones, which may bridge a number of slip planes, tend to be unreliable. Furthermore, there were only four strain gauges employed in the force monitoring system and hence the loss of any one of the gauges in a yielded zone would prevent a correct interpretation of the force components. This problem of strain measurement in zones of discontinuous yield was recognised by Birnstiel in a study of a biaxially loaded steel columns [6.12]. The solution which he adopted was the use of long gauges (65mm gauge length) which straddled a significant number of adjacent slip planes. The resulting strain readings were then effectively an average plastic strain over the length of the gauge. This method appeared to work well in Birnstiel's studies. Due to the unreliable performance of strain gauges in yield zones, it was evident that more than the absolute minimum of four gauges would be preferable. Work carried out by Lightfoot [6.13] has shown how so called 'redundant' gauges can be incorporated into strain data analysis to generate the strain profile in structural steel sections more accurately. A method has been developed by Gibbons [6.14] for measuring the forces and moments in structural steel sections in both the elastic and the elastic-plastic regions which used four gauges on the top and bottom flanges and two gauges on the column web. The method involves the mathematical treatment of readings from the redundant strain gauges to improve the accuracy of the strain measurement under elastic stress conditions. A close correspondence of the results was obtained with the predicted result of a finite element program in his study. Thus it is clear that the use of more strain gauges should be included in future experimental studies.

## **6.4.8 Tests to Failure of Beams**

### **6.4.8.1 Accidental Failure of Beam 6**

After the two columns had been loaded to failure, test 3 was carried out in order to fail each of the beams. The load history of this test is shown in Table 6.8. All beams were loaded to their full dead load (scan 7) and the applied loads on beams 2, 3, 4 and 6 were then increased to design load value in six increments (scan 13). From the BRE report [6.9], beams 2 and 3 were accidentally unloaded during a change of loading to beam 6. This causes failure to occur in beam 6 under an applied axial load of 128 kN. Unfortunately, no reading was taken to indicate the unloading of beams 2 and 3 in the data file. After that beams 2 and 3 were reloaded to their design load values of 116 kN, and beam 6 was loaded to 128 kN for a second time. Three scans of readings were then taken at this level of load. Failure was observed in that beam, all beams were then unloaded to their dead plus imposed loads and subsequently dead loads before all applied loads were released. A detailed discussion is presented in the author's progress reports [6.7].

### **6.4.8.2 Failure of Beams 3, 4 and 5**

The aims of failing each beam was not reached in test 3 and therefore a further test (test 4) was carried out in order to fail beams 3, 4 and 5 individually. Table 6.9 shows the load history in test 4. All beams were first loaded to their full dead load (scan 3). After two further load increments, beam 3, 4 and 6 were loaded to their design loads which was achieved in scan 5. Beam 3 was the first beam to be loaded up to failure. After four more increments of load were applied (scan 9), it was found that the beam was unable to take further load showing that failure was approached. The load on beam 3 was kept at its failure value and beam 5 was then loaded up to failure. This occurred in beam 5 after five increments of applied load. Finally, the same procedure was applied to beam 4 with the failure load being maintained on beams 3 and 5. Failure occurred in beam 4 after six increments of applied beam load at a recorded applied beam load of 147 kN.

Figures 6.24 to 6.26 show the load vs moment plots for beams 3 to 5 in test 4. Linear load moment relationships were obtained for beams 3 and 4 at different locations up to applied beam loads of 120 kN, and consequently the load moment relationship was linear only up to a level of load lower than their design load (1.4 D.L. + 1.6 L.L.). In Figure 6.26, a decrease of the moment can be observed at the two loading points whilst an increase of moment can be seen at the two ends of the beam when beam 5 was under its dead load. This was due to the effect of increasing the applied load on beams 2, 3, 4 and 6 with no

change of applied load to beam 5. The rotation of the column forces an increase of the joint rotation and thus increases the connection moment and reduces the mid-span moment. A larger increase of moment is produced in three of the beams with a corresponding increase of applied load after the applied beam load exceeded 120 kN in beam 3, 110 kN in beam 5 and 130 kN in beam 4. The shedding of moment to the mid-spans of three beams was a result of the plastic hinges nearly formed at the beam ends.

Figure 6.27 shows the load deflection curves on a single plot in beams 3 to 5 in test 4. This figure shows the relationship for beam 3 which followed a linear route up to high applied loads (120 kN). Subsequently, the variation to non-linear curves, having larger increments of deflection for corresponding increases of the applied load, reflected a loss of stiffness with higher applied load. The failure occurred at an applied beam load of 146 kN with a mid-span deflection of 38 mm. This figure also shows a linear response up to an applied beam load of 130 for beam 4 after which it changes to a non-linear curve with a larger increments of deflection for corresponding increases of the applied load. The plot indicates that failure was reached at an applied beam load of 147 kN with a corresponding maximum mid-span deflection which was recorded as 36 mm. This figure shows a reduced deflection was observed at constant applied dead load in beam 5. This was explained in the section 6.4.4. and was due to the effect of load being applied to other beams.

## **6.5 Tests to Failure - Frame 4**

### **6.5.1 Test Observations**

Test 3 was used to investigate the behaviour of the frame up to the failure of the two columns in the non-sway mode under a combination of beam and column loads. After two scans of readings were taken at zero load (one with the hydraulic pump off and one with the pump on), load was then applied to all beams up to their dead load values. Beams 1, 2, 3, 4 and 6 were then loaded to their full design load with the load on beam 5 remaining at its dead load. As for Frame 3, displacement rather than load was employed to control the hydraulic system used at the head of columns. All columns were first axially shortened by 3 mm (approximately 150 kN). The column in position 1 was then axially shortened by 1 mm (50 kN) increments and finally 0.5 mm (25 kN) increments up to failure of that column. After failure of column in position 1, a similar procedure was used to fail the central column in position 2 with a very high but sustainable load remaining in the already failed column in position 1. After failure of the two columns, the axial displacement applied to all columns

was released and all the beam loads were reduced to about 53 kN before taking all load off the frame.

As in frame 3, there was a problem of erratic records of applied column load again due to the use of an uncorrected calibration factor adopted in this frame tests [6.10,6.11]. The same method as was used for frame 3 was again employed to solve this problem. Table 6.10 provides a corrected load history for this test. The axial load in each column lift during the test and determined by the strain gauges is recorded in Table 6.11 and a comparison of the applied beam and column loads in each storey and the axial load measured in the column at this level are shown in Table 6.12. A discrepancy of up to 7 % was determined at scan 42 (failure of the central column). This was again due to the combined effect of unreliable nature of results obtained from strain gauges after material yield as discussed in progress report no.7 (Frame 3) and the errors in the axial displacement resulting from the rotation of the column head and the eccentricity of the devices.

Based on the records of Davison [6.1], the lateral movement of joint C with the maximum value of 1 mm was monitored using a theodolite throughout the test which verified that the frame was effectively braced.

### 6.5.2 Bending Moments on Beams

Figures 6.28 to 6.33 show the load against moment plots for all six beams in test 3. For moderate loads, non-linear curves were obtained for all beams at the beam ends and near the connections and consequently the load moment relationships were non-linear. Figure 6.34 displays the bending moment distribution for scans 4, 6, 8, 10, 12 and 13 which cover the beam loading phase. At the load level corresponding to the design load for beam, the connections sustained a moment in a range 17 - 20 % of the mid-span free bending moment.

After the axial column load was applied (Figures 6.28 to 6.33), an increase of the moment in two loading points for each beam was observed with no increase in applied beam load. Thus, it may be concluded that the failure of the column required either further rotation or relaxation of the connection with a consequent shift of moment to the mid-span of beam.



### 6.5.3 Relationship of Load-Deflection in Beams

Figure 6.35 shows the load deflection curves in a single plot for all six beams in test 3. All curves shown follow a slightly non-linear route up to the end of the beam loading phase. After that, an increase in the mid-span deflection for each beam was observed with no further increase of the applied beam load. As explained in section 6.5.2., the failure of the columns required either further rotation or relaxation of the connection with an increase in the mid-span deflection of the beam. Deflections of 25 to 32 mm were observed in beams 1, 2, 3, 4 and 6 when they were under their design load before the application of any applied column load. Compared with the results determined in test 2 of Frame 3, a little higher mid-span deflection was obtained in this test at the same level of applied beam load. This may be due to reduced restraint provided to the beams by the adjacent minor axis columns. These deflections compare with the mid-span deflection of a simply supported beam which are typically about 33 mm. Thus the result of this frame test showed a reduction of up to 24 % in the mid-span deflection of the beams due solely to the restraint provided by the semi-rigid joints.

### 6.5.4 Bending Moment Distribution around the Frame

Figures 6.36 to 6.38 show the distribution of bending moment around the frame. In Figure 6.36, the moments at three levels of load are plotted on the same graph in order to compare the variation of frame moment at different locations and at various levels of loads. Scan number 7, which corresponds to the dead load (D.L.), scan number 10, which corresponds to the dead plus imposed loads (D.L. + L.L.) and scan number 16 which corresponds to the design load (1.4 D.L. + 1.6 L.L.) are used. The upper stories of two external columns 1 and 7 were subjected to quite high moment and thus caused considerable deflection (Figure 6.40). Due to the flexibility of the two external columns in the upper stories, less moment was attracted to the connections A and H. Conversely, the presence of two adjacent beams at the central column enable larger restraint to occur with higher moments attracted at the same load level but with very little moment being transferred to the column due to the balanced beam moments introduced at the two sides. A detailed analysis of the behaviour of the joints in the test will be discussed in section 6.5.10. Figure 6.39 shows the moment distribution at the intersection of the beam and column at the end of the beam loading phase. Most of the intersection points indicated that the apparent out-of-balance is small, less than 1.72 kNm. This out of balance is probably due to the additional moment induced at the column centreline by the eccentricity of the beam end reaction. Figures 6.37 and 6.38 show the frame moment at the level of loads corresponding to the failure of

columns in positions 1 (scan 33) and 2 (scan 43). In Figure 6.37, very high moment was observed in the top of column 1. The high moment existing at this point was not anticipated and may be due to the rotation of the column head under the applied beam load which causes the load applied to the top of the column stub to induce both an axial load and a bending moment. This effect can be improved by modifying the connection from the column head and the loading system by inserting a captive roller bearing. Figure 6.38 shows the bending moment distribution at scan 43. Very little moment existed at the top of column 4 which was due to the balanced beam moments introduced at the two sides. Examining the results shown that a plastic hinge have formed at the mid-height of column in the second lift (column 5). A detailed analysis of the test to failure of two columns will be discussed next.

#### **6.5.5 Deflected Shape of the Frame**

Figures 6.40 to 6.42 show the deflection of the frame at different load levels. In Figure 6.40, the deflections during the beam loading phase are plotted on the same loading scan as in Figure 6.36. The change of deflection of beams and columns at the different level of loads are thus illustrated. The mid-span deflections for beams and columns increased approximately in proportion to the applied load. In Figures 6.41 and 6.42, the deflected shapes of the frame at failure of the column in positions 1 and 2 (scans 33 and 43) are plotted and frame distortions at the failure of the columns are thus clearly demonstrated. In Figure 6.41, very large mid-height deflection was observed in the top lift of the edge column in position 1. In Figure 6.42, the largest deflection was observed at the mid-height of the column in the second lift (column 5) due to the formation of a plastic hinge.

#### **6.5.6 Failure of Column in Position 1**

Figure 6.43 shows the total load against the mid-height deflection for the three column lifts in position 1. Observation of this figure shows that deflection increase with the increase of the axial load during the beam loading phase. After the load was applied to the head of the edge column, it is evident that there is a large increase in the mid-height deflection of columns 1 and 2 and a reversal of mid-height deflection was produced in column 3. The marked change of slope in the load-deflection behaviour at the end of the beam loading phase and the commencement of axial load applied to the column head can be observed for both upper column lengths. Failure occurred when the edge column was unable to sustain a steady axial column load. As the failure was approached, the recorded applied column load

was 468 kN and the strain gauged cross sections gave the total axial load in columns 1, 2 and 3 as 520 kN, 547 kN and 632 kN respectively. These values correspond to 529 kN, 587 kN and 646 kN as computed from 468 kN plus half of the loads applied to each connecting beam above the section.

It is noted in Figure 6.43 that larger deformation in the mid-height of column 1 suggests that failure occurred in this floor level. Figure 6.44 shows the axial load plotted against the bending moment at the top of columns 1, 2 and 3. When load was applied to the head of the edge column, column 1 exhibited a loss of stiffness until failure was produced in that column segment. A reversal of moment occurred in column 2 but the head moment in column 3 saw no significant change. Thus failure was reached in column 1, evident by a loss of stiffness, due to the application of the highest out of balance beam moment transferred to the column head. This phenomenon was due to the discontinuity of the beam on the adjacent side and exacerbated because no column extended above that column. After the application of applied axial column loads, large bending moments were produced at the top of the column as shown in Figure 6.37.

#### 6.5.7 Failure of Column in Position 2

Figure 6.45 shows the total load against the mid-height deflection of the lifts 4, 5 and 6 in columns position 2. It is observed in this figure that the largest mid-height deflection of 9 mm observed in column 5 and this coincided with the formation of a plastic hinge formed at the mid-height of that column lift due to out of balance moment introduced by two adjacent beams (beams 2 and 5). The appearance of the characteristic progressive loss of stiffness in columns 5 and 6 suggested that failure was also imminent in these two column lengths.

Figure 6.46 shows the axial load against the bending moment at the mid-height of columns 4, 5 and 6. An irregular curve was observed in column 4. The mid-height moment in column 5 increased steadily and rapidly until a plastic hinge had formed in this location under the axial load of 550 kN. A moment reversal was produced in column 6 after the axial load of 400 kN and a large increase in moment to 19 kNm was observed in that position at the maximum applied load. Failure occurred when the central column was unable to sustain a steady axial column load. As the failure was approached, the recorded applied column load was 404 kN and the strain gauged cross sections gave the total axial load in columns 4, 5 and 6 as 530 kN, 628 kN and 808 kN respectively. These values correspond

to 524 kN, 610 kN and 728 kN as computed from 404 kN plus half of the loads applied to each connecting beam above the section.

Failure was reached in the central column at the first and second lifts (columns 5 and 6) and flattening out of the load deflection plots was observed (Figure 6.45). The presence of a plastic hinge and the largest deformation observed at the mid-height of column 5 confirm this point and thus the column could not sustain higher axial load.

When the axial load was compared with the failure load obtained from the load cell (Table 6.12), a large discrepancy was found after scan 17. As discussed in frame 3, at high levels of load the axial loads predicted by the strain gauge are higher than those from the load cells due to partial yielding at strain gauge positions. The readings from strain gauges in yield zones, which may bridge a number of slip planes, tend to be unreliable. Furthermore, there were only four strain gauges employed in the force monitoring system and hence the loss of any one of the gauges in a yielded zero would prevent a correct interpretation of the force components. A detail discussion and the method used to counter this problem have been described in section 6.4.7.2.

### **6.5.8 Test to Failure of the Edge Columns in Position 3**

Test 4 was used to investigate the behaviour of the frame up to failure of the edge column in position 3 under a combination of beam and column loads applied to the test frame. After two scans of readings were taken at zero load (one with the hydraulic pump off and one with the pump on), load was then applied to all beams up to their dead load. Beams 2, 3, 5 and 6 were loaded to their full design load with the load on beams 1 and 4 remaining at its dead load in order to reduce the amount of displacement and rotation at the column head. As a result, the moment induced into the column by eccentricity of the loading system could be reduced. Table 6.13 summarises the load levels applied to the beams. The column in position 3 was axially shortened by 1 mm increment (approximately 50 kN). After two loading scans, the column load was reset and the column was axially shortened by 1 mm increments up to failure. However, the displacement transducer that controlled the load applied to the top of column in position 3 was observed to run out of travel at scan 27 and had to be reset. Then the column was accidentally failed due to additional applied load. After failure of this column, the axial displacement applied to all columns was released and all the beam loads were reduced to about 53 kN before taking all load off the frame. After the test, permanent deflection of 11 mm was observed at the

mid-height of column as shown in Figure 6.47.

### 6.5.9 Behaviour of Joints in Frame 3

Figures 6.48 to 6.51 illustrate the moment-rotation curves of the connections as measured in test 2 together with the smoothed curve from results of a test on isolated cruciform joint. The moment-rotation plots obtained from the experiment include not only the loading section but also the unloading part which may be used to derive the stiffness of the joint. The slope of the unloading curve and the initial tangent can be seen to be parallel in most of the joints i.e. joints C, E, F, G, I and K. The initial and unloaded stiffnesses found from each joint together with some analysis using new design approaches will be discussed in chapter 10.

The device at joint D developed a fault during the test and thus will not be discussed further. Some distortion was observed in some of the joints after the test, especially these on the central columns 5 and 6.

During the beam loading phase, all the connections behaved as expected exhibiting a reasonably smooth moment rotation response. The connections to the internal column were able to sustain 12 - 16 kNm while those connected to the external column were able to sustain moments in the range 14 - 18 kNm. Consider the behaviour of the internal joints F, I and K. Figure 6.50 shows joint I on the internal column at the second floor level. From Figures 6.17 and 6.18, it can be seen that the central column rotated anti-clockwise during the beam loading phase. As axial load was applied to the central column, an opposite sign of rotation was produced which thus reduced the rotation of column. This produced an increase of joint rotation up to  $18 \times 10^{-3}$  (rad.) for one of the connections attached at joint F whilst the opposite phenomenon was observed in the adjacent joint (K) of the first floor level. The relevant column 6 rotated clockwise (Figure 6.17) during the beam load phase, the joint was forced to open as further rotation was produced in that column as further axial load was applied. Thus the connection moment reduced as the connection opened and the joint was unloaded as can be seen in Figure 6.50. A different form of response was observed in Joint F (Figure 6.49) with the connection closing continuously during both the beam loading and the axial loading phases. However, an unexpected and unexplained connection moment drop was found in this curve after the axial load was applied to the head of the central column.

For the external column, a similar phenomenon relating to the opening and closing of joints was observed. Examination of the joints on the external column in position 3 (joints H, J and L in Figure 6.51) clearly demonstrates the change of the moment rotation behaviour at the different levels of load. At joint H, the column rotated anti-clockwise during the beam loading phase. Under the application of axial load to the external column, an increase of the column rotation was observed which lead to a 'opening' of the joint. Thus the joint was unloaded and its rotation reduced. An unclear moment-rotation curve was observed in joint J which was difficult to interpret. However, the joint was forced to open as column failure was approached. A curve similar to that of joint H was observed for joint L. Due to the action of joint K (Figure 6.50) which reduced its moment after column load applied, joint L was forced to open after the axial load applied to the edge column.

#### 6.5.10 Behaviour of Joints in Frame 4

Figures 6.52 to 6.55 illustrate the moment-rotation curves of the connections as measured in test 3. From the analysis of the moment-rotation plot obtained from the experiment, it is observed in these figures that joint stiffness from the slope of the unloading curve and the initial tangent gave similar values in most of the joints i.e. joints B, C, D, E, F, G, I, J, K and L. The determined initial and unloaded stiffness in each joint together with some analysis using new design approaches will be presented in chapter 10.

During the beam loading phase, all the connections behaved as expected exhibiting a smooth moment rotation response with the exception of joint A which performed rather erratically. Those connected to the internal column (joints B, D, F, G, I and K) were able to sustain quite high moments of 15 - 24 kNm. Those connected to the external column (joint A, C, E, H, J and L) sustained moments in the range 10 - 15 kNm. The difference may be attributed to the flexibility of the edge columns and the absence of restraint from adjacent beams.

Consider the behaviour of the external joints to the column in position 1. A similar phenomenon to that seen in frame 3 relating to the connection opening and closing of joints was observed. Examination of the joints on the external column in position 1 (joints A, C and E in Figure 6.52) clearly demonstrates the change of the moment rotation behaviour at the different levels of load. At joint A, the column rotated clockwise during the beam loading phase (see Figure 6.40). Under the application of axial load to the external column, an increase of the column rotation was observed which to a 'opening' of the joint (Figure

6.41). Thus the joint was unloaded and its rotation reduced. A curve similar to that of joint A was observed for joint E. A different form of response was observed in Joint C with the connection closing continuously during both the beam loading and the axial loading phases. A sympathetic action in the connections B, D and F at the opposite ends of beams 1 to 3 was observed in Figure 6.53. Due to slip occurring in joint B at scans 16 and 17, moment in this connection dropped and then the joint attempted to pick up more moment after more load was applied to the column head.

Turning to the behaviour of the internal joints F, I and K shown in Figures 6.53 and 6.54. Figure 6.54 shows joint I, an internal beam to column joint at the second floor level. From Figures 6.40 and 6.42, it can be seen that the central column rotated anti-clockwise during the beam loading phase. As axial load was applied to the central column, an opposite sign of rotation was produced which thus reduced the rotation of column. The relevant column 6 rotated clockwise (Figure 6.40) during the beam load phase, joint K (Figure 6.54) was forced to open as additional rotation was produced in that column as further axial load was applied. Thus the connection moment reduced as the connection open and the joint was unloaded. A different form of response was observed in Joint F (Figure 6.53) with the connection closing continuously during both the beam loading and the axial loading phases. The connections on the adjacent side of the column behaved in the opposite way. This is best illustrated by comparing the response of connection D and I, F and K. As joint D opened, joint I closed. As joint F closed, joint K opened.

It is interesting to note that all the joints in frame 3 exhibited a similar initial stiffness to the joint tests. The maximum moment in the external joints sustained a slightly higher value than the joints test whilst the internal joints sustained a similar moment. Turning to compare with the  $M-\phi$  curves in frame 4, a lower initial stiffness was observed in the external joint whilst the initial joints showed a similar value to the joint tests. The moment in the internal joints attained a higher value than the joint tests.

This phenomenon may be due to the same arrangement of the joint tests and the internal joints in the two frame tests (cruciform). Due to the different load path mechanism of the internal and external joints, a different connection stiffness and strength may be obtained. It is the author's opinion that this phenomenon was one of the most important observations from the study - specially the external joints showed a less stiffness than the internal joints. It could be effected the behaviour of the structures in analysis when the  $M-\phi$  curves in different locations are adopted. A more detailed explanation for this connection behaviour and a parameter study concerned of the column capacity due to the variation of

the  $M-\phi$  response will be subjected to a further investigation in chapter 9. Moreover, both the joint and frame  $M-\phi$  curves employed the new approach to predict the deformation of steel frames in the serviceability limit state will be addressed in chapter 10.

## 6.6 Concluding Remarks on the Study

Throughout this study, the behaviour of the two Sheffield frames has been considered. Errors in the recorded value of the load cell which one were discovered during the analysis of frame 3 which was due to the adoption of an incorrect calibration factor during the test. Three methods were considered by the author to solve this problem. After a comparison with the applied column load determined from three different methods, method 3 is thought to be best. This method is based on using a computer program to convert the incorrect data back to voltages which are then used as the independent variable in a polynomial expression for the load. This method is then used to correct the applied column load for other tests.

Somewhat high values of axial loads and moments determined in the edge columns were probably due to a rather high value of elastic modulus ( $E$ ) measured in the stub column test in frame 3. Some values obtained from the strain gauges after the yield of sections were found and it was suggested that more strain gauges should be included in the sections for future frame tests in order to obtain more accurate results.

The tests illustrated that the rotational stiffness of the flange cleat connection significantly influences the distribution of moments around the frame, leading to reduce beam deflections and enhance column capacities when compared to traditional pinned joint concepts. The semi-rigid action transfers larger moments from the beam through to the column. Thus, it increases the moment and deflection of the column relative to the same member with true pinned connections when only beam loading is applied. When utilising the semi-rigid joint effect, part of the mid-span moment is transferred to the column. Hence, a smaller mid-span beam deflection will be encountered. In addition, the reduced mid-span moment can allow larger applied beam moments to be carried or the beam size may be reduced with a consequent improvement in economy. During failure of the column, the connection on either side rotated in the same direction thus causing unloading of one and continued loading of the other. The unloading connection has the greater stiffness and hence restrains the column more than the adjacent, loading connection.

The eccentricity of the applied load produced at the head of the column is due to



the rotation of the column head during the beam load phase. This problem is difficult to overcome since stable and safe test arrangements are required. It may have been prudent to have applied lower load to the third floor beams and hence reduce the rotation of the head of the column.

In chapter 8, the result of the frame tests are compared with the prediction of in house finite element analysis programs. A parametric study to investigate how the variation of the  $M-\phi$  response to effect the ultimate capacity of column is performed in chapter 9. New design methods will be developed and checked using all test results as addressed in chapter 10.

## References

- [6.1] Davison, J. B., 'Strength of Beam-Columns in Flexibly Connected Steel Frames', Ph.D. Thesis, University of Sheffield, June, 1987.
- [6.2] Roeder C. W. and Dailey, R. H., 'The Results of Experiments on Seated Beam Connections', Engineering Journal, American Institute of Steel Construction, INC, 3rd Quarter, 1989 , Vol. 26, No. 3.
- [6.3] British Standards Institution BS 5950: Part 1: 'Structural Use of Steelwork in Building', BSI, London, British Standards Institution, 1990.
- [6.4] British Standards Institution BS 449: Part 2: 'The Use of Structural Steel in Building', British Standards Institution, 1969.
- [6.5] Nethercot, D. A. and Lawson, R. M., 'Lateral Stability of Steel Beams and Columns - Common Cases of Restraint', The Steel Construction Institute, P093, 1992.
- [6.6] Jennings, D. A., Moore, D. B. and Sims, P. A. C., 'Instrumenting and Testing Bolted Steel Frame Structures', Proceedings, Determination of Dangerous Stress Levels and Safe Operation Condition, Edinburgh, August, 1986.
- [6.7] Lau, S. M., 'Full Scale Frame Tests with Semi-Rigid Connections', Progress Report no.6, Department of Civil and Structural Engineering, University of Sheffield.
- [6.8] Lau, S. M., 'Full Scale Frame Tests with Semi-Rigid Connections', Progress Report no.7, Department of Civil and Structural Engineering, University of Sheffield.
- [6.9] Moore, D. B., 'Full-Scale Steel Frame Tests: Load Tests on Frame no.3', Building Research Establishment, Report No. N59/87.
- [6.10] Lennon, T., 'Full-Scale Steel Frame Tests: Calibration of Instrumentation for Frame 5', Building Research Establishment, Report No. N71/88.
- [6.11] Lennon, T., 'Full-Scale Steel Frame Tests: Calibration of Instrumentation', Building Research Establishment, Report No. N61/87.
- [6.12] Birnstiel, C., 'Experiments on H-Columns under Biaxial Bending', Journal of Structural Division, ASCE, Vol. 94, 1968, pp. 2429-2449.
- [6.13] Lightfoot, F., 'The Statistical Interpretation of Strain Gauge Readings', Journal of Strain Analysis, 1965, 1, pp. 27-30.

- [6.14] Gibbons, C. et al., 'The Experimental Assessment of the Force Components within Structural Steel 'H' Sections', Journal of Strain Analysis, Vol. 26, No. 1, I.Mech.E., 1991.
- [6.15] Price, G., ' On the Use of Electro-levels to Measure Bending Moments and Axial Loads in Steel Framed Structures', In press.

Total Load per Beam (kN)	Comments
10.0	
20.0	
30.0	
40.4	
53.0	unfactored dead load only (1.0 D.L.)
60.0	
74.2	factor dead load only (1.4 D.L.)
79.5	unfactored dead + imposed load (1.0 D.L. + 1.0 L.L.)
90.0	
100.7	factored dead + unfactored imposed load (1.4 D.L. + 1.0 L.L.)
116.6	factored dead + factored imposed load (1.4 D.L. + 1.6 L.L.)

Table 6.1 : Load Increments for the Applied Beam Loads in Frames 3 and 4

SCAN	APPLIED LOAD (kN)							COMMENTS
	BEAM NO.					COLUMN POSITION		
	2	3	4	5	6	2	3	
1	0.0	0.0	0.0	0.0	0.0	0.0	0.0	Zero load
2	0.0	0.0	0.0	0.0	0.0	0.0	0.0	
3	8.7	8.0	8.8	8.8	8.8	0.0	0.0	Dead load 'equally'
4	18.9	18.1	19.1	19.5	19.6	0.0	0.0	
5	29.0	28.2	29.3	30.2	30.4	0.0	0.0	
6	39.2	38.4	39.5	40.8	40.9	0.0	0.0	
7	52.3	51.6	52.8	54.7	54.4	0.0	0.0	
8	59.5	58.7	59.9	54.7	55.2	0.0	0.0	
9	59.5	58.7	59.9	54.7	61.6	0.0	0.0	Pattern beam loading
10	73.9	73.2	74.5	54.7	76.4	0.0	0.0	
11	79.3	78.6	79.8	54.7	81.8	0.0	0.0	
12	90.0	89.3	90.6	54.7	92.7	0.0	0.0	
13	100.7	100.0	101.3	54.7	103.5	0.0	0.0	
14	117.0	116.2	117.7	54.7	120.0	0.0	0.0	
15	117.1	116.1	117.6	54.7	119.8	44.0	45.1	Columns 2 & 3 loaded 'equally'
16	117.1	116.1	117.6	54.7	119.7	104.0	105.4	
17	117.1	116.1	117.6	54.7	119.8	165.7	165.3	
18	117.1	116.1	117.6	54.7	119.8	244.2	223.1	
19	117.1	116.1	117.6	54.7	119.8	315.8	279.5	
20	117.2	116.1	117.5	54.7	119.7	390.2	271.3	
21	117.1	116.1	117.5	54.7	119.7	472.4	271.4	Column 2 loaded to failure
22	117.2	116.1	117.6	54.7	119.8	490.3	266.2	
23	117.2	116.1	117.6	54.7	119.8	501.5	263.4	
24	117.2	116.1	117.5	54.7	119.8	512.9	261.4	
25	117.2	116.1	117.5	54.7	119.8	441.4	265.1	
26	117.1	116.1	117.5	54.7	119.7	438.6	329.1	
27	117.1	116.1	117.5	54.7	119.7	440.1	397.4	
28	117.1	116.1	117.5	54.7	119.7	441.1	454.1	
29	117.1	116.1	117.5	54.7	119.7	439.7	510.3	
30	117.1	116.1	117.5	54.6	119.7	437.9	545.0	
31	117.1	116.1	117.6	54.6	119.7	433.8	572.3	
32	117.1	116.1	117.6	54.6	119.7	433.1	590.2	
33	117.1	116.1	117.7	54.6	119.7	432.3	606.0	
34	117.1	116.1	117.6	54.6	119.7	435.2	619.7	
35	117.1	116.1	117.6	54.6	119.7	435.1	634.0	
36	117.1	116.2	117.6	54.7	119.7	434.7	647.6	
37	117.1	116.2	117.6	54.6	119.7	433.8	660.4	
38	117.1	116.2	117.6	54.6	119.7	433.8	670.1	
39	117.1	116.1	117.6	54.6	119.7	433.4	654.4	Unloaded of members
40	117.1	116.2	117.4	54.6	119.7	88.4	448.2	
41	117.1	116.2	117.6	54.6	119.7	-7.8	1.4	
42	52.6	51.6	52.5	54.6	54.1	-8.3	0.5	
43	0.4	0.1	5.1	-0.1	1.3	2.6	0.2	

Table 6.2 : Load History of Frame 3 Test 2 (uncorrected)

Scan	Applied Column Axial Load (kN)						Comments
	Column in Position 2			Column in Position 3			
	Method			Method			
	1	2	3	1	2	3	
15	41.4	54.2	35.2	41.9	55.3	45.4	
16	97.8	114.7	90.6	98.0	120.7	104.4	
17	155.8	175.4	150.4	153.7	184.3	160.6	
18	229.5	250.8	226.2	207.5	244.4	214.0	
19	296.9	317.0	292.7	259.9	302.1	265.8	
20	366.8	380.3	358.9	252.3	293.0	258.2	
21	444.1	453.4	429.8	252.4	293.0	258.4	
22	460.9	470.2	445.0	247.6	287.8	253.6	
23	471.4	480.3	454.6	245.0	284.6	251.0	
24	482.1	490.6	464.3	243.1	282.1	249.2	Failure of Column 2
25	414.9	422.2	403.1	246.5	285.3	252.6	
26	412.3	419.6	400.7	306.1	350.6	311.4	
27	413.7	422.0	402.0	369.6	418.7	374.3	
28	414.6	422.5	402.8	422.3	469.2	426.4	
29	413.3	421.4	401.6	474.6	521.8	477.6	
30	411.6	419.5	400.0	506.9	552.8	509.1	
31	407.8	415.7	396.6	532.2	578.5	533.6	
32	407.1	415.1	395.9	548.9	594.6	549.8	
33	406.4	414.4	395.3	563.6	609.1	563.7	
34	409.1	417.4	397.7	576.3	622.0	575.8	
35	409.0	417.6	397.6	589.6	635.4	588.5	
36	408.6	417.4	397.3	602.3	648.1	600.4	
37	407.8	416.3	396.5	614.2	662.4	611.6	
38	407.8	416.1	396.2	623.2	673.2	620.1	Failure of Column 3
39	407.4	414.7	394.9	608.6	659.4	606.3	
40	83.1	95.4	75.9	416.8	446.2	421.0	
41	-7.3	5.6	-4.2	1.3	9.2	1.5	
42	-7.8	-1.3	-4.3	0.5	1.8	0.5	
43	2.4	30.4	2.2	0.2	0.0	0.3	

Table 6.3 : Comparison with Different Methods to predict the Applied Column Axial Loads in Test 2

Scan	Total Load in the Upper Level (kN)		
	Axial Load from Strain Gauges	Method (1)	Method (3)
15	220.2	200.9	198.2
19	729.8	674.6	676.1
24	883.4	843.1	831.0
38	1200.0	1148.2	1133.9

Remark : Total Load in the Upper Level in Method (1) and (3)  
= Beam Load + Applied Column Load

Table 6.4 : Comparison the Total Axial Loads in the Upper Storey with the Results obtained from Methods (1) and (3)

	AXIAL LOAD (kN)							
	COLUMN NO.							
	2	3	4	5	6	7	8	9
1	0.0	0.0	0.0	0.0	0.0	0.0	0.0	0.0
2	0.2	0.0	0.3	0.0	0.0	-0.3	-0.1	0.0
3	5.9	11.2	-4.2	5.3	14.0	-0.5	4.8	9.4
4	12.3	24.9	1.2	21.9	41.0	4.7	16.2	26.4
5	19.3	39.1	6.8	38.9	67.9	10.6	27.6	43.5
6	26.3	54.1	11.9	54.6	93.0	16.2	40.1	61.9
7	35.0	72.5	18.3	75.4	127.0	23.6	55.4	84.0
8	39.9	82.2	21.9	83.5	139.4	27.6	59.3	88.7
9	39.8	82.1	22.1	83.7	143.2	27.4	59.4	91.4
10	49.7	102.5	29.3	98.7	172.4	35.5	67.6	107.9
11	53.3	110.1	31.8	104.2	183.2	38.5	70.3	113.8
12	60.7	125.1	37.4	115.7	205.4	44.4	76.2	125.7
13	68.1	140.0	42.8	126.9	227.5	50.4	82.1	137.6
14	79.1	162.8	51.6	144.6	261.3	59.1	90.7	155.4
15	78.9	163.2	105.8	198.8	313.9	114.4	144.0	208.8
16	79.2	163.7	166.3	259.6	373.1	179.8	209.1	273.3
17	79.9	164.0	227.0	320.4	432.2	243.4	272.5	336.1
18	80.0	164.4	302.4	395.8	505.6	303.5	332.4	395.5
19	80.3	164.9	368.6	462.1	576.7	361.2	389.8	452.2
20	80.7	165.6	431.9	526.0	650.6	352.1	380.9	443.4
21	80.0	164.1	505.0	605.9	742.7	352.4	380.0	442.6
22	80.3	164.5	521.8	622.8	763.4	346.9	374.5	437.2
23	80.5	164.8	531.9	633.2	776.8	343.7	371.7	434.6
24	80.3	164.7	542.2	643.7	789.2	341.2	369.4	432.3
25	80.1	164.4	473.8	575.1	724.0	344.4	373.0	435.5
26	80.1	164.2	471.2	572.8	721.8	409.7	438.5	500.5
27	80.0	164.2	473.6	574.8	723.9	477.8	505.9	566.7
28	80.1	164.0	474.1	575.9	725.3	528.3	557.5	618.0
29	80.0	164.1	473.0	574.8	724.7	580.9	610.2	672.8
30	79.9	163.9	471.1	573.0	723.2	611.9	641.2	709.3
31	79.8	163.8	467.3	569.1	720.0	637.6	669.5	743.2
32	79.8	163.6	466.7	568.5	719.6	653.7	687.2	761.6
33	79.9	163.9	466.0	568.0	719.2	668.2	706.5	780.9
34	80.1	164.0	469.0	571.0	722.4	681.1	722.4	803.2
35	80.1	163.9	469.2	570.9	722.5	694.5	738.2	825.4
36	80.1	164.0	469.0	570.7	722.8	707.2	754.0	847.4
37	80.3	164.1	467.9	569.8	722.0	721.5	768.9	869.8
38	80.2	164.2	467.7	569.4	721.8	732.3	781.7	890.7
39	80.1	164.1	466.3	568.1	720.4	718.5	769.1	883.4
40	78.7	162.6	147.4	248.6	408.7	505.3	556.5	674.0
41	78.6	162.2	57.2	157.6	319.5	68.3	119.9	241.2
42	35.3	74.7	24.5	87.6	182.2	31.4	85.6	171.1
43	-0.3	1.7	32.9	37.3	77.5	2.6	26.4	83.2

Table 6.5 : Axial Load in Columns of Frame 3 Test 2  
(Computed from Strain Gauge Readings)



Scan	Total Load (kN)					
	Upper Columns		Middle Columns		Lower Columns	
	Applied	Axial	Applied	Axial	Applied	Axial
1	0.0	0.0	0.0	0.0	0.0	0.0
2	0.0	0.0	0.0	0.1	0.0	0.0
3	8.8	-4.7	26.3	16.0	43.1	34.6
4	19.1	5.9	57.5	50.4	95.2	92.3
5	29.3	17.4	88.5	85.8	147.1	150.5
6	39.5	28.1	119.5	121.0	198.8	209.0
7	52.8	41.9	159.8	165.8	265.8	283.5
8	59.9	49.5	174.1	182.7	288.0	310.3
9	59.9	49.5	174.1	182.9	294.4	316.7
10	74.5	64.8	203.1	216.0	352.7	382.8
11	79.8	70.3	213.8	227.8	374.2	407.1
12	90.6	81.8	235.3	252.6	417.3	456.2
13	101.3	93.2	256.7	277.1	460.2	505.1
14	117.7	110.7	289.4	314.4	525.6	579.5
15	198.2	220.2	370.0	421.7	605.9	685.9
16	312.6	346.1	484.4	547.9	720.2	810.1
17	428.6	470.4	600.4	672.8	836.3	932.3
18	557.8	605.9	729.6	808.2	965.5	1065.5
19	676.1	729.8	847.9	932.2	1083.8	1193.8
20	734.6	784.0	906.5	987.6	1142.3	1259.6
21	805.7	857.4	977.5	1065.9	1213.3	1349.4
22	816.2	868.7	988.1	1077.6	1224.0	1365.1
23	823.2	875.6	995.1	1085.4	1231.0	1376.2
24	831.0	883.4	1002.9	1093.4	1238.8	1386.2
25	773.2	818.2	945.1	1028.2	1181.0	1323.9
26	829.6	880.9	1001.4	1091.4	1237.2	1386.5
27	893.8	951.4	1065.6	1160.7	1301.4	1454.8
28	946.7	1002.4	1118.5	1213.5	1354.3	1507.3
29	996.7	1053.9	1168.5	1265.0	1404.3	1561.6
30	1026.6	1083.0	1198.3	1294.1	1434.1	1596.4
31	1047.8	1104.9	1219.5	1318.4	1455.3	1627.0
32	1063.3	1120.4	1235.0	1335.5	1470.8	1644.8
33	1076.7	1134.2	1248.4	1354.4	1484.2	1664.0
34	1091.1	1150.1	1262.8	1373.5	1498.6	1689.6
35	1103.7	1163.7	1275.4	1389.2	1511.2	1711.8
36	1115.3	1176.2	1287.1	1404.8	1523.0	1734.2
37	1125.7	1189.4	1297.4	1419.0	1533.3	1755.9
38	1133.9	1200.0	1305.6	1431.3	1541.5	1776.7
39	1118.8	1184.8	1290.5	1417.3	1526.3	1767.9
40	614.3	652.7	786.0	883.8	1021.9	1245.3
41	114.9	125.5	286.6	356.1	522.5	722.9
42	48.7	55.9	155.9	208.5	261.6	428.0
43	7.6	35.5	7.9	63.4	9.3	162.4

Table 6.6 : Comparison of Total Applied Load and Axial Load in Columns above Different Storeys in Test 2

SCAN	APPLIED LOAD (kN)							COMMENTS
	BEAM NO.					COLUMN POSITION		
	2	3	4	5	6	2	3	
1	0.0	0.0	0.0	0.0	0.0	0.0	0.0	Zero load
2	0.0	0.0	0.0	0.0	0.0	0.0	0.0	
3	8.7	8.0	8.8	8.8	8.8	0.0	0.0	Dead load 'equally'
4	18.9	18.1	19.1	19.5	19.6	0.0	0.0	
5	29.0	28.2	29.3	30.2	30.4	0.0	0.0	
6	39.2	38.4	39.5	40.8	40.9	0.0	0.0	
7	52.3	51.6	52.8	54.7	54.4	0.0	0.0	
8	59.5	58.7	59.9	54.7	55.2	0.0	0.0	
9	59.5	58.7	59.9	54.7	61.6	0.0	0.0	
10	73.9	73.2	74.5	54.7	76.4	0.0	0.0	
11	79.3	78.6	79.8	54.7	81.8	0.0	0.0	
12	90.0	89.3	90.6	54.7	92.7	0.0	0.0	
13	100.7	100.0	101.3	54.7	103.5	0.0	0.0	Columns 2 & 3 loaded 'equally'
14	117.0	116.2	117.7	54.7	120.0	0.0	0.0	
15	117.1	116.1	117.6	54.7	119.8	35.2	45.4	
16	117.1	116.1	117.6	54.7	119.7	90.6	104.4	
17	117.1	116.1	117.6	54.7	119.8	150.4	160.6	
18	117.1	116.1	117.6	54.7	119.8	226.2	214.0	
19	117.1	116.1	117.6	54.7	119.8	292.7	265.8	
20	117.2	116.1	117.5	54.7	119.7	358.9	258.2	
21	117.1	116.1	117.5	54.7	119.7	429.8	258.4	
22	117.2	116.1	117.6	54.7	119.8	445.0	253.6	
23	117.2	116.1	117.6	54.7	119.8	454.6	251.0	Column 2 loading reduced
24	117.2	116.1	117.5	54.7	119.8	464.3	249.2	
25	117.2	116.1	117.5	54.7	119.8	403.1	252.6	Column 3 loaded to failure
26	117.1	116.1	117.5	54.7	119.7	400.7	311.4	
27	117.1	116.1	117.5	54.7	119.7	402.0	374.3	
28	117.1	116.1	117.5	54.7	119.7	402.8	426.4	
29	117.1	116.1	117.5	54.7	119.7	401.6	477.6	
30	117.1	116.1	117.5	54.6	119.7	400.0	509.1	
31	117.1	116.1	117.6	54.6	119.7	396.6	533.6	
32	117.1	116.1	117.6	54.6	119.7	395.9	549.8	
33	117.1	116.1	117.7	54.6	119.7	395.3	563.7	
34	117.1	116.1	117.6	54.6	119.7	397.7	575.8	
35	117.1	116.1	117.6	54.6	119.7	397.6	588.5	
36	117.1	116.2	117.6	54.7	119.7	397.3	600.4	
37	117.1	116.2	117.6	54.6	119.7	396.5	611.6	
38	117.1	116.2	117.6	54.6	119.7	396.2	620.1	
39	117.1	116.1	117.6	54.6	119.7	394.9	606.3	
40	117.1	116.2	117.4	54.6	119.7	75.9	421.0	
41	117.1	116.2	117.6	54.6	119.7	-4.2	1.5	
42	52.6	51.6	52.5	54.6	54.1	-4.3	0.5	
43	0.4	0.1	5.1	-0.1	1.3	2.2	0.3	

Table 6.7 : Load History of Frame 3 Test 2 (corrected)

SCAN	APPLIED LOAD (kN)					COMMENTS
	BEAM NO.					
	2	3	4	5	6	
1	0.0	0.0	0.0	0.0	0.0	Zero load
2	0.0	0.0	0.0	0.0	0.0	
3	8.0	8.4	9.1	9.7	9.4	
4	18.2	18.5	19.4	20.3	19.8	
5	28.3	28.6	29.6	31.1	30.2	
6	38.5	38.8	39.9	41.8	40.6	
7	51.7	52.0	53.1	55.6	54.1	Dead load on each beam
8	58.8	59.2	60.3	55.6	61.4	
9	73.3	73.7	74.8	55.6	76.1	
10	78.6	79.1	80.2	55.6	81.5	
11	89.4	89.9	91.0	55.6	92.5	
12	100.1	100.6	101.7	55.6	103.3	
13	116.4	116.8	118.0	55.6	119.7	Beams 2, 3, 4 and 6 subject to design load
14	116.4	116.8	118.0	55.6	128.3	Failure of beam 6
15	116.4	116.8	118.0	55.6	128.2	
16	116.5	116.7	118.0	55.6	128.0	
17	78.9	79.1	80.2	55.6	80.9	
18	51.9	52.1	53.0	55.6	53.6	
19	0.0	-0.1	-0.1	-0.1	0.0	

Table 6.8 : Load History of Frame 3 Test 3

SCAN	APPLIED LOAD (kN)					COMMENTS
	BEAM NO.					
	2	3	4	5	6	
1	0.0	0.0	0.0	0.0	0.0	Zero load
2	47.1	53.1	50.3	55.7	54.8	
3	51.9	52.0	53.2	55.6	54.1	
4	78.9	79.1	80.3	55.6	81.6	
5	116.6	116.8	118.1	55.6	119.9	
6	116.6	125.4	118.1	55.6	119.7	
7	116.6	135.5	118.1	55.6	119.7	
8	116.7	140.5	118.2	55.7	119.8	
9	116.6	145.4	118.1	55.7	119.7	Failure of beam 3
10	116.7	145.5	118.2	84.0	119.7	
11	116.7	145.5	118.2	106.5	119.7	
12	116.7	145.5	118.2	123.5	119.7	
13	116.7	145.5	118.2	132.4	119.7	
14	116.7	145.5	118.2	137.7	119.7	Failure of beam 5
15	116.7	145.5	121.6	137.7	119.7	
16	116.7	145.5	126.8	137.7	119.7	
17	116.7	145.5	131.8	137.7	119.7	
18	116.7	145.5	137.0	137.7	119.7	
19	116.7	145.5	141.9	137.7	119.7	
20	116.7	145.5	147.0	137.7	119.6	Failure of beam 4
21	74.5	74.5	75.6	79.1	76.4	
22	49.2	49.2	50.2	52.5	50.8	
23	0.0	-0.1	0.0	-0.3	0.2	

Table 6.9 : Load History of Frame 3 Test 4

SCAN	APPLIED LOAD (kN)									COMMENTS	
	BEAM NO.						COLUMN POSITION				
	1	2	3	4	5	6	1	2	3		
1	0.0	0.0	0.0	0.0	0.0	0.0	0.0	0.0	0.0	0.0	Zero load
2	0.0	0.0	0.0	0.0	0.0	0.0	0.0	0.0	0.0	0.0	
3	9.3	8.5	8.6	8.5	8.9	8.6	0.0	0.0	0.0	0.0	Dead load 'equally'
4	19.9	18.7	18.7	18.7	19.6	19.1	0.0	0.0	0.0	0.0	
5	30.5	28.8	28.9	28.9	30.3	29.7	0.0	0.0	0.0	0.0	
6	41.0	39.0	39.1	39.1	41.0	40.1	0.0	0.0	0.0	0.0	
7	54.7	52.2	52.3	52.4	54.9	53.5	0.0	0.0	0.0	0.0	
8	62.1	59.5	58.5	59.6	54.9	60.8	0.0	0.0	0.0	0.0	Pattern beam loading
9	77.0	73.9	73.9	74.1	54.9	75.5	0.0	0.0	0.0	0.0	
10	82.5	79.3	79.4	79.5	54.9	80.9	0.0	0.0	0.0	0.0	
11	93.6	90.1	90.1	90.3	54.9	91.7	0.0	0.0	0.0	0.0	
12	104.6	100.8	100.7	101.2	54.9	102.6	0.0	0.0	0.0	0.0	
13	121.3	117.1	116.8	117.5	54.9	118.9	0.0	0.0	0.0	0.0	Columns loaded 'equally'
14	121.3	117.2	116.7	117.5	54.8	118.6	0.0	0.0	0.0	0.0	
15	121.3	117.2	116.7	117.5	54.9	118.6	0.0	0.0	0.0	0.0	
16	121.3	117.2	116.8	117.5	54.9	118.6	0.0	0.0	0.0	0.0	
17	121.3	117.2	116.8	117.5	54.9	118.6	42.9	13.9	53.6		
18	121.3	117.2	116.8	117.5	54.9	118.6	96.2	42.7	105.5		
19	121.2	117.2	116.8	117.5	54.8	118.6	145.1	77.4	159.0		
20	121.2	117.2	116.8	117.5	54.8	118.6	139.1	131.7	152.8		
21	121.3	117.2	116.8	117.5	54.8	118.6	188.5	130.6	151.1		
22	121.3	117.2	116.8	117.5	54.8	118.6	241.7	130.5	149.6	Column 1 loaded to failure	
23	121.3	117.2	116.8	117.5	54.8	118.6	288.4	130.3	150.5		
24	121.3	117.2	116.9	117.5	54.8	118.6	330.8	131.3	155.7		
25	121.3	117.2	116.9	117.5	54.9	118.6	351.2	132.4	156.8		
26	121.2	117.2	116.8	117.5	54.8	118.6	375.0	134.0	153.5		
27	121.3	117.2	116.8	117.5	54.9	118.6	395.2	133.7	150.9		
28	121.3	117.2	116.8	117.5	54.9	118.6	412.6	134.4	150.0		
29	121.3	117.2	116.9	117.5	54.9	118.6	431.2	136.5	148.3		
30	121.3	117.2	116.9	117.5	54.8	118.6	442.5	138.2	146.5		
31	121.3	117.2	116.9	117.5	54.9	118.6	436.2	139.2	145.6		
32	121.3	117.2	116.9	117.5	54.9	118.6	454.8	139.0	143.6		
33	121.3	117.2	116.9	117.5	54.9	118.6	468.1	139.7	141.9		
34	121.3	117.2	116.9	117.5	54.9	118.5	457.9	142.8	141.4	Column 1 loading reduced	
35	121.3	117.2	116.9	117.5	54.8	118.6	451.4	201.2	148.0	Column 2 loaded to failure	
36	121.3	117.2	116.8	117.5	54.8	118.6	448.0	253.6	146.3		
37	121.3	117.2	116.8	117.5	54.8	118.6	445.2	279.0	144.6		
38	121.3	117.2	116.9	117.5	54.9	118.6	442.9	302.5	143.6		
39	121.3	117.2	116.9	117.5	54.9	118.6	442.2	325.2	142.5		
40	121.3	117.2	117.0	117.5	54.9	118.6	441.2	346.9	141.3		
41	121.3	117.2	116.9	117.4	54.9	118.5	440.1	367.3	141.1		
42	121.3	117.2	116.9	117.4	54.9	118.5	438.5	388.2	141.0		
43	121.3	117.2	116.9	117.4	54.9	118.5	436.7	404.4	140.4		
44	121.2	117.2	116.9	117.4	54.9	118.5	385.0	397.5	143.4		Unloaded of members
45	121.3	117.1	117.1	117.5	54.9	118.5	-14.9	79.4	167.		
46	121.3	117.1	117.0	117.4	54.9	118.5	-15.6	2.4	0.1		
47	82.3	79.6	79.3	79.7	54.9	80.4	-15.8	2.4	-7.5		
48	54.4	52.6	52.3	52.7	54.9	53.2	-15.9	15.9	-7.6		
49	-0.2	3.4	-0.2	0.0	-0.2	0.3	-16.1	34.9	30.2		

Table 6.10 : Load History of Frame 4 Test 3

SCAN	AXIAL LOAD (kN)								
	COL 1	COL 2	COL 3	COL 4	COL 5	COL 6	COL 7	COL 8	COL 9
1	0.0	0.0	0.0	0.0	0.0	0.0	0.0	0.0	0.0
2	0.0	0.0	0.0	0.0	0.0	0.0	0.0	0.0	0.0
3	1.6	5.4	9.1	10.2	20.1	30.6	2.1	6.4	10.3
4	3.9	12.5	20.7	22.0	43.8	65.7	5.3	14.6	23.5
5	6.7	20.1	33.8	32.7	65.6	97.5	9.0	24.1	39.0
6	11.0	29.5	48.3	43.6	87.1	129.3	13.5	34.2	54.7
7	17.1	42.9	68.1	57.2	113.5	169.4	19.3	48.4	76.2
8	20.6	49.9	78.9	64.9	125.0	188.3	22.8	52.0	83.8
9	27.5	64.2	100.4	80.2	147.8	226.2	30.5	59.6	99.3
10	30.1	69.4	108.5	85.8	156.3	240.6	33.2	62.4	105.1
11	35.3	80.0	124.3	97.1	173.0	268.5	38.7	68.2	116.5
12	40.5	90.7	140.4	108.6	189.7	296.3	44.2	73.9	127.8
13	48.0	106.4	164.0	125.7	215.4	336.4	52.6	82.5	145.5
14	47.4	105.8	163.1	125.6	215.3	335.7	52.2	82.3	145.2
15	47.4	105.7	163.1	125.6	215.4	335.7	52.3	82.3	145.3
16	44.3	101.5	158.5	125.6	215.6	336.0	59.6	89.7	152.5
17	93.0	151.8	209.3	141.0	231.2	351.9	116.9	147.4	210.8
18	142.7	201.3	258.6	174.5	264.6	385.2	173.8	205.2	268.3
19	190.2	249.0	306.2	212.7	303.1	423.2	233.0	264.6	327.6
20	184.6	244.8	301.0	268.1	357.6	477.3	226.0	257.5	320.6
21	233.5	292.4	349.5	267.3	357.0	478.0	223.3	254.6	317.8
22	281.4	339.9	395.6	267.7	357.6	478.0	221.4	252.6	315.9
23	325.2	383.7	443.3	268.0	358.0	479.0	222.7	253.8	316.9
24	364.5	422.5	486.2	269.3	359.7	481.1	228.0	259.1	322.2
25	384.2	441.3	507.8	270.7	361.2	482.7	229.1	259.9	323.2
26	404.9	458.9	528.7	272.3	362.8	484.6	225.2	256.3	319.5
27	429.1	477.8	550.3	272.4	362.9	485.0	222.1	253.0	316.3
28	450.8	493.7	568.9	273.4	363.8	486.2	221.8	252.5	315.7
29	472.4	511.7	588.9	276.0	366.4	488.9	219.3	250.0	313.4
30	486.2	522.2	603.0	277.6	368.1	490.9	217.4	248.3	311.6
31	485.0	515.7	599.2	278.7	369.1	492.1	216.2	247.1	310.4
32	504.9	534.1	618.9	279.0	369.5	492.8	214.0	244.8	308.2
33	520.4	546.7	632.4	280.4	370.9	494.3	212.0	242.9	306.2
34	513.8	536.0	624.3	283.0	373.5	497.0	213.6	244.8	308.3
35	509.0	529.8	618.2	336.0	426.3	552.1	218.9	249.8	313.3
36	508.1	526.6	615.1	385.6	476.3	607.5	217.3	248.1	311.8
37	506.4	523.7	612.4	410.0	501.4	636.5	215.4	246.3	310.0
38	504.9	521.5	610.3	432.6	524.7	664.2	214.1	245.1	309.0
39	504.6	520.7	609.8	454.4	547.9	692.1	213.0	243.7	308.0
40	504.3	519.9	609.0	475.9	570.7	722.2	211.9	243.0	306.9
41	503.9	519.0	608.1	495.6	592.1	751.4	211.7	242.9	307.0
42	503.1	517.5	606.7	513.5	610.9	778.0	212.0	243.0	307.1
43	501.6	515.8	604.9	529.5	627.5	807.6	211.3	242.5	306.8
44	449.9	463.0	552.2	523.2	621.2	807.5	214.6	245.4	309.9
45	91.5	106.8	191.8	210.2	310.9	498.5	239.1	270.0	333.6
46	91.2	106.4	191.7	131.4	232.2	418.6	52.8	81.8	145.5
47	74.6	72.5	140.6	86.5	167.1	309.9	35.7	65.6	110.7
48	61.0	46.8	101.7	88.3	154.2	267.4	22.6	53.0	83.7
49	31.6	-5.6	22.3	41.1	49.0	107.1	32.6	34.5	36.2

Table 6.11 : Axial Load of Frame 4 Test 3

Scan	Total Load (kN)					
	Upper Columns		Middle Columns		Lower Columns	
	Applied	Axial	Applied	Axial	Applied	Axial
1	0.0	0.0	0.0	0.0	0.0	0.0
2	0.0	0.0	0.0	0.0	0.0	0.0
3	17.8	13.9	35.2	31.9	52.4	50.0
4	38.6	31.2	76.9	70.9	114.7	109.9
5	59.4	48.4	118.5	109.8	177.1	170.3
6	80.1	68.1	160.1	150.8	239.3	232.3
7	107.1	93.6	214.2	204.8	320.0	313.7
8	121.7	108.3	236.1	226.9	355.4	351.0
9	151.1	138.2	279.9	271.6	429.3	425.9
10	162.0	149.1	296.2	288.1	456.5	454.2
11	183.9	171.1	328.9	321.2	510.7	509.3
12	205.8	193.3	361.5	354.3	564.8	564.5
13	238.8	226.3	410.8	404.3	646.5	645.9
14	238.8	225.2	410.8	403.4	646.1	644.0
15	238.8	225.3	410.9	403.4	646.2	644.1
16	238.8	229.5	410.9	406.8	646.3	647.0
17	349.2	350.9	521.3	530.4	756.7	772.0
18	483.2	491.0	655.3	671.1	890.7	912.1
19	620.2	635.9	792.2	816.7	1027.6	1057.0
20	662.3	678.7	834.3	859.9	1069.7	1098.9
21	709.0	724.1	881.0	904.0	1116.4	1145.3
22	760.6	770.5	932.6	950.1	1168.0	1189.5
23	808.0	815.9	980.0	995.5	1215.4	1239.2
24	856.6	861.8	1028.6	1041.3	1264.1	1289.5
25	879.2	884.0	1051.3	1062.4	1286.8	1313.7
26	901.2	902.4	1073.2	1078.0	1308.6	1332.8
27	918.6	923.6	1090.7	1093.7	1326.1	1351.6
28	935.8	946.0	1107.9	1110.0	1343.3	1370.8
29	954.8	967.7	1126.9	1128.1	1362.4	1391.2
30	966.0	981.2	1138.0	1138.6	1373.5	1405.5
31	959.8	979.9	1131.9	1131.9	1367.4	1401.7
32	976.2	997.9	1148.3	1148.4	1383.8	1419.9
33	988.5	1012.8	1160.6	1160.5	1396.1	1432.9
34	980.9	1010.4	1153.0	1154.3	1388.4	1429.6
35	1039.4	1063.9	1211.4	1205.9	1446.9	1483.6
36	1086.7	1111.0	1258.7	1251.0	1494.1	1534.4
37	1107.6	1131.8	1279.6	1271.4	1515.0	1558.9
38	1127.8	1151.6	1299.9	1291.3	1535.4	1583.5
39	1148.7	1172.0	1320.8	1312.3	1556.3	1609.9
40	1168.2	1192.1	1340.3	1333.6	1575.9	1638.1
41	1187.2	1211.2	1359.3	1354.0	1594.7	1666.5
42	1206.4	1228.6	1378.5	1371.4	1613.9	1691.8
43	1220.2	1242.4	1392.3	1385.8	1627.7	1719.3
44	1164.5	1187.7	1336.6	1329.6	1572.0	1669.6
45	470.4	540.8	642.4	687.7	878.0	1023.9
46	225.6	275.4	397.6	420.4	633.1	755.8
47	141.1	196.8	275.6	305.2	435.3	561.2
48	99.5	171.9	207.0	254.0	312.5	452.8
49	48.8	105.3	52.0	77.9	52.1	165.6

Table 6.12 : Comparison of Total Applied Load and Axial Load in Columns above Different Storeys in Test 3 of Frame 4

SCAN	APPLIED LOAD (kN)									COMMENTS
	BEAM NO.						COLUMN POSITION			
	1	2	3	4	5	6	1	2	3	
1	0.0	0.0	0.0	0.0	0.0	0.0	0.0	0.0	0.0	Zero load
2	0.0	0.0	0.0	0.0	0.0	0.0	0.0	0.0	0.0	
3	9.0	8.7	8.2	9.5	8.7	8.8	0.0	0.0	0.0	Dead load 'equally'
4	19.6	18.9	18.3	19.7	19.4	19.2	0.0	0.0	0.0	
5	30.2	29.1	28.5	29.9	30.1	29.6	0.0	0.0	0.0	
6	40.8	39.3	38.7	40.1	40.8	40.0	0.0	0.0	0.0	
7	54.4	52.5	51.9	53.4	54.7	53.4	0.0	0.0	0.0	
8	54.4	59.7	59.0	53.4	62.2	60.7	0.0	0.0	0.0	Pattern beam load
9	54.4	74.2	73.5	53.4	77.4	75.4	0.0	0.0	0.0	
10	54.4	79.5	78.9	53.4	83.0	80.8	0.0	0.0	0.0	
11	54.4	90.3	89.6	53.4	94.2	91.7	0.0	0.0	0.0	
12	54.4	101.0	100.3	53.4	105.4	102.5	0.0	0.0	0.0	
13	54.4	117.3	116.5	53.4	122.4	118.9	0.0	0.0	0.0	
14	54.4	117.4	116.5	53.5	122.5	118.8	0.0	0.0	0.0	
15	54.4	117.5	116.6	53.5	122.5	118.8	0.0	0.0	0.0	Column 3 loaded to failure
16	54.4	117.4	116.5	53.6	122.4	118.7	0.0	0.0	46.6	
17	54.4	117.4	116.5	53.6	122.4	118.7	0.0	0.0	123.8	
18	54.5	117.5	116.5	53.6	122.5	118.8	0.0	0.0	79.2	
19	54.5	117.5	116.5	53.7	122.5	118.8	0.0	0.0	131.0	
20	54.4	117.5	116.5	53.6	122.5	118.7	0.0	0.0	185.2	
21	54.4	117.4	116.5	53.6	122.4	118.7	0.0	0.0	239.2	
22	54.4	117.5	116.5	53.6	122.5	118.7	0.0	0.0	294.0	
23	54.4	117.5	116.5	53.7	122.5	118.7	0.0	0.0	350.4	
24	54.4	117.5	116.5	53.7	122.5	118.8	0.0	0.0	406.5	
25	54.4	117.5	116.5	53.6	122.5	118.7	0.0	0.0	458.2	
26	54.4	117.5	116.5	53.6	122.5	118.7	0.0	0.0	480.0	
27	54.4	117.5	116.6	53.7	122.6	117.8	0.0	0.0	38.6	Unloaded of members
28	54.4	52.9	52.0	53.6	54.7	52.2	0.0	0.0	32.5	
29	0.0	0.0	0.0	0.0	0.0	0.2	0.0	0.0	61.0	

Table 6.13 : Load History of Frame 4 Test 4



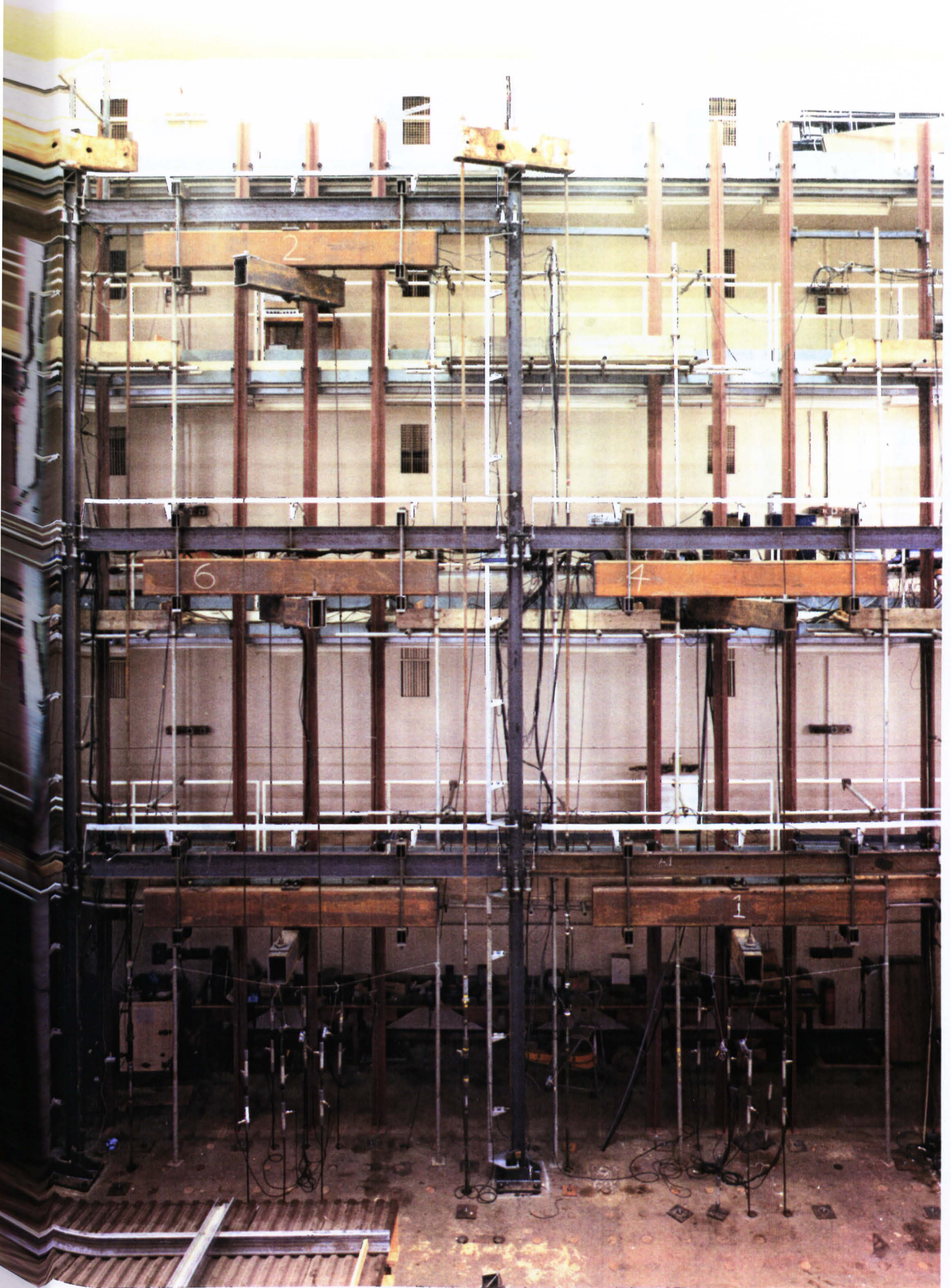


Figure 6.1 : Frame 3 viewed towards the Balcony

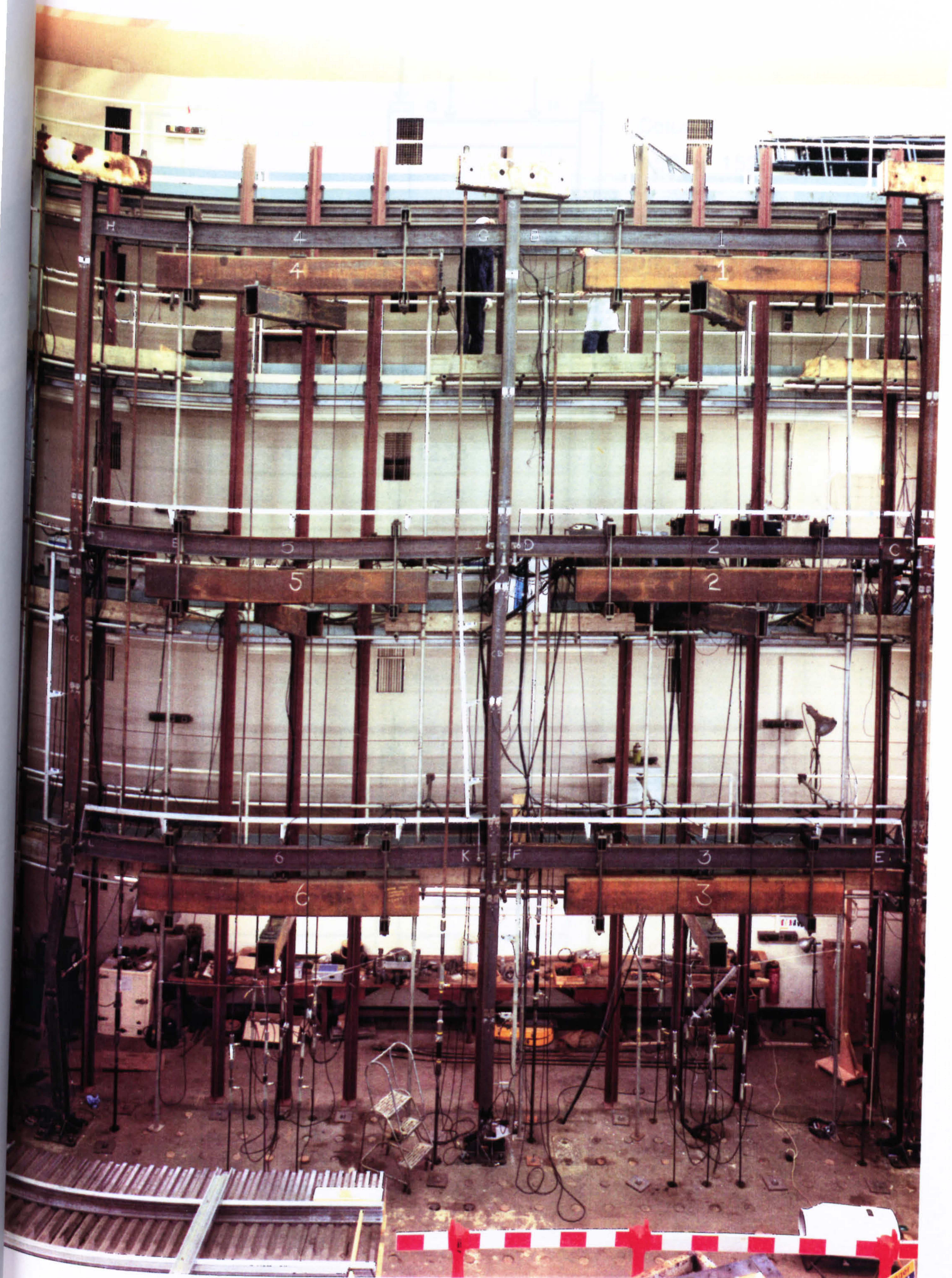


Figure 6.2 : Frame 4 viewed towards the Balcony

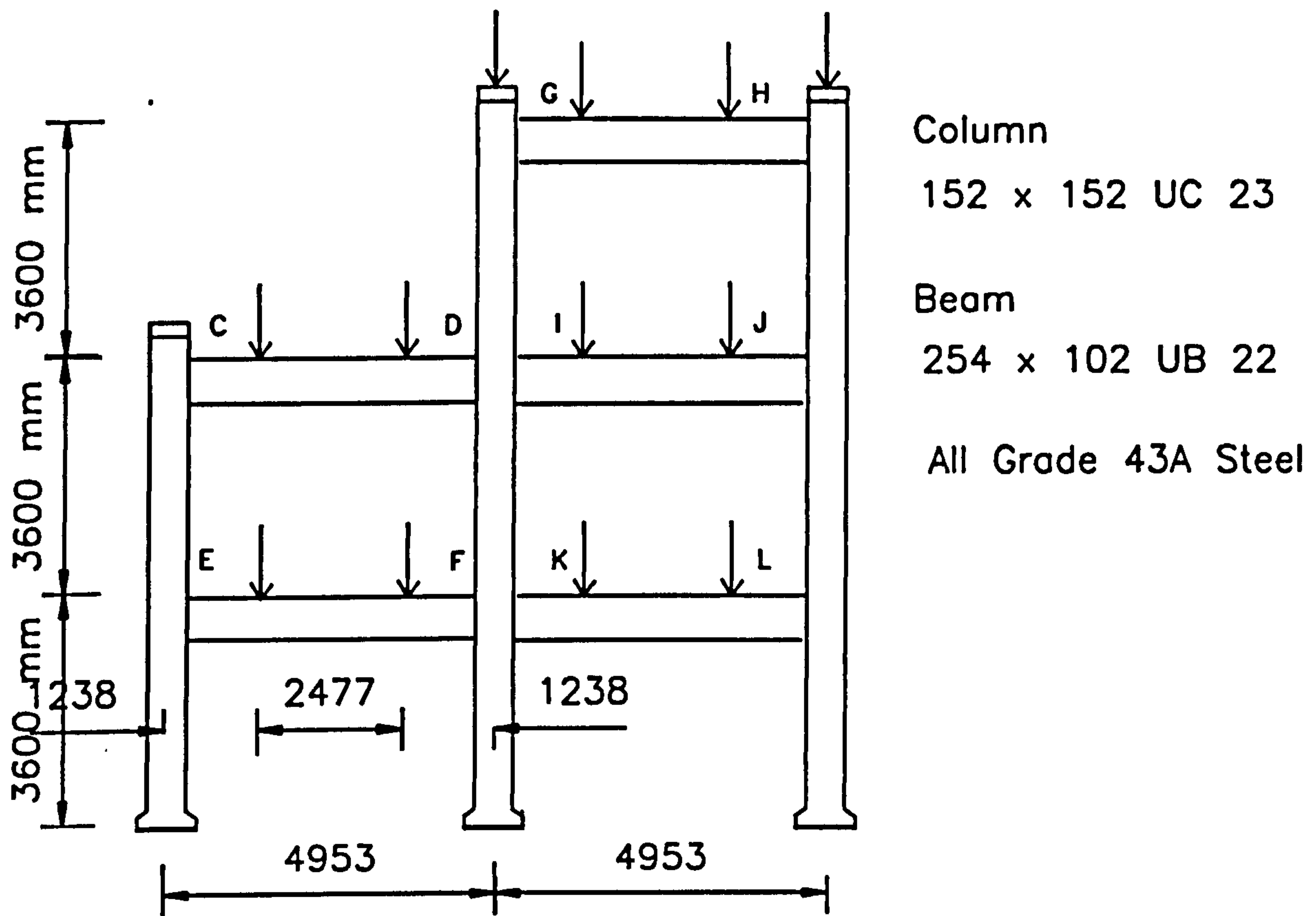


Figure 6.3 : General Arrangement of Frame 3 (Major Axis Frame)

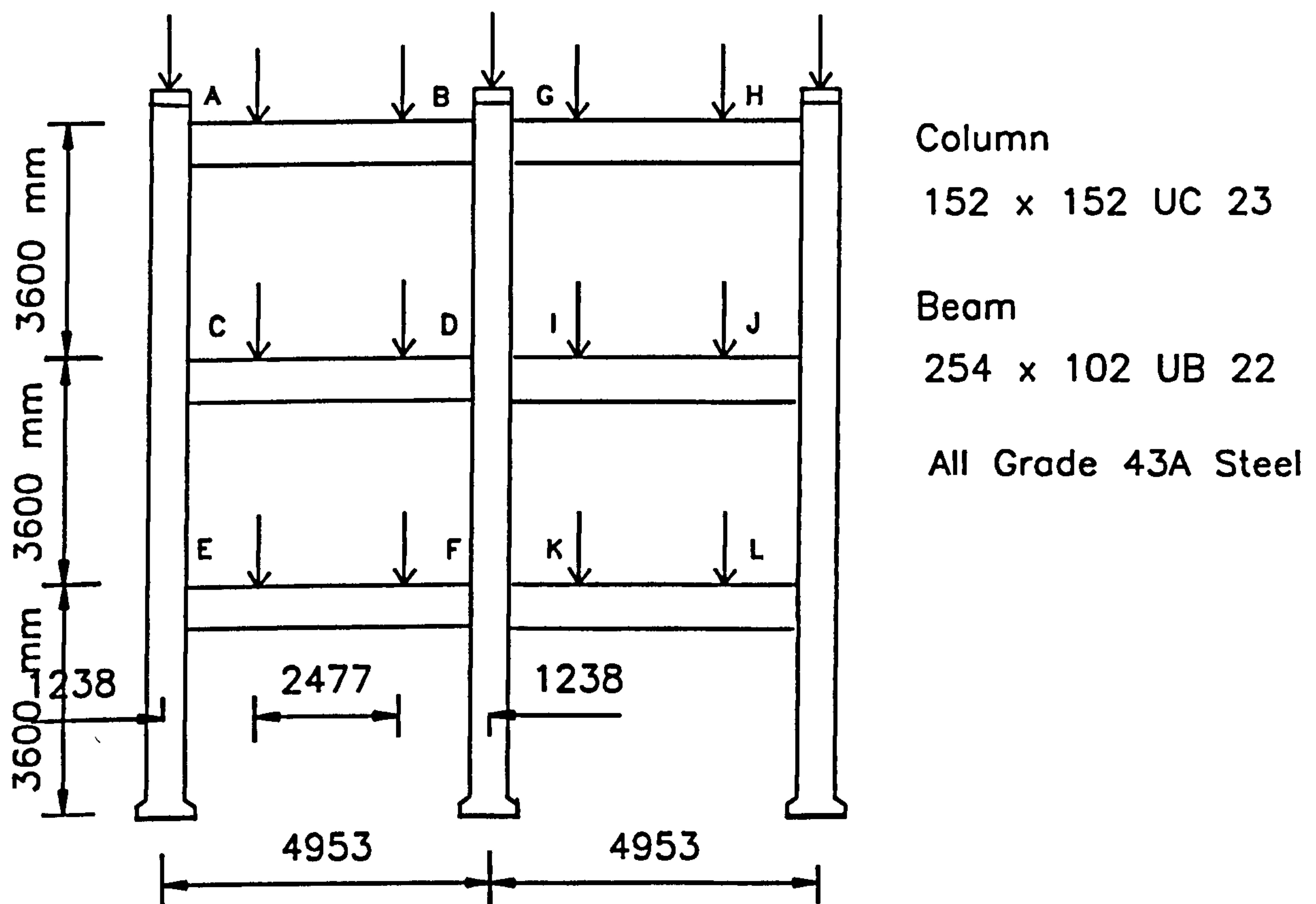


Figure 6.4 : General Arrangement of Frame 4 (Minor Axis Frame)

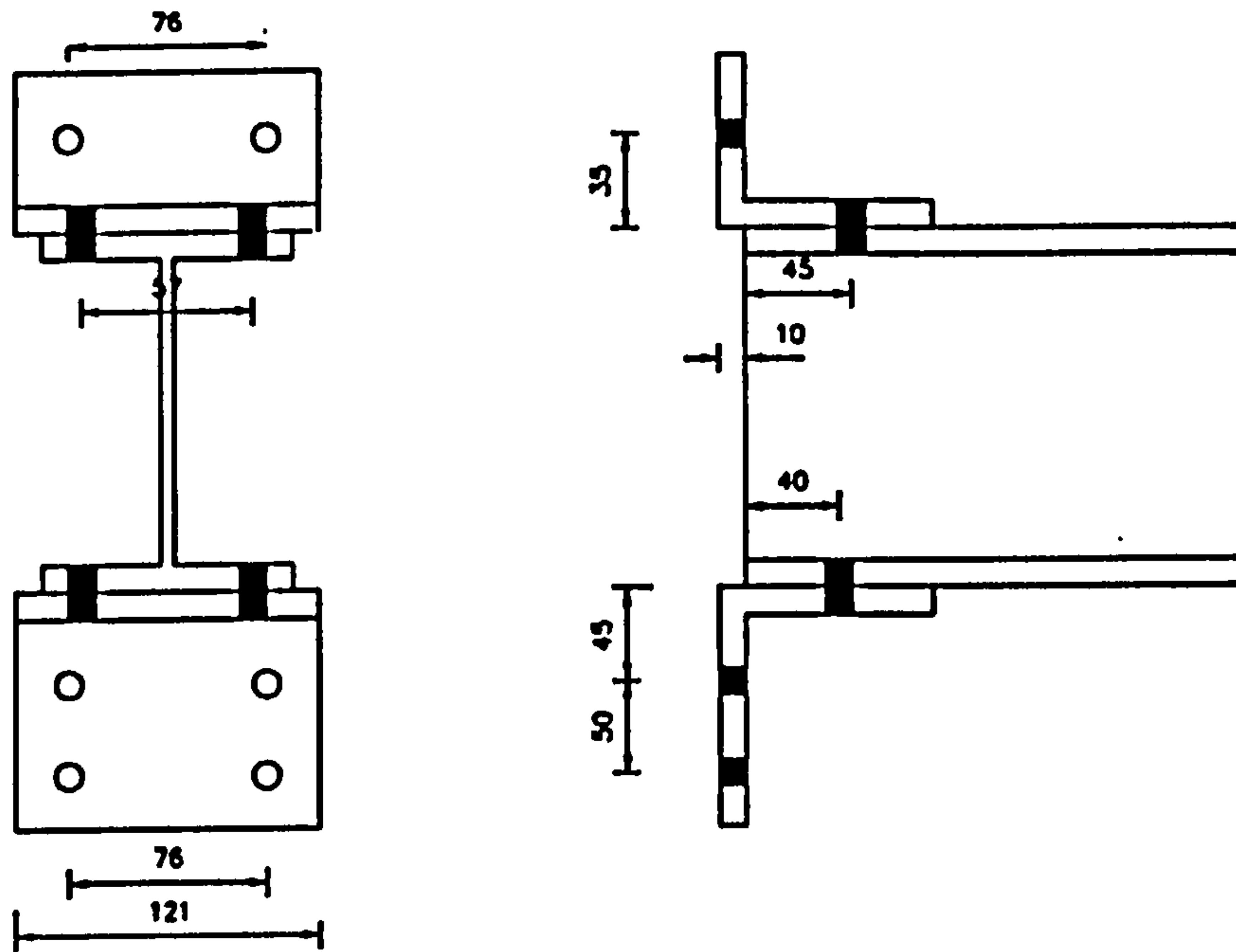


Figure 6.5 : Flange Cleat Connection used in Frames 3 and 4

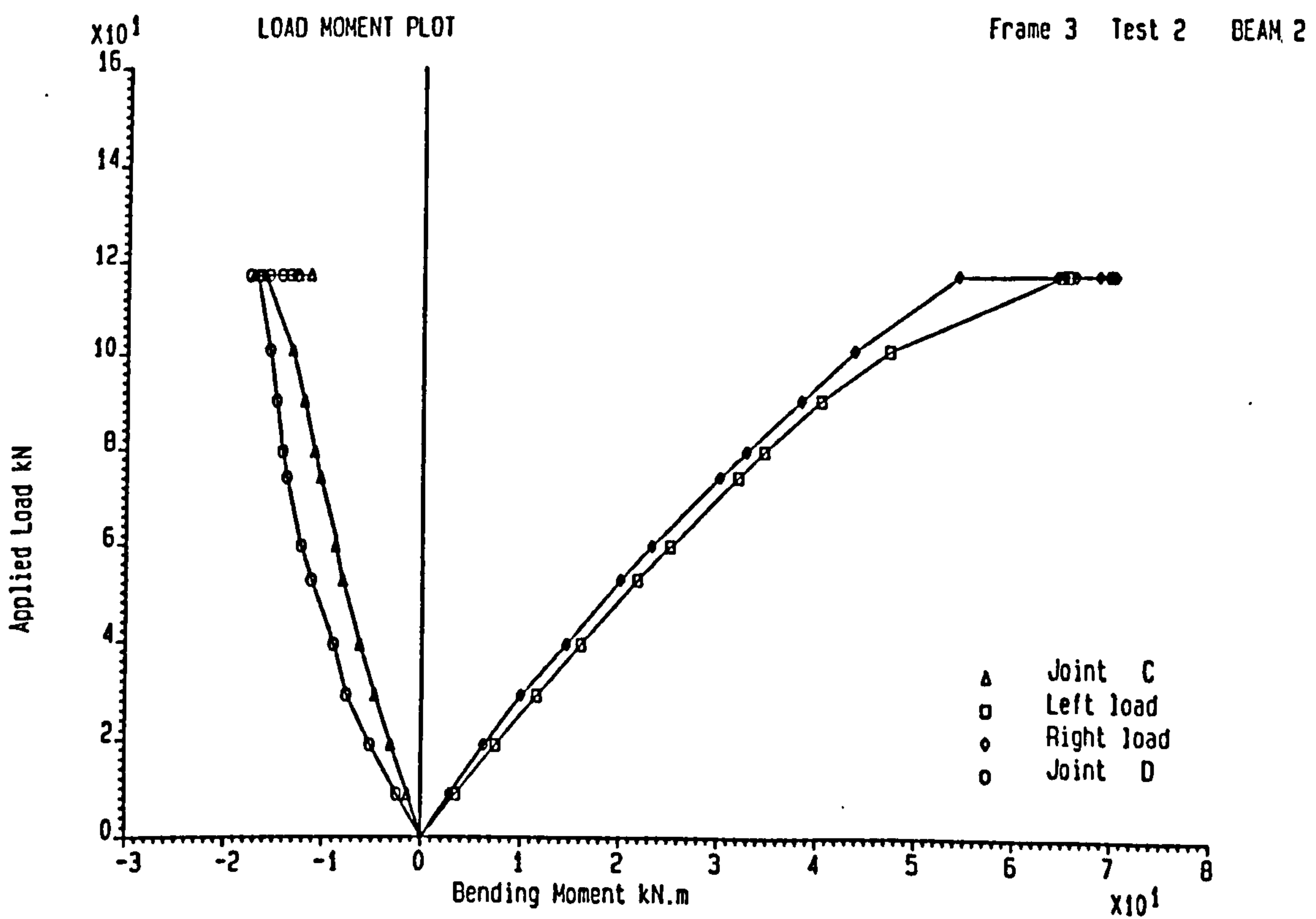


Figure 6.6 : Total Applied Load against Bending Moment on Beam 2 in Test 2 of Frame 3

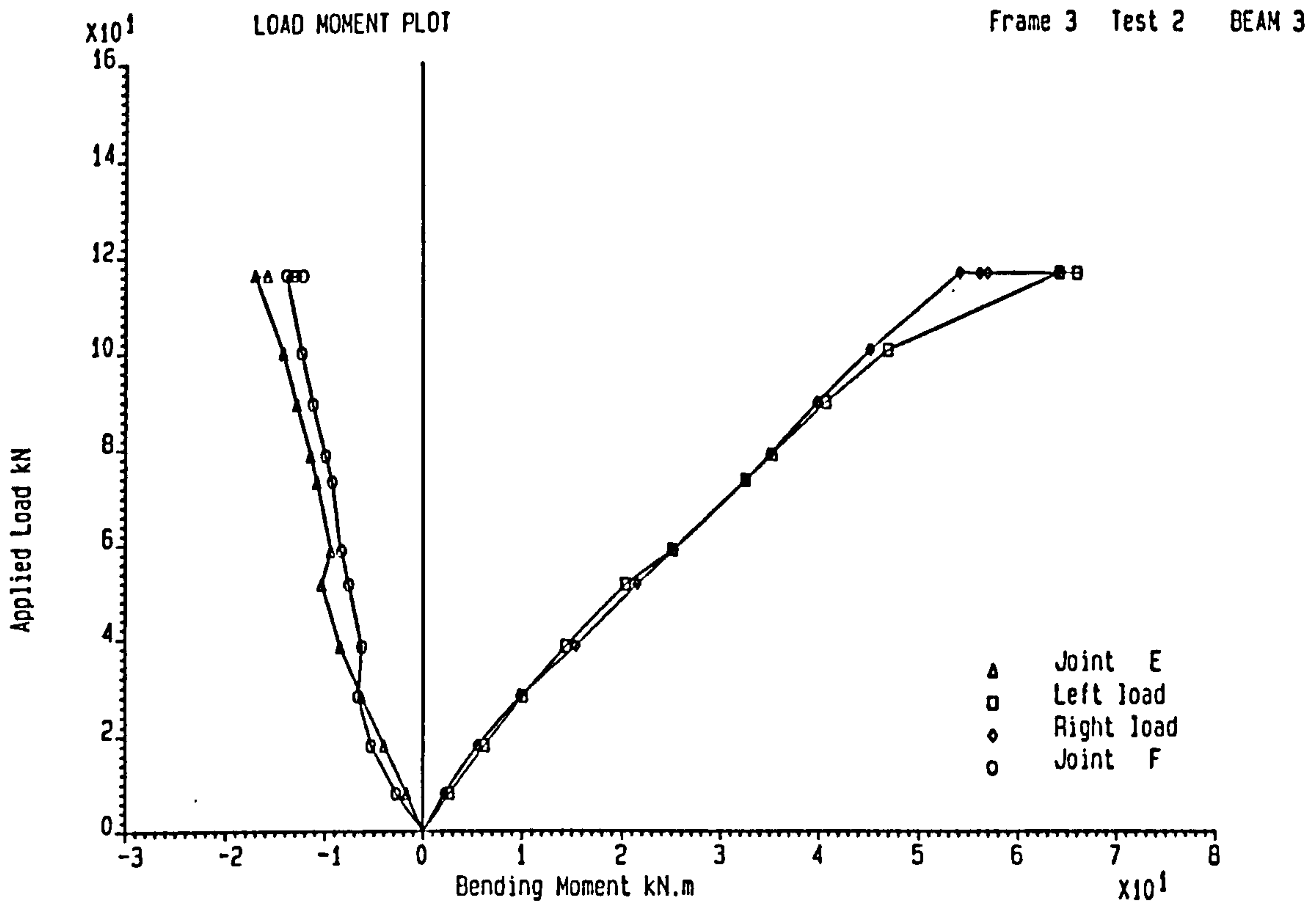


Figure 6.7 : Total Applied Load against Bending Moment on Beam 3  
in Test 2 of Frame 3

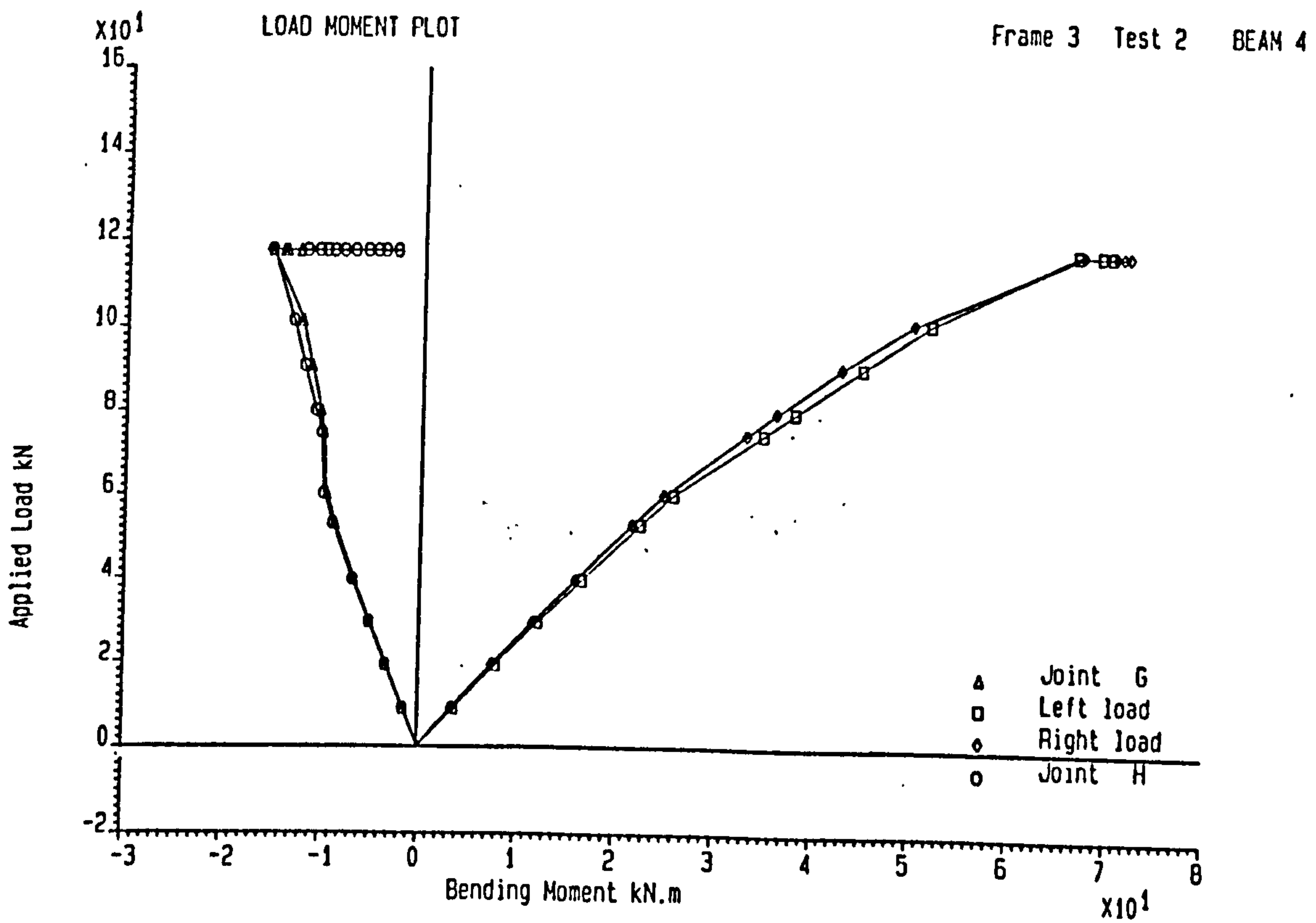


Figure 6.8 : Total Applied Load against Bending Moment on Beam 4  
in Test 2 of Frame 3

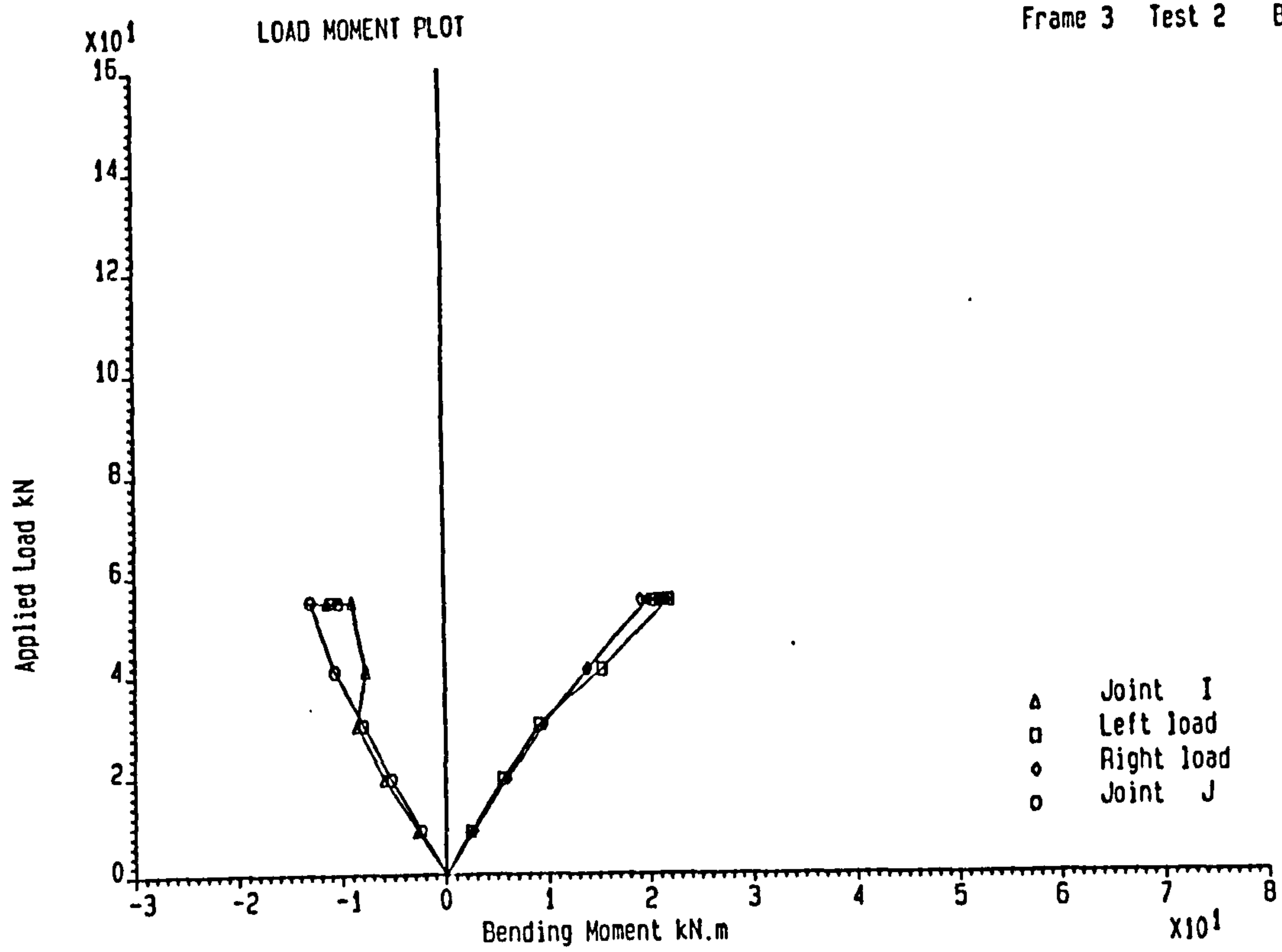


Figure 6.9 : Total Applied Load against Bending Moment on Beam 5 in Test 2 of Frame 3

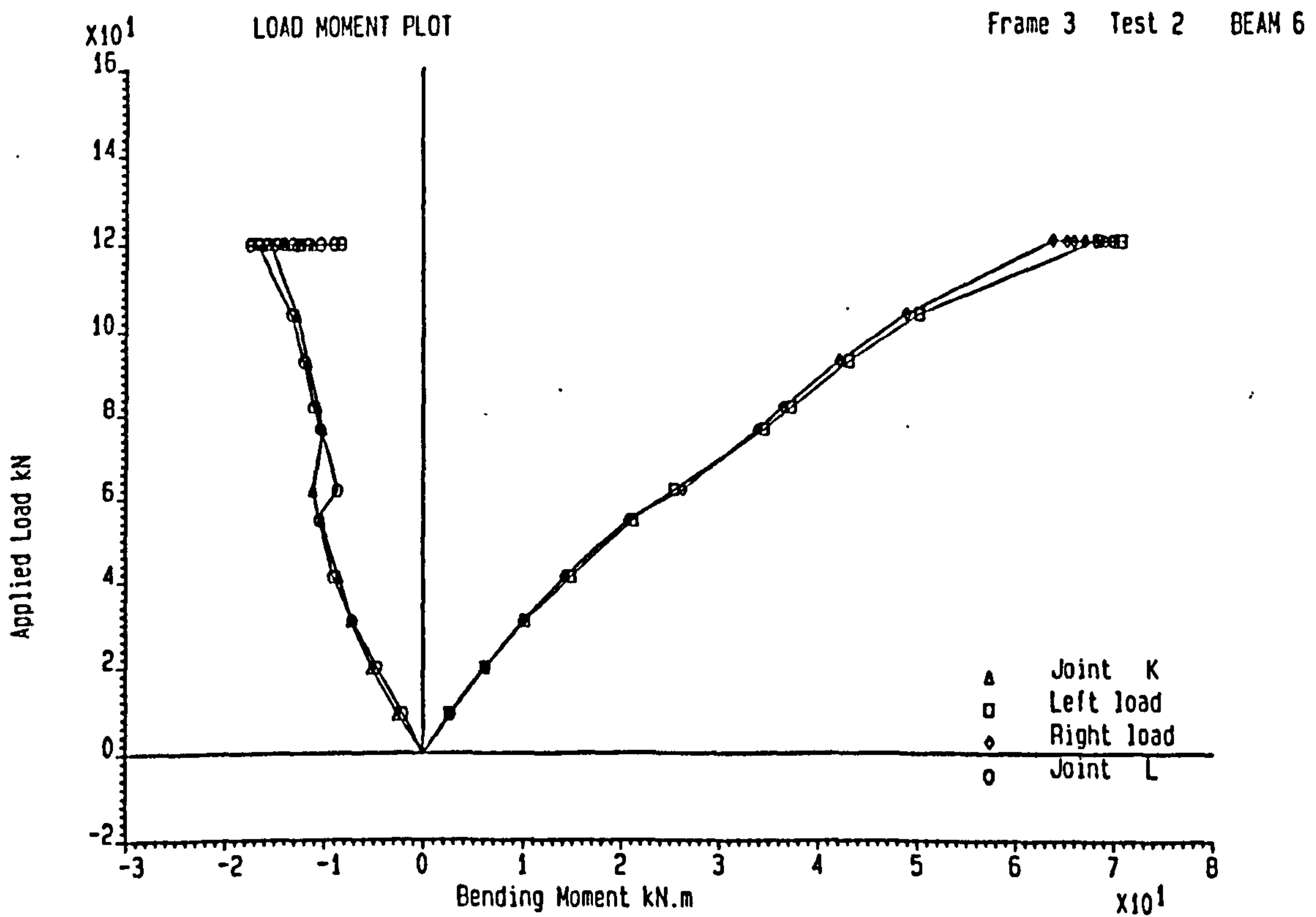
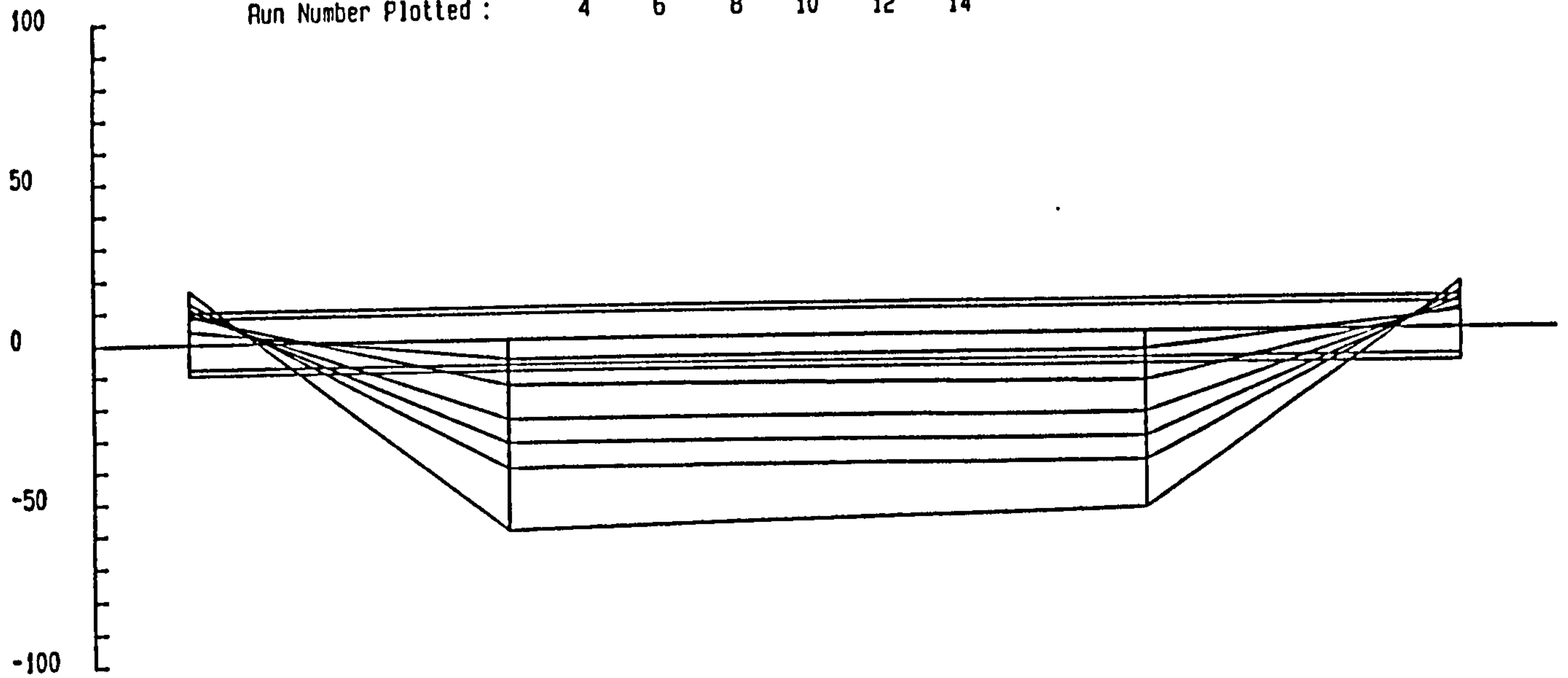


Figure 6.10 : Total Applied Load against Bending Moment on Beam 6 in Test 2 of Frame 3

Bending Moment kN.m

Run Number Plotted : 4 6 8 10 12 14



SUPERIMPOSED BENDING MOMENT

Figure 6.11 : Bending Moment Distribution around Beam 3 in Test 2 of Frame 3 up to End of Beam Load

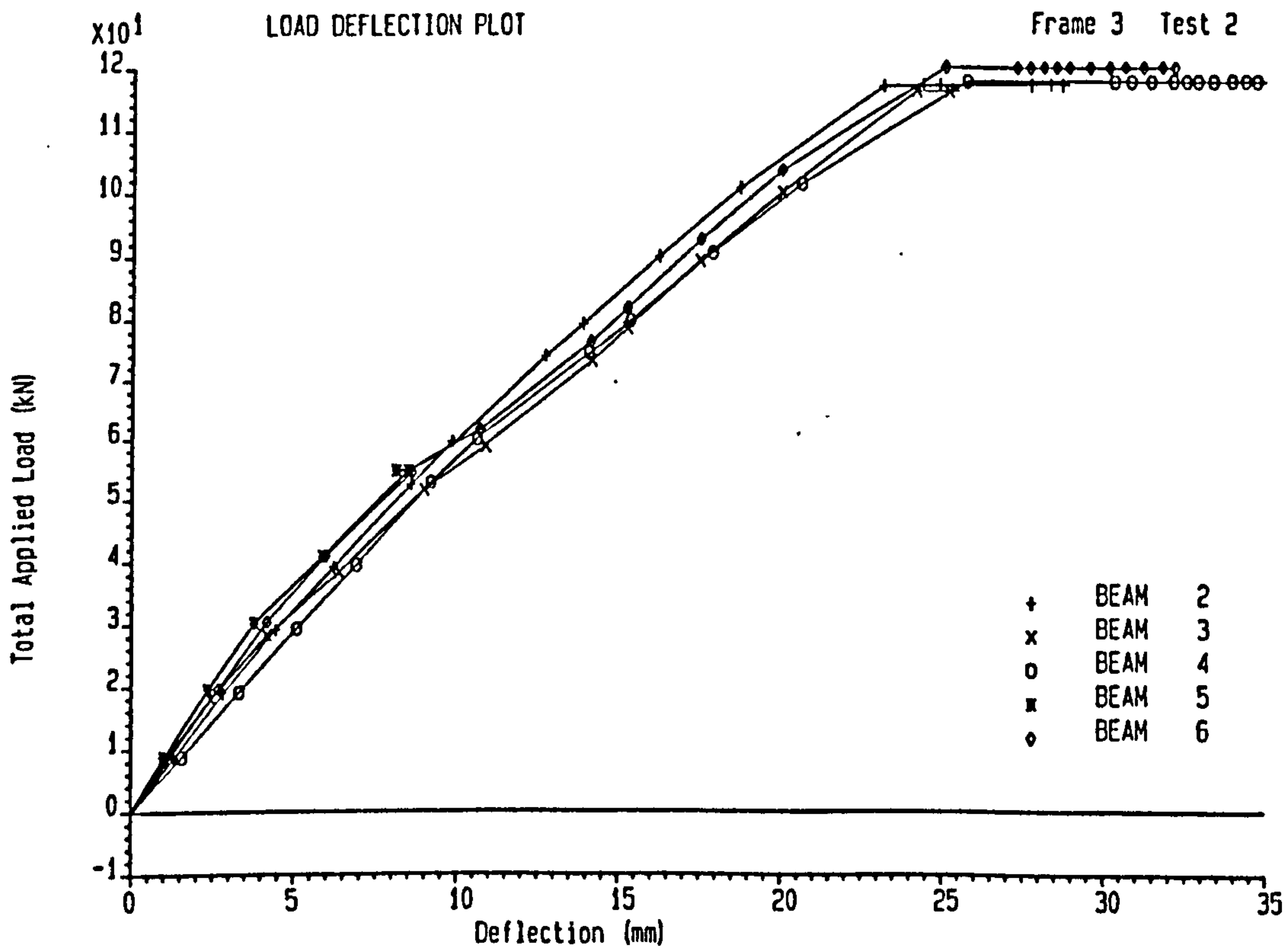
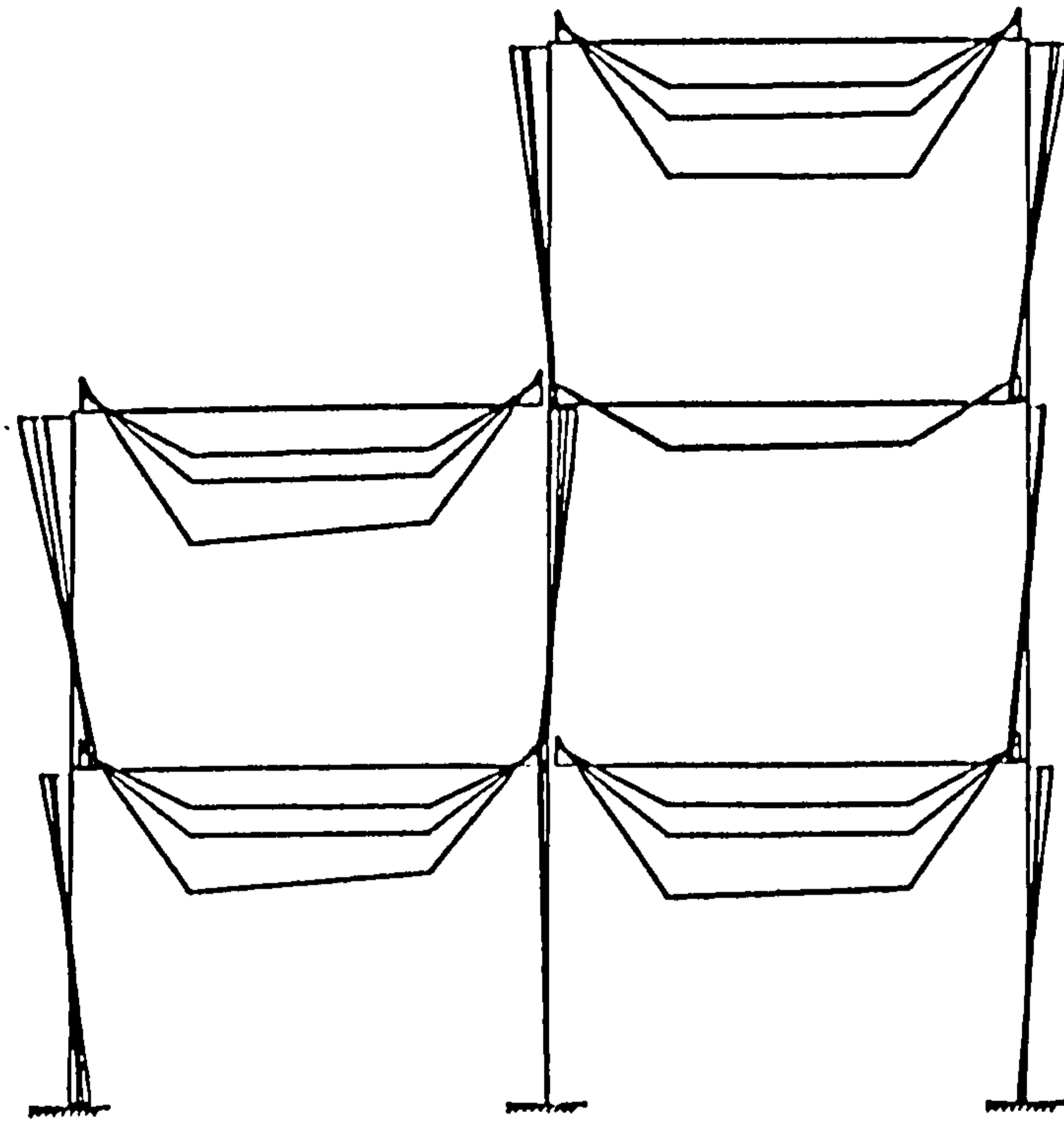


Figure 6.12 : Total Applied Load against Mid-Span Deflection on Five Beams in Test 2 of Frame 3

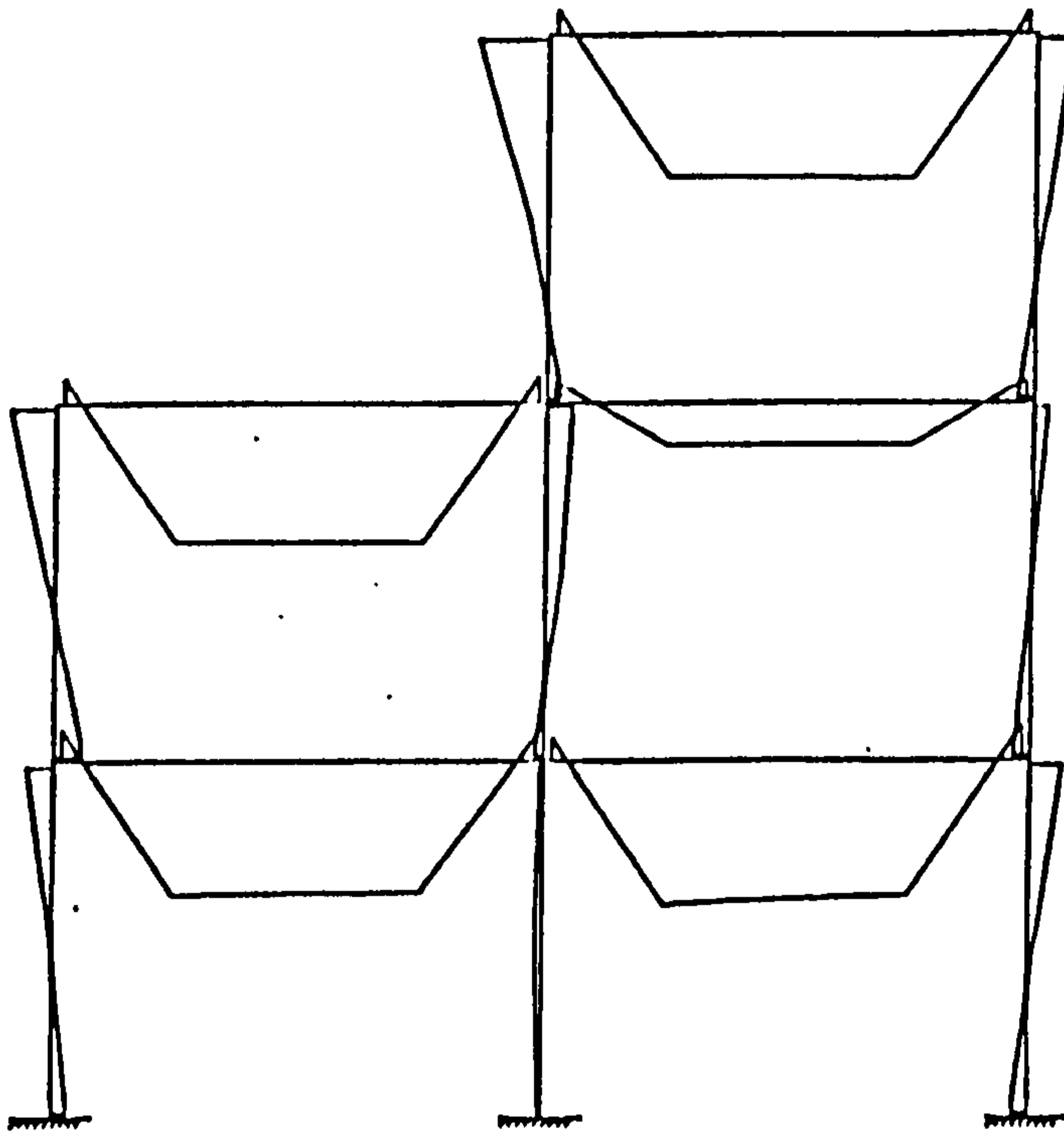


Scale : 0 50 100  
in kNm

Frame 3 Test 2

Run Numbers Plotted : 7 11 14

Figure 6.13 : Frame Moment around the Frame in Test 2 of Frame 3 up to End of Beam Load



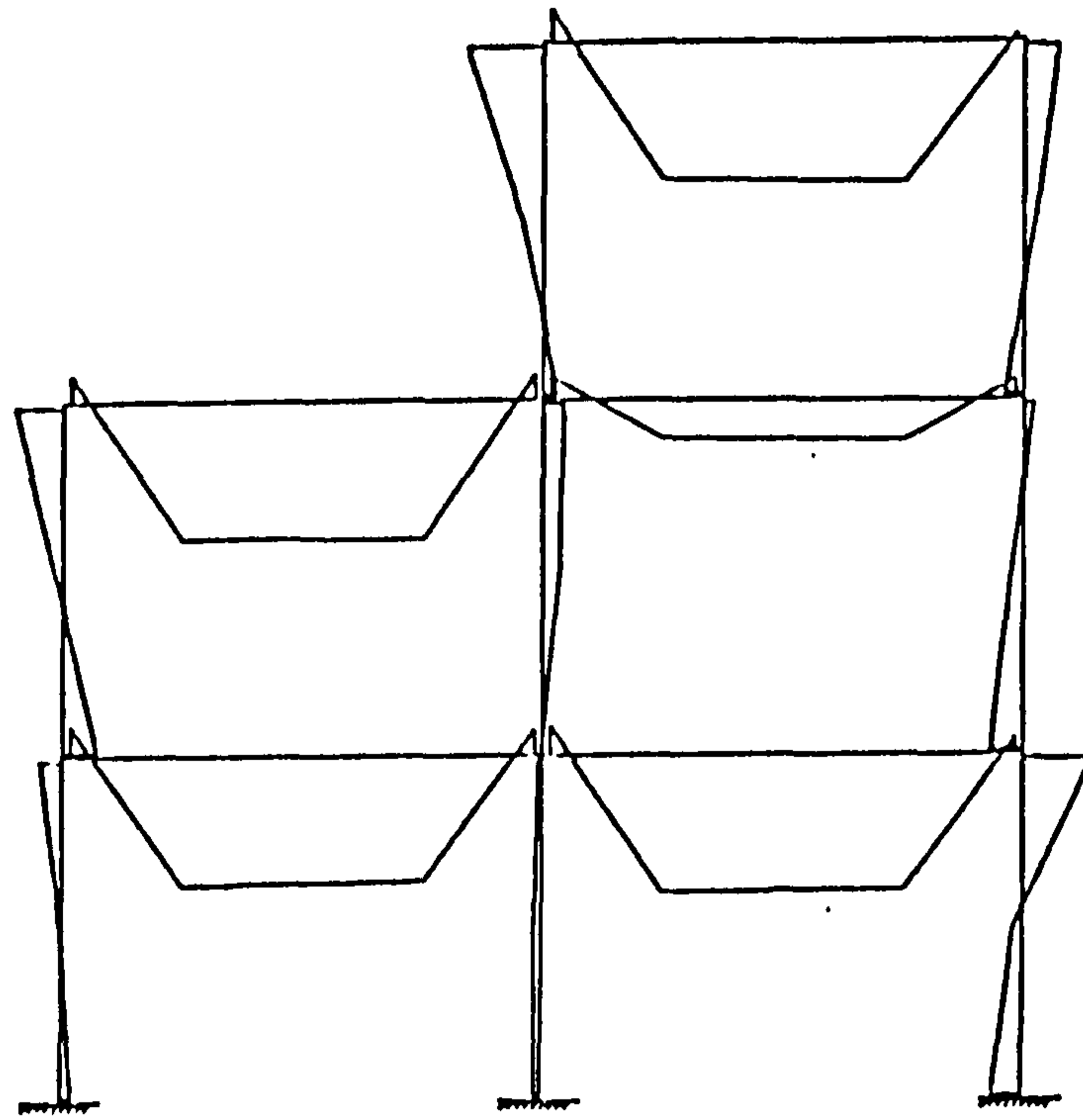
Scale : 0 50 100  
in kNm

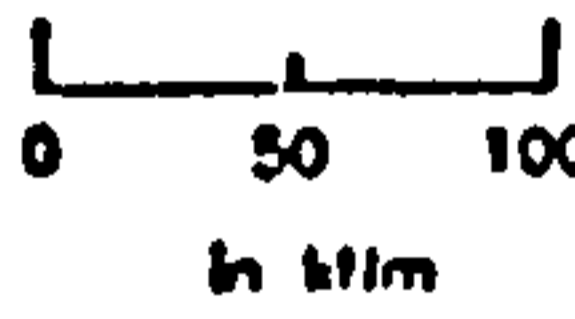
Frame 3 Test 2

Run Numbers Plotted : 24

Figure 6.14 : Frame Moment around the Frame in Test 2 of Frame 3 in Failure of the Central Column in Position 2

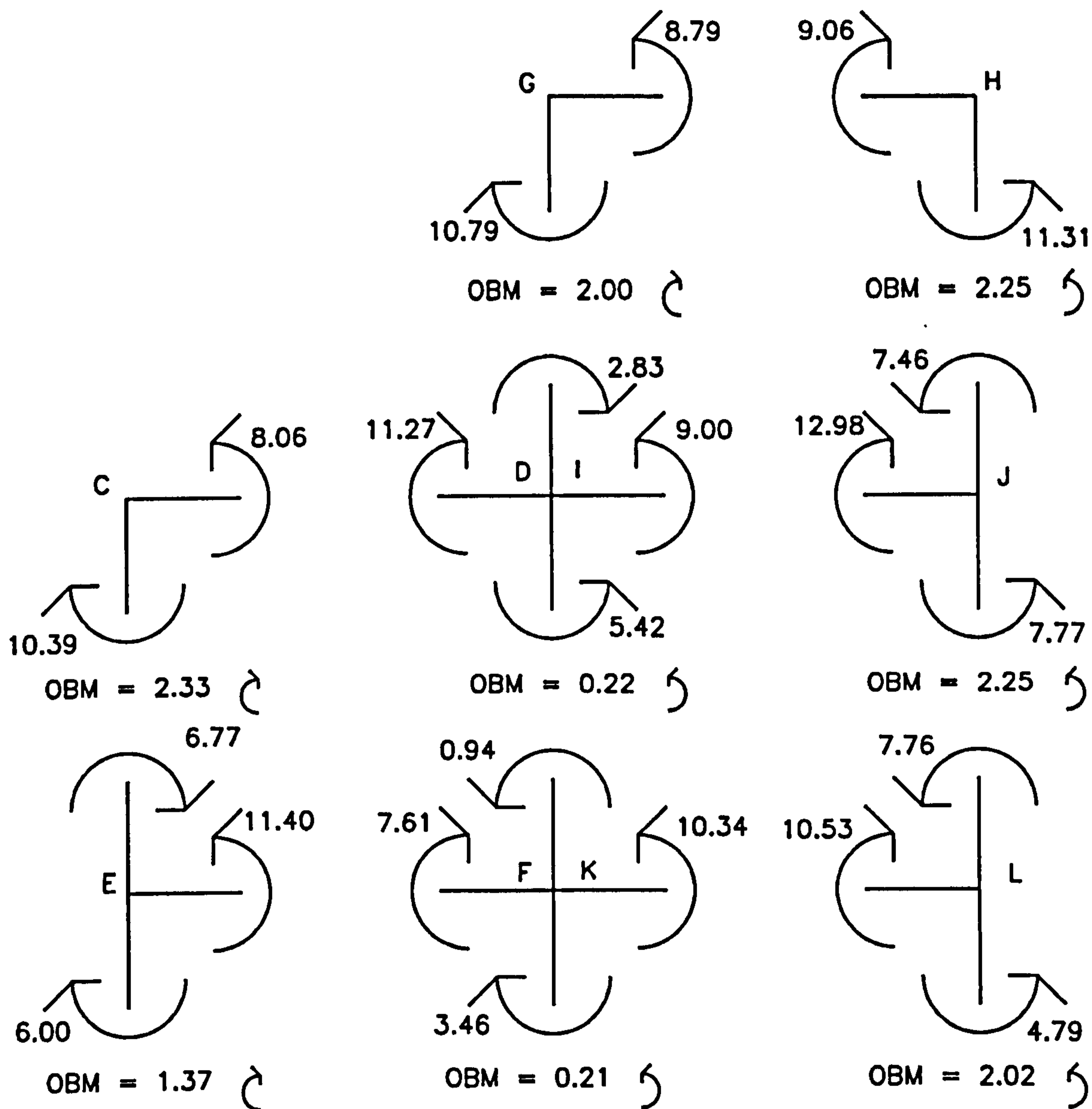




Scale :  0 50 100  
in mm  
Run Numbers Plotted : 38

Frame 3 Test 2

Figure 6.15 : Frame Moment around the Frame in Test 2 of Frame 3  
in Failure of the Edge Column in Position 3



OBM = Out of balance moment

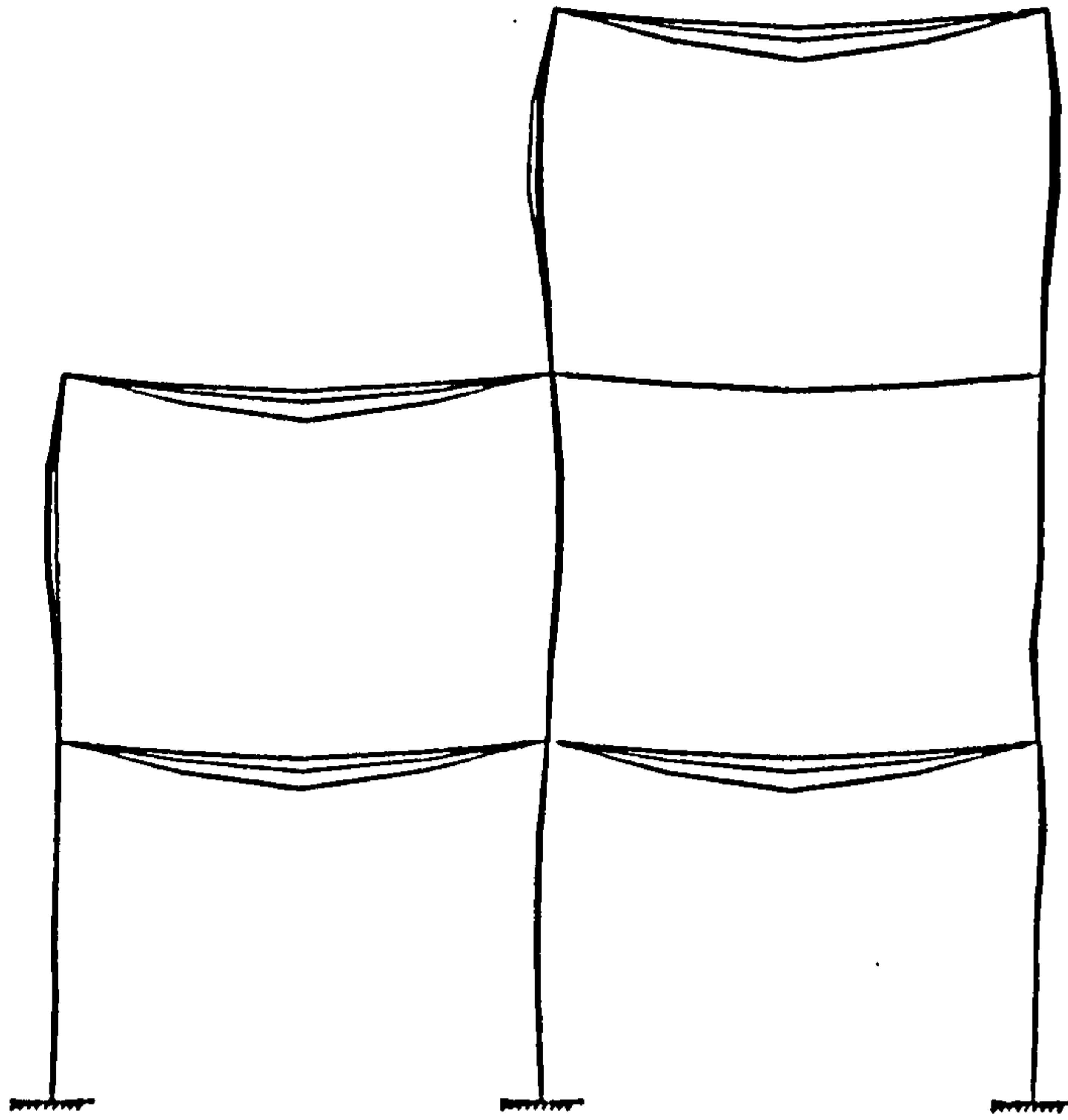
All values in kN.m units

FRAME 3

TEST 2

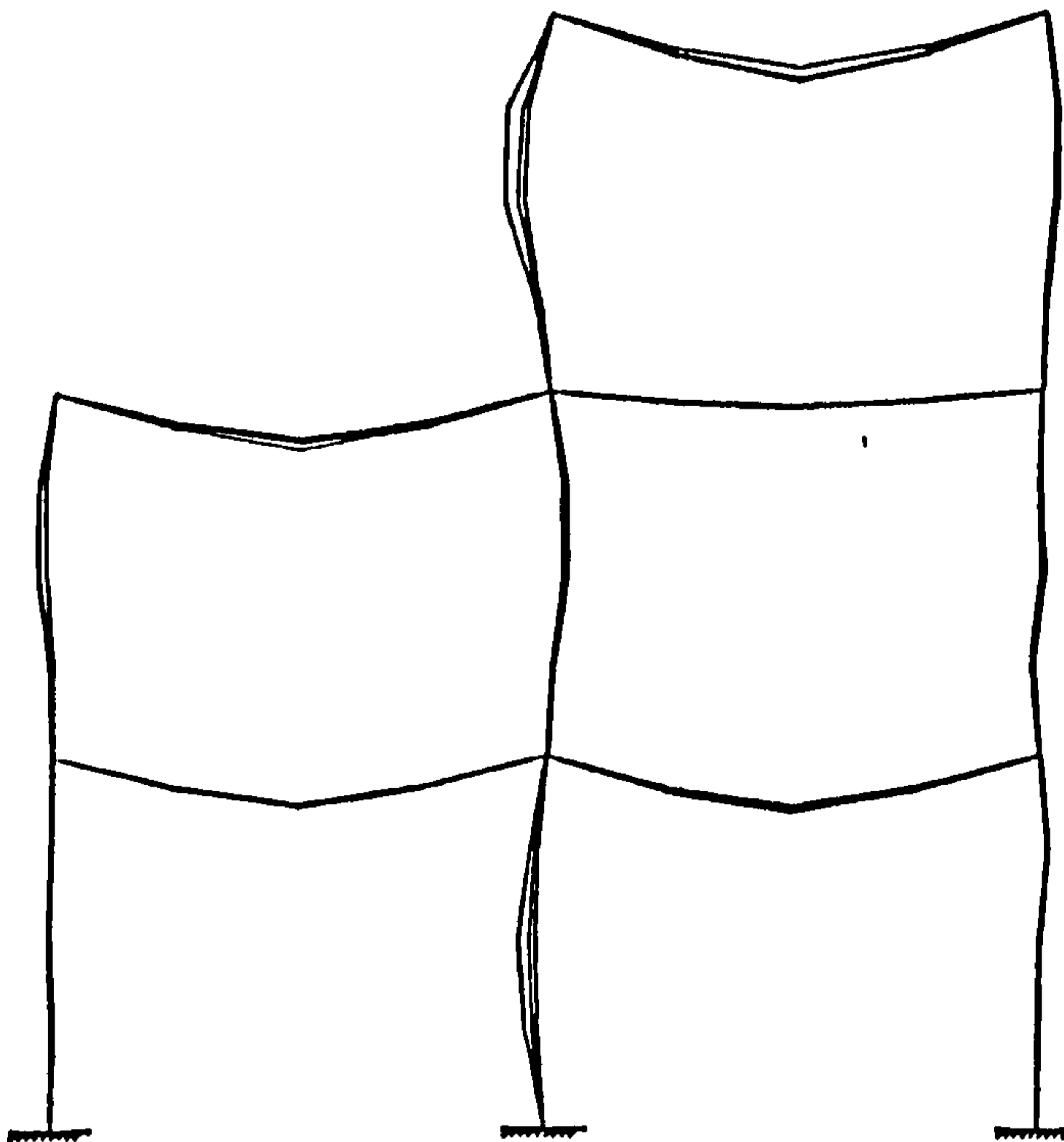
SCAN 7

Figure 6.16 : Moment Equilibrium Check in Frame 3 Test 2



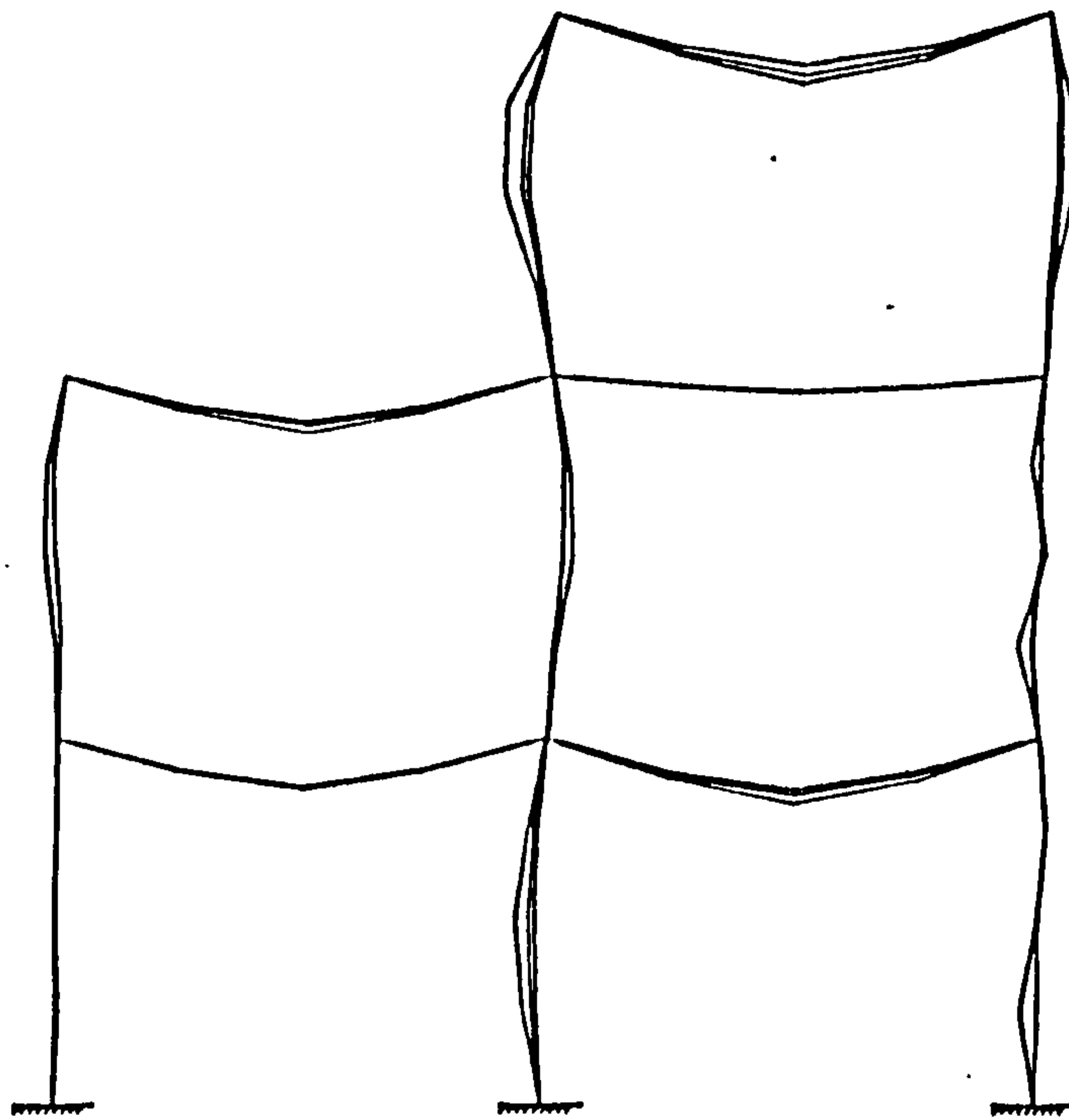
Horizontal deflections of  $\frac{12.5}{25}$   
 Vertical deflections of  $\frac{50}{100}$  in mm  
 Frame 3 Test 2  
 Run Numbers Plotted : 7 11 14

Figure 6.17 : Frame Deformation around the Frame in Test 2 of Frame 3 up to End of the Beam Load



Horizontal deflections of  $\frac{12.5}{25}$   
 Vertical deflections of  $\frac{50}{100}$  in mm  
 Frame 3 Test 2  
 Run Numbers Plotted : 14 19 24

Figure 6.18 : Frame Deformation around the Frame in Test 2 of Frame 3 in Failure of the Central Column in Position 2



Horizontal deflections 0 | 12.5 | 25  
 Vertical deflections 0 | 50 | 100 in mm  
 Run Numbers Plotted : 14 19 38  
 Frame 3 Test 2

Figure 6.19 : Frame Deformation around the Frame in Test 2 of Frame 3  
 in Failure of the Edge Column in Position 3

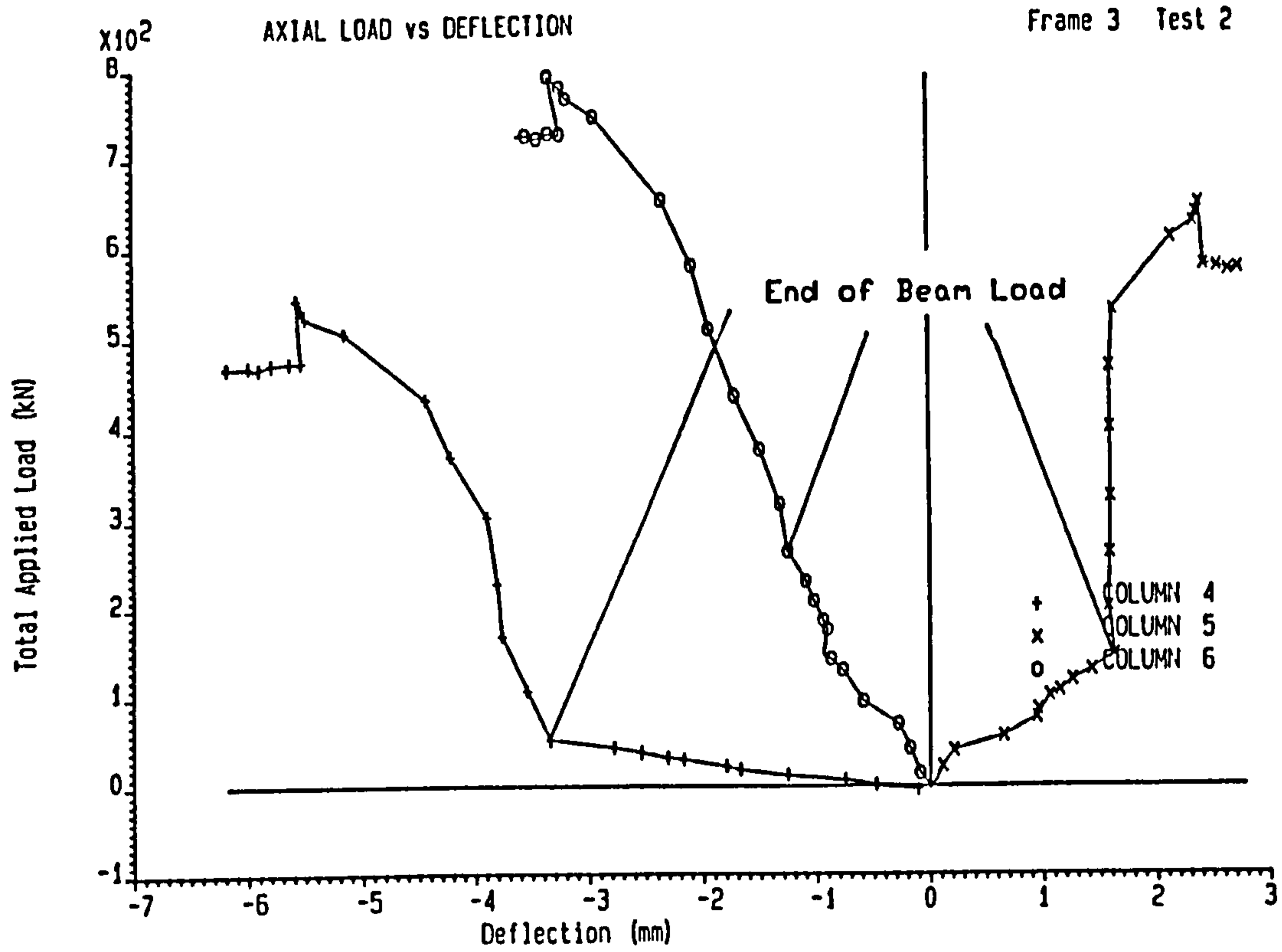


Figure 6.20 : Total Axial Load against the Mid-Height Deflection at Three Lifts of the Central Column (Position 2) in Test 2 of Frame 3

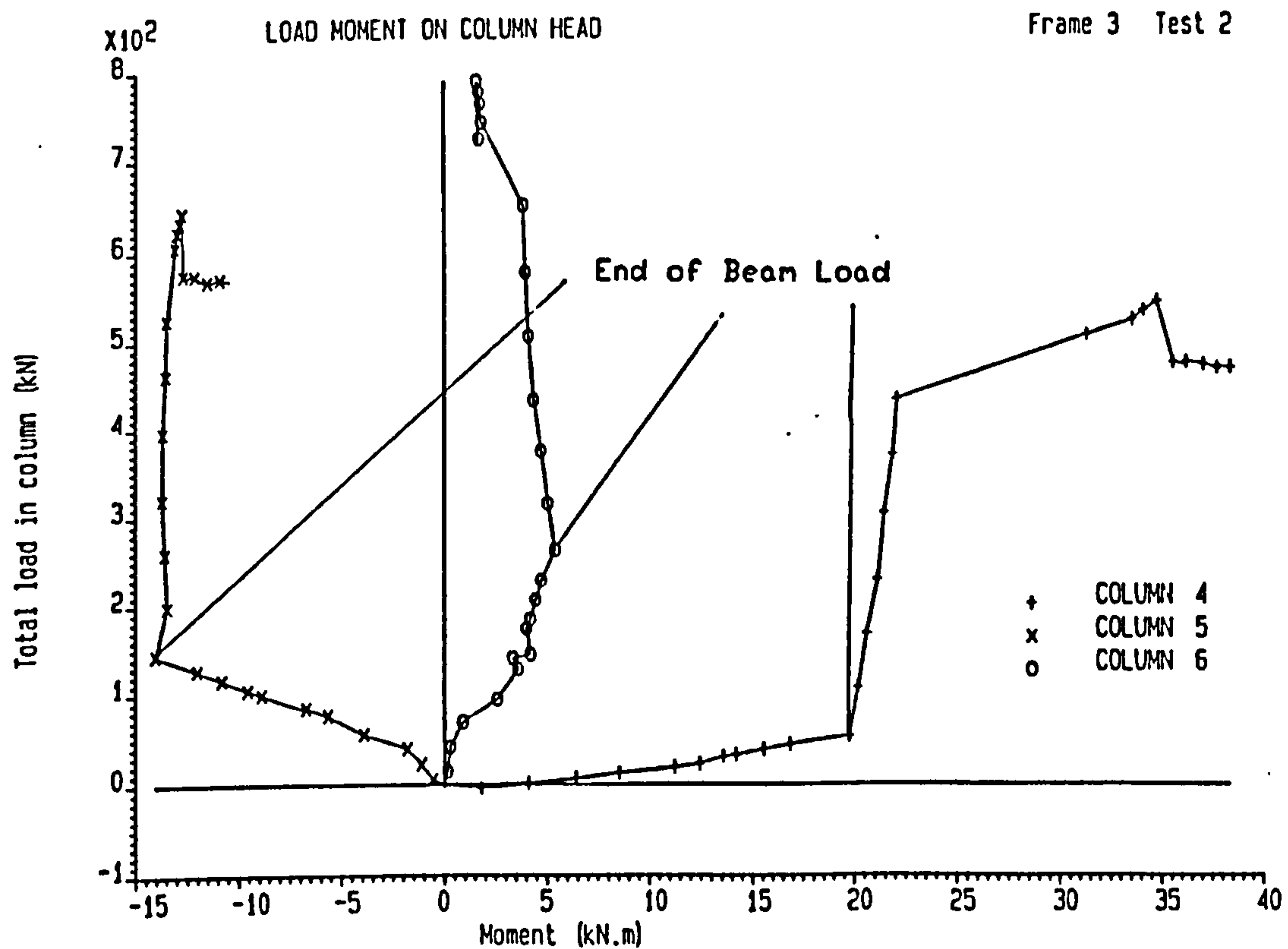


Figure 6.21: Total Axial Load against the Column Head Moments at Three Lifts of the Central Column (Position 2) in Test 2 of Frame 3

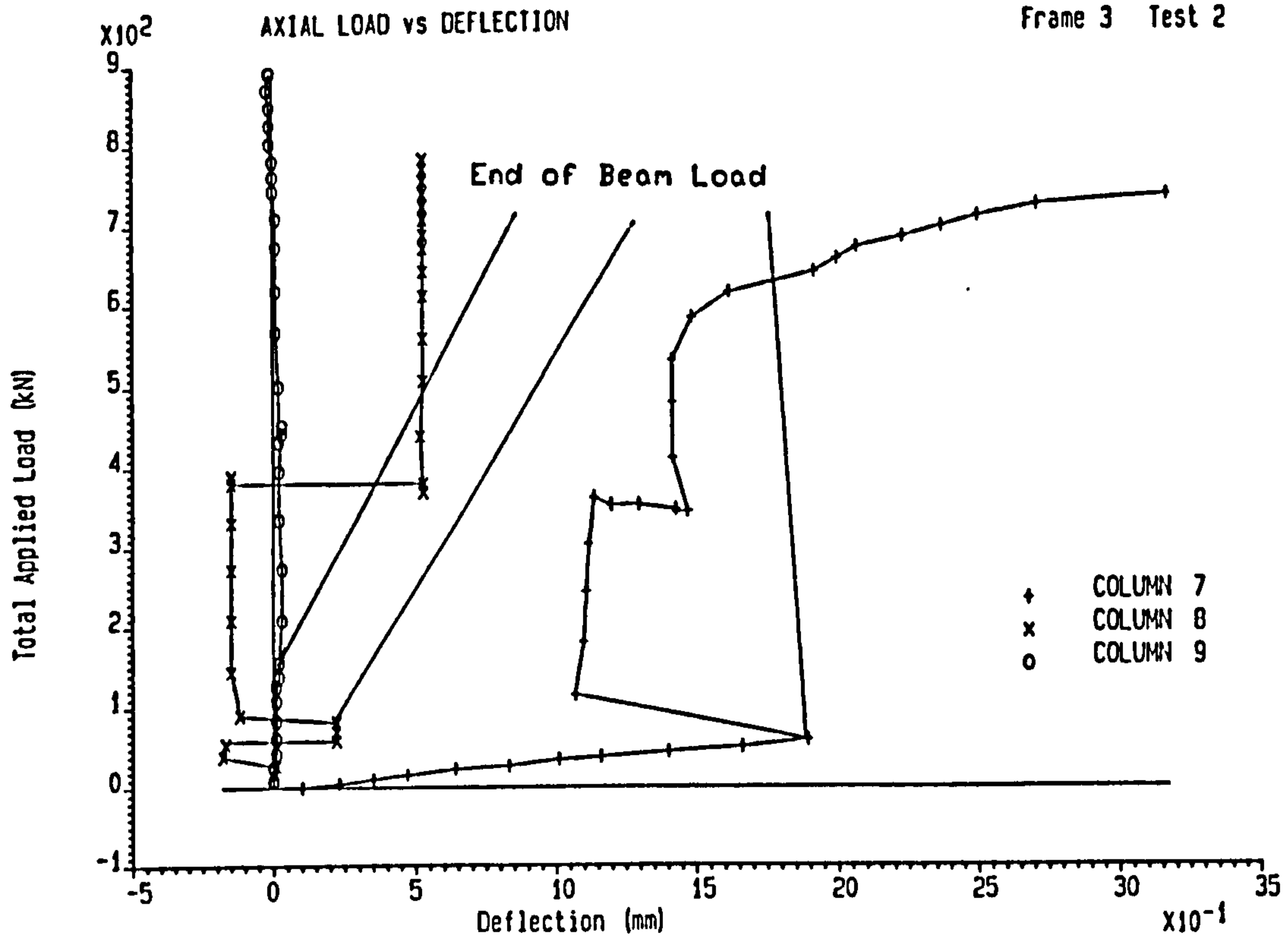


Figure 6.22 : Total Axial Load against the Mid-Height Deflection at Three Lifts of the Edge Column (Position 3) in Test 2 of Frame 3

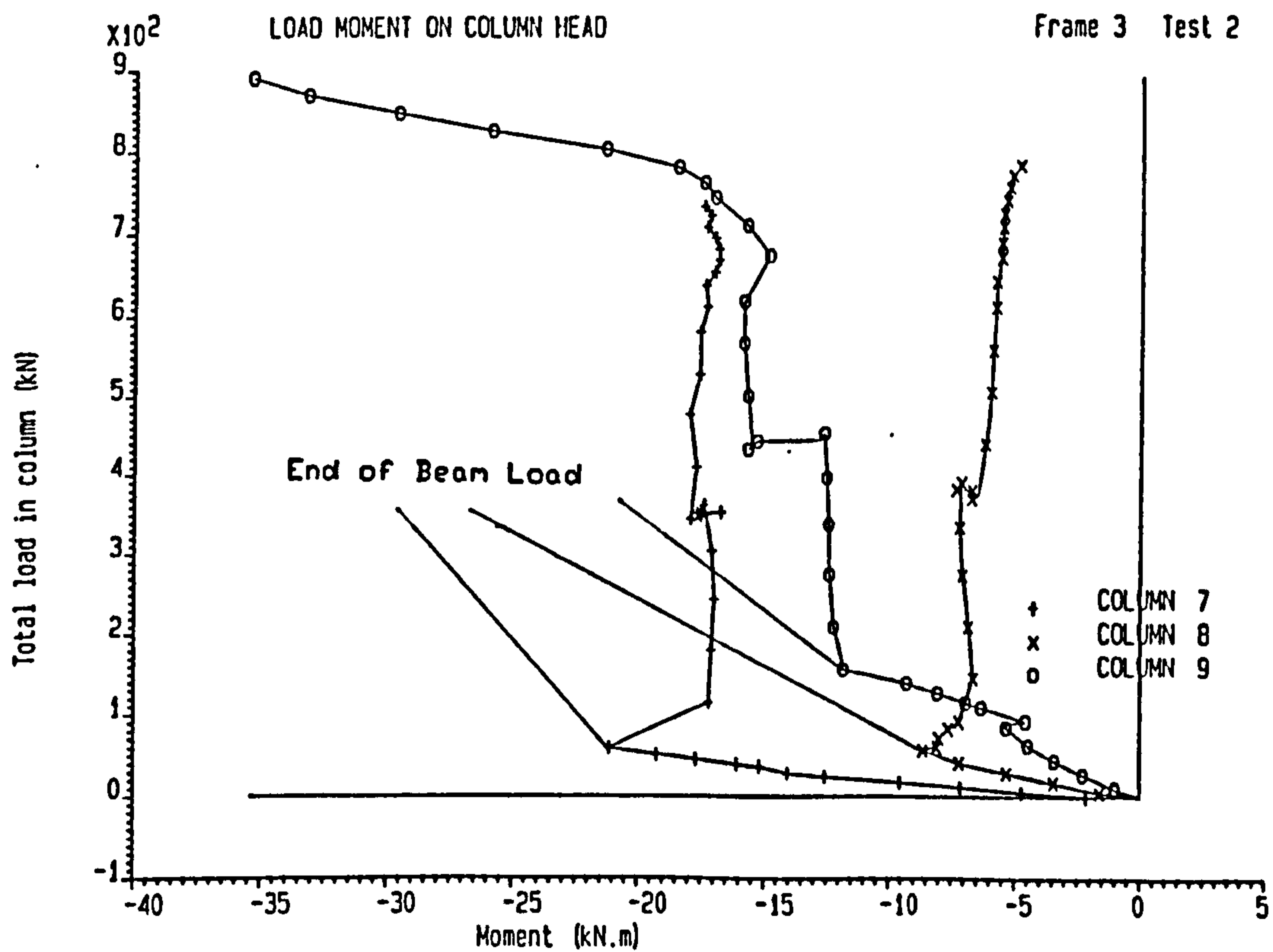


Figure 6.23: Total Axial Load against the Column Head Moments at Three Lifts of the Edge Column (Position 3) in Test 2 of Frame 3

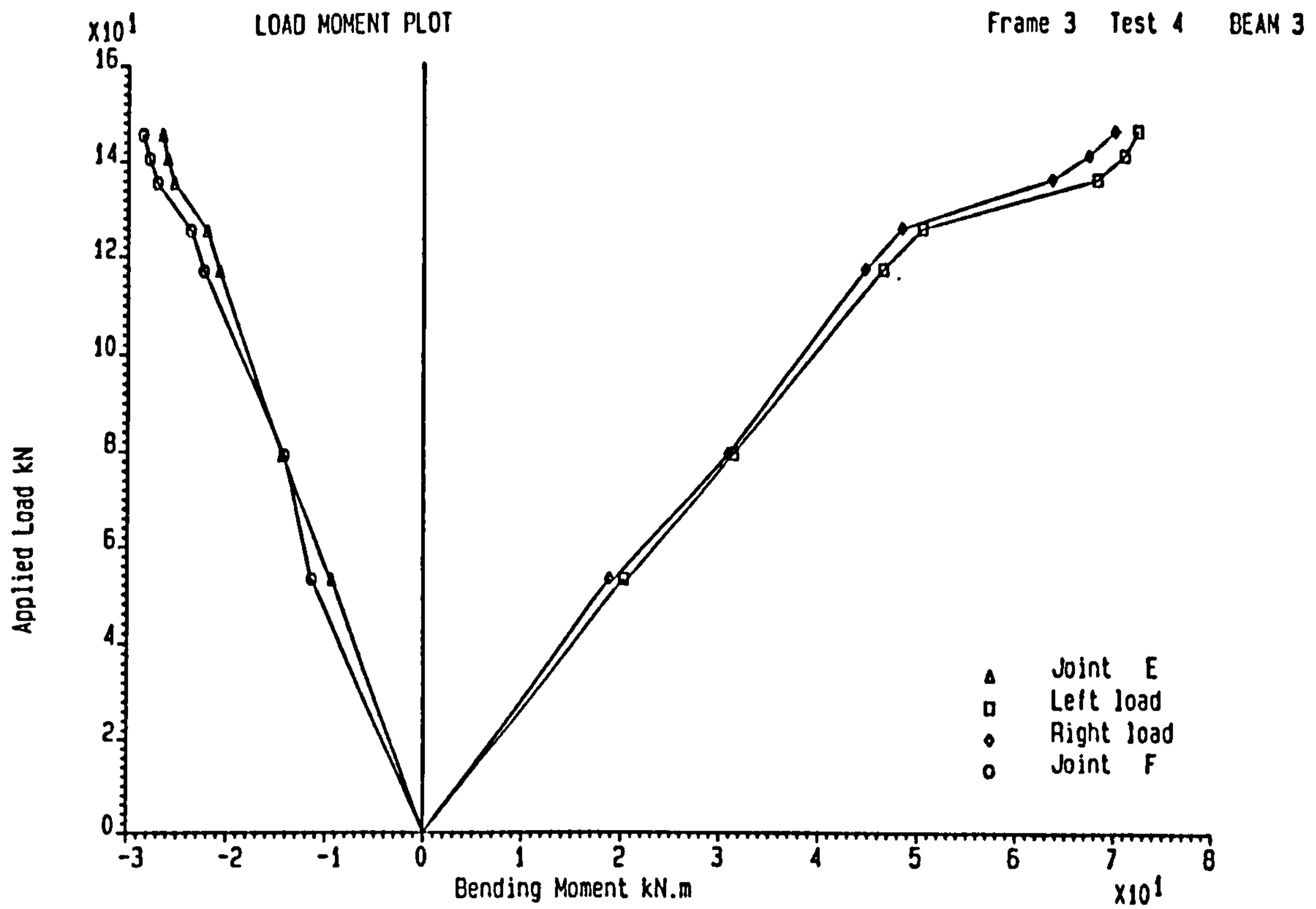


Figure 6.24 : Total Applied Load against Bending Moment on Beam 3 in Test 4 of Frame 3

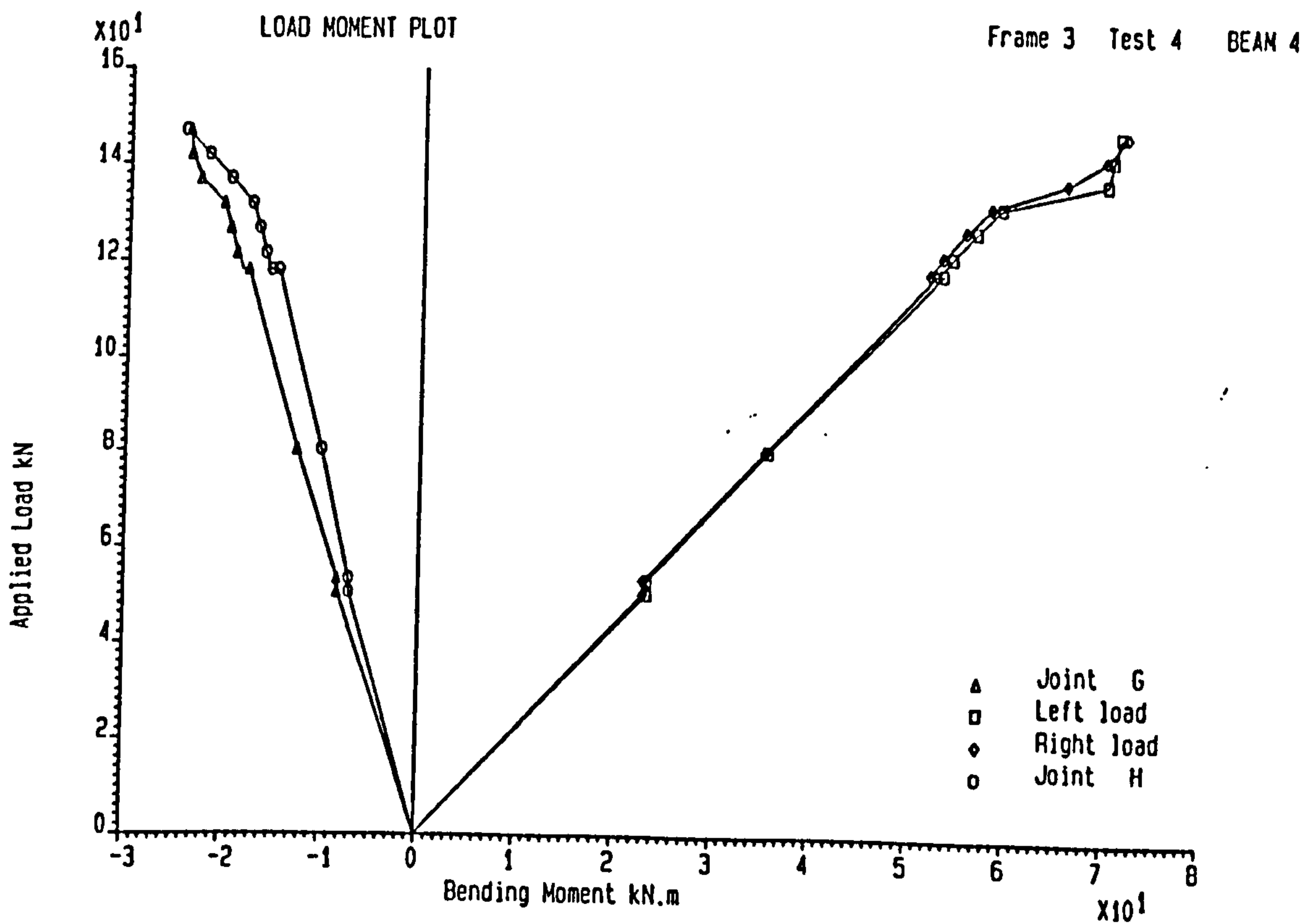


Figure 6.25 : Total Applied Load against Bending Moment on Beam 4 in Test 4 of Frame 3

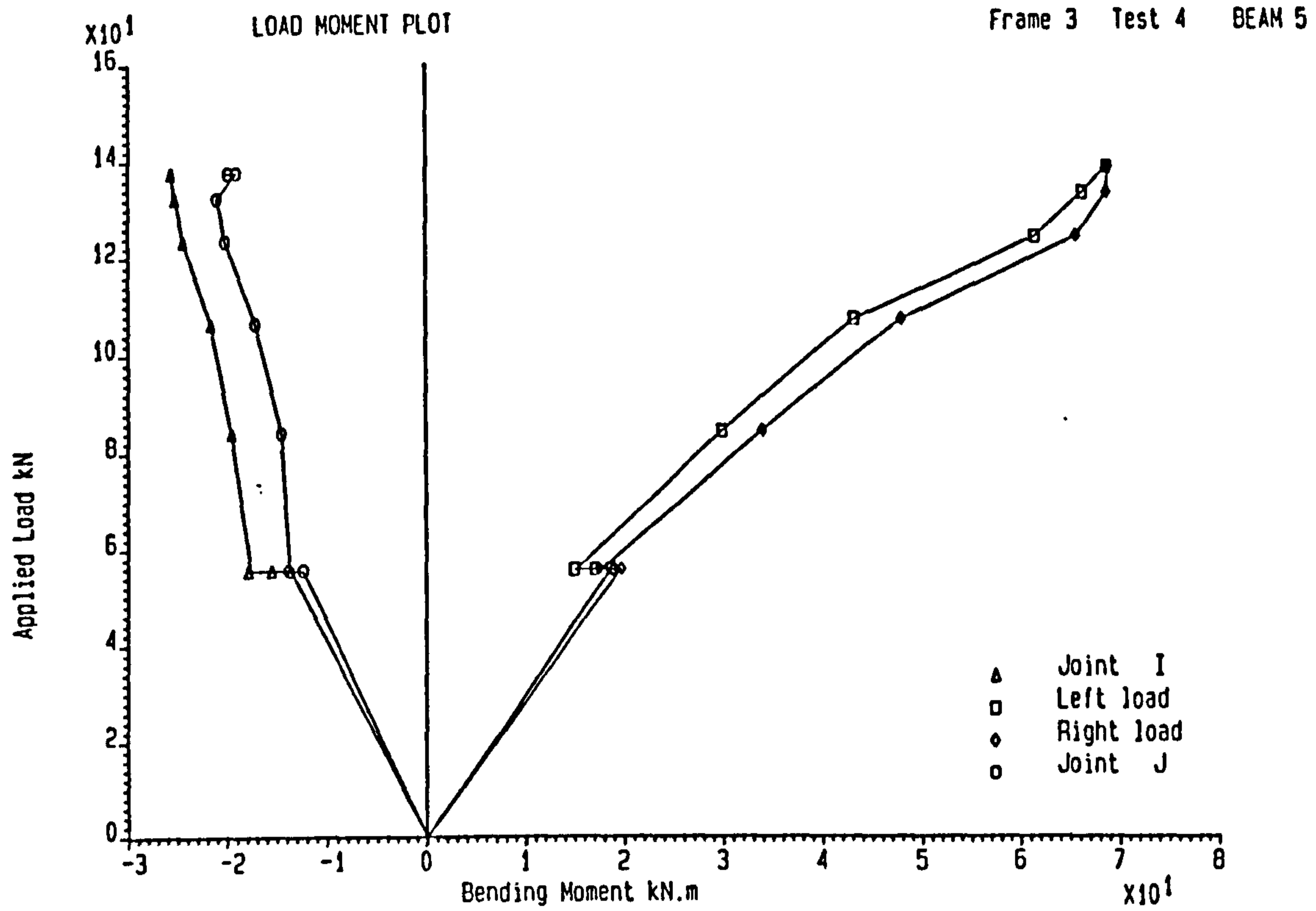


Figure 6.26 : Total Applied Load against Bending Moment on Beam 5 in Test 4 of Frame 3

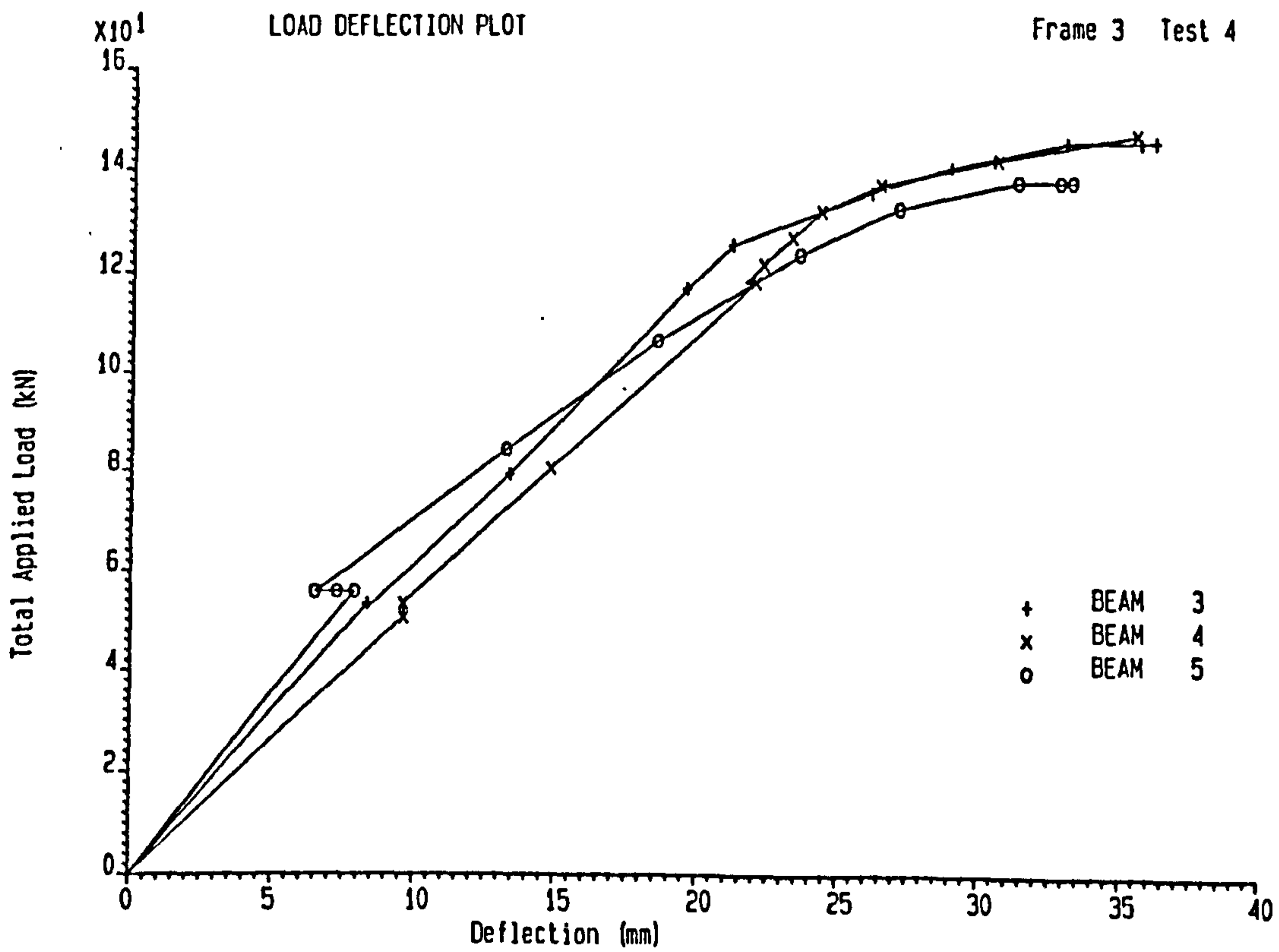


Figure 6.27 : Total Applied Load against Mid-Span Deflection on Beams 3, 4 and 5 in Test 4 of Frame 3



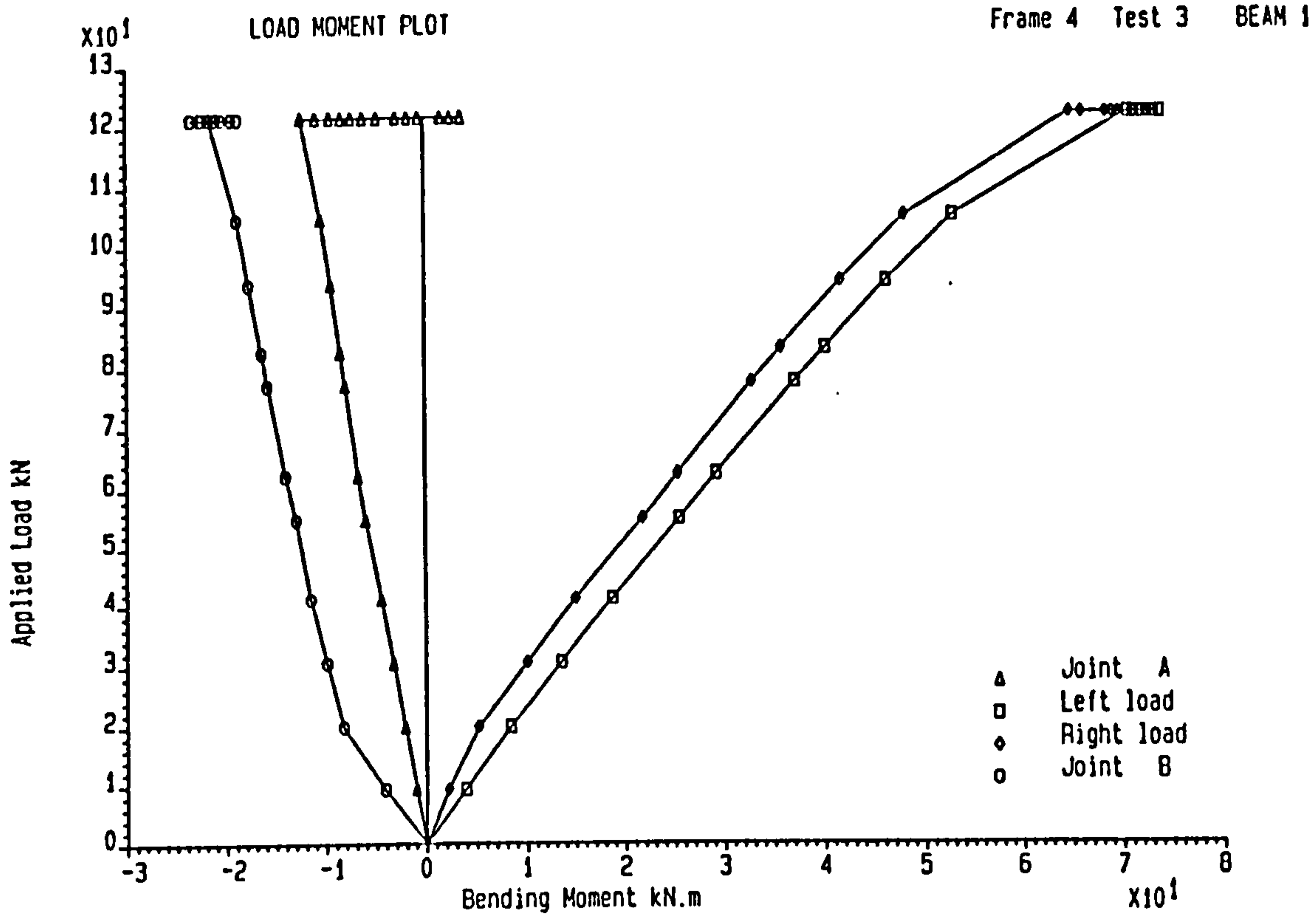


Figure 6.28 : Total Applied Load against Bending Moment on Beam 1 in Test 3 of Frame 4

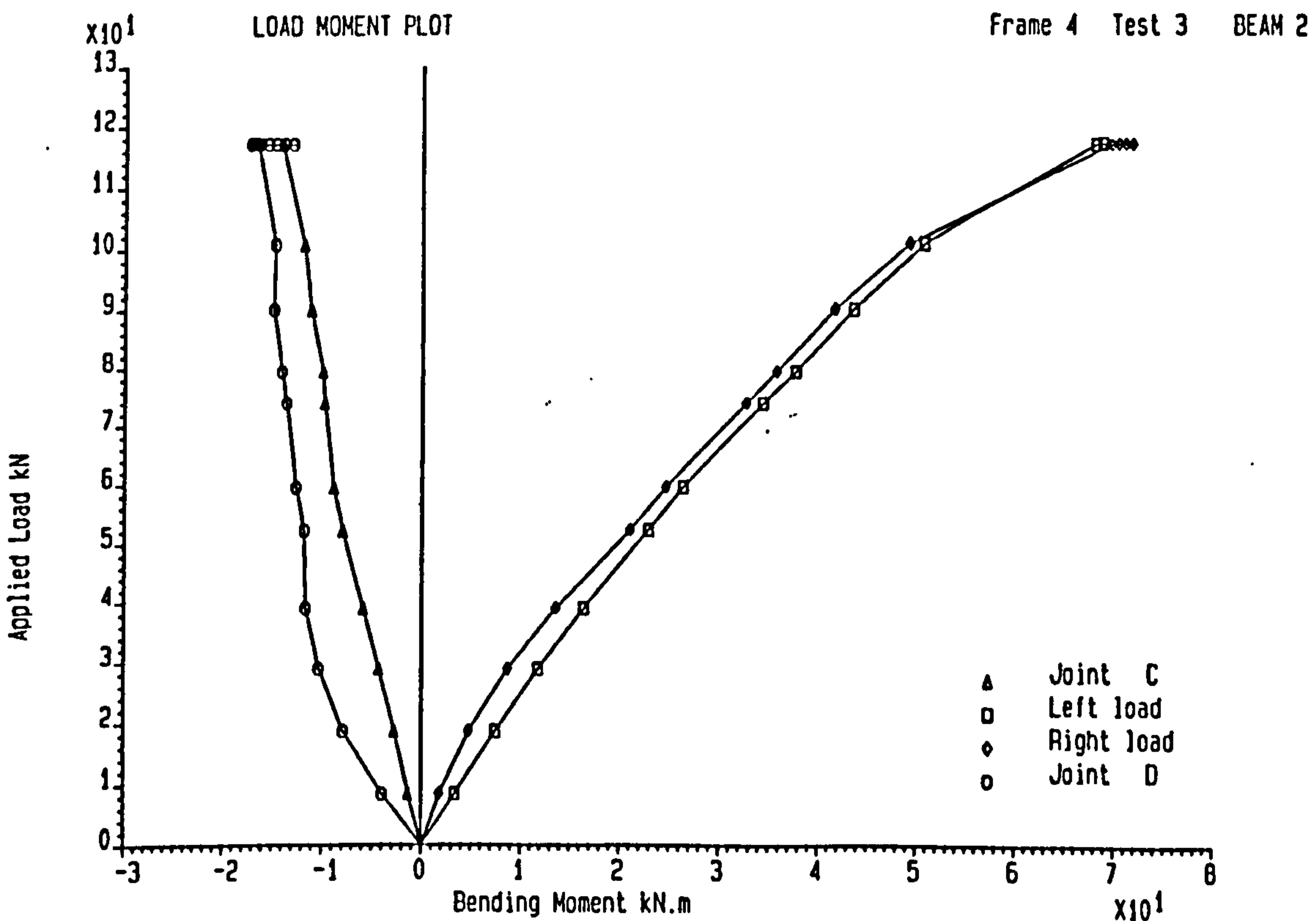


Figure 6.29 : Total Applied Load against Bending Moment on Beam 2 in Test 3 of Frame 4

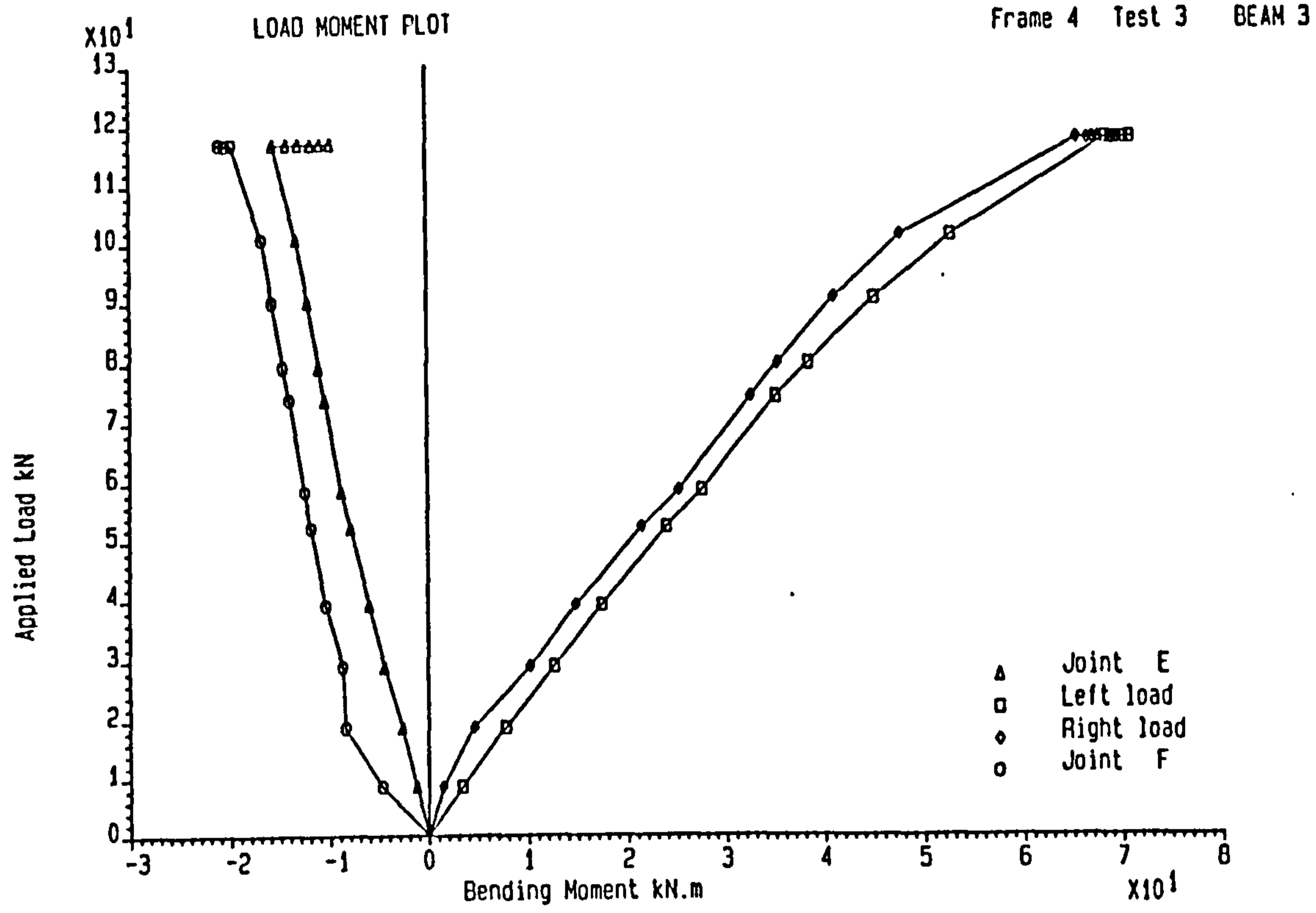


Figure 6.30 : Total Applied Load against Bending Moment on Beam 3 in Test 3 of Frame 4

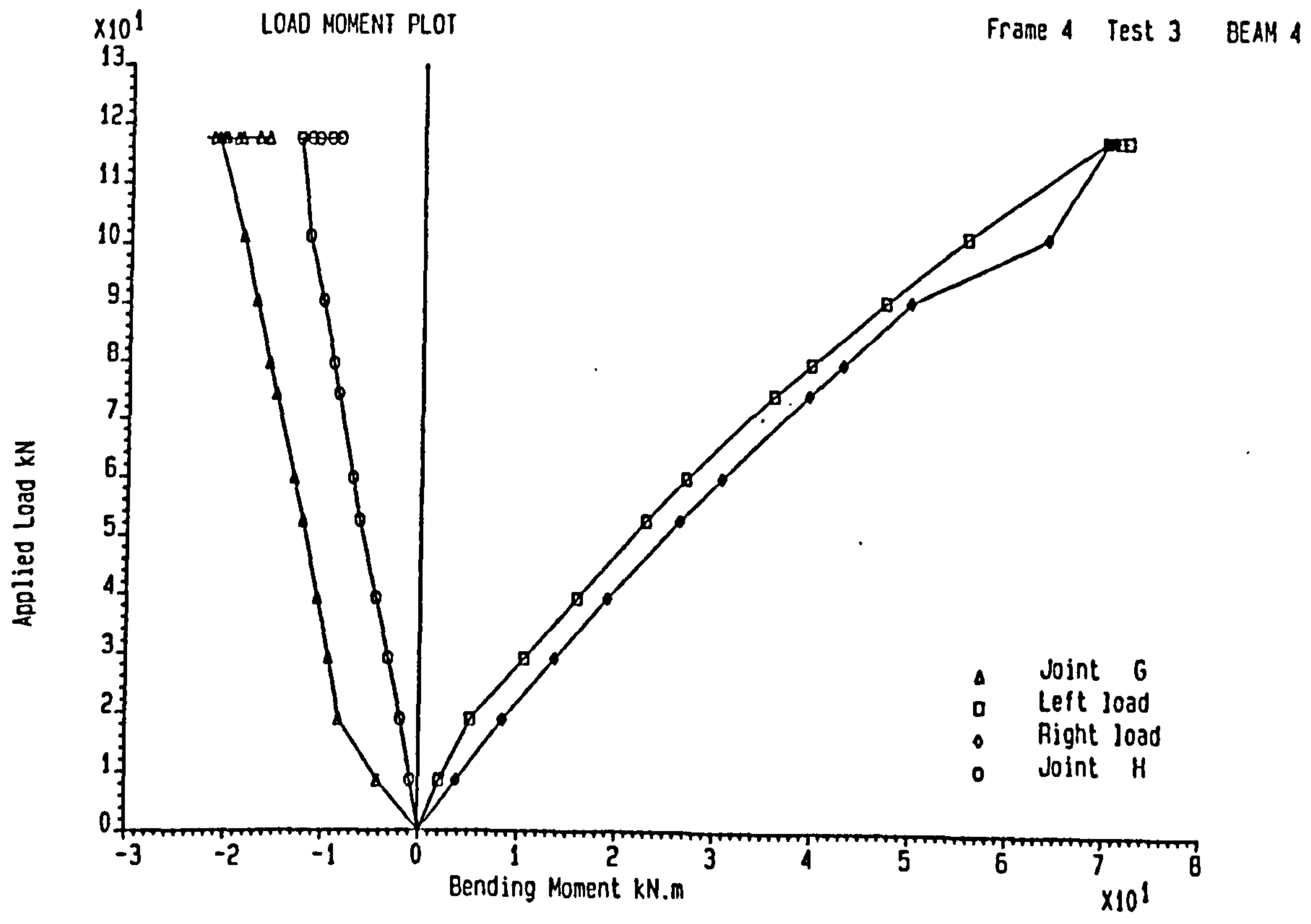


Figure 6.31 : Total Applied Load against Bending Moment on Beam 4 in Test 3 of Frame 4

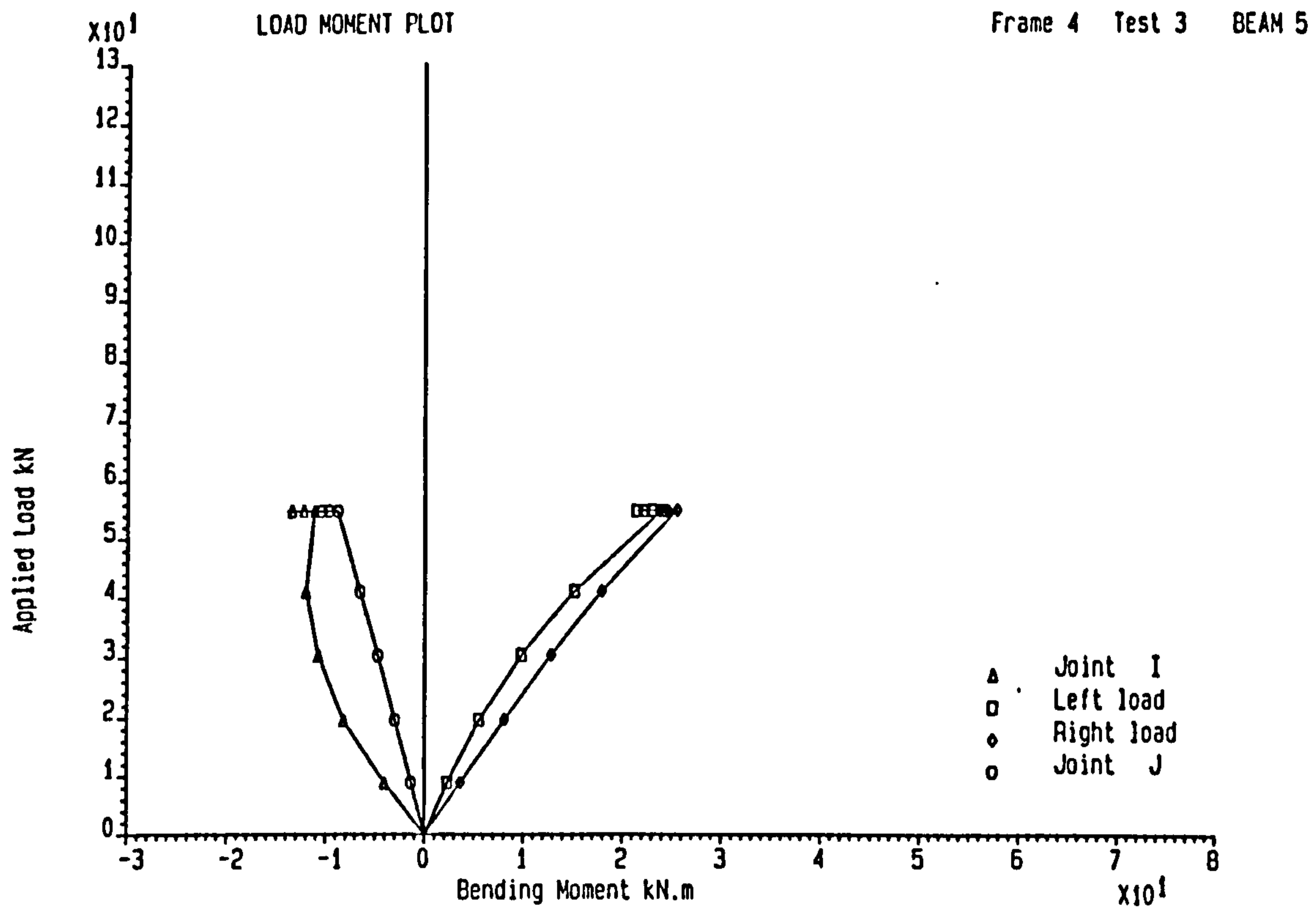


Figure 6.32 : Total Applied Load against Bending Moment on Beam 5 in Test 3 of Frame 4

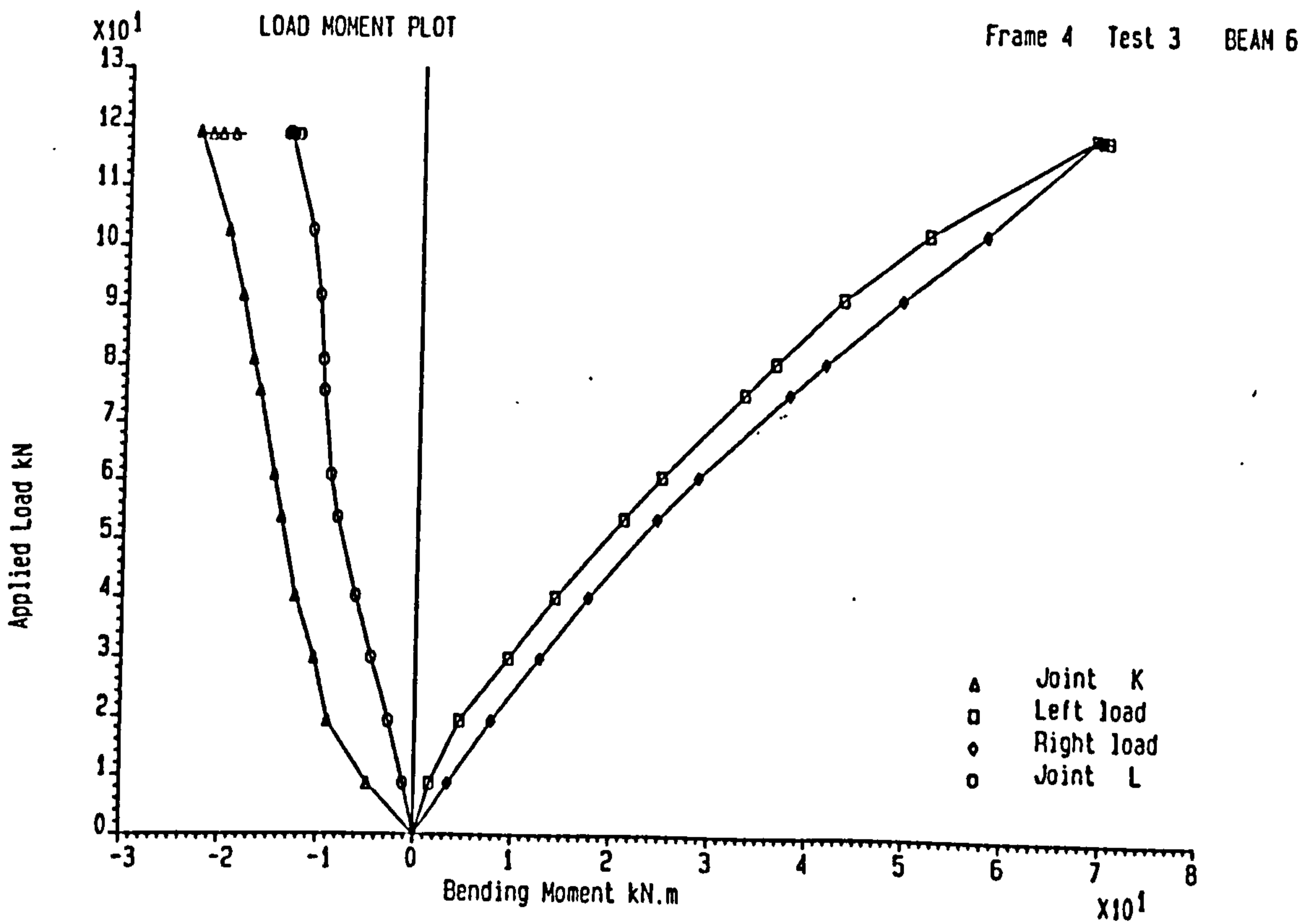


Figure 6.33 : Total Applied Load against Bending Moment on Beam 6 in Test 3 of Frame 4

Bending Moment kN.m

Frame 4 Test 3BEAM 3

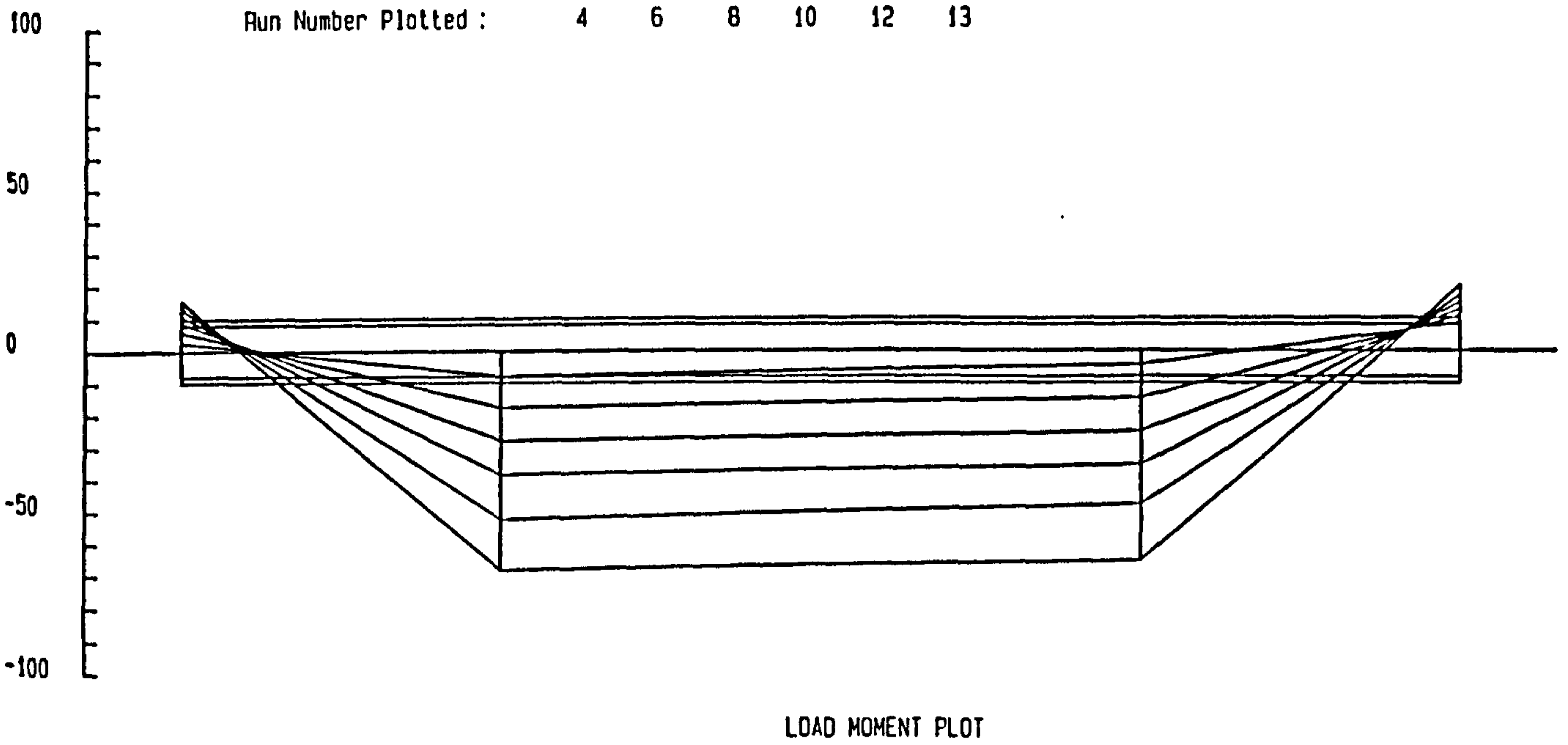


Figure 6.34 : Bending Moment Distribution around Beam 3 in Test 3 of Frame 4 up to End of Beam Load

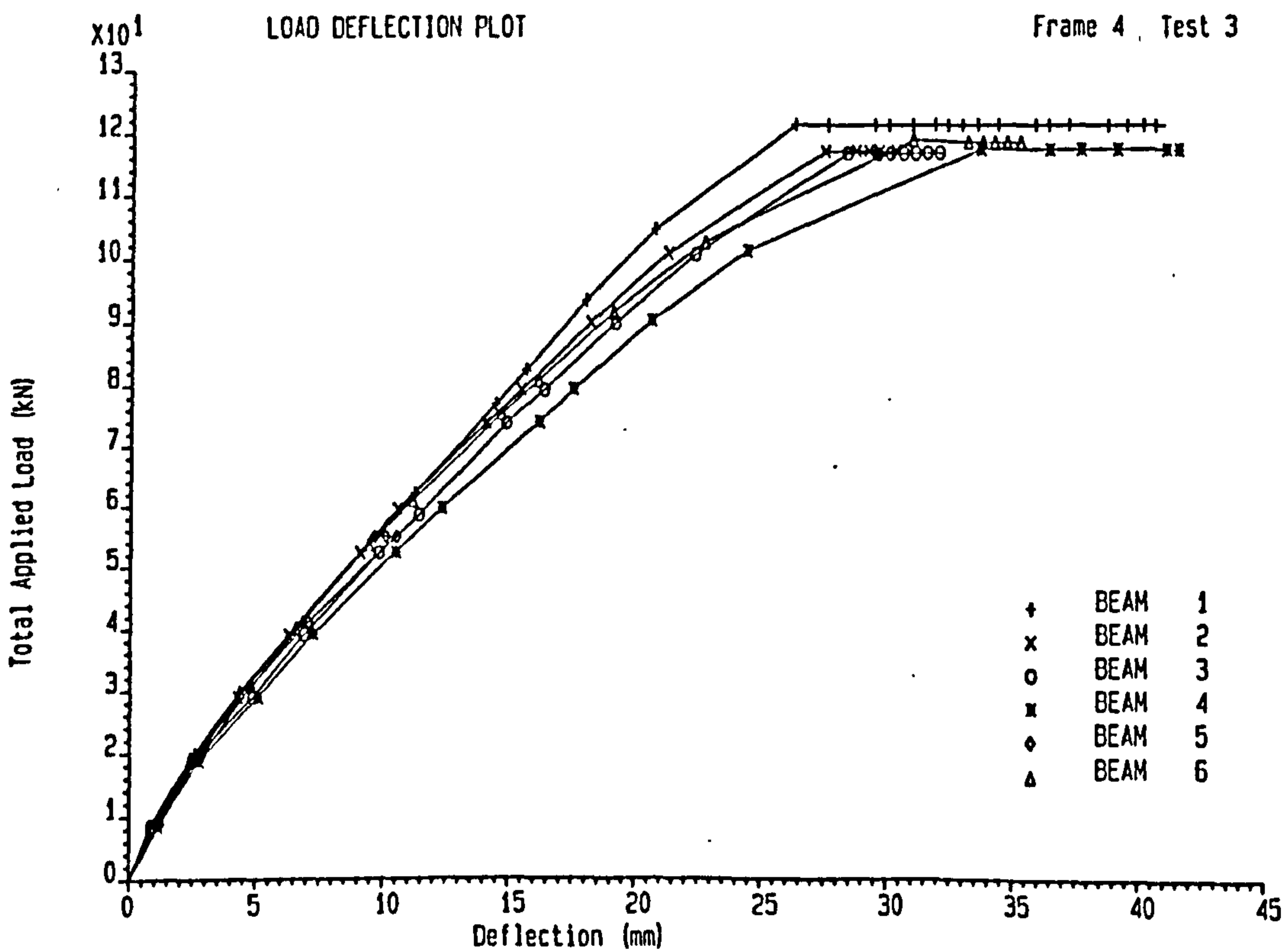
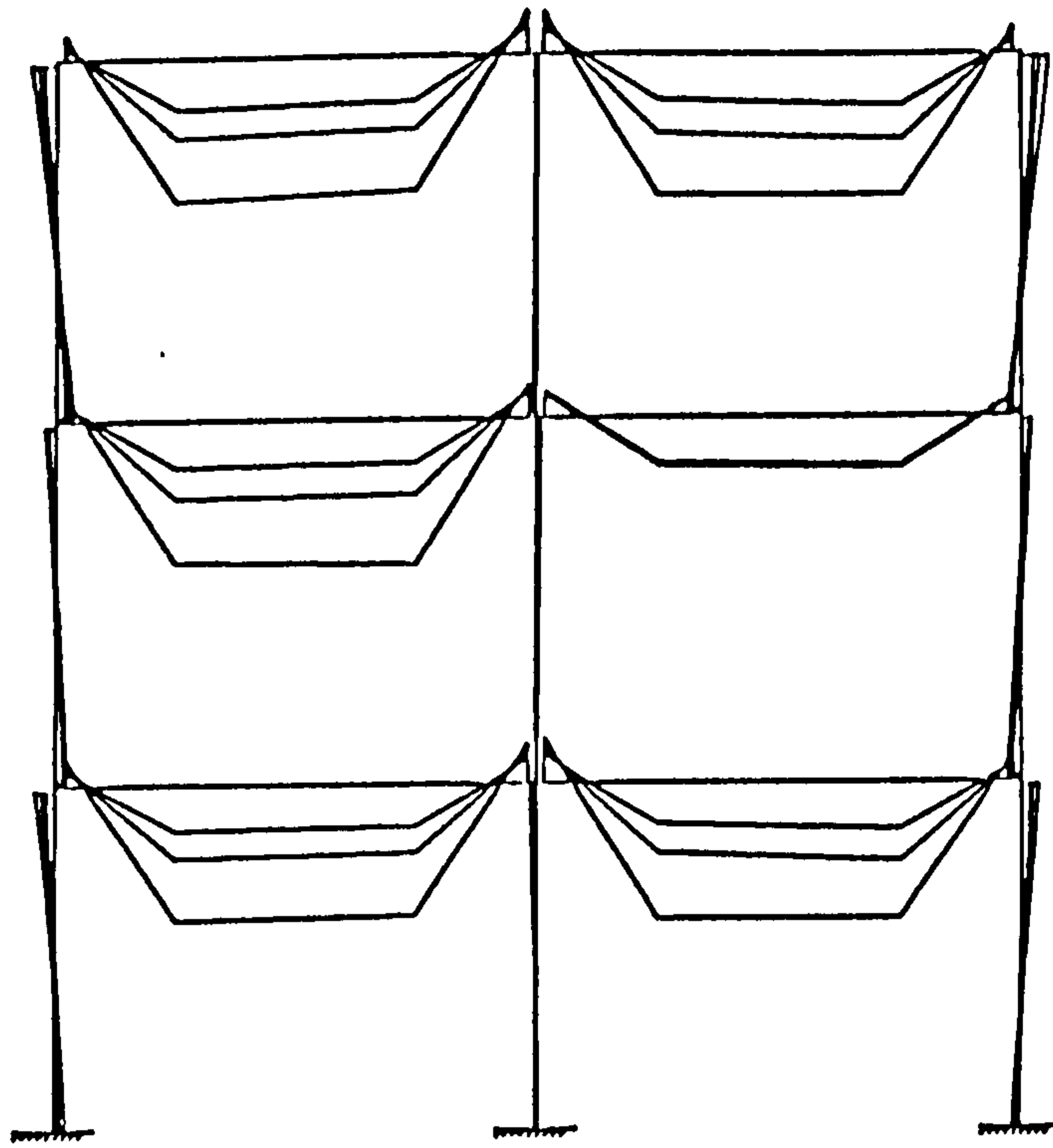
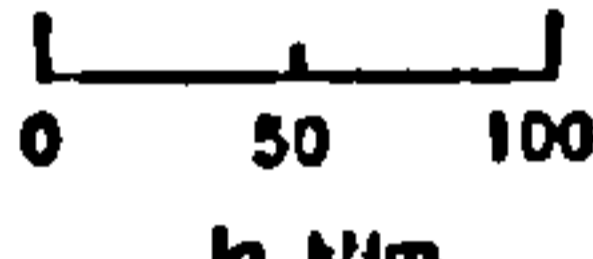


Figure 6.35 : Total Applied Load against Mid-Span Deflection on Six Beams in Test 3 of Frame 4

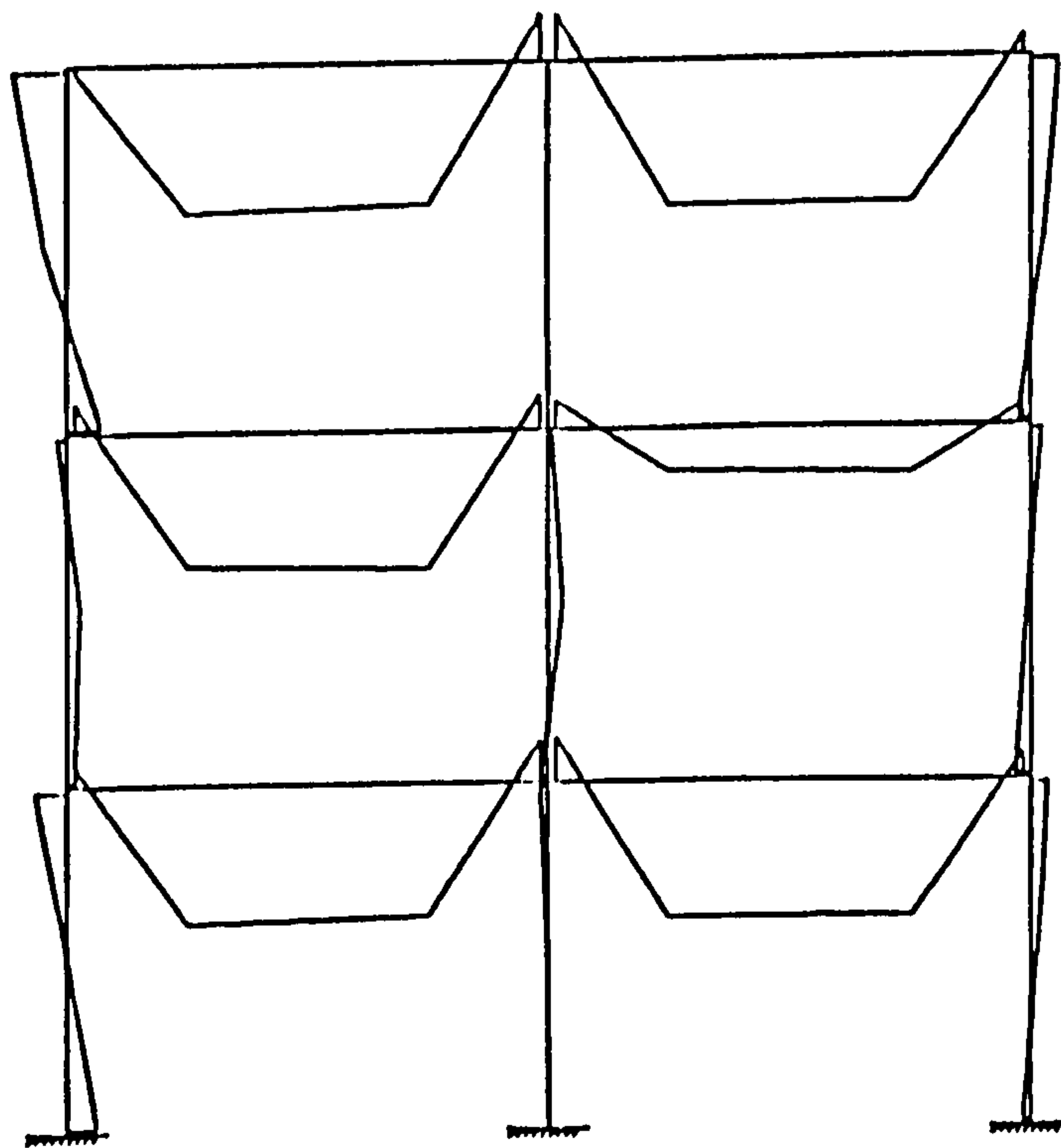


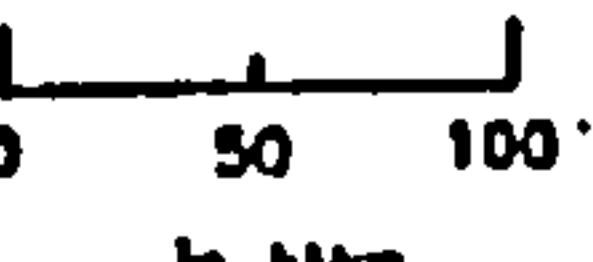
Scale :  0 50 100  
In kNm

Frame 4 Test 3

Run Numbers Plotted : 7 10 16

Figure 6.36 : Frame Moment around the Frame in Test 3 of Frame 4 up to End of Beam Load

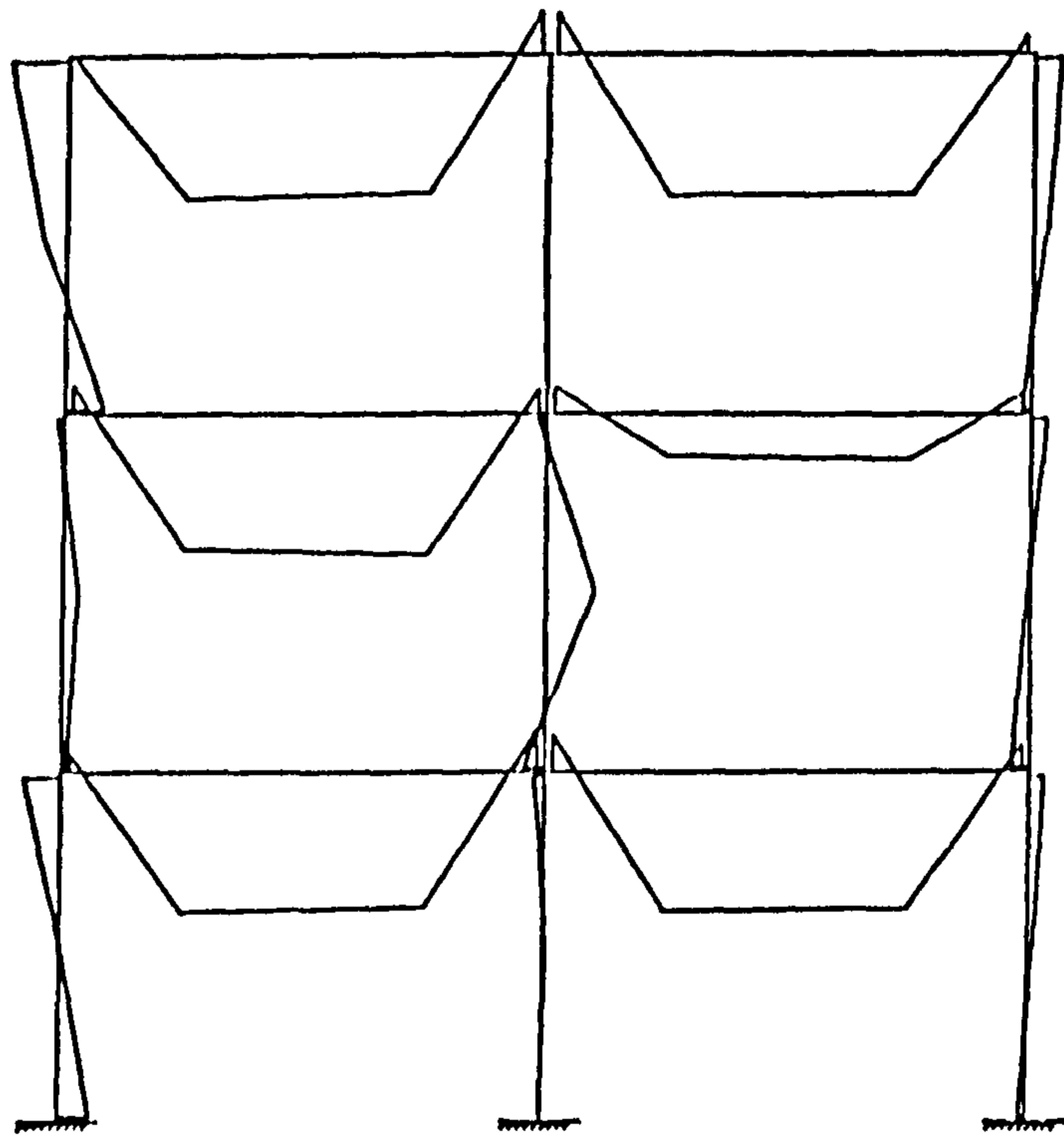


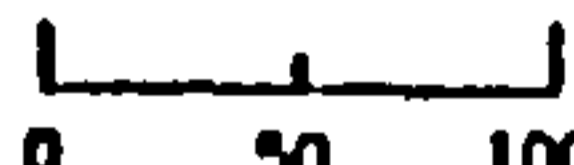
Scale :  0 50 100  
In kNm

Frame 4 . Test 3

Run Numbers Plotted : 33

Figure 6.37 : Frame Moment around the Frame in Test 3 of Frame 4 in Failure of the Edge Column in Position 1

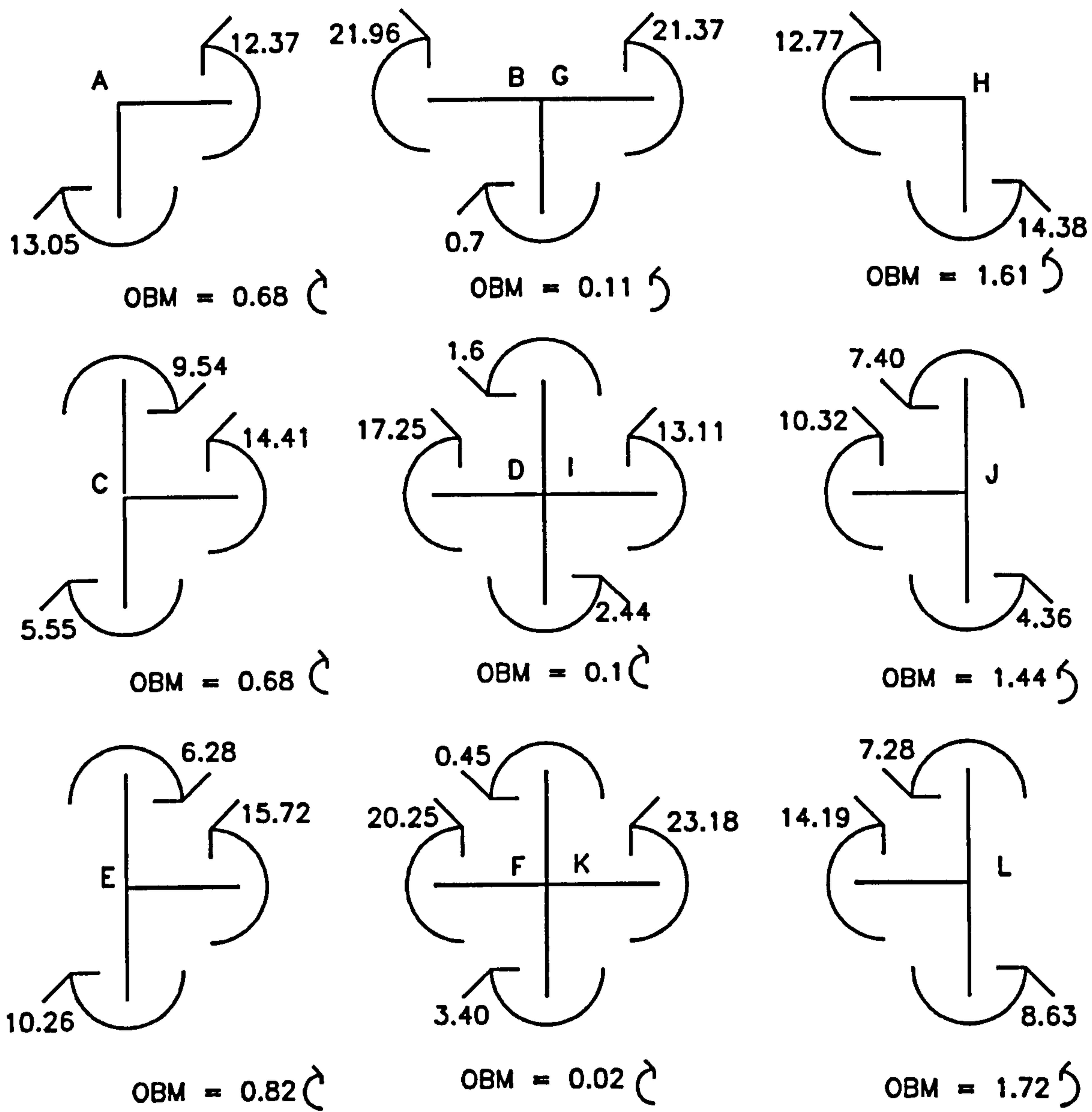


Scale :   
in kNm

Run Numbers Plotted : 43

Frame 4 Test 3

**Figure 6.38 : Frame Moment around the Frame in Test 3 of Frame 4  
in Failure of the Central Column in Position 2**



OBM = Out of balance moment

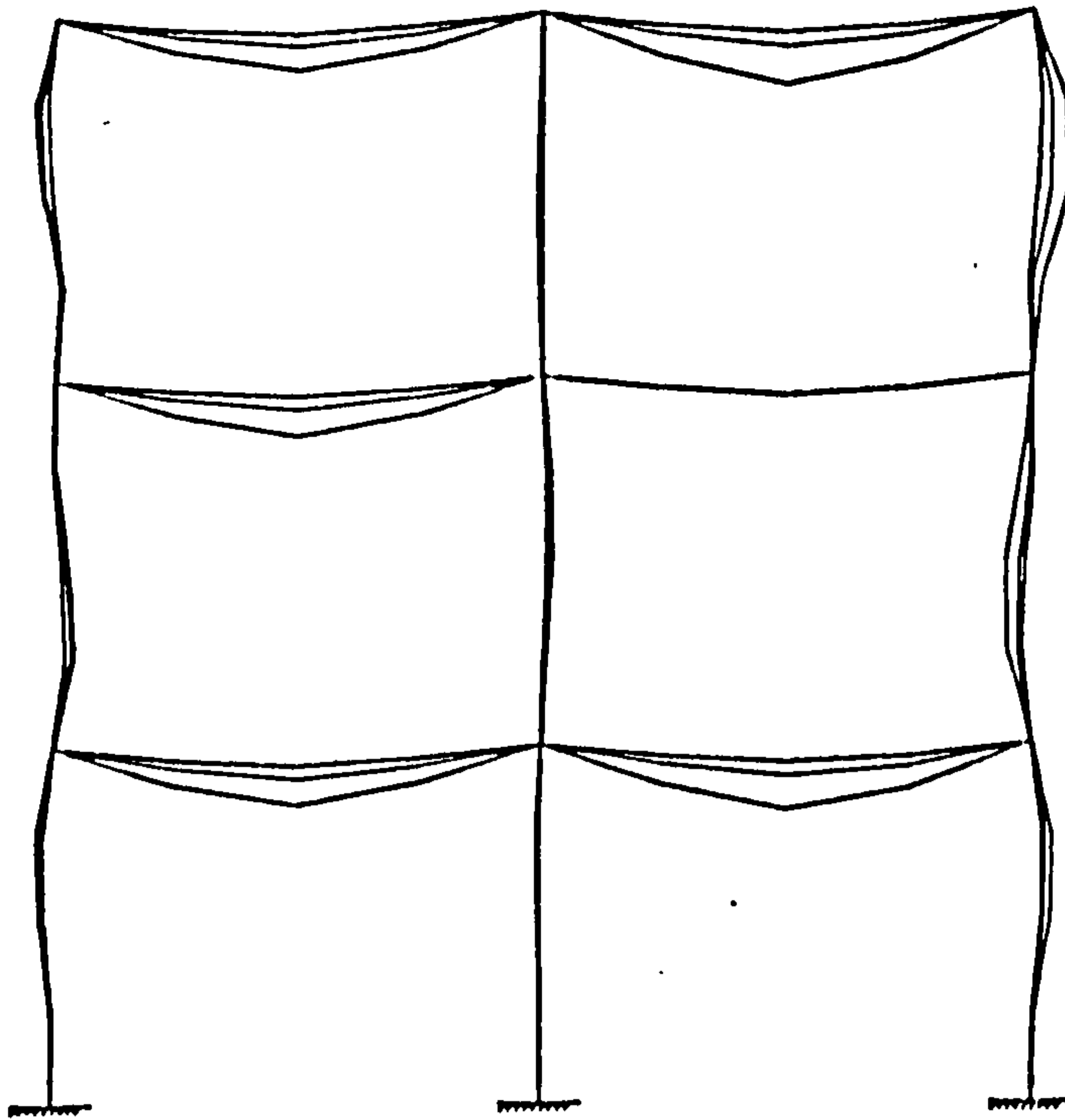
All values in kN.m units

FRAME 4

TEST 3

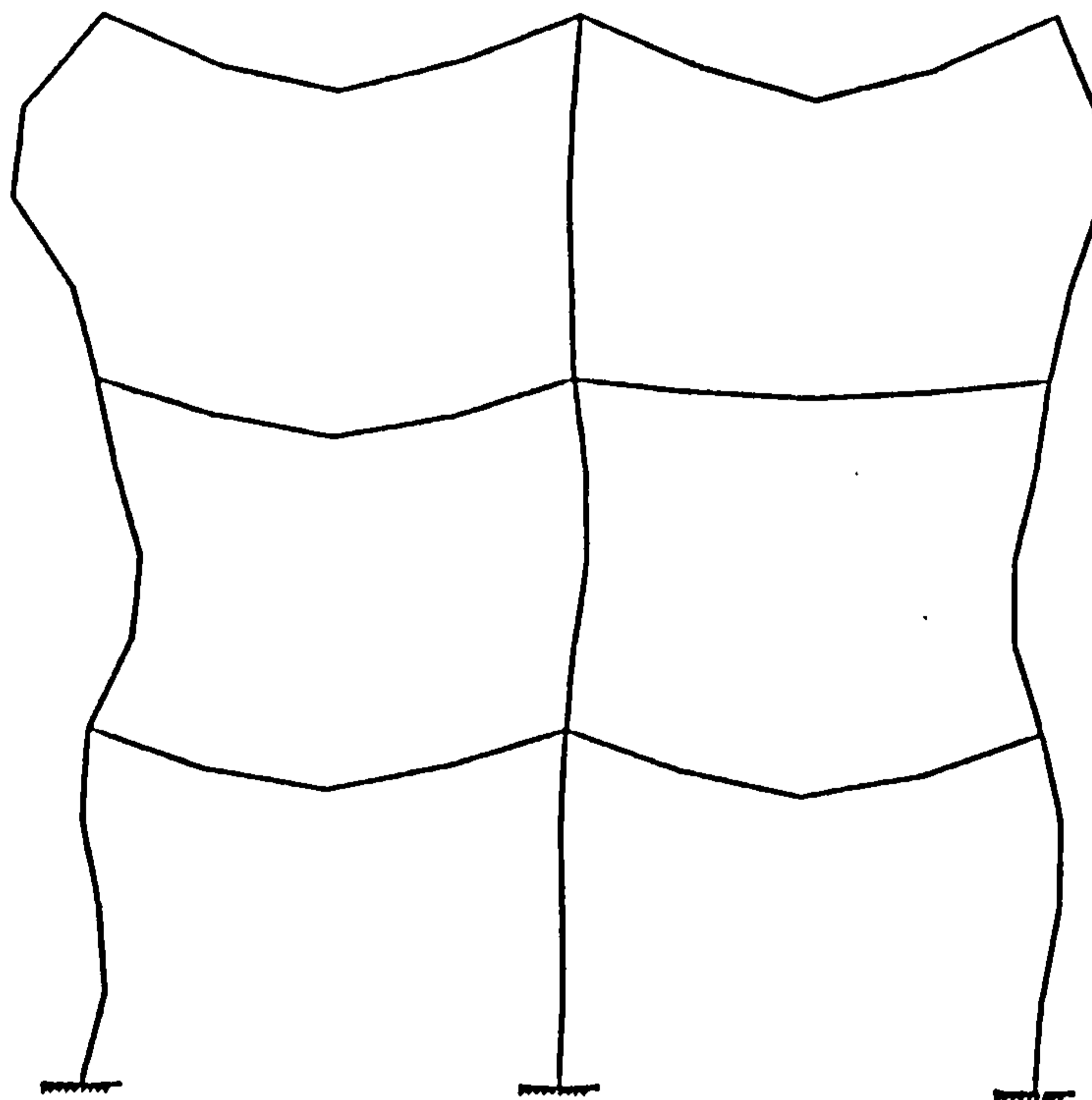
SCAN 16

Figure 6.39 : Moment Equilibrium Check in Frame 4 Test 3



Horizontal deflections 0 | 12.5 | 25  
 Vertical deflections 0 | 50 | 100 in mm  
 Run Numbers Plotted : 7 10 16  
 Frame 4 Test 3

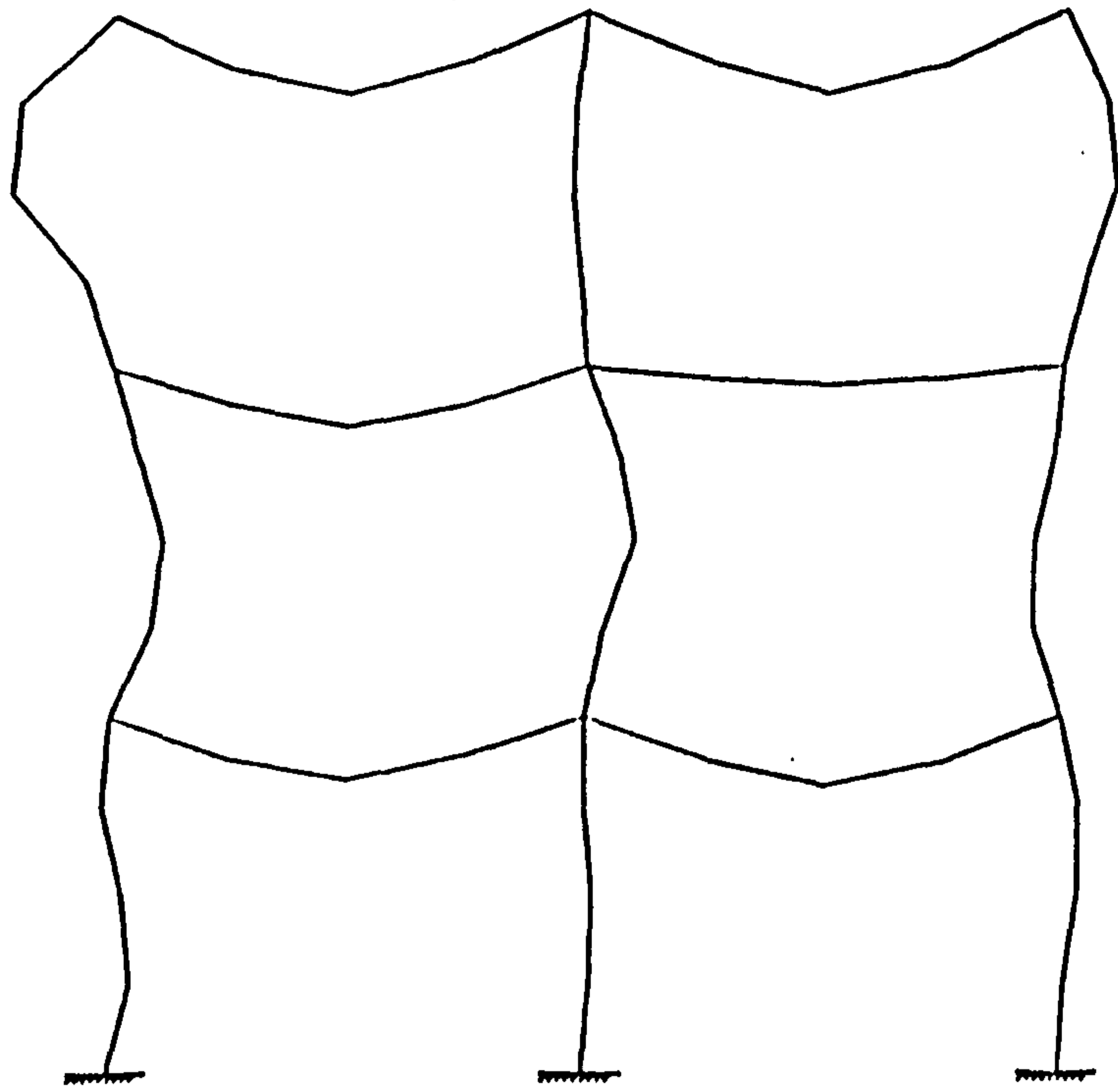
Figure 6.40 : Frame Deformation around the Frame in Test 3 of Frame 4 up to End of the Beam Load



Horizontal deflections 0 | 12.5 | 25  
 Vertical deflections 0 | 50 | 100 in mm  
 Run Numbers Plotted : 33  
 Frame 4 Test 3

Figure 6.41 : Frame Deformation around the Frame in Test 3 of Frame 4 in Failure of the Edge Column in Position 1





Horizontal deflections 0 | 12.5 | 25  
Vertical deflections 0 | 50 | 100 in mm Frame 4 Test 3  
Run Numbers Plotted : 43

Figure 6.42 : Frame Deformation around the Frame in Test 3 of Frame 4  
in Failure of the Central Column in Position 2

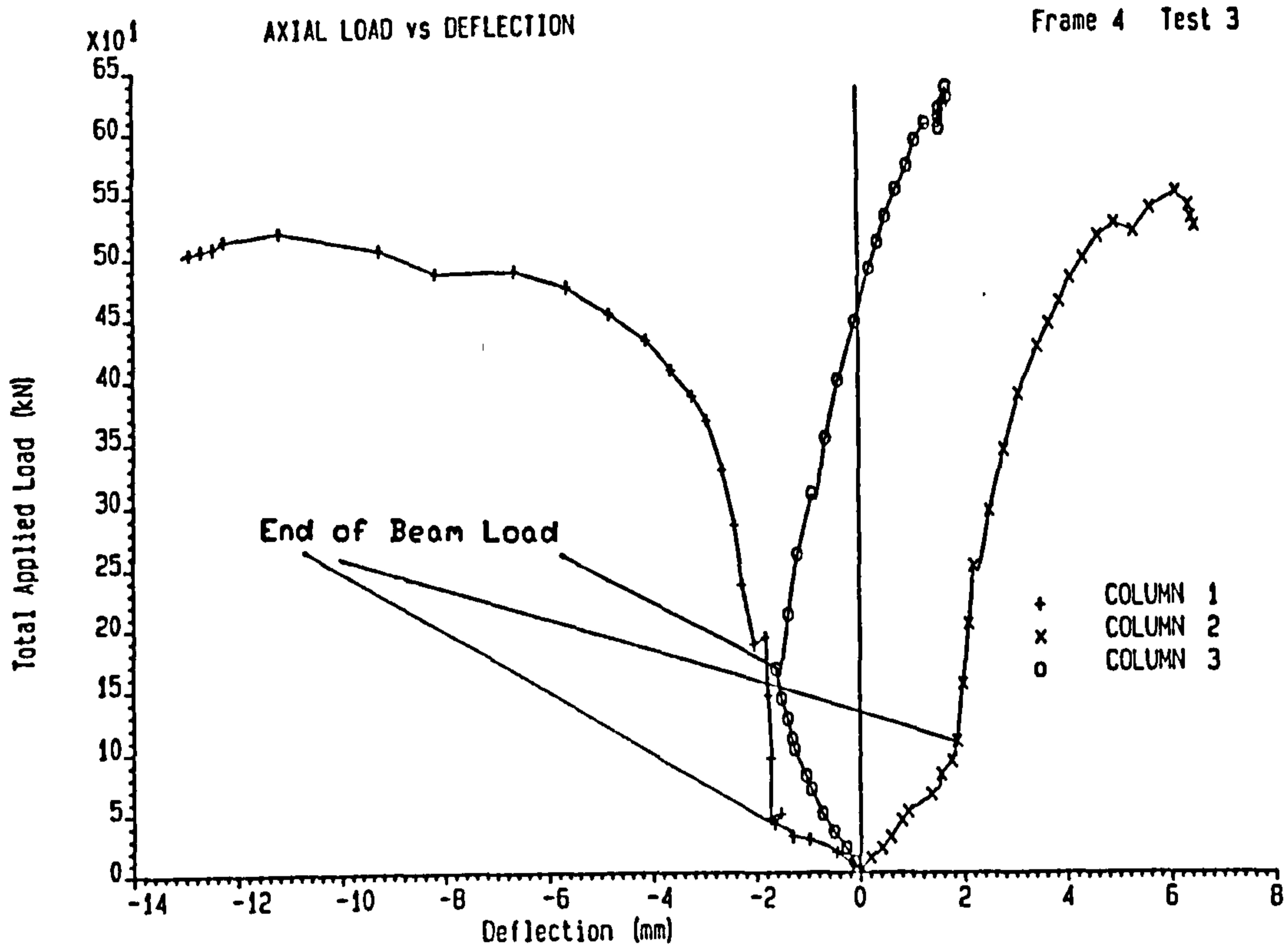


Figure 6.43 : Total Axial Load against the Mid-Height Deflection at Three Lifts of the Edge Column (Position 1) in Test 3 of Frame 4

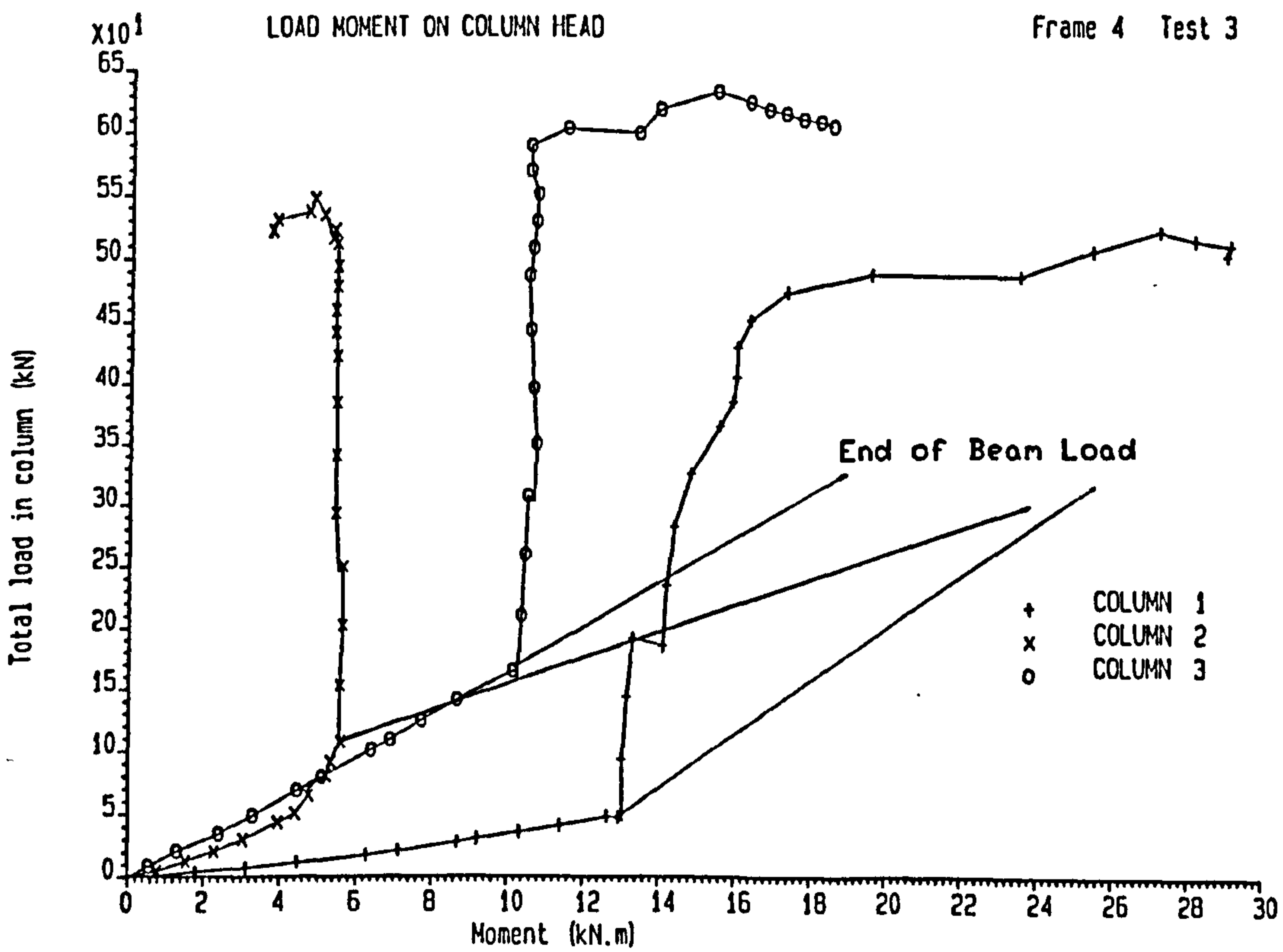


Figure 6.44 : Total Axial Load against the Column Head Moments at Three Lifts of the Edge Column (Position 1) in Test 3 of Frame 4

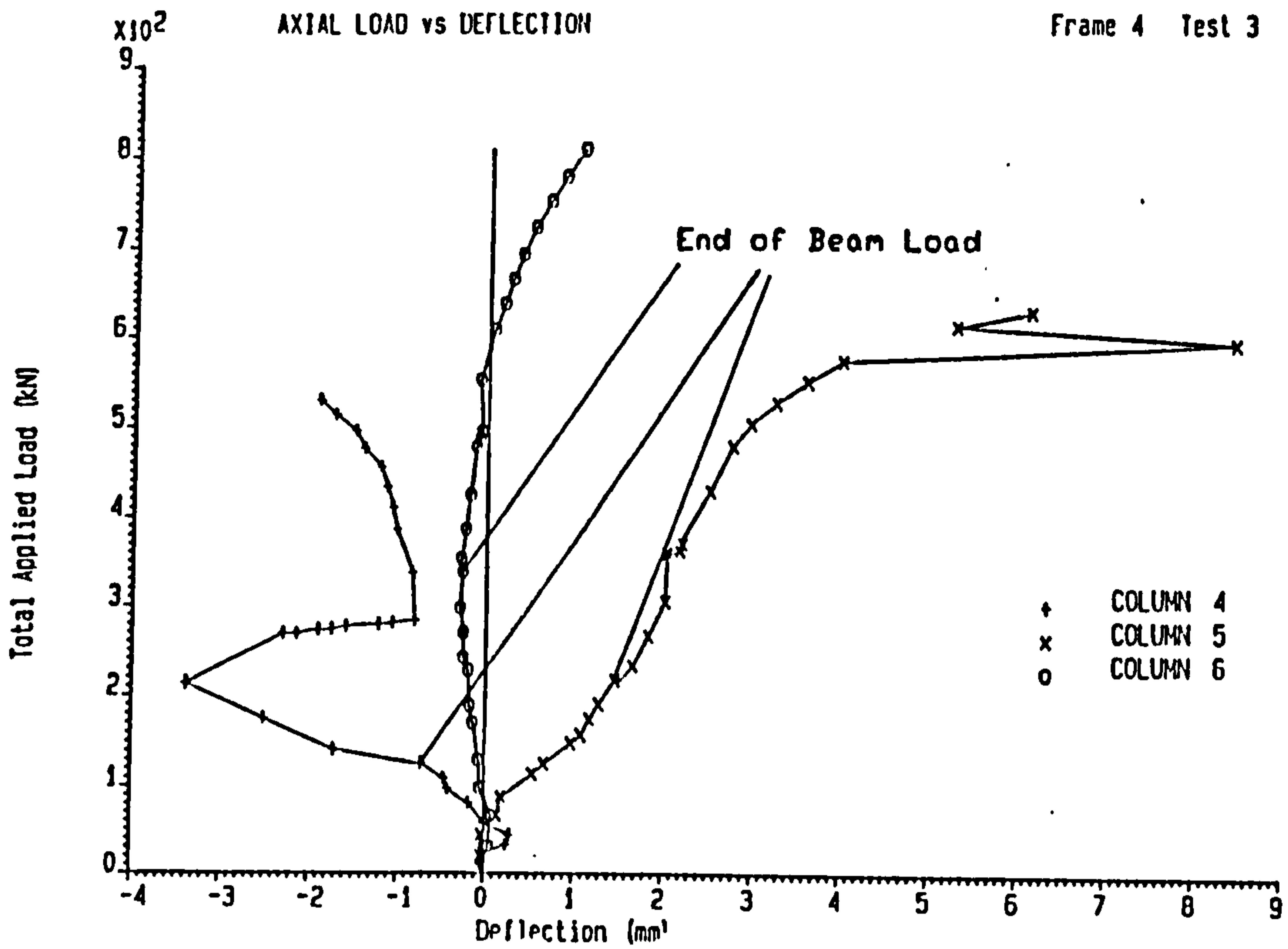


Figure 6.45 : Total Axial Load against the Mid-Height Deflection at Three Lifts of the Central Column (Position 2) in Test 3 of Frame 4

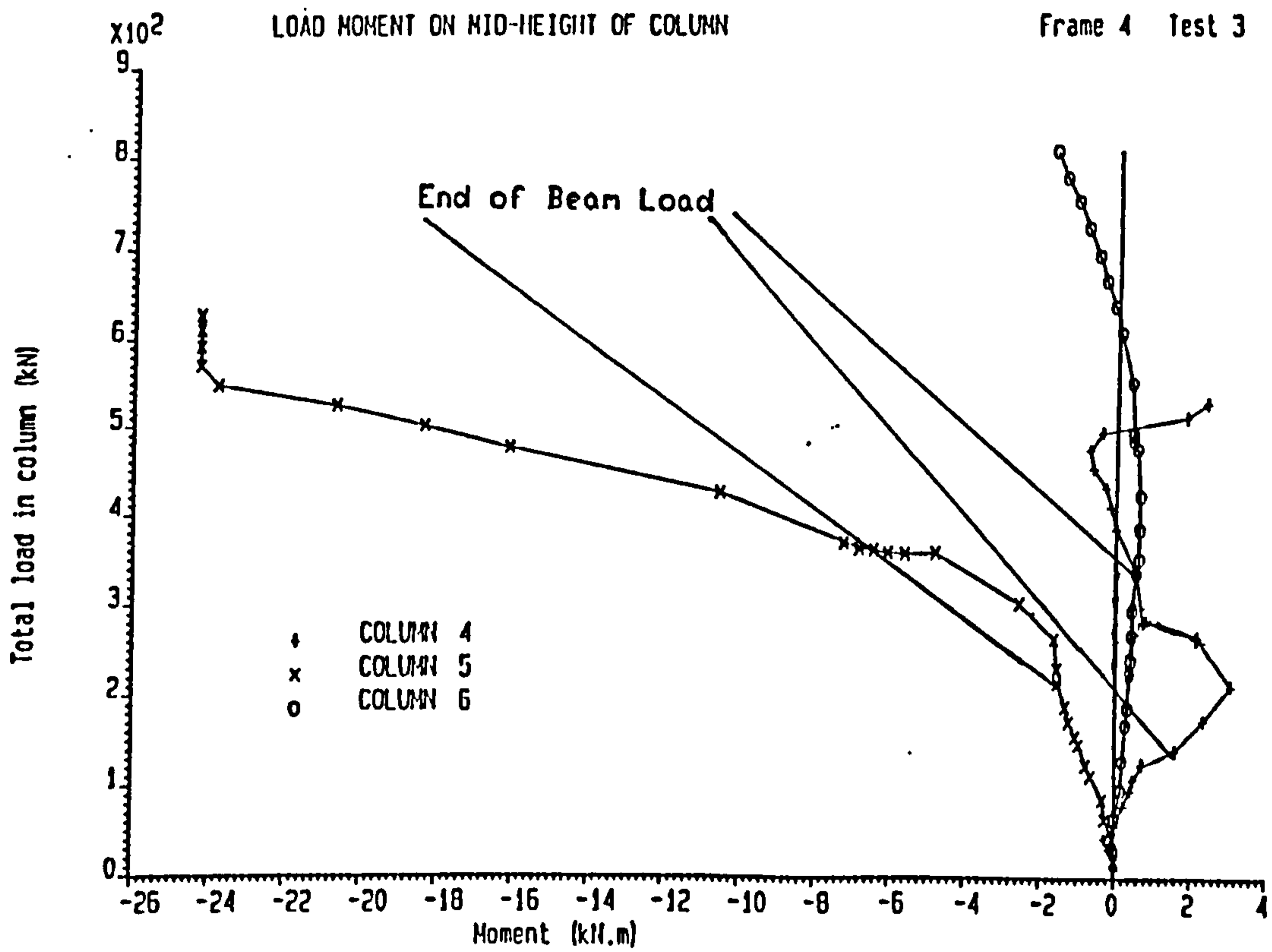


Figure 6.46 : Total Axial Load against the Mid-Height Column Moments at Three Lifts of the Central Column (Position 2) in Test 3 of Frame 4

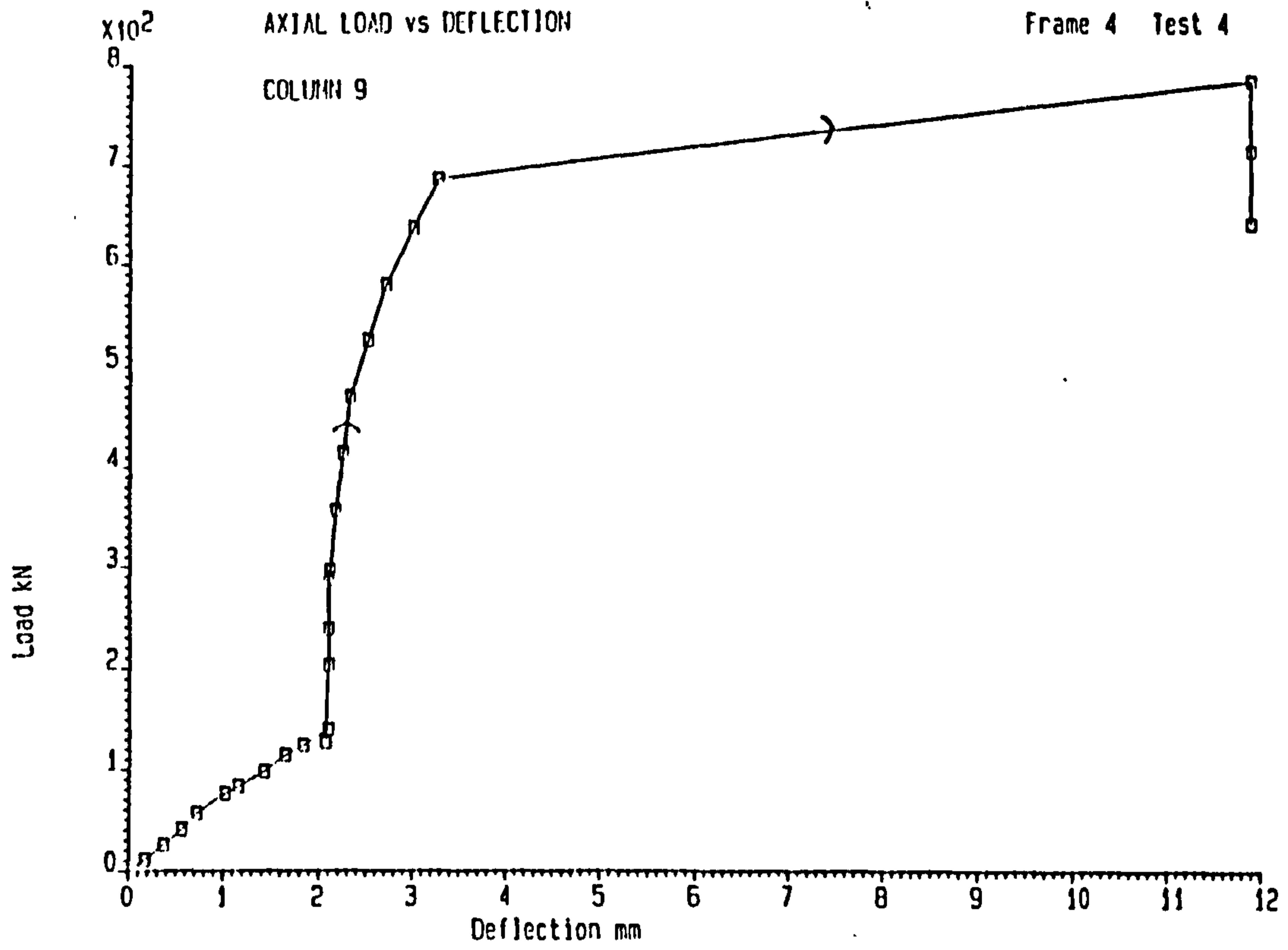


Figure 6.47 : Total Axial Load against the Mid-Height Deflection at Column 9 of the Edge Column (Position 3) in Test 4 of Frame 4

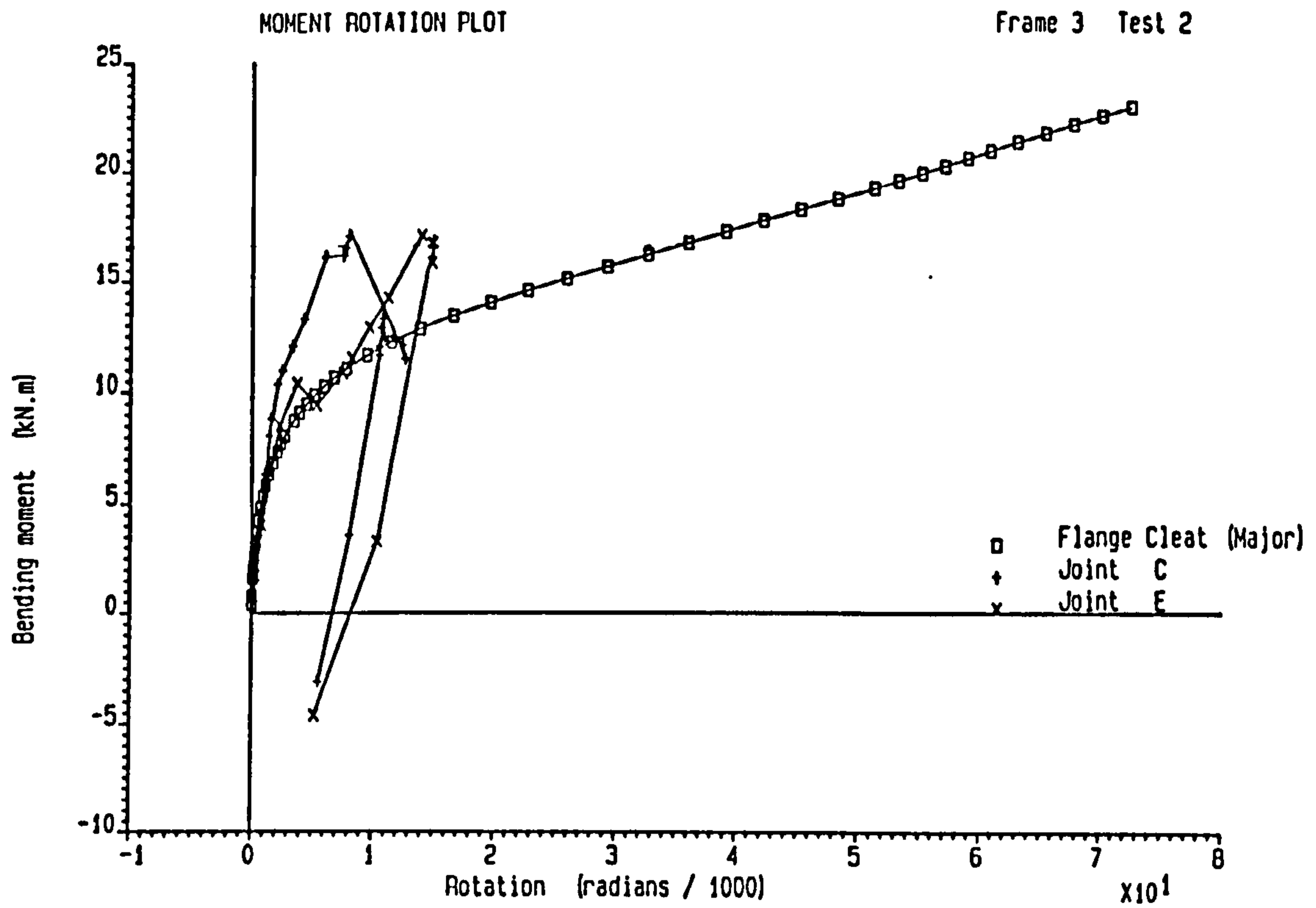


Figure 6.48 : Moment Rotation Curve for Test 2 of Frame 3  
(External Joints C and E)

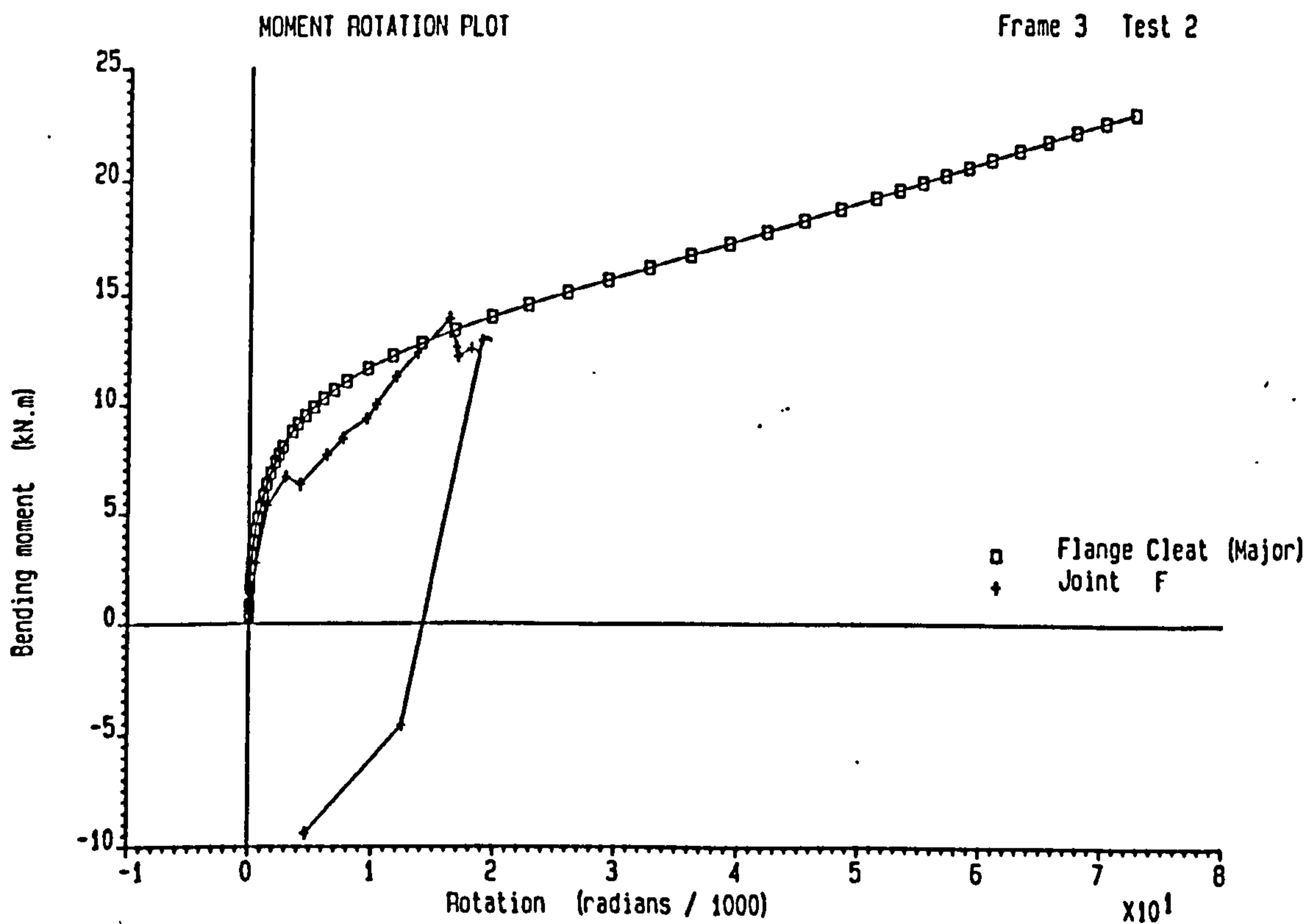


Figure 6.49 : Moment Rotation Curve for Test 2 of Frame 3  
(Internal Joint F)

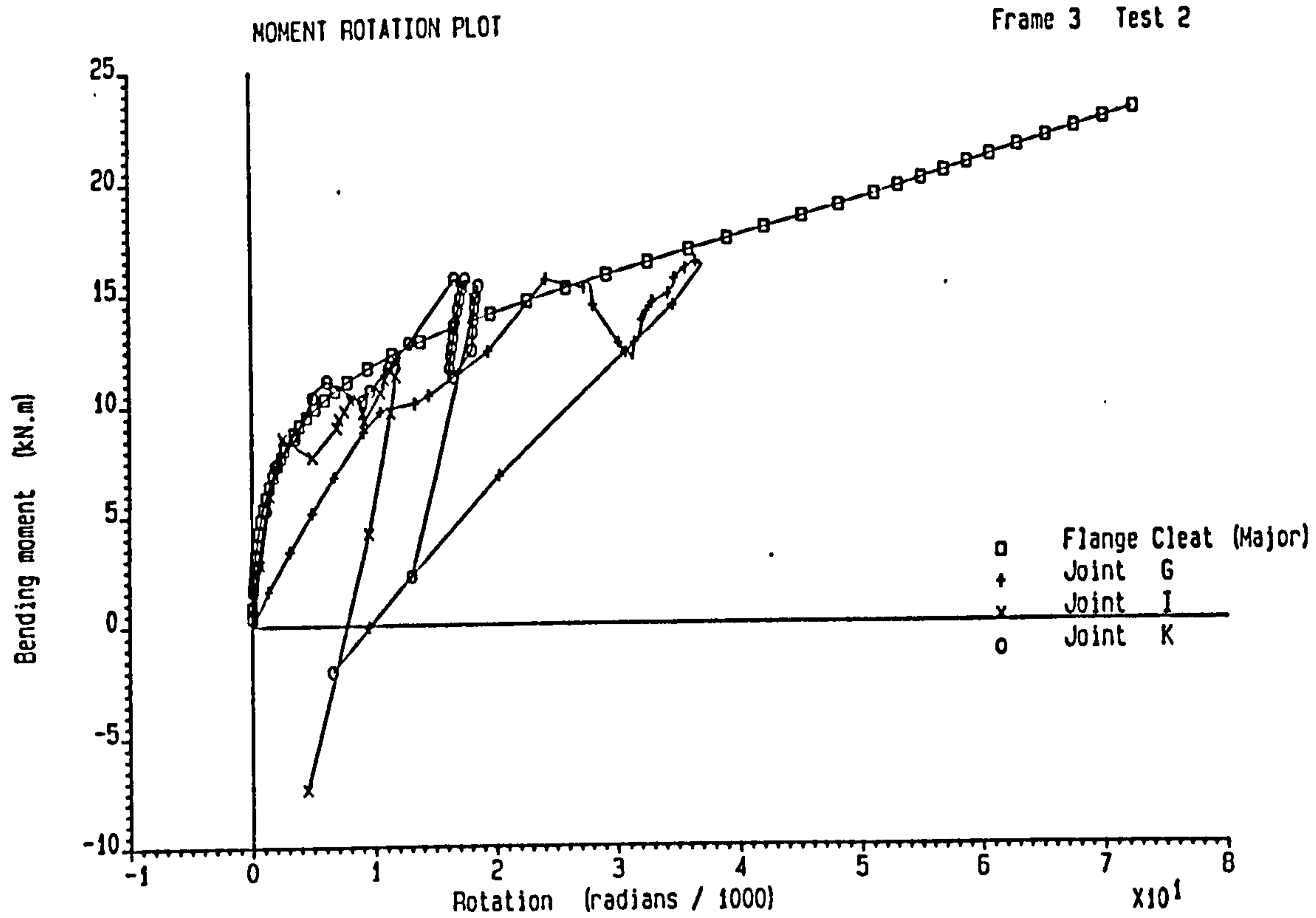


Figure 6.50 : Moment Rotation Curve for Test 2 of Frame 3  
(Internal Joints G, I and K)

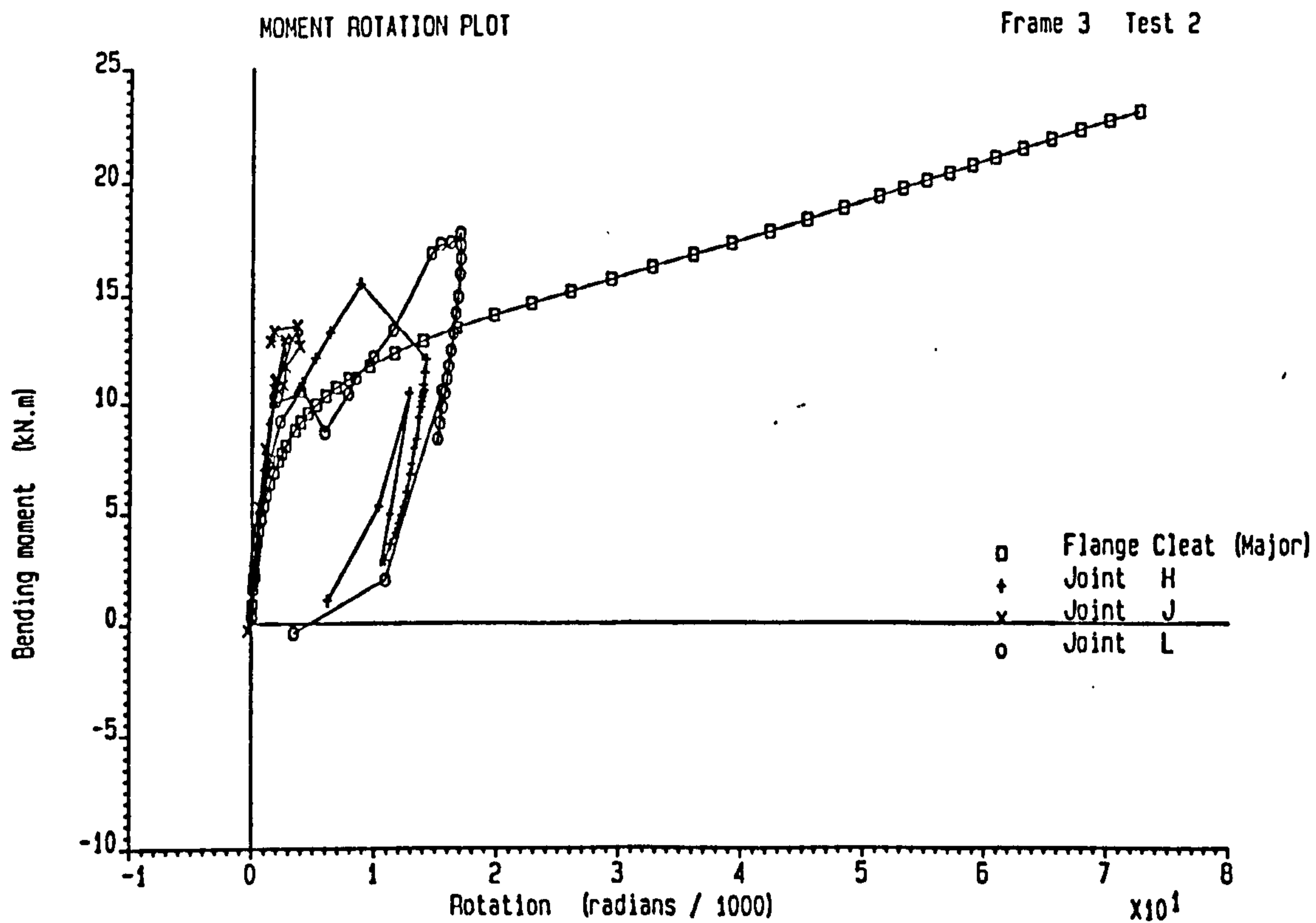
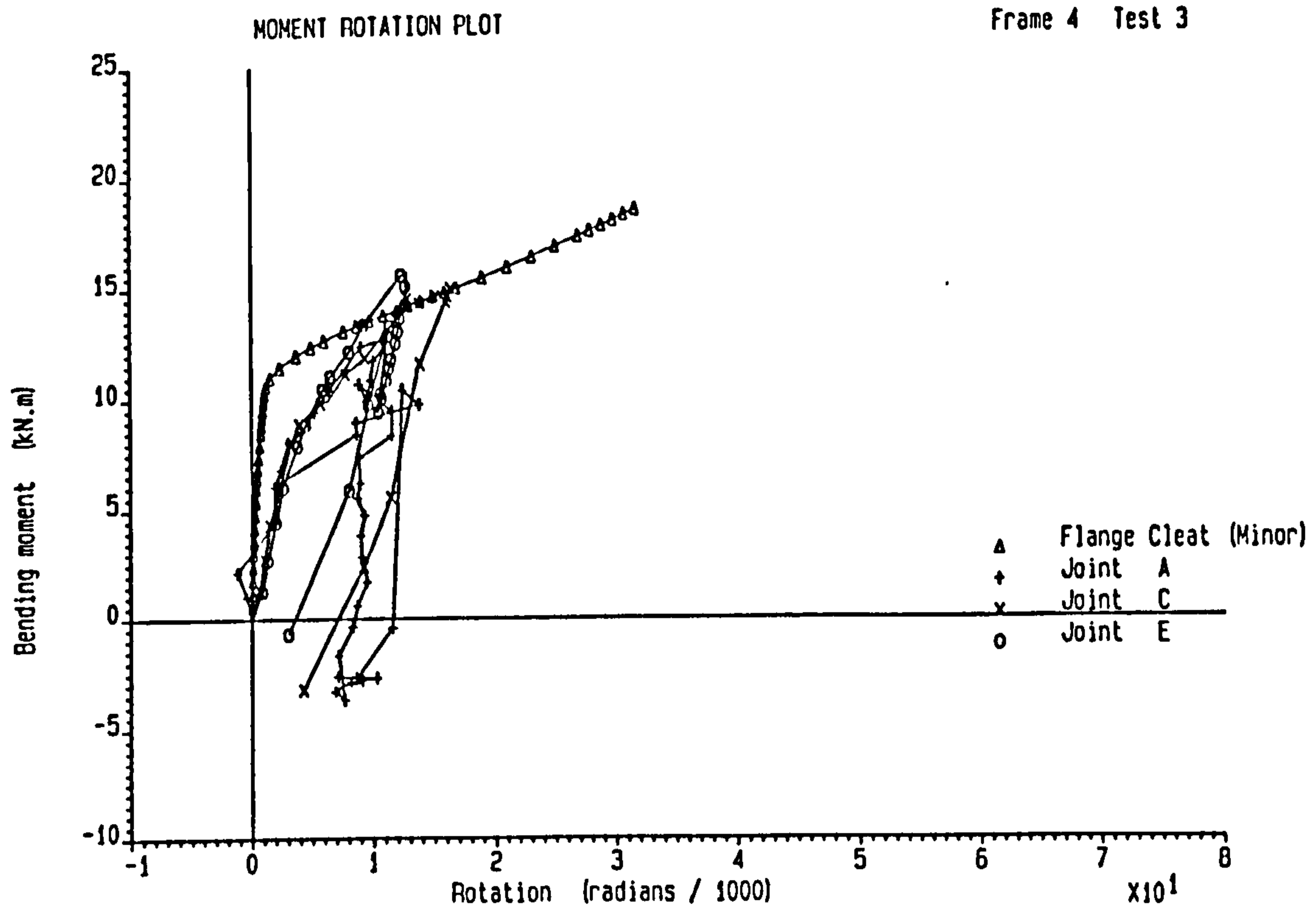
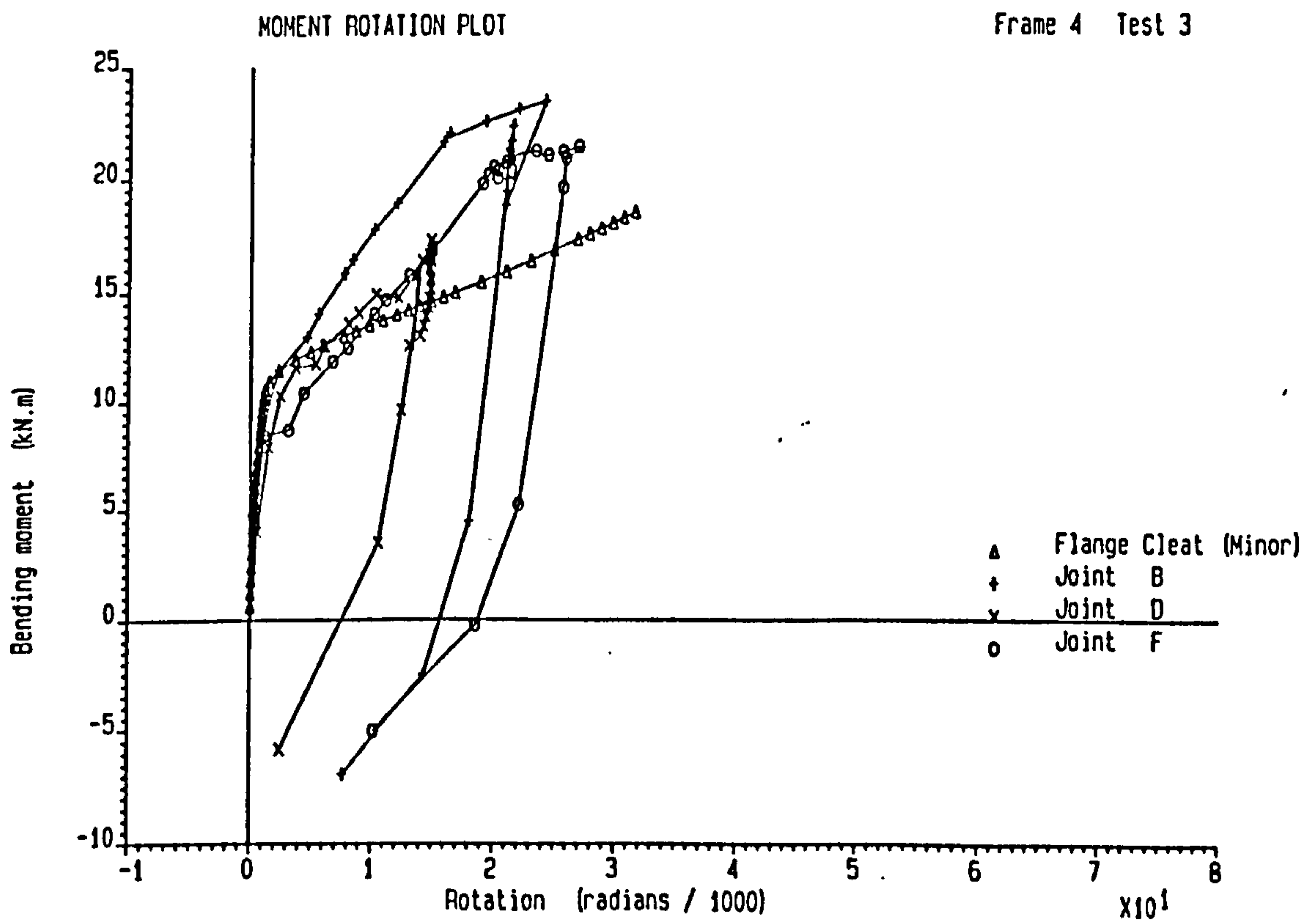


Figure 6.51 : Moment Rotation Curve for Test 2 of Frame 3  
(External Joints H, J and L)



**Figure 6.52 : Moment Rotation Curve for Test 3 of Frame 4  
(External Joints A, C and E)**



**Figure 6.53 : Moment Rotation Curve for Test 3 of Frame 4  
(Internal Joints B, D and F)**

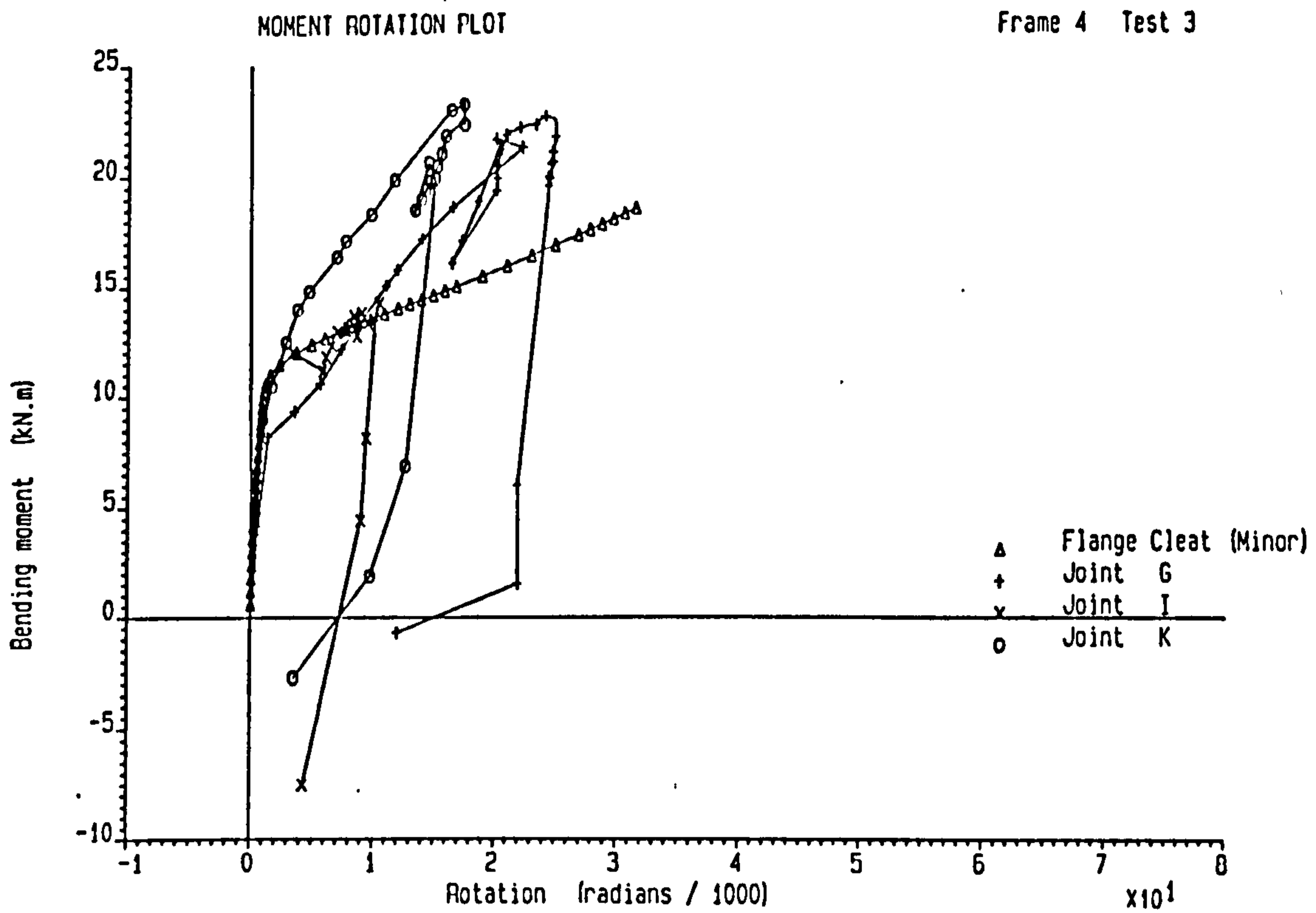


Figure 6.54 : Moment Rotation Curve for Test 3 of Frame 4  
(Internal Joints G, I and K)

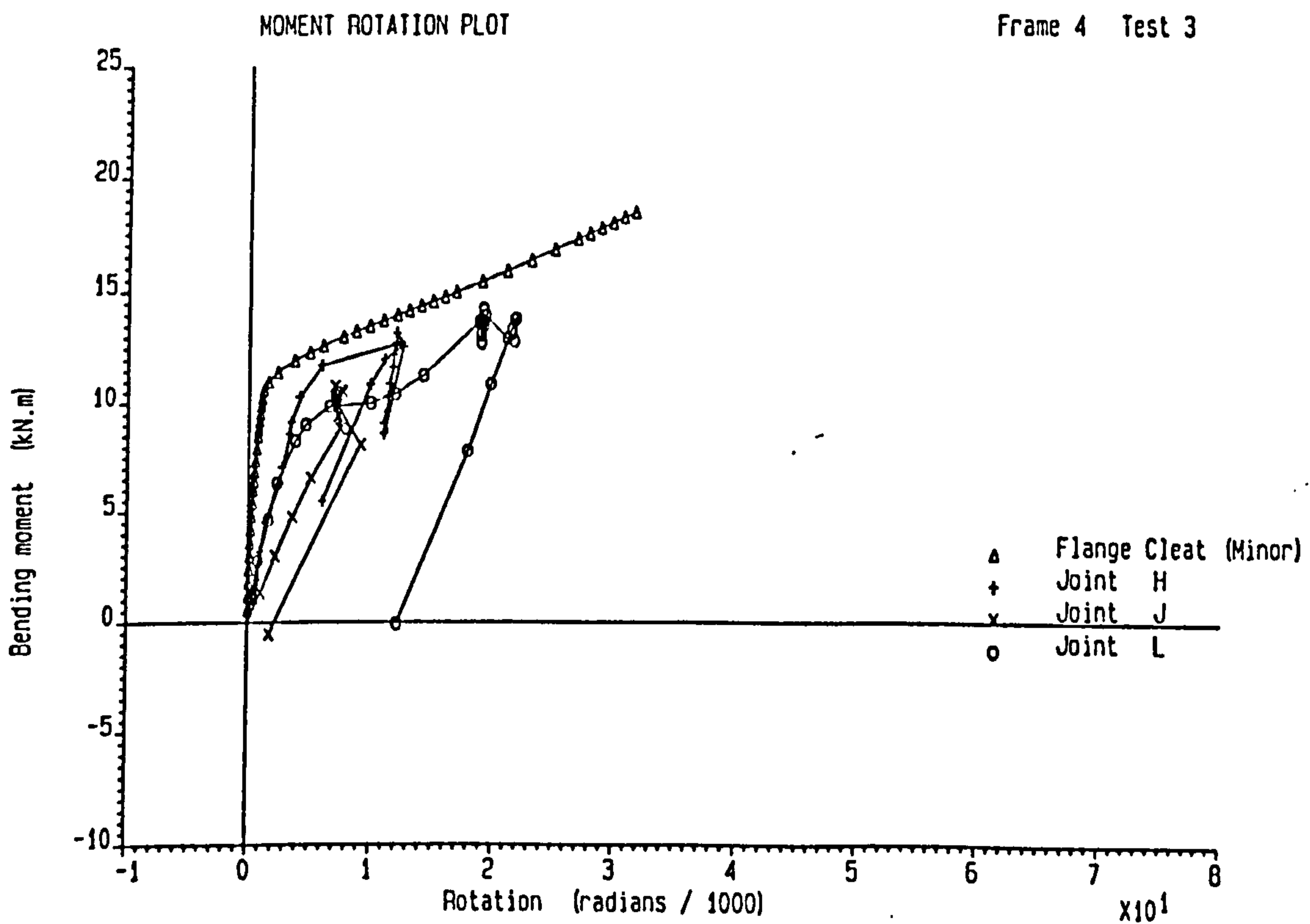


Figure 6.55 : Moment Rotation Curve for Test 3 of Frame 4  
(External Joints H, J and L)



## Chapter 7

# Behaviour of a Symmetrical Frame with End-Plate Connection

### 7.1 Introduction

Frame 5 was the last of the series of full scale tests and was designed and tested by BRE [7.1]. The objective of this test was to enable the different effects of the two different sizes of beams and end-plate connections on the behaviour of the structure to be investigated. The frame is introduced and the test set up described. After the loading tests are discussed, the test to failure are analysed in detail and the total axial resistance in the columns are compared Design Code predictions.

### 7.2 Test Configuration

Frame 5, shown in Figure 7.1, was a three storey structure of approximate overall dimension 10 m wide x 11 m high. Figure 7.2 shows the general arrangement of this frame and identifies the joint nomenclature.

The frame was constructed using 152 x 152 UC 37 sections for the columns. Each column has a 554 mm upstand, which facilitates load application through a jacking system. The thickness of capping plate was 10 mm. Two sizes of beams are adopted for each bay - 254 x 146 UB 37 sections for the beams in the left hand bay and 254 x 102 UB 28 sections for the beams in the right hand bay (as viewed in Figure 7.2). The reason for using beams of different sections for each bay was to enable them to be designed for a different load level and thus alternative connections could be adopted. The larger section beams were then

designed to have flush end-plate connections (joint A to F) whilst the smaller section of beams were designed with extended end-plate connections (joints G to L). Details of the connections used are shown in Figure 7.3. All the columns had a fixed base detail with heavy base plates bolted to the laboratory floor through the existing grid of holes spaced at 381 mm centres.

As in the two Sheffield frames [7.2], frame 5 had no stiffeners in the column. The frame was tested in-plane and in a non-sway condition using the bracing system as for frames 1 to 4. In common with the other frames tested, stiffeners were used at the loading points in all beams in order to prevent web buckling due to applied loads. The load configuration of the previous frames was again adopted for frame 5.

Each beam was loaded at its quarter and three-quarter points using the loading system similar to that described in the chapter 4. A pattern of beam load was applied in increments to a pre-determined value and column loads were then applied, by using displacement to control the hydraulic system, to fail the central column (Test 17). A detailed description of the instrumentation is recorded in the reference [7.3] and also presented in chapter 4.

### **7.3 Tests for Frame 5**

A total of 14 tests were conducted on this frame and Table 7.1 gives a simple description of each individual test. The tests on this frame can be divided into 3 stages.

#### **1. Stage 1 : Preliminary Testing**

Low loads (below 10 kN) were applied to each beam individual in order that the instrumentation and equilibrium could be checked carefully.

#### **2. Stage 2 : Loading Test**

Two series tests are included in this series. In the first series, a load of 50 kN was applied to each beam individual. In the second stage, loads of about 80 kN were applied to two beams at each storey.

#### **3. Stage 3 : Test to Failure**

Loads up to about 200 kN were applied. Column load was then applied at the head of the central column to cause the failure of the frame.

A description of the loading history for each test and the checking for each device and strain gauge is included in tabular form as presented in the progress report no.8 [7.4].

## 7.4 Loading Tests

A study of the different pattern loads, including load applied to each beam individually and load applied to all beams together, was studied in frame 2 as discussed in chapter 5. The results showed that a higher value of the mid-span deflection was recorded when loads were applied to each beam individually due to lesser restraint provided by the adjacent beam. However, the values recorded are significantly lower than those for a simply supported beam. The author has investigated in greater detail how the different pattern loads affect the behaviour of frame. Frame 5 contained a series of tests under individual beam loads, loads applied to the pair of beams at each floor level and all beams loaded together. Thus a more detailed comparison can be made together with the value computed for a simply supported beam with the same level of applied loads.

The mid-span beam deflection of a simply supported beam was computed and compared with the test results. Table 7.2 shows the mid-span deflection of beams under different pattern load conditions under total beam loads of 50 kN. It is clear from this table that the mid-span deflection recorded in the second stage of first series tests are generally slightly greater than those recorded in other pattern load tests the exception being beam 1 due to lack of the restraint by the columns extended above. This is due to reduced restraint provided by the adjacent beam when compared with other pattern loading tests. In fact, the column deformation and rotation due to loads applied to the storey above (test 17) will affect the mid-span beam deflection. However, the differences are quite small when they are compared with magnitudes of the deflections induced in each storey (the second stage of second series tests). As a result, deflection determined in the second stage of first series tests (beam loaded individually) should be considered for the beam deformation check in the serviceability limit state.

The mid-span deflection of 7.6 mm in beams 1 to 3 and 10.5 mm in beams 4 to 6 are computed from a simply supported beam with the same applied loads. It is noted in Table 7.2 that the actual values are between 4.5 to 4.9 mm for beams 1 to 3 and 4.3 to 5.7 mm for beams 4 to 6. A minimum reduction of 40 % was determined for all beams in tests. It implied that the potential savings to be incorporated in semi-rigid action than the simple design method. A fully examine the existing approaches to predict the mid-span deflection in serviceability together with the proposed method will be discussed in chapter 10.

Column design in a simply multi-storey frame is covered by BS 5950 : part 1 clause 4.7.7 [7.5]. This clause clearly states that in a structure of simple multi-storey construction

it is not necessary to consider the effect on columns of pattern loading. For the purpose of column design, all beams supported by a column at any one level may be assumed to be fully loaded. Clause 4.7.1 recommends that the column head moment is the eccentrically induced moment. However, the semi-rigid action causes the transfer of moments from the beam through to the column which vary for different pattern loads. A more detailed investigation of the axial resistance for the column using different methods to determine the column head moment will be presented in section 7.5.6.

Table 7.3 records the beam moments in stages 2 and 3 tests at load levels of about 50 kN. A comparison of the frame moment can thus be made for different load patterns. It can be observed that similar moments were attracted to both ends of each beam when the beams were loaded individually (second stage of first series test) whilst higher moments were attracted to the beam ends near the internal joints in the second stage of second series tests due to larger restraint provided by the adjacent beams. When the beam moment determined in the second stage of second series tests are compared with the values determined in stage 3 test (test 17) under load together with same applied load, it is observed no significant difference.

At the total applied load of 50 kN in a beam, the free bending moment is determined as 31.0 kNm. For the test frame, moments were attracted to connections due the stiffness of end-plate leading a reduction in the mid-span moment. The results shown in Table 7.3 indicate that beam ends with flush end-plate connection sustain a minimum of 17 % free bending moment and 25 % for the extended end-plate connected beams. It further confirms the potential saving to be taken accounting the semi-rigid action than the simple design method.

## **7.5 Test of Failure**

### **7.5.1 Test Observations**

Test 17 was used to investigate the behaviour of the frame up to the failure of the central column in the non-sway mode under a combination of beam and column loads. After one scan of readings was taken at zero load, load was applied to all beams up to about 200 kN in 25 increments. The central column in position 2 was then axially shortened by 1 mm increments (corresponding about 50 kN) and finally 0.2 mm (corresponding 10 kN increments) up to failure of that column. At scan 32 the column was accidentally unloaded

- the column was then reloaded to about 350 kN in one increment. Failure occurred in scan 38 with a record of applied column axial load of 490 kN. After failure of that central column, the axial displacement applied to all columns was released and all the beams unloaded in 30 kN increments. Table 7.4 summarises the load levels applied to the beams.

The axial load in each column lift during the test, as determined by the strain gauges, is recorded in Table 7.5. A comparison of the applied beam and column loads in each storey and the axial load measured in the columns at this level is shown in Table 7.6 and low discrepancy of the axial load with a maximum value of 4 % was determined up to scan 38 (failure of the central column). A large discrepancy was determined after that due to either irrecoverable deformation of the steel section due to yield of the material or to damage of the strain gauges after failure of the central column. The correlation between loads calculated from the measured applied loading and these determined from the strain gauges reading indicates that the instrumentation was working correctly.

### 7.5.2 Bending Moments on Beams

Figures 7.4 to 7.9 show the load against moment plots for all six beams in test 17. The value of load plotted on the vertical axis is the sum of both loads on the beam as measured by the load cells in the loading rods. All joints attracted significant moment due to the stiffness of connections. For moderate loads, non-linear curves were obtained for all beams at the beam ends due to the connection response and consequently all the load moment relationships were non-linear.

Figure 7.10 shows the distribution of moment in beam 3 as the applied beam load increased. This figure displays the bending moment distribution for scans 5, 10, 15, 20 and 25 which cover the beam loading phase. At the load level corresponding to the design load of the beam, the connections sustained about 22 % of the free moment in beams 1 to 3 and 46 % in beams 4 to 6. It is showed in Table 7.7 that the internal joints attracted higher moments than the external one.

### 7.5.3 Relationship of Load-Deflection in Beams

Figure 7.11 shows a single plot of load against deflection curve for all six beams, thus the deflection for each bay of beams could be compared. In this test frame, beams 1 to 3 used a larger section and a comparable weaker flush end-plate connection than beams 4 and

6. All curves shown follow a slightly non-linear route up to the end of the beam load phase (the maximum total applied load). After that, an increase in the mid-span deflection for each beam was observed as load was applied to column 2 whilst the applied beam load were maintained at constant value. As discussed in chapter 6, the failure of the columns required either further rotation or relaxation of the connection with an increase of the mid-span deflection of the beam. Deflections of 18 to 23 mm were observed in beams 1 to 3 and 23 to 27 mm in the remaining beams in which they were under their design load and before the application of any column axial load.

#### 7.5.4 Bending Moment Distribution around the Frame

Figure 7.12 shows the distribution of bending moments around the frame. In this figure, the moments at two levels of load are plotted on the same graph in order to compare the variation of frame moment at different locations and at various levels of loads. Scan number 25, which corresponds to the end of the beam load phase (design load) and scan number 38 which corresponds to the failure of the central column, are plotted. The upper stories of two external columns 1 and 7 were subjected to quite high moment and thus caused considerable deflection (Figure 7.16).

Figure 7.13 illustrates a frame moment diagram in scan 38 and clearly shows that with the application of the column axial load, there was a reduction of the column moment. This is largely attributed to the development of plasticity within the column due to the increased axial load and the consequent increase the rotation of the end of column. The shedding of moments from joints F (Figure 7.6) and K (Figure 7.9) to the beam spans provided an evidence of this phenomenon. A detailed analysis for the change of the column moment during the test will be discussed in next section.

Figure 7.14 shows the moment distribution at the intersection of the beam and column at the end of beam load phase. Most of the intersection points indicated the apparent out-of-balance with a maximum of 16.43 kNm. This out of balance is probably due to the additional moment induced at the column centreline by the eccentricity of the beam end reaction. A detailed analysis of the test to failure will be discussed in section 7.5.6.

### 7.5.5 Deflected Shape of the Frame

Deflections were recorded at the mid-span, quarter and three-quarter points of the beams and the mid-height of the columns. Figure 7.15 shows the deflection of the frame of two different load levels, corresponding to the scans as described in Figure 7.12 of section 7.5.4 and Figure 7.16 show the frame deformation diagram in scan 38. There is no significant change in the mid-span deflections for beams and nor of the columns during the application of the column load.

### 7.5.6 Failure of Column in Position 2

Figures 7.17 to 7.19 show the major axis moment at three locations (1/4 point, mid-height and 3/4 point) in column lifts 4 to 6 (the central column) plotted against the respective total column axial load measured from the strain gauge sections. It is evident from these plots that the major axis moment of all three columns shows no change of the stiffness associated with a column subjected to beam load only. During the application of the column axial load very little change of moment was observed. It is evident that column 6 experienced a sudden loss of stiffness measured as change in moment per increment of applied column load, showing that the column had failed (see Figure 7.19). Undoubtedly, the curves of load against moment on the head of columns 4, 5 and 6 shown in Figure 7.20 exhibits the failure of that column. It is noted in this figure that only column 6 exhibited a sudden loss of stiffness whilst other columns show no significant change of moment at failure indicating failure in the bottom section. Figure 7.21 shows the deflection in three locations of column 6 against its total axial load. The mid-height deflection in that column exhibits a sudden loss of stiffness with a maximum recorded value of 1.3 mm in lowest segment. This confirms that failure occurred of the column in position 2 - column 6.

Failure was deemed to have occurred when the central column was unable to sustain a steady axial column load. As the failure was approached, the recorded applied column head load was 490 kN and the strain gauged cross sections gave the total axial load in columns 4, 5 and 6 as 725 kN, 944 kN and 1093 kN respectively. These values agree quite well with values of 705 kN, 893 kN and 1100 kN as computed from the applied column head load of 490 kN plus half of the loads applied to each connecting beam above the section. A close inspection of the strain gauge reading after the test further confirmed that failure had occurred in the column in the bottom lift (column 6).

The axial resistance predicted by BS 5950: part 1 clause 4.8.3.3 [7.5] for the central

column has been calculated and is given for three different assumptions of the co-existing moment in Table 7.8. In case 1, the moment is the eccentrically induced moment recommended by clause 4.7.1 i.e. half the beam load times half the column depth plus 100 mm. Case 2 used for the difference of the beam end moment measured in the test at scan 38. Finally, case 3 used for the column end moment measured in the test at scan 38. Different effective length ratios were assumed and used to compute the axial resistance of the central column. Value of 1 and 0.85 were considered for columns 4 and 5, with values of 0.85 and 0.7 being adopted for column 6.

For the lowest storey, the simplified approach in clause 4.8.3.3.1 calculated the maximum axial load in case 1 as 1147 kN based on the effective length factor of 0.85. This is about 5 % more than the measured axial load whilst in case 2, which uses the difference of beam moment, the calculated load was 1052 kN, about 96 % of the actual load. A predicted value of 1099 kN was determined in case 3, which used the test moment in the column head and was 1 % higher than the axial load determined from the strain gauges in the column. Using the effective length factor of 0.7 to repeat the predicted failure load due to lesser restraint to be taken account, higher ultimate capacity was thus determined (Table 7.8). A same conclusion is drawn.

Also on Table 7.8, the ultimate capacity determined for a pin ended column under axial load  $P_{pin}$  only is recorded. The failure load of lowest column lift occurs at a value of 1093 kN and a similar result of the  $P_{pin}$  value is determined. It further supported the  $\alpha_{pin}$  approach [7.6] which is indicated that the beneficial effect of restraint provided by the beams through the semi-rigid connection outweighs the disadvantage effect of the moment transmitted through the connection. As other two column lifts (column 4 and 5) did not attain failure, no comment was drawn.

The above method only concentrated to adopt assumed effective ratios to predict the ultimate capacity of columns. Taking into account the semi-rigid action of the connection, a new design approach to predict the effective length ratio is suggested and this method is fully examined using the results of frames 3, 4 and 5 in chapter 10



## 7.6 Moment Rotation Behaviour in Joints

### 7.6.1 General Behaviour of Connections

The behaviour of a beam-to-column connection is dependent on a number of different parameters including the type of connection, the grade of steel, the size of the beam and the column and the axis of bending. The behaviour of the connection is best illustrated by the relationship between the moment transmitted by the connection and the corresponding rotation. As in frames 1 and 2, two types of connections, flush end-plate and extended end-plate, were used in this frame. The moment rotation curves will be compared with the results determined from reported by Chakraborti cruciform joint tests [7.7] but with a lower initial stiffness and moment capacity.

### 7.6.2 Discussion of Results

#### 1. Flush End-Plate

Figures 7.22 and 7.23 show the moment rotation plot for the connections in the external column (joint A, C and E) and internal column (B, D and F). The curves of joints A and C (Figure 7.22) show a similar in form response to the cruciform test result. The unloading stiffness was observed to be sensibly parallel to the initial stiffness. Joint E showed a lower initial stiffness up to a moment of 10 kNm due to the lack-of-fit in the joint, but it started to pick up more moment after that. It is noted in Figure 7.23 that the behaviour of the joints B, D and F matched quite well with the response obtained from the joint tests. They show very similar response to the cruciform test results.

#### 2. Extended End-Plate

The moment rotation curves of the extended end-plate connections are shown in Figures 7.24 and 7.25. The behaviour of the extended end-plate connections had significantly higher stiffness and sustained higher moment than the flush end-plate connections. Joints G, I and K, shown in Figure 7.24, performed consistently with an almost identical initial stiffness and matched well with the response obtained from the joint test. The behaviour of joint G developed a result almost coincident with the joint test with a maximum sustained moment of 65 kNm. Other joints showed a slightly lower sustained moment of 55 kNm. But this is irrelevant if it merely indicates that they were not called up to carry higher moments.

The instrumentation for which joints J and L response was obtained developed a fault, a usable curve was only determined in joint H from the external column of the extended end-plate connections (Figure 7.25). This joint was observed to fall below the joint test result and sustained a quite low moment of 56 kNm as explained above.

### 7.6.3 Loading and Unloading Stiffness

Loading and unloading stiffness of connections are determined for the slopes as determined from Figure 5.23 and the results are recorded in Table 7.9. A low initial stiffness determined from some joints were thought due to lack-of-fit in the connections. After that the connection stiffness increased to a higher value with increase in the applied load. This may be due a closing of the gap between the column flange and the end-plate as the connection loaded. Thus a maximum stiffness in the loading stage for each joint was determined in order to compare it with the initial and unloading stiffnesses. The results, shown in Table 7.9, that indicated similar maximum and unloading stiffnesses were observed in most of the joints. The internal joints show a slightly larger stiffness than the external joint. A detailed explanation of the connection behaviour will be presented in chapter 9.

### 7.6.4 Comparison of the Connection Moment to the Rigid Moment

The behaviour of connections play an important role in the design of a steel frame and it is interesting to compare the test moments in the connections to those expected in a rigid frame. A rigid jointed plane frame analysis program, developed by Dr Burgess in the University of Sheffield, was used to determined the connection moment for an identical fully rigid frame. The value of the elastic modulus, yield stress and section properties were obtained from reference [7.1]. Two levels of loads are considered in this study. Scan number 12 corresponds to the level of load in the maximum elastic region - this point was determined from the behaviour of the load-deflection (Figure 7.11) and the moment rotation responses (Figures 7.22 to 7.25) in test 17 - and scan 25 which corresponds to the end of the beam load phase (design load). The connection moments obtained in the test and the predictions at two loadings are listed in Table 7.10.

It is clear to note that the flush end-plate connections attracted an average of 47 % of the rigid moment in scan 12 whilst a slightly lower ratio of 33 % in scan 25. Extended end-plate connections show a higher stiffness with an average of 70 % rigid moment in scan 12 and 77 % in scan 25. The ability of extended end-plate of this type considered in this

frame to function as rigid appears highly questionable.

Analysis of the results of frames 1 and 2 where thick end-plates with column stiffeners were employed and the results showed that the extended end-plate connection used could be regarded as 'rigid'. Here lighter end-plate without column stiffener were used, the sort commonly regarded as being capable of transmitting shear only. If the extended end-plate joints have regarded as semi-rigid, the additional fabrication required, together with the inconvenience of using a joint that extended beyond the beam depth, would seem to point to change to a flush end-plate arrangement.

## 7.7 Connection Moment and Bolt Forces

### 7.7.1 Objectives

The use of semi-rigid partial strength connections in a steel frame requires the formation of a plastic hinge within the connection at loads less than the factored design loads. The philosophy adopted in the design method is to allow each bolt row to attain its design strength i.e. resulting in progressive yielding of the connection. Existing methods to design a frame with end-plate connections to the column flange, it is assumed that the centre of rotation is in line with the compression flange of the beam. The distribution of tensile strain due to moment is assumed to be linear. This phenomenon is clearly shown in the analysis of the previous frames in section 5.6.7. The study in frames 1 and 2 showed that most of the tension force was sustained in the top row of bolts of the flush end-plate connection with very small compression or tension force observed in the lowest row. For the extended end-plate connection, the middle row sustained a highest tensile force. As the flush end-plate connections, the lowest row attracted the lowest tensile or compression force. As a result, the bolt force could be computed for each row using this approach. It is also shown by frames 1 and 2 that the connection attains its ultimate limit state when the uppermost bolt row for the flush end-plate connections and middle row for the extended end-plate connections reach their design strength. Thus they are most critical in design. The aims of this study are to further investigate the distribution of the bolt force during the tests.

Figures 7.26 to 7.37 present the resulting moment bolt force plots for each bolt of the connections in test 17. All six bolts in each connection are plotted in a single graph in order to compare the distribution of the axial force in each bolt for a connection during the test.

Joints A to F used the flush end-plate connections and joints G to L used the extended end-plate connections in frame 5. The position of these bolt rows in flush end-plate and extended end-plate connections was defined as Figure 5.3. Tables 7.11 and 7.12 give the average maximum recorded bolt forces in each row in this test. The results for the internal and external joints for each type of connections will be discussed separately in next section.

## 7.7.2 General Discussions

### 1. Flush End-Plate Connections

#### (a) External Joints A, C and E

Examination of the plots of joint A (Figure 7.26), bolts 1 and 4 (top row) show a linear response of bolt force vs moment up to moment of 12 kNm, after which the plots varied non-linearly for the corresponding moment increments. Other bolts had shown a linear response with increase of their connection moment in the test. It is noted that the maximum tensile force was observed in the top row ( $T_1$ ) with a record of 57 kN whilst the second row sustained a much lower value of 17 kN. As frames 1 and 2, the lowest row ( $T_3$ ) sustained a lowest tension force of 7 kN. For joint C (Figure 7.27), a similar response was observed in all bolts. It is interesting to note that in this joint, bolt 3 was initially subjected to a compression force up to the connection moment of 8 kNm. After that it changed to become subjected to a tensile force. The initial compression forces in the bolts may be due to release of some tension from pre-load of bolts. It perhaps due to lack-of-fit of connections. All the bolts in Joint E (Figure 7.28) are subjected to tensile force (see Table 7.11).

#### (b) Internal Joints B, D and F

First consider the upper joint B (Figure 7.29), the average axial force for rows 1, 2 and 3 was recorded in Table 7.11. It is noted that an increase in the axial force for all bolts without increase of the connection moment occurred at a recorded moment of 31 kNm. This implies that this joint already attained its ultimate limit state as a plastic hinge had formed in the connection. The moment rotation plot in joint B (Figure 7.29) reinforced this point.

All bolts in joint D (Figure 7.30) gave a linear response up to about the connection moment of about 16 kNm after which non-linearity occurred. The

lowest row of bolts was first subjected to small compression up to connection moment of 21 kNm and changed to under tensile force after that. The maximum axial force in  $T_1$ ,  $T_2$  and  $T_3$  was 64, 15 and 6 kN.

Finally, all the bolts in joint F (Figure 7.31) were subjected to tension with a record of 66, 22 and 19 kNm in three rows.

## 2. Extended End-Plate Connections

### (a) Internal Joints G, I and K

Consider the behaviour of the upper joints G (Figure 7.32), it is noted that the top row  $T_2$  (bolts A and B) sustained a highest tensile force of 65 kN whilst a slightly lesser tension of 52 kN was observed in  $T_1$  (bolts C and D). Bolts E and F in the lowest row were subjected to a low tensile force of 3 kN.

All the bolts in joints I and K (Figures 7.33 and 7.34) had shown a same behaviour with a quite similar force sustained in two top rows. The bottom row was observed under a very low tensile force and the value can be negligible.

### (b) External Joints H, J and L

Turning to discuss the external joints H, J and L (Figures 7.35, 7.36 and 7.37), they show a similar response to the internal joints in the test. Due to fault developed in bolt 6 of joint L, no usable result is discussed. However, it is not deemed to effect for this study.

## 7.7.3 General Behaviour of Bolts in Different Connections

For the test results shown in Table 7.11 that the upper row of the flush end-plate connection was used to sustain most of the tension force, the middle row may sustain lesser tension force. The lowest row  $T_3$  was used to transfer lowest tension or even compression force to the column flange. The distribution of strain was not with rotation about far from a triangle. It reinforced that in section 7.7.1, the connections attain their ultimate limit state when the uppermost bolts reach their design strength and thus they are the most critical in design.

A difference was found from the extended end-plate connection. It is noted that in Table 7.12  $T_1$  was observed under a very similar tension but slightly higher value than  $T_2$

in connections G, J and L. The lowest row was used to sustain a very low axial force. Connections H and K were subjected to a similar tension in  $T_1$  and  $T_2$ . As discussed in chapter 5, due to the larger restraining force provided by the adjacent beam in internal column, the bending of the connection was different. The larger bolt force in the upper row of connection I was thought due to increasing bending in the top of plate. As the result, the middle row  $T_1$  for the extended end-plate is more critical for design. A detailed explanation of the philosophy and methods for the end plate connection design will be discussed in chapter 10. The EC 3 annex J method [7.8] to predict the  $M-\phi$  characteristics for the end-plate connection will be examined and the predictions are compared with the frame and joint test results.

## 7.8 Concluding Remarks on the Study

This study has considered a full scale two dimensional frame test and column capacity calculated used the method outlined in BS 5950 Part 1. The load applied to individual beams were observed a larger mid-span beam deflection than other load combinations in this instant. Thus it is suggested that this type of pattern load should be considered for the beam deformation check in the serviceability limit state.

The tests illustrated that the rotational stiffness of the end-plate connection significantly influences the distribution of moments around the frame, leading to a reduction of beam deflections when compared to traditional pinned joint concepts. The semi-rigid action transfers large moments from the beam through to the column. Thus, it increases the moments and the deflection of the column relative to the same member with true pinned connections.

When utilising the semi-rigid joint effect, part of the mid-span moment is transferred to the column. Hence, a smaller mid-span beam deflection will be encountered. In addition, the reduced mid-span moment can allow larger applied beam moments to be carried or the beam size may be reduced with a consequent improvement in economy.

Although flush end plates are usually consider to operate in shear only, they can be classified as semi-rigid. The stiffness observed indicates that the significant reductions in beam span moments and deflections are observed. However, the moments at beam end are significant lower than rigid moment. From frames 1 and 2, thicker end-plate with the column stiffeners adopted in the extended end-plate connection, this connections used could

be regarded as rigid. Frame 5 used thin end-plate without column stiffeners in the connections, the joint response is similar to semi-rigid. It indicates that the behaviour of extended end-plate connections variety dependent on the different design conditions i.e. thickness of plates and are not all suitable classified as 'rigid'. If extended end-plate joints have to be regarded as semi-rigid, the additional fabrication required, together with the inconvenience of using a joint that extended beyond the beam depth, would seem to point to change to a flush end-plate arrangement.

There was significant non-linearity in some of the  $M-\phi$  curves obtained which in part may be due to lack of fit occurring in connections. The maximum stiffness in the loading stage was found parallel to the unloading stiffness.

Observed behaviour was always superior so that predicted by BS 5950 Part 1, take clearly demonstration that exploitation of semi-rigid joint action will lead to economies in design. Taking into account the semi-rigid action, a new approach for the non-sway column design will be proposed and examined in chapter 10.

The result of the frame tests are compared with the prediction of in house finite element analysis programs in chapter 8. The method presented in EC 3 annex J to predict the  $M-\phi$  characteristics for end-plate connections will be examined and new design methods for the laterally restrained beams in serviceability and ultimate limit states will be developed and checked using all test results as addressed in chapter 10.

## References

- [7.1] Lennon, T., 'Full-Scale Steel Frame Tests: Load Tests on Frame No.5', Building Research Establishment, Report No. N71/88.
- [7.2] Davison, J. B., 'Strength of Beam-Columns in Flexibly Connected Steel Frames' Ph.D. Thesis, University of Sheffield, June, 1987.
- [7.3] Jennings, D. A., Moore, D. B. and Sims, P. A. C., 'Instrumenting and Testing Bolted Steel Frame Structures', Proceedings, Determination of Dangerous Stress Levels and Safe Operation Condition, Edinburgh, August, 1986.
- [7.4] Lau, S. M. 'Full Scale Frame Test with Semi-Rigid Connections', Progress Report no.8, Department of Civil & Structural Engineering, University of Sheffield, April, 1992.
- [7.5] British Standards Institution BS 5950: Part 1: Structural Use of Steelwork in Building. BSI, London, British Standards Institution 1985.
- [7.6] Kirby, P. A., Bitar, S. S. and Gibbons, C., 'Design of Column in Non-Sway Semi-Rigidly Connected Frames', Constructional Steel Design, World Developments, Elsevier Applied Science, 1992, pp. 54-63.
- [7.7] Chakrabarti, B., 'Tests of Unstiffened End-Plate Beam-Column Connection', Building Research Establishment, Report No. N123/87.
- [7.8] Eurocode 3 - ENV 1993-1-1 : Design of Steel Structures Part 1.1 : General Rules and Rules for Building (together with United Kingdom National Application Document', European Committee for Standardization, 1992.



Stage	Test	Data File	Load Position	Loaded Members	Max. Load	No. of Increments
1	1	BRE1.DAT	1/4 pts.	BEAM 3	10 kN	7
1	2	BRE2.DAT	1/4 pts.	BEAM 3	10 kN	4
1	3	BRE3.DAT	1/4 pts.	BEAM 2	10 kN	6
1	4	BRE4.DAT	1/4 pts.	BEAM 1	10 kN	5
1	5	BRE5.DAT	1/4 pts.	BEAM 6	10 kN	5
2	6	BRE6.DAT	1/4 pts.	BEAM 1	50 kN	11
2	8	BRE8.DAT	1/4 pts.	BEAM 3	50 kN	13
2	9	BRE9.DAT	1/4 pts.	BEAM 4	50 kN	13
2	10	BRE10.DAT	1/4 pts.	BEAM 5	50 kN	13
2	11	BRE11.DAT	1/4 pts.	BEAM 6	50 kN	13
2	12	BRE12.DAT	1/4 pts.	BEAMS 1 & 4	80 kN	13
2	13	BRE13.DAT	1/4 pts.	BEAMS 2 & 5	80 kN	13
2	14	BRE14.DAT	1/4 pts.	BEAMS 3 & 6	80 kN	9
3	17	BRE17.DAT	1/4 pts.	ALL BEAMS and COLUMN 2	FAILURE	47

Remark : The numbering of tests are referred to the number of the data files

Table 7.1 : Description of Tests in Frame 5

Stage	Series	Test	Mid-Span Deflection of Beam (mm)					
			1	2	3	4	5	6
2	1	6	4.5	-	-	-	-	-
		8	-	-	4.9	-	-	-
		9	-	-	-	5.2	-	-
		10	-	-	-	-	4.9	-
		11	-	-	-	-	-	5.7
2	2	12	4.6	-	-	5.2	-	-
		13	-	4.8	-	-	4.5	-
		14	-	-	4.7	-	-	5.3
3	-	17	4.7	4.8	4.8	5.0	4.3	5.2

Table 7.2 : Mid-Span Deflection of Beams in Different Tests

Stage	Series	Test	Beam	Moment (kNm)			
				Left End	Left Load	Right Load	Right End
2	1	6	1	-5.20	21.45	20.40	-7.50
		8	3	-7.87	22.79	22.09	-7.82
		9	4	-13.92	18.61	20.22	-9.86
		10	5	-13.61	16.31	16.63	-12.76
		11	6	-15.52	17.48	21.13	-8.17
2	2	12	1	-5.99	25.33	21.88	-13.58
		13	2	-6.77	23.96	21.49	-11.65
		14	3	-10.82	33.00	29.02	-16.35
		12	4	-17.70	15.57	19.14	-9.58
		13	5	-17.30	14.02	16.24	-12.51
		14	6	-26.07	20.64	29.58	-8.43
3	-	17	1	-6.94	24.34	22.79	-10.32
		2	2	-7.92	23.62	23.06	-9.26
		3	3	-8.96	24.34	22.79	-10.32
		4	4	-17.66	15.20	18.10	-11.05
		5	5	-17.01	13.66	14.67	-14.58
		6	6	-19.70	14.62	20.63	-7.60

Table 7.3 : Beam Moment Distribution in Different Tests

SCAN	APPLIED LOAD (KN)									COMMENTS
	BEAM NO.						COLUMN POSITION			
	1	2	3	4	5	6	1	2	3	
1	0.0	0.0	0.0	0.0	0.0	0.0	0.0	0.0	0.0	
2	8.6	7.6	7.8	7.2	7.4	7.2	0.2	0.2	0.1	
3	17.9	16.6	16.7	15.8	15.5	15.5	0.2	0.3	0.1	
4	27.3	25.5	25.7	24.4	23.7	23.8	0.2	0.3	0.1	
5	36.8	34.6	34.7	33.1	32.0	32.2	0.2	0.4	0.1	
6	46.2	43.6	43.7	41.6	40.1	40.5	0.3	0.5	0.2	
7	55.6	52.5	52.6	50.2	48.3	48.9	0.4	0.5	0.2	
8	65.0	61.5	61.6	58.9	56.5	57.3	0.4	0.6	0.3	
9	74.5	70.5	70.6	67.5	64.7	65.7	0.5	0.7	0.4	
10	83.9	79.6	79.5	76.0	72.8	74.0	0.4	0.6	0.3	
11	93.4	88.7	88.6	84.7	81.3	82.4	0.5	0.7	0.3	
12	102.8	97.6	97.4	93.3	89.6	90.8	0.5	0.7	0.3	
13	112.2	106.6	106.4	101.9	97.9	99.2	0.6	0.8	0.4	
14	121.7	115.6	115.4	110.4	106.0	107.5	0.6	0.8	0.4	
15	131.1	124.6	124.4	119.0	114.2	115.9	0.5	0.7	0.4	
16	140.7	133.7	133.5	127.7	122.2	124.4	0.5	0.7	0.3	
17	149.6	142.6	142.4	136.3	127.8	132.8	0.5	0.8	0.4	
18	159.0	151.7	151.5	144.8	134.6	141.1	0.5	0.7	0.4	
19	168.4	160.7	160.5	153.5	143.5	149.5	0.5	0.7	0.4	
20	177.9	169.8	169.5	162.2	147.0	158.0	0.5	0.7	0.3	
21	187.4	178.8	178.6	170.8	160.3	166.4	0.5	0.8	0.4	
22	196.7	178.9	187.5	179.3	166.9	174.7	0.6	0.8	0.4	
23	206.1	178.9	196.5	187.9	176.2	183.1	0.6	0.8	0.4	
24	215.6	179.0	205.6	196.6	180.0	191.4	0.6	0.8	0.4	End of
25	225.2	179.0	214.6	205.0	191.7	199.7	0.6	0.8	0.4	beam load
26	225.0	179.1	214.6	205.0	191.0	199.7	0.5	32.2	0.4	Column 2
27	225.0	179.1	214.7	205.0	191.0	199.8	0.5	71.2	0.4	loaded
28	225.1	179.1	214.7	205.0	189.1	199.4	0.5	110.8	0.4	to failure
29	225.0	179.1	214.7	205.0	188.9	199.8	0.5	150.4	0.4	
30	225.0	179.1	214.7	205.0	189.4	199.9	0.5	231.1	0.4	
31	225.0	179.1	214.7	205.0	190.7	199.8	0.5	307.4	0.4	
32	225.0	179.1	214.7	205.0	193.8	199.6	0.5	17.1	0.4	Unloaded
33	225.3	179.2	214.7	205.0	197.0	199.9	0.5	349.0	0.4	
34	225.3	179.2	214.7	205.0	197.0	198.9	0.6	388.0	0.4	
35	225.2	179.2	214.7	205.0	197.0	199.9	0.6	422.4	0.4	
36	225.2	179.2	214.7	205.0	197.0	199.9	0.6	471.3	0.4	
37	225.3	179.2	214.7	205.0	197.0	199.9	0.6	480.6	0.4	
38	225.3	179.2	214.7	205.0	197.0	199.9	0.6	489.7	0.4	Failure
39	225.3	179.2	214.7	205.0	197.0	199.9	0.6	262.7	0.4	Unloaded of
40	225.4	179.2	214.7	205.0	197.0	200.0	0.6	33.2	0.4	members
41	225.4	179.2	214.7	205.0	197.0	200.0	0.6	1.1	0.4	
42	187.7	179.2	178.8	170.7	164.2	166.7	0.6	1.0	0.5	
43	150.0	143.2	142.8	136.2	131.2	133.2	0.6	1.0	0.4	
44	112.4	107.3	106.8	101.8	98.1	99.7	0.6	1.0	0.4	
45	74.6	71.2	70.8	67.3	65.0	66.1	0.7	1.0	0.5	
46	37.0	35.3	34.8	32.7	31.5	32.4	0.7	1.1	0.5	
47	-0.3	-0.4	-0.2	-0.5	-0.3	-0.3	0.6	1.0	0.5	

Table 7.4 : Load History of Frame 5 Test 17

SCAN	AXIAL LOAD (kN)								
	COL 1	COL 2	COL 3	COL 4	COL 5	COL 6	COL 7	COL 8	COL 9
1	0.0	0.0	0.0	0.0	0.0	0.0	0.0	0.0	0.0
2	4.5	8.8	12.9	8.6	16.8	23.9	3.8	7.6	10.9
3	9.4	18.1	27.1	18.2	36.3	51.6	8.4	16.2	23.3
4	14.1	27.4	41.1	27.9	55.7	79.5	13.0	24.7	35.7
5	18.6	36.7	55.1	37.6	75.5	107.7	17.6	33.1	47.8
6	23.2	46.0	69.2	47.3	95.1	136.1	22.2	41.4	59.9
7	27.9	55.1	83.1	57.1	115.1	164.8	26.7	49.8	71.9
8	32.4	64.3	97.0	67.1	135.0	193.6	31.2	58.3	83.8
9	37.2	73.3	110.9	76.7	154.8	222.4	35.9	66.6	95.7
10	41.9	82.4	124.7	86.5	174.6	251.0	40.2	74.6	107.4
11	46.3	91.3	138.4	96.5	194.9	280.2	44.6	82.9	119.3
12	50.9	100.3	152.3	106.5	214.4	308.1	49.3	91.3	131.8
13	55.6	109.5	166.6	116.3	233.5	335.3	54.0	100.1	144.7
14	60.3	118.8	180.8	125.8	252.3	362.1	58.7	108.6	157.4
15	65.0	128.2	194.9	135.6	271.5	391.7	63.4	117.0	170.5
16	69.7	137.5	209.4	145.4	291.1	419.6	68.1	125.7	183.5
17	74.1	146.4	223.2	154.9	310.1	446.8	73.1	134.5	196.7
18	79.0	155.8	237.6	164.7	329.4	474.4	77.7	143.3	209.4
19	83.6	165.0	251.8	174.5	348.7	503.2	82.5	152.3	222.7
20	88.1	174.4	266.2	184.3	368.0	530.7	87.3	161.3	235.8
21	92.9	183.7	280.4	194.0	387.1	557.2	92.2	170.3	249.0
22	97.3	188.0	289.9	203.5	401.2	578.5	96.8	179.1	262.0
23	101.9	192.9	299.6	213.2	415.9	600.1	101.7	188.5	275.3
24	106.8	197.8	309.3	222.9	430.4	622.0	106.7	197.9	288.5
25	111.5	202.2	318.8	232.0	444.6	643.4	111.3	206.9	301.3
26	111.2	202.5	319.0	264.6	477.2	674.7	111.5	207.7	302.4
27	111.5	202.7	319.4	303.6	515.6	713.7	111.9	208.3	303.0
28	111.8	203.2	319.8	343.2	555.4	753.4	112.2	208.6	303.2
29	111.9	203.4	320.2	382.8	594.2	794.4	112.4	208.9	303.8
30	112.3	203.7	321.0	463.2	674.6	882.2	112.9	210.0	305.1
31	112.4	204.2	321.9	540.3	750.9	968.4	113.2	210.6	306.3
32	112.0	203.2	320.3	251.4	467.1	683.2	112.3	208.9	304.2
33	112.6	204.9	322.6	584.1	793.3	1016.6	113.5	211.2	307.2
34	112.7	205.1	322.9	622.8	831.7	1060.7	113.8	211.5	307.7
35	113.0	205.2	323.4	657.3	866.2	1084.8	114.0	211.8	308.3
36	113.4	205.5	324.2	706.2	916.2	1103.8	114.5	213.2	310.1
37	113.4	206.0	324.5	715.5	930.7	1099.4	114.7	213.5	310.9
38	113.7	206.1	324.7	724.8	943.6	1093.0	114.7	213.9	311.5
39	112.9	205.2	323.5	504.7	730.8	973.9	113.7	212.2	309.4
40	112.3	204.4	322.6	275.4	505.2	846.3	113.1	210.8	307.7
41	112.3	204.0	322.4	240.4	470.6	824.1	112.8	210.8	307.5
42	94.9	187.1	286.5	201.5	413.0	764.0	96.0	177.8	259.1
43	77.3	151.6	231.7	162.5	335.7	692.0	79.0	145.1	210.5
44	59.4	115.9	176.5	123.8	259.1	619.6	61.6	111.5	161.5
45	40.3	78.0	118.3	86.1	182.7	533.8	43.3	76.7	110.9
46	21.0	40.2	59.7	49.8	108.4	444.0	24.8	41.1	58.9
47	2.2	3.1	3.2	14.3	32.1	340.3	4.9	4.7	7.7

Table 7.5 : Axial Load of Frame 5 Test 17

Scan	Total Load (kN)					
	Upper Columns		Middle Columns		Lower Columns	
	Beam	Axial	Beam	Axial	Beam	Axial
1	0.0	0.0	0.0	0.0	0.0	0.0
2	16.0	16.9	31.0	33.2	46.0	47.7
3	34.0	36.0	66.1	70.6	98.3	102.0
4	52.0	55.0	101.2	107.8	150.7	156.3
5	70.3	73.8	136.9	145.3	203.8	210.6
6	88.3	92.7	172.0	182.5	256.2	265.2
7	106.3	111.7	207.1	220.0	308.6	319.8
8	124.5	130.7	242.5	257.6	361.4	374.4
9	142.7	149.8	277.9	294.7	414.2	429.0
10	160.5	168.6	312.9	331.6	466.4	483.1
11	178.8	187.4	348.8	369.1	519.8	537.9
12	196.8	206.7	384.0	406.0	572.2	592.2
13	214.9	225.9	419.4	443.1	625.0	646.6
14	232.9	244.8	454.5	479.7	677.4	700.3
15	250.8	264.0	489.6	516.7	729.9	757.1
16	269.1	283.2	525.0	554.3	782.9	812.5
17	286.7	302.1	557.1	591.0	832.3	866.7
18	304.5	321.4	590.8	628.5	883.4	921.4
19	322.6	340.6	626.8	666.0	936.8	977.7
20	340.8	359.7	657.6	703.7	985.1	1032.7
21	359.0	379.1	698.1	741.1	1043.1	1086.6
22	376.8	397.6	722.6	768.3	1084.8	1130.4
23	394.8	416.8	749.9	797.3	1129.5	1175.0
24	413.0	436.4	772.0	826.1	1169.0	1219.8
25	431.0	454.8	801.7	853.7	1216.0	1263.5
26	462.2	487.3	832.3	887.4	1246.6	1296.1
27	501.2	527.0	871.3	926.6	1285.8	1336.1
28	540.9	567.2	909.1	967.2	1323.2	1376.4
29	580.4	607.1	948.4	1006.5	1362.9	1418.4
30	661.1	688.4	1029.6	1088.3	1444.2	1508.3
31	737.4	765.9	1107.2	1165.7	1521.7	1596.6
32	447.1	475.7	820.0	879.2	1234.3	1307.7
33	779.3	810.2	1155.5	1209.4	1570.1	1646.4
34	818.3	849.3	1194.5	1248.3	1608.1	1691.3
35	852.6	884.3	1228.8	1283.2	1643.4	1716.5
36	901.5	934.1	1277.7	1334.9	1692.3	1738.1
37	910.9	943.6	1287.1	1350.2	1701.7	1734.8
38	920.0	953.2	1296.2	1363.6	1710.8	1729.2
39	693.0	731.3	1069.2	1148.2	1483.8	1606.8
40	463.6	500.8	839.8	920.4	1254.5	1476.6
41	431.5	465.5	807.7	885.4	1222.4	1454.0
42	359.4	392.4	702.8	777.9	1048.3	1309.6
43	287.2	318.8	561.6	632.4	837.6	1134.2
44	215.2	244.8	420.6	486.5	627.1	957.6
45	142.9	169.7	279.1	337.4	416.0	763.0
46	70.8	95.6	137.6	189.7	204.8	562.6
47	0.2	21.4	-0.5	39.9	-1.0	351.2

Table 7.6 : Comparison of Total Applied Beam Load and Axial Load in Columns above Different Storeys in Test 17

Beam	% of Free Moment				Beam
	L.H.S.	R.H.S.	L.H.S.	R.H.S.	
1	17	25	51	41	4
2	20	25	46	42	5
3	22	23	49	44	6

Table 7.7 : End Moment as percentage of Free Moment at Design Load in Test 17 of Frame 5

Column	$\frac{L_E}{L}$	Maximum Axial Load (kN)				
		case 1	case 2	case 3	Test Result	$P_{pin}$ Value
4	1	1082	884	1016	725	1104
	0.85	1133	925	1064		
5	1	1084	1027	1060	944	1104
	0.85	1145	1076	1110		
6	0.85	1147	1052	1099	1093	1104
	0.7	1192	1096	1144		

Note:

case 1. Using simplified approach of the moment assuming eccentric end reaction

case 2. Using simplified approach of the difference of beam end moment

case 3. Using simplified approach of the column head moment measured in the frame test

$P_{pin}$  indicated the ultimate capacity of a pin ended column under axial load

Table 7.8 : Comparison of the Collapse Load from the Test and BS5950 for the Central Column

Joint	Stiffness (kN/millirad)			Maximum Moment (kNm)
	Initial	Maximum	Unloading	
A	3.33	3.60	3.60	20
B	2.99	4.42	4.69	30
C	2.22	2.22	2.64	20
D	2.00	4.19	4.55	31
E	0.63	3.17	3.85	30
F	2.27	3.87	4.21	27
G	-	-	12.50	65
H	6.67	6.67	5.88	56
I	9.52	9.52	9.26	55
J	-	-	-	-
K	9.09	9.09	10.00	55
L	6.06	6.06	-	-

Table 7.9 : Comparison of the Stiffness and Sustained Moment in Connections in Test 17

Joint	Moment (kNm)					
	Scan 12			Scan 25		
	Test	Rigid	Test/Rigid	Test	Rigid	Test/Rigid
A	13.2	21.7	0.61	21.1	50.9	0.41
B	24.4	56.6	0.43	30.7	125.6	0.24
C	13.4	32.9	0.41	20.3	64.4	0.32
D	19.8	49.0	0.40	31.4	93.3	0.34
E	15.4	27.3	0.57	27.3	64.3	0.42
F	21.0	51.9	0.41	28.1	114.8	0.24
G	33.8	54.2	0.62	63.4	120.8	0.52
H	20.4	21.9	0.93	51.1	43.5	1.17
I	32.5	46.4	0.70	57.0	92.1	0.62
J	25.6	32.0	0.80	52.5	67.0	0.78
K	36.4	47.1	0.77	60.8	110.2	0.55
L	10.4	28.5	0.37	55.0	56.6	0.97

Table 7.10 : Comparison of the Rigid connected Frame Moments in Scans 12 and 25 of Test 17

Connection	Row	Maximum Load (kN)
A	1	57
	2	17
	3	7
C	1	55
	2	15
	3	6
E	1	63
	2	18
	3	5
B	1	91
	2	33
	3	7
D	1	64
	2	15
	3	6
F	1	66
	2	22
	3	19

Table 7.11 Maximum Loads for Bolts in Test 17 (Flush End-Plate)

Connection	Row	Maximum Load (kN)
G	2	52
	1	65
	3	3
I	2	63
	1	52
	3	9
K	2	60
	1	60
	3	14
H	2	39
	1	34
	3	3
J	2	54
	1	57
	3	11
L	2	26
	1	50
	3	-5

Table 7.12 Maximum Loads for Bolts in Test 17 (Extended End-Plate)



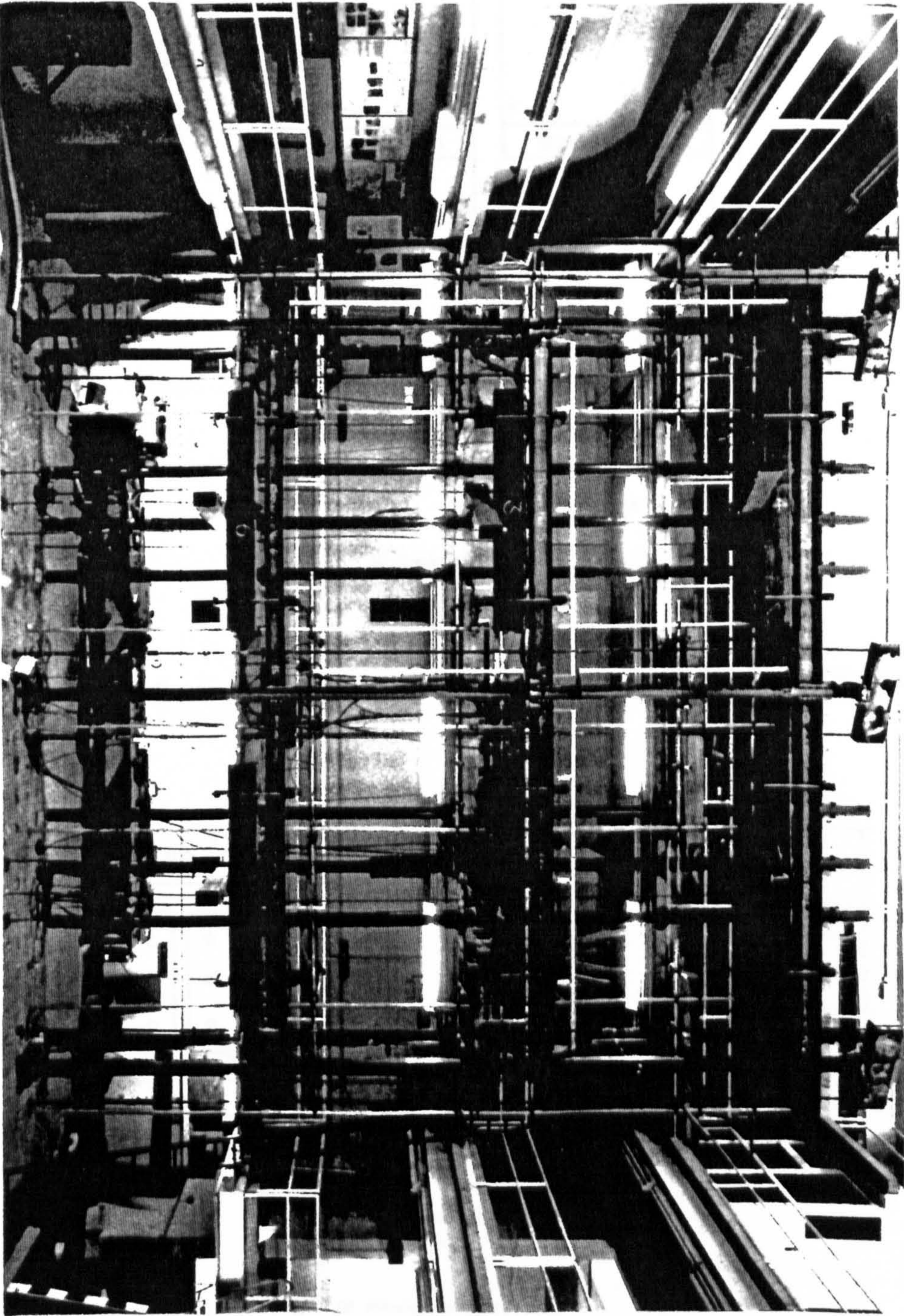
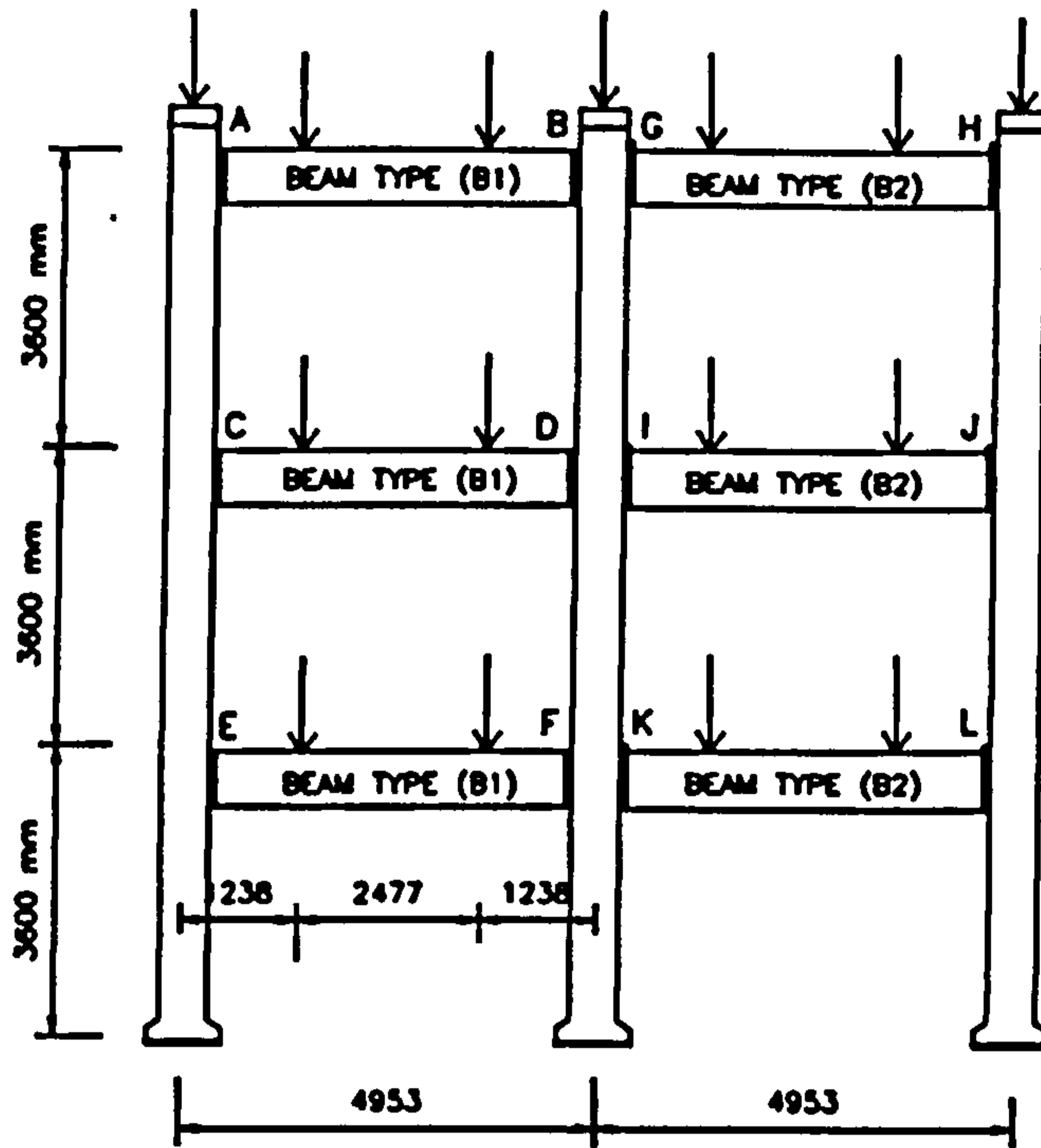


Figure 7.1 : Frame 5 viewed towards the Balcony



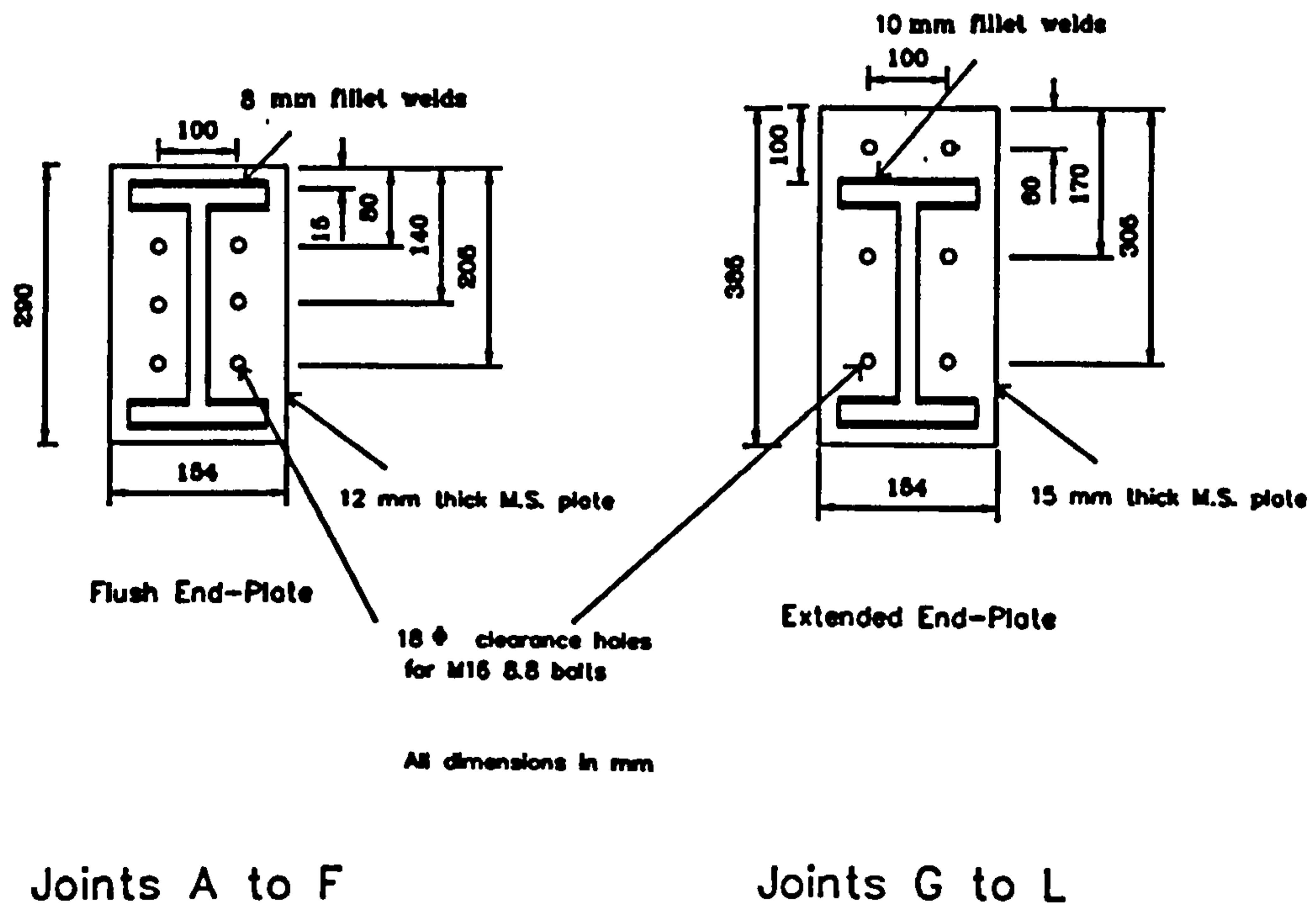
Column 152 X 152 UC 37

Beam (B1) 254 X 146 UB 37

(B2) 254 X 102 UB 28

All Grade 43A Steel

Figure 7.2 : General Arrangement of Frame 5 viewed from the Balcony



Joints A to F

Joints G to L

Figure 7.3 : Connection Detail in Frame 5

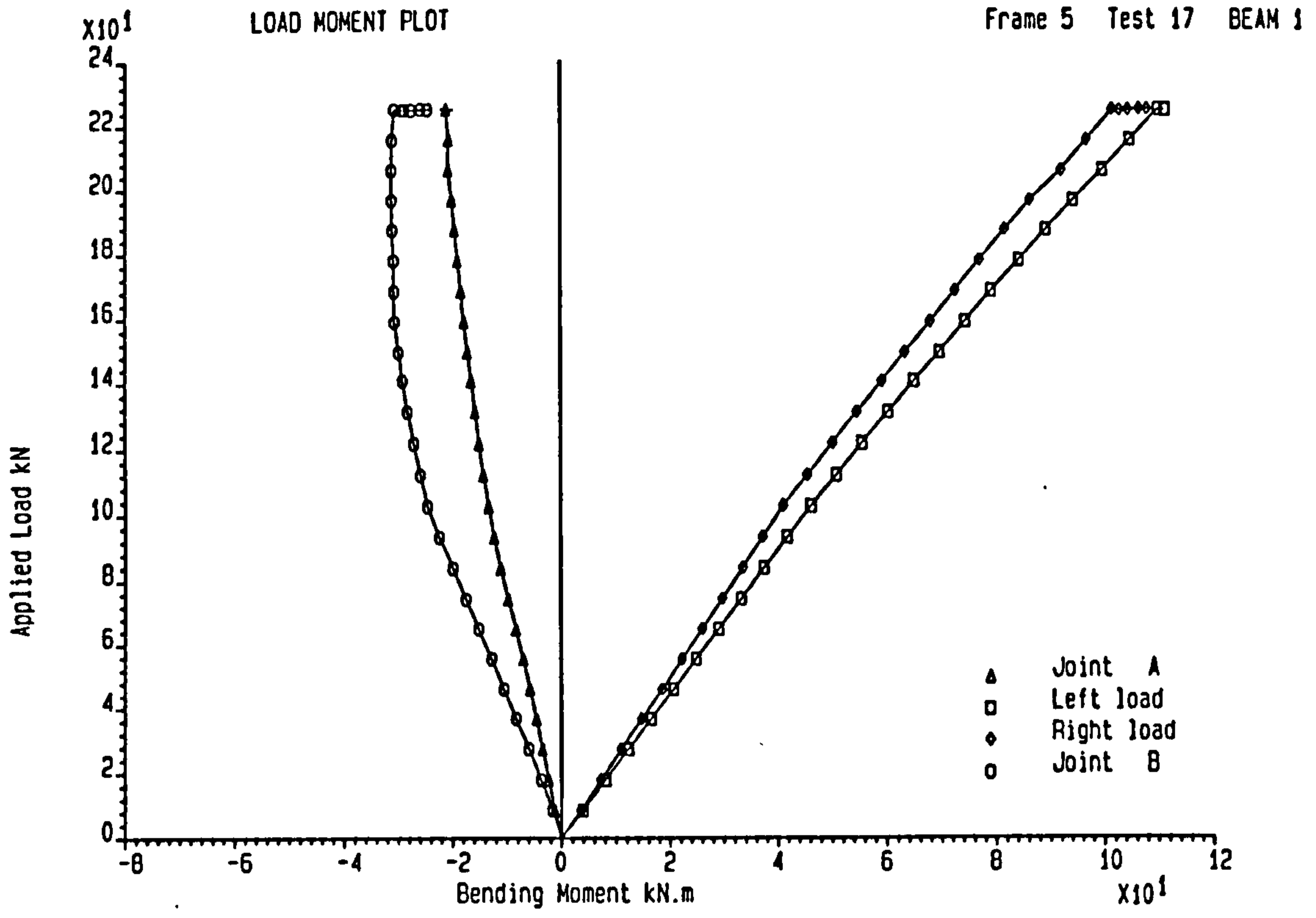


Figure 7.4 : Total Applied Load against Bending Moment on Beam 1  
in Test 17 of Frame 5

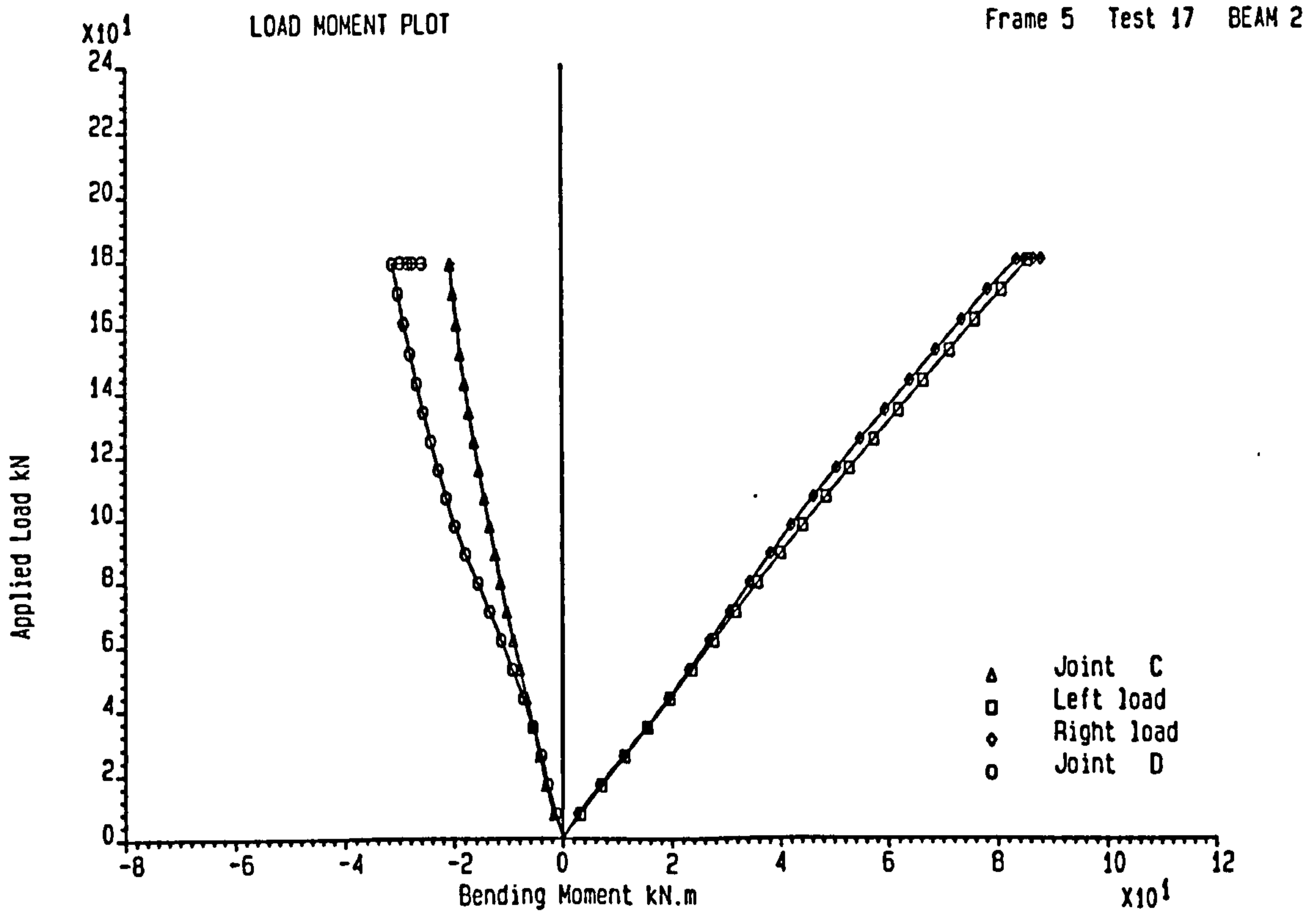


Figure 7.5 : Total Applied Load against Bending Moment on Beam 2  
in Test 17 of Frame 5

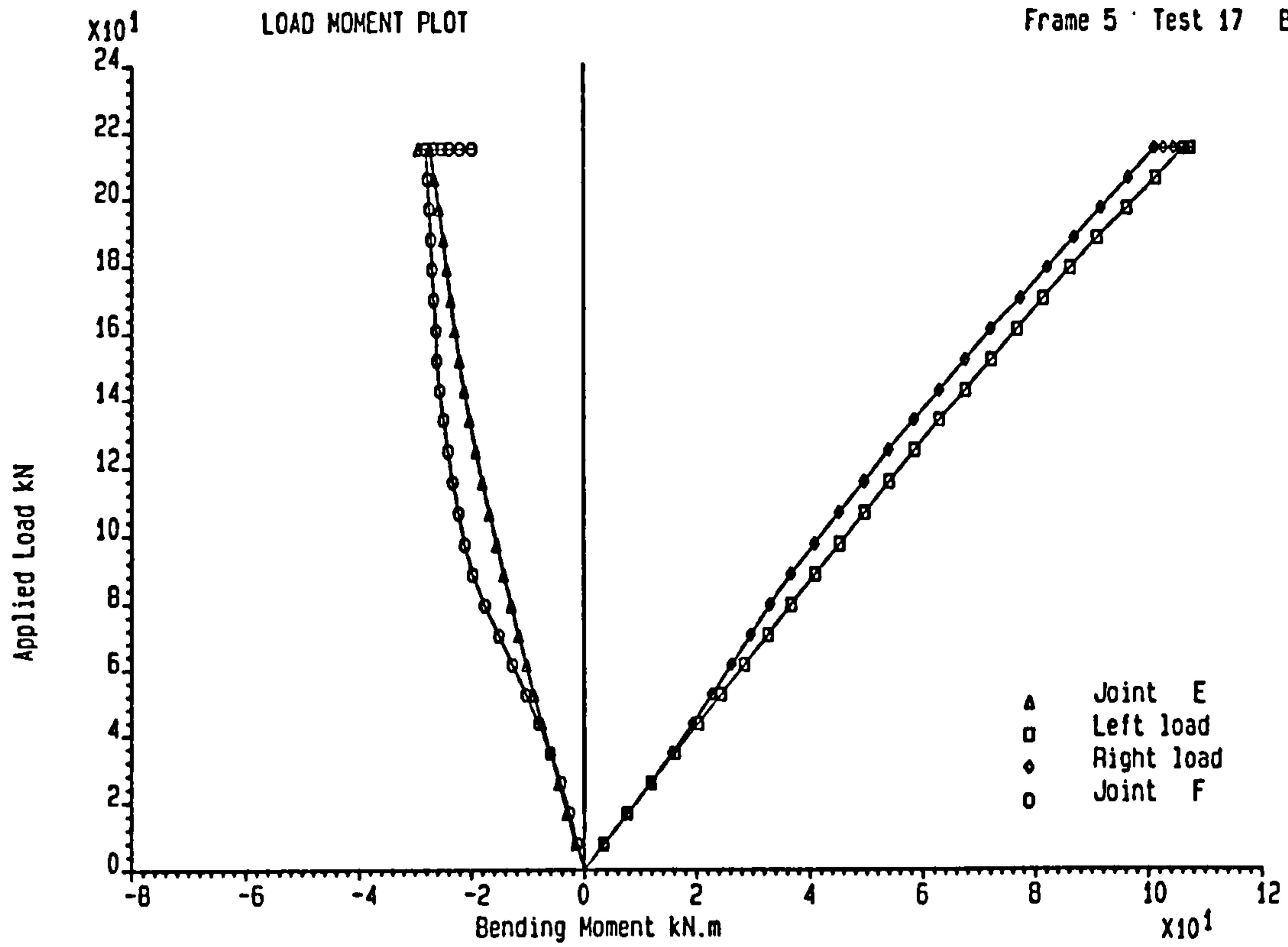


Figure 7.6 : Total Applied Load against Bending Moment on Beam 3  
in Test 17 of Frame 5

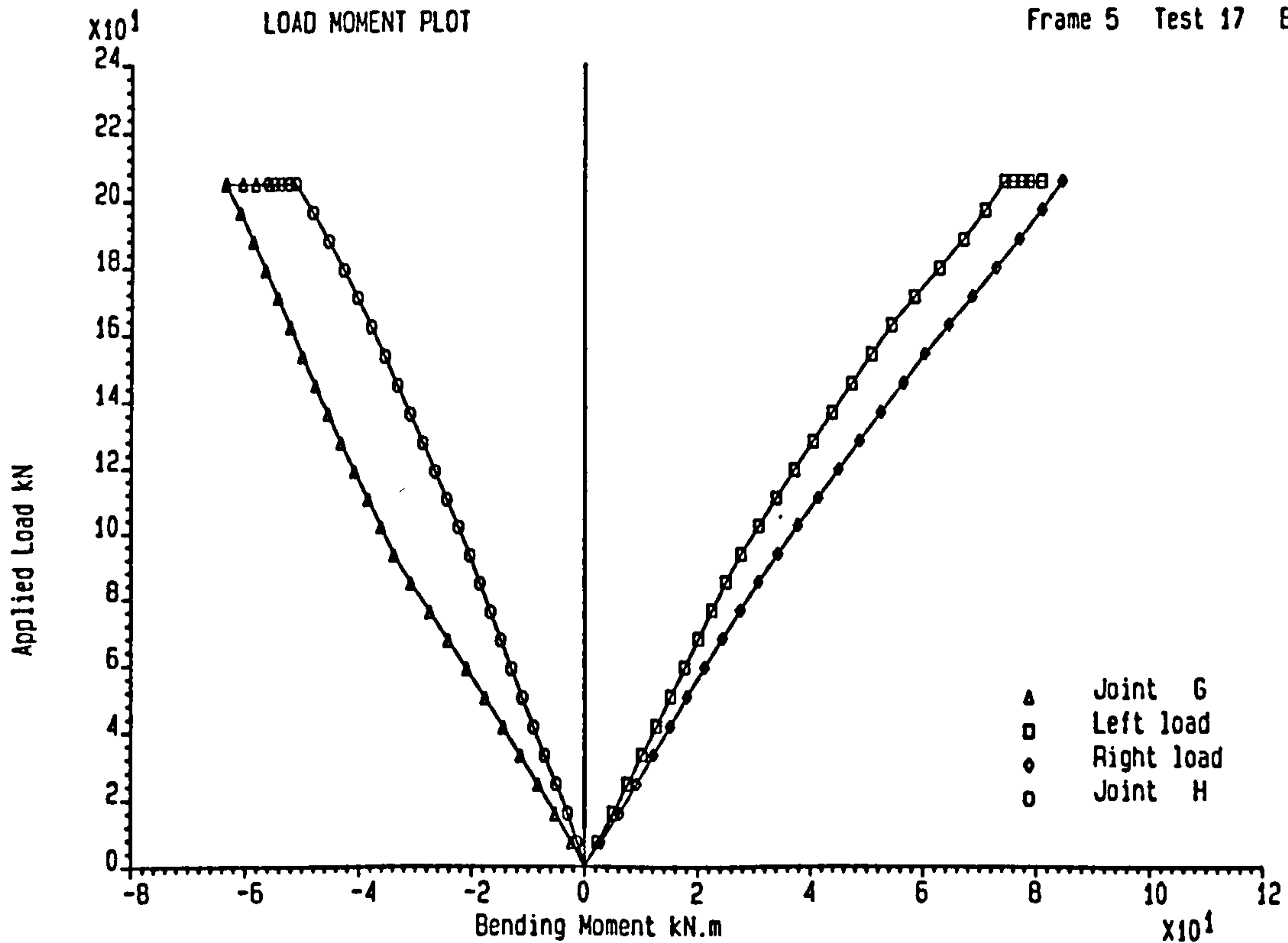


Figure 7.7 : Total Applied Load against Bending Moment on Beam 4  
in Test 17 of Frame 5

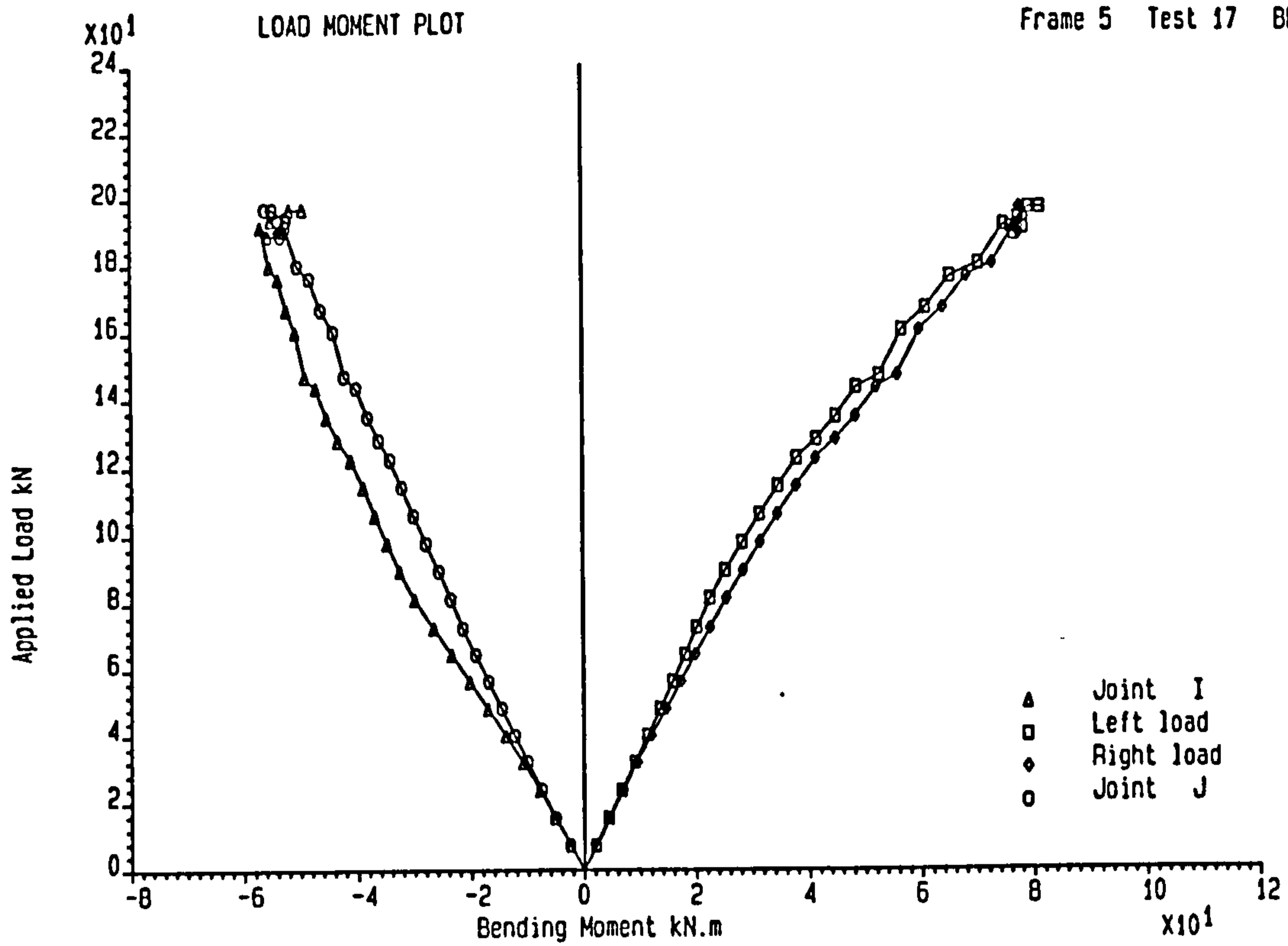


Figure 7.8 : Total Applied Load against Bending Moment on Beam 5  
in Test 17 of Frame 5

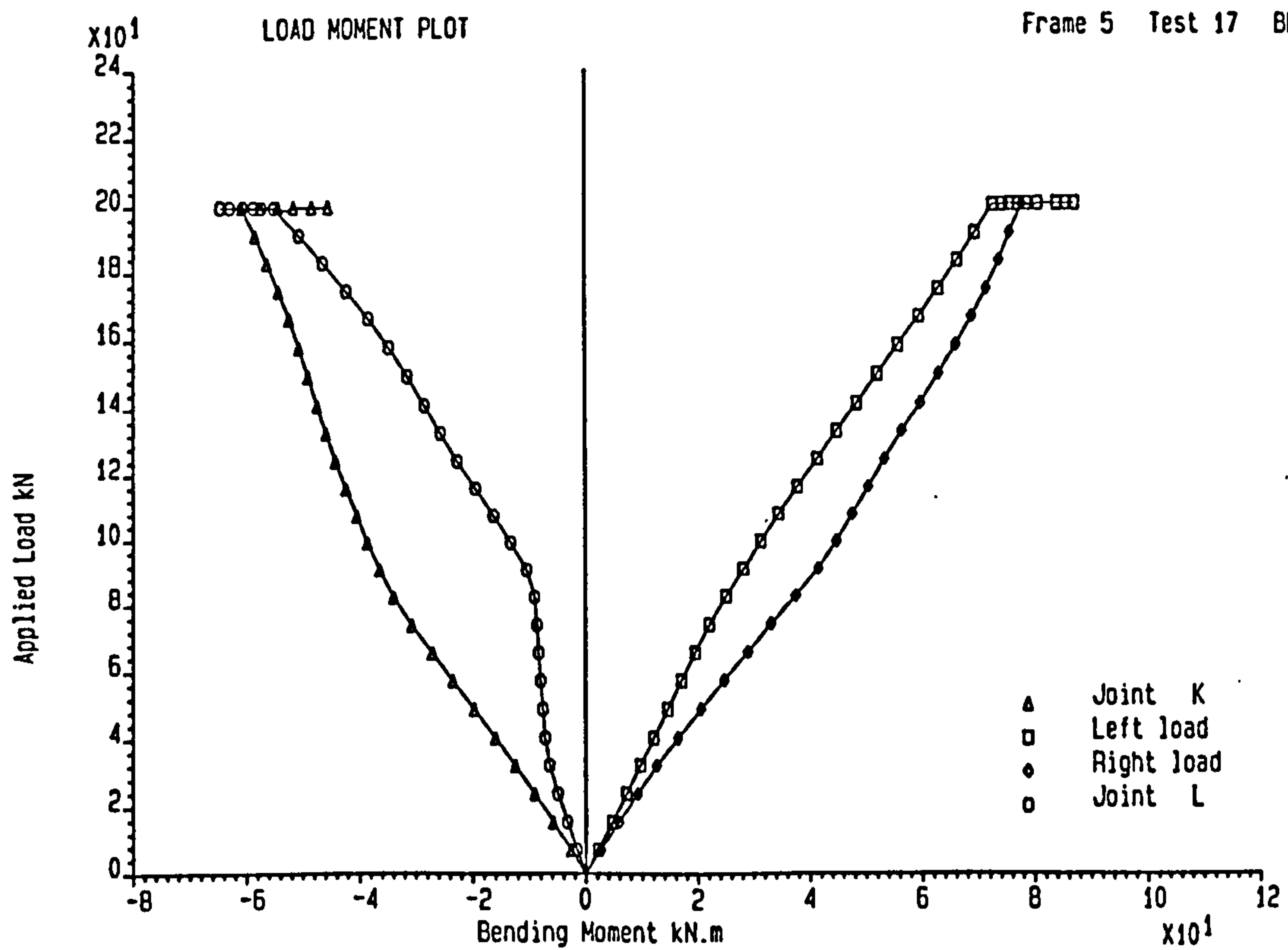


Figure 7.9 : Total Applied Load against Bending Moment on Beam 6  
in Test 17 of Frame 5

Run Number Plotted : 5 10 15 20 25

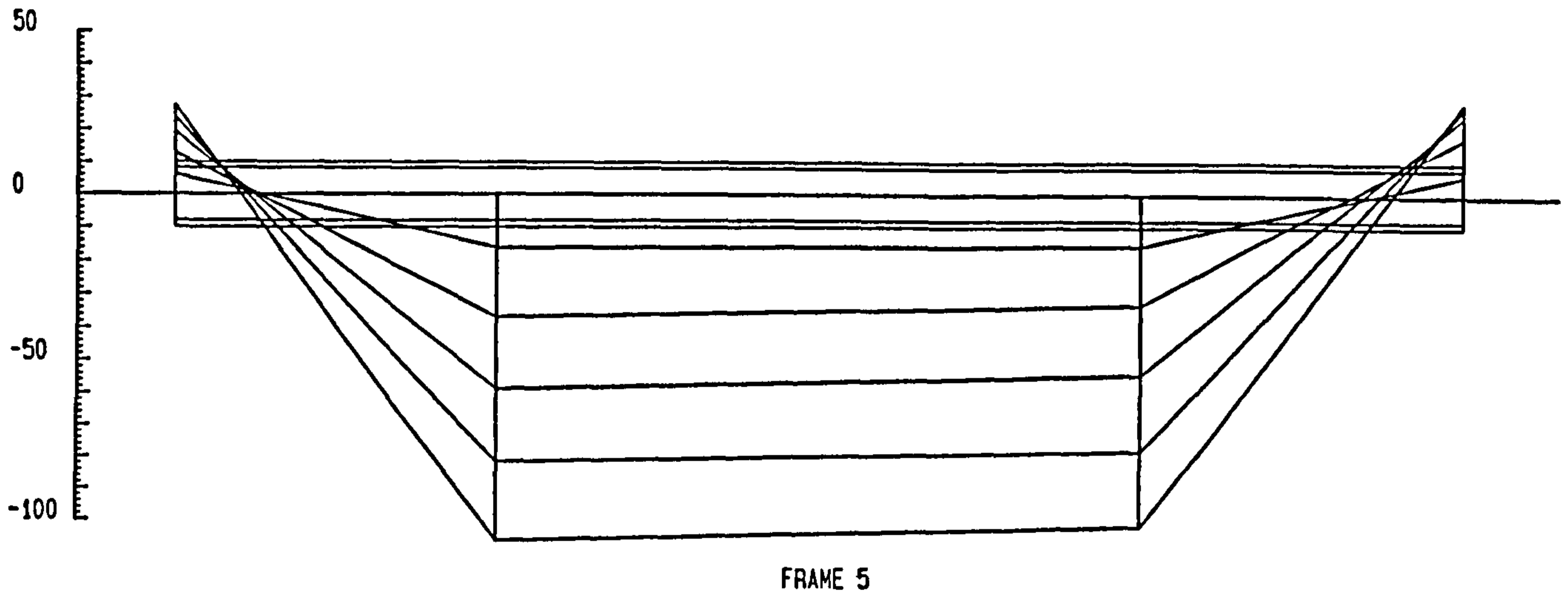


Figure 7.10 : Bending Moment Distribution around Beam 3 in Test 17 of Frame 5 up to End of Beam Load

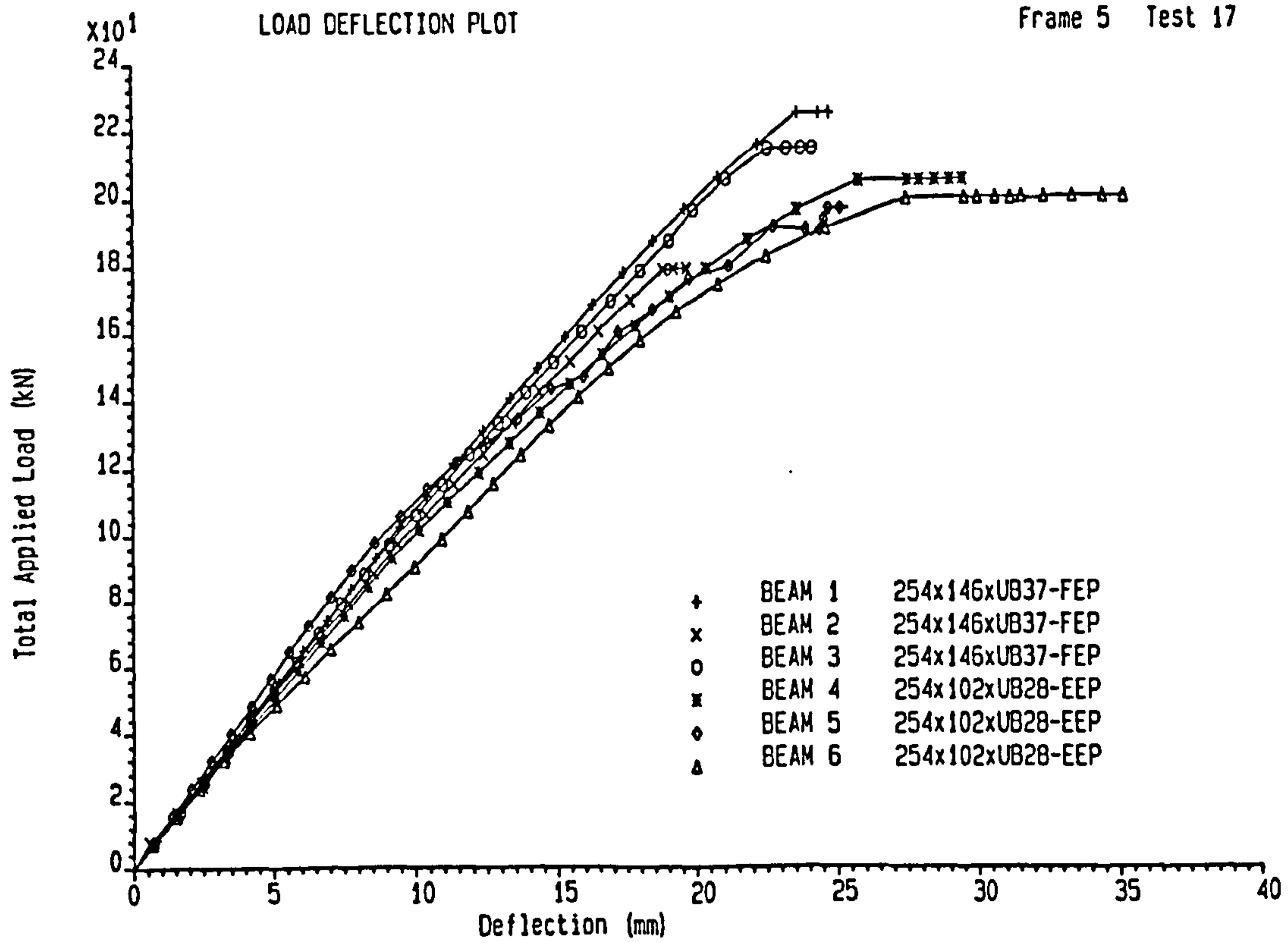
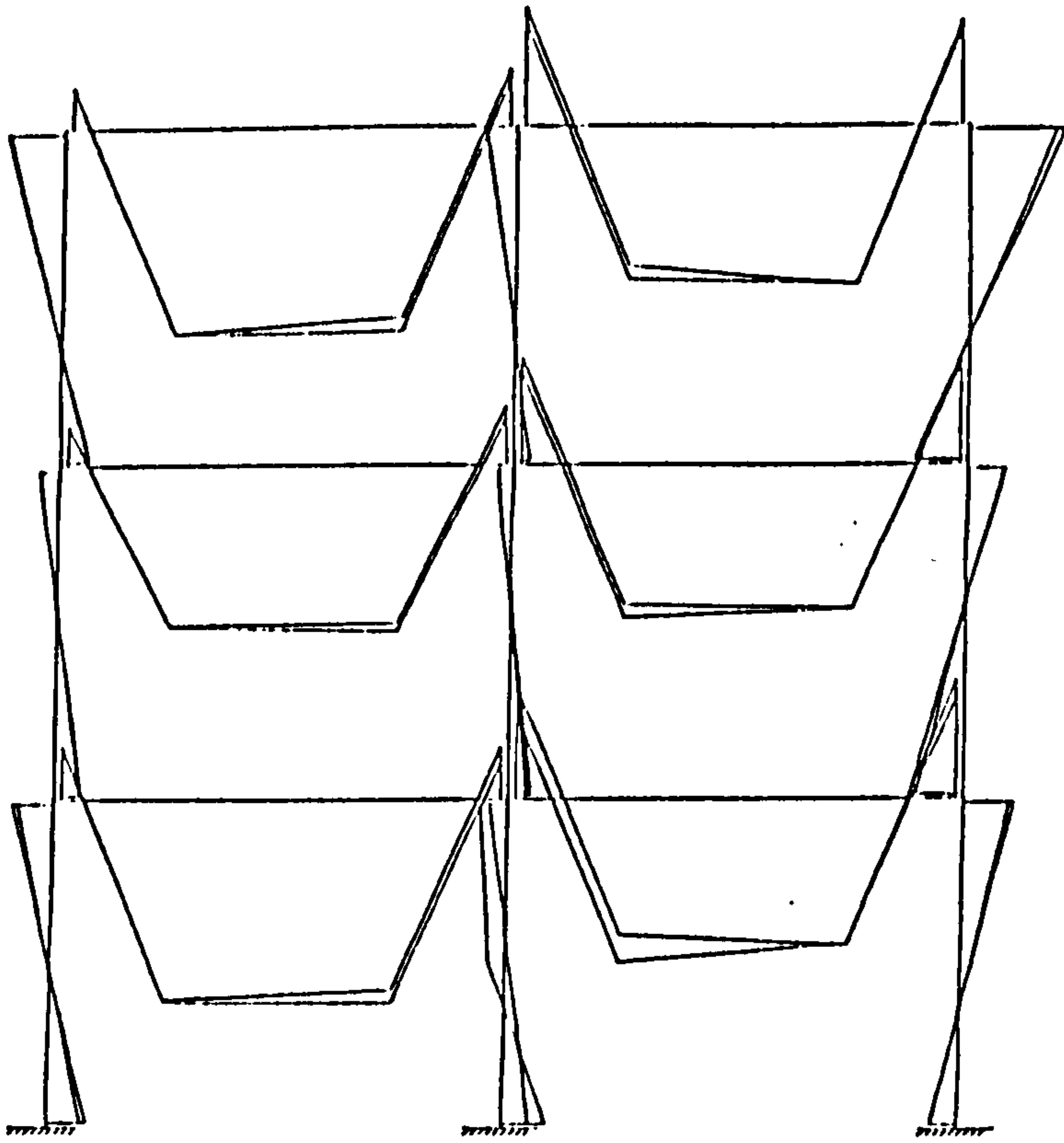


Figure 7.11 : Total Applied Load against Mid-Span Deflection on Six Beams in Test 17 of Frame 5

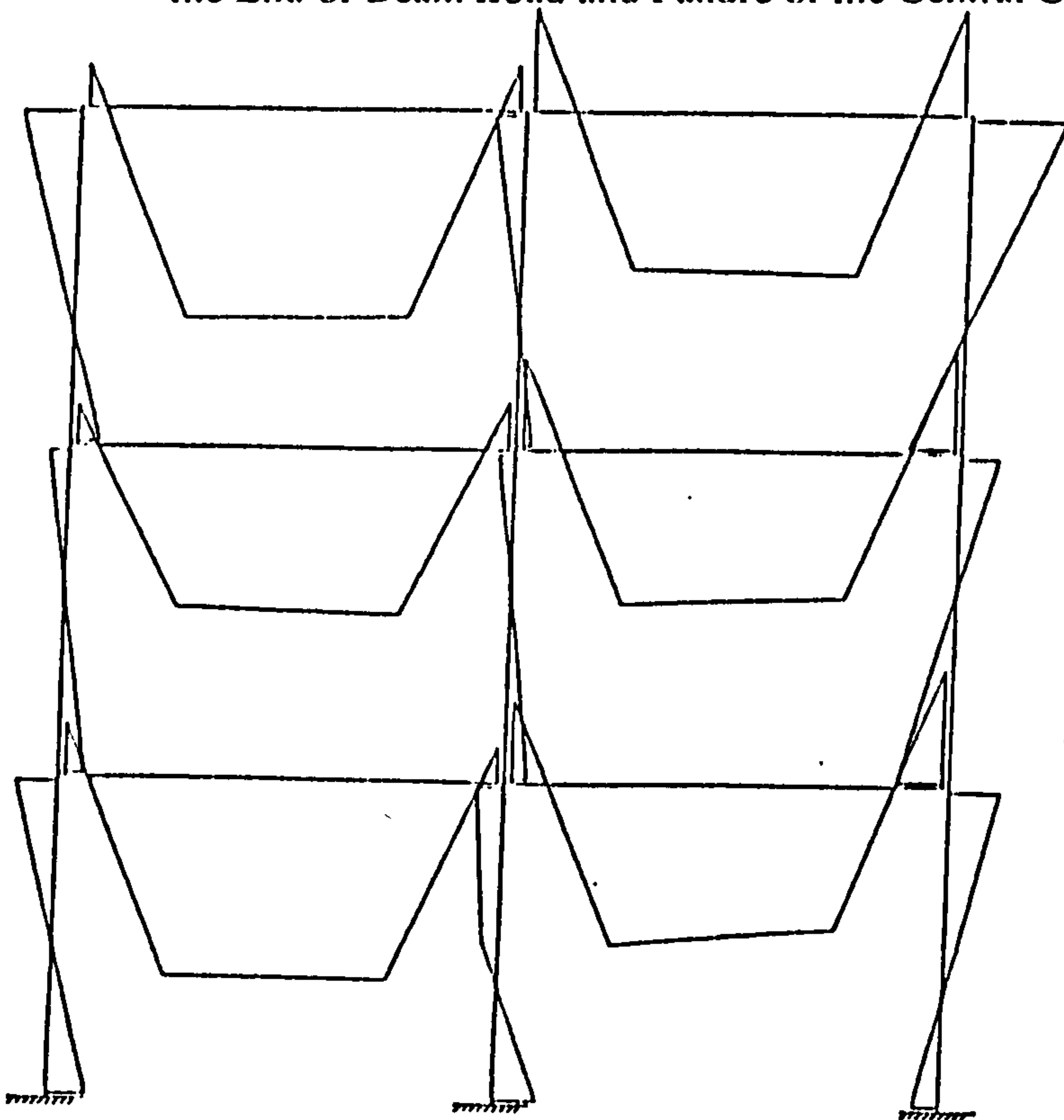


Scale : 0 50 100  
In kNm

Frame 5 Test 17

Run Numbers Plotted : 25 30

Figure 7.12 : Frame Moment around the Frame in Test 17 of Frame 5 in the End of Beam Load and Failure of the Central Column

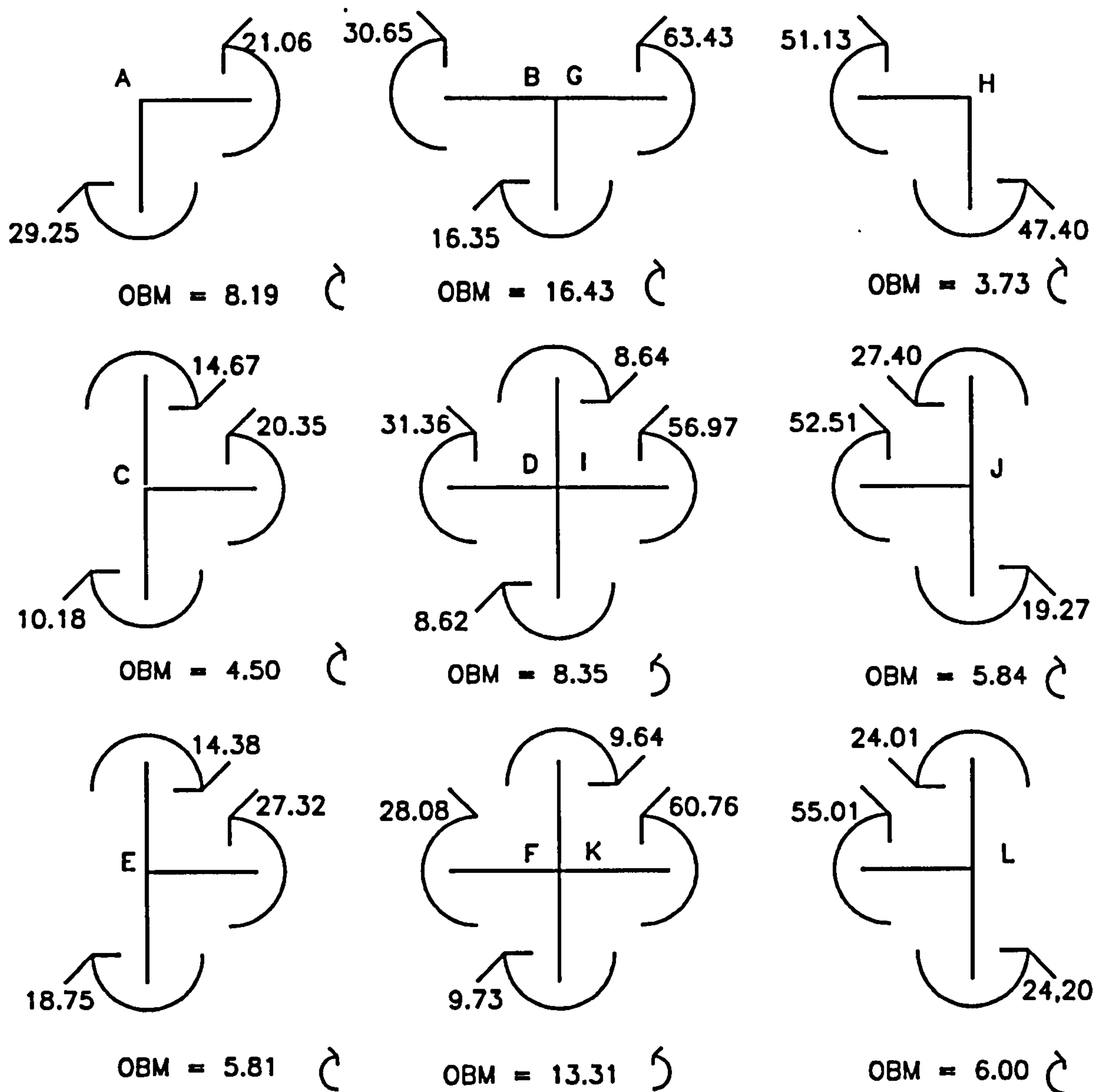


Scale : 0 50 100  
In kNm

Frame 5 Test 17

Run Numbers Plotted : 30

Figure 7.13 : Frame Moment around the Frame in Test 17 of Frame 5 in Failure of the Central Column



OBM = Out of balance moment

All values in kN.m units

FRAME 5

TEST 17

SCAN 25

Figure 7.14 : Moment Equilibrium Check in Frame 5 Test 17



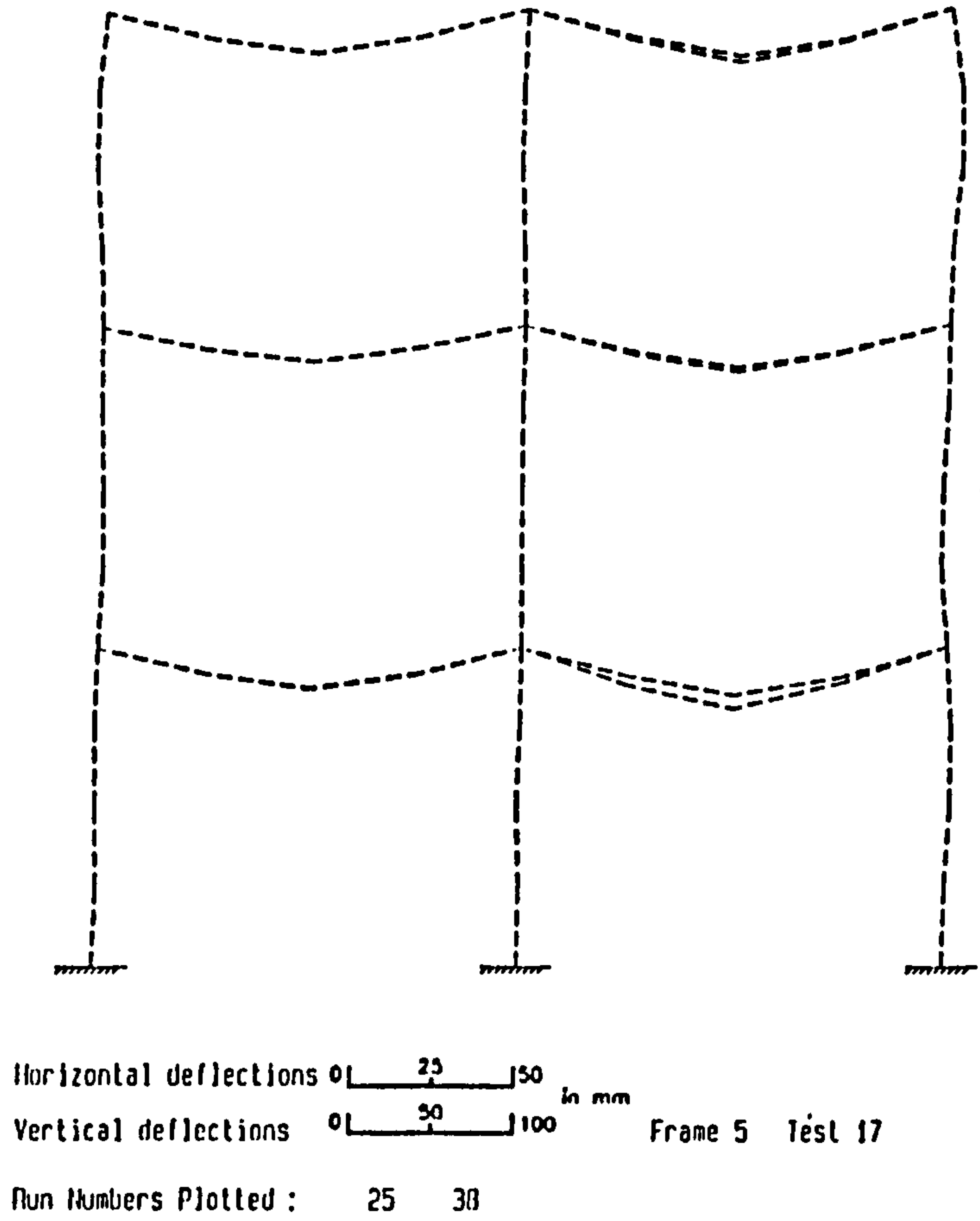


Figure 7.15 : Frame Deformation around the Frame in Test 17 of Frame 5 in the End of the Beam Load and Failure of the Central Column

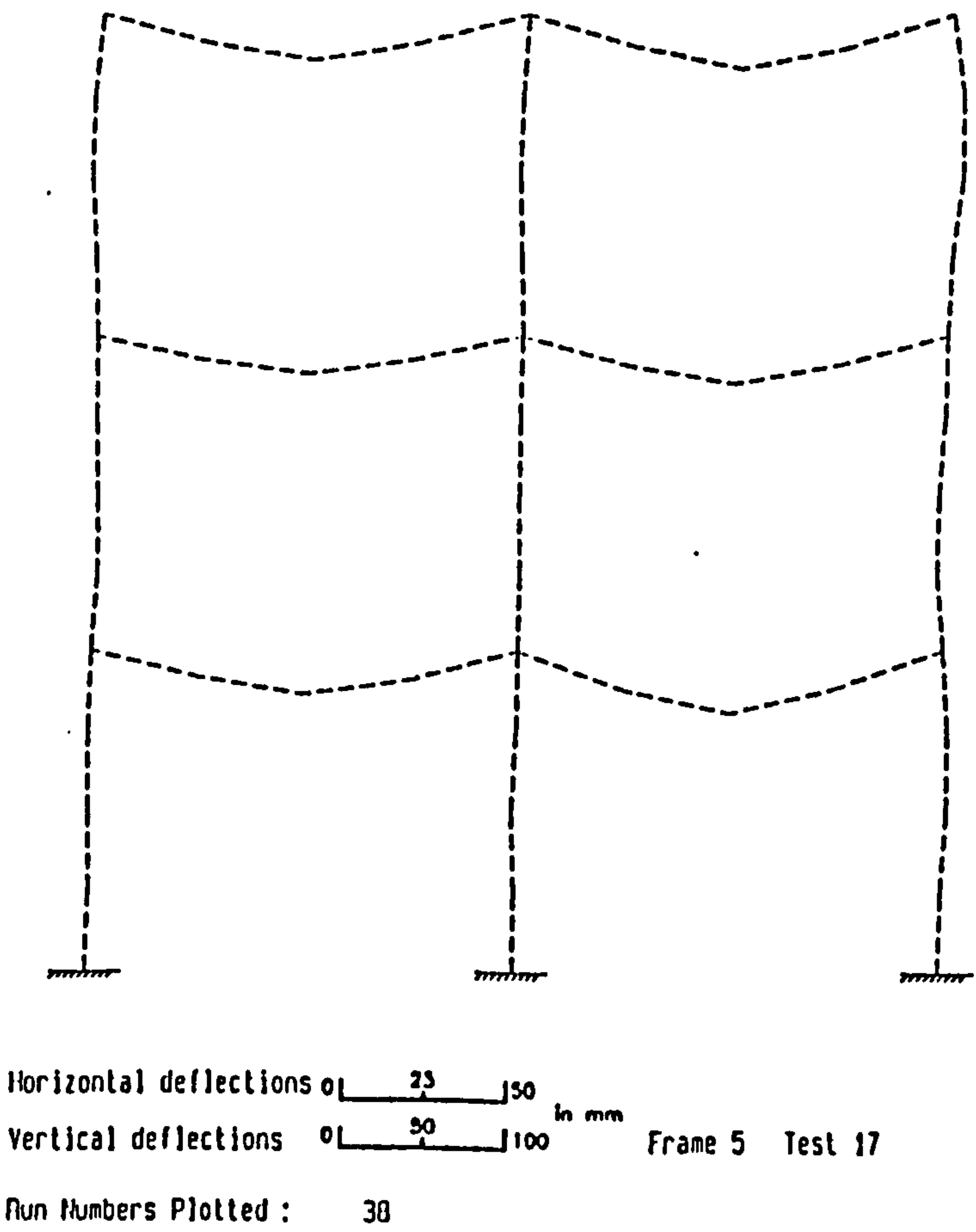


Figure 7.16 : Frame Deformation around the Frame in Test 17 of Frame 5 in Failure of the Central Column

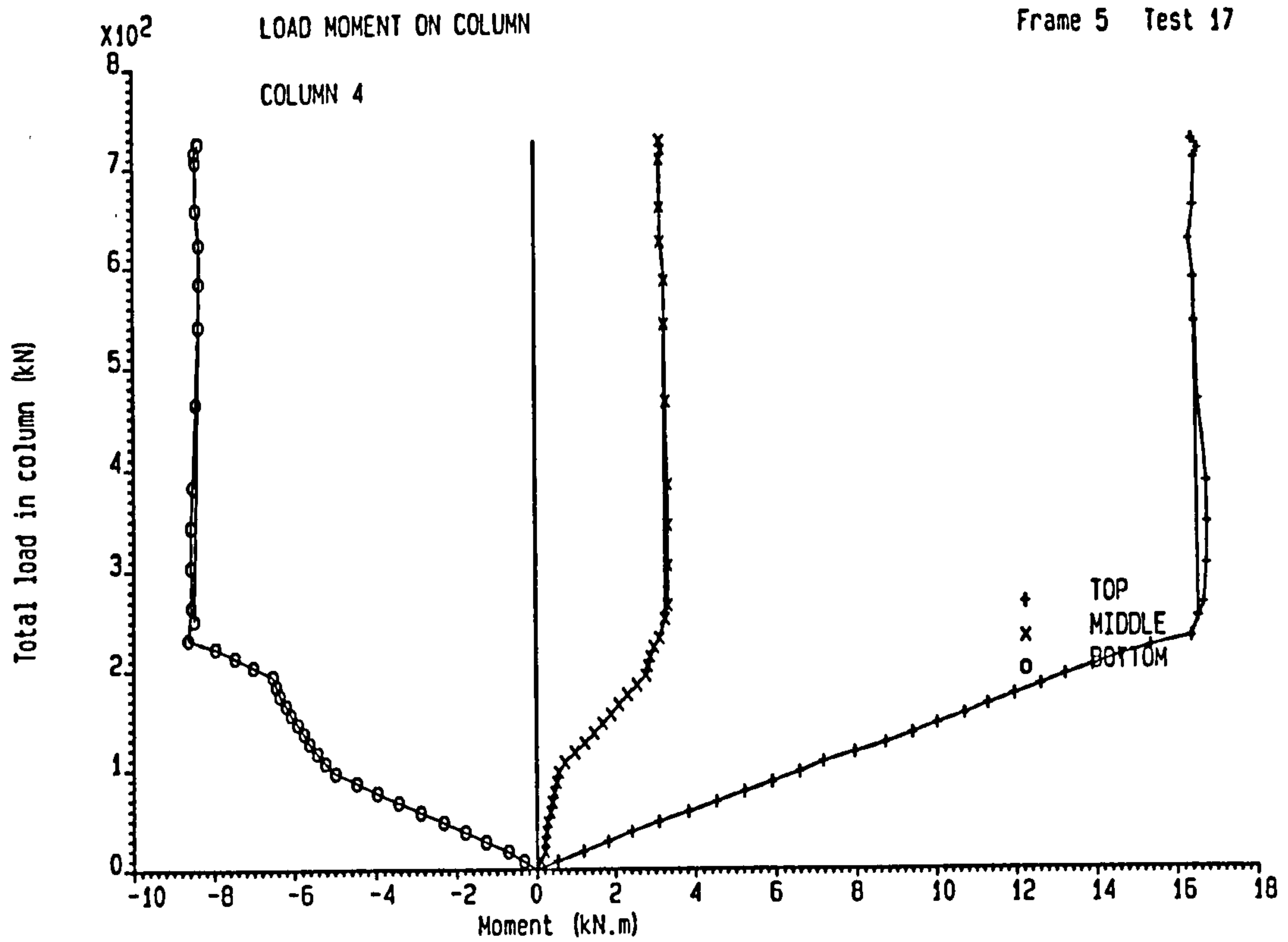


Figure 7.17 : Total Axial Load against the Column Moments at Different Locations at Column 4 in Test 17 of Frame 5

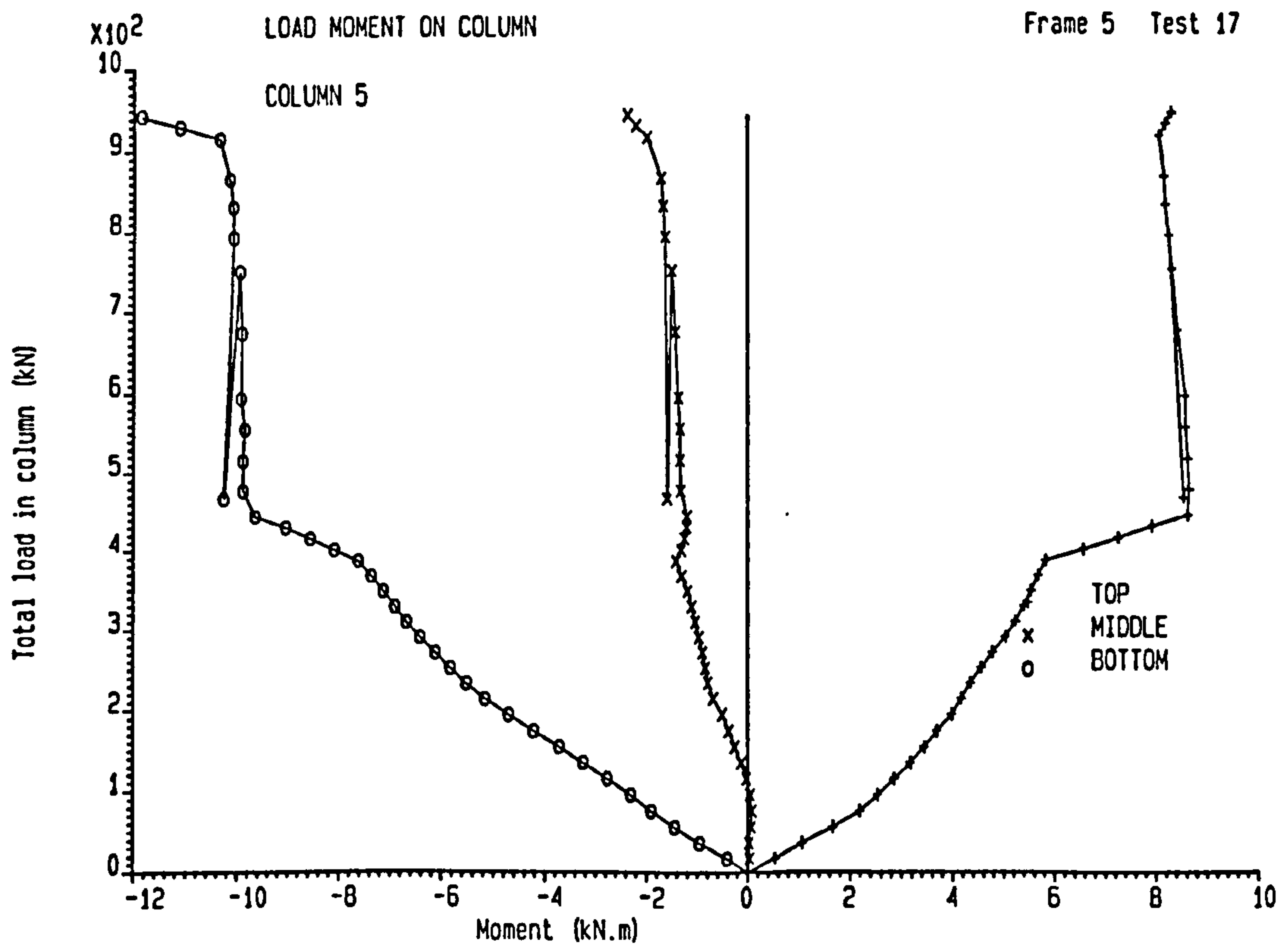


Figure 7.18 : Total Axial Load against the Column Moments at Different Locations at Column 5 in Test 17 of Frame 5

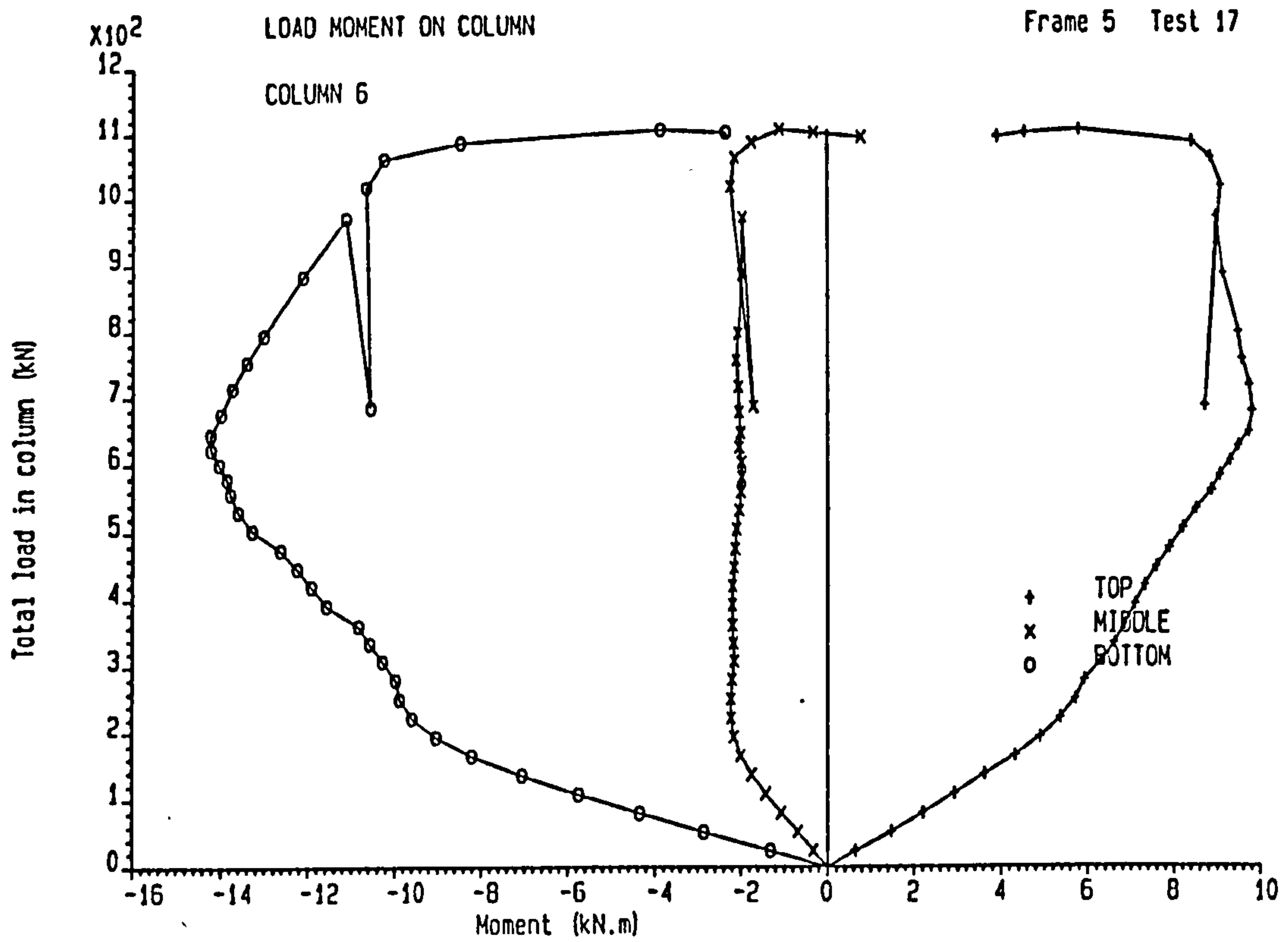


Figure 7.19 : Total Axial Load against the Column Moments at Different Locations at Column 6 in Test 17 of Frame 5

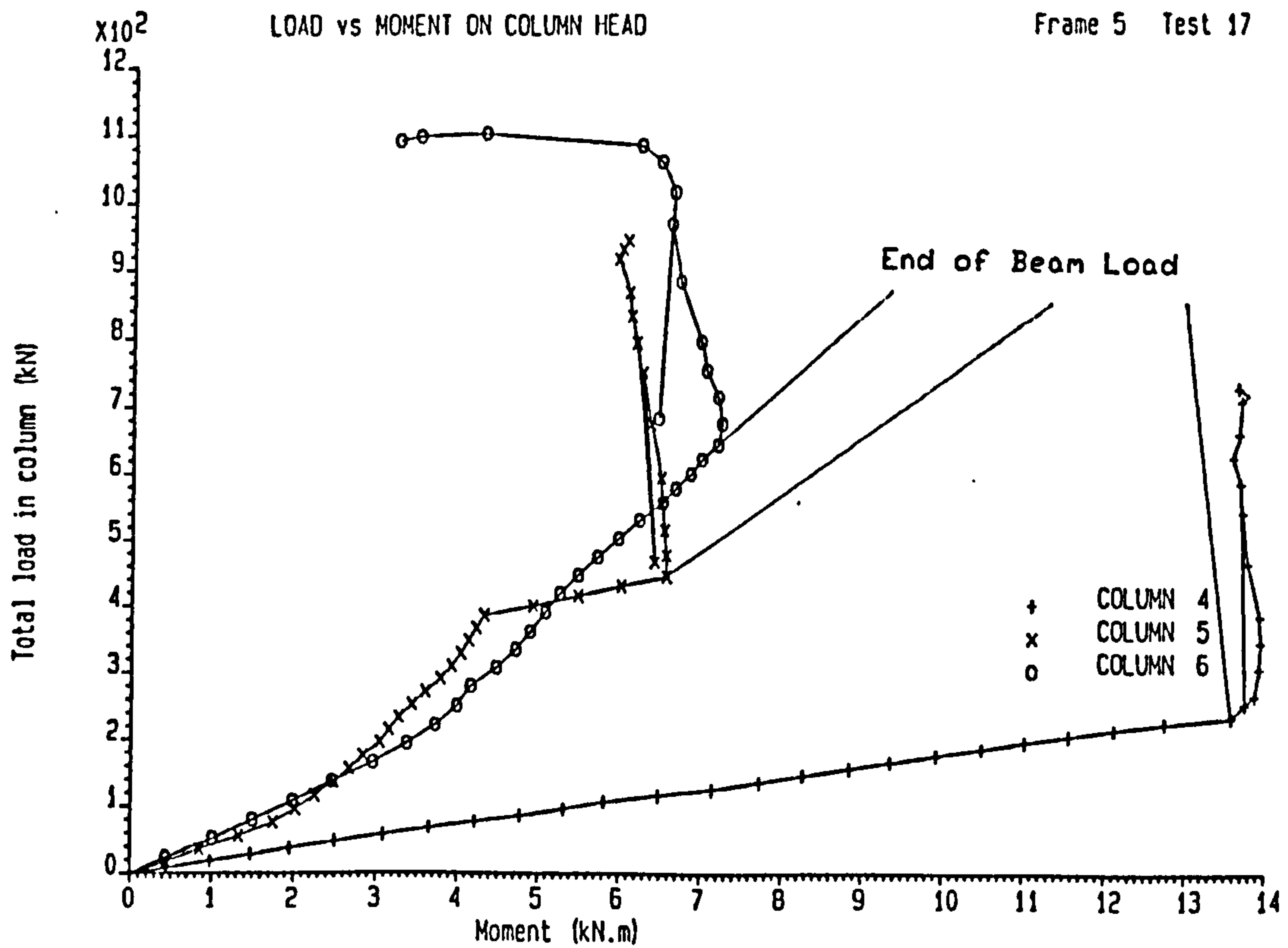


Figure 7.20 : Total Axial Load against the Column Head Moments at Three Lifts of the Central Column (Position 2) in Test 17 of Frame 5

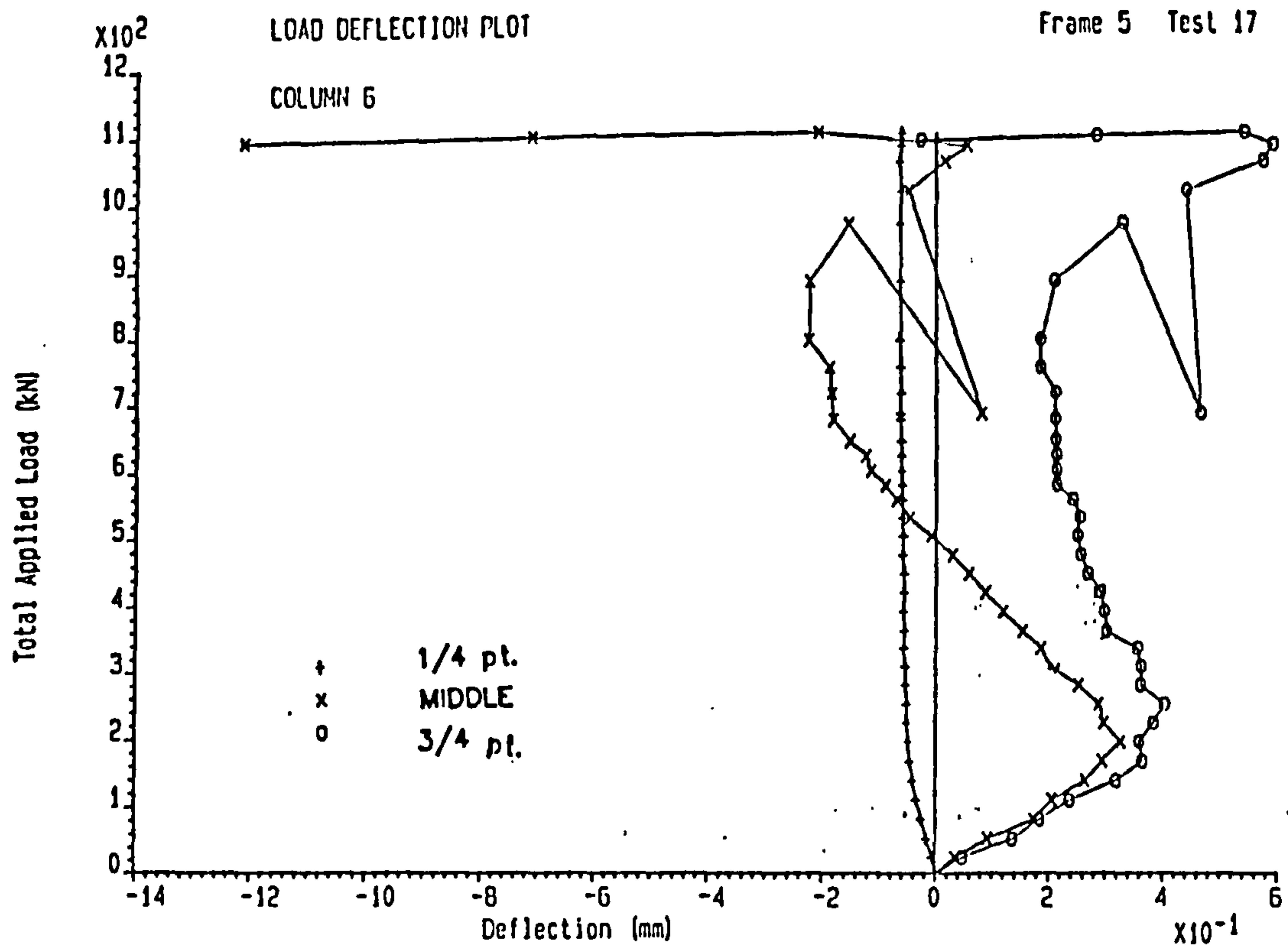


Figure 7.21 : Total Axial Load against the Column Deflections at Different Locations at Column 6 in Test 17 of Frame 5

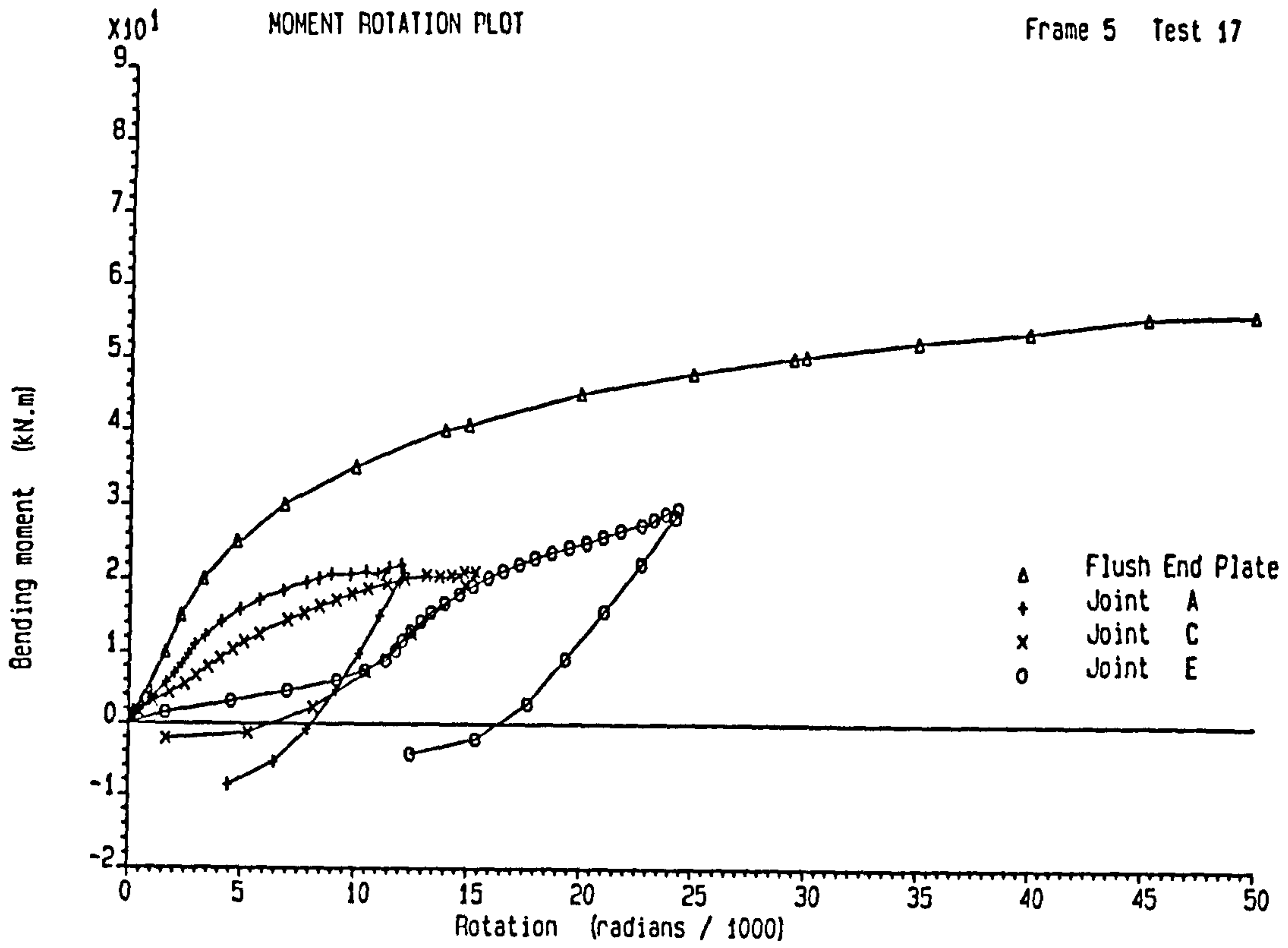


Figure 7.22 : Moment Rotation Curve for Test 17 of Frame 5  
(External Joints A, C and E)

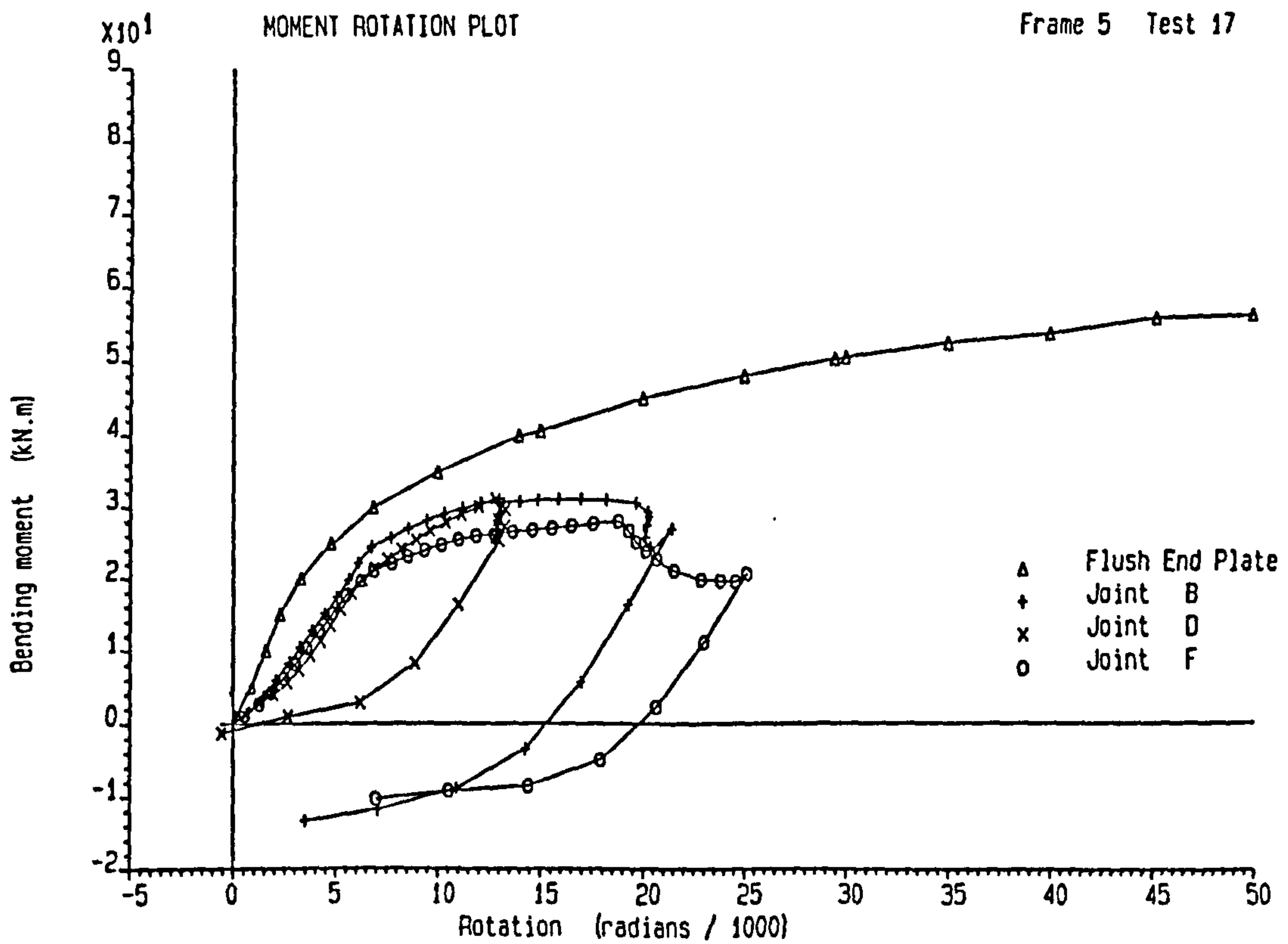


Figure 7.23 : Moment Rotation Curve for Test 17 of Frame 5  
(Internal Joints B, D and F)

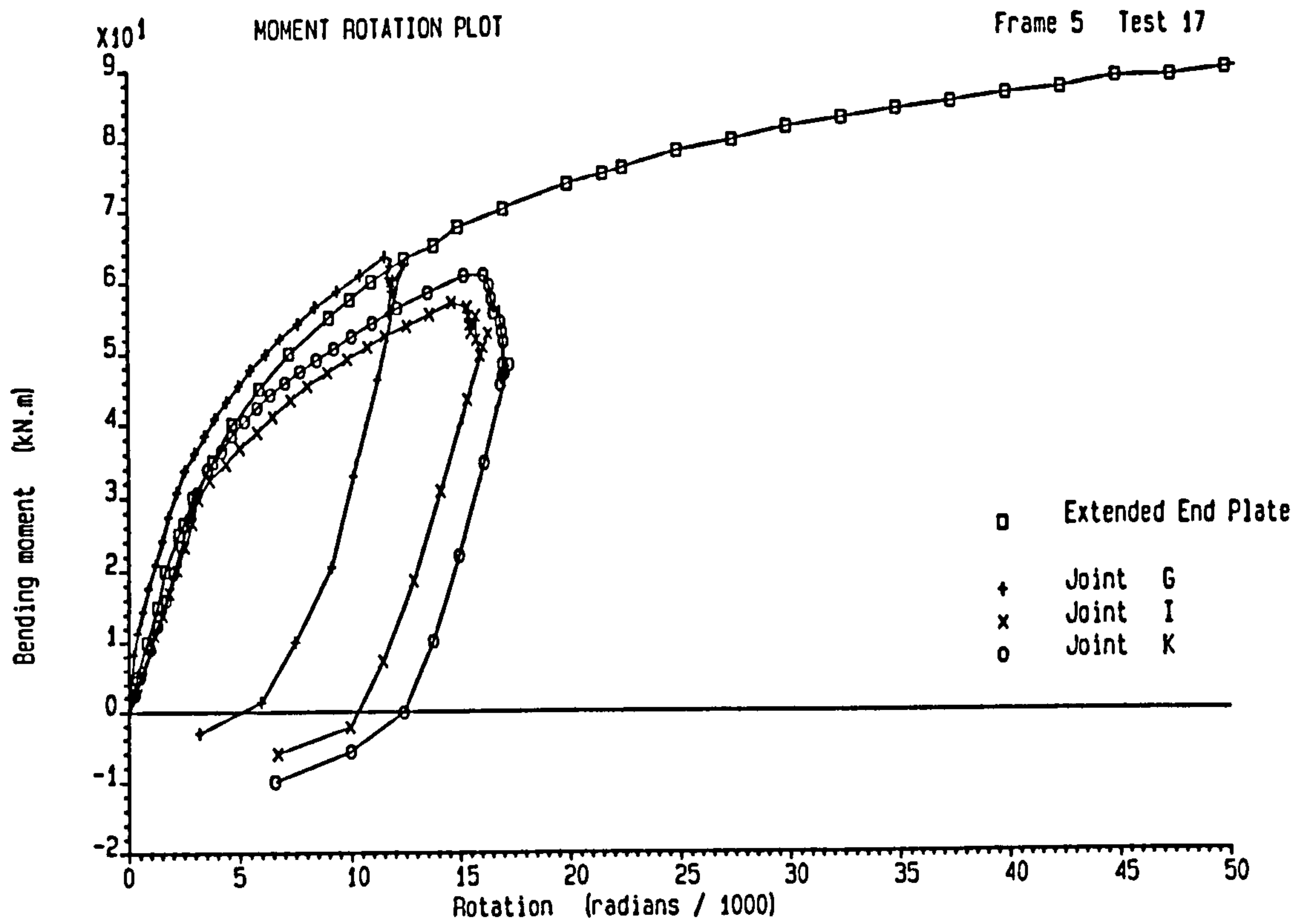


Figure 7.24 : Moment Rotation Curve for Test 17 of Frame 5  
(Internal Joints G, I and K)

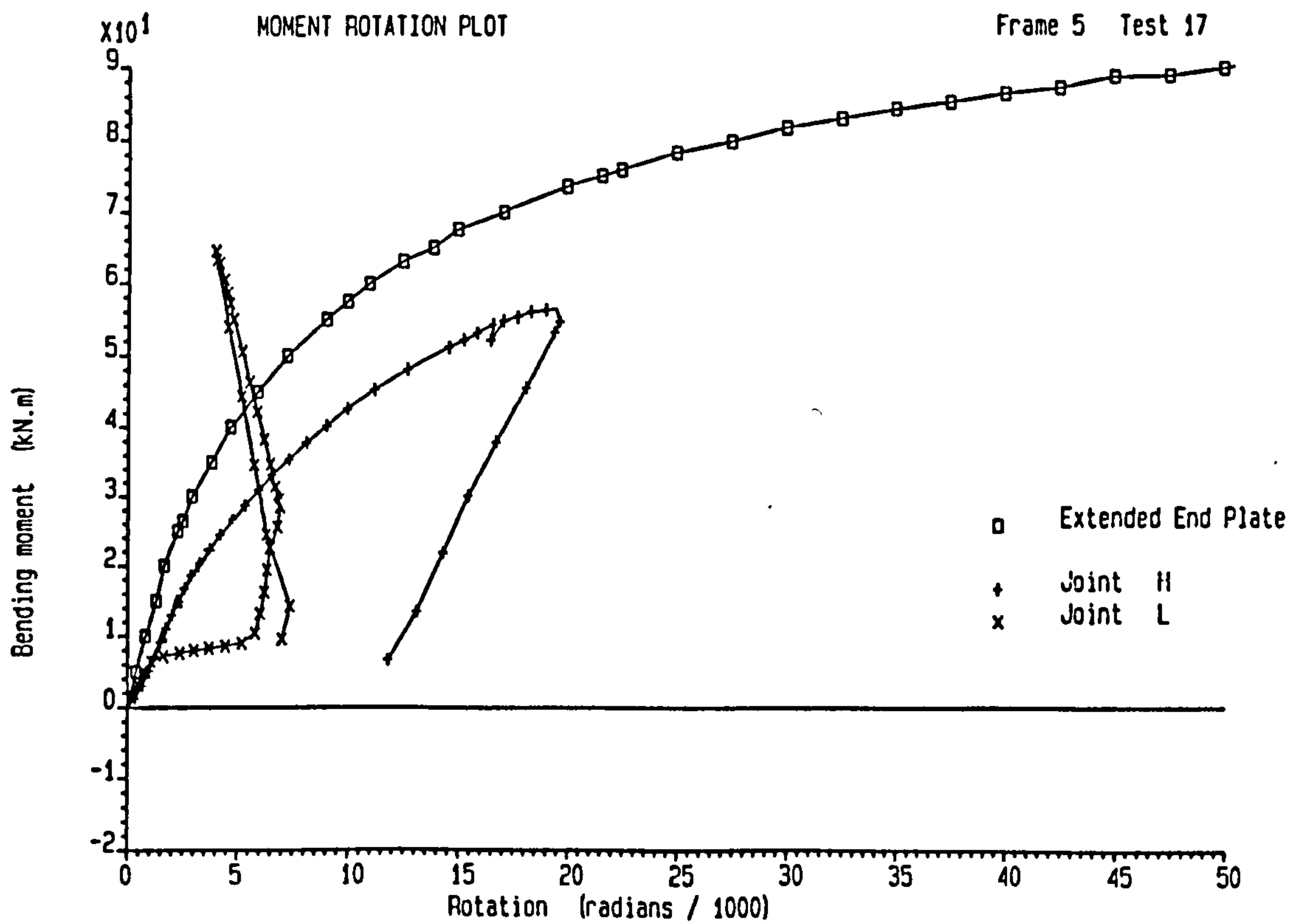


Figure 7.25 : Moment Rotation Curve for Test 17 of Frame 5  
(External Joints H and L)

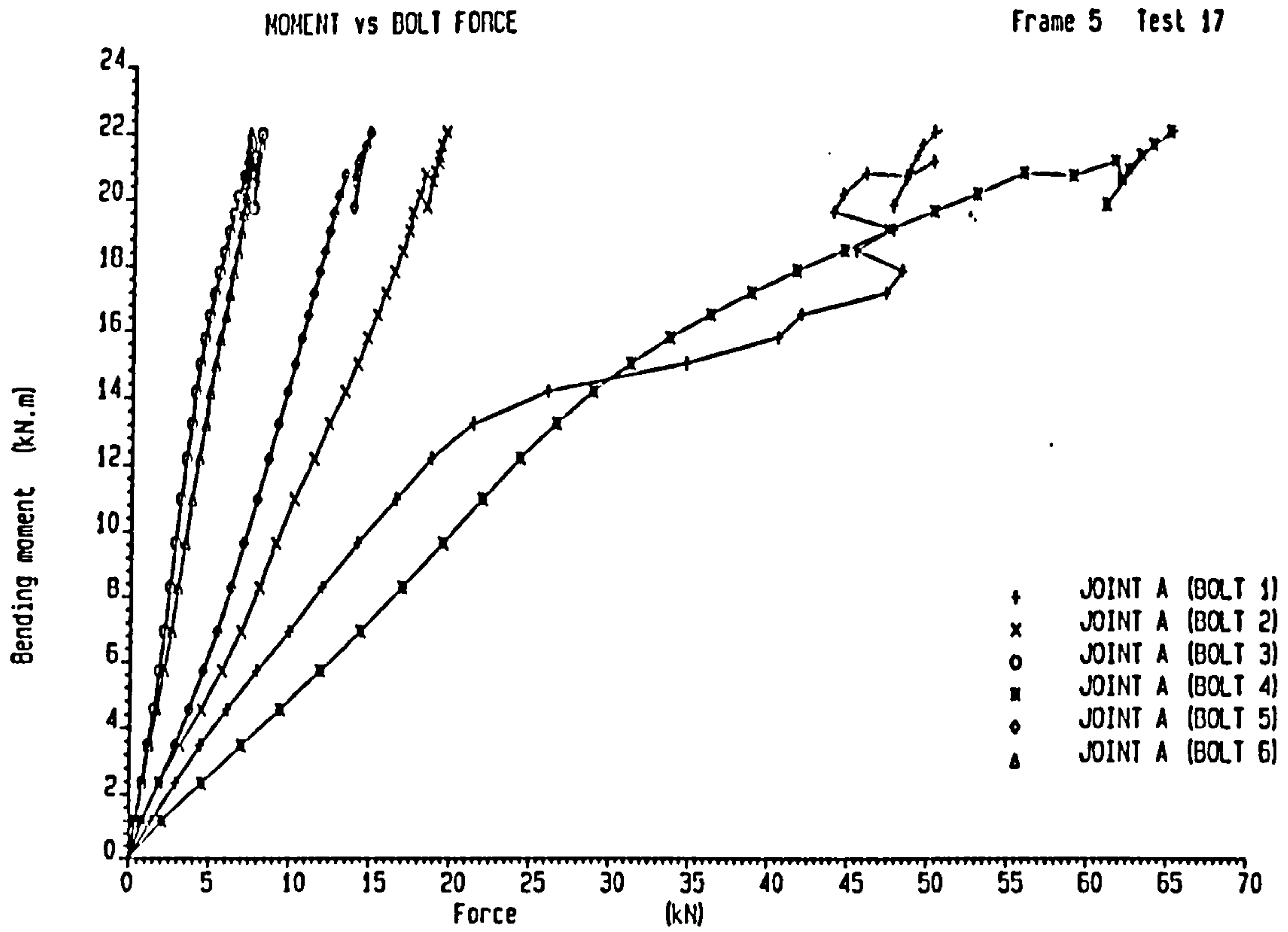


Figure 7.26 : Moment against Bolt Forces at Joint A for Test 17 of Frame 5

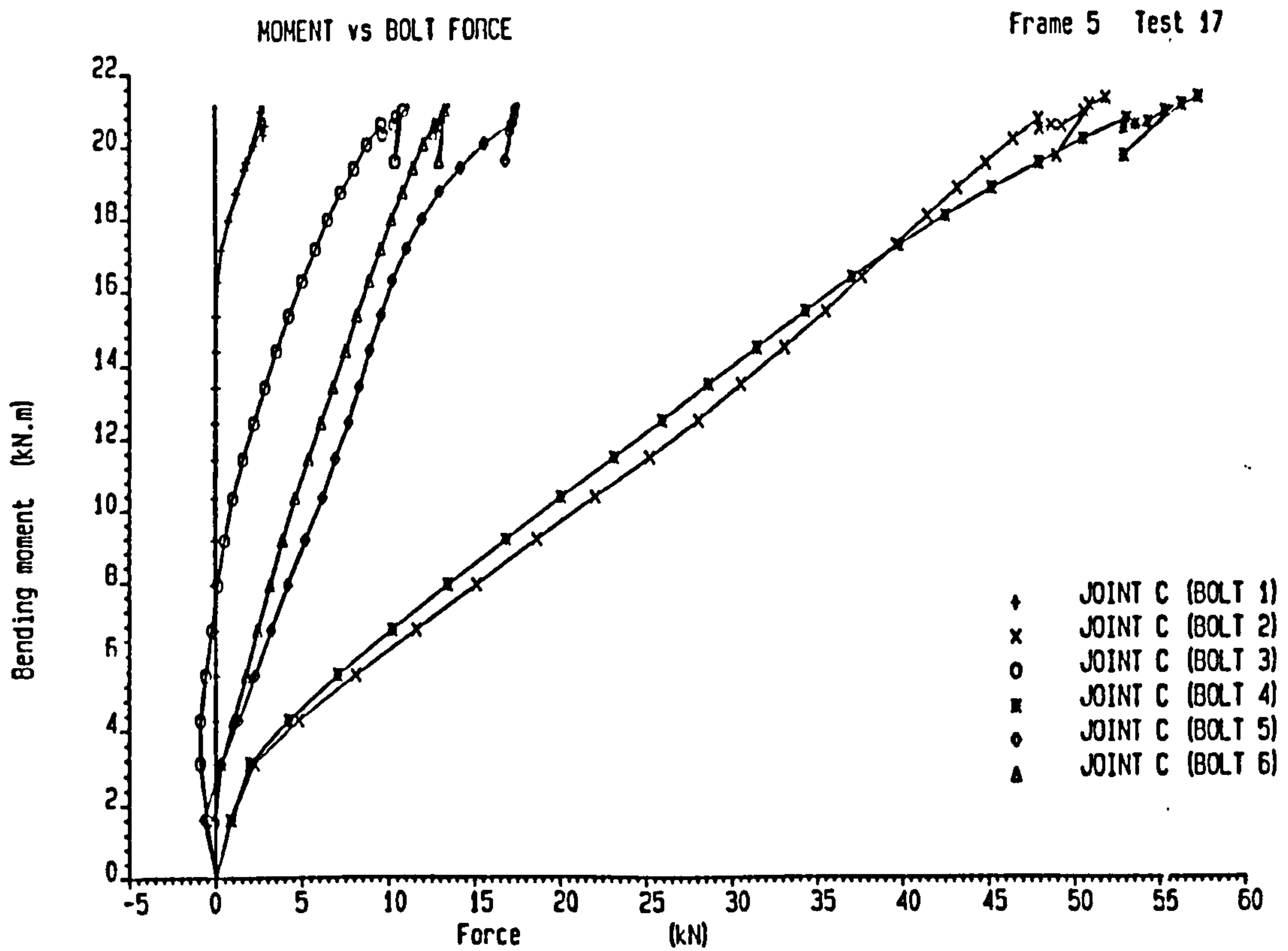


Figure 7.27 : Moment against Bolt Forces at Joint C for Test 17 of Frame 5

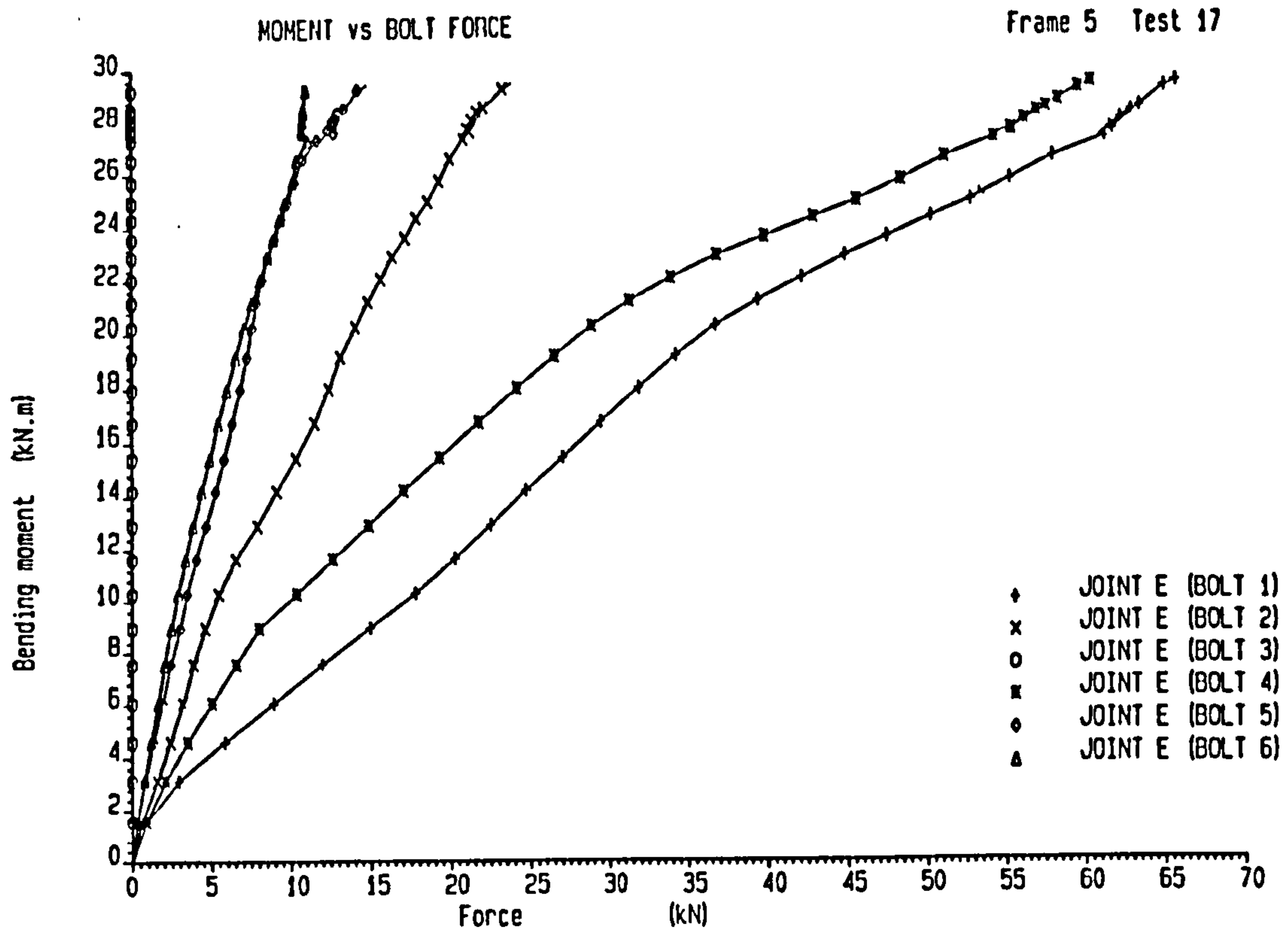


Figure 7.28 : Moment against Bolt Forces at Joint E for Test 17 of Frame 5

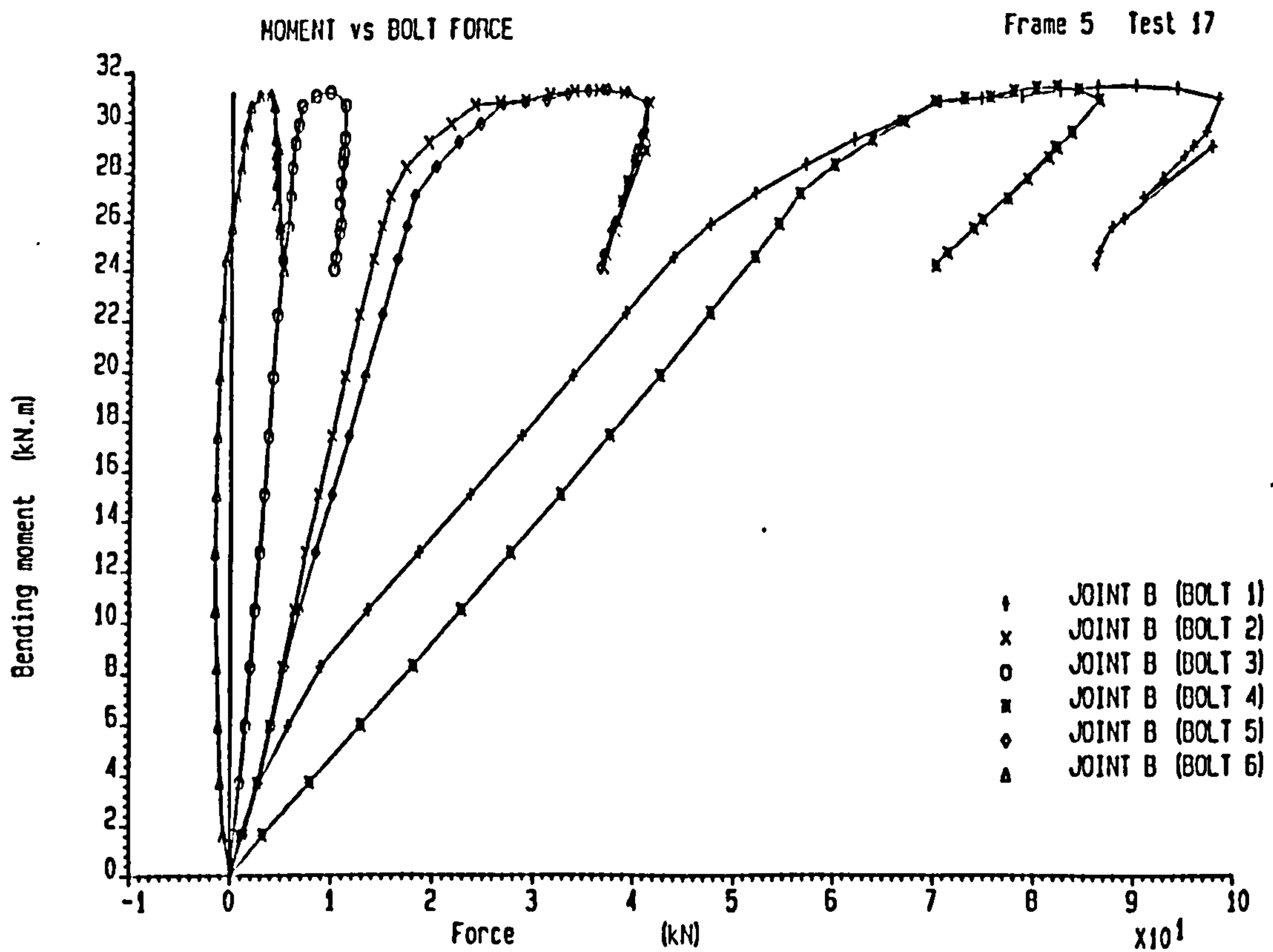


Figure 7.29 : Moment against Bolt Forces at Joint B for Test 17 of Frame 5



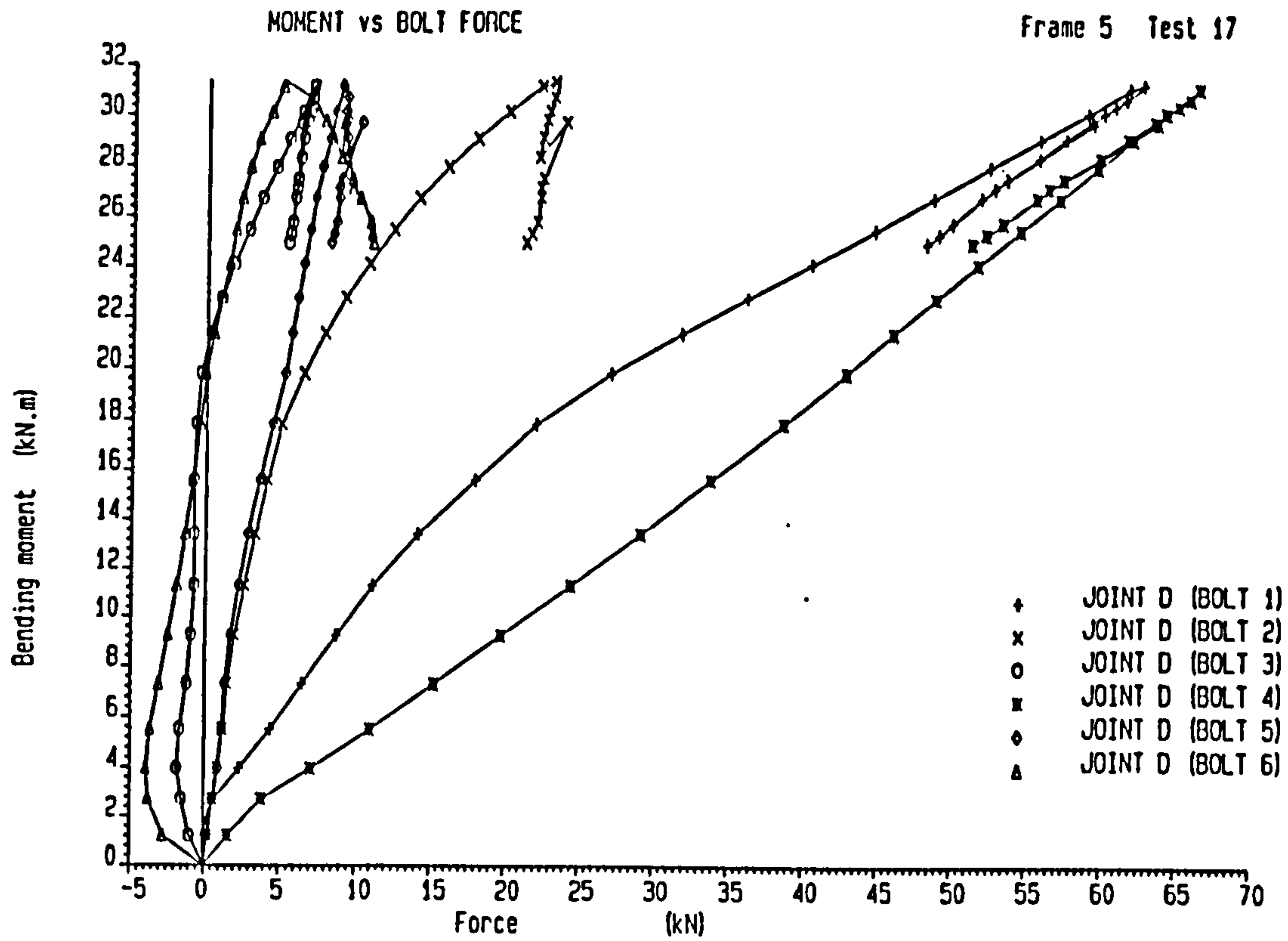


Figure 7.30 : Moment against Bolt Forces at Joint D for Test 17 of Frame 5

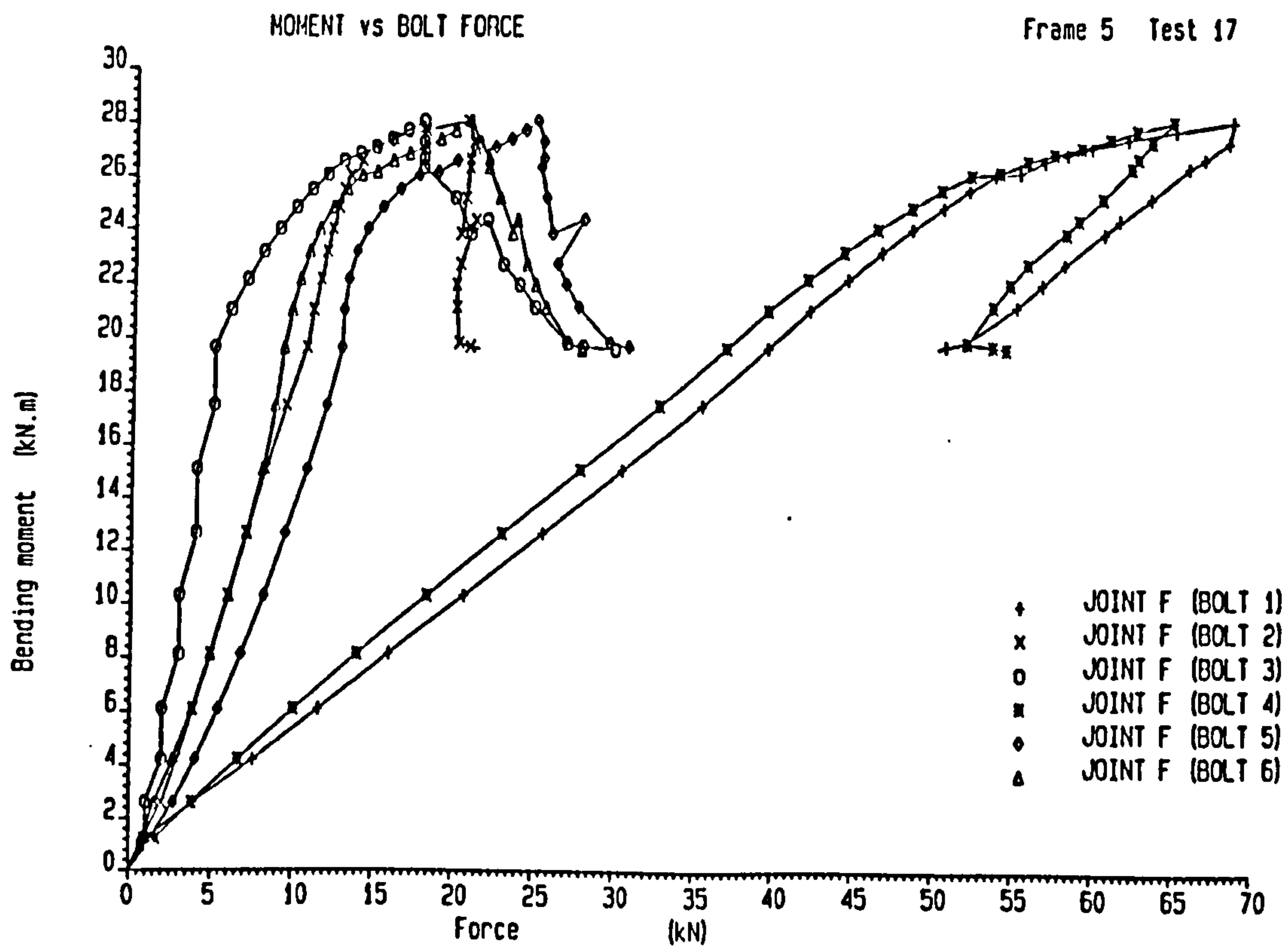


Figure 7.31 : Moment against Bolt Forces at Joint F for Test 17 of Frame 5

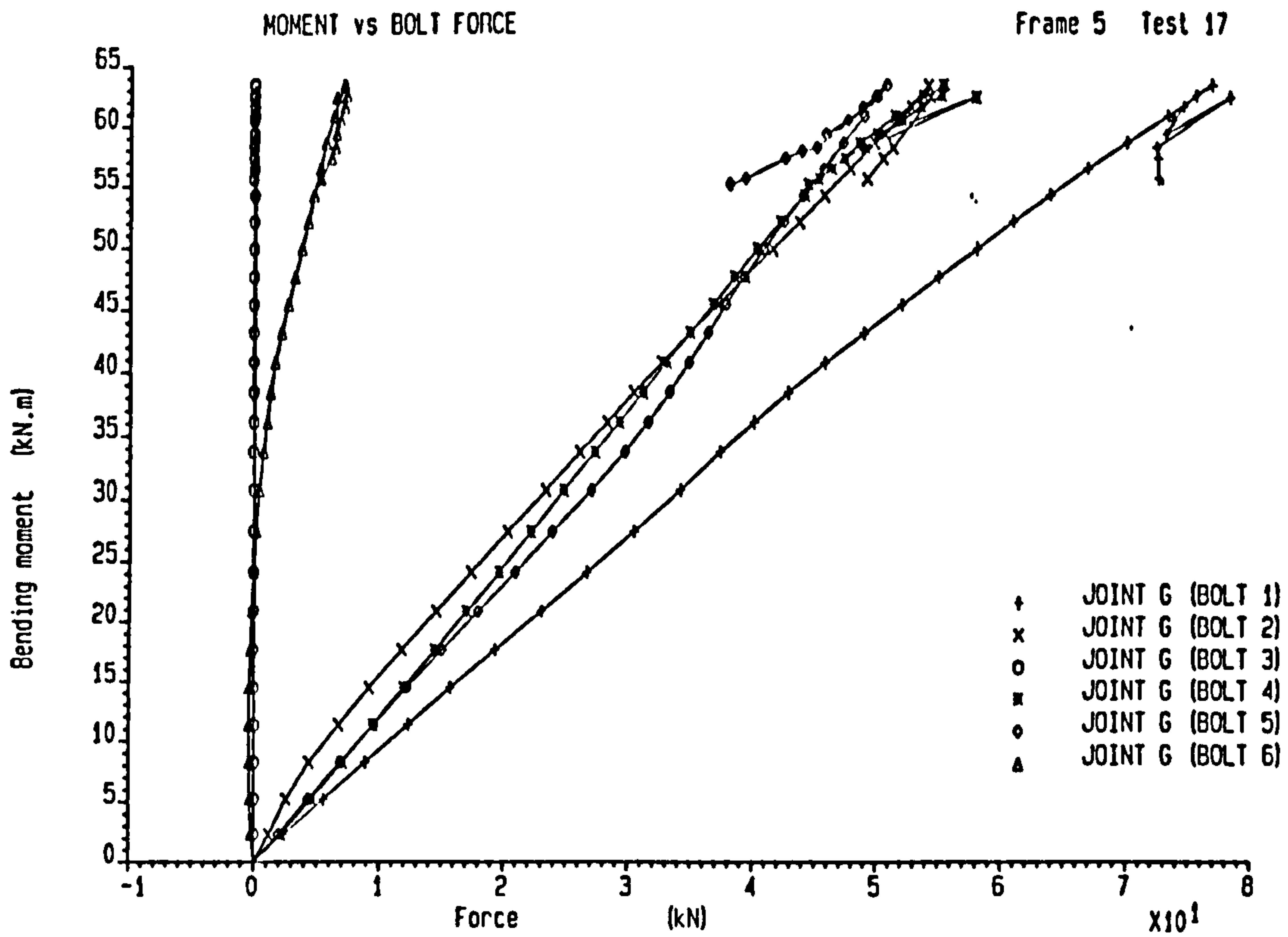


Figure 7.32 : Moment against Bolt Forces at Joint G for Test 17 of Frame 5

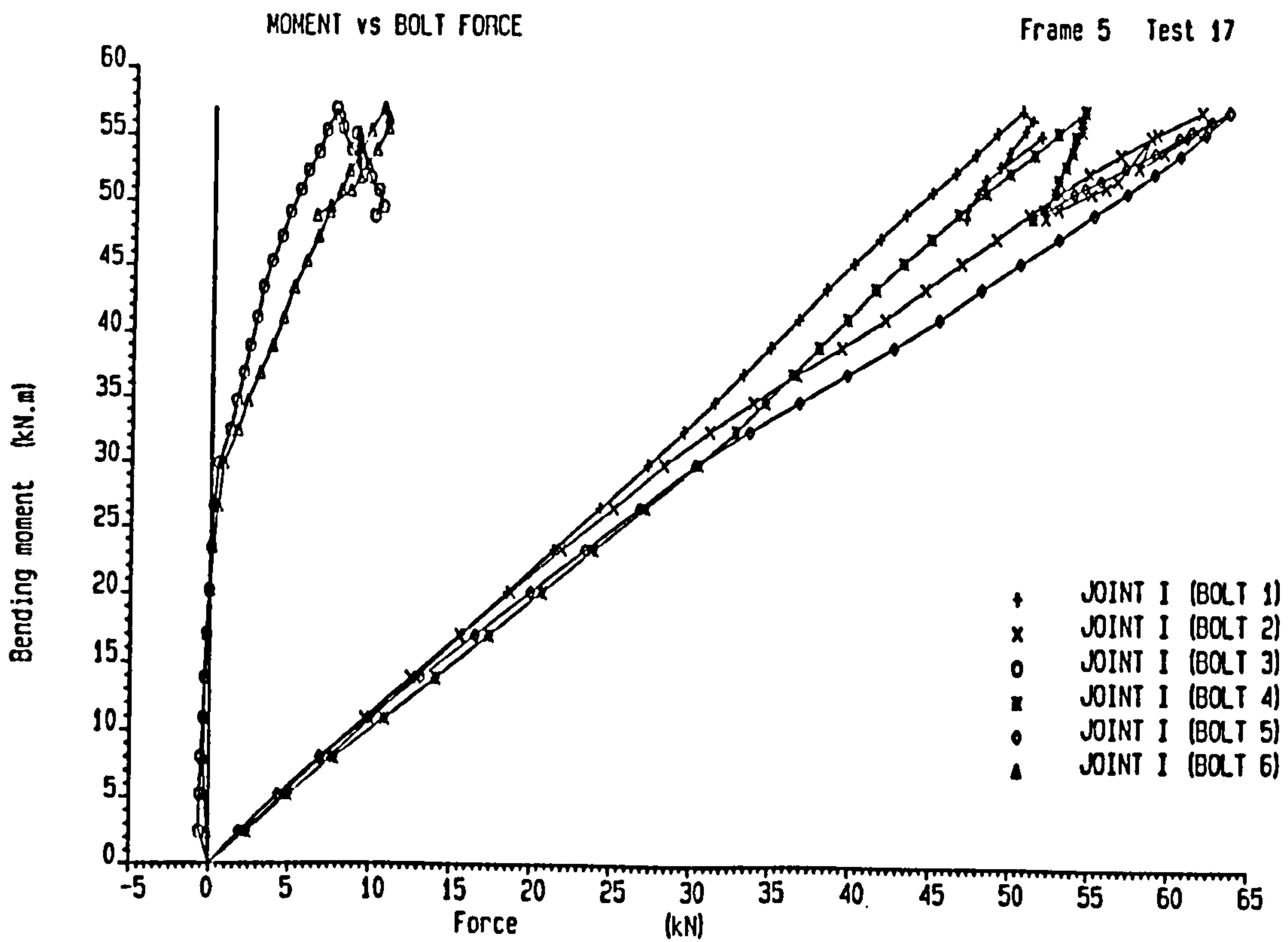


Figure 7.33 : Moment against Bolt Forces at Joint I for Test 17 of Frame 5

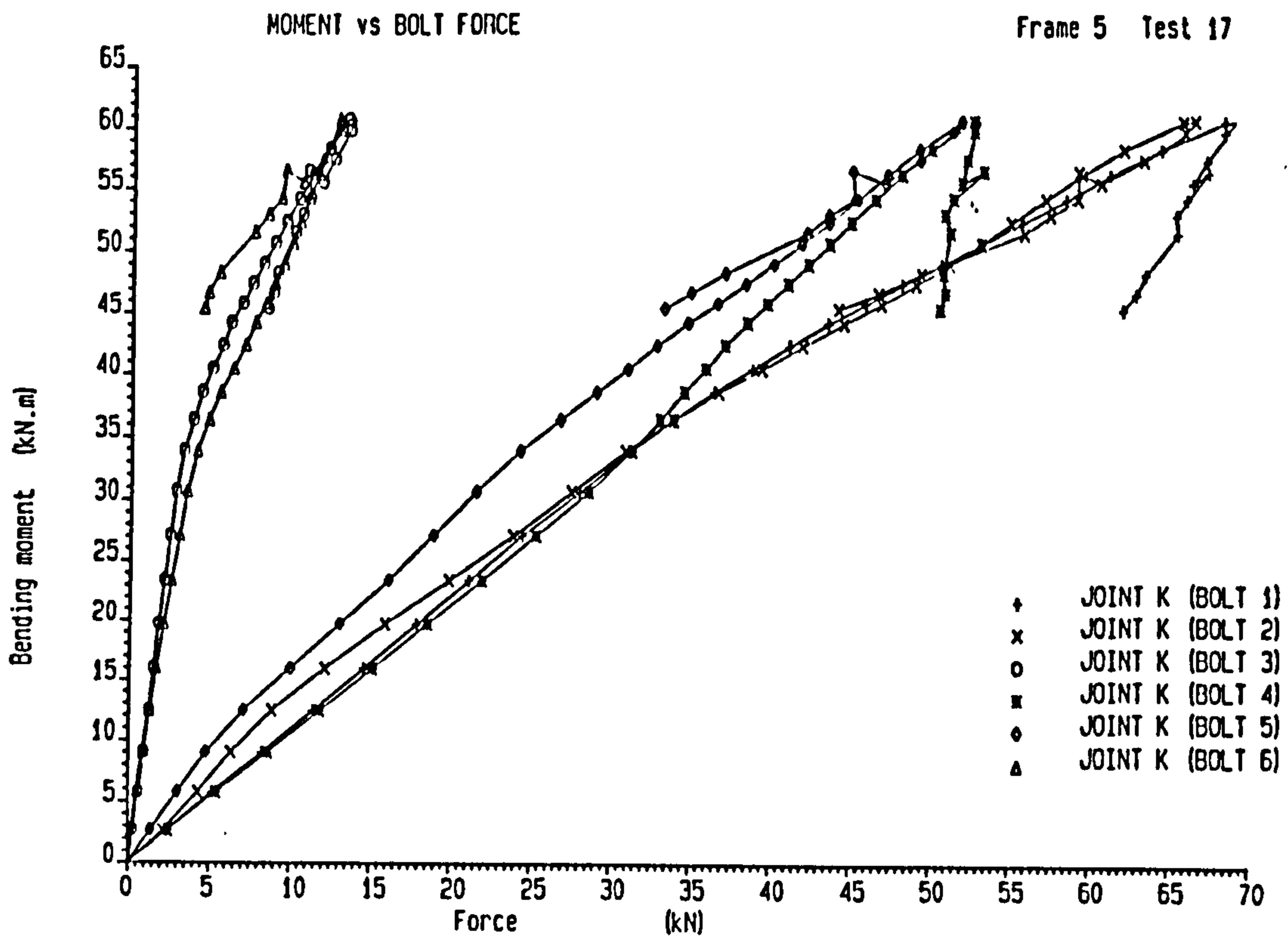


Figure 7.34 : Moment against Bolt Forces at Joint K for Test 17 of Frame 5

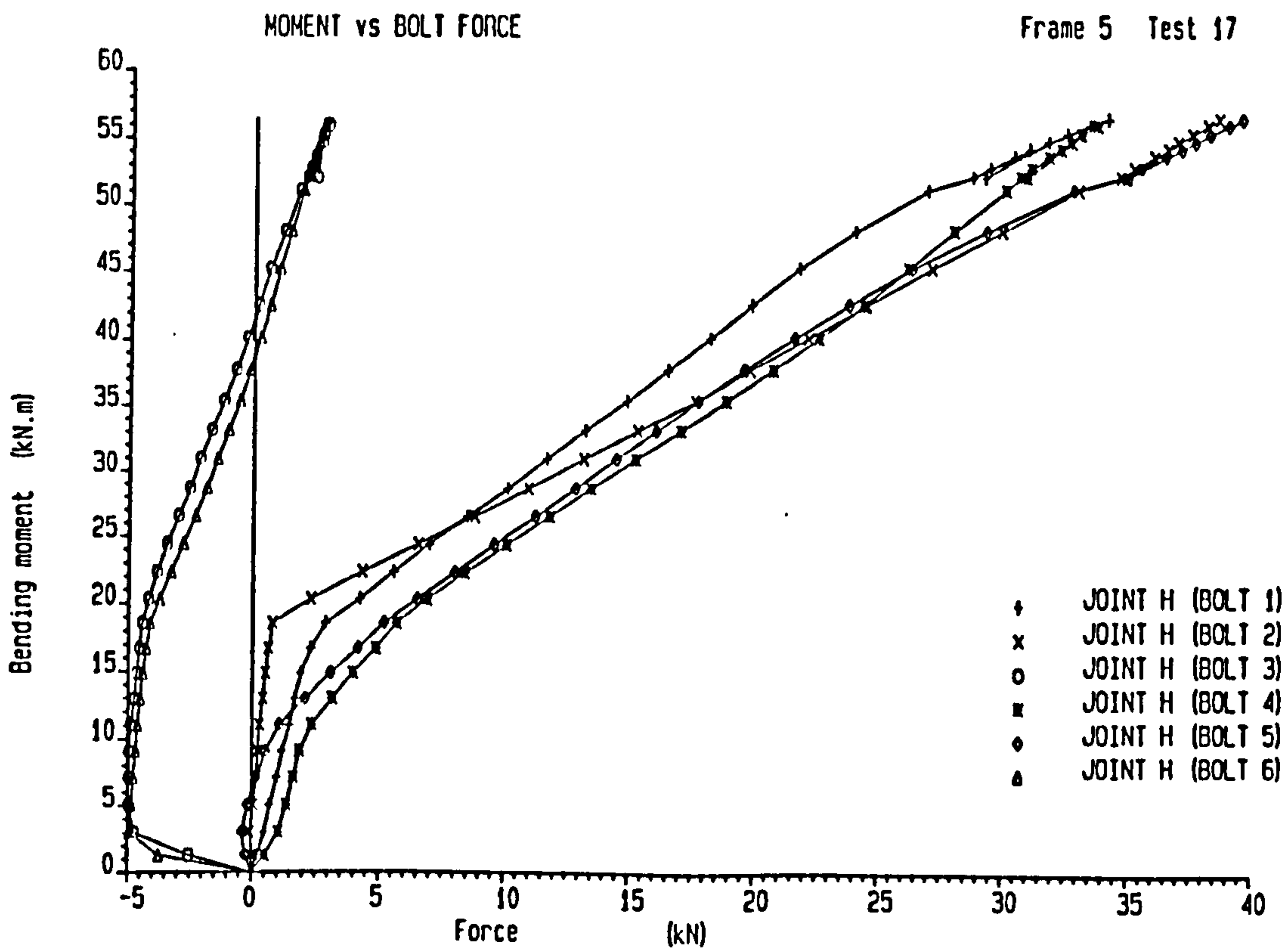


Figure 7.35 : Moment against Bolt Forces at Joint H for Test 17 of Frame 5

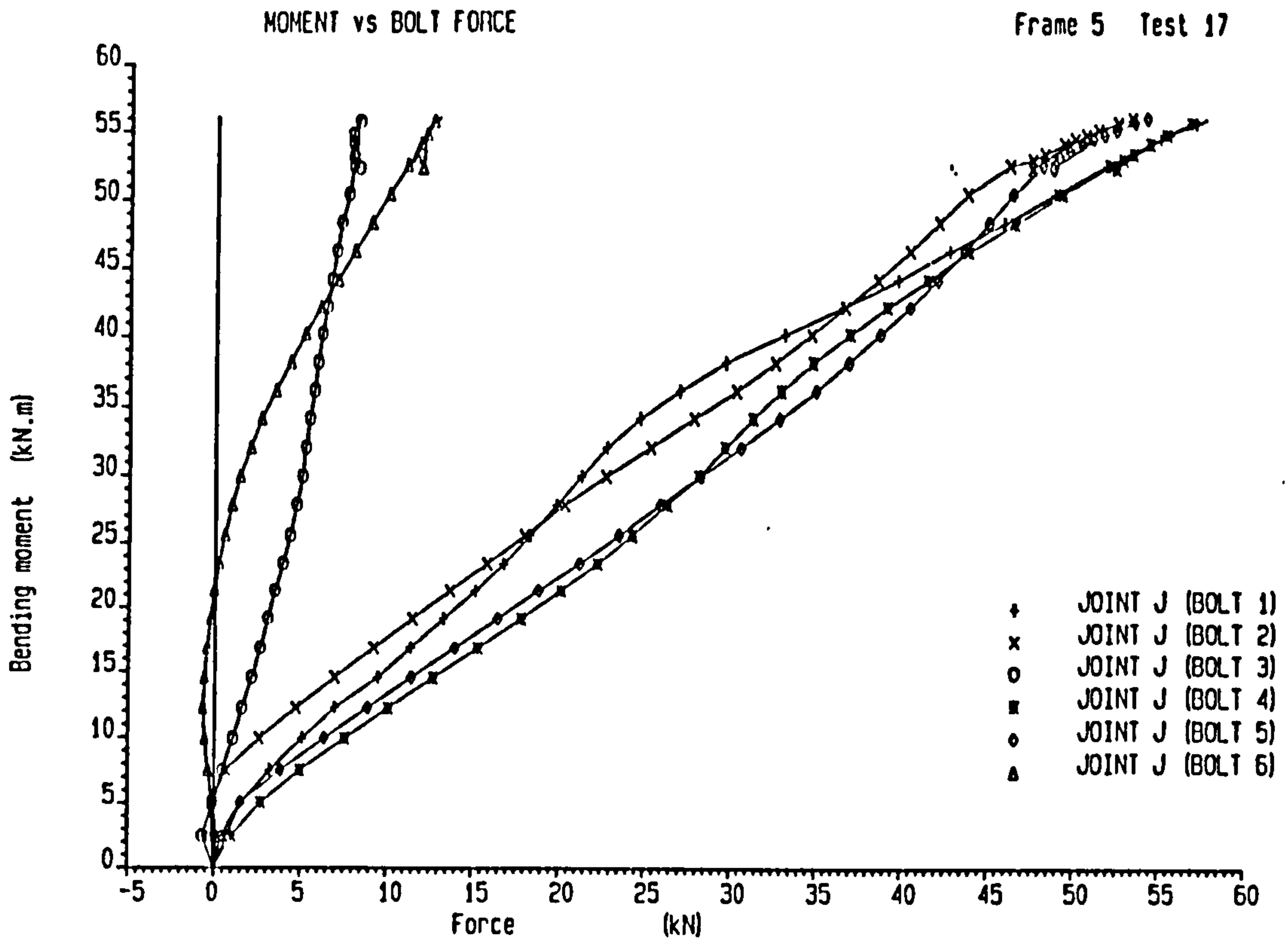


Figure 7.36 : Moment against Bolt Forces at Joint J for Test 17 of Frame 5

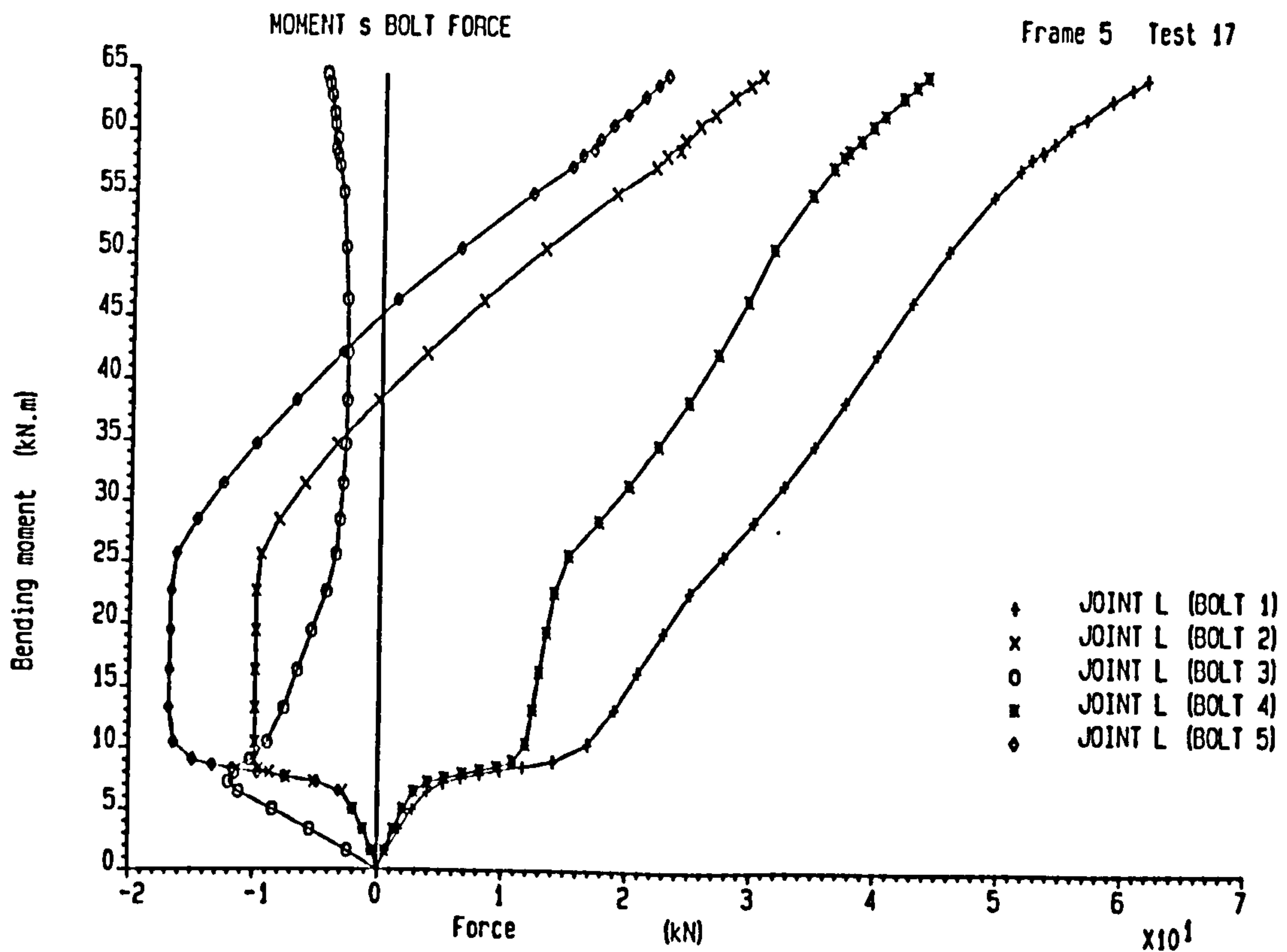


Figure 7.37 : Moment against Bolt Forces at Joint L for Test 17 of Frame 5